Evolutionäre Quanten-Spieltheorie im Kontext sozio-ökonomischer Systeme

Evolutionary Quantum Game Theory in the Context of Socio-Economic Systems

D I S S E R T A T I O N

zur Erlangung des akademischen Grades

Dr. rer. pol.
im Fach Wirtschaftswissenschaften

eingereicht an der
Wirtschaftswissenschaftlichen Fakultät
Goethe-Universität Frankfurt am Main

von
Dr. phil. nat. Matthias Hanauske
02.11.1970 Frankfurt am Main

Präsident der Goethe-Universität Frankfurt am Main:
Prof. Dr. Werner Müller-Esterl

Dekan der Wirtschaftswissenschaftlichen Fakultät:
Prof. Dr. Alfons Weichenrieder

Gutachter:
1. Prof. Dr. Wolfgang König
2. Prof. Dr. Matthias Blonski

eingereicht am: 10.12.2010
Tag der mündlichen Prüfung: 14.02.2011

Inhaltsverzeichnis

1. Deutsche Zusammenfassung **1**

1.1. Einführung 1

1.1.1. Motivation und Zielsetzung 1

1.1.2. Struktur und Fokus 3

1.2. Evolutionäre Quanten-Spieltheorie 4

1.2.1. Spieltheorie 5

1.2.2. Evolutionäre Spieltheorie 9

1.2.3. Evolutionäre Entwicklung sozio-ökonomischer Netzwerke . 12

1.2.4. Quanten-Spieltheorie 14

1.2.5. Exemplarische Beispiele 25

1.2.6. Resultate 46

1.3. Zusammenfassung und Ausblick 53

2. Introductory Paper: Evolutionary Quantum Game Theory **55**

2.1. Introduction 55

2.2. Classical Game Theory 57

2.2.1. Introduction 57

2.2.2. Definition and key aspects of classical game theory 60

2.3. Classical Evolutionary Game Theory 66

2.3.1. Definition and key aspects of classical evolutionary game theory 66

2.3.2. Classes of evolutionary games 69

2.3.3. Results for symmetric games 71

2.3.4. Results for unsymmetric games 81

2.4. Quantum Game Theory 94

2.4.1. Introduction 94

2.4.2. Definition and key aspects of quantum game theory . . . 98

2.4.3. Results for symmetric quantum games 106
2.5. Evolutionary Quantum Game Theory 117
2.6. Applications 118
2.6.1. Article 1: Quantum Game Theory and Open Access Publishing 118
2.6.2. Article 2: Evolutionary Quantum Game Theory and Scientific Communication 118
2.6.3. Article 3: Doves and Hawks in Economics Revisited: An evolutionary quantum game theory-based analysis of financial crises 119
2.6.4. Article 4: Experimental Validation of Quantum Game Theory 119
2.6.5. Article 5: Evolutionary Game Theory and Complex Networks of Scientific Information 119
2.7. Summary 120

3. Article 1: Quantum Game Theory and Open Access Publishing 123
3.1. Introduction 124
3.2. The Classical Game of Open Access 126
3.2.1. Formalization of the Game 126
3.2.2. Potential Game Settings 128
3.3. The Quantum Game of Open Access 130
3.3.1. Formalization of the Quantum Game 131
3.3.2. Potential Game Settings 134
3.3.3. Manifestation of Quantum Strategies 143
3.4. Summary 144

4. Article 2: Evolutionary Quantum Game Theory and Scientific Communication 147
4.1. Introduction 148
4.2. Definitions and key aspects of classical evolutionary game theory 149
4.3. Evolutionary Quantum Game Theory 152

5. Article 3: Doves and Hawks in Economics Revisited 157
5.1. Introduction 158
5.2. The financial crisis as Hawk-Dove game 161

5.3. The classical evolutionary game of doves and hawks 164
5.4. The quantum game of doves and hawks 172
5.4.1. Quantum Dove Strategies 175
5.4.2. Quantum Hawk Strategies 181
5.5. The quantum evolutionary game of doves and hawks 185
5.6. Interpretation and consequences 188
5.7. Summary 190

6. Article 4: Experimental Validation of Quantum Game Theory 193
6.1. Introduction 194
6.2. Mathematics of QGT 195
6.3. Quantum Cooperation Indicators 198
6.4. Classical vs. Quantum Cooperation Indicators 203
6.5. Experimental Validation 205
6.6. Summary 210

7. Article 5: Evolutionary Game Theory and Networks of Scientific Information 211
7.1. Introduction 211
7.2. Evolutionary Game Theory 214
7.2.1. Game theory: A simple example 214
7.2.2. Definition and key aspects of evolutionary game theory . 218
7.2.3. Classes of evolutionary games 225
7.3. Applications 241
7.3.1. Scientific communication and the open access decision . . 241
7.3.2. Evolution of Hubs- and Spokes Communication Networks 244
7.4. Summary and Outlook 246

Anhang A 249
A.I. Analytische Lösung des Barabasi-Albert Modell 249

Appendix B 251
B.I. Payoff transformations and strategic equivalent games 251
B.I.1. Positive affine transformations 251
B.I.2. Local payoff shifts 253
B.II. Results for classical symmetric (2x2) games 256

B.III.Results for classical symmetric (2x3) games 269
B.IV.Results for classical unsymmetric (2x2) games 278
B.V. Analytical expression for the γ-thresholds 289
B.V.1. Entanglement threshold γ_1 289
B.V.2. Entanglement threshold γ_2 290
B.VI.Results for symmetric (2x2) quantum games 292

1. Deutsche Zusammenfassung

1.1. Einführung

1.1.1. Motivation und Zielsetzung

Im Jahre 1928 veröffentlichte Johann (John) von Neumann eine mathematische Analyse mit dem Titel „Zur Theorie der Gesellschaftsspiele“ [234]. Die Frage, deren Beantwortung die Arbeit von John von Neumann anstrebte lautet:
„N Spieler ($\mathcal{I} = \{1, 2, ..., N\}$) spielen ein gegebenes Gesellschaftsspiel Γ. Wie muss einer dieser Spieler spielen, um dabei ein möglichst günstigstes Resultat zu erzielen?“ (siehe Einleitung in [234])
Eine Fußnote innerhalb dieser Arbeit lässt die, von John von Neumann damals schon erkannte, umfassende Anwendung auf ökonomische Fragestellungen erahnen:
„Es ist das Hauptproblem der klassischen Nationalökonomie: was wird, unter gegebenen äußeren Umständen, der absolut egoistische ‚homo oeconomicus‘ tun?“ (siehe zweite Fußnote in [234])
Neben dieser Arbeit, die man als den Ursprungsartikel der formalen Spieltheorie auffassen kann[1], befasste sich von Neumann in dieser Zeit hauptsächlich mit den mathematischen Grundlagen der Quanten Theorie. In seinem, 1932 erschienenen Lehrbuch „Mathematische Grundlagen der Quantenmechanik“ [232], befasste sich von Neumann mit der „einheitlichen, mathematisch einwandfreien Darstellung

[1] Die Ursprünge der Spieltheorie reichen genaugenommen bis ins 18.Jahrhundert zurück. Antoine-Augustin Cournot (1801–1877) und Francis Ysidro Edgeworth (1845–1926) analysierten schon damals ökonomische Gesellschaftsspiele unter Berücksichtigung der Interaktion der Wirtschaftssubjekte [80]. Desweiteren ist der im Jahre 1913 erschienene Aufsatz des Mathematikers Ernst Zermelo hervorzuheben [244], welcher die Analyse des Schachspiels mittels Rückwärtsinduktion betrachtete. Die noch heute benutzte Nomenklatur und mathematisch formale Beschreibung der Spieltheorie wurde jedoch erst im Jahre 1928 von John von Neumann vorgestellt [234].

der neuen Quantenmechanik“. Die von ihm eingeführte Theorie der hermiteschen Operatoren auf abstrakten Hilberträumen diente von damals an als mathematisches Grundgerüst der gesamten quantentheoretischen Beschreibung elementarer physikalischer Prozesse. 1933 emigrierte von Neumann in die USA und arbeitete am „Institute for Advance Study“ in Princeton. Gemeinsam mit Oskar Morgenstern veröffentlichte er im Jahre 1947 das erste Lehrbuch über Spieltheorie [233]. Im Jahre 1950, ebenfalls am „Institute for Advance Study“ in Princeton forschend, vollendete John Forbes Nash Jr. seine Dissertation und entwickelte in mehreren wissenschaftlichen Artikeln [141, 142, 143, 144] ein wichtiges, später nach ihm benanntes Gleichgewichtskonzept – das so genannte „Nash-Gleichgewicht“. Im Jahre 1972 erkannte J. Maynard Smith, dass sich die stationären Lösungen evolutionärer Differentialgleichungen auf die Spieltheorie und speziell auf die dem Spiel zugrundeliegenden Nash-Gleichgewichte zurückführen lassen [216]. In den darauf folgenden Jahren, wurde diese, so genannte „Evolutionäre Spieltheorie“ [213, 214, 198, 166, 222, 198, 21, 108] auf die unterschiedlichsten Systeme angewendet. So wurden unter anderem biologische [209, 226, 148, 78, 171, 172] und sozio-ökonomische Systeme, wie z.B. „Öffentliche Gut“ Spiele [51], kulturelle und moralische Entwicklungen [68, 121], die Evolution der Sprache [177], soziales Lernen [68], die Evolution von sozialen Normen [23, 175], Finanzkrisen [114] und die Evolution von komplexen sozio-ökonomischen Netzwerken [222, 139, 67] mittels der evolutionären Spieltheorie untersucht. Die durch Agenten-basierte Computersimulation erzielten numerischen Resultate der evolutionären Entwicklung sozio-ökonomischer Systeme stellen ein aktuelles, interdisziplinäres Forschungsfeld dar (näheres siehe Kapitel 1.2.3).

Im selben Jahr (1933) als von Neumann in die USA emigrierte, floh auch Albert Einstein nach Princeton und arbeitete von da an ebenfalls am „Institute for Advance Study“. Einstein forschte in dieser Zeit schon an einer einheitlichen Formulierung der gesamten Physik, welche die von ihm und David Hilbert entwickelte Allgemeine Relativitätstheorie mit den anderen bekannten Wechselwirkungen (speziell dem Elektromagnetismus) vereinen sollte. Neben diesem Forschungsschwerpunkt arbeitete Einstein auch an den Interpretationsvarianten der Quantentheorie. Gemeinsam mit Boris Podolsky und Nathan Rosen veröffentlichte er im Jahre 1935 eine Arbeit [64], die als das Ursprungswerk des Begriffes der Quantenverschränkung aufzufassen ist, und die in den folgenden

Jahren unter dem Stichwort „EPR-Paradoxon“ diskutiert wurde. Die, in diesem Artikel angesprochene Verletzung des klassischen Prinzips des lokalen Realismus durch die Quantentheorie, veranlassten Albert Einstein dazu der gesamten nichtkommutativen Quantentheorie skeptisch gegenüber zu stehen. Die durch eine mögliche Quantenverschränkung entstehenden Phänomene bezeichnete A. Einstein als eine „Spukhafte Fernwirkung“. Die experimentelle Bestätigung der Verschränkung von Quantenzuständen wurde erst nach Einsteins Tot in den 70er Jahren realisiert, die praktische Anwendung findet sich heutzutage z.B. in der Quantenkryptografie und im Quantencomputer wieder. Die Quantenverschränkung liefert zusätzlich die Basis für ein weiteres Forschungsfeld, nämlich das der Quanten-Spieltheorie. Im Jahre 1999 veröffentlichte Jens Eisert die erste Arbeit über Quanten-Spieltheorie [66] und vereinigte dadurch die beiden von John von Neumann formulierten Theorien der Spiel- und Quanten Theorie mit den Einstein'schen Konzepten der Quantenverschränkung.

Das Hauptanliegen dieser Arbeit liegt in einer zusammenfassenden, mathematisch einwandfreien Darstellung der Theorie der Gesellschaftsspiele auf quantentheoretischen, abstrakten Hilbertschen Räumen. Die Arbeit gibt einen Überblick über die methodischen Grundlagen der Quanten-Spieltheorie, der in dieser Zusammenstellung und ausführlichen Form noch nicht in der wissenschaftlichen Literatur zu finden ist. Da die, seit den Ursprüngen der Quanten-Spieltheorie maßgeblich in physikalischen wissenschaftlichen Zeitschriften veröffentlichten Artikel für Wirtschaftswissenschafter nur mit großen Anstrengungen zu verstehen sind, ist der vorliegende Überblick stark an die spieltheoretische Nomenklatur und Thematik angelehnt. Ein Hauptziel der Arbeit besteht somit darin, mathematisch interessierten Sozial- und Wirtschaftswissenschaftlern einen verständlichen Überblicksartikel über die Quanten-Spieltheorie zu liefern. Neben diesem Überblick über den Themenbereich, liegt ein weiteres Ziel der Arbeit in der Präsentation von möglichen Anwendungsbeispielen der Theorie.

1.1.2. Struktur und Fokus

Diese kumulative Dissertation besteht, neben dieser deutschen Zusammenfassung, aus insgesamt sechs separaten Arbeiten, wobei der erste eine umfassende Einführung in die Evolutionäre Quanten-Spieltheorie darstellt (siehe „Introductory

Paper“ [110]).

- Introductory Paper: Evolutionary Quantum Game Theory [110]
- Artikel 1: Quantum Game Theory and Open Access Publishing [111]
- Artikel 2: Evolutionary Quantum Game Theory and Scientific Communication [118]
- Artikel 3: Doves and hawks in economics revisited:
  An evolutionary quantum game theory-based analysis of financial crises [114]
- Artikel 4: Experimental Validation of Quantum Game Theory [112]
- Artikel 5: Evolutionary Game Theory and Complex Networks of Scientific Information [117]

Die Artikel 1, 2 und 5 wenden die Theorie auf den Markt für wissenschaftliche Fachinformationen an, Artikel 3 beschreibt die, während der Promotionsdauer aufgetretende Finanzmarktkrise, als evolutionäres Quantenspiel und Artikel 4 diskutiert erste Ansätze einer experimentellen Bestätigung der Quanten-Spieltheorie.

Der gesamte Aufbau der Arbeit verfolgt zunächst das Anliegen die theoretischen, mathematischen Konstrukte so allgemein wie möglich einzuführen (siehe „Introductory Paper“ [110]), wobei ein gewisser thematischer Fokus nötig war. Die in dieser Arbeit diskutierten (evolutionären) Spiele sind unter dem Stichwort „(N Personen) - (m Strategien) Spiele in strategischer Form“ zusammenzufassen, wobei der Hauptteil der Arbeit sich mit der Klassifikation von „(2 Personen) - (2 Strategien) Quantenspielen“ beschäftigt. Quantenspiele in extensiver Form und der gesamte Themenbereich der kooperativen Spieltheorie wird in dieser Arbeit nicht behandelt.

1.2. Evolutionäre Quanten-Spieltheorie

Dieses Kapitel vermittelt die wesentlichen Konzepte der evolutionäre Quanten-Spieltheorie und fasst die erzielten Ergebnisse und betrachteten Anwendungsfelder der vorliegenden kumulativen Dissertation in komprimierter Form, in deutscher

Sprache zusammen. Eine ausführliche, in englischer Sprache verfasste Darstellung der Theorie der evolutionären Quantenspiele findet sich in dem „Introductory Paper“ der Dissertation. Eine eingehende Untersuchung und Diskussion der betrachteten Anwendungsfelder ist den fünf beigefügten Artikeln zu entnehmen.

Die ersten beiden Unterkapitel befassen sich mit den Grundlagen der klassischen (evolutionären) Spieltheorie. Unterkapitel 1.2.3 gibt einen kurzen Einblick in das aktuelle Forschungsgebiet der evolutionären Entwicklung von sozio-ökonomischen Netzwerken und motiviert Unterkapitel 1.2.4, welches sich mit der Theorie der Quantenspiele befasst. Das Unterkapitel 1.2.5 stellt die abstrakte mathematische Theorie der evolutionären Quanten-Spieltheorie an mehreren Beispielen exemplarisch dar. Die formalen Ergebnisse der Arbeit und die in der gesamten kumulativen Dissertation behandelten Anwendungsfelder werden in Unterkapitel 1.2.6 zusammengefasst und kurz diskutiert.

1.2.1. Spieltheorie

Dieses Unterkapitel stellt die wesentlichen Definitionen und Konzepte der klassischen Spieltheorie vor, beschränkt sich jedoch auf das Teilgebiet der sogenannten „gemischten Erweiterung von simultanen (N Spieler)-(m Strategien) Spiele in strategischer Form“. Die formale mathematische Definition eines solchen Spiels lautet (siehe z.B. [198]):

N-Spieler Spiel:

$$\Gamma := (\mathcal{I}, \mathcal{S}, \$) \tag{1.1}$$

Menge der Spieler:

$\mathcal{I} = \{1, 2, ..., N\}$

Raum der reinen Strategien der Spieler:

$\mathcal{S} = \mathcal{S}^1 \times \mathcal{S}^2 \times ... \times \mathcal{S}^N$

Menge der reinen Strategien des Spielers $\mu \in \mathcal{I}$:

$\mathcal{S}^\mu = \left\{(s_1^\mu, s_2^\mu, ..., s_{m_\mu}^\mu)\right\}$

Raum der gemischten Strategien der Spieler:

$\tilde{\mathcal{S}} = \tilde{\mathcal{S}}^1 \times \tilde{\mathcal{S}}^2 \times ... \times \tilde{\mathcal{S}}^N$

Gemischte Strategie des Spielers $\mu \in \mathcal{I}$:

$$\tilde{\mathcal{S}}^{\mu} = \left\{ (\tilde{s}_1^{\mu}, \tilde{s}_2^{\mu}, ..., \tilde{s}_{m_\mu}^{\mu}) \mid \sum_{i=1}^{m_\mu} \tilde{s}_i^{\mu} = 1, \tilde{s}_i^{\mu} \geq 0, i = 1, 2, ..., m_\mu \right\}$$

Anzahl der für Spieler $\mu \in \mathcal{I}$ möglichen reinen Strategien:

$$m_\mu$$

Gemischtes Strategienprofil des Spielers $\mu \in \mathcal{I}$:

$$\tilde{s}^{\mu} = \left(\tilde{s}_1^{\mu}, \tilde{s}_2^{\mu}, ..., \tilde{s}_{m_\mu}^{\mu} \right)^T \in \tilde{\mathcal{S}}^{\mu}$$

Vektorwertige Auszahlungsfunktion der Spieler:

$$\$ = \left(\$^1, \$^2, ..., \$^N \right) : \mathcal{S} \to \mathbb{R}^N$$

Vektorwertige gemischte Auszahlungsfunktion der Spieler:

$$\tilde{\$} = \left(\tilde{\$}^1, \tilde{\$}^2, ..., \tilde{\$}^N \right) : \tilde{\mathcal{S}} \to \mathbb{R}^N$$

Gemischte Auszahlungsfunktion des Spielers $\mu \in \mathcal{I}$:

$$\tilde{\$}^{\mu}(\tilde{s}^1, \tilde{s}^2, ..., \tilde{s}^N) = \sum_{i_1=1}^{m_1} \sum_{i_2=1}^{m_2} ... \sum_{i_N=1}^{m_N} \$^{\mu}(s_{i_1}^1, s_{i_2}^2, ..., s_{i_N}^N) \prod_{\nu=1}^{N} \tilde{s}_{i_\nu}^{\nu}$$

Die Menge der Spieler $\mathcal{I}$ kann unter Umständen aus unterschiedlichen Teilmengen bestehen, die ihrerseits unterschiedliche Strategiemengen $\mathcal{S}$ besitzen. In sozioökonomischen Netzwerken stellen die Spieler die jeweiligen Knoten des Netzwerkes dar (näheres siehe Kapitel 1.2.3). Definition (1.1) sagt im wesentlichen aus, dass man für die Definition eines solchen N Personen Spiels lediglich drei Angaben benötigt. Ein Spiel $\Gamma := (\mathcal{I}, \mathcal{S}, \$)$ ist für die klassische Spieltheorie hinreichend definiert, wenn die Menge $\mathcal{I}$ der Spieler, die Menge (der Raum) $\mathcal{S}$ der Strategien der Spieler und ihre Auszahlungsfunktion $\$$ bekannt sind. Um diese formale Definition im einzelnen zu erklären, beschränken sich die folgenden Darlegungen auf den einfachsten Fall des simultanen (2 Spieler)-(2 Strategien) Spiels.

Abbildung 1.1 stellt den Spielbaum eines simultanen (2 Personen)-(2 Strategien) Spiels dar. Beide Spieler (Spieler A und Spieler B) treffen die Entscheidung, welche der beiden reinen Strategien (s_1 und s_2) sie auszuwählen gedenken, zur gleichen Zeit, d.h. beim Zeitpunkt der Entscheidung wissen beide Spieler nicht, welche der Strategien der andere Spieler auswählt. $\$^{\mu}$ ($\mu = A, B$) bezeichnet die Auszahlung, welche den Spielern nach Bekanntgabe ihrer Entscheidung ausgezahlt wird. Definition (1.1) vereinfacht sich in einem solchen (2×2) Spiel somit wie

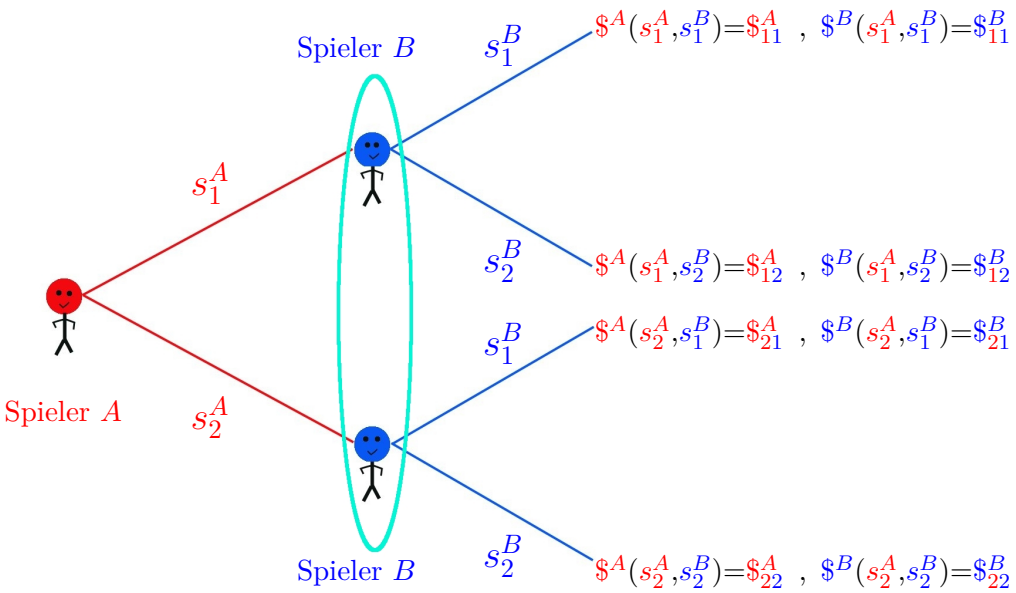

Abbildung 1.1.: Spielbaum eines (2 Personen)-(2 Strategien) Spiels mit den Auszahlungsfunktionen für Spieler A ($\$^A$) und Spieler B ($\$^B$).

folgt:

$$
\begin{aligned}
&(2\times 2) \text{ Spiel:}\\
&\Gamma := \left(\{A,B\}, \mathcal{S}^A \times \mathcal{S}^B, \hat{\$}_A, \hat{\$}_B\right)\\
&\text{Menge der reinen Strategien des Spielers A und B:}\\
&\mathcal{S}^A = \left\{s_1^A, s_2^A\right\}\ ,\ \mathcal{S}^B = \left\{s_1^B, s_2^B\right\}\\
&\text{Menge der gemischten Strategien des Spielers A und B:}\\
&\tilde{\mathcal{S}}^A = \left\{\tilde{s}_1^A, \tilde{s}_2^A\right\}\ ,\ \tilde{\mathcal{S}}^B = \left\{\tilde{s}_1^B, \tilde{s}_2^B\right\}\\
&\text{Auszahlungsmatrix der Spieler A und B:}\\
&\hat{\$}_A = \begin{pmatrix} \$^A_{11} & \$^A_{12} \\ \$^A_{21} & \$^A_{22} \end{pmatrix},\ \hat{\$}_B = \begin{pmatrix} \$^B_{11} & \$^B_{12} \\ \$^B_{21} & \$^B_{22} \end{pmatrix}
\end{aligned}
\tag{1.2}
$$

Die Menge der gemischten Strategien des Spielers A ($\tilde{\mathcal{S}}^A$) und B ($\tilde{\mathcal{S}}^B$) kann als eine mathematische Verallgemeinerung der Menge der reinen Strategien ($\mathcal{S}^A$ und $\mathcal{S}^B$) verstanden werden. Die einzelnen Elemente der Menge der gemischten Strategien eines Spielers $\mu = A, B$ ($\tilde{\mathbf{s}}^\mu = (\tilde{s}_1^\mu, \tilde{s}_2^\mu) \in \mathcal{S}^\mu$) besteht aus zwei reellwertigen Zahlen

($\tilde{s}_1^\mu \in [0,1]$ und $\tilde{s}_2^\mu \in [0,1]$) und kann als die Wahrscheinlichkeit des Spielers μ zur Wahl der Strategie 1 ($\tilde{s}_1^\mu$) bzw. der Strategie 2 ($\tilde{s}_2^\mu$) interpretiert werden. Desweiteren gilt die folgende Normalisierungsbedingung: $\tilde{s}_1^\mu + \tilde{s}_2^\mu = 1 \; \forall \, \mu = A, B$.

Unter Verwendung der Auszahlungsmatrizen des Spielers A ($\hat{\$}_A$) und B ($\hat{\$}_A$) schreibt sich die gemischte Auszahlungsfunktion des Spielers $\mu = A, B$ wie folgt:

$$\begin{aligned} &\tilde{\$}^\mu : \left(\tilde{\mathcal{S}}^A \times \tilde{\mathcal{S}}^B\right) \to \mathbb{R} \\ &\tilde{\$}^\mu((\tilde{s}_1^A, \tilde{s}_2^A), (\tilde{s}_1^B, \tilde{s}_2^B)) = \$_{11}^\mu \tilde{s}_1^A \tilde{s}_1^B + \$_{12}^\mu \tilde{s}_1^A \tilde{s}_2^B + \$_{21}^\mu \tilde{s}_2^A \tilde{s}_1^B + \$_{22}^\mu \tilde{s}_2^A \tilde{s}_2^B \end{aligned} \tag{1.3}$$

Aufgrund der Normalisierungsbedingung vereinfacht sich die Funktion in Gleichung (1.3) wie folgt:

$$\begin{aligned} &\tilde{\$}^\mu : ([0,1] \times [0,1]) \to \mathbb{R} \\ &\tilde{\$}^\mu(\tilde{s}^A, \tilde{s}^B) = \$_{11}^\mu \tilde{s}^A \tilde{s}^B + \$_{12}^\mu \tilde{s}^A (1 - \tilde{s}^B) + \$_{21}^\mu (1 - \tilde{s}^A) \tilde{s}^B + \$_{22}^\mu (1 - \tilde{s}^A)(1 - \tilde{s}^B) \end{aligned} \tag{1.4}$$

, wobei $\tilde{s}^A := \tilde{s}_1^A$, $\tilde{s}^B := \tilde{s}_1^B$, $\tilde{s}_2^A = 1 - \tilde{s}_1^A$ und $\tilde{s}_2^B = 1 - \tilde{s}_1^B$. Im Folgenden werden zwei fundamentale Gleichgewichtskonzepte der Spieltheorie vorgestellt.

Eine Strategienkombination $(\tilde{s}^{A\dagger}, \tilde{s}^{B\dagger})$ ist ein Gleichgewicht in dominanten Strategien, wenn die folgenden Bedingungen erfüllt sind:

$$\begin{aligned} &\text{Gleichgewicht in dominanten Strategien:} \\ &\tilde{\$}^\mu(\tilde{s}^{A\dagger}, \tilde{s}^{B\dagger}) \;\geq\; \tilde{\$}^\mu(\tilde{s}^A, \tilde{s}^B) \quad \forall \; \mu = A, B \text{ und } \tilde{s}^A, \tilde{s}^B \in [0,1] \end{aligned} \tag{1.5}$$

Eine Strategienkombination $(\tilde{s}^{A*}, \tilde{s}^{B*})$ nennt man ein Nash-Gleichgewicht, falls die folgenden Bedingungen erfüllt sind:

$$\begin{aligned} &\text{Nash-Gleichgewicht:} \\ &\tilde{\$}^A(\tilde{s}^{A*}, \tilde{s}^{B*}) \;\geq\; \tilde{\$}^A(\tilde{s}^A, \tilde{s}^{B*}) \quad \forall \; \tilde{s}^A \in [0,1] \\ &\tilde{\$}^B(\tilde{s}^{A*}, \tilde{s}^{B*}) \;\geq\; \tilde{\$}^B(\tilde{s}^{A*}, \tilde{s}^B) \quad \forall \; \tilde{s}^B \in [0,1] \end{aligned} \tag{1.6}$$

Ein Spezialfall des Nash-Gleichgewichts besteht, falls die partielle Ableitung der gemischten Auszahlungsfläche verschwindet. Man nennt dann ein solches Nash-Gleichgewicht $(\tilde{s}^{A\star}, \tilde{s}^{B\star})$ ein internes Nash-Gleichgewicht bzw. ein Nash-

Gleichgewicht in gemischten Strategien.

$$\text{Nash-Gleichgewicht in gemischten Strategien:} \tag{1.7}$$
$$\left.\frac{\partial \tilde{\$}^A(\tilde{s}^A, \tilde{s}^B)}{\partial \tilde{s}^A}\right|_{\tilde{s}^B=\tilde{s}^{B\star}} = 0 \quad \forall\ \tilde{s}^A \in [0,1]\ ,\ \tilde{s}^{B\star} \in]0,1[$$
$$\left.\frac{\partial \tilde{\$}^B(\tilde{s}^A, \tilde{s}^B)}{\partial \tilde{s}^B}\right|_{\tilde{s}^A=\tilde{s}^{A\star}} = 0 \quad \forall\ \tilde{s}^B \in [0,1]\ ,\ \tilde{s}^{A\star} \in]0,1[$$

1.2.2. Evolutionäre Spieltheorie

Dieses Unterkapitel fasst die wesentlichen Konzepte der deterministischen evolutionäre Spieltheorie zusammen und fokussiert speziell auf das Teilgebiet der Reproduktionsdynamik. Weiterführende Konzepte wie z.B. die stochastische evolutionäre Spieltheorie und adaptive oder rationale Lernprozesse werden in diesem Unterkapitel nicht beschrieben (näheres siehe [196]). Die Darstellung beschränkt sich auf die Reproduktionsdynamik und betrachtet andere mögliche Dynamiken (wie z.B. nichtlineare Auszahlungsfunktionen, allgemeine Imitationsdynamiken, Bestantwortdynamiken, Logit Dynamiken und Brown-von Neumann-Nash Dynamiken) nicht (näheres hierzu siehe [196, 128]). Eine Miteinbeziehung von zugrundeliegenden komplexen Netzwerkstrukturen in die evolutionären Gleichungen, unter Verwendung von Agenten-basierten Simulationen, wird kurz in Unterkapitel 1.2.3 angesprochen (eine detaillierte Darstellung findet sich z.B. in [222, 128]).

Die Reproduktionsdynamik der evolutionären Spieltheorie untersucht das zeitliche Verhalten einer großen Anzahl von individuellen Spielern, der sogenannten Population (siehe [235, 198, 109]). Betrachtet man ein wiederholtes Spiel innerhalb eines Netzwerks von individuellen Entscheidungsknoten, so sollten die gemittelten Werte der Entscheidungen der Spieler im Grenzfall großer, zufälliger Netzwerke in die Gleichungen der evolutionären Spieltheorie übergehen.

Gegeben sei die strategische Form eines, zunächst noch im Allgemeinen unsymmetrischen (2 Personen)-(2 Strategien) Spiels Γ (siehe Definition (1.2)). $x_i^\mu(t)$ ($i = 1, 2$ und $\mu = A, B$) seien die zeitabhängigen, gemittelten Anteile der Spieler innerhalb der Spielergruppe $\mu = A, B$, die die Strategie 1 ($x_1^\mu(t)$) bzw. die Strategie 2 ($x_2^\mu(t)$) wählen. Diese gruppenspezifischen Populationsvek-

toren ($\vec{x}^A(t) = (x_1^A(t), x_2^A(t))$ und $\vec{x}^B(t) = (x_1^B(t), x_2^B(t))$) unterliegen folgender Normalisierungsbedingung:

$$x_i^\mu(t) \geq 0 \quad \text{und} \quad \sum_{i=1}^{2} x_i^\mu(t) = 1 \quad \forall\, i = 1, 2\,,\ t \in \mathbb{R},\ \mu = A, B \tag{1.8}$$

Aufgrund dieser Bedingung lassen sich die beiden Komponenten der zweidimensionalen gruppenspezifischen Populationsvektoren auf eine Komponente reduzieren ($x_2^A = 1 - x_1^A$ und $x_2^B = 1 - x_1^B$). Das zeitliche Verhalten der Komponenten der Populationsvektoren (Gruppe A: $x(t) := x_1^A(t)$ und Gruppe B: $y(t) := x_1^B(t)$) wird in der Reproduktionsdynamik mittels des folgenden Systems von Differentialgleichungen beschrieben (näheres siehe z. B. [21, 198, 166, 196, 128, 109]):

$$\begin{aligned}
\frac{dx(t)}{dt} &= \left(\$_{11}^A + \$_{22}^A - \$_{12}^A - \$_{21}^A\right)\left(x(t) - (x(t))^2\right) y(t) + \\
&\quad + \left(\$_{12}^A - \$_{22}^A\right)\left(x(t) - (x(t))^2\right) =: g_A(x, y) \\
\frac{dy(t)}{dt} &= \left(\$_{11}^B + \$_{22}^B - \$_{12}^B - \$_{21}^B\right)\left(y(t) - (y(t))^2\right) x(t) + \\
&\quad + \left(\$_{12}^B - \$_{22}^B\right)\left(y(t) - (y(t))^2\right) =: g_B(x, y)
\end{aligned} \tag{1.9}$$

Gleichung (1.9) beschreibt die zeitliche Entwicklung des strategischen Verhaltens der beiden Teilpopulationen A und B in einem allgemeinen unsymmetrischen Bimatrix Spiel. Der Anteil der Spieler in Teilgruppe A, die zum Zeitpunkt t die Strategie s_1 wählen ist mittels der Größe $x(t)$ quantifiziert, wohingegen $y(t)$ denselben Anteil in Teilgruppe B beschreibt. Die zeitliche Entwicklung des Systems von gekoppelten Differentialgleichungen (1.9) hängt neben den beiden Funktionen $g_A(x, y)$ und $g_B(x, y)$ von den jeweiligen Anfangswerten der Populationsvektoren $x(t = 0)$ und $y(t = 0)$ ab.

Unter Annahme einer symmetrischen Auszahlungsmatrix ($\hat{\$}^A \equiv \left(\hat{\$}^B\right)^T$, $\$_{lk} := \$_{lk}^A = \$_{kl}^B$) vereinfacht sich das System der Differentialgleichungen (1.9) und es lässt sich leicht erkennen, dass nun die jeweiligen Populationsvektoren $\vec{x}^A(t)$ und $\vec{x}^B(t)$ (bzw. $x(t)$ und $y(t)$) identisch sind. Bezeichnet man den gemeinsamen Populationsvektor mit $x(t)$, so ist sein dynamisches Verhalten durch folgende

Differentialgleichung gegeben (näheres siehe [21, 198, 166, 109]):

$$\begin{aligned}\frac{dx}{dt} &= x\left[\$_{11}(x-x^2)+\$_{12}(1-2x+x^2)+\$_{21}(x^2-x)+\$_{22}(2x-x^2-1)\right] \\ &= x\left[(\$_{11}-\$_{21})(x-x^2)+(\$_{12}-\$_{22})(1-2x+x^2)\right] =: g(x) \qquad (1.10)\end{aligned}$$

wobei: $\quad x = x(t) := x_1(t) \quad \rightarrow \quad x_2(t) = (1-x(t))$

$x(t)$, der Anteil der Spieler die zum Zeitpunkt t die Strategie s_1 spielen, hängt neben der Funktion $g(x)$ von dem Anfangswert $x(t=0)$ ab. Die stationären Lösungen des asymptotischen Verhaltens des Populationsvektors ($\lim_{t\to\infty}(x(t))$) werden mittels eines weiteren Gleichgewichtskonzeptes, das der evolutionär stabilen Strategie (ESS) beschrieben. Gegeben sei ein allgemeines zwei Personen Spiel Γ (gemischte Auszahlungsfunktionen: $\tilde{\$}^A$ und $\tilde{\$}^B$). Eine Strategienkombination $(\tilde{s}^{A*}, \tilde{s}^{B*}) \in ([0,1]\times[0,1])$ bezeichnet man als eine evolutionär stabile Strategie, falls

a) $(\tilde{s}^{A*}, \tilde{s}^{B*})$ ist ein Nash-Gleichgewicht des Spiels Γ

b) $\tilde{\$}^A(\tilde{s}^A, \tilde{s}^B) \leq \tilde{\$}^A(\tilde{s}^{A*}, \tilde{s}^B) \qquad \forall \quad \tilde{s}^A \in r^A(\tilde{s}^{B*}), \;\; \tilde{s}^B \neq \tilde{s}^{B*}$
$\tilde{\$}^B(\tilde{s}^A, \tilde{s}^B) \leq \tilde{\$}^B(\tilde{s}^A, \tilde{s}^{B*}) \qquad \forall \quad \tilde{s}^B \in r^B(\tilde{s}^{A*}), \;\; \tilde{s}^A \neq \tilde{s}^{A*}$

$r^B(\tilde{s}^A)$ bzw. $r^A(\tilde{s}^B)$ ist die Abbildung der besten Antwort des Spielers B auf die Strategie $\tilde{s}^A$ bzw. des Spielers A auf die Strategie $\tilde{s}^B$. Eine ESS $(\tilde{s}^{A*}, \tilde{s}^{B*})$ des Spiels Γ besteht somit, falls diese ein Nash-Gleichgewicht ist (notwendige Bedingung) und zusätzlich (hinreichende Bedingung) die Ungleichungen in b) für alle Strategiekombinationen $(\tilde{s}^A, \tilde{s}^B)$ innerhalb der Menge der Bestantwort $r^B(\tilde{s}^A)$ bzw. $r^A(\tilde{s}^B)$ erfüllt sind.

Die dargestellten Gleichungen der Reproduktionsdynamik und die Definition der ESS lassen sich nach Spezifikation der Auszahlungsmatrix $\hat{\$}$ auf unterschiedlichste Populationsspiele anwenden. Generell lassen sich symmetrische (2×2) Spiele und somit die Lösungen der Gleichung (1.10) in drei unterschiedliche Spielklassen gliedern: dominanten Spiele, Koordinationsspiele und Anti-Koordinationsspiele. Unsymmetrische (2×2) Spiele und somit die Lösungen der Gleichung (1.9) lassen sich hingegen in die folgenden Spielklassen gliedern: die Eckenspiele (engl.: „corner class games“), die Sattelspiele (engl.: „saddle class games“) und die Zentrumsspiele

(engl.: „center class games“). Die Eigenschaften dieser unterschiedlichen Klassen von Spielen sind im „Introductory Paper“ [110] dieser Dissertation im Detail beschrieben, wobei einige der betrachteten Beispiele zusätzlich im Unterkapitel 1.2.5 diskutiert werden.

1.2.3. Evolutionäre Entwicklung sozio-ökonomischer Netzwerke

Eine bedeutende Einschränkung der deterministischen, evolutionären Spieltheorie ist deren zugrundeliegende Netzwerkstruktur (Netzwerktopologie). Die jeweiligen Spieler der betrachteten Population suchen in jeder Spielperiode einen neuen Spielpartner, wobei sie hierbei zufällig vorgehen (zufälliges Netzwerk) und vom Prinzip her mit jedem Spieler innerhalb der Population potentiell das zugrundeliegende Spiel spielen können (vollständig verbundenes Netzwerk)[2]. Betrachtet man sich jedoch real existierende sozio-ökonomische Netzwerke, so zeigt sich, dass diese Annahme oft nicht erfüllt ist (siehe [18, 218]). Personen kennen oft nur eine Teilmenge von Spielern innerhalb der Population (kein vollständig verbundenes Netzwerk) und die Wahl der potentiellen Spielpartner erfolgt oft auch nicht nach zufälligen Mustern. Die Theorie der komplexen Netzwerke bildet die Grundlage zur Beschreibung einer Vielzahl von unterschiedlichen biologischen und sozio-ökonomischen Systemen. Die Verknüpfung der Theorie komplexer Netzwerke mit der evolutionären (Quanten) Spieltheorie stellt ein vielversprechendes mathematisches Modell dar, welches sowohl der interdisziplinären Grundlagenforschung, als auch der angewandten, empirischen Netzwerkforschung dienen kann. Im Folgenden wird die Vorgehensweise einer Miteinbeziehung komplexer Netzwerktopologien in die evolutionäre Spieltheorie beschrieben. Der Schwerpunkt der Darstellung liegt in der mathematischen Konstruktion des zugrundeliegenden Netzwerkmodells (siehe Anhang A.I). Die dann auf einem solchen komplexen Netzwerk ablaufenden Entscheidungsprozesse können in den meisten Fällen lediglich mittels nummerischer, Agenten-basierter Computersimulationen veranschaulicht werden. Die vom Autor dieser Dissertation geschriebene Java-Simulation der Entwicklung des Marktes für wissenschaftliche Fachinformation ist ein Beispiel eines solchen dynamischen Entscheidungsprozesses auf einem komplexen Netz-

[2] In Bimatrix Spielen suchen sich die Spieler der Teilpopulation A einen zufälligen Spielpartner aus Gruppe B (bzw. umgekehrt).

werk. Die detaillierte Beschreibung der Vorgehensweise und die Diskussion der Ergebnisse dieser Computersimulationen ist nicht Gegenstand dieser Dissertation (siehe hierzu die Artikel [32, 29, 152, 30] und die Projektberichte [3, 7, 4]).

Die mathematische Beschreibung sozialer Netzwerke ist in mehreren Übersichtsartikel (siehe z.B. [18, 218]) zusammengefasst[3]. Physikalische bzw. soziale Interaktionen werden hierbei durch Verbindungskanten zwischen den jeweiligen Netzwerkknoten beschrieben. In der Literatur werden grob vier unterschiedliche Netzwerktypen beschrieben – die „zufälligen“, die „kleine Welt“, die „exponentiellen“ und die „skalenfreien“ Netzwerke [99, 100, 101]. Die theoretische Netzwerkforschung befasst sich mit der Entstehung und Beschreibung dieser Netzwerke. Bei einigen Modellnetzwerken können analytische Ergebnisse gewonnen werden [217]. Die Anwendung der Theorie auf real existierende Netzwerkstrukturen ist ebenfalls in den Übersichtsartikeln [18, 218] zusammengefasst. Neben sozialen Netzwerken wie z. B. wissenschaftliche Kollaborationen, Koautorenschaften und Zitationsverflechtungen wissenschaftlicher Artikel [191, 158, 101, 100], Kommunikationsnetzwerken wie dem Internet [19] und diversen weiteren sozio-ökonomischen Netzwerkstrukturen (siehe z.B. [58, 189, 93, 85, 192, 208, 37, 245, 124, 185, 225, 201]) werden mit Hilfe des mathematischen Modells der komplexen Netzwerke auch biologische Netzwerken wie z.B. neuronale oder Proteinnetzwerke beschrieben und analysiert [209, 226, 148, 78, 171, 172, 83].

Die Annahme des vollständig verbundenen, zufälligen Netzwerks, welches die Grundlage der deterministischen evolutionären Spieltheorie bildet, ist in realen sozialen Netzwerken oft nicht erfüllt. In skalenfreien Netzwerken z.B. ist die Verbindung der Spieler untereinander extrem heterogen (siehe Verteilungsfunktion $P(k)$ in Gleichung (A.3) im Anhang A.I) – einige Spieler besitzen sehr viele Verbindungen zu anderen Spielern, wohingegen die meisten Spieler nur wenige Verbindungslinien zu anderen Spieler aufweisen. In realen sozialen Netzwerken bilden sich oft weitgehend abgeschlossene Cluster von miteinander verbundenen Spielern, die zu anderen Clustern nur bedingt bzw. selten Kontakt haben. Diese Art von Clusterbildung kann zu einer unterschiedlichen Ausprägung von sozialen Normen innerhalb der einzelnen Teilgruppen führen. Soziale Normen können sich somit herausbilden, die den einzelnen Spielern neben ihrem „homo ökonomischen“

[3] Auf eine sozialwissenschaftliche Untersuchung und Beschreibung sozialer Netzwerkstrukturen wird im Folgenden nicht eingegangen.

Interesse auch den Blick auf das Wohl der eigenen Gruppe nahelegen. Eine solche Art von induziertem Gruppeninteresse wird im folgenden Unterkapitel mittels des Ansatzes der Quanten-Spieltheorie mathematisch in die deterministischen Gleichungen der evolutionären Spieltheorie eingearbeitet.

1.2.4. Quanten-Spieltheorie

Die erste formale Beschreibung der Quanten-Spieltheorie wurde im Jahre 1999 von Eisert et al. vorgestellt [66]. Diese oft zitierte Arbeit betrachtet die quantentheoretische Erweiterung eines Gefangenendilemma Spiels und zeigt auf, dass die Spieler dem Dilemma entkommen können, falls der strategische Verschränkungswert oberhalb einer dem Spiel eigenen Grenze liegt. Im selben Jahr (1999) analysierte D. A. Meyer das „Penny Flip“ Spiel und erweiterte dieses mittels quantentheoretischer Konzepte [165]. In seinem Artikel betrachtete er den unrealistischen Fall, dass einer der Spieler das im Spiel benutzte Geldstück in einem überlagerten Quantenzustand positionieren könne und zeigte, dass dieser Spieler stets das Spiel gewinnen wird, falls sein Gegenspieler eine rein klassische Strategie benutzt.[4] Im Jahre 2000 wendeten Marinatto & Weber [162] die quantentheoretischen Konzepte auf das „Kampf der Geschlechter (battle of sexes)“ Spiel an und zeigten, dass durch die Verschränkung der Spielerstrategien ein eindeutiges Gleichgewicht möglich ist. In den folgenden Jahren wurden die quantenspieltheoretischen Konzepte auf weitere Spiele ausgedehnt; so analysierte R.V. Mendes die Quantenversion des „Ultimatum Spiels“, Hogg et al. betrachteten das „Öffentliche Gut“ Spiel [48], eine Version des „Quanten Koordinationsspiels“ [134] und analysierten „Quanten Auktionen“ [131]. Benjamin & Hayden [28] erweiterten im Jahre 2001 den Formalismus der Quanten-Spieltheorie auf mehr als zwei Spieler (siehe auch [50]). Im Jahre 2002 benutzten Piotrowski & Sladkowsky [178] die quantenspieltheoretischen Konzepte um Eigenschaften im Verhalten von Märkten zu erklären. Im Jahre 2006 analysierten Hanauske et al. [111] das „Open Access“-Publikationsverhalten wissenschaftlicher Autoren mittels des quantentheoretischen Ansatzes. Bereits im Jahre 2001 wurde das erste Quantenspiel auf einem Quantencomputer realisiert [62], wobei sich die

[4] Im Jahre 2000 kommentierte S.J. van Enk die Arbeit von D. A. Meyer [228] und zeigte, dass Meyer's Behauptung nicht sonderlich beeindruckend ist, da er nur einem der Spieler einen größeren Strategienraum erlaubt.

vorhergesagten Eigenschaften bestätigten. Die Resultate dieser Experimente wurden im Jahre 2007 von A. Zeilinger erneut bestätigt [190]. Die ersten Ansätze einer Anwendung der Quanten-Spieltheorie auf sozio-ökonomische Experimente wurden nach 2007 veröffentlicht [49, 176, 112, 242, 38]. Die Anzahl der seit 1999 veröffentlichten Artikel in diesem Forschungsfeld liegt im Bereich 200–300, wobei der Großteil der Artikel in wissenschaftlichen Zeitschriften veröffentlicht ist die dem Fachgebiet der Physik zugeordnet sind.

Neben diesen, vornehmlich theoretischen Arbeiten, entwickelte sich im Bereich der Psychologie in den vergangenen Jahren ein weiterer wissenschaftlicher Forschungszweig, welcher quantentheoretische Konzepte zur Erklärung von experimentellen Daten benutzt [40, 41, 187, 188, 14, 9, 8, 15, 12, 11, 9, 16, 42, 241, 55]. Diese Arbeiten zeigen, dass viele, zunächst nicht erklärbare experimentelle Befunde im Bereich der Psychologie, sich mittels quantenlogischer Konzepte beschreiben lassen. Einige dieser Arbeiten werden kurz im Unterkapitel 2.4.2 des „Introductory Papers“ diskutiert, da sie eine erste, beeindruckende Bestätigung der Quanten-Spieltheorie darstellen. Zusätzlich zu den bereits erwähnten Artikeln sind die folgenden Arbeiten hervorzuheben: Arbeiten über Koordinationsproblemen [133, 147], Eigenschaften der Quantenverschränkung [61], experimentelle Realisierung von Quantenspielen [200, 20], evolutionäre Quanten-Spieltheorie [135, 221, 160, 168], klassische Spiele mit zusätzlichen Quantensignalen [38, 159, 155, 49, 134] und in die Theorie einführende und zusammenfassende Arbeiten [151, 75, 97, 240, 180, 179, 181].

Die bei der quantentheoretischen Formulierung benutzten mathematischen Ansätze können grob in zwei Hauptströme gegliedert werden. Der Dichtematrix Ansatz der Quantenspieltheorie (siehe Marinatto & Weber [162]) und den quanteninformationstheoretischen Ansatz von Eisert et al. [66]. Der auf quanteninformationstheoretischen Konzepten aufbauende Ansatz (Eisert et al. [66]) hat einerseits den Vorteil, dass die neu entstehenden Quantenstrategien in einem reduzierten Quanten-Strategienraum visualisiert und interpretiert werden können, andererseits baut der Ansatz die Möglichkeit einer Quantenverschränkung in mathematisch eleganter Weise in die Theorie ein, so dass man die Stärke einer möglichen Strategienverschränkung der Spieler mittels eines zusätzlichen Parameters (γ) im Modell variieren kann. In den ersten Jahren nach seiner Veröffentlichung wurde der Eisert'sche Ansatz von Benjamin & Hayden [27] und S.J. van Enk [229]

angegriffen und kritisch diskutiert. Die damals erhobenen Vorwürfe stellten sich jedoch im Laufe der Zeit als nicht auf die Eisert'sche Theorie anwendbar heraus.[5] Im Folgenden wird das Konzept der Quanten-Spieltheorie (in der Eisert'schen, quanten-informationstheoretischen Nomenklatur) im Detail beschrieben.

In der Quanten-Spieltheorie kann der Entscheidungszustand der beteiligten Akteure, im Gegensatz zur klassischen Spieltheorie, eine gemeinsame Strategienverschränkung aufweisen. Durch das Konzept dieser möglichen quantentheoretischen Verschränkung der Entscheidungswege im imaginären Raum aller denkbaren Quantenstrategien können gemeinsame, durch kulturelle oder moralische Normen entstandene Denkrichtungen, mit in die klassische Theorie einbezogen werden. Eine der grundlegenden Folgerungen aus einer solchen gemeinsamen Strategienverschränkung ist, dass die beteiligten Akteure eine erhöhte Kooperationsbereitschaft aufweisen, da sie dann eine Optimierung des gemeinsamen Zwei-Spielerzustandes $|\Psi\rangle$ anstreben (näheres siehe z.B. [104]).

Um die mathematische Beschreibung eines evolutionären, quantenspieltheoretischen Modells zu verdeutlichen, wird im Folgenden zunächst ein (2 Personen)-(2 Strategien) Quantenspiel betrachtet. Der spieltheoretische, binäre Entscheidungsprozess der Akteure soll durch folgende allgemeine Auszahlungsmatrix bestimmt sein:

A\B	s_1^B	s_2^B
s_1^A	($\$_{11}^A$,$\$_{11}^B$)	($\$_{12}^A$,$\$_{21}^B$)
s_2^A	($\$_{21}^A$,$\$_{12}^B$)	($\$_{22}^A$,$\$_{22}^B$)

Tabelle 1.1.: Allgemeine 2×2 Auszahlungsmatrix der Spieler A und B, wobei zwei reine Strategien (s_1 und s_2) pro Spieler möglich sind.

Die Quanten-Spieltheorie beschreibt den Entscheidungszustand eines Spielers $\mu = A, B$, bevor dieser die endgültige Wahl der reinen Strategie getroffen hat, als eine komplexwertige Größe (Spinor) in einem zweidimensionalen[6] Zustandsraum, dem sogenannten Hilbertraum $\mathcal{H}_\mu$. Die in dieser Arbeit verwendete mathematische Repräsentation dieses Spinors wird mit Hilfe des Entscheidungsoperators

[5] Sie Diskussion am Ende dieses Unterkapitels.
[6] Bei m Strategien ist der zugrundeliegende komplexwertige Zustandsraum m-dimensional.

$\widehat{\mathcal{U}}_\mu(\theta_\mu, \varphi_\mu)$ konstruiert, der auf einen Anfangszustand (hier speziell $|s_1^\mu\rangle$) wirkt. Ein allgemeiner Entscheidungszustand des Spielers A wird somit wie folgt mathematisch konstruiert:

$$|\psi_A\rangle = \psi_1^A \left|s_1^A\right\rangle + \psi_2^A \left|s_2^A\right\rangle = \begin{pmatrix} \psi_1^A \\ -\psi_2^A \end{pmatrix} \in \mathcal{H}_A$$

$$\left|s_1^A\right\rangle = \begin{pmatrix} 1 \\ 0 \end{pmatrix}, \ \left|s_2^A\right\rangle = \begin{pmatrix} 0 \\ -1 \end{pmatrix}, \ \psi_1^A = e^{i\,\varphi_A}\cos(\tfrac{\theta_A}{2}), \ \psi_2^A = \sin(\tfrac{\theta_A}{2})$$

$$|\psi_A\rangle = \widehat{\mathcal{U}}(\theta_A, \varphi_A)\left|s_1^A\right\rangle = \begin{pmatrix} e^{i\,\varphi_A}\cos(\frac{\theta_A}{2}) \\ -\sin(\frac{\theta_A}{2}) \end{pmatrix} \tag{1.11}$$

Die reinen Zustände $\left|s_1^A\right\rangle$ und $\left|s_2^A\right\rangle$ bilden die Basis des Hilbertraums $\mathcal{H}_A$ des Spielers A und repräsentieren die reinen Strategien s_1^A und s_2^A des Spiels. Der Entscheidungsoperator des Spielers μ hängt von den beiden Entscheidungswinkeln θ_μ und φ_μ ab und ist explizit wie folgt definiert:

$$\widehat{\mathcal{U}}_\mu(\theta_\mu, \varphi_\mu) := \begin{pmatrix} e^{i\,\varphi_\mu}\cos(\frac{\theta_\mu}{2}) & \sin(\frac{\theta_\mu}{2}) \\ -\sin(\frac{\theta_\mu}{2}) & e^{-i\,\varphi_\mu}\cos(\frac{\theta_\mu}{2}) \end{pmatrix} \tag{1.12}$$
$$\forall \quad \theta_\mu \in [0, \pi] \ \wedge \ \varphi_\mu \in [0, \tfrac{\pi}{2}] \qquad .$$

Durch die Festlegung der Entscheidungswinkel θ_μ und φ_μ wählt der Spieler seine Quantenstrategie. Die klassische, reine Strategie s_1 legt der Spieler durch die Wahl $\theta = 0$ und $\varphi = 0$ fest:

$$\widehat{s_1} := \hat{\mathcal{U}}(0, 0) = \begin{pmatrix} 1 & 0 \\ 0 & 1 \end{pmatrix} \quad , \tag{1.13}$$

wohingegen die reine Strategie s_2 durch $\theta = \pi$ und $\varphi = 0$ festgelegt ist:

$$\widehat{s_2} := \hat{\mathcal{U}}(\pi, 0) = \begin{pmatrix} 0 & 1 \\ -1 & 0 \end{pmatrix} \quad . \tag{1.14}$$

Zusätzlich zu diesen reinen, klassischen Strategien ist die Quantenstrategie $\widehat{Q}$ wie folgt definiert

$$\widehat{Q} := \hat{\mathcal{U}}(0, \pi/2) = \begin{pmatrix} i & 0 \\ 0 & -i \end{pmatrix} \quad . \tag{1.15}$$

Um den Operatorformalismus der Quanten-Spieltheorie und das Konzept der Quantenstrategien besser zu verstehen, veranschaulicht Abbildung 1.2 die reellwertigen und imaginären Komponenten ψ_1^A und ψ_2^A des zweidimensionalen Quantenspinors $|\psi\rangle_A$ des Spielers A.

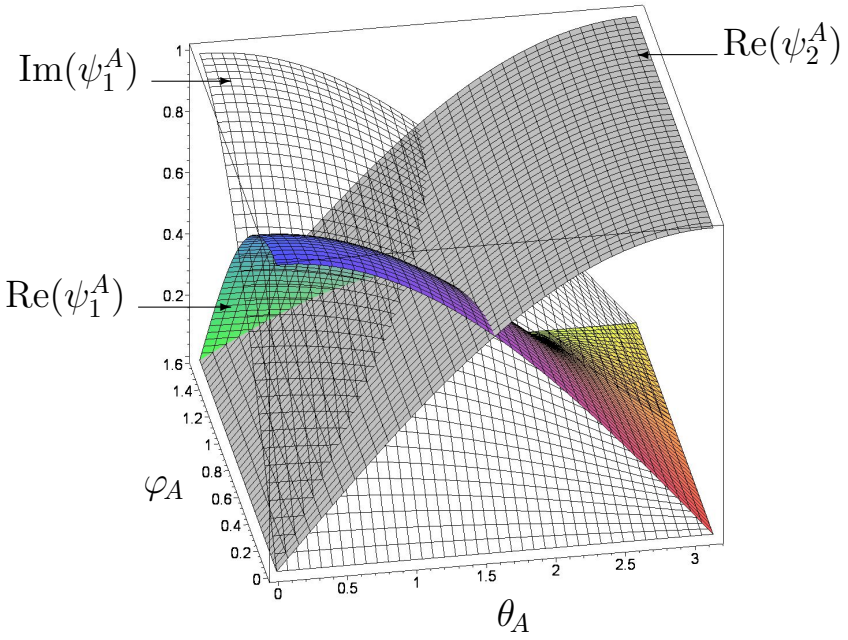

Abbildung 1.2.: Reellwertige und imaginäre Komponenten des zweidimensionalen Quantenspinors $|\psi\rangle_A = \widehat{\mathcal{U}}(\theta_A, \varphi_A)\left|s_1^A\right\rangle$ des Spielers A als Funktion der Quantenstrategien θ_A und φ_A.

Die farbige, untransparente Fläche in Abbildung 1.2 veranschaulicht den reellwertigen Anteil der ersten Spinorkomponente ($\mathrm{Re}(\psi_1^A)$), die durchsichtige graue Fläche beschreibt dessen imaginären Anteil ($\mathrm{Im}(\psi_1^A)$) und die graue undurchsichtige Fläche zeigt den reellwertigen Teil der zweiten Spinorkomponente ($\mathrm{Re}(\psi_2^A)$) in Abhängigkeit der Winkel θ_A und φ_A. Da die zweite Spinorkomponente lediglich reellwertige Anteile besitzt veranschaulicht Abbildung 1.2 lediglich drei Flächen. Die Menge der klassischen gemischten Strategien des Spielers A ($\tilde{\mathcal{S}}^A = \left\{\tilde{s}_1^A, \tilde{s}_2^A\right\}$) ist eine echte Teilmenge des strategischen Hilbertraums des Spielers A ($\mathcal{H}_A$) und

wird formal realisiert, indem man den Winkel φ_A auf null setzt:

$$\tilde{\mathcal{S}}^A = \left\{ |\psi\rangle_A = \widehat{\mathcal{U}}(\theta_A, \varphi_A) \left| s_1^A \right\rangle \mid \varphi_A \equiv 0\,,\ \theta_A \in [0, \pi] \right\} \subsetneq \mathcal{H}_A \quad . \tag{1.16}$$

In diesem Fall ($\varphi_A \equiv 0$) verschwinden alle imaginären Anteile des Zustandes $|\psi\rangle_A$ und als Folge dessen können die klassischen gemischten Strategien durch Variation des Winkels $\theta \in [0, \pi]$ realisiert werden (siehe Abbildung 1.2). Für $\varphi_A > 0$ verschwinden jedoch die imaginären Anteile nicht und diese Art von Quantenstrategien haben kein Pendant in der klassischen Spieltheorie. Da der Entscheidungsoperator auf den reinen Anfangszustand der Strategie s_1 wirkt, entstehen mögliche imaginäre Anteile im Zustand $|\psi\rangle_A$ lediglich in der ersten Spinorkomponente und man nennt deshalb diese Teilmenge von Quantenstrategien die sogenannten s_1-Quantenstrategien.

Die quantentheoretische Beschreibung des Entscheidungszustandes des Spielers A kurz vor der definitiven Auswahl und Bekundung der reinen Strategie besitzt demnach im Allgemeinen neben den reellwertigen auch imaginäre Anteile. Bei s_1-Quantenstrategien kann sich der Spieler nur im imaginären Raum der ersten Strategie gedanklich bewegen. Eine grundlegende Eigenschaft der gesamten Quantentheorie ist die prinzipielle Unbeobachtbarkeit des Quantenzustandes. Diese Eigenschaft spiegelt sich in der Quanten-Spieltheorie in der Unbeobachtbarkeit des Gedankenprozesses wider. Die einzelnen Inhalte, Gedankenwege und gefühlsauslösende Überlegungen, die während des Entscheidungsprozesses im Gehirn des Spielers (bewusst oder unterbewusst) ablaufenden, können nicht direkt gemessen werden. s_1-Quantenstrategien können als der gedankliche Weg während des Entscheidungsprozesses interpretiert werden, welcher vom gedanklichen Ursprung her von der klassischen Strategie s_1 startet und hypothetisch, gebunden an die Wünsche und Ängste des Spielers, den Gedankenweg weiterbildet. Aus diesem Grund besitzen die s_1-Quantenstrategien (bzw. s_2-Quantenstrategien), die speziell bei einer der reinen klassischen Strategien starten ($\{(\theta_A \equiv 0, \varphi_A) \mid \varphi_A \in [0, \frac{\pi}{2}]\}$), eine besondere Bedeutung.

Die quantenspieltheoretische Erweiterung beschreibt somit den Entscheidungszustand eines Spielers A als einen im komplexen Hilbertraum definierten Zustandsvektor. Der Spielbaum eines (2 Personen)-(2 Strategien) Quantenspiels ist in Abbildung 1.3 visualisiert. Der Zwei-Spielerzustand $|\Psi\rangle$ ist ein vierkomponentiger

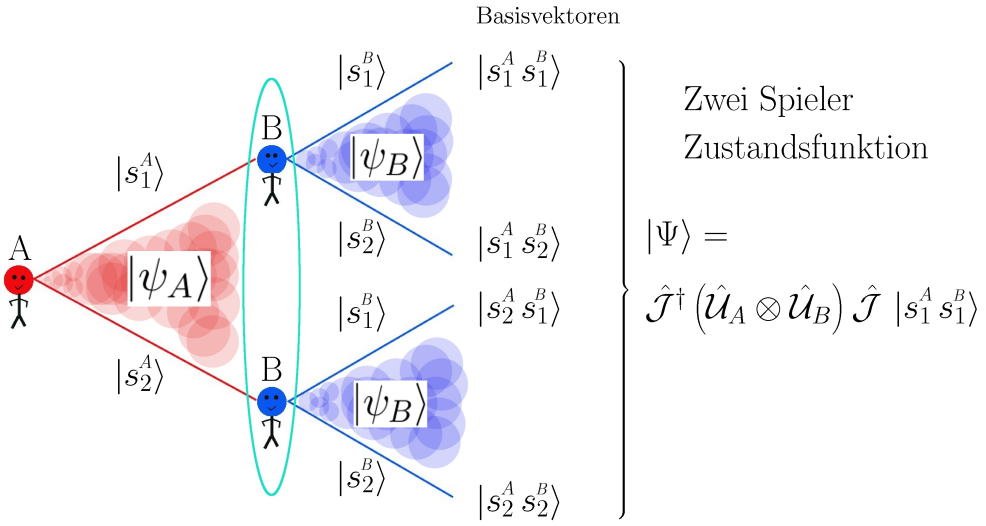

Abbildung 1.3.: Spielbaum eines (2 Personen)-(2 Strategien) Quantenspiels.

Spinor, welcher auf dem gemeinsamen Hilbertraum der Spieler ($\mathcal{H} := \mathcal{H}_A \otimes \mathcal{H}_B$) definiert ist. Die Basisvektoren dieses vierdimensionalen komplexwertigen Raumes werden durch die vier möglichen, klassischen Strategienkombinationen (messbaren Eigenzustände des Quantensystems) gebildet ($\left|s_1^A s_1^B\right\rangle := (1,0,0,0)$, $\left|s_1^A s_2^B\right\rangle := (0,-1,0,0)$, $\left|s_2^A s_1^B\right\rangle := (0,0,-1,0)$ and $\left|s_2^A s_2^B\right\rangle := (0,0,0,1)$).

Der finale Zwei-Spielerzustand eines simultanen Zwei-Strategien-'One Shot'-Quantenspiels wird somit durch den vierkomponentigen Quantenzustand $|\Psi\rangle$ beschrieben, welcher sich in der Eisert'schen Repräsentation (siehe [66]) wie folgt aus dem Anfangszustand $\left|s_1^A s_1^B\right\rangle$ (siehe Gleichung (1.19)) entwickelt

$$|\Psi\rangle = \hat{\mathcal{J}}^\dagger \left(\hat{\mathcal{U}}_A \otimes \hat{\mathcal{U}}_B\right) \hat{\mathcal{J}} \left|s_1^A s_1^B\right\rangle \quad , \tag{1.17}$$

wobei $\hat{\mathcal{J}} := (J_{\alpha\beta}), \alpha, \beta = 1...4$ die von dem Parameter γ abhängige Verschrän-

kungsmatrix (bzw. den Verschränkungsoperator) beschreibt

$$\widehat{\mathcal{J}} := e^{i\frac{\gamma}{2}(\widehat{s_1}\otimes\widehat{s_1})} = \begin{pmatrix} \cos\left(\frac{\gamma}{2}\right) & 0 & 0 & i\sin\left(\frac{\gamma}{2}\right) \\ 0 & \cos\left(\frac{\gamma}{2}\right) & -i\sin\left(\frac{\gamma}{2}\right) & 0 \\ 0 & -i\sin\left(\frac{\gamma}{2}\right) & \cos\left(\frac{\gamma}{2}\right) & 0 \\ i\sin\left(\frac{\gamma}{2}\right) & 0 & 0 & \cos\left(\frac{\gamma}{2}\right) \end{pmatrix}, \ \gamma \in [0, \frac{\pi}{2}]\,. \tag{1.18}$$

$\hat{\mathcal{U}}_A := (U^A_{\alpha\beta}), \alpha, \beta = 1...2$ und $\hat{\mathcal{U}}_B := (U^B_{\alpha\beta}), \alpha, \beta = 1...2$ stellen die von den Winkeln θ_A, φ_A und θ_B, φ_B abhängigen Entscheidungsmatrizen (Entscheidungsoperatoren) der Spieler A und B dar. Der Zwei-Spieleranfangszustand $\left|s_1^A s_1^B\right\rangle$ bildet sich durch das äußere Produkt der Ein-Spieler Zustände $\left|s_1^A\right\rangle$ und $\left|s_1^B\right\rangle$. Die vektorielle Repräsentation der allgemeinen Ein-Spieler Zustände $|\psi_A\rangle$, bzw. $|\psi_B\rangle$ ist wie folgt durch die Basen der reinen Zustände definiert:

$$|\psi_A\rangle := \begin{pmatrix} \psi_1^A \\ -\psi_2^A \end{pmatrix} = \psi_1^A \left|s_1^A\right\rangle + \psi_2^A \left|s_2^A\right\rangle \tag{1.19}$$

$$|\psi_B\rangle := \begin{pmatrix} \psi_1^B \\ -\psi_2^B \end{pmatrix} = \psi_1^B \left|s_1^B\right\rangle + \psi_2^B \left|s_2^B\right\rangle$$

$$\text{wobei:} \quad |s_1^\mu\rangle = \begin{pmatrix} 1 \\ 0 \end{pmatrix} \quad |s_2^\mu\rangle = \begin{pmatrix} 0 \\ -1 \end{pmatrix}$$

$$\left|s_1^A s_1^B\right\rangle := \left|s_1^A\right\rangle \otimes \left|s_1^B\right\rangle = \begin{pmatrix} 1 \\ 0 \\ 0 \\ 0 \end{pmatrix}$$

Der Erwartungswert der Auszahlungen der Spieler wird zusätzlich durch die Spielmatrix (Tabelle 1.1) mitbestimmt:

$$\begin{aligned} \$_A &= \$^A_{11} P_{11} + \$^A_{12} P_{12} + \$^A_{21} P_{21} + \$^A_{22} P_{22} \\ \$_B &= \$^B_{11} P_{11} + \$^B_{21} P_{12} + \$^B_{12} P_{21} + \$^B_{22} P_{22} \\ \text{mit:} \quad & P_{kl} = \left|\left\langle s_k^A\, s_l^B|\Psi\right\rangle\right|^2 , \quad k,l = \{1,2\} \end{aligned} \tag{1.20}$$

Dieser Erwartungswert der Auszahlungen stellt eine Erweiterung des aus der klassischen Spieltheorie bekannten Konzepts der Auszahlungsfunktion in gemischten Strategien dar (siehe Gleichung (1.5)). Um die Auswirkungen des quantenspieltheoretischen Konzepts auf die dem Spieler ratsame Wahl der Entscheidung zu untersuchen, wird im Folgenden die Struktur der quantenspieltheoretisch erweiterten gemischten Auszahlungsfunktion (siehe Gleichung (1.20)) untersucht. Im Unterschied zur klassischen Auszahlungsfunktion ($\tilde{\$}^{\mu}(\tilde{s}^A, \tilde{s}^B)$, siehe Gleichung (1.5)), die lediglich von den gemischten Strategien des Spielers A ($\tilde{s}^A$) und des Spielers B ($\tilde{s}^B$) abhängt, hängt die quantentheoretische Erweiterung der Auszahlungsfunktion im Allgemeinen von fünf Parametern ab: Die vier Winkel der Entscheidungsoperatoren ($\theta_A, \varphi_A, \theta_B$ und φ_B) und der Parameter γ, welcher die Stärke der Strategienverschränkung quantifiziert. Um die Auszahlungsfunktion dennoch als Fläche in einem dreidimensionalen Raum zu visualisieren, reduziert man deren Abhängigkeiten, indem man einerseits den Verschränkungsparameter γ fixiert und die Menge der Quantenstrategien auf diejenigen beschränkt, die vom Ursprung der reinen, klassischen s_1-Strategie starten. Die Abhängigkeiten des vierkomponentigen Zwei-Spieler Quantenzustand $|\Psi\rangle$ werden durch die Einführung zweier neuer Parameter (τ_A und τ_B) reduziert: $|\Psi\rangle = |\Psi(\theta_A, \varphi_A, \theta_B, \varphi_B)\rangle \rightarrow |\Psi(\tau_A, \tau_B)\rangle$. Die für jeden Spieler wählbaren Entscheidungswinkel θ und φ werden dadurch auf einen einzigen Parameter $\tau \in [-1, 1]$ reduziert[7]. Positive τ-Werte entsprechen den klassischen gemischten Strategien, wohingegen negative τ-Werte Quantenstrategien mit $\theta = 0$ und $\varphi > 0$ repräsentieren. Der gesamte quantentheoretische Strategienraum wird dadurch in vier separate Regionen unterteilt: in den absolut klassischen Bereich (*ClCl*: $\tau_A, \tau_B \geq 0$), den absoluten Quantenbereich (*QuQu*: $\tau_A, \tau_B < 0$) und in die beiden semi-klassischen Quantenbereiche (*ClQu*: $\tau_A \geq 0 \wedge \tau_B < 0$ und *QuCl*: $\tau_A < 0 \wedge \tau_B \geq 0$). Durch diese (τ_A, τ_B)-Repräsentation wird die Menge der möglichen Quantenstrategien auf die folgende Untermenge reduziert:

$$\underbrace{\{(\tau\,\pi, 0) \mid \tau \in [0, 1]\}}_{\text{klassischer Bereich } Cl} \quad \wedge \quad \underbrace{\{(0, \tau\,\frac{\pi}{2}) \mid \tau \in [-1, 0[\}}_{\text{Quantenbereich } Qu} \tag{1.21}$$

Abbildung 1.4 stellt die vier Regionen des Visualisierungsraums der quanten-

[7] Der Parameter τ entspricht dem Parameter t in dem Artikel [66].

theoretischen Auszahlungsfunktion dar. Die absolut klassische Region (*ClCl*, $\varphi_A, \varphi_B \equiv 0$) befindet sich im vorderen Bereich, die Region in welchem beide Spieler eine Quantenstrategie wählen (*QuQu*: $\tau_A, \tau_B < 0$) ist im hinteren Bereich des Diagramms zu finden und die semi-klassischen Quantenregionen befinden sich seitlich in dem rechten und linken Bereich.

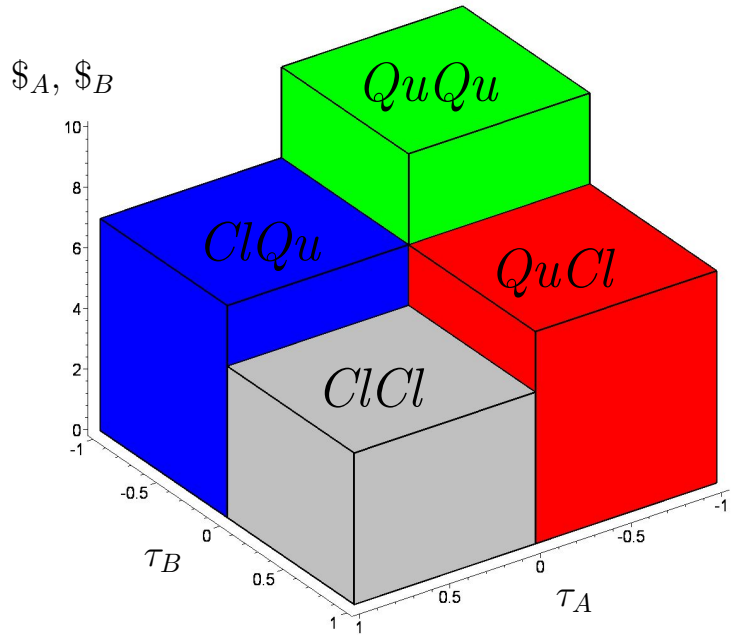

Abbildung 1.4.: Visualisierungsraum der quantentheoretisch erweiterten Auszahlung \$ als Funktion der reduzierten s_1-Quantenstrategien τ_A des Spielers A und τ_B des Spielers B.

Bei der im nächsten Unterkapitel (Unterkapitel 1.2.5) folgenden Diskussion der exemplarischen Beispiele wird dieser Visualisierungsraum benutzt werden, um die Resultate der Quanten-Spieltheorie zu verdeutlichen.

Der Eisert'sche Ansatz wurde in der wissenschaftlichen Literatur, in den ersten Jahren nach seiner Veröffentlichung, kritisch diskutiert. Bereits im Jahre 2000 kommentierten beispielweise Benjamin & Hayden den Eisert'schen Ansatz (siehe [27]) und behaupteten, dass die benutzte Matrix-Repräsentation der Quanten-

Entscheidungsoperatoren der Spieler (siehe Gleichung (1.12)) eine unzulässige Einschränkung darstelle. Definiert man die Quanten-Entscheidungsoperatoren auf einer allgemeinen $SU(2)$-Gruppe, so die Behauptung, dann entstehen keine neuen Nash-Gleichgewichte im Quantenbereich der Strategien (siehe hierzu auch [56]). Benjamin & Hayden begründeten diese Behauptung, indem sie zeigten, dass die beste Antwort auf das von Eisert definierte Quanten Nash-Gleichgewicht ($\widehat{Q} = \hat{\mathcal{U}}(0, \pi/2)$) die zusammengesetzte Entscheidungsoperation ($\hat{\mathcal{U}}(0, \pi/2)\hat{\mathcal{U}}(\pi, 0)$) ist. Dies ist zwar mathematisch richtig, entspricht jedoch nicht dem Verständnis der in dieser Arbeit benutzten Formalisierung der Quanten-Spieltheorie. Die Einschränkung der Quanten-Entscheidungsoperatoren durch die Matrix-Repräsentation der Gleichung (1.12), in Verbindung mit der Reduktion auf s_1-Quantenstrategien (bzw. s_2-Quantenstrategien)[8] spiegelt die, während des Entscheidungsprozesses durchdachten gedanklichen Pfade des jeweiligen Spielers wider. Zusammengesetzte, simultane Gedankenwege wie ($\hat{\mathcal{U}}(0, \pi/2)\hat{\mathcal{U}}(\pi, 0)$) würden einem schizophren artigen Gedankenprozess entsprechen, indem der Spieler während des Entscheidungsprozesses in zwei separate Persönlichkeiten (A1 und A2) unterschiedlicher Denkrichtungen geteilt ist ($\widehat{\mathcal{U}}_{A1}(0, \pi/2)$ und $\widehat{\mathcal{U}}_{A2}(\pi, 0)$) – dies ist im Eisert'schen Ansatz nicht möglich.

Im Jahre 2002 kommentierten S.J. van Enk & R. Pike [229] den Eisert'schen quantenspieltheoretischen Ansatz und behaupteten, dass (2 Personen)-(2 Strategien) Quantenspiele äquivalent zu einem klassischen (2 Personen)-(3 Strategien) Spiel seien, wobei die dritte, klassische Strategie der Quantenstrategie $\widehat{Q}$ entsprechen soll. Das Verschwinden der dominanten Strategie im Gefangenendilemma und die Vorteilhaftigkeit der neuen dominanten $\widehat{Q}$-Strategie im (2 Personen)-(3 Strategien) Spiel sei nach van Enk & Pike nicht beeindruckend, da es sich um unterschiedliche Spiele handelt. Diese Aussage ist nicht richtig, da das zugrundeliegende, beobachtbare Spiel auch in einer quantentheoretisch erweiterten Form ein (2 Personen)-(2 Strategien) bleibt. Die gewählten, beobachtbaren Strategienentscheidungen der Spieler sind auch bei Quantenspielen die beiden reinen Strategien. Die von van Enk & Pike aufgezeigte Analogie kann man lediglich als pädagogische Veranschaulichung der Quantenstrategie verstehen. Die Vorteilhaftigkeit des durch die $\widehat{Q}$-Strategie erweiterte Strategienraum steigt bei zunehmender Verschränkung der

[8] Eine ausführliche Darstellung der s_1- und s_2-Quantenstrategien ist in Kapitel 5 am Beispiel der „Tauben"- und „Falken"-Quantenstrategien diskutiert.

Parameter-sätze	Spiel-klasse	$\$_{11}$	$\$_{12}$	$\$_{21}$	$\$_{22}$	Nash-Gleichgewichte
Set_A	Dominantes Spiel	10	4	12	5	Ein reines Nash-Gleichgewicht (s_2^A, s_2^B)
Set_B	Koordinations-spiel	10	4	9	5	Zwei reine NEs, ein internes NE $(s^\star = \frac{1}{2})$
Set_C	Anti-Koordinations-spiel	10	7	12	5	Zwei reine NEs, ein internes NE $(s^\star = \frac{1}{2})$

Tabelle 1.2.: Parameterwerte der drei symmetrischen Beispielspiele

Spielerstrategien. Liegt dieser Verschränkungswert unterhalb einer spieleigenen, definierten Grenze, so können die Spieler die Vorteilhaftigkeit des Gedankenweges $\widehat{Q}$ nicht erkennen und bleiben als Folge dessen im Dilemma des (2 Personen)-(2 Strategien) Spiels gefangen. Liegt die Stärke der Strategienverschränkung jedoch oberhalb der definierten Barriere, so erscheint der Gedankenweg $\widehat{Q}$ ihnen als vorteilhaft. Die neue, dominante Strategie $\widehat{Q}$ stellt jedoch keine real existierende Strategie dar, da diese stets als eine der beiden reinen Strategie beobachtet wird (im Falle des Gefangenendilemmas als kooperierende Strategie).

1.2.5. Exemplarische Beispiele

Dieses Unterkapitel illustriert das Konzept der Quanten-Spieltheorie an mehreren Beispielen. Zunächst werden drei Beispiele von symmetrischen Quantenspielen diskutiert. Das danach folgende Spiel illustriert die allgemeine Vorgehensweise einer quantentheoretischen Erweiterung unsymmetrischer (Bimatrix) Spiele.

Symmetrische Quantenspiele

Tabelle 1.2 fasst die Auszahlungsparameter der im Folgenden diskutierten symmetrischen Spiele zusammen. Symmetrische (2 Personen)-(2 Strategien) Spiele lassen sich formal in drei unterschiedliche Spielklassen separieren [110]. Die Abgrenzung dieser Spielklassen erfolgt formal durch eine Transformation der

Auszahlungsmatrix, bei welcher die vier Auszahlungsparameter auf zwei relevante, die Spielklasse definierende Größen (a und b) reduziert werden. Diese transformierten Auszahlungsgrößen hängen wie folgt von den ursprünglichen Auszahlungsparametern ab: $a = \$_{11} - \$_{21}$ und $b = \$_{22} - \$_{12}$.
Die dominanten Spiele ($a < 0$, $b > 0$ oder $a > 0$, $b < 0$) besitzen lediglich ein Nash-Gleichgewicht in reinen Strategien, welches ebenfalls die einzige evolutionär stabile Strategie des evolutionären Spiels ist.
Koordinationsspiele ($a, b > 0$) besitzen zwei symmetrische Nash-Gleichgewichte in reinen Strategien und ein internes Nash-Gleichgewicht in gemischten Strategien. Der jeweilige explizite Wert des gemischten Nash-Gleichgewichts des Spiels hängt von den Werten der Auszahlungsparameter ab:

$$\text{Nash-Gleichgewicht in gemischten Strategien:} \qquad (1.22)$$
$$(\tilde{s}^{A\star}, \tilde{s}^{B\star}) = \left(\frac{\$_{22}-\$_{12}}{\$_{11}-\$_{21}+\$_{22}-\$_{12}}, \frac{\$_{22}-\$_{12}}{\$_{11}-\$_{21}+\$_{22}-\$_{12}}\right)$$

Koordinationsspiele besitzen zwei mögliche evolutionär stabile Strategien, die den zwei symmetrischen Nash-Gleichgewichten entsprechen. In welcher ESS die Population schließlich endet, hängt von dem Anfangswert des Populationsvektors ab.
Anti-Koordinationsspiele ($a, b < 0$) besitzen zwei asymmetrische Nash-Gleichgewichte in reinen Strategien und ein internes Nash-Gleichgewicht in gemischten Strategien. Das interne NE, welches sich bei dem in Gleichung (1.22) definierten Wert befindet, ist die einzige ESS des Anti-Koordinationsspiels.

Dominante Spiele

Das durch Parametersatz Set_A[9] definierte Spiel gehört der Klasse der dominanten Spiele an. Das Nash-Gleichgewicht in reinen Strategien befindet sich bei der Strategienkombination, bei welcher beide Spieler die Strategie s_2 spielen (s_2^A, s_2^B). Abbildung 1.5 visualisiert die klassische Auszahlungsfläche (siehe Gleichung (1.5)) als Funktion der gemischten Strategie des Spielers A ($\tilde{s}^A$) und des Spielers B ($\tilde{s}^B$). Anhand der Abbildung 1.5 lässt sich leicht zeigen, dass es sich bei dem durch Parametersatz Set_A bestimmtem Spiel um ein dominantes Spiel handelt. Unabhängig welche gemischte Strategie Spieler B spielt ($\tilde{s}^B \in [0, 1]$), die beste Antwort für Spieler A ist stets die reine Strategie $s_2^A \hat{=} (\tilde{s}^A = 0)$, da die Auszahlungsfläche

[9] Der Parametersatz Set_A entspricht dem Parametersatz Set_3 des „Introductory Papers“ [110].

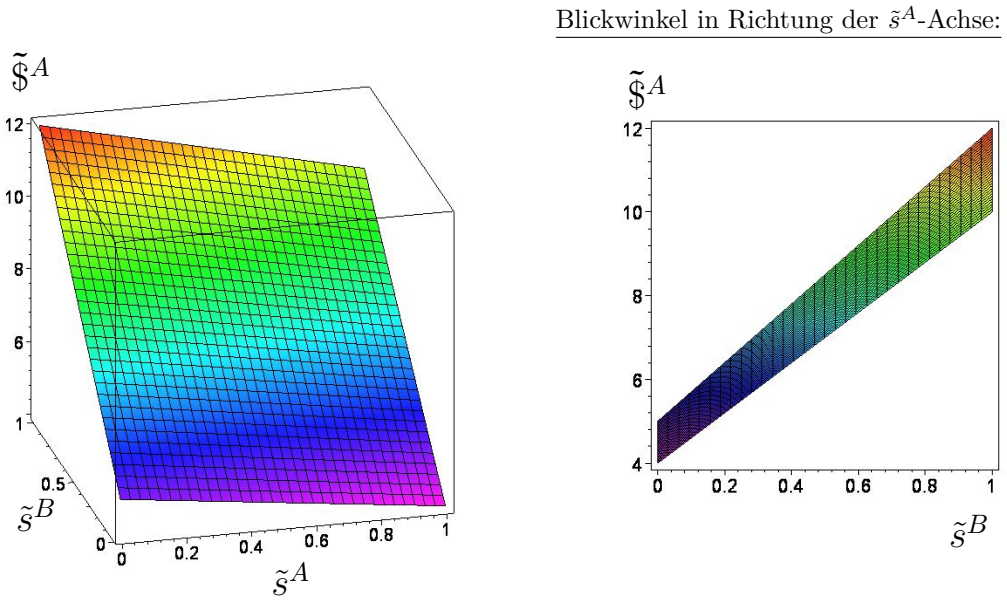

Abbildung 1.5.: Parametersatz Set_A: Auszahlungsfunktion $\tilde{\$}^A(\tilde{s}^A, \tilde{s}^B)$ des Spielers A als Funktion der gemischten Strategie des Spielers A ($\tilde{s}^A$) und des Spielers B ($\tilde{s}^B$).

des Spielers A ($\tilde{\$}^A$) bei festem, beliebigem $\tilde{s}^B$ den größten Wert bei $\tilde{s}^A = 0$ annimmt. Das alleinige Nash-Gleichgewicht $((s_2^A, s_2^B) \hat{=} (\tilde{s}^A = 0, \tilde{s}^B = 0))$ ist somit die dominante und evolutionär stabile Strategie des Spiels. Das betrachtete dominante Spiel besitzt zudem die Eigenschaft eines Dilemmas, da die zugrundeliegende dominante Strategienkombination eine weit niedrigere Auszahlung $(\tilde{\$}^A(\tilde{s}^A = 0, \tilde{s}^B = 0) = 5)$ besitzt, als die Strategienkombination in welcher beide Spieler die reine Strategie s_1 gewählt hätten $(\tilde{\$}^A(\tilde{s}^A = 1, \tilde{s}^B = 1) = 10)$. Das durch Parametersatz Set_A bestimmte Spiel ähnelt demnach einem „Gefangenen Dilemma“. In Abbildung 1.5 ist zusätzlich die Projektion der Auszahlungsfläche in Richtung der $\tilde{s}^A$-Achse veranschaulicht. Das Fehlen eines weiteren internen Nash-Gleichgewichts kann mittels dieses Blickwinkels einfach nachgewiesen werden. Da die partielle Ableitung bei internen Nash-Gleichgewichten verschwindet (siehe Gleichung (1.7)), sollte sich bei dieser Projektion die Fläche scheinbar auf einen Punkt zusammenziehen. Da ein solcher Fokuspunkt nicht existiert,

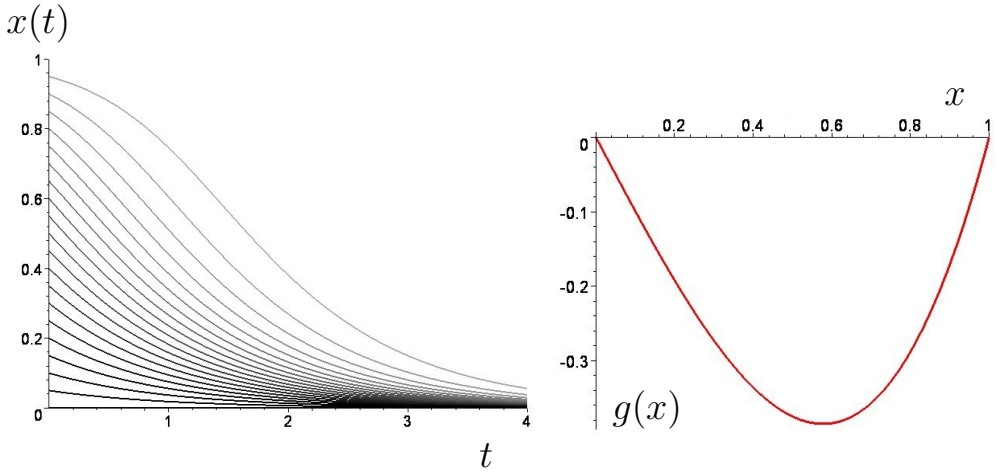

Abbildung 1.6.: Links: $x(t)$, Anteil der Spieler die zurzeit t die Strategie s_1 wählen für unterschiedliche Anfangswerte berechnet im Parametersatz Set_A. Rechts: $g(x)$, Reproduktionsdynamik bestimmende Funktion.

besitzt das betrachtete dominante Spiel kein Nash-Gleichgewicht in gemischten Strategien.

Die rechte Seite der Abbildung 1.6 veranschaulicht die Funktion $g(x)$, welche die evolutionäre, strategische Populationsentwicklung maßgeblich beeinflusst (siehe Gleichung (1.10)). Die linke Seite hingegen zeigt die numerischen Resultate der Reproduktionsdynamik (Gleichung (1.10)) für unterschiedliche Anfangswerte des Populationsvektors ($x(t=0) = 0, 0.05, 0.1, ..., 0.95$). Da die Funktion $g(x)$ für alle $x \in]0,1[$ negativ ist, ist der Anteil der Spieler die die Strategie s_1 wählen ($x(t)$) streng monoton fallend. Unabhängig von der ursprünglichen Anfangsbedingung wird demnach die gesamte Population sich zwangsläufig zur evolutionär stabilen Strategie entwickeln, bei der alle Spieler die Strategie s_2 spielen ($x(t \to \infty) = 0$)).

Die bisher besprochenen Resultate des exemplarischen Beispiels des Parametersatzes Set_A bedienten sich allein der Theorie der klassischen evolutionären Spieltheorie. Die nun folgenden Ergebnisse benutzen die theoretischen Erkenntnisse der Quanten-Spieltheorie. Abbildung 1.7 stellt die quantentheoretisch erweiterte Auszahlung $\$_A$ des Spielers A (untransparente Fläche) und $\$_B$ des Spielers B (transparente Fläche) als Funktion der reduzierten s_1-Quantenstrategien τ_A des

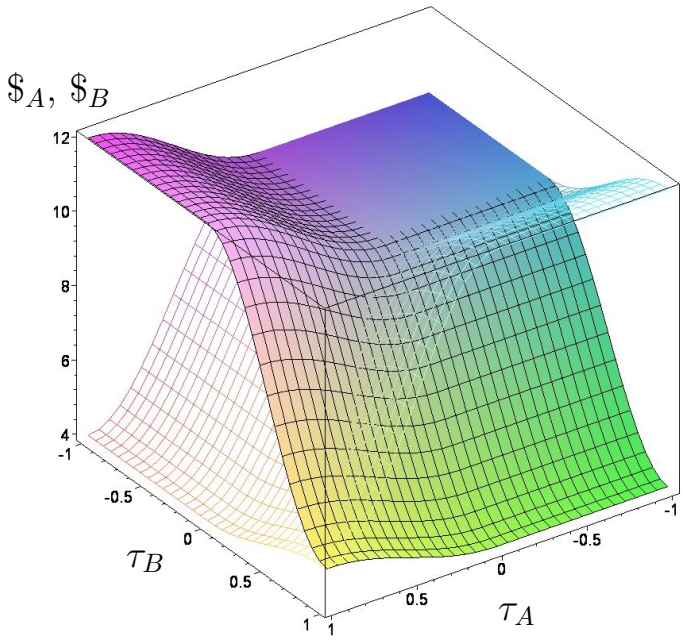

Abbildung 1.7.: Quantentheoretisch erweiterte Auszahlung $\$_A$ des Spielers A (untransparente Fläche) und $\$_B$ des Spielers B (transparente Fläche) als Funktion der reduzierten s_1-Quantenstrategien τ_A des Spielers A und τ_B des Spielers B in einem unverschränktem Quantenspiel ($\gamma = 0$) unter Verwendung des Parametersatzes Set_A.

Spielers A und τ_B des Spielers B dar. Als zugrundeliegender Parametersatz wurde Set_A verwendet und die Stärke der Quantenverschränkung der Spielerstrategien wurde auf null gesetzt ($\gamma = 0$). Als Visualisierungsraum wurde der in Abbildung 1.4 beschriebene Raum verwendet, wobei der absolute Quantenbereich *QuQu*, bei dem beide Spieler eine Quantenstrategie benutzen, im hinteren Teil des Diagramms zu finden ist und die rein klassische Region *ClCl* nach vorne projiziert wurde. Die Abbildung zeigt deutlich, dass das unverschränkte Quantenspiel identisch mit der klassischen Version des Spiels ist. Im Bereich, in dem beide Spieler eine Quantenstrategie wählen ($\tau_A < 0 \wedge \tau_B < 0$), ist die Auszahlung der Spieler gleich der Auszahlung, als wenn die Spieler die klassische Strategie s_1 gewählt hätten ($\$_A(\tau_A = 0, \tau_B = 0) = 10$, $\$_B(\tau_A = 0, \tau_B = 0) = 10$). Das

Nash-Gleichgewicht des klassischen Spiels ((s_2^A, s_2^B), die dominante Strategie) entspricht den folgenden τ-Werten: $(s_2^A, s_2^B) \hat{=} (\tau_A = 1, \tau_B = 1)$ und bleibt auch im unverschränkten Quantenspiel bestehen.

Die beiden Diagramme in Abbildung 1.8 stellen die quantentheoretisch erweiterte Auszahlungsfunktion bei mittleren Verschränkungswerten dar. Die Struktur der Auszahlungsflächen innerhalb der vollständig klassischen Region *ClCl* verändert ihr Erscheinungsbild bei ansteigendem γ-Wert nicht, wohingegen die anderen Bereiche (*ClQu*, *QuCl* und *QuQu*) durch die Stärke der Verschränkung beeinflusst werden. Bei dem, durch den ansteigenden γ-Wert verursachten Übergang vom linken ($\gamma = \frac{\pi}{10} \approx 0.31$) zum rechten ($\gamma = \frac{\pi}{5} \approx 0.63$) Diagramm der Abbildung 1.8, verschwindet zunächst das ursprüngliche im klassischen Spiel existierende Nash-Gleichgewicht und danach entsteht ein neues Nash-Gleichgewicht bei der Quantenstrategie ($(\widehat{Q}, \widehat{Q}) \hat{=} (\tau_A = -1, \tau_B = -1)$). Diese beiden separaten Eigenschaften, die bei den γ-Grenzwerten γ_1 und γ_2 entstehen, werden im Folgenden kurz näher erläutert. Für Strategienverschränkungen γ, die größer sind als die erste γ-Barriere ($\gamma_1 \approx 0.361$), ist die beste Antwort des Spielers A auf die $s_2^B \hat{=} (\tau_B = 1)$-Strategie des Spielers B nicht mehr die Strategie $s_2^A \hat{=} (\tau_A = 1)$, sondern die Quantenstrategie $\tau_A = -1$, da die Auszahlung $\$_A(\tau_A = -1, \tau_B = 1) \approx 5.05$ für diese Strategie nun größer ist als die Auszahlung im klassischen Nash-Gleichgewicht ($\$_A(\tau_A = 1, \tau_B = 1) = 5$). Das ursprüngliche Nash-Gleichgewicht verschwindet demnach für $\gamma > \gamma_1$. Ab der zweiten γ-Barriere ($\gamma_2 \approx 0.524$) ist die beste Antwort des Spielers A auf die Strategie $\widehat{Q}_B \hat{=} (\tau_B = -1)$ des Spielers B nicht mehr die klassische Strategie $s_2^A \hat{=} (\tau_A = 1)$ sondern die Quantenstrategie $\widehat{Q}_A \hat{=} (\tau_A = -1)$, da die Auszahlung $\$_A(\tau_A = 1, \tau_B = -1) \approx 9.96$ bei einem Wert $\gamma \approx 0.524$ niedriger ist als die Auszahlung für den Fall, wenn beide Spieler die Quantenstrategie $\widehat{Q}$ spielen ($\$_A(\tau_A = -1, \tau_B = -1) = 10$). Ein neues Nash-Gleichgewicht, welches dann die dominante Strategie des Spiels ist, entsteht demnach für $\gamma > \gamma_2$. Die exakten Werte der beiden γ-Barrieren können für symmetrische (2 Personen)-(2 Strategien) Quantenspiele analytisch, in Abhängigkeit der Auszahlungsparameter angegeben werden (siehe Anhang im „Introductory Paper“ [110]).

Die Resultate der Abbildung 1.8 zeigen somit, dass durch die quantentheoretische Erweiterung eines Gefangenendilemma-ähnlichen Spiels die Spieler dem Dilemma entkommen können, falls der Wert der Stärke der Verschränkung über einem

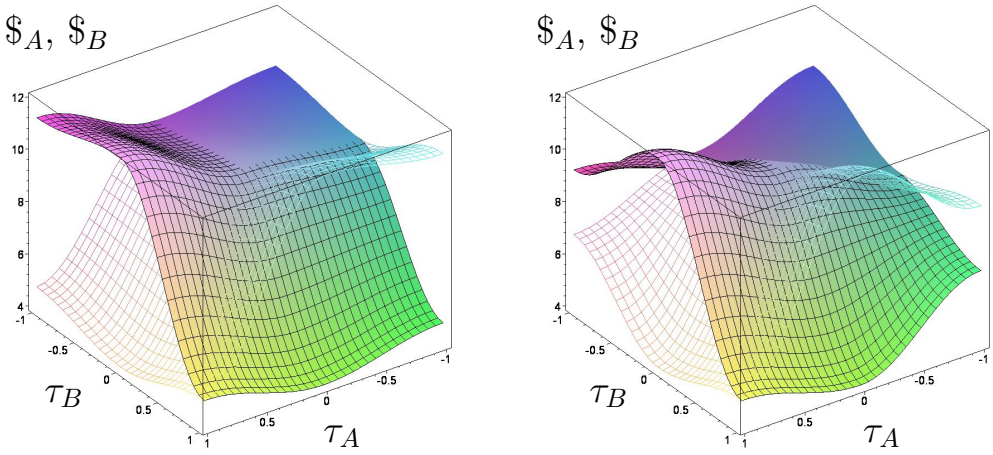

Abbildung 1.8.: Quantentheoretisch erweiterte Auszahlungsfunktion (wie in Abbildung 1.7 beschrieben). Die beiden Diagramme stellen die Resultate von Quantenspielen im Parametersatz Set_A mit einem mittleren Verschränkungswert dar (linke Seite: $\gamma = \frac{\pi}{10}$, rechte Seite: $\gamma = \frac{\pi}{5}$).

definierten γ-Grenzwert liegt. Liegt der γ-Wert der Strategienverschränkung oberhalb der dem Spiel eigenen γ-Barriere (siehe z.B. rechtes Diagramm der Abbildung 1.8), so hat sich die klassische dominante Strategie für die Spieler aufgelöst und eine neue vorteilhafte, dominante Strategiekombination $(\widehat{Q}_A, \widehat{Q}_B)$ ist für die Spieler entstanden. Da die Projektion dieser dominanten Quantenstrategienkombination $(\widehat{Q}_A, \widehat{Q}_B)$ auf den messbaren, realen Raum der klassischen Strategienkombination (s_1^A, s_1^B) entspricht, entkommen die Spieler dem Dilemma des Spiels.

Abbildung 1.9 stellt die quantentheoretisch erweiterte Auszahlungsfunktion bei hohen Verschränkungswerten dar (links $\gamma = \frac{3\pi}{10} \approx 0.94$, rechts $\gamma = \frac{\pi}{2} \approx 1.57$). Die beiden Diagramme zeigen, dass sich die Vorteilhaftigkeit der neuen dominanten Quantenstrategie bei weiter ansteigenden γ-Werten verbessert und somit dessen Dominanz weiter zunimmt.

Neben diesem exemplarischen Beispiel eines dominanten Quantenspiels können

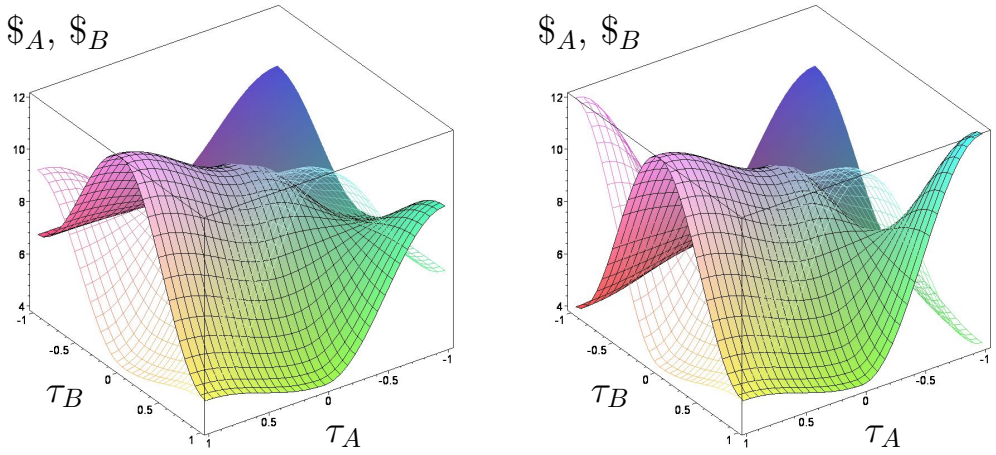

Abbildung 1.9.: Quantentheoretisch erweiterte Auszahlungsfunktion (wie in Abbildung 1.7 beschrieben). Die beiden Diagramme stellen die Resultate von Quantenspielen im Parametersatz Set_A mit einem hohen Verschränkungswert dar (linke Seite: $\gamma = \frac{3\pi}{10}$, rechte Seite: $\gamma = \frac{\pi}{2}$).

im Allgemeinen die Folgenden Aussagen bewiesen werden (siehe „Introductory Paper“ [110]).

- Die quantentheoretische Erweiterung eines dominanten, symmetrischen (2 Personen)-(2 Strategien) Spiels mit Dilemma löst das zugrundeliegende Dilemma des Spiels ab einer definierten γ-Barriere auf.
- Die quantentheoretische Erweiterung eines dominanten, symmetrischen (2 Personen)-(2 Strategien) Spiels ohne Dilemma liefert keine weiteren Nash-Gleichgewichte. Die ursprüngliche dominante Strategie des Spiels bleibt auch bei maximaler Strategienverschränkung bestehen.

Koordinationsspiele

Das durch Parametersatz Set_B[10] definierte Spiel gehört der Klasse der Koordinationsspiele an. Im Vergleich zum Set_A hat sich der Wert $\$_{21}$ von 12 auf 9 verringert,

[10]Der Parametersatz Set_A entspricht dem Parametersatz Set_4 des „Introductory Papers“ [110].

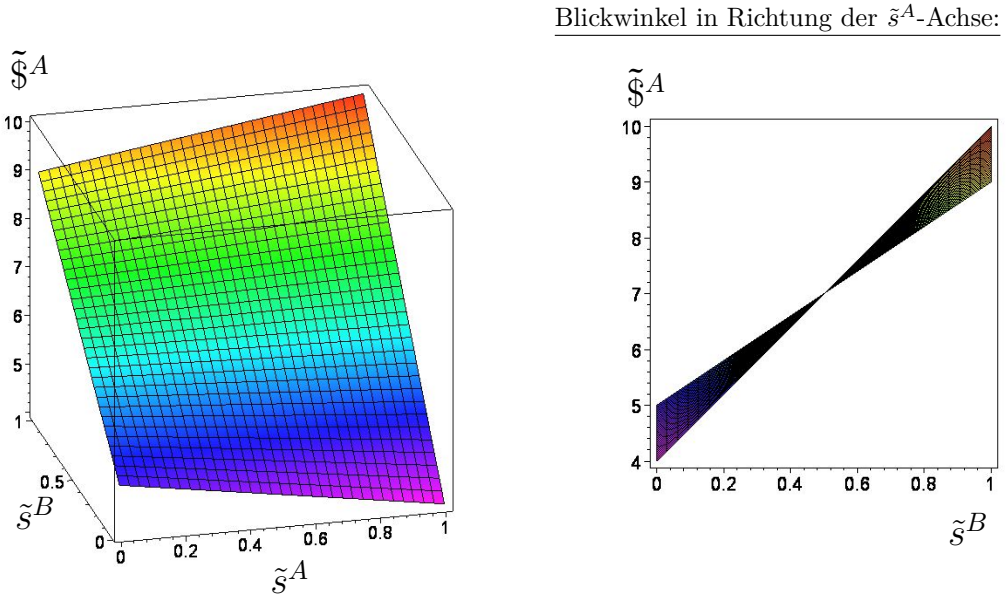

Abbildung 1.10.: Parametersatz Set_B: Auszahlungsfunktion $\tilde{\$}^A(\tilde{s}^A, \tilde{s}^B)$ des Spielers A als Funktion der gemischten Strategie des Spielers A ($\tilde{s}^A$) und des Spielers B ($\tilde{s}^B$).

was den Übergang vom dominanten Spiel hin zu der Klasse der Koordinationsspiele bewirkte. Das Spiel hat nun zwei symmetrische Nash-Gleichgewichte in reinen Strategien $((s_1^A, s_1^B) \hat{=} (\tilde{s}^A = 1, \tilde{s}^B = 1)$ und $(s_2^A, s_2^B) \hat{=} (\tilde{s}^A = 0, \tilde{s}^B = 0))$ und ein internes Nash-Gleichgewicht bei der gemischten Strategienkombination $((\tilde{s}^{A\star}, \tilde{s}^{B\star}) = (\frac{1}{2}, \frac{1}{2}))$. Die beiden reinen Nash-Gleichgewichte können anhand des linken Diagramms der Abbildung 1.10 veranschaulicht werden. Falls Spieler A annimmt, dass Spieler B eine gemischte Strategie $\tilde{s}^B > s^\star$ wählt, ist die Bestantwort für Spieler A die reine Strategie $s_1^A \hat{=} (\tilde{s}^A = 1)$. Andererseits, für den Fall, dass Spieler B $\tilde{s}^B < s^\star$ wählt, ist die beste Antwort die andere reine Strategie $(s_2^A \hat{=} (\tilde{s}^A = 0))$. Das gemischte Nash-Gleichgewicht ist mittels der speziellen Projektion der Auszahlungsfläche (in Blickrichtung der $\tilde{s}^A$-Achse) im rechten Diagramm der Abbildung 1.10 einfach zu erkennen. Da in diesem Nash-Gleichgewicht die partielle Ableitung der Auszahlungsfunktion verschwindet, zieht sich die gesamte Fläche bei der gewählten $\tilde{s}^A$-Projektion auf einen Punkt

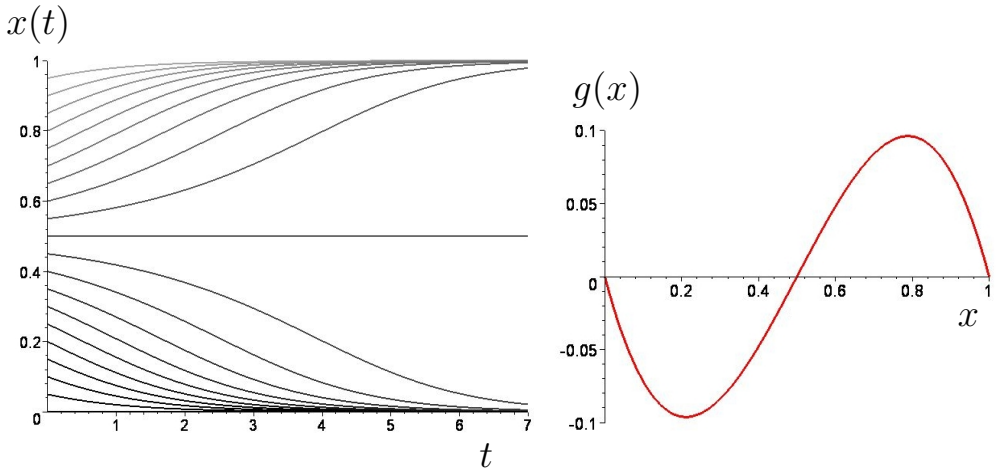

Abbildung 1.11.: Links: $x(t)$, Anteil der Spieler die zurzeit t die Strategie s_1 wählen für unterschiedliche Anfangswerte berechnet im Parametersatz Set_B. Rechts: $g(x)$, Reproduktionsdynamik bestimmende Funktion.

zusammen.

Der Wert des gemischten Nash-Gleichgewichts $\tilde{s}^\star = \frac{1}{2}$ besitzt zusätzlich die Eigenschaft die Nullstelle der Funktion $g(x)$ zu definieren ($g(x = \tilde{s}^\star) \equiv 0$, vergleiche rechte Seite der Abbildung 1.11). Allgemein besitzt die Funktion $g(x)$ bei Koordinationsspielen einen negativen Bereich ($g(x) < 0 \; \forall \; x \in]0, s^\star[$) und einen positiven Bereich ($g(x) > 0 \; \forall \; x \in]s^\star, 1[$), dessen Grenze durch den Wert des gemischten Nash-Gleichgewichts definiert ist. Aufgrund dieser Eigenschaft existieren bei Koordinationsspielen stets zwei mögliche evolutionär stabile Strategien ($x(t \to \infty) = 0$ und $x(t \to \infty) = 1$). Zu welcher dieser Endzustände sich die gesamte Population der Spieler entwickeln wird, hängt von der Anfangsbedingung $x(t = 0)$ ab (vergleiche linke Seite der Abbildung 1.11). Falls der Anteil der s_1-Strategie Spieler zurzeit $t = 0$ unterhalb des Wertes des gemischten Nash-Gleichgewichts liegt ($x(0) < s^\star$), wird sich die Strategienwahl der Population zur ESS entwickeln, bei welcher alle Spieler ausschließlich die Strategie s_2 wählen ($\lim_{t\to\infty}(x(t)) = 0$). Befindet sich der Anfangswert dagegen oberhalb ($x(0) > s^\star$), so entwickelt sich die Strategienwahl der Population hin zur anderen ESS ($\lim_{t\to\infty}(x(t)) = 1$), bei welche alle Spieler die s_1-Strategie wählen. Die

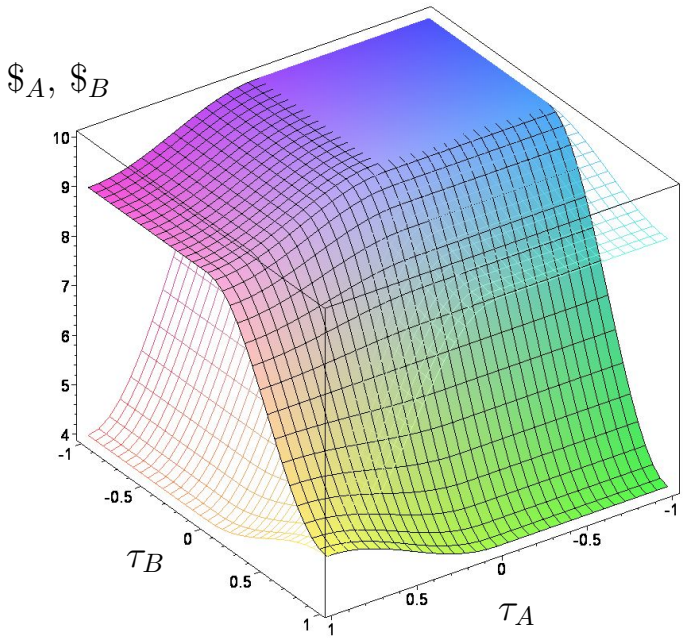

Abbildung 1.12.: Quantentheoretisch erweiterte Auszahlung $\$_A$ des Spielers A (untransparente Fläche) und $\$_B$ des Spielers B (transparente Fläche) als Funktion der reduzierten s_1-Quantenstrategien τ_A des Spielers A und τ_B des Spielers B in einem unverschränktem Quantenspiel ($\gamma = 0$) unter Verwendung des Parametersatzes Set_B.

horizontale Linie bei $x(0.5) = 0.5$ in der linken Seite der Abbildung 1.11 ist ein Artefakt der benutzten nummerischen Simulationsmethode und entspricht keiner stabilen evolutionären Bahn, da diese schon bei infinitesimal kleinen Störungen instabil wird.

Die quantentheoretisch erweiterte Auszahlung $\$_A$ des Spielers A (untransparente Fläche) und $\$_B$ des Spielers B (transparente Fläche) des Parametersatzes Set_B ist in Abbildung 1.12 für den unverschränkten Fall ($\gamma = 0$) dargestellt. Die Abbildung zeigt wiederum, dass das unverschränkte Quantenspiel des Parametersatzes Set_B identisch mit dem klassischen Koordinationsspiel ist. Falls beide Spieler eine Quantenstrategie wählen ($\tau_A < 0 \wedge \tau_B < 0$),

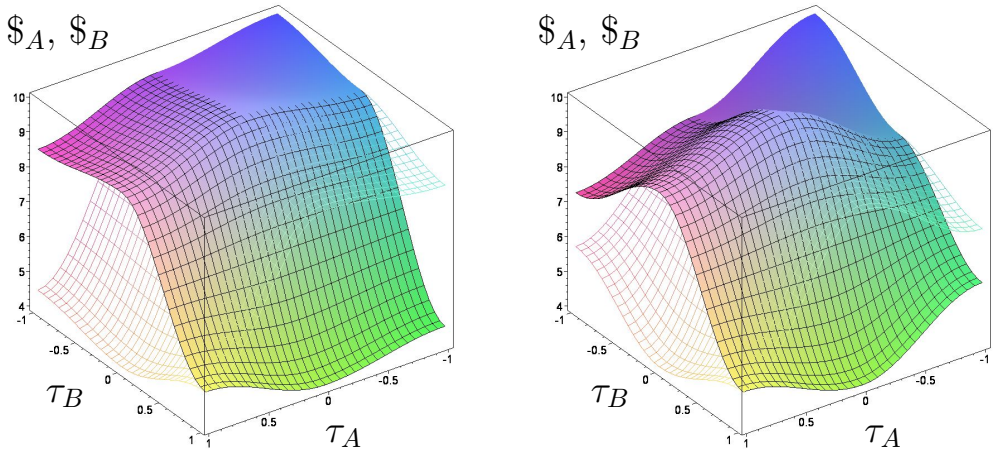

Abbildung 1.13.: Quantentheoretisch erweiterte Auszahlungsfunktion (wie in Abbildung 1.12 beschrieben). Die beiden Diagramme stellen die Resultate von Quantenspielen im Parametersatz Set_B mit einem mittleren Verschränkungswert dar (linke Seite: $\gamma = \frac{\pi}{10}$, rechte Seite: $\gamma = \frac{\pi}{5}$).

ist deren erzielte Auszahlung gleich dem Fall, in welchem beide Spieler die klassische Strategie s_1 spielen ($\$_A(\tau_A = 0, \tau_B = 0) = 10$), und entspricht der größt möglichen Auszahlung des zugrundeliegenden Koordinationsspiels. Die zwei reinen Nash-Gleichgewichte entsprechen den folgenden τ-Strategien: $(s_1^A, s_1^B) \hat{=} (\tau_A = 0, \tau_B = 0)$ und $(s_2^A, s_2^B) \hat{=} (\tau_A = 1, \tau_B = 1)$. Der $\tau^\star$-Wert des internen Nash-Gleichgewichts in gemischten Strategien ($s^\star$) berechnet sich unter Verwendung der Gleichung (1.11)[11]

$$s^\star = \psi_1(\psi_1)^* = \left(\cos(\frac{\theta^\star}{2})\right)^2 = \left(\cos(\frac{\pi\,\tau^\star}{2})\right)^2 \Leftrightarrow \tau^\star = \frac{2}{\pi}\arccos(\sqrt{s^\star}) \;, \quad (1.23)$$

und befindet sich somit bei $\tau^\star = \frac{2}{\pi}\arccos(\sqrt{\frac{1}{2}}) = \frac{1}{2}$.

Die Auszahlungsflächen der Abbildung 1.13 zeigen die Ergebnisse des betrachteten Quanten-Koordinationsspiels für zwei mittelmäßig verschränkte Situationen

[11] $(\psi_1)^*$ steht hierbei für den konjugiert komplexen Wert der Zustandskomponente ψ_1.

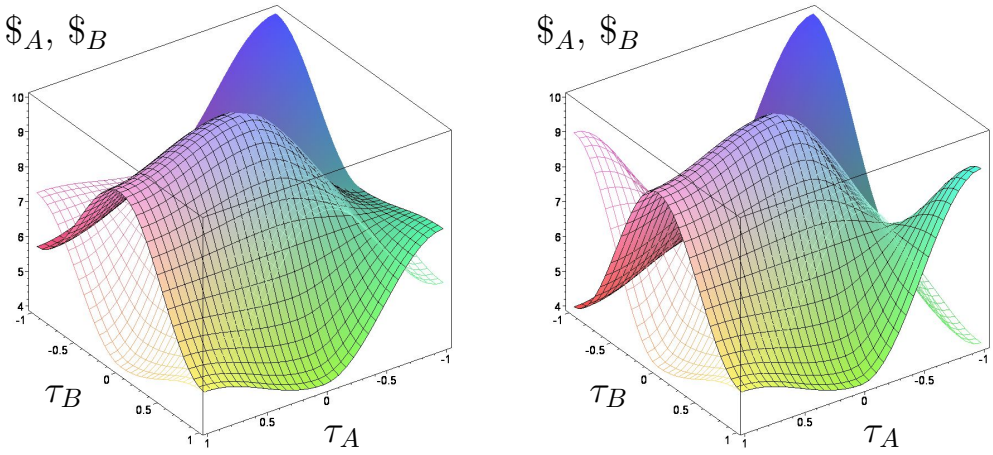

Abbildung 1.14.: Quantentheoretisch erweiterte Auszahlungsfunktion (wie in Abbildung 1.12 beschrieben). Die beiden Diagramme stellen die Resultate von Quantenspielen im Parametersatz Set_B mit einem hohen Verschränkungswert dar (linke Seite: $\gamma = \frac{3\pi}{10}$, rechte Seite: $\gamma = \frac{\pi}{2}$).

(linke Seite: $\gamma \approx 0.31$, rechte Seite: $\gamma \approx 0.63$). Abbildung 1.13 zeigt, dass selbst bei minimaler Verschränkung ein neues Nash-Gleichgewicht bei der Quanten-Strategienkombination $((\widehat{Q}, \widehat{Q}) \hat{=} (\tau_A = -1, \tau_B = -1))$ entsteht. Formal erhält man dieses Resultat durch die Berechnung der γ_2-Barriere (siehe Anhang im „Introductory Paper“ [110]), die bei Koordinationsspielen rein imaginär ist und somit formal den reellen Wert $\gamma_2 = 0$ besitzt. Die Auflösung des klassischen, reinen Nash-Gleichgewichts mit geringer Auszahlung $(s_2^A, s_2^B) \hat{=} (\tau_A = 1, \tau_B = 1)$ im Parametersatz Set_B entsteht bei Verschränkungswerten die oberhalb der γ_1-Barriere liegen $\gamma > \gamma_1 \approx 0.4636$. Spieler, die sich in einer Situation des linken Diagramms der Abbildung 1.13 befinden, können somit dem Dilemma des Koordinationsspiels nicht entkommen, wohingegen sich für die Spieler des rechten Diagramms das zweite reine Nash-Gleichgewicht mit geringer Auszahlung aufgelöst hat. In einem evolutionären Koordinationsspiel existiert demnach oberhalb der γ_1-Barriere nur noch die evolutionär stabile Quantenstrategie, welche projiziert auf die reelle Achse bedeutet, dass die Spieler der Population ausschließlich die s_1-Strategie

wählen und somit dem Koordinationsproblem des Spiels entkommen. Wie in Abbildung 1.14 illustriert, ändert sich bei weiter ansteigendem γ-Wert an diesem Sachverhalt nichts.

Neben diesem exemplarischen Beispiel eines Quanten-Koordinationspiels kann im Allgemeinen gezeigt werden (siehe „Introductory Paper“ [110]), dass in einer quantentheoretischen Erweiterung eines symmetrischen (2 Personen)-(2 Strategien) Koordinationspiels das dem Spiel zugrundeliegende Koordinationsproblem ab einer definierten γ-Barriere verschwindet.

Anti-Koordinationsspiele

Im Parametersatz Set_C[12] hat sich im Vergleich zum Set_A der Wert $\$_{12}$ von 4 auf 7 erhöht, was einen Übergang vom dominanten Spiel hin zu der Klasse der Anti-Koordinationsspiele bewirkte. Das Spiel besitzt nun zwei unsymme-

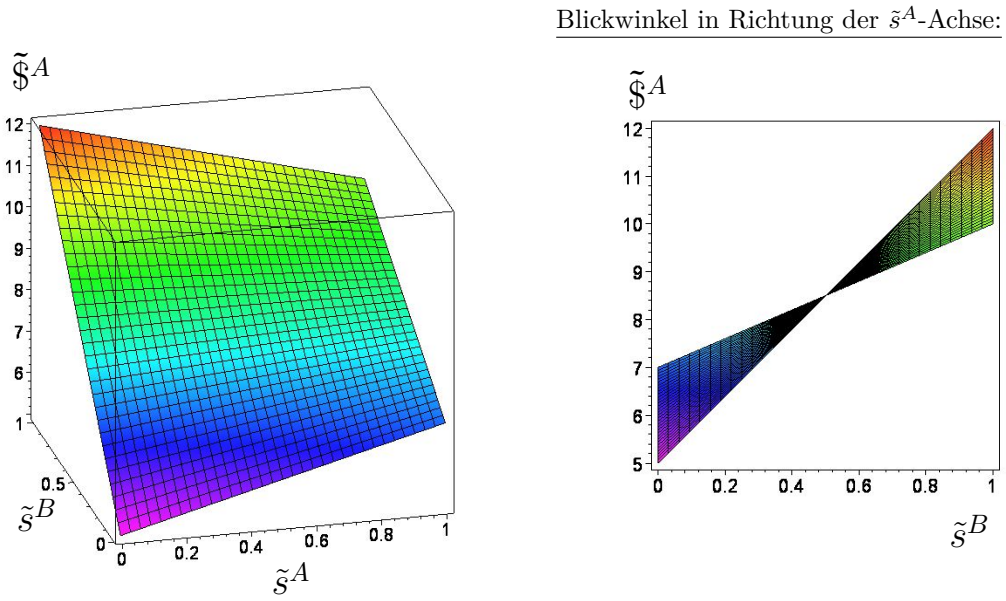

Abbildung 1.15.: Parametersatz Set_C: Auszahlungsfunktion $\tilde{\$}^A(\tilde{s}^A, \tilde{s}^B)$ des Spielers A als Funktion der gemischten Strategie des Spielers A ($\tilde{s}^A$) und des Spielers B ($\tilde{s}^B$).

[12] Der Parametersatz Set_C entspricht dem Parametersatz Set_8 des „Introductory Papers“ [110].

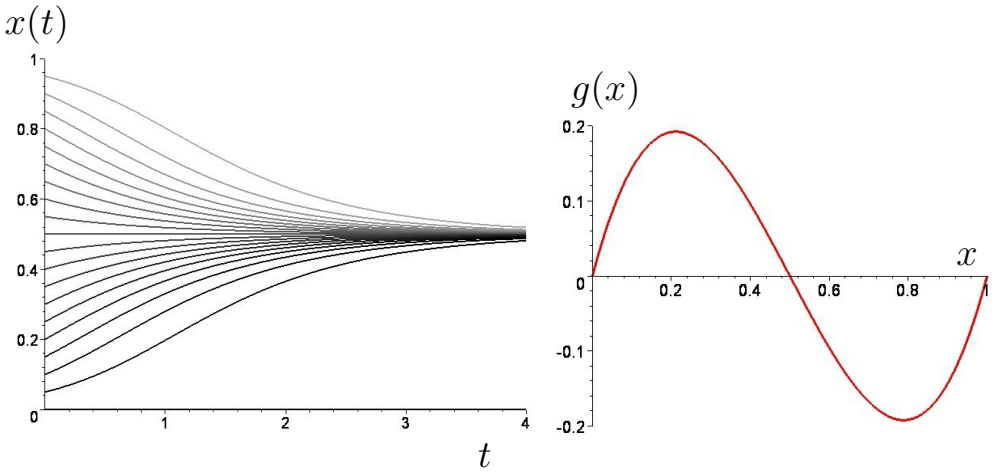

Abbildung 1.16.: Links: $x(t)$, Anteil der Spieler die zurzeit t die Strategie s_1 wählen für unterschiedliche Anfangswerte berechnet im Parametersatz Set_C. Rechts: $g(x)$, Reproduktionsdynamik bestimmende Funktion.

trische Nash-Gleichgewichte in reinen Strategien ($(s_1^A, s_2^B) \hat{=} (\tilde{s}^A = 1, \tilde{s}^B = 0)$ und $(s_2^A, s_1^B) \hat{=} (\tilde{s}^A = 0, \tilde{s}^B = 1)$) und ein internes Nash-Gleichgewicht bei der gemischten Strategienkombination ($(\tilde{s}^{A\star}, \tilde{s}^{B\star}) = (\frac{1}{2}, \frac{1}{2})$). Die beiden reinen Nash-Gleichgewichte können wiederum durch die Struktur der Auszahlungsfläche, anhand des linken Diagramms der Abbildung 1.15 illustriert werden. Falls Spieler A annimmt, dass Spieler B eine gemischte Strategie $\tilde{s}^B > s^\star$ wählt, ist die Bestantwort für Spieler A die reine Strategie $s_2^A \hat{=} (\tilde{s}^A = 0)$. Andererseits, für den Fall, dass Spieler B $\tilde{s}^B < s^\star$ wählt, ist die beste Antwort die andere reine Strategie ($s_1^A \hat{=} (\tilde{s}^A = 1)$). Das gemischte Nash-Gleichgewicht ist abermals mittels der speziellen Projektion der Auszahlungsfläche (in Blickrichtung der $\tilde{s}^A$-Achse) im rechten Diagramm der Abbildung 1.15 einfach zu erkennen.

Wie im betrachteten Koordinationsspiel besitzt der Wert des gemischten Nash-Gleichgewichts $\tilde{s}^\star = \frac{1}{2}$ zusätzlich die Eigenschaft die Nullstelle der Funktion $g(x)$ zu definieren ($g(x = \tilde{s}^\star) \equiv 0$, vergleiche rechte Seite der Abbildung 1.16). Allgemein besitzt die Funktion $g(x)$ bei Anti-Koordinationsspielen einen negativen Bereich ($g(x) < 0 \; \forall \; x \in]s^\star, 1[$) und einen positiven Bereich ($g(x) > 0 \; \forall \; x \in]0, s^\star[$), dessen Grenze durch den Wert des gemischten Nash-Gleichgewichts

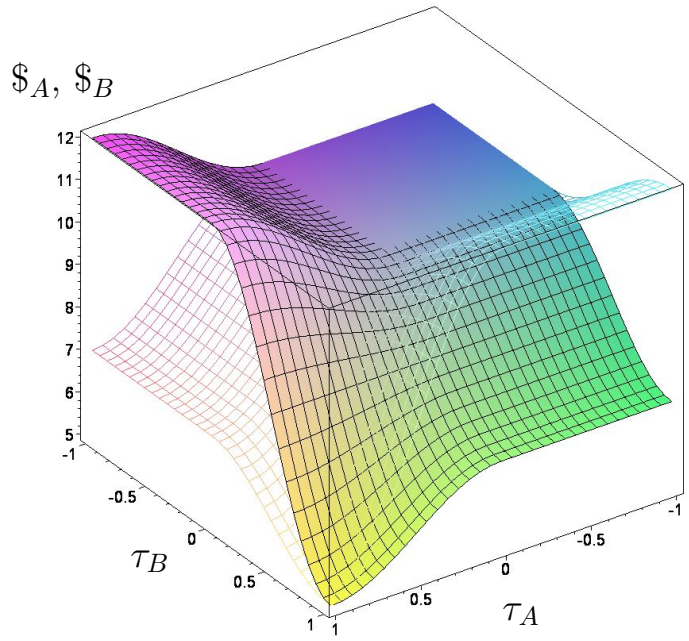

Abbildung 1.17.: Quantentheoretisch erweiterte Auszahlung $\$_A$ des Spielers A (untransparente Fläche) und $\$_B$ des Spielers B (transparente Fläche) als Funktion der reduzierten s_1-Quantenstrategien τ_A des Spielers A und τ_B des Spielers B in einem unverschränktem Quantenspiel ($\gamma = 0$) unter Verwendung des Parametersatzes Set_C.

definiert ist. Aufgrund dieser Eigenschaft existiert bei Anti-Koordinationsspielen stets nur eine mögliche evolutionär stabile Strategie, die sich (unabhängig von der zugrundeliegenden Anfangsbedingung) beim Wert des gemischten Nash-Gleichgewichts befindet ($x(t \to \infty) = s^\star$, siehe linken Seite der Abbildung 1.16). Die stabile evolutionäre Strategie bei Anti-Koordinationsspielen ist demnach ein dynamisches evolutionäres Gleichgewicht. Obwohl sich die durchschnittliche Anzahl der Spieler, die eine s_1-Strategie wählen, sich im Gleichgewichtszustand nicht weiter ($(x(t \to \infty) = s^\star)$ verändert, können einzelne Spieler ihre Strategie verändern.

Die quantentheoretisch erweiterten Auszahlungen der Spieler dieses exemplari-

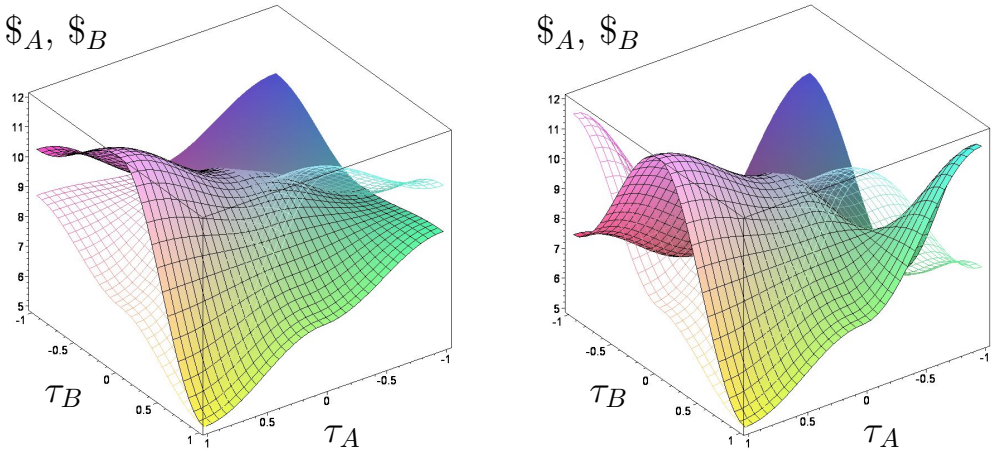

Abbildung 1.18.: Quantentheoretisch erweiterte Auszahlungsfunktion (wie in Abbildung 1.17 beschrieben). Die beiden Diagramme stellen die Resultate von Quantenspielen im Parametersatz Set_C mit einem mittleren (linke Seite: $\gamma = \frac{\pi}{5}$) und einem hohen (rechte Seite: $\gamma = \frac{2\pi}{5}$) Verschränkungswert dar.

schen Anti-Koordinationsspiels sind in Abbildung 1.17 für den unverschränkten Fall ($\gamma = 0$) dargestellt. Wiederum zeigt die Abbildung, dass der unverschränkte Fall identisch mit dem klassischen Spiel ist. Falls beide Spieler eine Quantenstrategie wählen ($\tau_A < 0 \wedge \tau_B < 0$), ist die erzielte Auszahlung gleich dem Fall, in welchem beide Spieler die klassische Strategie s_1 spielen ($\$_A(\tau_A = 0, \tau_B = 0) = 10$). Die zwei reinen unsymmetrischen Nash-Gleichgewichte des Anti-Koordinationsspiel entsprechen den folgenden τ-Strategien: $(s_1^A, s_2^B) \hat{=} (\tau_A = 0, \tau_B = 1)$ und $(s_2^A, s_1^B) \hat{=} (\tau_A = 1, \tau_B = 0)$. Der $\tau^\star$-Wert des internen Nash-Gleichgewichts in gemischten Strategien ($s^\star$) berechnet sich wie beim Koordinationsspiel (siehe Gleichung (1.23)) zu $\tau^\star = \frac{2}{\pi}\arccos(\sqrt{\frac{1}{2}}) = \frac{1}{2}$.

Die Auszahlungsflächen der Abbildung 1.18 zeigen die Ergebnisse des betrachteten Quanten-Koordinationsspiels für ein mittelmäßig (linke Seite: $\gamma = \frac{\pi}{5}$) und stark (rechte Seite: $\gamma = \frac{2\pi}{5}$) verschränktes Spiel. Schon bei minimaler

Verschränkung entsteht bei Anti-Koordinationsspiele bei der Strategienkombination ($\tau_A = 1, \tau_B = -1$) bzw. ($\tau_A = -1, \tau_B = 1$) ein neues unsymmetrisches Nash-Gleichgewicht. Formal erhält man dieses Resultat durch die Berechnung der γ_1-Barriere (siehe Anhang im „Introductory Paper“ [110]), die bei Anti-Koordinationsspielen rein imaginär ist, und somit formal den reellen Wert $\gamma_1 = 0$ liefert. Bei Verschränkungsstärken die höher als die γ_2-Barriere ($\gamma_2 \approx 0.685$) sind, entsteht bei Anti-Koordinationsspielen (zusätzlich zur klassischen ESS) eine neue evolutionär stabile Quantenstrategie, bei welcher die gesamte Population, auf den reellen Raum projiziert, die s_1-Strategie wählt.

Neben diesem exemplarischen Beispiel eines Quanten-Anti-Koordinationspiels kann im Allgemeinen gezeigt werden (siehe „Introductory Paper“ [110]), dass in einer quantentheoretischen Erweiterung eines symmetrischen (2 Personen)-(2 Strategien) Anti-Koordinationspiels ab einer definierten γ-Barriere eine neue, evolutionär stabile Quantenstrategie entsteht. Welche der beiden evolutionär stabile Strategien in einer dynamischen Populationsentwicklung realisiert wird, ist durch die Struktur der zeitabhängigen, quantentheoretisch erweiterten Differentialgleichungen (siehe Unterkapitel 2.5) bestimmt.

Unsymmetrische Quantenspiele

Die Darstellung der Resultate des vorigen Unterkapitels betrachtete ausschließlich die evolutionäre Entwicklung symmetrischer Quantenspiele, bei welcher die zugrundeliegende Population der Spieler eine homogene Gruppe ununterscheidbarer Akteure bildete. Bei unsymmetrischen (2 Personen)-(2 Strategien) Spielen (Bimatrix Spiele) separiert sich die zu beschreibende Population zwangsläufig in zwei separate Gruppen. Die klassische evolutionäre Entwicklung solcher Spiele ist durch die gekoppelte Differentialgleichung (siehe Gleichung (1.9)) formalisiert, wobei dessen Lösungen in die drei Hauptklassen der Eckenspiele, Sattelspiele und Zentrumsspiele gegliedert werden. Die Eigenschaften elf exemplarischer Beispiele dieser Klassen sind im „Introductory Paper“ [110] dieser Dissertation beschrieben und sollen innerhalb dieser Zusammenfassung nicht erneut im Detail diskutiert werden. Die quantentheoretische Erweiterung von Bimatrix Spielen wird hingegen im Folgenden mittels eines Beispiels exemplarisch erläutert.

Im Allgemeinen lässt sich die quantentheoretische Erweiterung von Bimatrix Spielen auf die zugrundeliegenden Eigenschaften der symmetrischen Quantenspiele der beiden Teilpopulationen zurückführen. Dies wird im Folgenden anhand eines unsymmetrischen Sattelspiels veranschaulicht, welcher dem Parametersatz Set_7^{us} des „Introductory Papers“ [110] entspricht. Die Auszahlungsparameter der Teilpopulationen A und B sind in Tabelle 1.3 zusammengefasst.

A\B	s_1^B	s_2^B
s_1^A	(10,10)	(4,7)
s_2^A	(9,4)	(5,5)

Tabelle 1.3.: (2×2)-Auszahlungsmatrix der Spieler A und B im Parametersatz Set_7^{us}.

Beide Teilpopulationen sind einem Koordinationsspiel unterworfen, so dass sich eine Sattelklasse des gemeinsamen Bimatrix Spiels ergibt. Aufgrund der unsymmetrischen Auszahlungsstruktur unterscheiden sich die internen, gemischten Nash-Gleichgewichte der Teilspiele und man erhält für die interne Nash-Gleichgewichtsstrategienkombination den folgenden Wert: $(\tilde{s}^{A\star}, \tilde{s}^{B\star}) = (\frac{1}{2}, \frac{1}{4})$. Die linke Seite der Abbildung 1.19 veranschaulicht die Auszahlungsflächen der Spieler A und B, wohingegen die rechte Seite der Abbildung, die das dynamische Verhalten des evolutionären Spiels determinierenden Funktionen $g_x(x, y)$ und $g_y(x, y)$ veranschaulicht. Das gemischte Nash-Gleichgewicht $(\tilde{s}^{A\star}, \tilde{s}^{B\star})$ befindet sich gerade an dem Punkt, bei welchem die beiden Funktionen $g_x(x, y)$ und $g_y(x, y)$ die Nullfläche (siehe weiße Fläche im rechten Diagramm der Abbildung 1.19) treffen.

Die deterministische, evolutionäre Entwicklung des strategischen Verhaltens der beider Gruppen ist in Abbildung 1.20 für drei unterschiedliche Anfangsbedingungen $(x(0), y(0))$ veranschaulicht. Die sich von den Anfangsbedingungen aus entwickelnden Trajektorien $(x(t), y(t))$ sind in einem Phasendiagramm dargestellt, wobei die Komponente $x(t)$ den Anteil der Spieler aus Gruppe A, die die Strategie s_1 spielen, und $y(t)$ denselben Anteil der Spieler aus Gruppe B bezeichnet. Die drei farbigen Trajektorien sind in ein Felddiagramm eingebettet, wobei die kleinen grauen Pfeile den „strategischen Populationswind“ veranschau-

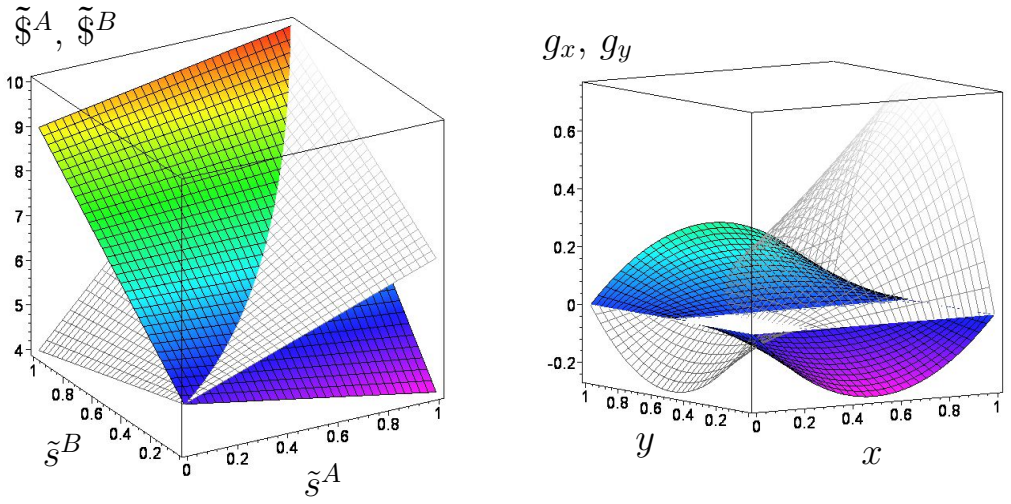

Abbildung 1.19.: Linke Seite: Auszahlungsfunktion in gemischten Strategien für Spieler A ($\tilde{\$}^A(\tilde{s}^A, \tilde{s}^B)$, farbige Fläche) und Spieler B ($\tilde{\$}^B(\tilde{s}^A, \tilde{s}^B)$, graue Fläche) berechnet im unsymmetrischen Parametersatz Set_7^{us} als Funktion der gemischten Strategien des Spielers A ($\tilde{s}^A$) und Spielers B ($\tilde{s}^B$). Rechte Seite: $g_x(x, y)$ (farbige Fläche) und $g_y(x, y)$ (transparente graue Fläche) in Abhängigkeit der durchschnittlichen strategischen Wahl der Teilpopulation A (x) und B (y).

lichen, den die gesamte Population im Laufe ihrer Entwicklung zu folgen hat. Die drei Anfangsbedingungen sind durch farbige Punkte am Anfang der jeweiligen Trajektorien gekennzeichnet. Die farbigen Pfeile auf den Trajektorien entsprechen der strategischen Populationsentwicklung für eine feste Zeitspanne δt, wobei die Länge der Pfeile somit ein Maß für die Änderungsgeschwindigkeit der mittleren strategischen Entscheidung der Population ist. Da diese strategischen Änderungsgeschwindigkeiten für die drei dargestellten Trajektorien sehr unterschiedlich sind, wurden die δt-Werte in Abbildung 1.20 unterschiedlich gewählt. Während für die rote und grüne Trajektorie ein gemeinsamer Wert ($\delta t = 0.35$) gewählt wurde, sind die farbigen Pfeile auf der blauen (langsamsten) Trajektorie eine Zeitspanne $\delta t = 2$ auseinander. Die blaue Trajektorie startet bei dem Anfangswert $(x(0) = 0.7, y(0) = 0.1)$ und endet in dem symmetrischen

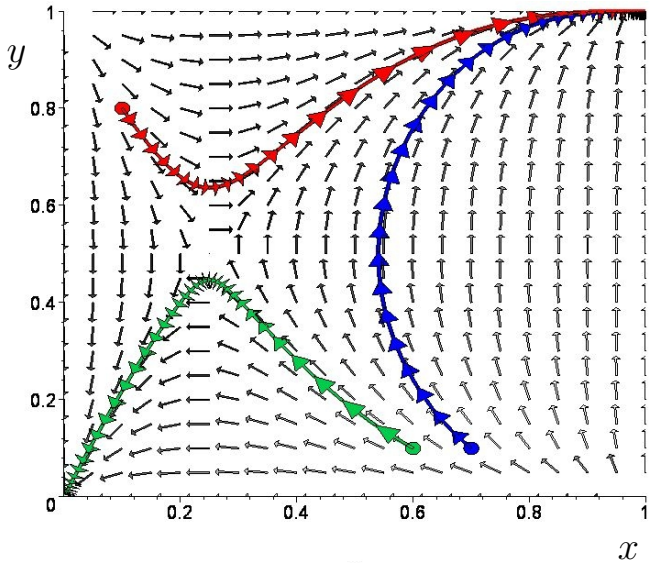

Abbildung 1.20.: Phasendiagramm der xy-Trajektorien für drei unterschiedliche Anfangsbedingungen im Parametersatz Set_7^{us}. x beschreibt den Anteil der Spieler aus Gruppe A, die die Strategie s_1 wohingegen y denselben Anteil der Spieler aus Gruppe B bezeichnet.

Nash-Gleichgewicht $(s_1^A, s_1^B) \hat{=} (\tilde{s}^{A*} = 1, \tilde{s}^{B*} = 1)$ (alle Spieler wählen die s_1-Strategie). Während der Anteil der s_1-Spieler innerhalb der Gruppe B stetig monoton ansteigt, sinkt der Anteil der s_1-Spieler innerhalb der Gruppe A zunächst, um dann nach einem Umkehrpunkt stetig anzusteigen. Bei der roten Trajektorie, welche bei $(x(0) = 0.1, y(0) = 0.8)$ startet, ist diese Eigenschaft gerade umgekehrt. Der Anteil der s_1-Spieler innerhalb der Gruppe A steigt hier stetig monoton an, wohingegen er in Gruppe B zunächst fällt, um danach wieder anzusteigen. Am Umkehrpunkt der roten Trajektorie verlangsamt sich die strategische Änderungsgeschwindigkeit sehr, da der Pfad der Entwicklung dem gemischten Nash-Gleichgewicht sehr nahe kommt. Obwohl die Anfangsbedingungen der roten und blauen Trajektorie sehr unterschiedlich sind, enden beide in der evolutionär stabilen Strategie $(s_1^A, s_1^B) \hat{=} (\tilde{s}^{A*} = 1, \tilde{s}^{B*} = 1)$. Obwohl der Anfangswert der grünen Trajektorie $(x(0) = 0.6, y(0) = 0.1)$ nur ein wenig unterschiedlich von dem der blauen Trajektorie ist, entwickelt sich die grüne hin zu der anderen evolutionär stabilen Strategie $(s_2^A, s_2^B) \hat{=} (\tilde{s}^{A*} = 0, \tilde{s}^{B*} = 0)$ (alle Spieler wählen

die s_2-Strategie). Hier sinkt der Anteil der s_1-Spieler innerhalb der Gruppe A monoton, wobei der Anteil innerhalb der Gruppe B zunächst steigt und nach dem Umkehrpunkt stetig fällt. Ähnlich wie bei der roten Trajektorie verlangsamt sich die Änderungsgeschwindigkeit der strategischen Wahl am Umkehrpunkt, da sie dem internen, gemischten Nash-Gleichgewicht sehr nahe kommt.

Die bisherigen Darlegungen innerhalb dieses Unterkapitels bezogen sich ausschließlich auf die klassische Version des Spiels, wobei im Folgenden die quantentheoretische Erweiterung des exemplarischen, durch den Parametersatz Set_7^{us} definierten Sattelspiels, erläutert wird. Das nichtverschränkte Bimatrixspiel ($\gamma = 0$) ist wiederum identisch mit der klassischen Version des Spiels, wobei die beiden reinen Nash-Gleichgewichte und das interne Nash-Gleichgewicht den folgenden τ-Strategien entsprechen:

$$(s_1^A, s_1^B) \hat{=} (\tau_A = 0, \tau_B = 0) \ , \quad (s_2^A, s_2^B) \hat{=} (\tau_A = 1, \tau_B = 1)$$
$$(\tilde{s}^{A\star}, \tilde{s}^{B\star}) \hat{=} (\tau_A = \frac{2}{\pi}\arccos(\sqrt{\frac{1}{2}}), \tau_B = \frac{2}{\pi}\arccos(\sqrt{\frac{1}{4}}))$$

Da die Teilpopulation A eine γ-Barriere von $\gamma_1^A \approx 0.4636$ und die Teilpopulation B eine γ-Barriere von $\gamma_1^A \approx 0.6155$ besitzt, geht die Spielklasse des gemeinsamen Bimatrixspiel schon bei einem γ-Wert $\gamma > \gamma_1^A$ in die Klasse der Eckspiele über. Für $\gamma_1^B > \gamma > \gamma_1^A$ besitzt die Teilpopulation A nur noch die dominante Strategie s_1, so dass sich als alleinige evolutionär stabile Strategie des Eckspiels die Strategienkombination (s_1^A, s_1^B) ergibt. Bei noch höheren γ-Werten ($\gamma > \gamma_1^B > \gamma_1^A$) besitzen beide Teilpopulationen die dominante Strategie s_1.

In gleicher Weise können die Eigenschaften anderer Klassen von Bimatrixspielen durch die quantentheoretische Erweiterung der Teilpopulationsspiele illustriert werden. Aufgrund der Fülle der möglichen Übergangsmöglichkeiten ist eine umfassende Darstellung solchen Quanten-Bimatrixspiele nicht Gegenstand dieser Dissertation.

1.2.6. Resultate

Dieses Unterkapitel fasst die formalen Ergebnisse der Arbeit anhand der betrachteten Anwendungsfelder zusammen. Innerhalb dieser Zusammenfassung

A\B	o	ø
o	$(r+\delta,r+\delta)$	$(r-\alpha,r+\beta)$
ø	$(r+\beta,r-\alpha)$	(r,r)

Tabelle 1.4.: Allgemeine Auszahlungsmatrix des „Open Access“-Publikationsspiels.

werden die den Anwendungsfeldern zugrundeliegenden inhaltlichen Hintergründe der jeweiligen Spiele nicht beschrieben – diese sind den jeweiligen Artikeln zu entnehmen. Die Zusammenstellung der Resultate konzentriert sich hingegen ausschließlich auf die Ergebnisse der quantenspieltheoretischen Erweiterung der betrachteten Anwendungsfelder und bringt diese in Zusammenhang mit den in Unterkapitel 1.2.5 dargestellten Ergebnissen.

Erster Artikel: Quanten-Spieltheorie und „Open Access“-Publikation (Quantum Game Theory and Open Access Publishing)

Die Spieler der betrachteten Population sind die Autoren wissenschaftlicher Artikel, wobei die zwei reinen Strategien die Autorenentscheidung zwischen einer „Open Access“ (o) und „nicht Open Access“ (ø) Publikation darstellen. Tabelle 1.4 stellt die Parametrisierung der Auszahlungsmatrix des zugrundeliegenden symmetrischen (2 Personen)-(2 Strategien) Spiels dar. Der Parameter r bezeichnet den Reputationszuwachs der Autoren durch die Veröffentlichung ihres neuen Artikels, der Parameter δ stellt einen zusätzlichen Gewinn dar, falls beide Autoren die „Open Access“-Strategie wählen (größere Nutzung und erhöhte Zitation der Artikel). Die Parameter α und β stellen den Reputationsverlust bzw. Reputationsgewinn dar, falls einer der Autoren die „Open Access“-Strategie wählt, der andere sich jedoch dagegen entscheidet. Die Spielklasse determinierenden Parameter a und b hängen wie folgt von den Auszahlungsparametern ab: $a = \delta - \beta$ und $b = \alpha$. Durch die Wahl des Ansatzes der in Tabelle 1.4 definierten Auszahlungsmatrix ist ein Anti-Koordinationsspiel nicht möglich ($b = \alpha > 0$). Für $\delta > \beta$ gehört das Spiel der Klasse der Koordinationsspiele an, wohingegen für $\delta < \beta$ die Struktur eines dominanten Spiels mit Dilemma vorliegt.

Der erste Artikel dieser kumulativen Dissertation betrachtet die quantentheo-

retische Erweiterung des symmetrischen (2 Personen)-(2 Strategien) „Open Access“-Spiels anhand von drei Beispielen. Die ersten beiden Beispiele gehören der Klasse der dominanten Spiele mit Dilemma an, wobei das erste Spiel ein Nullsummenspiel ist ($r = 0$, $\delta = 0$ und $\alpha = \beta = 1$) und das zweite Spiel einem Gefangenendilemma entspricht ($r = 3$, $\delta = 1$ und $\alpha = \beta = 2$). Das dritte Beispiel ($r = 3$, $\delta = 1$, $\alpha = 2$ und $\beta = 0$) dagegen entspricht einem Hirschjagd Spiel, welches der Klasse der Koordinationsspiele zuzuordnen ist. Die in Unterkapitel 1.2.5 dargestellten Ergebnisse der quantentheoretischen Erweiterung der dominanten Spiele mit Dilemma (Set_A) und der Klasse der Koordinationsspiele (Set_B) können auf das „Open Access“-Publikationsspiel angewendet werden. Im dominanten Nullsummenspiel berechnen sich die beiden γ-Barrieren zu $\gamma_1 = \gamma_2 = \frac{\pi}{4}$, im „Open Access“-Gefangenendilemma ergeben sich die Werte $\gamma_1 = 2 \arctan\left(\frac{\sqrt{3}-1}{\sqrt{3}+1}\right)$ und $\gamma_2 = \frac{\pi}{4}$ und im „Open Access“-Hirschjagdspiel berechnet man $\gamma_1 = \frac{\pi}{2}$ und $\gamma_2 = 0$. Das betrachtete Hirschjagd Spiel stellt demnach ein spezielles Koordinationsspiel dar, bei dem die γ-Kooperationsbarriere erst beim maximal möglichen Wert $\gamma = \frac{\pi}{2}$ erreicht wird.

Der erste Artikel betrachtet die Forschungsfrage, warum lediglich in einigen wissenschaftlichen Teilcommunities das „Open Access“-Modell erfolgreich angewendet wird. Das zugrundeliegende klassische spieltheoretische Modell, welches formal mittels der in Tabelle 1.4 definierten Auszahlungsmatrix beschrieben ist, wird anhand von drei Parametersätzen diskutiert und es wird hierbei aufgezeigt, dass sich die Wissenschaftler in der klassischen Version des Spiels in einem Dilemma befinden. In der quantentheoretische Erweiterung des „Open Access“-Publikationsspiels können die Wissenschaftler diesem Dilemma jedoch entkommen, falls der Wert ihrer Strategienverschränkung oberhalb des definierten Grenzwertes liegt. Die Resultate des Artikels liefern demnach eine mögliche Erklärung warum die Autoren in einigen wissenschaftlichen Teilcommunities (z.B. Physik) „Open Access“ publizieren. Die Verschränkung der Publikationsstrategien von Autoren in ausschließlich traditionell publizierenden Teilcommunities befindet sich dagegen unterhalb der definierten γ-Kooperationsbarriere, so dass diese weiterhin im klassischen Nash-Gleichgewicht (ø,ø) gefangen sind.

Zweiter Artikel: Evolutionäre Quanten-Spieltheorie und wissenschaftliche Kommunikation (Evolutionary Quantum Game Theory and Scientific Communication)

Der zweite Artikel dieser kumulativen Dissertation betrachtet ebenfalls das „Open Access"-Publikationsspiel, erweitert die Beschreibung jedoch durch einen evolutionären spieltheoretischen Kontext. Die zugrundeliegende Auszahlungsmatrix des Spiels ist wiederum durch Tabelle 1.4 gegeben, wobei jedoch die folgende zusätzliche Bedingung angenommen wird: $\alpha \equiv \beta < \delta$. Aufgrund dieser zusätzlichen Bedingung gehört das betrachtete „Open Access"-Spiel der Klasse der Koordinationsspiele an ($a = \delta - \alpha > 0$ und $b = \alpha > 0$). Die Ergebnisse des klassischen evolutionären Spiels, als auch dessen quantentheoretische Erweiterung, werden anhand eines gewählten Parametersatzes ($r = 5, \delta = 3$ und $\alpha = 2$) illustriert. Es wird gezeigt, dass ab einer definierten γ-Barriere ($\gamma_1 = \frac{\pi}{4}$), das klassische evolutionär stabile Gleichgewicht mit geringer Reputationsauszahlung (ø,ø) verschwindet und für $\gamma > \frac{\pi}{4}$ die wissenschaftliche Gemeinschaft einer einzigen evolutionär stabilen Strategie zustrebt, die dann, projiziert auf die reelle Achse, dem Nash-Gleichgewicht (o,o) entspricht.

Fünfter Artikel: Evolutionäre Quanten-Spieltheorie und komplexe Netzwerke wissenschaftlicher Informationen (Evolutionary Game Theory and Complex Networks of Scientific Information)

Im fünften Artikel dieser kumulativen Dissertation werden zunächst die Ergebnisse der klassischen Spiele des „Introductory Papers" und die klassischen Resultate der ersten beiden Artikel zusammengefasst. Als zusätzliche Anwendung wird das klassische Bimatrixspiel des interagierenden Netzwerks, bestehend aus wissenschaftlichen Journalen und Autoren diskutiert. Die Spieler der betrachteten Teilpopulationen sind die Autoren wissenschaftlicher Artikel (Teilpopulation A) und die wissenschaftlichen Journale (Teilpopulation B). Die Wissenschaftler besitzen wiederum die Strategiemöglichkeiten $\{s_1^A, s_2^A\} = \{o,ø\} \hat{=} \{$*„Open Access"-Veröffentlichung*, *Traditionelle Veröffentlichung*$\}$, wobei die Journale die folgenden reinen Strategien besitzen: $\{s_1^B, s_2^B\} = \{o,ø\} \hat{=} \{$*„Open Access" akzeptieren*, *„Open Access" nicht akzeptieren*$\}$. Der Ansatz der Auszahlungsmatrix des Spiels ist in

der folgenden Tabelle zusammengefasst.

A\B	o	ø
o	$(r+\delta+I \ , \ r-\kappa)$	$(r+\delta \ , \ 0)$
ø	$(r+I \ , \ r)$	$(r-P+I \ , \ r+P)$

Tabelle 1.5.: Allgemeine Auszahlungsmatrix des „Autoren(A)-Journal(B)“ „Open Access“-Bimatrixspiels.

Wie in den beiden ersten Artikeln, bezeichnet der Parameter r den Reputationszuwachs der Autoren durch die Veröffentlichung ihres neuen Artikels und der Parameter δ stellt einen zusätzlichen Gewinn dar, falls beide Autoren die „Open Access“-Strategie o wählen. Der Parameter I bezeichnet den zusätzlichen Reputationszuwachs für die Autoren, wenn diese ihren Artikel in dem wissenschaftlichen Journal veröffentlichen können, und kann somit z.B. als der „Impakt Faktor“ des Journals interpretiert werden. Der Parameter κ quantifiziert die hypothetische Auszahlungsminderung (Gewinneinbußen) der Journale, die in einem Markt entstehen können, der die „Grüne Open Access“-Strategie vollkommen implementiert hat, und der Parameter P bezeichnet die Auszahlungserhöhung der Journale, die durch eine ungewöhnlich hohe Preissteigerung in einem vollkommen traditionellen Markt verursacht werden kann.

Im Artikel fünf dieser Dissertation wird gezeigt, dass durch den Ansatz der Auszahlungsmatrix (siehe Tabelle 1.5) nur zwei der drei möglichen Hauptklassen von Bimatrixspielen möglich sind. Die Klasse der Zentrumsspiele ist im vorliegenden „Autoren-Journal Open Access“-Bimatrixspiel nicht möglich, da die die Spielklasse bestimmenden Parameter wie folgt von den Auszahlungsparametern abhängen: $a^A = \delta \geq 0$, $b^A = I - P - \delta$, $a^B = r - \kappa$ und $b^B = P \geq 0$. Für $b^A, a^B > 0$ ($r > \kappa, I > P + \delta$) gehört das Spiel der Klasse der Sattelspiele an und besitzt zwei reine, symmetrische Nash-Gleichgewichte ($(s_1^A, s_1^B) \hat{=}$(o,o) and $(s_2^A, s_2^B) \hat{=}$(ø,ø)) und ein internes Nash-Gleichgewicht in gemischten Strategien ($(\tilde{s}^{A\star}, \tilde{s}^{B\star}) = (\frac{P}{r-\kappa+P}, \frac{I-P-\delta}{I-P})$). Die Eigenschaften eines solchen Spiels entsprechen dem im Unterkapitel 1.2.5 diskutierten Bimatrixspiels (Parametersatz Set_7^{us}). Alle anderen Parameterkonstellationen gehören der Klasse der Eckenspiele an. Für ($b^A < 0$ and $a^B > 0$) ergibt sich das alleinige Nash-Gleichgewicht (o,o),

für ($b^A > 0$ und $a^B < 0$) ergeben sich Eckenspiele, die in (ø,ø) enden, und für ($a^B, b^A < 0$) existiert das unsymmetrische Nash-Gleichgewicht (o,ø). Eine quantentheoretische Erweiterung wurde im fünften Artikel nicht dargestellt, diese kann jedoch, wie im Unterkapitel 1.2.5 beschrieben, auf die jeweiligen Teilspiele zurückgeführt werden.

Dritter Artikel: Neue Erkenntnisse im Falke-Taube Spiel: *Eine auf quantenspieltheoretischen Konzepten basierende Analyse der Finanzkrise* (Doves and hawks in economics revisited: *An evolutionary quantum game theory-based analysis of financial crises*)

Die Spieler der betrachteten Population sind nun Investmentbanker, wobei diese die folgenden zwei reinen Strategien besitzen. Die „Falke"-Strategie stellt eine aggressive Verkaufsstrategie dar. Investmentbanker, die diese Strategie wählen, verkaufen sehr risikovolle Produkte mit einem hohen Gewinn. Die „Taube"-Strategie dagegen stellt eine nicht-aggressive Strategie dar, in welcher die verkauften Produkte einen moderaten Gewinn bei niedrigem Risiko versprechen. In jeder Spielrunde kämpfen zwei Investmentbanker um einen Investor. Die Auszahlungsmatrix des zugrundeliegenden symmetrischen (2 Personen)-(2 Strategien) Spiels wurde wie folgt parametrisiert:

A\B	Falke	Taube
Falke	$(\frac{p_h-d}{2}, \frac{p_h-d}{2})$	$(p_h,0)$
Taube	$(0,p_h)$	$(\frac{p_m}{2}, \frac{p_m}{2})$

Tabelle 1.6.: Auszahlungsmatrix der Investmentbanker A und B im Falke-Taube Spiel.

Der Parameter p_h bezeichnet die hohe Gewinnauszahlung bei Wahl der „Falke"-Strategie, der Parameter p_m bezeichnet den moderaten Gewinn bei Wahl der „Taube"-Strategie und der Parameter d beschreibt den absoluten Betrag des negativen Auszahlungswerts, der in einer Kampfsituation zweier „Falken"-Investmentbanker entsteht. Um die formale Struktur eines Falke-Taube Spiels zu garantieren, wurde die folgende zusätzliche Bedingung gefordert: $p_h > p_m > 0 > \frac{p_h-d}{2}$.

Die Spielklasse bestimmenden Parameter des zugrundeliegenden Falke-Taube Spiels ($a = \frac{p_h - d}{2} < 0$ und $b = \frac{p_m - p_h + d}{2} < 0$) sind beide negativ, so dass es sich um ein Anti-Koordinationsspiel handelt. Das klassische Spiel besitzt somit zwei unsymmetrische reine Nash-Gleichgewichte ($(s_1^A, s_2^B) \hat{=} (\tilde{s}^A = 1, \tilde{s}^B = 0) \hat{=}$(Falke,Taube)) und $(s_2^A, s_1^B) \hat{=} (\tilde{s}^A = 0, \tilde{s}^B = 1) \hat{=}$(Taube,Falke)) und ein internes Nash-Gleichgewicht bei der gemischten Strategienkombination $((\tilde{s}^{A\star}, \tilde{s}^{B\star}) = (\frac{p_m - 2p_h}{p_m - p_h - d}, \frac{p_m - 2p_h}{p_m - p_h - d}))$.

Im dritten Artikel werden zunächst die Resultate des klassischen evolutionären spieltheoretischen Modells anhand von drei Parametrisierungen diskutiert und dann die quantentheoretische Erweiterung vollzogen. Die diskutierten Ergebnisse sind vergleichbar mit dem in Unterkapitel 1.2.5 besprochenen Parametersatz Set_C, wobei zusätzlich auf die Unterschiede von s_1-(Falken) und s_2-(Tauben) Quantenstrategien eingegangen wird. Desweiteren wird bewiesen, dass es sich bei dem, bei hohen Verschränkungswerten auftretendem Quanten Nash-Gleichgewicht, um eine evolutionär stabile Strategie handelt. Die Population der Investmentbanker kann somit bei hohen strategischen Verschränkungswerten in einem Gleichgewichtszustand enden, bei dem alle beteiligten Spieler eine nicht-aggressive „Taube“-Strategie wählen.

Vierter Artikel: Experimentelle Bestätigung der Quanten-Spieltheorie (Experimental Validation of Quantum Game Theory)

Im vierten Artikel dieser kumulativen Dissertation werden die quantenspieltheoretischen Vorhersagen mit den Werten aus zwei experimentellen Studien (siehe [34, 25]) verglichen. Die übernommenen Resultate aus beiden experimentellen Studien stellen den durchschnittlichen Anteil an kooperierenden Spielern C_p in einem wiederholt durchgeführten Gefangenendilemma Spiel dar. Beide Studien benutzten unterschiedliche Auszahlungsparametrisierungen von Gefangenendilemma Spielen und unterschiedliche Werte der Abbruchswahrscheinlichkeit des Spiels. Für jede der experimentell realisierten Auszahlungsparametrisierungen wurden die entsprechenden γ-Barrieren (γ_1 und γ_2) berechnet. Zusätzlich zu diesen quantentheoretischen Kooperationsindikatoren wurden zwei weitere Größen definiert und für jede Parametrisierung berechnet. γ_*, der erste neu definierte quantentheoretischen Kooperationsindikator stellt die Nullstelle einer Funktion

$\mathcal{N}(\gamma)$ dar, die die Vorteilhaftigkeit der Quantenstrategie gegenüber der Nicht-Kooperationsstrategie im Gefangenendilemma quantifiziert. $\mathcal{N}$, der zweite neu definierte Quanten-Kooperationsindikator, berechnet sich durch das Integral der Funktion über den gesamten möglichen Verschränkungsbereich. Der vierte Artikel definiert zunächst diese vier quantentheoretischen Kooperationsindikatoren und vergleicht diese mit klassischen Kooperationsindikatoren. Danach werden die experimentellen Befunde der unterschiedlichen Gefangenendilemma Spiele mit den quantenspieltheoretischen Vorhersagen verglichen. Es zeigt sich, dass mittels der Quanten-Spieltheorie die experimentell ermittelten Kooperationsanteile C_p gut beschrieben werden können.

1.3. Zusammenfassung und Ausblick

Die vorliegende kumulative Dissertation stellt eine Erweiterung der klassischen Theorie der Gesellschaftsspiele dar. Sie liefert einen zusammenfassenden Überblick der Spieltheorie auf quantentheoretischen, abstrakten Hilbertschen Räumen. Die quantentheoretischen Vorhersagen unterschiedlicher Spielklassen werden berechnet, und im Detail, anhand von mehreren exemplarischen Beispielen, diskutiert. Neben diesem theoretischen Überblick werden unterschiedliche Anwendungsbeispiele der Quanten-Spieltheorie vorgestellt und innerhalb der beigefügten fünf Artikel diskutiert.

Die dargestellte quantenspieltheoretische Beschreibung liefert ein mathematisches Grundgerüst für eine enorme Fülle an aufbauenden Forschungsvorhaben, die sowohl für die Wissenschaft als auch für die Praxis von großem Wert sein können. Aufgrund der im „Introductory Paper“ benutzten allgemeinen Formulierung, ist es möglich, die zugrundeliegenden, konstruierten Computerprogramme ohne weitere Umstände auf jedes evolutionäre (2 Personen)-(2 Strategien) Spiel auszudehnen. Die aktuell laufenden Berechnungen konzentrieren sich inhaltlich auf die Evolution sozialer Normen in Firmen [115] und die Entwicklung von Hubs- und Spokes Netzwerken innerhalb der Unternehmenssoftwarebranche [113]. Eine Verknüpfung der Theorie der komplexen Netzwerke mit der evolutionären Quanten-Spieltheorie stellt ein vielversprechendes mathematisches Modell dar, welches sowohl der interdisziplinären Grundlagenforschung, als auch der angewandten empirischen

Netzwerkforschung dienen kann.

2. Introductory Paper: Evolutionary Quantum Game Theory

2.1. Introduction

Starting a review article about "Evolutionary Quantum Game Theory" (EQGT) is not an easy task. Several concepts of different scientific disciplines are together combined in one single model, which is from now on called EQGT. The classical[1] version of this model is known as "Evolutionary Game Theory" (EGT). EGT is a time dependent dynamical extension of "Game Theory" (GT), which itself is a mathematical toolbox to explain interdependent decision processes happening in biological or socio-economic systems. "Quantum Game Theory" (QGT), which is an amplification of GT uses mathematical models developed in "Quantum Theory" (QT). This review article might have been started from the physical perspective, explaining the conceptual framework of QT—however, as this article is used as a summary paper of a cumulative PhD thesis, submitted to the economic department of the *Johann Wolfgang Goethe University*, it begins with classical GT.

In 1928 the main inventor of GT—Johann (John) von Neumann—published the first article on GT [234]. The first book about GT was published in 1944 by von Neumann and Morgenstern [233]. EGT (see e.g. [216, 213, 214, 198, 166, 222, 198, 21, 108] was developed after J.M. Smith had found that the stationary solutions of the evolutionary differential equations are connected with game theory [212]. In the following years applications in respect to biological

[1] Following the scientific classification of the physical literature, the notation "classical" is used to describe the scientific sub discipline that do not use "quantum" concepts to describe the underlying natural processes (example in physics: *Classical Mechanics* vs. *Quantum Mechanics*).

[209, 226, 148, 78, 171, 172] and socio-economic systems, e.g. "public good"-games [51], cultural or moral developments [68, 121], the evolution of languages [177], social learning [68], the evolution of social norms [23, 175], the financial crisis [114] and the evolution of social networks [222, 139, 67] came into the focus of research. In 1999 the first two articles on quantum games where published [165, 66]. In 2001 the first quantum game was realized on a quantum computer [62] (see also [190]). The extension to more than two players [28], the application to social networks [178, 111], social experiments [49, 176, 112] and first approaches towards an EQGT [169, 95, 114][2] followed.

Within this article *Evolutionary Quantum Game Theory* the framework of EGT is described in detail. After a general introduction and a brief literature review, the groundings of GT (section 2.2) and EGT (section 2.3) are explained in detail. The formal mathematical model, the different concepts of equilibria and the various classes of evolutionary games will be defined, explained and visualized to understand the main ideas of EGT.

QGT is a mathematical and conceptual amplification of classical game theory. The space of all conceivable decision paths is extended from the purely rational, measurable space in the Hilbertspace of complex numbers. Through the concept of a potential entanglement of the imaginary quantum strategy parts, it is possible to include corporate decision path, caused by cultural or moral standards. If this strategy entanglement is large enough, then, additional Nash equilibria can occur, previously present dominant strategies could become nonexistent and new evolutionary stable strategies might appear.

This article summarizes the main results of classical and quantum game theory and focuses on the different game categories of (2 player)-(2 strategy) evolutionary games. After a general introduction into quantum game theory (see section 2.4), the formal mathematical model is explained and visualized. Additionally, in section 2.6 five different applications are discussed (the underlying five papers of these applications are attached to this article).

- Article 1: Quantum Game Theory and Open Access Publishing (see subsection 2.6.1)

[2] — which is mathematically, most likely formulated with the use of the *von Neumann equation* —

- Article 2: Evolutionary Quantum Game Theory and Scientific Communication (see subsection 2.6.2)
- Article 3: Doves and hawks in economics revisited: *An evolutionary quantum game theory-based analysis of financial crises* (see subsection 2.6.3)
- Article 4: Experimental Validation of Quantum Game Theory (see subsection 2.6.4)
- Article 5: Evolutionary Quantum Game Theory and Complex Networks of Scientific Information (see subsection 2.6.5)

Section 2.7 finally summarizes the main outcomes of this article.

All the materials presented within this chapter are mainly based on a lecture the author had given in the year 2009 in Lyon ("Advances in evolutionary game theory", `http://evolution.wiwi.uni-frankfurt.de/Lyon2009/`), published works/working papers [118, 119, 114, 112, 111] and on several conference talks [103, 106, 105, 107, 104, 102].

2.2. Classical Game Theory

2.2.1. Introduction

This section is dedicated to introduce the necessary definitions and fundamental basics of classical GT. The main part of this section (subsection 2.2.2) deals with the mathematical description of GT, however this introduction explains the use of these game theoretical concepts with one simple example:

Two persons (Emma and Hans) have to make a decision. Each of them has to choose between two possible actions. For both of them it is an important decision, as they might get a great benefit (or a punishment) if they choose the "right" (or "wrong") decision. The amount of the potential benefit depends on the decisions of both persons and not only on the action of one. Unfortunately they do not have any possibility to communicate with the other one to coordinate their actions.

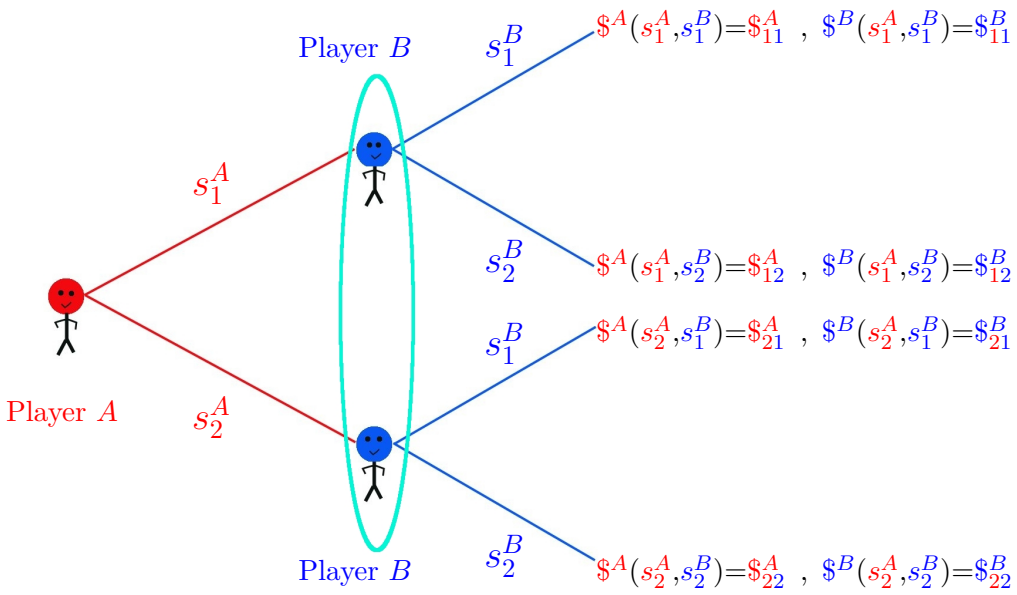

Figure 2.1.: Game tree of a (2 person)-(2 strategy) game with payoff for player A ($\$^A$) and player B ($\$^B$).

GT is a mathematical concept to analyze such decision states. Every quantitative mathematical model, which tries to explain processes happening in nature, begins with a definition of the necessary parameters. In the following, the parameter A or B (later also μ) will be used to describe a person, a player, a decision maker or even a firm or an animal. In the above example the parameter A means "Emma" and the parameter B means "Hans". The parameter $\mathcal{S}^A$ will be used to describe the set of possible strategies (actions) available to Emma, whereas $\mathcal{S}^B$ describes the set of available actions of player "Hans". In the above example this would be written as $\mathcal{S}^A = \left\{s_1^A, s_2^A\right\}$, as Emma can only choose between two possible actions, namely strategy one (s_1^A) and strategy two (s_2^A). The strategy space of Hans is written in a similar form: $\mathcal{S}^B = \left\{s_1^B, s_2^B\right\}$. The parameter \$ is used to quantify the potential benefit (or the amount of punishment) given to the persons after they had announced their final decisions.

GT, in its classical version, does not focus on the specific stories of the underlying game, but gives a mathematical framework to analyze and predict the game outcomes. Nevertheless, to introduce the concepts of GT, a specific story is chosen within this article:

Emma (Player A) is separated from Hans (Player B) and they do not have any possibility to communicate. Both have to make a binary decision. The binary decision could be "To stay" or "To go", or it could be simply to choose between two strategies (e.g. $(\{buy, don't\, buy\},\ \{left, right\},\ (\{above, below\},\ \{s_1, s_2\})$. The benefit if both choose the strategy s_1 is very good for both of them and the parameter $\$_{11}$ is used in the following to quantify this benefit. If Emma and Hans choose the strategy s_2, it will be bad for both of them and the parameter $\$_{22}$ quantifies the value of punishment for both of them. If Emma decides to stay (s_1^A) and Hans goes, the outcome for Hans will be even slightly better than the situation for him if both stay ($\$_{11}^B < \$_{12}^B$); the same holds true for Emma: ($\$_{11}^A < \$_{21}^A$). However if Emma chooses the strategy s_2^A and Hans stays (strategy s_1^A), the outcome for Hans will be extremely bad ($\$_{21}^B << \$_{22}^B$); the same holds true for Emma: ($\$_{12}^A << \$_{22}^A$).

GT analyses such decision states, using mathematically defined equilibrium concepts. The most famous concept of this kind is called the "Nash equilibrium" (NE). As player B does not know for sure what player A will do, he starts to think what would be the best for him, if player A chose the strategy s_1^A (staying): *"It would be good for me, if player A stays and I stay, but in this case, it would be even better for me to go."*. After remaining a moment at this thought, player B starts to think in the other direction: *"If player A goes and I stay, it will be extremely bad for me—it is really advisable for me to go!"*. Within the framework of classical GT, the predicted outcome of this example is, that both players decide to go. In the language of game theory, the strategy s_2 is the only NE of this example, and as the game is a (two player)-(two strategy)-normal form game, s_2 is even a dominant strategy. To be more precise:

The strategy combination (s_2^A, s_2^B) is a Nash equilibrium, because:

$$\text{Nash equilibrium at } (s_2^A, s_2^B): \tag{2.1}$$
$$\$^A(s_2^A, s_2^B) = \$_{22}^A \ \geq\ \$^A(s^A, s_2^B) \quad \forall\ s^A \in \mathcal{S}^A = \left\{s_1^A, s_2^A\right\}$$
$$\$^B(s_2^A, s_2^B) = \$_{12}^B \ \geq\ \$^B(s_2^A, s^B) \quad \forall\ s^B \in \mathcal{S}^B = \left\{s_1^B, s_2^B\right\}$$

The tragedy of this game is, that after both players had made their decision, they are in a worse situation than when they had chosen the strategy s_1 ($\$_{22}^A < \$_{11}^A$

and $\$^B_{22} < \$^B_{11}$).

The attentive reader has certainly noticed, that the real outcome of the example might also depend on further characteristics of the specific story of the game. Who is Emma, who is Hans, where are they, why are they in such a decision state, what is the history of the game, ... The most obvious difference between QGT and classical GT is that there is one additional specific parameter in QGT. QGT in-cooperates specific factors of the underlying story and affiliates them into a new parameter called γ. In QGT players may cooperate, depending on the degree of strategic entanglement (γ) among players [119]. The meaning of γ will be explained within section 2.4, whereas classical GT is discussed in the following.

2.2.2. Definition and key aspects of classical game theory

As the variety of different concepts in GT is very large and the article is not meant to summarize only classical GT, the presented game theoretical concepts of this article will only focus on "strategic form (normal form) games"[3] and it do not discuss "extensive-form games" nor "cooperative games". In the following, the formal framework of the mixed extension of a (N player)-(m strategy) game

[3]The category of "strategic form games" is often also called "non-cooperative games".

in strategic form will be defined:

N-person game: (2.2)

$$\Gamma := \left(\mathcal{I}, \tilde{\mathcal{S}}, \tilde{\$}\right)$$

Set of players:

$$\mathcal{I} = \{1, 2, ..., N\}$$

Pure strategy space:

$$\mathcal{S} = \mathcal{S}^1 \times \mathcal{S}^2 \times ... \times \mathcal{S}^N$$

Pure strategy space of player $\mu \in \mathcal{I}$:

$$\mathcal{S}^\mu = \left\{(s_1^\mu, s_2^\mu, ..., s_{m_\mu}^\mu)\right\}$$

Mixed strategy space:

$$\tilde{\mathcal{S}} = \tilde{\mathcal{S}}^1 \times \tilde{\mathcal{S}}^2 \times ... \times \tilde{\mathcal{S}}^N$$

Mixed strategy space of player $\mu \in \mathcal{I}$:

$$\tilde{\mathcal{S}}^\mu = \left\{(\tilde{s}_1^\mu, \tilde{s}_2^\mu, ..., \tilde{s}_{m_\mu}^\mu) \mid \sum_{i=1}^{m_\mu} \tilde{s}_i^\mu = 1, \tilde{s}_i^\mu \geq 0, i = 1, 2, ..., m_\mu\right\}$$

Number of strategies available for player $\mu \in \mathcal{I}$:

$$m_\mu$$

Mixed strategy profile of player $\mu \in \mathcal{I}$:

$$\tilde{s}^\mu = \left(\tilde{s}_1^\mu, \tilde{s}_2^\mu, ..., \tilde{s}_{m_\mu}^\mu\right)^T \in \tilde{\mathcal{S}}^\mu$$

Vector function of mixed payoffs:

$$\tilde{\$} = \left(\tilde{\$}^1, \tilde{\$}^2, ..., \tilde{\$}^N\right) : \tilde{\mathcal{S}} \to \mathbb{R}^N$$

Mixed payoff for player $\mu \in \mathcal{I}$:

$$\tilde{\$}^\mu(\tilde{s}^1, \tilde{s}^2, ..., \tilde{s}^N) = \sum_{i_1=1}^{m_1} \sum_{i_2=1}^{m_2} ... \sum_{i_N=1}^{m_N} \$^\mu(s_{i_1}^1, s_{i_2}^2, ..., s_{i_N}^N) \prod_{\nu=1}^{N} \tilde{s}_{i_\nu}^\nu$$

For two person games ($N = 2$) the definition (2.2) reduces to:

Two person game: (2.3)

$$\Gamma := \left(\mathcal{I}, \tilde{\mathcal{S}}, \tilde{\$}\right)$$

Set of players:

$$\mathcal{I} = \{1, 2\} \hat{=} \{A, B\}$$

Pure strategy space:

$$\mathcal{S} = \mathcal{S}^A \times \mathcal{S}^B$$

Pure strategy space of player $\mu \in \mathcal{I}$:

$$\mathcal{S}^\mu = \left\{(s_1^\mu, s_2^\mu, ..., s_{m_\mu}^\mu)\right\}$$

Mixed strategy space:

$$\tilde{\mathcal{S}} = \tilde{\mathcal{S}}^A \times \tilde{\mathcal{S}}^B$$

Mixed strategy space of player $\mu \in \mathcal{I}$:

$$\tilde{\mathcal{S}}^\mu = \left\{(\tilde{s}_1^\mu, \tilde{s}_2^\mu, ..., \tilde{s}_{m_\mu}^\mu) \mid \sum_{i=1}^{m_\mu} \tilde{s}_i^\mu = 1, \tilde{s}_i^\mu \geq 0, i = 1, 2, ..., m_\mu\right\}$$

Number of strategies available for player A, B:

$$m_A\,,\ m_B$$

Mixed strategy profile of player $\mu \in \mathcal{I}$:

$$\tilde{s}^\mu = \left(\tilde{s}_1^\mu, \tilde{s}_2^\mu, ..., \tilde{s}_{m_\mu}^\mu\right)^T \in \tilde{\mathcal{S}}^\mu$$

Vector function of mixed payoffs:

$$\tilde{\$} = \left(\tilde{\$}^1, \tilde{\$}^2\right) : \tilde{\mathcal{S}} \to \mathbb{R}^2$$

Mixed payoff for player $\mu \in \mathcal{I}$:

$$\tilde{\$}^\mu(\tilde{s}^A, \tilde{s}^B) = \sum_{i_A=1}^{m_A} \sum_{i_B=1}^{m_B} \$^\mu(s_{i_A}^A, s_{i_B}^B) \prod_{\nu=A}^{B} \tilde{s}_{i_\nu}^\nu$$

Using the components of the two payoff matrices ($\hat{\$}^A$ and $\hat{\$}^A$)

$$\hat{\$}^A = \begin{pmatrix} \$^A_{11} & \$^A_{12} & ... & \$^A_{1m_B} \\ \$^A_{21} & \$^A_{22} & ... & \$^A_{2m_B} \\ ... & ... & ... & ... \\ \$^A_{m_A1} & \$^A_{m_A2} & ... & \$^A_{m_Am_B} \end{pmatrix} \quad : \text{Payoff matrices of player A} \tag{2.4}$$

$$\hat{\$}^B = \begin{pmatrix} \$^B_{11} & \$^B_{12} & ... & \$^B_{1m_B} \\ \$^B_{21} & \$^B_{22} & ... & \$^B_{2m_B} \\ ... & ... & ... & ... \\ \$^B_{m_A1} & \$^B_{m_A2} & ... & \$^B_{m_Am_B} \end{pmatrix} \quad : \text{Payoff matrices of player B}$$

$$\$^\mu_{ij} := \$^\mu(s^A_i, s^B_j) \quad : \text{Components of the payoff matrices}$$

the mixed payoffs of player A and player B can be formulated as follows

$$\tilde{\$}^A(\tilde{s}^A, \tilde{s}^B) = (\tilde{s}^A)^T \hat{\$}^A \tilde{s}^B \quad , \quad \tilde{\$}^B(\tilde{s}^A, \tilde{s}^B) = (\tilde{s}^A)^T \hat{\$}^B \tilde{s}^B \quad .$$

For $m_A = m_B = 2$ the equation reduces to the following explicit formulation:

$$\begin{aligned} \tilde{\$}^A(\tilde{s}^A, \tilde{s}^B) &= (\tilde{s}^A)^T \hat{\$}^A \tilde{s}^B = \left(\tilde{s}^A_1, \tilde{s}^A_2\right) \begin{pmatrix} \$^A_{11}\tilde{s}^B_1 + \$^A_{12}\tilde{s}^B_2 \\ \$^A_{21}\tilde{s}^B_1 + \$^A_{22}\tilde{s}^B_2 \end{pmatrix} = \\ &= \$^A_{11}\tilde{s}^B_1\tilde{s}^A_1 + \$^A_{12}\tilde{s}^B_2\tilde{s}^A_1 + \$^A_{21}\tilde{s}^B_1\tilde{s}^A_2 + \$^A_{22}\tilde{s}^B_2\tilde{s}^A_2 \\ \tilde{\$}^B(\tilde{s}^A, \tilde{s}^B) &= (\tilde{s}^A)^T \hat{\$}^B \tilde{s}^B = \left(\tilde{s}^A_1, \tilde{s}^A_2\right) \begin{pmatrix} \$^B_{11}\tilde{s}^B_1 + \$^B_{12}\tilde{s}^B_2 \\ \$^B_{21}\tilde{s}^B_1 + \$^B_{22}\tilde{s}^B_2 \end{pmatrix} = \\ &= \$^B_{11}\tilde{s}^B_1\tilde{s}^A_1 + \$^B_{12}\tilde{s}^B_2\tilde{s}^A_1 + \$^B_{21}\tilde{s}^B_1\tilde{s}^A_2 + \$^B_{22}\tilde{s}^B_2\tilde{s}^A_2 \end{aligned} \tag{2.5}$$

One of the main conceptions of evolutionary game theory is the concept of evolutionary stable strategies (ESS). An ESS can be defined as follows:

Taking a general 2-player game Γ (see definition (2.3)) with payoff matrices $\hat{\$}^A$ and $\hat{\$}^B$. A strategy $(\tilde{s}^{A*}, \tilde{s}^{B*}) \in \tilde{\mathcal{S}}^A \times \tilde{\mathcal{S}}^B$ is defined as an evolutionary stable strategy (ESS) if [198]
a) $(\tilde{s}^{A*}, \tilde{s}^{B*})$ is a Nash equilibrium of the game
b1) $\$^A(\tilde{s}^A, \tilde{s}^B) \leq \$^A((\tilde{s}^{A*}, \tilde{s}^B))$
$\forall\ (\tilde{s}^A, \tilde{s}^B) \in r^A(\tilde{s}^{A*}, \tilde{s}^{B*})\,,\ (\tilde{s}^A, \tilde{s}^B) \neq (\tilde{s}^{A*}, \tilde{s}^{B*})$
b2) $\$^B(\tilde{s}^A, \tilde{s}^B) \leq \$^B((\tilde{s}^A, \tilde{s}^{B*}))$
$\forall\ (\tilde{s}^A, \tilde{s}^B) \in r^B(\tilde{s}^{A*}, \tilde{s}^{B*})\,,\ (\tilde{s}^A, \tilde{s}^B) \neq (\tilde{s}^{A*}, \tilde{s}^{B*})$

$r^A(\tilde{s}^{A*}, \tilde{s}^{B*})$ and $r^B(\tilde{s}^{A*}, \tilde{s}^{B*})$ are the best response functions of player A and player B to the strategy $(\tilde{s}^{A*}, \tilde{s}^{B*})$ and $\$^A(\tilde{s}^A, \tilde{s}^B)$ and $\$^B(\tilde{s}^A, \tilde{s}^B)$ describes the mixed strategy payoff functions of player A and player B. An evolutionary stable strategy $\tilde{s}^* = (\tilde{s}^{A*}, \tilde{s}^{B*})$ therefore needs to be a NE of the game and additionally the inequations b1) and b2) should be fulfilled for any strategy $\tilde{s} = (\tilde{s}^A, \tilde{s}^B)$ belonging to the set of best responses to $(\tilde{s}^{A*}, \tilde{s}^{B*})$.

To be more precise, the following part of the article is constrained to the normal (strategic) form of an unsymmetric (or symmetric) (2 player)-(2 strategy) game Γ (for details see [108, 222]):

$$
\begin{aligned}
(2 \times 2) \text{ game:} \qquad & \Gamma := \left(\{A, B\}, \mathcal{S}^A \times \mathcal{S}^B, \hat{\$}_A, \hat{\$}_B\right) \\
\text{Set of pure strategies of player A and B:} \qquad & \mathcal{S}^A = \left\{s_1^A, s_2^A\right\}\ ,\ \mathcal{S}^B = \left\{s_1^B, s_2^B\right\} \\
\text{Set of mixed strategies of player A and B:} \qquad & \tilde{\mathcal{S}}^A = \left\{\tilde{s}_1^A, \tilde{s}_2^A\right\}\ ,\ \tilde{\mathcal{S}}^B = \left\{\tilde{s}_1^B, \tilde{s}_2^B\right\} \\
\text{Payoff matrix for player A and B:} \qquad & \hat{\$}_A = \begin{pmatrix} \$_{11}^A & \$_{12}^A \\ \$_{21}^A & \$_{22}^A \end{pmatrix} \\
& \hat{\$}_B = \begin{pmatrix} \$_{11}^B & \$_{12}^B \\ \$_{21}^B & \$_{22}^B \end{pmatrix}
\end{aligned} \tag{2.6}
$$

The set of mixed strategies of player A ($\tilde{\mathcal{S}}^A$) and player B ($\tilde{\mathcal{S}}^B$) is a mathematical amplification of the set of pure strategies ($\mathcal{S}^A$ and $\mathcal{S}^B$). The elements belonging to the set of mixed strategies ($\tilde{\mathbf{s}}^\mu = (\tilde{s}_1^\mu, \tilde{s}_2^\mu) \in \mathcal{S}^\mu$) of player $\mu = A, B$ consist of two real numbers ($\tilde{s}_1^\mu \in [0, 1]$ and $\tilde{s}_2^\mu \in [0, 1]$) and can be interpreted as the probability of player μ for choosing the strategy 1 ($\tilde{s}_1^\mu$) or 2 ($\tilde{s}_2^\mu$). For two strategy games the following normalization condition has to be fulfilled: $\tilde{s}_1^\mu + \tilde{s}_2^\mu = 1\ \forall\, \mu = A, B$.

The mixed strategy payoff function of player $\mu = A, B$ has the following structure:

$$\begin{aligned} &\tilde{\$}^{\mu} : \left(\tilde{\mathcal{S}}^{A} \times \tilde{\mathcal{S}}^{B}\right) \to \mathbb{R} \\ &\tilde{\$}^{\mu}((\tilde{s}_1^A, \tilde{s}_2^A), (\tilde{s}_1^B, \tilde{s}_2^B)) = \$_{11}^{\mu}\tilde{s}_1^A\tilde{s}_1^B + \$_{12}^{\mu}\tilde{s}_1^A\tilde{s}_2^B + \$_{21}^{\mu}\tilde{s}_2^A\tilde{s}_1^B + \$_{22}^{\mu}\tilde{s}_2^A\tilde{s}_2^B \end{aligned} \tag{2.7}$$

Due to the normalizing conditions it is possible to simplify the functional dependence of the mixed strategy payoff function

$$\begin{aligned} &\tilde{\$}^{\mu} : ([0,1] \times [0,1]) \to \mathbb{R} \\ &\tilde{\$}^{\mu}(\tilde{s}^A, \tilde{s}^B) = \$_{11}^{\mu}\tilde{s}^A\tilde{s}^B + \$_{12}^{\mu}\tilde{s}^A(1-\tilde{s}^B) + \$_{21}^{\mu}(1-\tilde{s}^A)\tilde{s}^B + \$_{22}^{\mu}(1-\tilde{s}^A)(1-\tilde{s}^B) \end{aligned} \tag{2.8}$$

, where $\tilde{s}^A := \tilde{s}_1^A$, $\tilde{s}^B := \tilde{s}_1^B$, $\tilde{s}_2^A = 1 - \tilde{s}_1^A$ and $\tilde{s}_2^B = 1 - \tilde{s}_1^B$.

In the following, two fundamental equilibrium concepts are defined, namely the *equilibrium in dominant strategies* and the *Nash equilibrium*.

A strategy combination $(\tilde{s}^{A\dagger}, \tilde{s}^{B\dagger})$ is an equilibrium in dominant strategies, if the following conditions are fulfilled:

$$\tilde{\$}^{\mu}(\tilde{s}^{A\dagger}, \tilde{s}^{B\dagger}) \;\geq\; \tilde{\$}^{\mu}(\tilde{s}^A, \tilde{s}^B) \quad \forall \;\; \mu = A, B \,\text{and}\, \tilde{s}^A, \tilde{s}^B \in [0,1] \tag{2.9}$$

A strategy combination $(\tilde{s}^{A*}, \tilde{s}^{B*})$ is called a Nash equilibrium, if:

$$\begin{aligned} \tilde{\$}^{A}(\tilde{s}^{A*}, \tilde{s}^{B*}) \;&\geq\; \tilde{\$}^{A}(\tilde{s}^A, \tilde{s}^{B*}) \quad \forall \;\; \tilde{s}^A \in [0,1] \\ \tilde{\$}^{B}(\tilde{s}^{A*}, \tilde{s}^{B*}) \;&\geq\; \tilde{\$}^{B}(\tilde{s}^{A*}, \tilde{s}^B) \quad \forall \;\; \tilde{s}^B \in [0,1] \end{aligned} \tag{2.10}$$

An interior (mixed strategy) NE $(\tilde{s}^{A\star}, \tilde{s}^{B\star})$ is a special case of condition (2.10), as the partial derivative of the mixed strategy payoff function vanishes at the value of the interior NE:

$$\begin{aligned} \left.\frac{\partial\tilde{\$}^{A}(\tilde{s}^A, \tilde{s}^B)}{\partial\tilde{s}^A}\right|_{\tilde{s}^B=\tilde{s}^{B\star}} &= 0 \quad \forall \;\; \tilde{s}^A \in [0,1] \;\;,\;\; \tilde{s}^{B\star} \in]0,1[\\ \left.\frac{\partial\tilde{\$}^{B}(\tilde{s}^A, \tilde{s}^B)}{\partial\tilde{s}^B}\right|_{\tilde{s}^A=\tilde{s}^{A\star}} &= 0 \quad \forall \;\; \tilde{s}^B \in [0,1] \;\;,\;\; \tilde{s}^{A\star} \in]0,1[\end{aligned} \tag{2.11}$$

2.3. Classical Evolutionary Game Theory

This section is dedicated to the introduction of the necessary definitions and fundamental basics of classical EGT.

2.3.1. Definition and key aspects of classical evolutionary game theory

The defined mathematical constructs of the previous section can be used to analyze one-shot (2×2) games, while the following equations will describe the time evolution of the strategic behavior of a large group of players (population). At each time increment all of the individual players of the population search randomly for a partner to play a (2×2) game. Then, after the persons have chosen their strategies and receive their payoffs they search again for the next game partner. To describe the time evolution of such a repeated version of the game Γ, *replicator dynamics* were developed. As the payoff matrices ($\hat{\$}_A$ and $\hat{\$}_B$) of the two persons playing the game are in general unsymmetric, the whole population of players separates into the two subpopulations "A" and "B". Replicator dynamics, formulated within a system of differential equations, defines in which way the population vector $\vec{x}^{\mu} = (x_1^{\mu}, x_2^{\mu})$ evolves in time. Each component $x_i^{\mu} = x_i^{\mu}(t)$ ($i = 1, 2$ and $\mu = A, B$) describes the time evolution of the fraction of different player types i in the μ-subpopulation, where a type-i player is understood as an actor μ playing strategy s_i^{μ}. Similar to the normalizing condition of the mixed strategies, the two population vectors $\vec{x}^A$ and $\vec{x}^B$ have to fulfill the normalizing conditions of a unity vector

$$x_i^{\mu}(t) \geq 0 \quad \text{and} \quad \sum_{i=1}^{2} x_i^{\mu}(t) = 1 \quad \forall\, i = 1, 2\,,\ t \in \mathbb{R},\ \mu = A, B. \tag{2.12}$$

The structure of the time evolution of the components of the two population vectors $\vec{x}^A(t) = (x_1^A(t), x_2^A(t)$ and $\vec{x}^B(t) = (x_1^B(t), x_2^B(t))$ is formulated through a system of differential equations, known as the equation of *Replicator Dynamics*

[21, 198, 166, 108, 222]:

$$\begin{aligned}
\frac{dx_i^A(t)}{dt} &= x_i^A(t)\left[\sum_{l=1}^{2} \$_{il}^A\, x_l^B(t) - \sum_{l=1}^{2}\sum_{k=1}^{2} \$_{kl}^A\, x_k^A(t)\, x_l^B(t)\right] \\
\frac{dx_i^B(t)}{dt} &= x_i^B(t)\left[\sum_{l=1}^{2} \$_{li}^B\, x_l^A(t) - \sum_{l=1}^{2}\sum_{k=1}^{2} \$_{lk}^B\, x_l^A(t)\, x_k^B(t)\right]
\end{aligned} \tag{2.13}$$

As the number of available strategies in our approach is restricted to two, it is possible to substitute the second strategy by using condition (2.12): $x_2^A = 1 - x_1^A$ and $x_2^B = 1 - x_1^B$. The system of differential equations (2.13) can therefore be formulated as follows ($x(t) := x_1^A(t)$, $y(t) := x_1^B(t)$):

$$\begin{aligned}
\frac{dx(t)}{dt} &= \left(\$_{11}^A + \$_{22}^A - \$_{12}^A - \$_{21}^A\right)\left(x(t) - (x(t))^2\right) y(t) + \\
&\quad + \left(\$_{12}^A - \$_{22}^A\right)\left(x(t) - (x(t))^2\right) =: g_A(x,y) \\
\frac{dy(t)}{dt} &= \left(\$_{11}^B + \$_{22}^B - \$_{12}^B - \$_{21}^B\right)\left(y(t) - (y(t))^2\right) x(t) + \\
&\quad + \left(\$_{12}^B - \$_{22}^B\right)\left(y(t) - (y(t))^2\right) =: g_B(x,y)
\end{aligned} \tag{2.14}$$

Equation (2.14) describes the time evolution of the strategic behavior of two separate subpopulations playing an unsymmetric bimatrix game. The fraction of players choosing strategy s_1 at time t of the subpopulation "A" is quantified by $x(t)$, whereas $y(t)$ describes the average strategic choice of subpopulation "B". The time evolution of the coupled system of differential equations (2.14) depend on the properties of the two functions $g_A(x,y)$ and $g_B(x,y)$ and on the initial conditions $x(t=0)$ and $y(t=0)$.

By restricting the underlying payoff matrix to be symmetric ($\hat{\$}^A \equiv \left(\hat{\$}^B\right)^T$, $\$_{lk} := \$_{lk}^A = \$_{kl}^B$), the two separate subpopulation (A and B) cannot be distinguished any more and the system of differential equations (2.13) simplifies as follows:

$$\begin{aligned}
\frac{dx_i^A(t)}{dt} &= x_i^A(t)\left[\sum_{l=1}^{2} \$_{il}\, x_l^B(t) - \sum_{l=1}^{2}\sum_{k=1}^{2} \$_{kl}\, x_k^A(t)\, x_l^B(t)\right] \\
\frac{dx_i^B(t)}{dt} &= x_i^B(t)\left[\sum_{l=1}^{2} \$_{il}\, x_l^A(t) - \sum_{l=1}^{2}\sum_{k=1}^{2} \$_{kl}\, x_l^A(t)\, x_k^B(t)\right]
\end{aligned} \tag{2.15}$$

Equation (2.15) indicates, that the mathematical structure of the two population vectors $\vec{x}^A$ and $\vec{x}^B$ are identical, which simply means, that a symmetric evolutionary game can be described by a single population vector $\vec{x} := \vec{x}^A = \vec{x}^B$. The system of differential equations (2.15) reduces therefore to one single equation:

$$\frac{dx_i(t)}{dt} = x_i(t)\left[\underbrace{\sum_{l=1}^{2} \$_{il}\, x_l(t)}_{:=f_i(t)} - \underbrace{\sum_{l=1}^{2}\sum_{k=1}^{2} \$_{kl}\, x_k(t)\, x_l(t)}_{:=\bar{f}(t)}\right] \tag{2.16}$$

where $f_i(t)$ is the fitness of type i and $\bar{f}(t) = \sum_{i=1}^{2} f_i(t)$ is the average fitness of the whole population. Again the overall vector $\vec{x} = (x_1(t), x_2(t))$ has to fulfill the normalizing conditions of a unity vector:

$$x_i(t) \leq 0 \;\; \forall\, i = 1,2 \quad \text{and} \quad \sum_{i=1}^{2} x_i(t) = 1 \;\; \forall\, t \in \mathbb{R} \quad . \tag{2.17}$$

For a symmetric game, equation (2.16) can therefore be simplified as follows:

$$\begin{aligned} \frac{dx}{dt} &= x\Big[\$_{11}(x - x^2) + \$_{12}(1 - 2x + x^2) + \$_{21}(x^2 - x) + \$_{22}(2x - x^2 - 1)\Big] \\ &= x\Big[(\$_{11} - \$_{21})(x - x^2) + (\$_{12} - \$_{22})(1 - 2x + x^2)\Big] =: g(x) \end{aligned} \tag{2.18}$$

with: $\qquad x = x(t) := x_1(t) \quad \rightarrow \quad x_2(t) = (1 - x(t))$

$x(t)$, the fraction of players choosing the strategy s_1 at time t, depends on the function $g(x)$ and on the initial starting value $x(t = 0)$. The stationary solutions of the asymptotic behavior $\lim_{t\to\infty}(x(t))$ depends also on $g(x)$ and on the initial condition and is formalized within the mathematical concept of the *Evolutionary Stable Strategy* (ESS). Taking a general 2-player game Γ with the mixed payoff functions $\tilde{\$}^A$ and $\tilde{\$}^B$. A strategy combination $(\tilde{s}^{A*}, \tilde{s}^{B*}) \in ([0,1] \times [0,1])$ is defined as an (ESS) if

a) $(\tilde{s}^{A*}, \tilde{s}^{B*})$ is a Nash equilibrium of the game

b) $\tilde{\$}^A(\tilde{s}^A, \tilde{s}^B) \leq \tilde{\$}^A(\tilde{s}^{A*}, \tilde{s}^B) \qquad \forall \quad \tilde{s}^A \in r^A(\tilde{s}^{B*})\,, \;\; \tilde{s}^B \neq \tilde{s}^{B*}$
$\tilde{\$}^B(\tilde{s}^A, \tilde{s}^B) \leq \tilde{\$}^B(\tilde{s}^A, \tilde{s}^{B*}) \qquad \forall \quad \tilde{s}^B \in r^B(\tilde{s}^{A*})\,, \;\; \tilde{s}^A \neq \tilde{s}^{A*}$

$r^B(\tilde{s}^A)$ and $r^A(\tilde{s}^B)$ is the best response function of player B and A to the strategy $\tilde{s}^A$ and $\tilde{s}^B$. An ESS $(\tilde{s}^{A*}, \tilde{s}^{B*})$ therefore needs to be a Nash equilibrium of the game and additionally the inequations b) should be fulfilled for any strategy combination $(\tilde{s}^A, \tilde{s}^B)$ belonging to the set of best responses to $(\tilde{s}^{A*}, \tilde{s}^{B*})$.

2.3.2. Classes of evolutionary games

Within this subsection the possible game classes of (2 player)-(2 strategy) games are defined. The first part of this subsection focuses on the game classes of the symmetric version of the game Γ, whereas the second part deals with the bimatrix version of games.

The set of Nash equilibria (see equation (2.20)) and the dynamical behavior of evolutionary games formulated within equation (2.18) are unaffected by positive affine payoff transformations and by additionally added constants, where the strategy choice of the other players are fixed (e.g. see [235] and appendix B.I). In the following the second kind of payoff transformation will be used to transform the payoff matrices in order to classify the underlying games in different categories.

Game classes of the symmetric (2 player)-(2 strategy) games

It is easy to see (details can be found in [235]), that the following payoff matrix describes a Nash-equivalent game of the symmetric version of the game Γ.

A\B	s_1^B	s_2^B
s_1^A	($\$_{11}$,$\$_{11}$)	($\$_{12}$,$\$_{21}$)
s_2^A	($\$_{21}$,$\$_{12}$)	($\$_{22}$,$\$_{22}$)

$\Longrightarrow$

A\B	${}^{Trafo}s_1^B$	${}^{Trafo}s_2^B$
${}^{Trafo}s_1^A$	($\underbrace{\$_{11}-\$_{21}}_{:=a}$,$\underbrace{\$_{11}-\$_{21}}_{:=a}$)	(0,0)
${}^{Trafo}s_2^A$	(0,0)	($\underbrace{\$_{22}-\$_{12}}_{:=b}$,$\underbrace{\$_{22}-\$_{12}}_{:=b}$)

Table 2.1.: Symmetric payoff matrix after payoff transformation.

Following the classification scheme of [235] (see also [222]) only three classes of games are possible, namely the dominant game class, the class of anti-coordination games and the coordination game class. For $a < 0$ and $b > 0$ the game belongs to the class of dominant games, having only one pure Nash equilibrium (s_1^A, s_1^B), which is also the dominant strategy and the only ESS of the game. For $a, b < 0$ the game Γ describes an anti-coordination game, having two pure non-symmetric Nash equilibria $((s_1^A, s_2^B)$ and $(s_2^A, s_1^B))$ and one symmetric interior mixed strategy NE $(\tilde{s}^{A\star}, \tilde{s}^{B\star}) = (\frac{b}{a+b}, \frac{b}{a+b})$, which is the only ESS of the game. For $a, b > 0$ the game belongs to the coordination game class, having two pure symmetric Nash equilibria $((s_1^A, s_1^B)$ and $(s_2^A, s_2^B))$, which are the two possible ESS's and one symmetric interior NE at $(\tilde{s}^{A\star}, \tilde{s}^{B\star}) = (\frac{b}{a+b}, \frac{b}{a+b})$. For $b < 0$ and $a > 0$ the game is again a dominant game, having only one pure NE and ESS at (s_2^A, s_2^B).

Game classes of the unsymmetric model

The following table describes a Nash-equivalent game of the unsymmetric version of the game Γ.

A\B	s_1^B	s_2^B
s_1^A	($\$_{11}^A$,$\$_{11}^B$)	($\$_{12}^A$,$\$_{12}^B$)
s_2^A	($\$_{21}^A$,$\$_{21}^B$)	($\$_{22}^A$,$\$_{22}^B$)

$\Longrightarrow$

A\B	${}^{Trafo}s_1^B$	${}^{Trafo}s_2^B$
${}^{Trafo}s_1^A$	($\underbrace{\$_{11}^A - \$_{21}^A}_{:=a^A}$,$\underbrace{\$_{11}^B - \$_{12}^B}_{:=a^B}$)	(0,0)
${}^{Trafo}s_2^A$	(0,0)	($\underbrace{\$_{22}^A - \$_{12}^A}_{:=b^A}$,$\underbrace{\$_{22}^B - \$_{21}^B}_{:=b^B}$)

Table 2.2.: Unsymmetric payoff matrix after payoff transformation.

Following the bimatrix classification scheme of Cressman (see also [222]) again only three major[4] classes are possible within the unsymmetric version of the game Γ, namely the corner class, the center class and the saddle class. The game belongs to the saddle class if all of the parameters are positive ($a^A, b^A, a^B, b^B > 0$). Saddle Class games have an interior mixed strategy Nash equilibrium at $(\tilde{s}^{A\star}, \tilde{s}^{B\star}) = (\frac{b^B}{a^B+b^B}, \frac{b^A}{a^A+b^A})$ and two pure symmetric Nash equilibria ((s_1^A, s_1^B) and (s_2^A, s_2^B)), which are the two ESS's of the game. For $a^A, b^A > 0$ and $a^B, b^B < 0$ (or $a^A, b^A < 0$ and $a^B, b^B > 0$) the game describes a center class game, having only one NE, the interior mixed strategy NE at $(\tilde{s}^{A\star}, \tilde{s}^{B\star}) = (\frac{b^B}{a^B+b^B}, \frac{b^A}{a^A+b^A})$. Center class games do not have any ESS and the population trajectories are closed cycles. Corner class games exist if the four parameters fulfill the following conditions: $a^A < 0 < b^A, b^B > 0, a^B \neq 0$ (or $a^B < 0 < b^B, b^A > 0, a^A \neq 0$). Such games have only one pure Nash equilibrium (s_2^A, s_2^B) (or (s_1^A, s_1^B)) which is the dominant strategy and the only ESS of the game.

2.3.3. Results for symmetric games

To illustrate these formal results and visualize the outcomes of the different game classes, this section is dedicated to present the numerical simulations

[4]Beside the three major (generic) classes there exist also degenerate cases, where one or more of the parameters a^A, b^A, a^B and b^B are zero (see [222]).

within different parameter settings of symmetric games. The parameter settings Set_1-Set_3 belong to the class of dominant games, parameter settings Set_4-Set_7 belong to the coordination game class

Set	Game class	$\$_{11}$	$\$_{12}$	$\$_{21}$	$\$_{22}$	a	b	Nash equilibria:
Set_1	Dominant Class	5	7	7	10	-2	3	One pure, symmetric Nash equilibrium (s_2^A, s_2^B)
Set_2	Dominant Class	10	7	7	5	3	-2	One pure, symmetric Nash equilibrium (s_1^A, s_1^B)
Set_3	Dominant Class	10	4	12	5	-2	1	One pure, symmetric Nash equilibrium (s_2^A, s_2^B)
Set_4	Coordination Class	10	4	9	5	1	1	Two pure, symmetric Nash equilibria and one interior NE at $s^\star = \frac{1}{2}$
Set_5	Coordination Class	10	4	7	5	3	1	Two pure, symmetric Nash equilibria and one interior NE at $s^\star = \frac{1}{4}$
Set_6	Coordination Class	10	2	9	5	1	3	Two pure, symmetric Nash equilibria and one interior NE at $s^\star = \frac{3}{4}$
Set_7	Coordination Class	15	2	14	5	1	3	Two pure, symmetric Nash equilibria and one interior NE at $s^\star = \frac{3}{4}$

Table 2.3.: Parameter values of the first seven different sets of symmetric games belonging to the dominant and coordination class.

, whereas the last four game settings describe different versions of anti-coordination

games.

Set	Game class	$\$_{11}$	$\$_{12}$	$\$_{21}$	$\$_{22}$	a	b	Nash equilibria:
Set_8	Anti-Coord. Class	10	7	12	5	-2	-2	Two pure, unsymmetric Nash equilibria and one interior NE at $s^\star = \frac{1}{2}$
Set_9	Anti-Coord. Class	10	9	12	5	-2	-4	Two pure, unsymmetric Nash equilibria and one interior NE at $s^\star = \frac{2}{3}$
Set_{10}	Anti-Coord. Class	10	6	12	5	-2	-1	Two pure, unsymmetric Nash equilibria and one interior NE at $s^\star = \frac{1}{3}$
Set_{11}	Anti-Coord. Class	15	6	17	5	-2	-1	Two pure, unsymmetric Nash equilibria and one interior NE at $s^\star = \frac{1}{3}$

Table 2.4.: Parameter values of the last four different sets of symmetric games belonging to the anti-coordination class.

The tables 2.3 and 2.4 summarize the different parameters of the eleven parameter sets.

Dominant Games

Figure 2.2 visualizes the mixed strategy payoff function $\tilde{\$}^A(\tilde{s}^A, \tilde{s}^B)$ (see equation (2.8)) for player A within parameter set Set_2. The right picture shows a special projection of the surface, in which the observer looks in direction of the $\tilde{s}^A$-axis. The figure shows that the game's category of parameter set Set_2 belongs to the class of dominant games and that only one pure NE exists ($(s_1^A, s_1^B) \hat{=} (\tilde{s}^A = 1, \tilde{s}^B = 1)$), which is the dominant strategy of the game. This property can be seen in the left picture of figure 2.2, if one fixes the mixed strategy of player B to an arbitrary value ($\tilde{s}^B \in [0, 1]$). The best response for player A will always

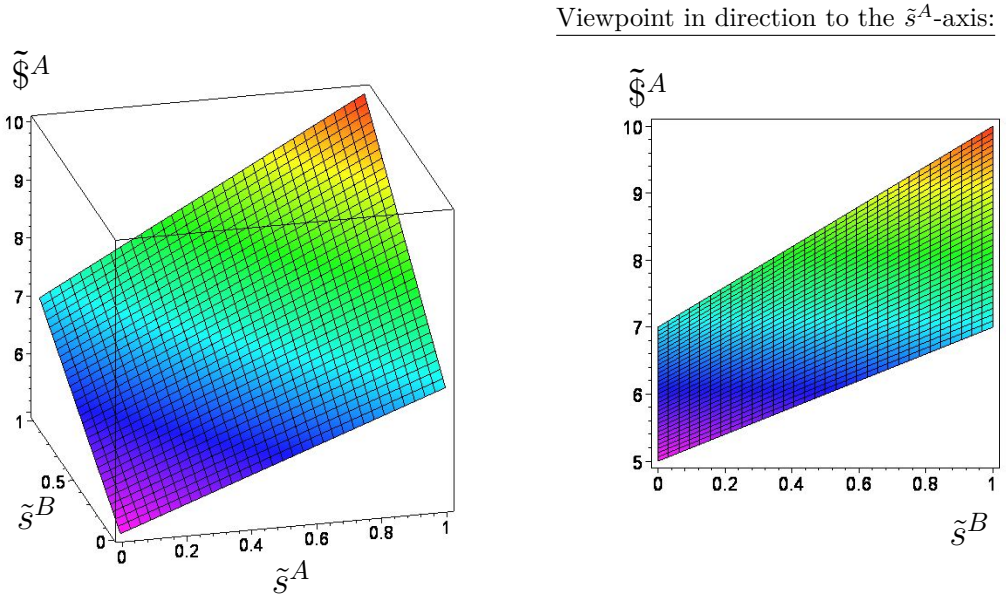

Figure 2.2.: Mixed strategy payoff function $\tilde{\$}^A(\tilde{s}^A, \tilde{s}^B)$ for player A within parameter set Set_2 as a function of the mixed strategies of player A ($\tilde{s}^A$) and B ($\tilde{s}^B$).

be the dominant strategy $s_1^A \hat{=} (\tilde{s}^A = 1)$. As no interior NE is present within parameter set Set_2 the partial derivative (see equation (2.11)) of $\tilde{\$}^A$ does not vanish within the given boundaries. The right picture of figure 2.2 visualizes this fact as no cord-up point was found within the special $\tilde{s}^A$-projection.

The right picture of figure 2.3 shows the function $g(x)$ within parameter set Set_2, whereas the left picture visualizes the numerical results of replicator dynamics ($x(t)$, see equation (2.18)) for several initial conditions of the population function ($x(t=0) = 0, 0.05, 0.1, ..., 0.95$). As the function $g(x)$ is positive for all $x \in]0, 1[$, the fraction of players choosing the strategy $s_1 = s_1^A = s_1^B$ ($x(t)$) will always increase until everybody chooses the strategy s_1, independently on the initial condition. The situation for parameter set Set_1 is similar, however the dominant strategy within this set is s_2 (see figure B.1 in appendix B.II).

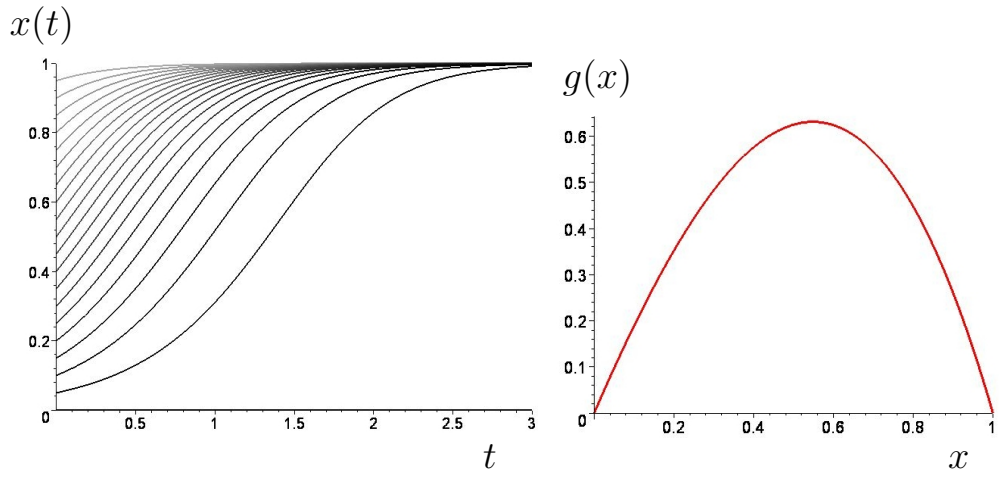

Figure 2.3.: $x(t)$, fraction of players choosing the strategy s_1 at time t for different initial conditions within parameter set Set_2 (left picture). The picture on the right shows the function $g(x)$, which determines the dynamical behavior of $x(t)$.

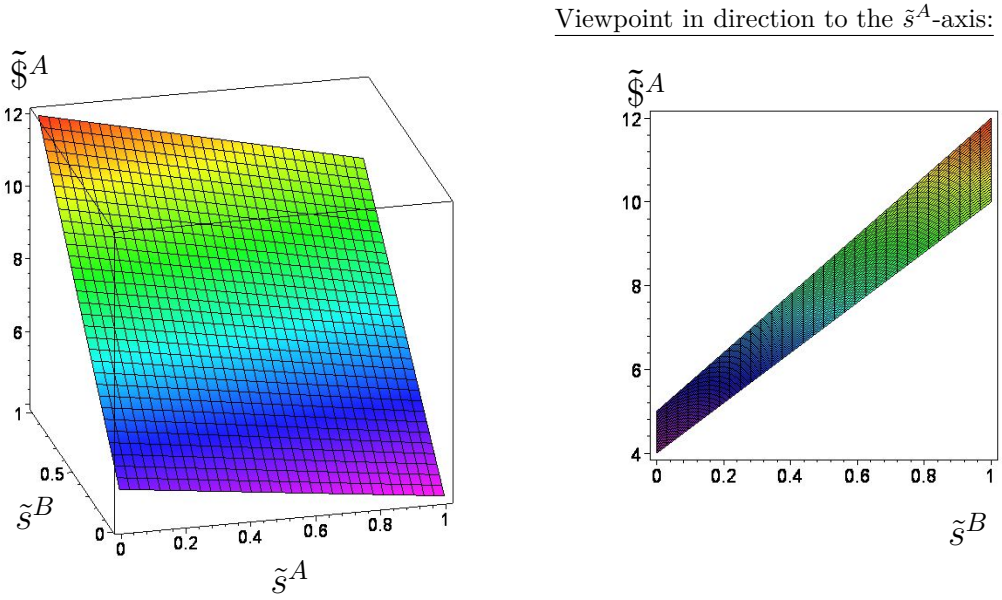

Figure 2.4.: Mixed strategy payoff function $\tilde{\$}^A(\tilde{s}^A, \tilde{s}^B)$ for player A within parameter set Set_3 as a function of the mixed strategies of player A ($\tilde{s}^A$) and B ($\tilde{s}^B$).

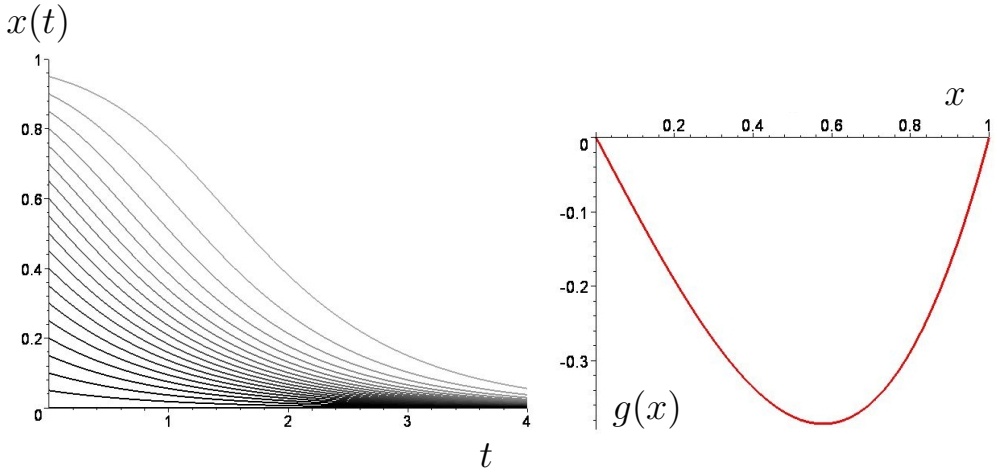

Figure 2.5.: $x(t)$, fraction of players choosing the strategy s_1 at time t for different initial conditions within parameter set Set_3 (left picture). The picture on the right shows the function $g(x)$, which determines the dynamical behavior of $x(t)$.

Set_3 belongs also to the class of dominant games, nevertheless here the underlying structure of the payoff matrix is different (see figure 2.4). Similar as in set Set_1, the only NE and the dominant strategy of the game is s_2, but for all that a dilemma appears within set Set_3. Within Set_1 the payoff of the dominant strategy was equal to the highest point of the surface (Set_1: $\tilde{\$}^A(\tilde{s}^A = 0, \tilde{s}^B = 0) = 10$), in set Set_3 however it is far below the highest point (Set_3: $\tilde{\$}^A(\tilde{s}^A = 0, \tilde{s}^B = 0) = 5$). The structure of the game within parameter set Set_3 is comparable to a "prisoner's dilemma" game. As the function $g(x)$ is negative for all $x \in]0, 1[$, the fraction of players choosing the strategy $s_1 = s_1^A = s_1^B$ will always decrease until everybody chooses the strategy s_2, independently on the initial condition (see figure 2.5). Set_3, which belongs to the class of dominant games with a dilemma is also comparable with the simple example explained in the introduction.

Coordination Games

Within parameter set Set_4 the payoff $\$_{21} = 9$ has decreased compared to the value of Set_3 ($\$_{21} = 12$). Due to this decrease, the game class has shifted from the class of dominant games to the coordination game class. The game

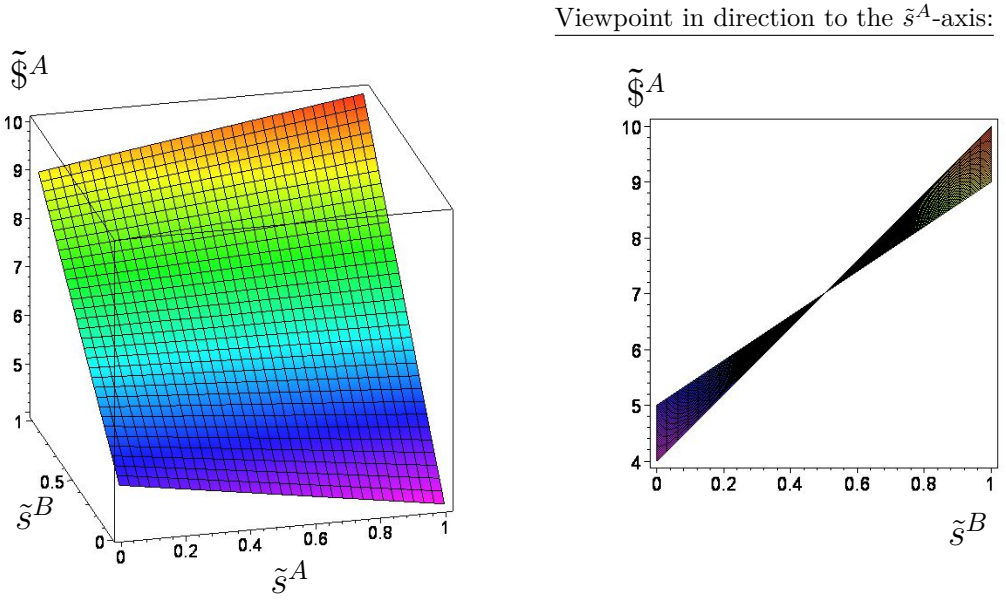

Figure 2.6.: Mixed strategy payoff function $\tilde{\$}^A(\tilde{s}^A, \tilde{s}^B)$ for player A within parameter set Set_4 as a function of the mixed strategies for player A ($\tilde{s}^A$) and B ($\tilde{s}^B$).

has now two pure symmetric Nash equilibria $((s_1^A, s_1^B) \hat{=} (\tilde{s}^A = 1, \tilde{s}^B = 1)$ and $(s_2^A, s_2^B) \hat{=} (\tilde{s}^A = 0, \tilde{s}^B = 0))$ and one interior mixed strategy Nash equilibrium $((\tilde{s}^{A\star}, \tilde{s}^{B\star}) = (\frac{1}{2}, \frac{1}{2}))$. The appearency of the two pure Nash equilibria are visualized within the left picture of figure 2.6. If player B is expected to choose a mixed strategy $\tilde{s}^B > s^\star$, the best response for player A is the pure strategy $s_1 \hat{=} \tilde{s}^A = 1$, whereas if player B is expected to choose a mixed strategy $\tilde{s}^B < s^\star$, the best response for player A is the pure strategy $s_1 \hat{=} \tilde{s}^A = 0$. The mixed strategy Nash equilibrium is visualized within the right picture of figure 2.6. Due to the fact, that the partial derivative of the payoff surface for player A vanishes at the value of the mixed strategy NE, the whole surface shrinks to one point if one projects the viewpoint in direction to the $\tilde{s}^A$-axis (see right picture of figure 2.6). The value of the mixed strategy Nash equilibrium is equal to the zero point of the function $g(x)$ (see right picture of figure 2.7). $g(x)$ (which determines the dynamical behavior of the population function $x(t)$) has,

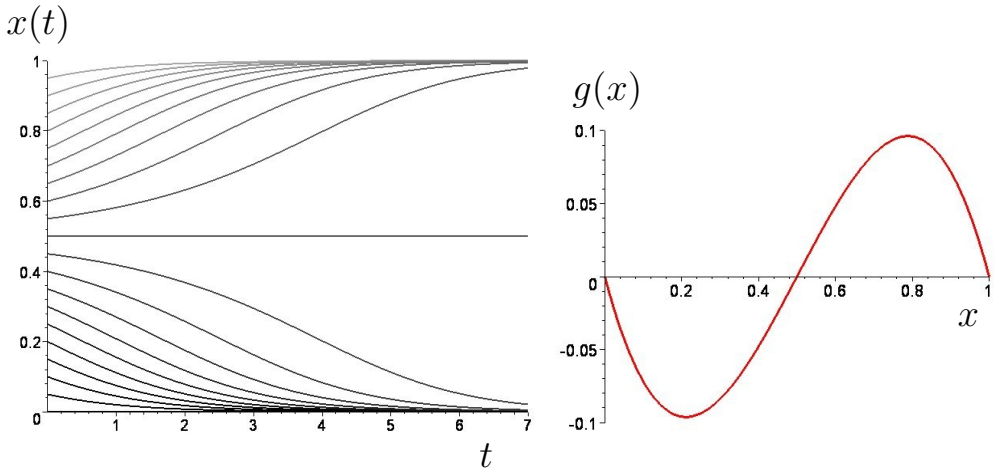

Figure 2.7.: $x(t)$, fraction of players choosing the strategy s_1 at time t for different initial conditions within parameter set Set_4 (left picture). The picture on the right shows the function $g(x)$, which determines the dynamical behavior of $x(t)$.

beside its negative region ($g(x) < 0 \; \forall \; x \in]0, s^\star[$) also a region where its value is positive ($g(x) > 0 \; \forall \; x \in]s^\star, 1[$). Due to this property two evolutionary stable strategies emerge ($x(t \to \infty) = 0$ and $x(t \to \infty) = 1$). To which of these ESS's the population will evolve depends on the initial condition. If the fraction of s_1-player types at the initial time $t = 0$ is below the value of the mixed strategy NE ($x(0) < s^\star = 0.5$) the population will evolve to the ESS $\lim_{t\to\infty}(x(t)) = 0$, which corresponds to a population sorely choosing the s_2-strategy. Only if the initial fraction is above the mixed strategy threshold ($x(0) > s^\star$) the population will end in the ESS $\lim_{t\to\infty}(x(t)) = 1$. The horizontal population path at $x(0.5) = 0.5$ is an artefact of the numerical simulation and is not an ESS, as the solution is unstable in respect to infinitely small perturbations.

The results within the other sets of coordination games are visualized in several pictures (see figures B.2, B.3 and B.4 in appendix B.II). Figure B.2 summarizes the results of parameter set Set_5. Due to a decrease of the parameter $\$_{21}$, the mixed strategy NE has also decreased its value (Set_5: $s^\star = 0.25$). Figure B.3 summarizes the results of parameter set Set_6. Due to an increase of parameter $\$_{12}$, the mixed strategy Nash equilibrium has now also increased (Set_6: $s^\star = 0.75$).

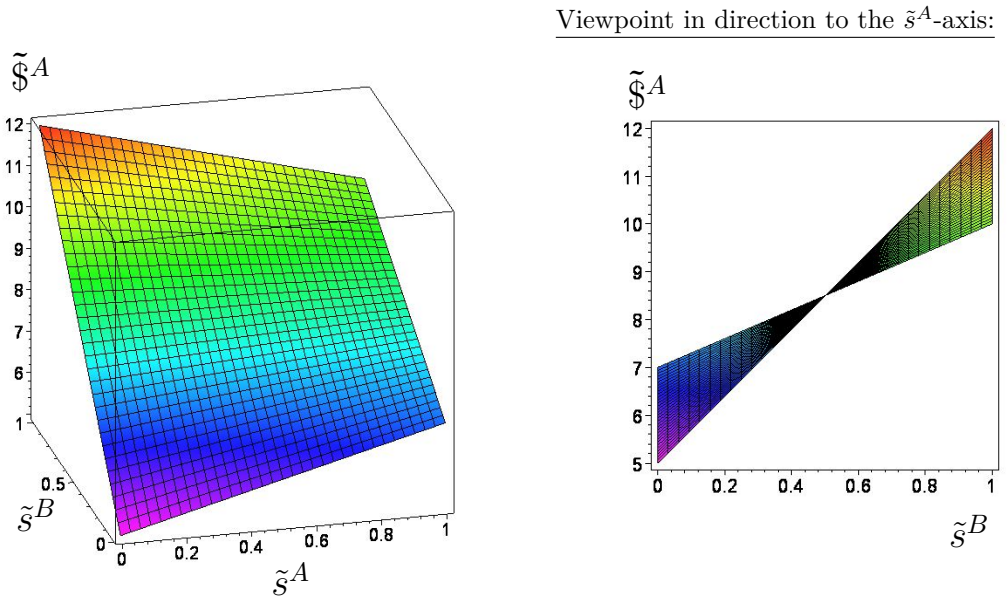

Figure 2.8.: Mixed strategy payoff function $\tilde{\$}^A(\tilde{s}^A, \tilde{s}^B)$ for player A within parameter set Set_8 as a function of the mixed strategies for player A ($\tilde{s}^A$) and B ($\tilde{s}^B$).

The strategy sets Set_6 and Set_7 have identical properties, as the payoff parameters of the payoff-transformed games ($a = 1$ and $b = 3$, see table 2.1) have the same values. The mixed strategy payoff surfaces for these two parameter sets are however quite different (see upper left picture in the figures B.3 and B.4).

Anti-Coordination Games

Within parameter set Set_8 the payoff $\$_{12} = 7$ has increased above the $\$_{22}$-value ($Set_8$: $\$_{22} = 5$). Due to this increase, the game class has shifted towards the class of anti-coordination games. Such games have two asymmetric pure Nash equilibria ((s_1^A, s_2^B) and (s_2^A, s_1^B)) and one interior mixed strategy Nash equilibrium, which is the only ESS of such games. The appearency of the two asymmetric Nash equilibria are visualized within the left picture of figure 2.8, whereas the mixed strategy Nash equilibrium (Set_8: $s^\star = 0.5$) is visualized within

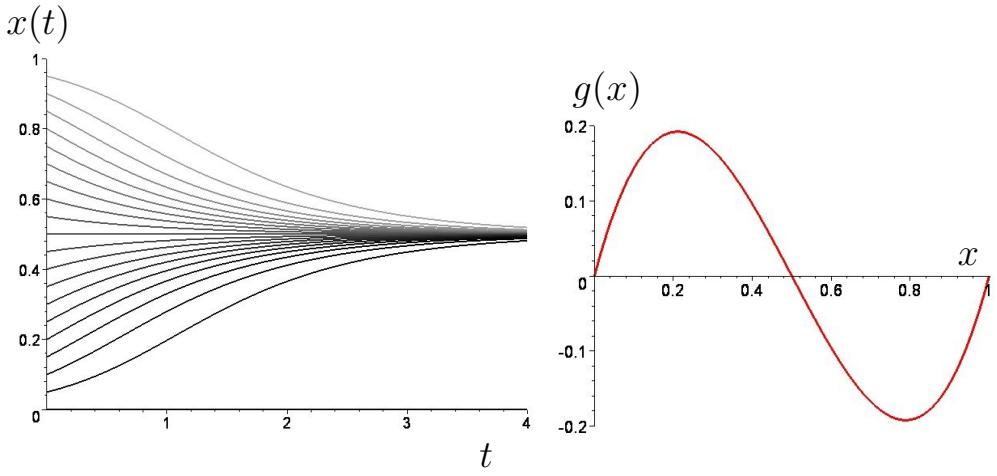

Figure 2.9.: $x(t)$, fraction of players choosing the strategy s_1 at time t for different initial conditions within parameter set Set_8 (left picture). The picture on the right shows the function $g(x)$, which determines the dynamical behavior of $x(t)$.

the right picture. The value of the mixed strategy NE is again equal to the zero point of the function $g(x)$ (see right picture of figure 2.9). $g(x)$ has now a positive region at $(g(x) > 0 \; \forall \; x \in]0, s^\star[)$ and a negative region at $(g(x) < 0 \; \forall \; x \in]s^\star, 1[)$. Independent on the specific value of the initial condition, the population will always end asymptotically in the ESS $x = s^\star = 0.5$ (see left picture of figure 2.9).

The results of the other anti-coordination game parameter settings are visualized in the appendix B.II (see figures B.5, B.6 and B.7).

An increase of parameter $\$_{12}$ (Set_9) shifts the mixed strategy NE and therefore the ESS to higher values (see figure B.5), whereas a decrease of $\$_{12}$ (Set_{10}) has the effect of decreasing the ESS-value (see figure B.6). The parameter sets Set_{10} and Set_{11} have identical properties however their payoff structure is different (see figures B.6 and B.7).

It was shown within this subsection, that symmetric (2×2)-games can be separated into three game classes. However, if the number of available strategies increases, the number of possible classes also needs to be extended. Zeeman has

defined 19 different game classes of symmetric (2×3)-games. Within the appendix B.III the properties and classification scheme of symmetric (2×3)-games are discussed and examples of the 19 possible classes are given.

2.3.4. Results for unsymmetric games

This subsection summarizes the numerical results of the unsymmetric model, where two separate subpopulations play an evolutionary bimatrix game. To illustrate the results and visualize the outcomes of the different game classes, the parameters where fixed within several different game settings (see the tables 2.5, 2.6, 2.7 and 2.8). The parameter settings Set_1^{us} - Set_6^{us} belong to the corner class of bimatrix games.

Set	μ	Class of μ	$\$_{11}^{\mu}$	$\$_{12}^{\mu}$	$\$_{21}^{\mu}$	$\$_{22}^{\mu}$	a^{μ}	b^{μ}	NE of Game μ	Game Class NE and ESS
Set_1^{us}	A:	Dom. Class	10	8	6	5	4	-3	One pure NE (s_1^A, s_1^B)	Corner Class
	B:	Dom. Class	10	6	8	5	4	-3	One pure NE (s_1^A, s_1^B)	One NE and ESS (s_1^A, s_1^B)
Set_2^{us}	A:	Dom. Class	10	4	14	5	-4	1	One pure NE (s_2^A, s_2^B)	Corner Class
	B:	Dom. Class	10	12	2	5	-2	3	One pure NE (s_2^A, s_2^B)	One NE and ESS (s_2^A, s_2^B)

Table 2.5.: Parameter values of the first two sets of unsymmetric games.

Set	μ	Class of μ	$\$_{11}^{\mu}$	$\$_{12}^{\mu}$	$\$_{21}^{\mu}$	$\$_{22}^{\mu}$	a^{μ}	b^{μ}	NE of Game μ	Game Class NE and ESS
Set_3^{us}	A:	Dom. Class	10	4	12	5	-2	1	One pure NE (s_2^A, s_2^B)	Corner Class
	B:	Coord. Class	10	9	4	5	1	1	Two pure NE, one int. NE $(s^\star = \frac{1}{2})$	One NE and ESS (s_2^A, s_2^B)
Set_4^{us}	A:	Dom. Class	10	7	7	5	3	-2	One pure NE (s_1^A, s_1^B)	Corner Class
	B:	Dom. Class	5	7	7	10	-2	3	One pure NE (s_2^A, s_2^B)	One NE and ESS (s_1^A, s_2^B)
Set_5^{us}	A:	Dom. Class	10	4	12	5	-2	1	One pure NE (s_2^A, s_2^B)	Corner Class
	B:	Anti-Co. Class	10	12	7	5	-2	-2	Two pure NE, one int. NE $(s^\star = \frac{1}{2})$	One NE and ESS (s_2^A, s_1^B)

Table 2.6.: Parameter values for set Set_{3-5}^{us} of unsymmetric games.

The sets Set_7^{us} - Set_9^{us} are saddle class games and the last two settings (Set_{10}^{us} and Set_{11}^{us}) describe games belonging to the center class.

Set	μ	Class of μ	$\$_{11}^{\mu}$	$\$_{12}^{\mu}$	$\$_{21}^{\mu}$	$\$_{22}^{\mu}$	a^{μ}	b^{μ}	NE of Game μ	Game Class NE and ESS
Set_6^{us}	A:	Dom. Class	10	4	12	5	-2	1	One pure NE (s_2^A, s_2^B)	Corner Class
	B:	Anti-Co. Class	10	12	6	5	-2	-1	Two pure as-NEs, one int. NE $(s^\star = \frac{1}{3})$	One NE and ESS (s_2^A, s_1^B)
Set_7^{us}	A:	Coord. Class	10	4	9	5	1	1	Two pure NE, one int. NE $(s^\star = \frac{1}{2})$	Saddle Class
	B:	Coord. Class	10	7	4	5	3	1	Two pure NE, one int. NE $(s^\star = \frac{1}{4})$	Two ESS's (s_1^A, s_1^B), (s_2^A, s_2^B)
Set_8^{us}	A:	Coord. Class	10	4	7	5	3	1	Two pure NE, one int. NE $(s^\star = \frac{1}{4})$	Saddle Class
	B:	Coord. Class	10	9	2	5	1	3	Two pure NE, one int. NE $(s^\star = \frac{3}{4})$	Two ESS's (s_1^A, s_1^B), (s_2^A, s_2^B)

Table 2.7.: Parameter values for set Set_{6-8}^{us} of unsymmetric games.

Set	μ	Class of μ	$\$_{11}^{\mu}$	$\$_{12}^{\mu}$	$\$_{21}^{\mu}$	$\$_{22}^{\mu}$	a^{μ}	b^{μ}	NE of Game μ	Game Class NE and ESS
Set_{9}^{us}	A:	Anti-Co. Class	10	7	12	5	-2	-2	Two pure NE, one int. NE ($s^{\star} = \frac{1}{2}$)	Saddle Class
	B:	Anti-Co. Class	10	12	9	5	-2	-4	Two pure NE, one int. NE ($s^{\star} = \frac{2}{3}$)	Two ESS's (s_1^A, s_2^B), (s_2^A, s_1^B)
Set_{10}^{us}	A:	Coord. Class	10	4	9	5	1	1	Two pure NE, one int. NE ($s^{\star} = \frac{1}{2}$)	Center Class
	B:	Anti-Co. Class	10	12	7	5	-2	-2	Two pure NE, one int. NE ($s^{\star} = \frac{1}{2}$)	Neither a NE nor an ESS
Set_{11}^{us}	A:	Coord. Class	10	4	7	5	3	1	Two pure NE, one int. NE ($s^{\star} = \frac{1}{4}$)	Center Class
	B:	Anti-Co. Class	10	12	9	5	-2	-4	Two pure NE, one int. NE ($s^{\star} = \frac{2}{3}$)	Neither a NE nor an ESS

Table 2.8.: Parameter values for set Set_{9-11}^{us} of unsymmetric games.

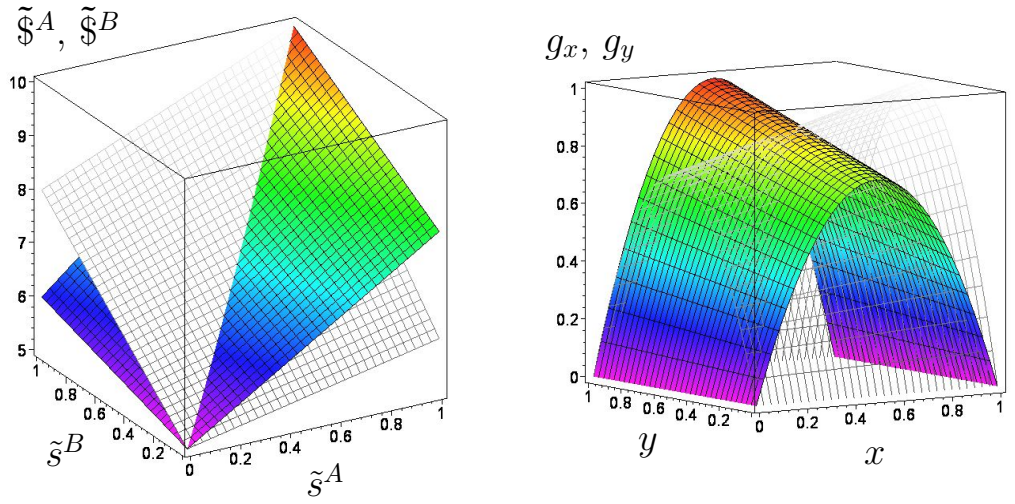

Figure 2.10.: Left picture: Mixed strategy payoff function for player A ($\tilde{\$}^A(\tilde{s}^A, \tilde{s}^B)$, colored surface) and player B ($\tilde{\$}^B(\tilde{s}^A, \tilde{s}^B)$, wired grey surface) within parameter set Set_1^{us} as a function of the mixed strategies of player A ($\tilde{s}^A$) and B ($\tilde{s}^B$). Right picture: $g_x(x, y)$ (colored surface) and $g_y(x, y)$ (wired grey surface) as a function of the strategic population fractions of group A (x) and group B (y).

The left picture of figure 2.10 visualizes the mixed strategy payoff function for player A ($\tilde{\$}^A(\tilde{s}^A, \tilde{s}^B)$: colored surface, see equation (2.8)) and player B ($\tilde{\$}^B(\tilde{s}^A, \tilde{s}^B)$: wired grey surface) within parameter set Set_1^{us}. This parameter set is similar to the symmetric parameter set Set_2, whereby the parameters $\$_{12}^{\mu}$ and $\$_{21}^{\mu}$ have different values. The game belongs still to the category of symmetric games, as the payoff matrix of player A is equal to the transposed payoff matrix of player B. The structure of the surfaces indicates, that both groups have only one NE, which is the dominant strategy $(s_1^A, s_1^B) \hat{=} (\tilde{s}^{A*} = 1, \tilde{s}^{B*} = 1)$. The right picture of figure 2.10 displays the two functions $g_x(x, y)$ and $g_y(x, y)$ that determine the dynamical behavior of the strategical decisions of group A ($x(t)$) and group B ($y(t)$) (see equation (2.14)). As the two surfaces are always above zero, the amount of players choosing strategy s_1 will monotonly increase in both groups as time goes by and will finally reach the only ESS ($x(t \to \infty) = 1$,$y(t \to \infty) = 1$), independent on the initial condition.

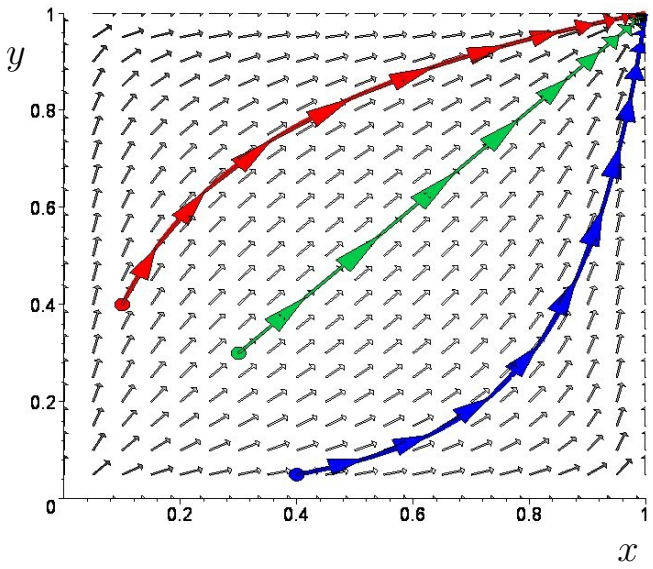

Figure 2.11.: Phase diagram of the xy-trajectories for three different initial conditions within parameter set Set_1^{us}. x describes the fraction of players within group A choosing the strategy s_1, while y is a similar fraction within group B.

The evolution of the strategic behavior of the two groups is visualized in figure 2.11. The plot describes the numerical results of equation (2.14) for three different initial conditions, displayed through the three colored curves (xy-trajectories). The three trajectories are embedded in a field plot phase diagram, where the little grey arrows describe the direction of a "strategic wind" the population has to follow during its time evolution. The three initial conditions $(x(0), y(0))$ are marked with colored circles at the beginning of the three curves. The several colored arrows, which are on top of the trajectories describe the populations movement for some intermediate time steps, where the length of arrows indicate the absolute value of the strategic change velocity within the population. Within figure 2.11 the difference in the intermediate time steps ($\delta t = 0.15$) is equal for all of the three trajectories. The red arrow for example begins at the initial condition $(x(0) = 0.1, y(0) = 0.4)$ and the head of the arrow ends at $(x(0.15) \approx 0.16, y(0.15) \approx 0.52)$ and the second green arrow starts at $(x(0.15) \approx 0.16, y(0.15) \approx 0.52)$ and its head ends at $(x(0.3) = 0.24, y(0.3) = 0.63)$.

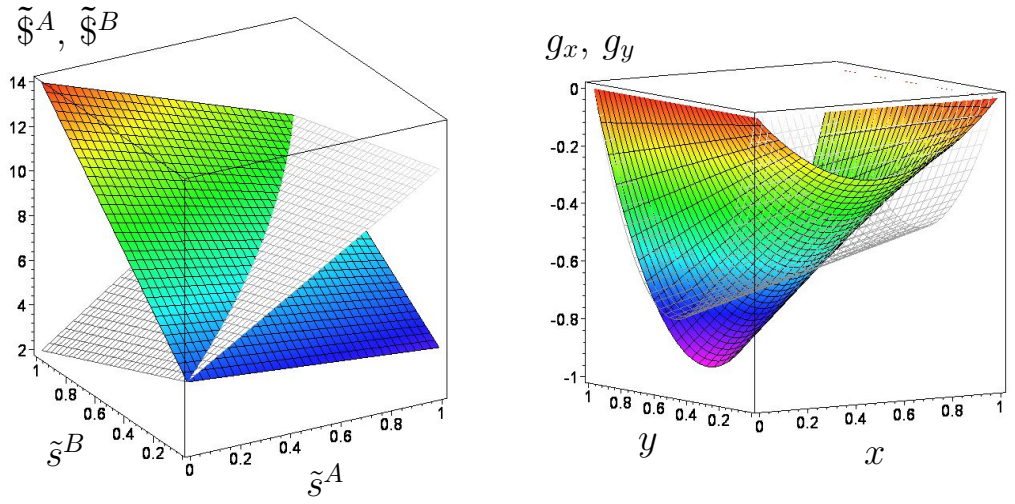

Figure 2.12.: Payoffs and functions $g_x(x, y)$ and $g_y(x, y)$ within set Set_2^{us}; similar description as in figure 2.10.

The interpretation of the results of figure 2.11 are comparable with the results of parameter set Set_1 of the symmetric model. Both population subgroups play a dominant game and the evolution of their strategical choice will finally—independent on the initial condition—reach a state, where everybody chooses the dominant strategy s_1. The game category belongs formally to the corner class. The velocity of the strategic change (length of the colored arrows) of the three trajectories differs slightly during the evolution. In the middle region of the trajectories the velocity is the highest, whereas at the end (near to the ESS) the strategic change slows down very much. Figure 2.11 shows that the two subpopulations behave identical, as all the trajectories are symmetric along the $(y = x)$-axis, which is due to the symmetry of the underlying parameter set. The properties of parameter set Set_1^{us} therefore could have been calculated using the more simple dynamic equation (2.18).

The left picture of figure 2.12 visualizes the mixed strategy payoffs within parameter set Set_2^{us}, which is similar to the symmetric parameter set Set_3 of a prisoner's dilemma game. In contrast to set Set_1^{us} the two game matrices for player A and B are unsymmetric ($\$_{12}^A = 4 \neq 2 = \$_{21}^B$ and $\$_{21}^A = 14 \neq 12 = \$_{12}^B$).

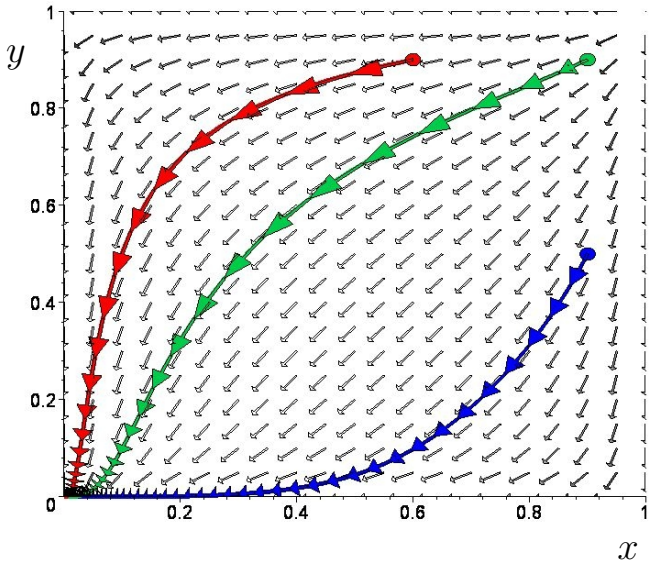

Figure 2.13.: Phase diagram for three different xy-trajectories within set Set_2^{us}; similar description as in figure 2.11.

The structure of the surfaces indicate that both groups have again only one NE, which is the dominant strategy $(s_2^A, s_2^B) \hat{=} (\tilde{s}^{A*} = 0, \tilde{s}^{B*} = 0)$. The right picture of figure 2.12 shows the two functions $g_x(x, y)$ (colored surface) and $g_y(x, y)$ (wired grey surface). The amount of players choosing strategy s_1 will in both groups monotony decrease and will—independent on the initial value—finally reach the only ESS $(x = 0, y = 0)$, because the two surfaces are always below or equal to zero $(g_x(x, y) \leq 0,\ g_y(x, y) \leq 0\ \forall\ x, y \in [0, 1])$. The game category belongs to the corner class.

The evolution of the strategic behavior of the two groups is visualized in figure 2.13. The intermediate time steps $(\delta t = 0.125)$ are equal for all of the three trajectories. The unsymmetric behavior of the trajectories is due to the unsymmetry of the parameter set. The green curve for example starts at an symmetric initial value $(x(0) = 0.9, y(0) = 0.9)$, but as time evolves, it follows an unsymmetric evolution. The interpretation of the results of figure 2.13 are comparable with the results of parameter set Set_3 of the symmetric model. Both population subgroups play a prisoner's dilemma game and the evolution of their strategical choice will finally—independent on the initial condition—reach a state, where

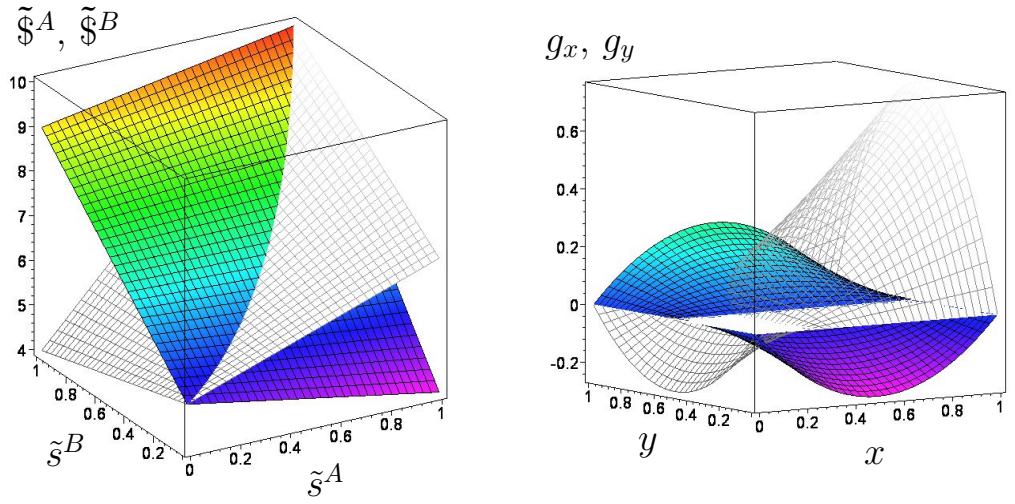

Figure 2.14.: Payoffs and functions $g_x(x, y)$ and $g_y(x, y)$ within set Set_7^{us}; similar description as in figure 2.10.

everybody chooses the dominant strategy s_2. Similar to the symmetric model, the players face a dilemma, as the two populations evolve towards a low payoff ESS ($\tilde{\$}^\mu(0,0) = 5 < 10 = \tilde{\$}^\mu(1,1)$).

Parameter set Set_4^{us} describes also a combination of two prisoner's dilemma games (Set_2 and Set_1). As the dominant strategies of the two games are not equal ($\tilde{s}^{A*} = 1$ and $\tilde{s}^{B*} = 0$), the ESS is situated at the unsymmetric lower-right corner of the phase diagram. The numerical results of this parameter set are visualized in figure B.14 within appendix B.IV.

Parameter set Set_3^{us} is a combination of a prisoner's dilemma game (subpopulation A) with a game belonging to the coordination class (subpopulation B). The resulting bimatrix game class is again the corner class with only one ESS $(s_2^A, s_2^B) \hat{=} (\tilde{s}^{A*} = 0, \tilde{s}^{B*} = 0)$ (see figure B.13 within the appendix B.IV). A combination of a dominant game with an anti-coordination game (parameter sets: Set_5^{us} and Set_6^{us}) results also in a corner class bimatrix game having only one asymmetric ESS (see figures B.15 and B.16 within the appendix B.IV).

Within parameter set Set_7^{us} both subpopulations play a coordination game, where

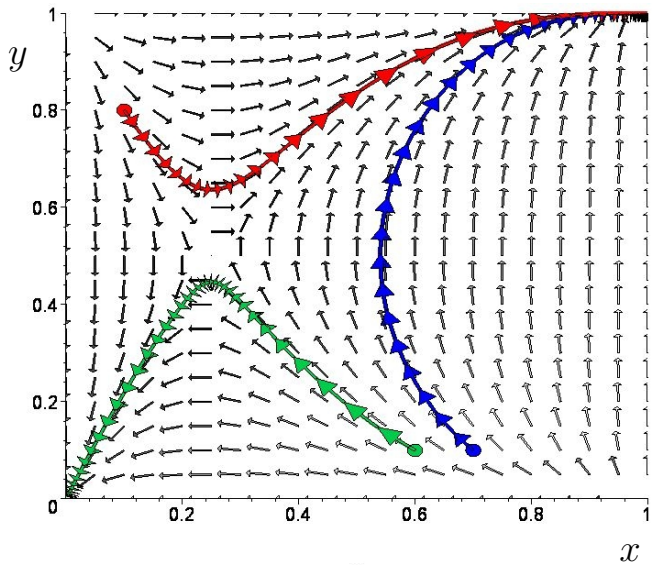

Figure 2.15.: Phase diagram for three different xy-trajectories within set Set_7^{us}; similar description as in figure 2.11.

the payoff of group A is equal to set Set_4 and the payoff for group B is equal to set Set_5. A bimatrix game, which is composed of two coordination games always results in a saddle class game. The structure of the payoff surfaces (see left picture in figure 2.14) indicates, that both groups have now two pure Nash equilibria ((s_1^A, s_1^B) and (s_2^A, s_2^B)). Additionally there exists an interior mixed strategy NE ($(\tilde{s}^{A\star}, \tilde{s}^{B\star}) = (\frac{1}{2}, \frac{1}{4})$). To indicate the zero-level, an additional white plane was added to figure 2.14 (right hand side). Within this parameter set, the two surfaces have regions where they have positive values ($g_x(x,y) > 0 \; \forall \; y \in]\tilde{s}^{B\star}, 1]$ and $g_y(x,y) > 0 \; \forall \; x \in]\tilde{s}^{A\star}, 1]$) and regions where they are negative ($g_x(x,y) < 0 \; \forall \; y \in]0, \tilde{s}^{B\star}[$ and $g_y(x,y) > 0 \; \forall \; x \in]0, \tilde{s}^{A\star}[$). The interior mixed strategy NE is exactly at the point, where all of the three surfaces intersect. As all of the parameters (a^A, a^B, b^A, b^B) are positive the game category belongs to the saddle class of bimatrix games and it has two symmetric ESS's.

The results of the evolutionary game of parameter set Set_7^{us} is visualized in figure 2.15. As the strategic change velocity within the three different trajectories are quite different, the time steps (δt) between the colored arrows are not the same for the three different population paths. The red and green trajectories have the same

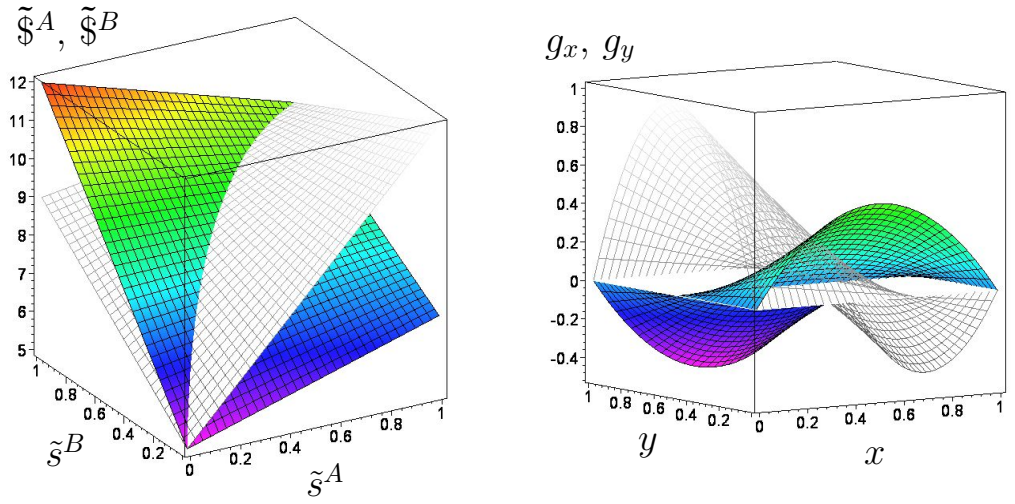

Figure 2.16.: Payoffs and functions $g_x(x, y)$ and $g_y(x, y)$ within set Set_9^{us}; similar description as in figure 2.10.

time increment ($\delta t = 0.35$), whereas the arrows on the blue path are separated by a time lag of $\delta t = 2$. The strategic change of the blue population path is the slowest; starting from an initial condition ($x(0) = 0.7, y(0) = 0.1$) the fraction of players who choose the s_1-strategy monotonically increases within group B ($y(t)$) while within group A ($x(t)$) the s_1-fraction first decreases and then increases, until the whole population finally ends in the ESS $(s_1^A, s_1^B) \hat{=} (\tilde{s}^{A*} = 1, \tilde{s}^{B*} = 1)$ (all players choose the s_1-strategy). The red trajectory, which starts at the initial condition ($x(0) = 0.1, y(0) = 0.8$) also ends within the ESS (s_1^A, s_1^B). Its strategic change velocity, however, slows down very much at the region near to the interior NE. The initial condition of the green trajectory ($x(0) = 0.6, y(0) = 0.1$) is only slightly different from the initial value of the blue curve, however its evolution is totally different. The s_1-fraction monotonically decreases within group A ($x(t)$) while within group B ($y(t)$) the s_1 fraction first increases and then decreases, until the whole population finally ends in the ESS $(s_2^A, s_2^B) \hat{=} (\tilde{s}^{A*} = 0, \tilde{s}^{B*} = 0)$ (all players choose the s_2-strategy). Similar to the red curve, the strategic change velocity slows down very much at the region near to the interior NE.

Set Set_8^{us}, which is also composed of two coordination games describes again a

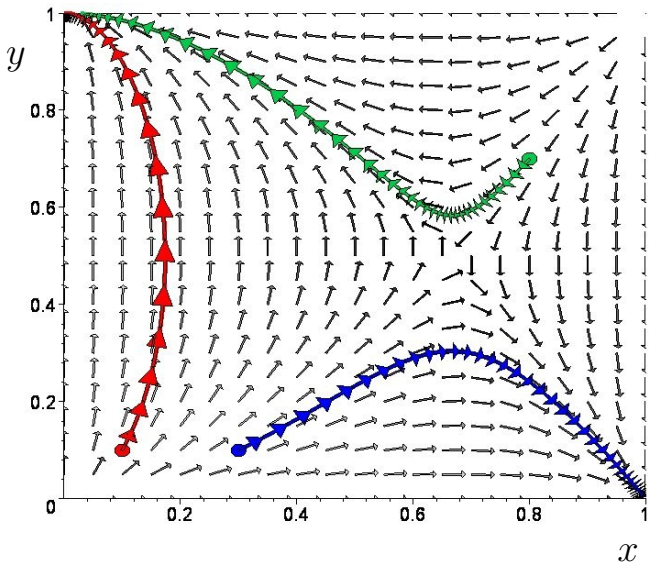

Figure 2.17.: Phase diagram for three different xy-trajectories within set Set_9^{us}; similar description as in figure 2.11.

saddle class game. The interior mixed strategy NE is situated at $((\tilde{s}^{A\star}, \tilde{s}^{B\star}) = (\frac{1}{4}, \frac{3}{4}))$. The results of this parameter set are visualized in figure B.17 within appendix B.IV.

Parameter set Set_9^{us} is a saddle class bimatrix game, where both subpopulations play an anti-coordination game (group A: set Set_8, group B: Set_9). The structure of the payoff surfaces (see left picture in figure 2.16) indicates that both groups have two asymmetric pure Nash equilibria $((s_1^A, s_2^B)$ and $(s_2^A, s_1^B))$ and one interior mixed strategy NE $((\tilde{s}^{A\star}, \tilde{s}^{B\star}) = (\frac{1}{2}, \frac{2}{3}))$. As all of the parameters (a^A, a^B, b^A, b^B) are negative the game category belongs to the saddle class of bimatrix games and has two asymmetric ESS's.

The results of the evolutionary game of parameter set Set_9^{us} is visualized in figure 2.17. The time steps (δt) between the colored arrow are the same for all of the three population paths $(\delta t = 0.125)$.

Finally, the last two parameter sets (Set_{10}^{us} and Set_{11}^{us}) belong to the category of center class games. Within parameter set Set_{11}^{us} the subpopulation A plays an coordination game (Set_4) while subpopulation B plays an anti-coordination

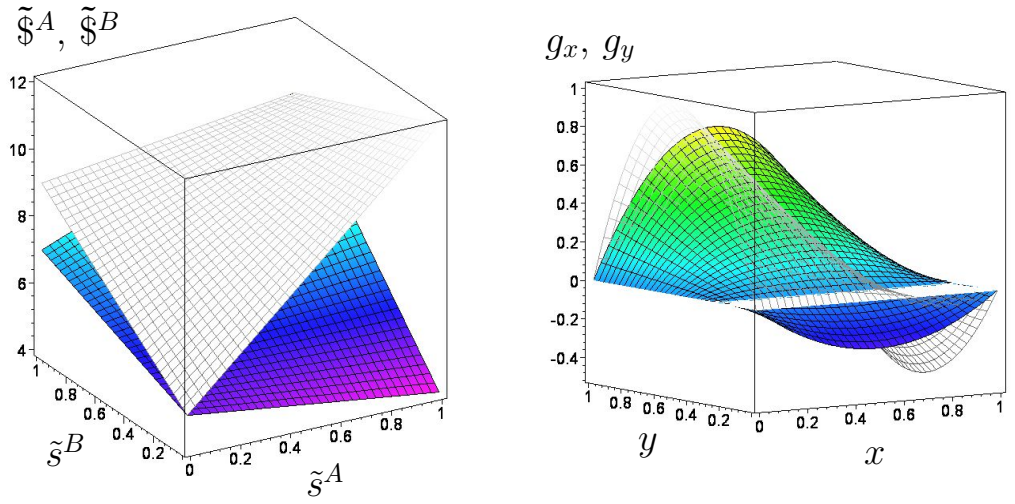

Figure 2.18.: Payoffs and functions $g_x(x, y)$ and $g_y(x, y)$ within set Set_{11}^{us}; similar description as in figure 2.10.

game (Set_9). The structure of the payoff surfaces (see left picture in figure 2.18) indicates that there is only one interior mixed strategy NE ($(\tilde{s}^{A\star}, \tilde{s}^{B\star}) = (\frac{1}{4}, \frac{2}{3})$).

The results of the evolutionary game of parameter set Set_{11}^{us} is visualized in figure 2.19 and show that all of the trajectories cycle around the interior NE and indicate the absence of an ESS. The time which is needed for one cycle is larger for bigger cycles and as a result the time steps (δt) between the colored arrow is the smallest for the blue trajectory ($\delta t = 6.5$) and the biggest for the red closed curve ($\delta t = 14.5$) (green: $\delta t = 8$).

The results of parameter set Set_{10}^{us} are visualized in figure B.18 within the appendix B.IV.

The mathematical formulation of QGT and its relevanz to EGT is briefly explained within the following two sections.

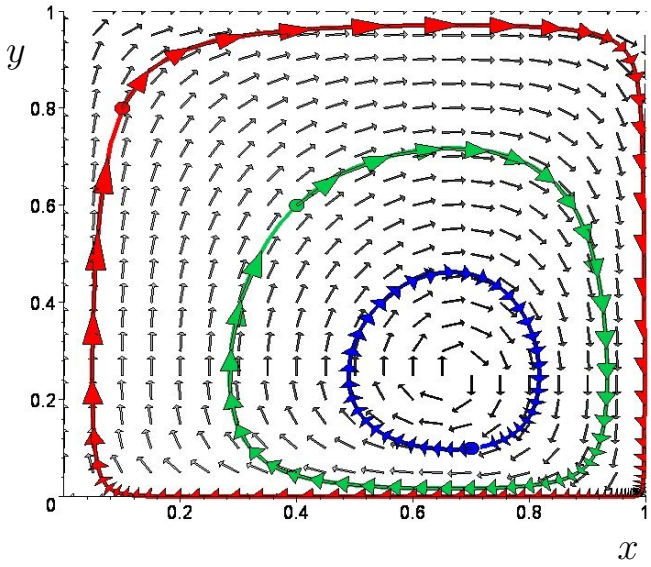

Figure 2.19.: Phase diagram for three different xy-trajectories within set Set_{11}^{us}; similar description as in figure 2.11.

2.4. Quantum Game Theory

2.4.1. Introduction

The discussion of quantum games started with the work of Eisert et al. (1999) [66] and Meyer (1999) [165]. Meyer analysed the "penny flip" game and showed, that a player who selects a quantum strategy always wins this game. Eisert et al. (1999) concentrated on the prisoner dilemma and demonstrated that the players of this game could escape this dilemma if the entanglement of the prisoners' wave function is above a certain value. Since these leadoff articles several further applications of quantum games have been published. Marinatto & Weber (2000) [162] applied quantum games to the "battle of sexes" showing that entangled strategies will lead to a unique solution of this game. R.V. Mendes analysed the "quantum ultimatum game" and Hogg et al. investigated the quantum treatment of several different games, namely the "quantum treatment of public good economics" [48], the "quantum coordination game" [134] and "quantum auctions" [131]. Benjamin & Hayden [28] amplified the quantum game approach

to a situation of multiple players. Piotrowski & Sladkowsky [178] used quantum games to examine market behaviour. In 2001 the first quantum game was realized on a quantum computer [62] (see also [190]). The application of quantum game theory to social experiments and experimental economics [49, 176, 112, 242, 38] and several review articles [97, 186, 240, 180, 155, 179, 181] followed. Hanauske et al. [111] based the analysis of the open access publishing behaviour in different scientific communities on a quantum game approach (see also [118]).

Within the previous two sections the main concepts of classical GT and EGT where discussed. It was shown for example, that games belonging to the class of dominant games with a dilemma (e.g. see results for parameter set Set_3) do have only one dominant strategy, which is also the only evolutionary stable strategy where the average strategic decision of the population of players will finally end. The tragedy of this game is that the population ends in a worse situation than when all players had chosen the other strategy.

Coming back to the example of section 2.2.1. The real outcome of the example might also depend on further characteristics of the specific story of the game. QGT in-cooperates specific factors of the underlying story and affiliates them into a new parameter called γ. Similar to classical GT, QGT also do not need to know "Who is Emma, who is Hans, where are they, why are they in such a decision state, ...", but it needs to know some characteristics of the underlying game—namely the value of strategic entanglement among the players. In order to explain this, the example is extended with the use of an additional little story. In principle the specific details of the story do not matter except one important value, in the following called the "γ-value of the story".

To give an example:
Emma (Player A) is separated from Hans (Player B) and they do not have any possibility to communicate. Both have to make a binary decision. The binary decision is simply to choose between the two strategies $\{s_1, s_2\}$ on a computer screen. The benefit if both choose the strategy s_1 is very good for both of them ($\$^A_{11} = 10$ and $\$^B_{11} = 10$). If Emma and Hans choose the strategy s_2 it will not be good for both of them ($\$^A_{22} = -5$ and $\$^B_{22} = -5$), as both need to give away 5. If Emma decides to use s^A_1 and Hans plays s^B_2, the outcome for Hans will be even slightly better than the situation for him if both choose s_1 ($\$^B_{11} = 10 < \$^B_{12} = 12$);

the same holds true for Emma: ($\$^A_{11} = 10 < \$^A_{21} = 12$). However if Emma chooses the strategy s^A_2 and Hans plays s^B_1, the outcome for Hans will be extremely bad ($\$^B_{21} = \alpha << \$^B_{22} = -5$); the same holds true for Emma: ($\$^A_{12} = \alpha << \$^A_{22} = -5$).

Without knowing any further details of the game and recalling the game theoretical results of classical games, it would be no wonder, if Emma and Hans would both choose the strategy s_2. It will be shown, that even for such extreme games there exists a γ-value for which both players choose the strategy s_1 and therefore escape the game's dilemma. For the above example the condition of the existence of a Nash equilibrium is written explicitly as follows:

The strategy combination (s^A_2, s^B_2) is a Nash equilibrium, because:

$$\begin{aligned} \$^A(s^A_2, s^B_2) = \$^A_{22} = -5 \ \geq \ \alpha = \$^A_{12} = \$^A(s^A_1, s^B_2) \\ \$^B(s^A_2, s^B_2) = \$^B_{22} = -5 \ \geq \ \alpha = \$^B_{21} = \$^B(s^A_2, s^B_1) \end{aligned} \tag{2.19}$$

The quantum game theoretical part of this article begins with an important, but also difficult quantum theoretical construct, namely the "quantum decision state" of player A ($|\psi\rangle_A$) and player B ($|\psi\rangle_B$). QGT is a mathematical and conceptual amplification of classical GT. The decision state of player A (and player B) is an amplification of the set of mixed strategies of player A ($\tilde{\mathbf{s}}^A$) (and of player B ($\tilde{\mathbf{s}}^B$)) and contains beside its real parts also imaginary values. Formally the state is constructed using an complex valued decision operator $\hat{\mathcal{U}}_A$ (for player B: $\hat{\mathcal{U}}_B$) which depends on two angles, namely θ_A and φ_A (for player B: θ_B and φ_B).

Starting from the theory of Nash equilibria, the players viewpoint of thinking begins from one of the two real valued eigenstates of the other person (for player A: $\left|s^B_1\right\rangle$ or $\left|s^B_2\right\rangle$ and for player B: $\left|s^A_1\right\rangle$ or $\left|s^A_2\right\rangle$). The mixed strategy payoff function is extended, using an reduced quantum strategy set which tries to model the variety of possible stories beginning from an s_1-perspective. The s_1-quantum extension of Nash equilibria is written as follows:

The strategy combination (τ^*_A, τ^*_B) is a called a quantum NE, if:

$$\begin{aligned} \$_A(\tau^*_A, \tau^*_B) \ \geq \ \$_A(\tau_A, \tau^*_B) \quad \forall \ \tau_A \in [-1, 1] \\ \$_B(\tau^*_A, \tau^*_B) \ \geq \ \$_B(\tau^*_A, \tau_B) \quad \forall \ \tau_B \in [-1, 1] \end{aligned} \tag{2.20}$$

The most important, but also most difficult mathematical concept in QGT is the two player quantum state $|\Psi\rangle$. It is formally constructed with the use of the decision operators $\hat{\mathcal{U}}_A$ and $\hat{\mathcal{U}}_B$ of player A and B and the entangling and disentangling operator $\hat{\mathcal{J}}$ and $\hat{\mathcal{J}}^\dagger$. $|\Psi\rangle$ is an spinor in a complex valued, 4-dimensional, abstract mathematical space called "Hilbertspace" $\mathcal{H}$. The space of all conceivable decision paths is extended from the purely rational, measurable space in the Hilbertspace of complex numbers. Through the concept of a potential entanglement of the imaginary quantum strategy parts, it is possible to include cooperate decision path, caused by cultural or moral standards. QGT is therefore a model which goes beyond *Homo Economicus* and the parameter γ, which is a measure for the strength of entanglement and fellow feeling, describes how strongly the players behave as *Homo Sociologicus* or *Homo Transzendentalis*.

In QGT players may cooperate, depending on the degree of entanglement among players. The notion of entanglement is perhaps most clearly expressed in terms of Adam Smith's classical concept of sympathy or "fellow feeling" which is a cornerstone of Smith's understanding of individual behavior [119]. In his "Theory of Moral Sentiments" (1759) [220] Smith claims that there is a general tendency for fellow-feeling among human beings, whereas the strength of fellow-feeling is greater the more closely related the individuals are. For example, there tends to be more fellow-feeling between friends than between acquaintances, and more between close relatives than between distant ones. Fellow-feeling as the human capacity to emphasize and become entangled with others is inversely related to the perceived and felt distance, whereas distance has been interpreted in terms of psychological and physical distance [194]. It can be shown that (even for the extreme game described in the additional story of the example) Emma and Hans are able to escape the dilemma if their strength of fellow feeling (strength of strategic entanglement) is high enough to overcome the game's γ-threshold.

To illustrate and explain the main differences between GT and QGT in more detail, the mathematical groundings of QGT are described in the following.

2.4.2. Definition and key aspects of quantum game theory

In QGT, the measurable pure classical strategies (s_1 and s_2) correspond to the orthonormal unit basis vectors $|s_1\rangle$ and $|s_2\rangle$ of the two dimensional complex space, the so called Hilbert space $\mathcal{H}_i$ of player i ($i = A, B$). A quantum strategy of a player i is represented as a general unit vector $|\psi\rangle_i$ in his strategic Hilbert space $\mathcal{H}_i$. The whole quantum strategy space $\mathcal{H}$ is constructed with the use of the direct tensor product of the individual Hilbert spaces: $\mathcal{H} := \mathcal{H}_A \otimes \mathcal{H}_B$. The main difference between classical and quantum game theory is that in the Hilbert space $\mathcal{H}$ correlations between the players' individual quantum strategies are allowed, if the two quantum strategies $|\psi\rangle_A \in \mathcal{H}_A$ and $|\psi\rangle_B \in \mathcal{H}_B$ are entangled. The overall state of the system we are looking at is described as a 2-player quantum state $|\Psi\rangle \in \mathcal{H}$. We define the four basis vectors of the Hilbert space $\mathcal{H}$ as the classical game outcomes ($\left|s_1^A s_1^B\right\rangle := (1,0,0,0)$, $\left|s_1^A s_2^B\right\rangle := (0,-1,0,0)$, $\left|s_2^A s_1^B\right\rangle := (0,0,-1,0)$ and $\left|s_2^A s_2^B\right\rangle := (0,0,0,1)$).

The setup of the quantum game begins with the choice of the initial state $|\Psi_0\rangle$. We assume that both players are in the state $|s_1\rangle$. The initial state of the two players is given by

$$|\Psi_0\rangle = \widehat{\mathcal{J}}\left|s_1^A s_1^B\right\rangle = \begin{pmatrix} \cos\left(\frac{\gamma}{2}\right) \\ 0 \\ 0 \\ i\sin\left(\frac{\gamma}{2}\right) \end{pmatrix}, \tag{2.21}$$

where the unitary operator $\hat{\mathcal{J}}$ (see equation (2.29)) is responsible for the possible entanglement of the 2-player system. The players' quantum decision (quantum strategy) is formulated with the use of a two parameter set of unitary 2×2 matrices:

$$\widehat{\mathcal{U}}(\theta,\varphi) := \begin{pmatrix} e^{i\,\varphi}\cos(\frac{\theta}{2}) & \sin(\frac{\theta}{2}) \\ -\sin(\frac{\theta}{2}) & e^{-i\,\varphi}\cos(\frac{\theta}{2}) \end{pmatrix} \tag{2.22}$$
$$\forall \quad \theta \in [0,\pi] \ \wedge \ \varphi \in [0,\tfrac{\pi}{2}]$$

By arranging the parameters θ and φ, a player chooses his quantum strategy. The classical strategy s_1 is selected by appointing $\theta = 0$ and $\varphi = 0$:

$$\widehat{s_1} := \hat{\mathcal{U}}(0,0) = \begin{pmatrix} 1 & 0 \\ 0 & 1 \end{pmatrix} \quad , \tag{2.23}$$

whereas the strategy s_2 is selected by choosing $\theta = \pi$ and $\varphi = 0$:

$$\widehat{s_2} := \hat{\mathcal{U}}(\pi,0) = \begin{pmatrix} 0 & 1 \\ -1 & 0 \end{pmatrix} \tag{2.24}$$

In addition, the quantum strategy $\widehat{Q}$ is given by

$$\widehat{Q} := \hat{\mathcal{U}}(0,\pi/2) = \begin{pmatrix} i & 0 \\ 0 & -i \end{pmatrix} \quad . \tag{2.25}$$

To illustrate the operator formalism of quantum game theory and the concept of quantum strategies, figure 2.20 displays the real and imaginary values of the two spinor components ψ_1^A and ψ_2^A of the of the state $|\psi\rangle_A$ of player A:

$$|\psi\rangle_A = \psi_1^A \left|s_1^A\right\rangle + \psi_2^A \left|s_2^A\right\rangle = \begin{pmatrix} \psi_1^A \\ -\psi_2^A \end{pmatrix} \in \mathcal{H}_A \tag{2.26}$$

$$\left|s_1^A\right\rangle = \begin{pmatrix} 1 \\ 0 \end{pmatrix}, \ \left|s_2^A\right\rangle = \begin{pmatrix} 0 \\ -1 \end{pmatrix}$$

$|\psi\rangle_A$, the decision state of player A, is formally constructed as a matrix-vector multiplication of the decision operator $\widehat{\mathcal{U}}(\theta_A, \varphi_A)$ acting on the initial state $\left|s_1^A\right\rangle$:

$$|\psi\rangle_A = \widehat{\mathcal{U}}(\theta_A, \varphi_A) \left|s_1^A\right\rangle = \begin{pmatrix} e^{i\,\varphi_A} \cos(\frac{\theta_A}{2}) \\ -\sin(\frac{\theta_A}{2}) \end{pmatrix} \tag{2.27}$$

$$\psi_1^A = e^{i\,\varphi_A} \cos(\frac{\theta_A}{2}) \,, \ \psi_2^A = \sin(\frac{\theta_A}{2})$$

The solid, colored surface in figure 2.20 depicts the real part of the first spinor component ($\mathrm{Re}(\psi_1^A)$), the wired grey surface describes its imaginary part ($\mathrm{Im}(\psi_1^A)$) and the solid grey surface shows the real part of the second component ($\mathrm{Re}(\psi_2^A)$) as a function of the two strategy angles θ_A and φ_A. As the imaginary part of ψ_2^A

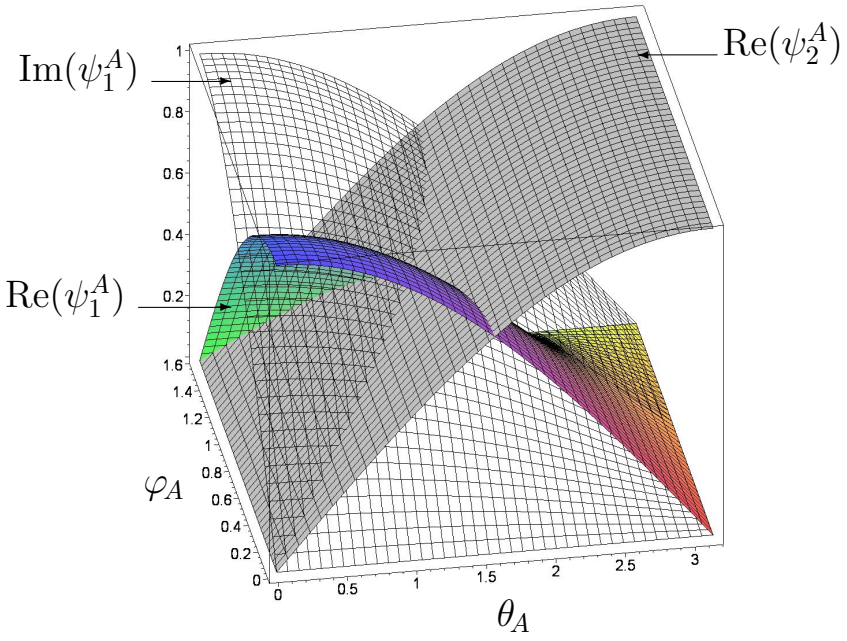

Figure 2.20.: Real and imaginary values of the spinor components of the state $|\psi\rangle_A = \widehat{\mathcal{U}}(\theta_A, \varphi_A) \left|s_1^A\right\rangle$ as a function of the two strategy angles θ_A and φ_A.

is identical to zero, figure 2.20 visualized only three surfaces.

The set of classical mixed strategies of player A ($\tilde{\mathcal{S}}^A = \left\{\tilde{s}_1^A, \tilde{s}_2^A\right\}$) is a subset of the Hilbertspace $\mathcal{H}_A$ (angle φ_A is identical zero):

$$\tilde{\mathcal{S}}^A = \left\{ |\psi\rangle_A = \widehat{\mathcal{U}}(\theta_A, \varphi_A) \left|s_1^A\right\rangle \;|\; \varphi_A \equiv 0\,,\; \theta_A \in [0, \pi] \right\} \subsetneq \mathcal{H}_A \tag{2.28}$$

The imaginary part of the state $|\psi\rangle_A$ is zero for $\varphi_A \equiv 0$ and as a result the different classical mixed strategies can be obtained by arranging the angle $\theta \in [0, \pi]$. However for $\varphi_A > 0$ the imaginary part of the first component ψ_1^A of the spinor $|\psi\rangle_A$ is not zero and these kind of quantum strategies cannot be found in the theory of classical games. As the imaginary part of the state $|\psi\rangle_A$ is only present within its first component ψ_1^A, these quantum strategies are named

s_1-quantum strategies. By exchanging the basis s_1 to s_2 it is possible to describe also s_1-quantum strategies (for details see section 2.6.3).

After the two players have chosen their individual quantum strategies ($\hat{\mathcal{U}}_A := \hat{\mathcal{U}}(\theta_A, \varphi_A)$ and $\hat{\mathcal{U}}_B := \hat{\mathcal{U}}(\theta_B, \varphi_B)$) the disentangling operator $\widehat{\mathcal{J}}^\dagger$ is acting to prepare the measurement of the players' state. The entangling and disentangling operator ($\widehat{\mathcal{J}}, \widehat{\mathcal{J}}^\dagger$; with $\hat{\mathcal{J}} \equiv \hat{\mathcal{J}}^\dagger$) depends on one additional single parameter γ which measures the strength of the entanglement of the system:

$$\widehat{\mathcal{J}} := e^{i\frac{\gamma}{2}(\widehat{s_1}\otimes\widehat{s_1})} \ , \quad \gamma \in [0, \frac{\pi}{2}] \tag{2.29}$$

In the used representation, the entangling operator $\widehat{\mathcal{J}}$ has the following explicit structure:

$$\widehat{\mathcal{J}} := \begin{pmatrix} \cos\left(\frac{\gamma}{2}\right) & 0 & 0 & i\sin\left(\frac{\gamma}{2}\right) \\ 0 & \cos\left(\frac{\gamma}{2}\right) & -i\sin\left(\frac{\gamma}{2}\right) & 0 \\ 0 & -i\sin\left(\frac{\gamma}{2}\right) & \cos\left(\frac{\gamma}{2}\right) & 0 \\ i\sin\left(\frac{\gamma}{2}\right) & 0 & 0 & \cos\left(\frac{\gamma}{2}\right) \end{pmatrix} \tag{2.30}$$

Finally, the state prior to detection can therefore be formulated as follows:

$$|\Psi\rangle = \hat{\mathcal{J}}^\dagger \left(\hat{\mathcal{U}}_A \otimes \hat{\mathcal{U}}_B\right) \hat{\mathcal{J}} \left|s_1^A s_1^B\right\rangle \tag{2.31}$$

The expected payoff within a quantum version of a general 2-player game depends on the payoff matrix (see table 2.6) and on the joint probability to observe the four observable outcomes P_{11}, P_{12}, P_{21} and P_{22} of the game

$$\begin{aligned} \$_A \quad &= \$_{11}^A P_{11} + \$_{12}^A P_{12} + \$_{21}^A P_{21} + \$_{22}^A P_{22} \\ \$_B \quad &= \$_{11}^B P_{11} + \$_{12}^B P_{12} + \$_{21}^B P_{21} + \$_{22}^B P_{22} \\ \text{with:} \quad & P_{\sigma\sigma'} = |\langle\sigma\sigma'|\Psi\rangle|^2 \ , \quad \sigma, \sigma' = \{s_1, s_2\} \quad . \end{aligned} \tag{2.32}$$

It should be pointed out here, that an entangled 2-player quantum state does not mean at all that the persons themselves (or even the players' brains) are entangled.

The process of quantum decoherence, with its quantum to classical transition, forbid such macroscopic entangled systems established from microscopic quantum particles [199, 140]. However, peoples' cogitation, represented as quantum strategies, could be associated within an abstract space. Although no measurable accord is present between the players' strategy choices, the imaginary parts of their strategy wave functions might interact, if their individual states are entangled. Such an interaction might be interpreted as a conjoint, psychological contract between the players aligning their strategies and possibly resulting from social norms, moral standards and other impacts of socio-economic context factors. Such an alignment is now formulated as the appearance of a strongly entangled strategy effectuating the players to act more like a collective state.

To analyze the different game classes of quantum games the extended mixed strategy payoff function of player A ($\$_A$) and player B ($\$_B$) (see equation (2.32)) will be visualized in the following. In contrast to the classical mixed payoff functions ($\tilde{\$}^A(\tilde{s}^A, \tilde{s}^B)$ and $\tilde{\$}^B(\tilde{s}^A, \tilde{s}^B)$), which depend only on the two parameters $\tilde{s}^A$ and $\tilde{s}^B$, the quantum version of the mixed strategy payoff function depends in general on five parameters; namely the four decision angles of player A and player B ($\theta_A, \varphi_A, \theta_B$ and φ_B) and the entangling parameter γ.

In order to visualize the payoff function as a surface in a three dimensional space it is necessary to reduce the set of parameters in the final state: $|\Psi\rangle = |\Psi(\theta_A, \varphi_A, \theta_B, \varphi_B)\rangle \rightarrow |\Psi(\tau_A, \tau_B)\rangle$. Within the following diagrams we have used the same specific parameterization as Eisert et al. [66], where the two strategy angles θ and φ depend only on a single parameter $\tau \in [-1, 1]$.[5] Positive τ-values represent pure and mixed classical strategies, whereas negative τ-values correspond to quantum strategies, where $\theta = 0$ and $\varphi > 0$. The whole strategy space is separated into four regions, namely the absolute classical region (*ClCl*: $\tau_A, \tau_B \geq 0$), the absolute quantum region (*QuQu*: $\tau_A, \tau_B < 0$) and the two partially classical-quantum regions (*ClQu*: $\tau_A \geq 0 \wedge \tau_B < 0$ and *QuCl*: $\tau_A < 0 \wedge \tau_B \geq 0$). It should be mentioned that within the (τ_A, τ_B)-representation the set of possible strategies $\{(\theta, \varphi) \mid \theta \in [0, \pi]\,,\ \varphi \in [0, \frac{\pi}{2}]\}$ is reduced to the

[5] The parameter τ corresponds to parameter t of [66].

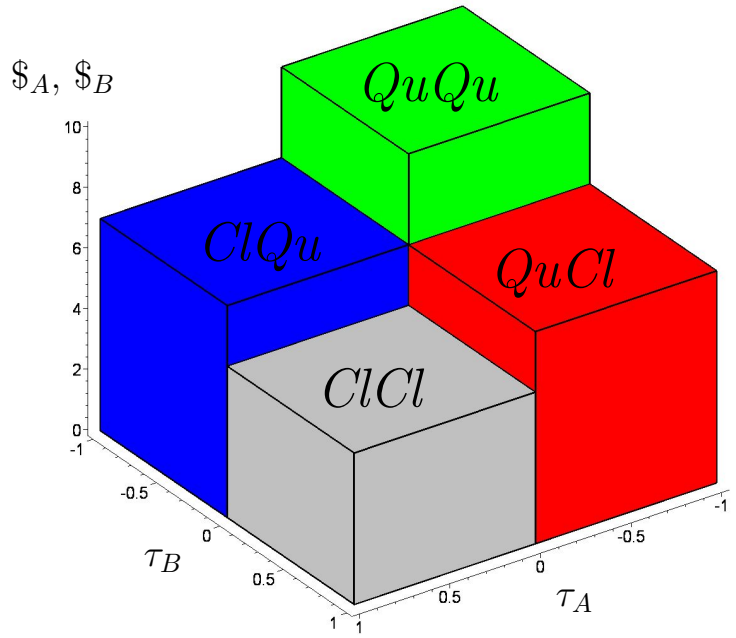

Figure 2.21.: Payoff visualization space as a function of the reduced s_1-quantum strategies τ_A of player A and τ_B of player B.

following specific subset:

$$\underbrace{\{(\tau\,\pi, 0) \mid \tau \in [0,1]\}}_{\text{classical region } Cl} \;\wedge\; \underbrace{\{(0, \tau\,\frac{\pi}{2}) \mid \tau \in [-1,0[\}}_{\text{quantum region } Qu} \tag{2.33}$$

Figure 2.21 visualizes the different regions of the reduced quantum strategy space τ_A and τ_B. The fully classical region in the front of the diagram ($ClCl$) describes the non-interfering classical outcome ($\varphi_A, \varphi_B \equiv 0$) and where the reduced strategies τ_A and τ_B describe the classical mixed strategies of player A and B. The visualization space of the extended mixed strategy payoff function of player A ($\$_A(\tau_A, \tau_B)$) and player B ($\$_B(\tau_A, \tau_B)$) will be displayed in the following sections within the reduced quantum strategy space of figure 2.21.

Before the presentation of the theoretical results of symmetric (two player)-(two

strategy) quantum games starts within the following subsection, a short summary of "Quantum Experimental Data in Psychology and Economics" [17] is mentioned. Some new articles in the field of psychology use quantum logical concepts to explain psychological experimental data. Their analysis puts forward a strong argument in favor of the validity of using the quantum formalism for modeling these psychological experimental data. The considered psychological experiments mostly belong to the field of human concept and decision theory.

D. Aerts and colleagues have analysed membership weights for concepts [17, 14, 9, 8, 15, 12, 11, 9, 16]. For example, the concepts "Home Furnishings" and "Furniture" and their disjunction "Home Furnishings or Furniture" were considered. Within their experiment they ask subjects if they think the item "Ashtray" belongs to these concepts. Subjects rated the membership weight of Ashtray for the concept "Home Furnishings" as 0.7 and for the concept "Furniture" as 0.3. However, the membership weight of Ashtray with respect to the disjunction "Home Furnishings or Furniture" was rated as only 0.25. For other concepts and items they have found a different situation. For example, the concepts "Fruits" and "Vegetables" and their disjunction "Fruits or Vegetables" and the item "Olive" were considered . Subjects rated the membership weight of Olive for the concept "Fruits" as 0.5 and for the concept "Vegetables" as 0.1, but however now, the membership weight of Olive with respect to the disjunction "Fruits or Vegetables" was rated as 0.8. Similar as in quantum game theory, D. Aerts and colleagues formulate the subjects (here subject μ) decision state with the use of a quantum wave function $|\psi\rangle_\mu$. They show that the experimental setting is similar to the famous "double-slit experiment" of quantum mechanics [9]. The situation where only one of the two slits are opened corresponds to singular concepts (e.g. concept "Fruits" and concept "Vegetables"), whereas the disjunction "Fruits or Vegetables" corresponds to the experimental situation where both slits are opened. Within the article "Experimental Evidence for Quantum Structure in Cognition" [13] the authors conclude their analysis with the following statement: "The violation of the classical weight structure is similar to the violation of the well-known Bell inequalities studied in quantum mechanics, and hence suggests that the quantum formalism and hence the modeling by quantum membership weights, as for example in [9], can accomplish what classical membership weights cannot do."

Psychological experiments in the field of decision science also indicate violations of "classical (rational)" decision theory (see e.g. [40, 41, 187, 188, 42, 241, 55]. J.R. Busemeyer and colleagues focus on two experimental tasks in psychology, namely the two-stage gambling game and the prisoner's dilemma game. The two-stage gambling game bases on an experimental setting performed by A. Tversky & E. Shafir in the year 1992 [227]: "Participants were told that they had just played a gamble (even chance to win 200 dollars or lose 100 dollars), and then they were asked to choose whether to play the same gamble a second time. In one condition, they knew they won the first play; in a second condition, they knew they lost the first play; and in a third condition, they did not know the outcome." Within their experimental study, Tversky & Shafir found that 69% of the participants accept the second gamble if they knew that they had won the first one, 59% accept the second gamble if they knew they had lost the first one, however when the outcome was unknown, the participants accepted the second gamble only with a percentage 39%. Within their article Tversky & Shafir conclude, that the experimental facts violate the Savage's-"sure-thing principle" [197][6] which is fundamental to classical decision theory—and they call this effect the "disjunction effect". In addition to this two-stage gambling game Tversky & Shafir also focus on another example of a disjunction effect in a one-shot prisoner's dilemma game. They compare the measured cooperation percentages in the sequential version with the cooperation percentage in the simultaneous version of the one-shot prisoner's dilemma game. They found that the rate of cooperation was 3% when subjects knew that the opponent had defected, and 16% when they knew that the opponent had cooperated. However, when subjects did not know whether their opponent had cooperated or defected, the rate of cooperation rose to 37%. Again, they conclude that the data suggest that the observed cooperation in a one-shot prisoner's dilemma game might be due to the disjunction effect. Within the article "A quantum probability explanation for violations of 'rational' decision theory" [187] E.M. Pothos & J.R. Busemeyer explained this effect by using a quantum theoretical description of the underlying decision problem and conclude that quantum probability provides a better framework for modeling human decision-making. Beside the presented

[6] Definition of the Savage's-"sure-thing principle" [197]: If x is preferred to y knowing that event A obtained, and if x is preferred to y knowing that A did not obtain, then x should be preferred to y even when it is not known whether A obtained.

studies, several other analysis have used a quantum theoretical model to explain experimental data in psychology and economics [112, 119, 241, 55] (see also the review articles [39, 17]).

2.4.3. Results for symmetric quantum games

This section is dedicated to summarize the results of the quantum version of symmetric (two player)-(two strategy) games. The main aim of this section is to compare the classical version of games with their quantum extensions and analyze the structure of the existing Nash equilibria of quantum games with different values of entanglement. The results of the quantum extension of the different classes of games, parameterized through the eleven sets of table 2.3, are summarized within the following three subsections. All of the diagrams discussed within the following subsections can be found in appendix B.VI.

Dominant games

The following diagram (figure 2.22) describes the payoff structure of player A (solid surface) and player B (wired surface) within parameter set Set_3 for a non-entangled quantum game ($\gamma = 0$). $\$_A$ and $\$_B$ are visualized as a function of the reduced s_1-quantum strategies τ_A of player A and τ_B of player B. In the figure the absolute quantum region $QuQu$ is projected in the back, whereas the absolute classical region $ClCl$ is projected to the front.

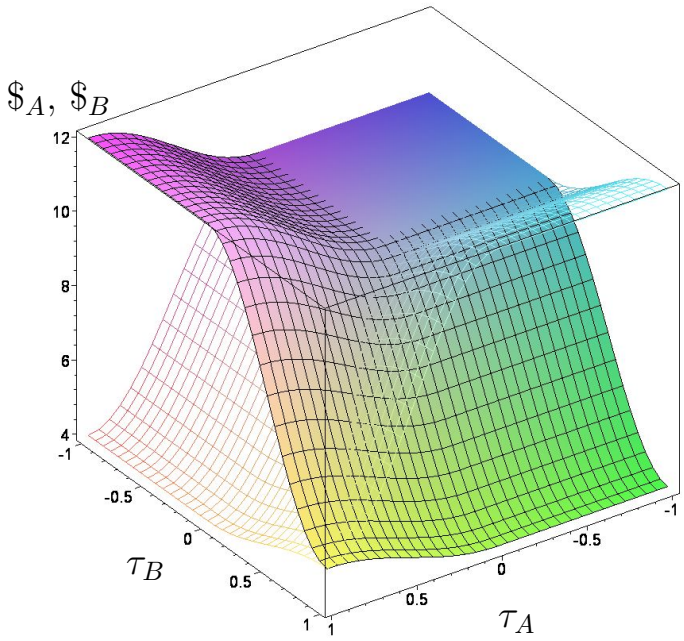

Figure 2.22.: Payoff surface of player A (solid) and player B (wired) as a function of their reduced s_1-quantum strategies τ_A and τ_B within a non-entangled quantum game ($\gamma = 0$) using the parameter setting Set_3 of the dominant prisoner's dilemma game.

The diagram clearly exhibits that the non-entangled quantum game simply describes the classical version of the prisoner's dilemma game parameterized through parameter set Set_3. For the case, that both players decide to play a quantum strategy ($\tau_A < 0 \wedge \tau_B < 0$) their payoff is equal to the case where both players choose the classical pure strategy s_1 ($\$_A(\tau_A = 0, \tau_B = 0) = 10$, $\$_B(\tau_A = 0, \tau_B = 0) = 10$). The classical NE ($(s_2^A, s_2^B)$, the dominant strategy) correspond to the following τ-values:$(s_2^A, s_2^B) \hat{=} (\tau_A = 1, \tau_B = 1)$.

Figure 2.23 shows the payoff surfaces within set Set_3 for a quantum game with a low value of entanglement. The corresponding value within the left picture is $\gamma = \frac{\pi}{10} \approx 0.31$, whereas the entanglement within the right picture is $\gamma = \frac{\pi}{5} \approx 0.63$. For the absolute classical region $ClCl$ the shape of the

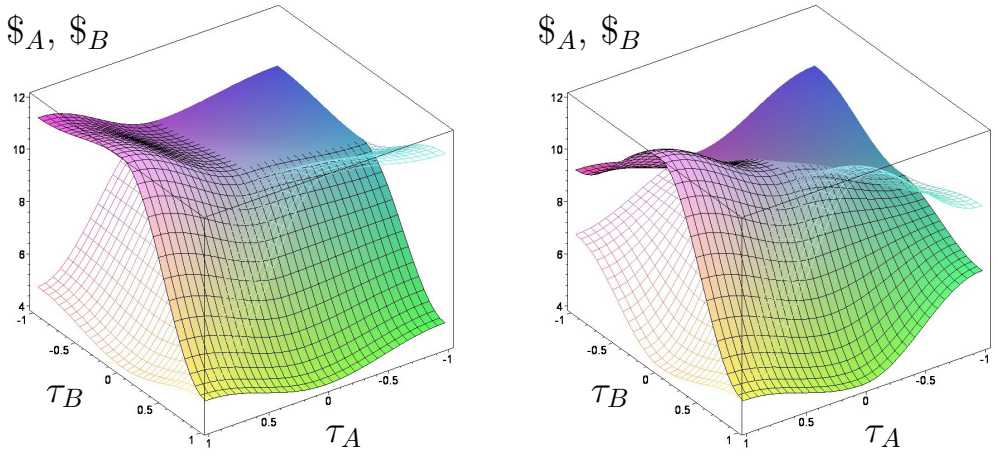

Figure 2.23.: Payoff surface of player A (solid) and player B (wired) as a function of their reduced s_1-quantum strategies τ_A and τ_B within two low-entangled quantum games (Left: $\gamma = \frac{\pi}{10}$, Right: $\frac{\pi}{5}$) using the parameter setting Set_3.

surfaces does not change, whereas for the partially classical-quantum (*ClQu* and *QuCl*) and absolute quantum (*QuQu*) regions the payoff structure changes, due to a possible interference of quantum strategies within Hilbertspace. The structure of Nash equilibria does not change for the left picture, whereas for the right picture the previously present dominant strategy of the prisoner's dilemma game has disappeared and a new, advisable quantum NE has appeared $(\widehat{Q}, \widehat{Q} \hat{=} (\tau_A = -1, \tau_B = -1))$. During the transition from the left to the right picture of figure 2.23 two separate phenomena have occurred. At first, for an entanglement value $\gamma_1 \approx 0.361$, the best response to the strategy $s_2^B \hat{=} \tau_B = 1$ for player A is no longer the strategy $s_2^A \hat{=} \tau_A = 1$, as $\$_A(\tau_A = -1, \tau_B = 1) \approx 5.05$ is now higher than $\$_A(\tau_A = 1, \tau_B = 1) = 5$. Secondly, for an entanglement value $\gamma_2 \approx 0.524$, the best response for player A to the strategy $\widehat{Q}_B \hat{=} \tau_B = -1$ is no longer the strategy $s_2^A \hat{=} \tau_A = 1$, as $\$_A(\tau_A = 1, \tau_B = -1) \approx 9.96$ is for $\gamma_2 \approx 0.524$ lower than $\$_A(\tau_A = -1, \tau_B = -1) = 10$. The exact values of the two entanglement thresholds γ_1 and γ_2 can be calculated for general symmetric

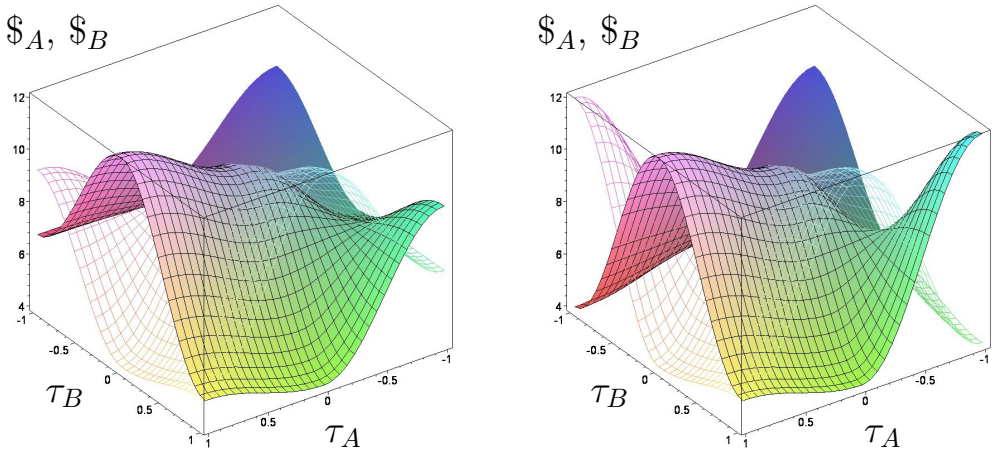

Figure 2.24.: Payoff surface of player A (solid) and player B (wired) as a function of their reduced s_1-quantum strategies τ_A and τ_B within two highly-entangled quantum games (Left: $\gamma = \frac{3\pi}{10}$, Right: $\frac{\pi}{2}$) using the parameter setting Set_3.

(two player)-(two strategy) games (see appendix B.V). The results show, that a quantum extension of a classical prisoner's dilemma game can change the structure of Nash equilibria and even previously present dominant strategies could become nonexistent if the value of entanglement increases further than a defined γ-threshold. Players with a strategic entanglement value $\gamma = \frac{\pi}{5} \approx 0.63$ (see right picture of figure 2.23) escape the dilemma as they see the advantage of the quantum strategy combination $(\widehat{Q}_A, \widehat{Q}_B)$, which is observed (measured) as both are playing the classical strategy s_1.

Figure 2.24 visualizes the payoff structure within set Set_3 for quantum games with a high value of entanglement (left picture $\gamma = \frac{3\pi}{10} \approx 0.94$, right picture $\gamma = \frac{\pi}{2} \approx 1.57$). The two pictures show, that the structure of the Nash equilibria does not change (in respect to the results for $\gamma = \frac{\pi}{5}$) if one increases γ even further.

Figure 2.25 shows the results of the non-entangled (left picture) and maximally entangled (right picture) quantum game of parameter set Set_2. Again, the non-

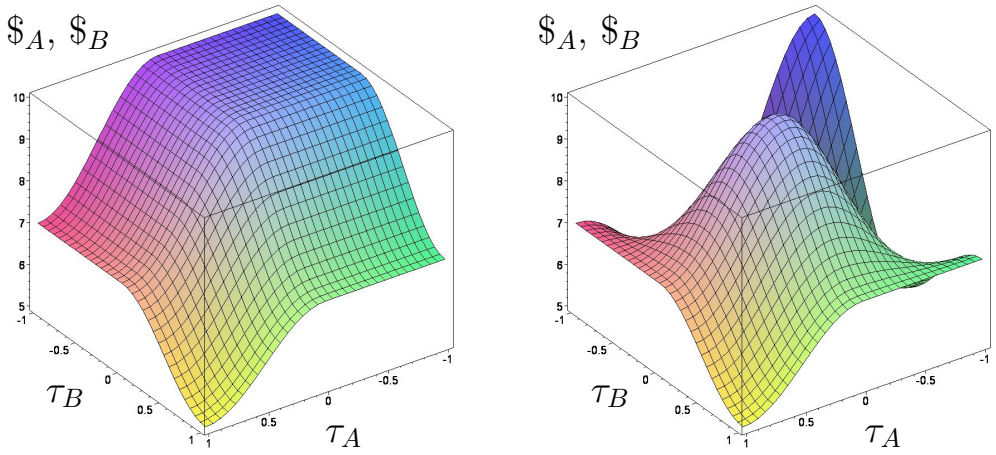

Figure 2.25.: Payoff surface of player A as a function of the reduced s_1-quantum strategies τ_A and τ_B within a non-entangled ($\gamma = 0$, left picture) and maximally entangled quantum game ($\gamma = \frac{\pi}{2}$, right picture) using the parameter setting Set_2.

entangled quantum version of Set_2 simply reproduces the results of the classical version of the game. The pure classical strategy s_1 remains to be the dominant strategy of the game. In contrast to the results of set Set_3, the dominant strategy also remains if one increases the value of γ (see figure B.20 in appendix B.VI). Even for the maximally entangled quantum game (see right picture of figure 2.25) the only NE and dominant strategy is the s_1-strategy, as the measured quantum strategy in the back of the *QuQu*-region ($\tau_A = -1, \tau_B = -1$) is also observed as an (s_1^A, s_1^B)-strategy combination. The underlying reason for this behavior is the lack of a dilemma within the dominant game of parameter set Set_2.

Figure 2.26 shows the results of the non-entangled (left picture) and maximally entangled (right picture) quantum game of set Set_1. Only because of a better visibility, the viewpoint of the three dimensional diagrams have been changed within the two pictures of figure 2.26: The *QuQu*-region is projected to the front, whereas the *ClCl*-region is now at the back. The dominant strategy within the non-entangled game is at ($\tau_A = 1, \tau_B = 1$) which corresponds to the

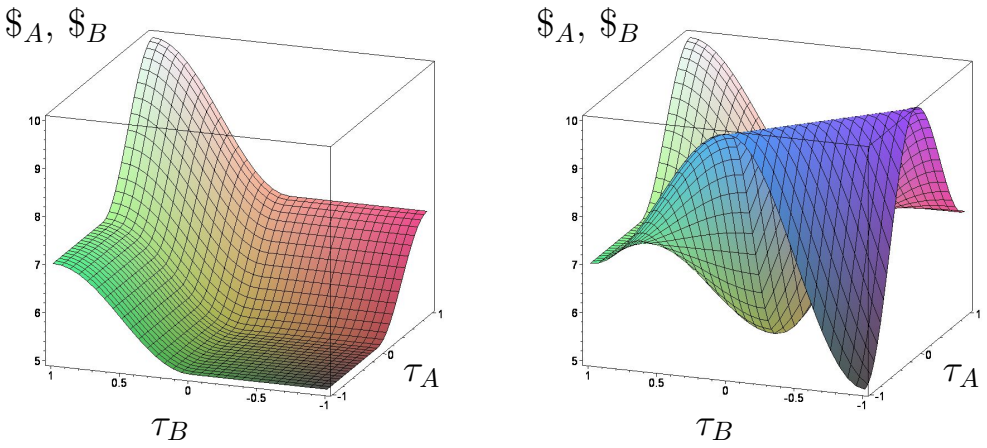

Figure 2.26.: Payoff surface of player A as a function of the reduced s_1-quantum strategies τ_A and τ_B within a non-entangled ($\gamma = 0$, left picture) and maximally entangled quantum game ($\gamma = \frac{\pi}{2}$, right picture) using the parameter setting Set_1.

classical dominant strategy (s_2^A, s_2^B) of parameter setting Set_1. Similar as in Set_2, an increase of entanglement does not change the structure of the existing Nash equilibria and dominant strategy of the game (see figure B.19 in appendix B.VI). The diagonal plateau of the payoff surface within the $QuQu$-region of the maximally entangled quantum game (see right picture of figure 2.26) is a so called s_2-plateau, as the observed strategy is for both players the s_2 strategy.

The study of quantum games within the dominant class of symmetric (two player)-(two strategy) games has shown, that only the subclass of dominant games with a dilemma change their NE structure when increasing the value of entanglement. The example of the prisoner's dilemma has indicated, that entanglement barriers exist (γ_1 and γ_2) where the games dilemma dissolves and a new quantum NE (dominant strategy) appears. The values of the entanglement threshold depend on the specific payoff parameters of the game and not only on the parameters on a and b of the transformed payoff matrix (see table 2.1).

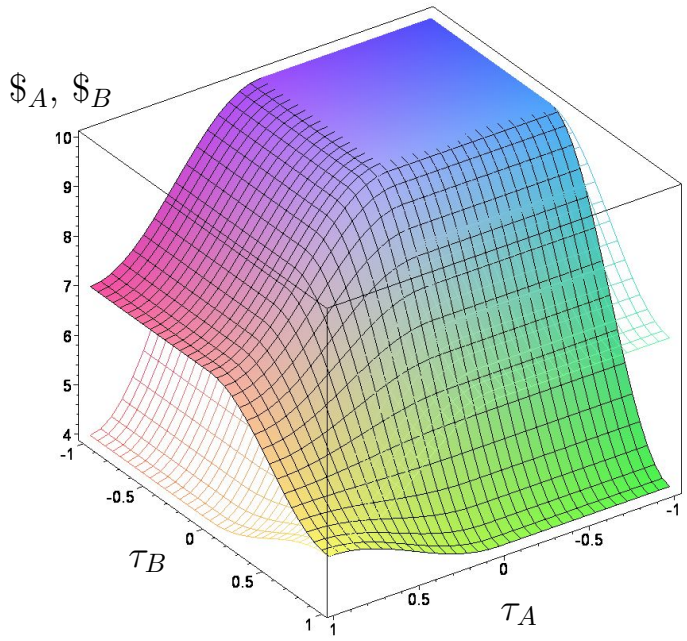

Figure 2.27.: Payoff surface of player A (solid) and player B (wired) as a function of their reduced s_1-quantum strategies τ_A and τ_B within a non-entangled quantum game ($\gamma = 0$) using the parameter setting Set_5 of an coordination game.

Coordination games

Figure 2.27 describes the payoff structure of player A (solid surface) and player B (wired surface) within parameter set Set_5 for a non-entangled quantum game ($\gamma = 0$). Again, the diagram clearly indicates that the non-entangled quantum game is identical to the classical version of the underlying coordination game parameterized through parameter setting Set_5. For the case, that both players decide to play a quantum strategy ($\tau_A < 0 \wedge \tau_B < 0$) their payoff is equal to the case where both players choose the classical pure strategy s_1 ($\$_A(\tau_A = 0, \tau_B = 0) = 10$), with the overall highest possible payoff. The classical pure Nash equilibria correspond to the following τ-values: $(s_1^A, s_1^B) \hat{=} (\tau_A = 0, \tau_B = 0)$ and $(s_2^A, s_2^B) \hat{=} (\tau_A = 1, \tau_B = 1)$, whereas the classical mixed strategy equilibrium is at: $\tau^\star = \frac{2}{\pi}\arccos(\sqrt{\frac{1}{4}}) = \frac{2}{3}$. The corresponding τ-value have been calculated as the

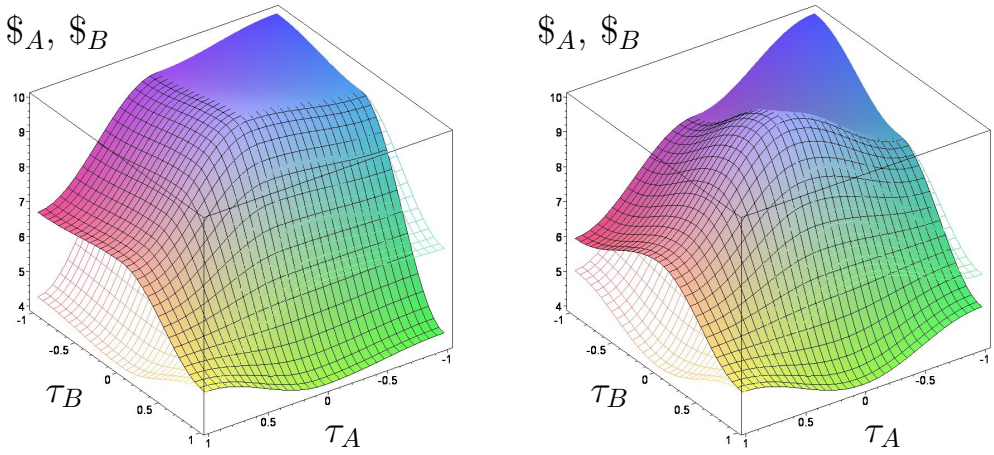

Figure 2.28.: Payoff surface of player A (solid) and player B (wired) as a function of their reduced s_1-quantum strategies τ_A and τ_B within two low-entangled quantum games (Left: $\gamma = \frac{\pi}{10}$, Right: $\frac{\pi}{5}$) using the parameter setting Set_5.

probability value $\psi_1(\psi_1)^*$ of measuring the classical s_1-strategy using equation (2.27):[7]

$$s^\star = \psi_1(\psi_1)^* = \left(\cos(\frac{\theta^\star}{2})\right)^2 = \left(\cos(\frac{\pi\,\tau^\star}{2})\right)^2 \Leftrightarrow \tau^\star = \frac{2}{\pi}\arccos(\sqrt{s^\star}) \qquad (2.34)$$

Figure 2.28 shows the payoff surfaces within set Set_5 for a quantum game with a low value of entanglement. The corresponding value within the left picture is $\gamma \approx 0.31$, whereas the entanglement within the right picture is $\gamma \approx 0.63$. Even for tiny values of entanglement (see left picture of figure 2.28) a new quantum NE appears ($\widehat{Q}, \widehat{Q} \hat{=} (\tau_A = -1, \tau_B = -1)$).[8] The strength of entanglement at the right picture of figure 2.28 is just slightly above the value, where the old low payoff NE disappears ($\gamma_1 \approx 0.6155$). For $\gamma \geq \gamma_1$ the game's only NE and ESS is the new quantum ESS.

[7] Here, $(\psi_1)^*$ is the conjugate value of ψ_1.

[8] The γ_2-value (see appendix B.V) has purely imaginary values, which means that coordination games in general have formally a γ_2-threshold of zero.

Figure 2.29 visualizes the payoff structure within set Set_5 for a quantum game with a high value of entanglement (left picture $\gamma = \frac{3\pi}{10} \approx 0.94$, right picture $\gamma = \frac{\pi}{2} \approx 1.57$. The two pictures show, that the structure of the Nash equilibria does not change again (in respect to the results for $\gamma = \frac{\pi}{5}$) if one increases γ even further.

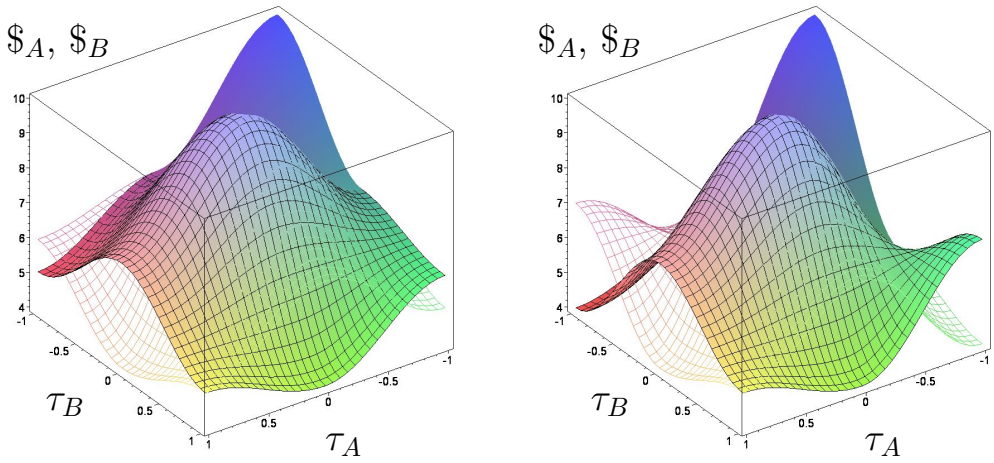

Figure 2.29.: Payoff surface of player A (solid) and player B (wired) as a function of their reduced s_1-quantum strategies τ_A and τ_B within two highly-entangled quantum games (Left: $\gamma = \frac{3\pi}{10}$, Right: $\frac{\pi}{2}$) using the parameter setting Set_5.

To illustrate that the existence of NE in quantum games is not invariant under linear payoff transformations (see table 2.1), the figures B.24 and B.25 compare the results for quantum games within parameter set Set_6 and Set_7. The figures show that the γ-threshold (and therefore the existence of quantum Nash equilibria) does depend on all payoff parameters and not only on a and b of the transformed game. While the outcome predictions of the classical version of Set_6 and Set_7 are identical, the quantum versions give different results for both parameter sets (Set_6: $\gamma_1 \approx 0.7137$ and Set_7: $\gamma_1 \approx 0.5236$). This difference could be tested experimentally (see also 2.6.4).

Anti-coordination games

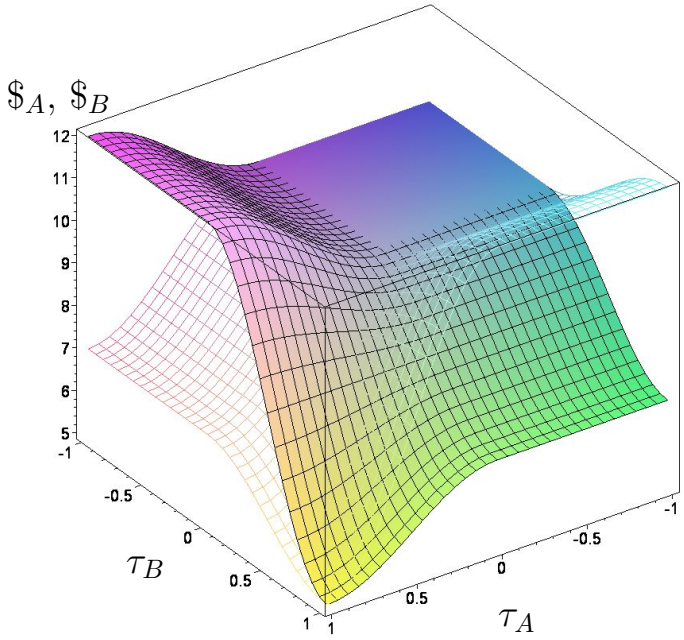

Figure 2.30.: Payoff surface of player A (solid) and player B (wired) as a function of their reduced s_1-quantum strategies τ_A and τ_B within a non-entangled quantum game ($\gamma = 0$) using the parameter setting Set_8 of an anti-coordination game.

Figure 2.30 describes the payoff structure of player A (solid surface) and player B (wired surface) within parameter set Set_8 for a non-entangled quantum game ($\gamma = 0$). Again, the diagram shows that the non-entangled quantum game is identical to the classical version of the underlying anti-coordination game parameterized through parameter setting Set_8. For the case, that both players decide to play a quantum strategy ($\tau_A < 0 \wedge \tau_B < 0$) their payoff is equal to the case where both players choose the classical pure strategy s_1 ($\$_A(\tau_A = 0, \tau_B = 0) = 10 = \$_B(\tau_A = 0, \tau_B = 0)$). The classical pure, asymmetric Nash equilibria correspond to the following τ-values: $(s_1^A, s_2^B) \hat{=} (\tau_A = 0, \tau_B = 1)$ and

$(s_2^A, s_1^B) \hat{=} (\tau_A = 1, \tau_B = 0)$, whereas the classical mixed strategy equilibrium is at: $\tau^\star = \frac{2}{\pi}\arccos(\sqrt{\frac{1}{2}}) = \frac{1}{2}$. The corresponding τ-value have been calculated as the probability value $\psi_1(\psi_1)^*$ of measuring the classical s_1-strategy using the equations (2.27) and (2.34).

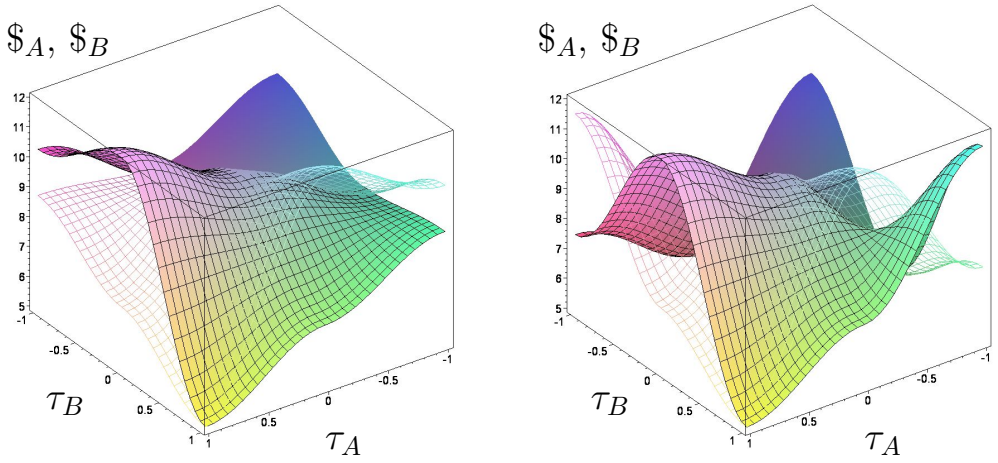

Figure 2.31.: Payoff surface of player A (solid) and player B (wired) as a function of their reduced s_1-quantum strategies τ_A and τ_B within a low-entangled (Left: $\gamma = \frac{\pi}{5}$) and a highly entangled quantum (Right: $\gamma = \frac{2\pi}{5}$) using the parameter setting Set_8.

The pictures within figure 2.31 show the results of parameter setting Set_8 for a low and medium value of entanglement. The results indicate, that beside the classical mixed strategy ESS a new quantum ESS appears at a specific γ-value ($\gamma_2 \approx 0.685$), which is between the γ-value of the left and right picture.[9] The results for the other parameter sets of anti-coordination games are summarized in appendix B.VI. A detailed description of a quantum extension of an anti-coordination game can be found in subsection 2.6.3.

[9] The γ_1-threshold (see appendix B.V) has purely imaginary values, which means that anti-coordination games in general have formally a γ_1-threshold of zero.

2.5. Evolutionary Quantum Game Theory

Within the previous section different versions of quantum games and the existence of new Nash equilibria and ESS's where discussed. However, the dynamical behavior of QGT and therefore the amplification of classical replicator dynamics (see equation (2.13)) was not addressed. Quantum replicator dynamics (QRD), recently developed and discussed by E.G. Hidalgo [95, 96] (see also Toor et. al. [138, 169]) was formulated within the density matrix approach of quantum game theory [162]. QRD employs the von Neumann equation, which describes how a quantum density operator evolves in time. In order to reveal that the von Neumann equation is simply a quantum amplification of classical replicator dynamics (see equation (B.10)), Hidalgo had reformulated equation (2.13) to a matrix equation. Constraining to only two possible pure strategies equation (2.13) can be formulated as follows [95]:

$$\frac{d}{dt}\widehat{X} = \left[\widehat{\Lambda}, \widehat{X}\right] \tag{2.35}$$

$$\widehat{X} := \begin{pmatrix} x_1 & \sqrt{x_1\, x_2} \\ \sqrt{x_2\, x_1} & x_2 \end{pmatrix} \quad \widehat{\Lambda} := \begin{pmatrix} \Lambda_{11} & \Lambda_{12} \\ \Lambda_{21} & \Lambda_{22} \end{pmatrix}$$

$$\Lambda_{ij} := \tfrac{1}{2} \sum_{k=1}^{n=2} \left(\$_{ik}\, x_k \sqrt{x_i\, x_j} - \sqrt{x_j\, x_i}\, \$_{jk}\, x_k \right)$$

, where the matrix $\widehat{X}$ is an amplification of the population vector $\vec{x} = (x_1, x_2)$, $\left[\widehat{a}, \widehat{b}\right] := \widehat{a}\widehat{b} - \widehat{b}\widehat{a}$ is the commutator of the two matrices $\widehat{a}$ and $\widehat{b}$ and $\widehat{\Lambda}$ is a payoff dependent (2×2)-matrix. The quantum amplification of classical replicator dynamics is realized by the substitution of $\widehat{X}$ to the density matrix $\widehat{\rho}$ and the interpretation of $\widehat{\Lambda}$ as the Hamilton Operator $\widehat{E}$ of the quantum system

$$E_{ij} := \frac{1}{2} \sum_{k=1}^{n=2} \left(\$_{ik}\, \rho_{kk}\, \rho_{ij} - \rho_{ji}\, \$_{jk}\, \rho_{kk} \right) \quad . \tag{2.36}$$

Quantum replicator dynamics as an extension of equation (2.13) and (2.35) is described with the "von Neumann equation"

$$\frac{d}{dt}\widehat{\rho} = \sigma \left[\widehat{E}, \widehat{\rho}\right] \quad , \tag{2.37}$$

where σ is a certain quantisation constant.[10] The mathematical structure of this approach has its origin in the Hamiltonian formulation of classical evolutionary game theory [127] and might be a special example of the multi-agent projector matrix formulation suggested by Gafiychuk and Prykarpatsky [82, 81]. The numerical simulation of equation (2.37) and therefore the time evolution of a quantum game will be addressed in a separate article.

2.6. Applications

Before the summarization of the main results of QGT and EQGT, several applications of the presented theory are discussed within this section.

2.6.1. Article 1: Quantum Game Theory and Open Access Publishing

The results of the first application where primarily, in the year 2006, released as a paper on the ArXiv-repository. After some improvements, the article was later published by *Physica A* [111].

In chapter 3 the article is attached to this dissertation. The main results are briefly discussed within subsection 1.2.6 of the German summary (chapter 1).

2.6.2. Article 2: Evolutionary Quantum Game Theory and Scientific Communication

The scientific article of the second application is available through the conference internetpage of the "Second Brasilian Workshop of the Game Theory Society *In honor of John Nash, on occasion of the 60th anniversary of Nash equilibrium* ", which was held in São Paulo (Brazil) from the 29th July until the 4th August in the year 2010. Additionally the article and further material is located at `http://evolution.wiwi.uni-frankfurt.de/BWGT2010/`.

[10] The von Neumann equation usually describes how a quantum density operator $\widehat{\rho}$ evolves over time, where $\sigma := \frac{1}{i\hbar}$. In quantum replicator dynamics σ shall be deemed to be a certain constant.

In chapter 4 the article is attached to this dissertation. The main results are briefly discussed within subsection 1.2.6 of the German summary (chapter 1).

2.6.3. Article 3: Doves and Hawks in Economics Revisited: An evolutionary quantum game theory-based analysis of financial crises

The results of the third application where primarily (April 2009) released as a paper on the ArXiv- (arXiv:0904.2113) and RePEc-repository (RePEc: pra:mprapa:14680). After some improvements, the article was updated at the SSRN-repository ($SSRN_{id}$:1597735). Finally, the article was accepted for publication *Physica A* [114] and will be published in November 2010.

In chapter 5 the article is attached to this dissertation. The main results are briefly discussed within subsection 1.2.6 of the German summary (chapter 1).

2.6.4. Article 4: Experimental Validation of Quantum Game Theory

The results of the fourth application where primarily, in the year 2007, released as a paper on the ArXiv-repository [112]. After some improvements, the article was later accepted as a paper at the conference *Logic and the Foundations of Game and Decision Theory* (LOFT 2008) which was held in the year 2008 in Amsterdam.

In chapter 6 the article is attached to this dissertation. The main results are briefly discussed within subsection 1.2.6 of the German summary (chapter 1).

2.6.5. Article 5: Evolutionary Game Theory and Complex Networks of Scientific Information

The fifth application applies the framework of evolutionary game theory on the market of scientific information. The article is going to be published as a chapter in the book *"Models of science dynamics—Encounters between complexity theory and information science", Spinger book in the Complexity series, Editors: Andrea Scharnhorst, Katy Börner and Peter van den Besselaar.*

In chapter 7 the article is attached to this dissertation. The main results are briefly discussed within subsection 1.2.6 of the German summary (chapter 1).

2.7. Summary

To summarize the main outcomes of this article, the *Theory of Evolutionary Quantum Games* is applied to the simple example of Emma and Hans (see subsections 2.2.1 and 2.4.1). Due to the payoff structure of the example, the underlying game class belongs to the class of dominant games with a dilemma ($a = -2 < 0$, and $b = -(\alpha + 5) >> 0$). The only classical Nash equilibrium and dominant strategy is the strategy combination (s_2^A, s_2^B) where both players get a negative payoff ($\$_{22}^A = \$_{22}^B = -5$). The results of QGT however show that there is a way out of the dilemma, if the strategic entanglement γ—their fellow feeling—is high enough to overshoot the games' γ-thresholds (see appendix B.V).

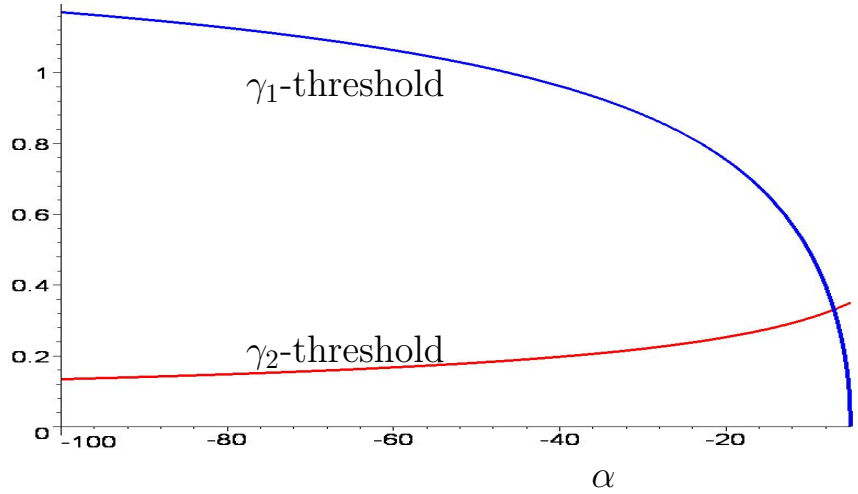

Figure 2.32.: The thresholds γ_1 (blue line) and γ_2 (red line) of the example game as a function of the payoff parameter α.

Figure 2.32 displays the γ-thresholds γ_1 and γ_2 as a function of the negative payoff parameter α. For $(-7 < \alpha < -5)$[11] the disappearance of the classical NE

[11]The lower boundary ($\alpha_L = -7$) was calculated using the intersection of the two γ-thresholds

happens at first ($\gamma_1 < \gamma_2$) however, as α is the parameter that models a very, very bad outcome ($\alpha << 0$), the opposite situation ($\gamma_1 > \gamma_2$) is valid for the example game. Emma and Hans therefore can escape the dilemma even for very low values of α, as the γ_1-threshold only approaches its maximal level in the limit of infinity ($\gamma_1(\alpha \to \infty) = \frac{\pi}{2}$).

Within this article *Evolutionary Quantum Game Theory* the framework of EGT was described in detail. After a general introduction and a brief literature review, the groundings of GT (section 2.2) and EGT (section 2.3) where explained in detail. The formal mathematical model, the different concepts of equilibria and the various classes of evolutionary games have been defined, explained and visualized to understand the main ideas of EGT.

Beside the results of classical EGT the article has focused on the different game categories of (2 player)-(2 strategy) evolutionary quantum games. After a general introduction into quantum game theory (see section 2.4), the formal mathematical model was explained and visualized. Additionally, in section 2.6 five different application where discussed (the underlying five papers of these applications have been attached to this article).

- Article 1: Quantum Game Theory and Open Access Publishing (see chapter 3)
- Article 2: Evolutionary Quantum Game Theory and Scientific Communication (see chapter 4)
- Article 3: Doves and hawks in economics revisited: *An evolutionary quantum game theory-based analysis of financial crises* (see chapter 5)
- Article 4: Experimental Validation of Quantum Game Theory (see chapter 6)
- Article 5: Evolutionary Quantum Game Theory and Complex Networks of Scientific Information (see chapter 7)

In summary, this article has shown that QGT is a mathematical and conceptual amplification of classical game theory. The space of all conceivable decision paths was extended from the purely rational, measurable space in the Hilbertspace

($\gamma_1(\alpha_L) = \gamma_2(\alpha_L)$).

of complex numbers. Through the concept of a potential entanglement of the imaginary quantum strategy parts it is possible to include cooperate decision path, caused by cultural or moral standards. It was shown, that if the strategy entanglement γ is large enough, then, additional Nash equilibria can occur, previously present dominant strategies could become nonexistent and new evolutionary stable strategies can appear.

3. Article 1: Quantum Game Theory and Open Access Publishing

ELSEVIER

Available online at www.sciencedirect.com
ScienceDirect

Physica A 382 (2007) 650–664

PHYSICA A

www.elsevier.com/locate/physa

Quantum game theory and open access publishing

Matthias Hanauske[a,*], Steffen Bernius[a], Berndt Dugall[b]

[a]*Institute of Information Systems, Johann Wolfgang Goethe-University, Mertonstr. 17, 60054 Frankfurt/Main, Germany*
[b]*Johann Christian Senckenberg University-Library, Bockenheimer Landstr. 134-138, 60325 Frankfurt/Main, Germany*

Received 29 December 2006
Available online 19 April 2007

Figure 3.1.: Published version of the article (Physica A 382 (2007) 650-664) [111].

Abstract

The digital revolution of the information age and in particular the sweeping changes of scientific communication brought about by computing and novel communication technology, potentiate global, high grade scientific information for free. The arXiv for example is the leading scientific communication platform, mainly for mathematics and physics, where everyone in the world has free access on. While in some scientific disciplines the open access way is successfully realized, other disciplines (e.g. humanities and social sciences) dwell on the traditional path, even though many scientists belonging to these communities approve the open access principle. In this paper we try to explain these different publication patterns by using a

game theoretical approach. Based on the assumption, that the main goal of scientists is the maximization of their reputation, we model different possible game settings, namely a zero sum game, the prisoners' dilemma case and a version of the stag hunt game, that show the dilemma of scientists belonging to "non-open access communities". From an individual perspective, they have no incentive to deviate from the Nash Equilibrium of traditional publishing. By extending the model using the quantum game theory approach it can be shown, that if the strength of entanglement exceeds a certain value, the scientists will overcome the dilemma and terminate to publish only traditionally in all three settings.

3.1. Introduction

In recent years the market of scientific publishing faces several forces that may cause a major change of traditional market mechanisms. First of all, the increase of digitalization brought a shift towards electronic publication. Furthermore, shrinking library budgets with a simultaneous rise of journal prices resulted in massive cancellations of journals and books [86, 224, 219, 163]. In consequence of this still lasting "journal crisis", alternative ways of publishing, in particular open access, received increasing attention [2, 173, 223]. Currently two main approaches have emerged. On the one hand, new open access journals are brought to being, either through transformation of traditional journals or through creation of new titles. This approach is often called the "Golden Road to Open Access". On the other hand, authors may self-archive their articles in Institutional Repositories, a model referred to as the "Green Road to Open Access" [123, 94].

In the following we understand open access publishing as the electronic publication of scientific information on a platform that provides access to this information for all potential users, without financial or other barriers. The realization of open access publishing differs between research disciplines [69]. The prime example of an adoption of the open access publishing paradigm is the arXiv server which is mainly used by physicists and mathematicians. Researchers in this fields normally self-archive their papers on the arXiv (so that everyone has free access to the work) and often additionally submit them to regular scientific journals, where these papers go through the traditional peer review process. Thus the

arXiv-model represents neither exactly the golden nor the green road of open access publishing.

In contrast most other scientific disciplines do not make use of open access publishing, even though they support this model if asked for [77, 203]. Instead, they submit research papers to traditional journals that do not provide free access to their articles. Considering that the majority of scientists regard open access publishing as superior to the traditional system, the question arises, why it is only adopted by few disciplines.

Based on the assumption, that the main goal of scientists is the maximization of their reputation, we try to answer this question from the perspective of the producers of scientific information by using a game theoretical approach. Scientific reputation originates mainly from two different sources: on the one hand the citations to the articles of a scientist and on the other hand the reputation of the journals he publishes his articles [57]. Starting from a general 2-Scientists-Game, where two authors have to decide whether they publish open access or not, three different possible game settings are developed. In each case the outcome of the game results in a dilemma, that cannot be solved within the static framework of classical game theory. Therefore we extend the model using the quantum game theoretical approach and show, that if choosing quantum strategies, the players can escape the dilemma.

The remainder of the paper is structured as follows. In section 3.2 the open access game is developed using the classical game theoretical notation. Firstly we define the general reputation payoff matrix of the game. The three settings of the game cover a zero sum game, the prisoners' dilemma case, and a variation of the so called stag hunt game. In section 3.3, after a brief introduction into the history of quantum game theory, we define the basic notations of the quantum version of the open access game and discuss the different game settings in detail. Our results are summarized in section 3.4.

3.2. The Classical Game of Open Access

3.2.1. Formalization of the Game

To describe the classical open access game we use a normal-form representation of a two-player [1] game Γ where each player (Player 1 $\hat{=}$ A, Player 2 $\hat{=}$ B) can choose between two strategies ($\mathcal{S}^A = \{s_1^A, s_2^A\}$, $\mathcal{S}^B = \{s_1^B, s_2^B\}$). In our case the two strategies represent the authors' choice between publishing open access (o) or not (ø). The game tree can therefore be visualized as in Fig. 3.2.

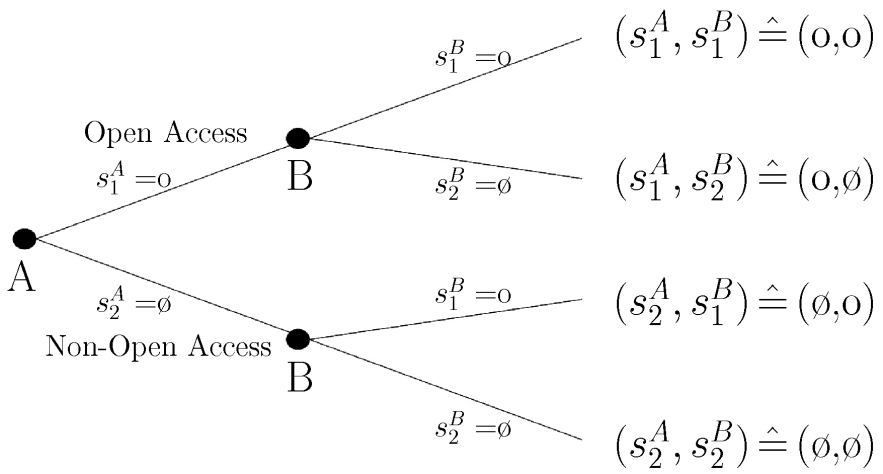

Figure 3.2.: Classical tree of the open access game.

The whole strategy space $\mathcal{S}$ is composed with use of a Cartesian product of the individual strategies of the two players (scientists):

$$\mathcal{S} = \mathcal{S}^A \times \mathcal{S}^B = \{(o,o), (o,ø), (ø,o), (ø,ø)\} \tag{3.1}$$

[1] In reality, the open access game consists of a lot of players. One can therefore understand Player B moreover as an overall construct of the probabilistic choice of the whole scientific community in which A is embedded.

As outlined in the introduction, we assume, that the main objective of scientists is the maximization of their reputation. In the following we focus on a situation, where the two scientists belong to a scientific community in which the open access paradigm is not yet broadly adopted and the publishers decline the acceptance of articles that are already accessible on an open access server. The payoff structure of this game can be described by the following matrix:

A\B	o	ø
o	$(r+\delta, r+\delta)$	$(r-\alpha, r+\beta)$
ø	$(r+\beta, r-\alpha)$	(r, r)

Table 3.1.: General open access payoff matrix.

The actual reputation of the two scientists is represented by a single parameter r [2]. If both players decide to publish their papers only in traditional journals (ø,ø), their reputation r does not change. If only one of the two players chooses the open access strategy ((ø,o) or (o,ø)) the parameters α and β ($\alpha, \beta \geq 0$) describe the decrease and the increase of the scientists' reputation, depending on the selected strategy. By modeling the payoff in this way, it is assumed that the reputation of the player, who performs open access, decreases if the other player simultaneously decides not to publish open access. This can be explained by the fact, that in "non-open access communities" reputation is mainly defined through the reputation of the journals a scientist publishes in. Thus if performing open access (by what a publication in traditional journals gets impossible), the scientist has no chance to gain journal-related reputation any more. On the other hand the parameter β describes the potential increase of reputation of a scientist that refuses to perform open access while the other player selects the open access strategy. By setting $\alpha = \beta$ the reputation is considered as a relative construct (see section 3.2.2). The parameter δ represents the potential benefit in the case that both players choose the open access strategy (o,o). The payoff for each player then is $r + \delta$. In this case it is assumed that if all players choose the open access strategy the publishers are forced to accept articles for publication

[2] By using this formalization, we assume that both scientists are on a similar level of reputation. It can be shown that if they have different "starting" reputation values, the outcome of the classical game would be the same.

even if they are already accessible. Then scientists can gain reputation both through the reputation of the journal they publish in and through the increase of citations due to a broader accessibility [157, 122, 70].

In the following we will describe three specific parameter settings of the open access game.

3.2.2. Potential Game Settings

Open Access as a Zero Sum Game

The most simple case of an open access game is realized by setting the free parameters of the games' payoff matrix to the following fixed values: $r = 0$, $\delta = 0$ and $\alpha = \beta = 1$. The starting reputation and the open access benefit of both players is set to zero, whereas the absolute value of the increase (β) and decrease (α) in reputation is taken to be equal. This setting therefore describes reputation as a relative quantity. A potential increase in reputation of one player results in an equivalent decrease of the other player's reputation. In this case, δ has to be zero because the total amount of reputation in the system cannot increase. The payoff matrix of this setting is illustrated in Table 3.2.

A\B	o	ø
o	(0,0)	(−1,1)
ø	(1,−1)	**(0,0)**

Table 3.2.: Open access payoff matrix with reputation as a relative quantity.

In this game each player has a dominant strategy (ø) and the Nash equilibrium is (ø,ø). Therefore no player has the incentive to deviate from the non-open access strategy ø.

The Open Access Game as a Prisoners' Dilemma

The game is similar to a classical prisoners' dilemma, if the assumption that reputation is a relative quantity is partially abrogated. If both players choose the open access strategy, the total amount of reputation will increase by δ ($\delta > 0$). In this case we have taken the following parameter settings: $r = 3$, $\delta = 1$ and $\alpha = \beta = 2$. Table 3.3 depicts the payoff of both players.

A\B	o	ø
o	(4,4)	(1,5)
ø	(5,1)	**(3,3)**

Table 3.3.: Open access payoff matrix within the prisoners' dilemma setting.

Although the payoff for both players would be higher if they choose the strategy set (o,o), they are stuck within the Nash equilibrium (ø,ø). This outcome describes the paradox situation of many scientific disciplines: Scientists on the one hand realize that they would benefit, if all players adopt open access, but on the other hand, no player has an individual incentive to change.

Open Access as a "Stag Hunt" Game

The stag hunt game in its original meaning describes the situation of two hunters, which have the choice between hunting a stag or a rabbit. If successful, bagging a stag provides more benefit than bagging a rabbit. The problem within this game is that hunting a stag can only be successful if both players go for the stag, whereas a rabbit can be easily bagged by only one hunter. In our case hunting a stag corresponds to the strategy of performing open access, and the non-open access strategy stands for hunting rabbits. Compared to the prisoners' dilemma only the parameter β is modified. To formulate the open access stag hunt game we have used the following parameter settings: $r = 3$, $\delta = 1$, $\alpha = 2$ and $\beta = 0$ (see Table 3.4) [3].

[3] In contrast to the original stag hunt game, where hunting a stag alone results in a payoff of zero, in this case the single open access performer gets a payoff of 1, simply because

A\B	o	ø
o	(4,4)	(1,3)
ø	(3,1)	(3,3)

Table 3.4.: Open access payoff matrix within the stag hunt setting.

In contrast to the other settings this game has two pure Nash equilibria ((o,o) and (ø,ø)) and one mixed strategy Nash equilibrium $\frac{2}{3}$(o,o). (o,o) is payoff dominant, whereas (ø,ø) is the risk dominant pure Nash equilibrium. The mixed strategy Nash equilibrium $\frac{2}{3}$(o,o) implies that one scientist has the incentive to choose non-open access if he expects the probability of the other player to choose non-open access as well, to be higher than $33.\overline{3}\,\%$.

In the following section we formulate the classical game settings described above within a quantum game theoretical framework.

3.3. The Quantum Game of Open Access

The basic principles of game theory were developed by J. von Neumann in the year 1928. Together with O. Morgenstern he applied this new theory to economics [233]. In addition to this outstanding scientific contribution he was also involved in the description of the mathematical foundations of quantum theory [232]. Keeping these historical facts in mind, it is surprising, that only recently game theory and quantum physics has been unified to one theory, the so called *Quantum Game Theory*.

The leadoff articles of quantum game theory where published by D. A. Meyer and J. Eisert et al. in the year 1999. Meyer illustrated a quantum version of the simple "Penny Flip" game and showed, that if one player uses a specific quantum strategy, whereas the other player persists in a classical one, the player who selects the quantum strategy will always win the game [165]. Just a few

a reputation value of zero is unrealistic. A reputation value of zero only makes sense, if reputation is seen as a relative quantity (see section 3.2.2).

weeks after Meyers' article was published, Eisert et al. focused on the well known prisoners' dilemma [66], unknowing Meyers' results. Within their quantum representation they where able to demonstrate, that prisoners could escape from the dilemma, if the entanglement of the prisoners' wave function is above a certain value. S. C. Benjamin and P. M. Hayden amplified the formal description of quantum games towards many players [28]. L. Marinatto and T. Weber applied the density matrix approach to the "Battle of Sexes" game and demonstrated, that entangled strategies lead to a unique solution of the game [162]. E. W. Piotrowski and J. Sladkowski disposed quantum game theory to market behaviors [178]. In 2001 J. Du et al. realized the first simulation of a quantum game; the experimental results confirmed their theoretical predictions [62]. Particularly they performed a prisoners' dilemma quantum game on their nuclear magnetic resonance quantum computer. Several other topics regarding quantum game theory have been addressed (e.g. overviews are given in [74, 90, 136]).

In the following subsection we summarize the main formal concepts of a two-player two-strategy quantum game. We follow the description of Eisert et al. [66, 65] and allow two parameter sets of quantum strategies [4].

3.3.1. Formalization of the Quantum Game

One can understand the concept of quantum strategies as an enlargement of mixed strategies towards an abstract complex strategy space. The measurable classical strategies (o and ø) correspond to the orthonormal unit basis vectors $|\mathrm{o}\rangle$ and $|\mathrm{ø}\rangle$ of the two dimensional complex space $\mathbb{C}^2$, the so called Hilbert space $\mathcal{H}_i$ of the player i ($i = A, B$). A quantum strategy of a player i is represented as a general unit vector $|\psi\rangle_i$ in his strategic Hilbert space $\mathcal{H}_i$. The whole quantum strategy space $\mathcal{H}$ is constructed with the use of the direct tensor product of the individual Hilbert spaces: $\mathcal{H} := \mathcal{H}_A \otimes \mathcal{H}_B$. The main difference between classical and quantum game theory is, that in the Hilbert space $\mathcal{H}$ correlations between the players' individual quantum strategies are allowed, if the two quantum strategies $|\psi\rangle_A$ and $|\psi\rangle_B$ are entangled. The overall state of the system we are looking at is described as a two-players quantum state $|\Psi\rangle \in \mathcal{H}$. The four basis vectors of

[4] This limitation of allowed quantum operations corresponds to the allowed set $S^{(TP)}$ in [65].

the Hilbert space $\mathcal{H}$ are chosen to be equal to the classical game outcomes ($|\text{oo}\rangle$, $|\text{o}\emptyset\rangle$, $|\emptyset\text{o}\rangle$ and $|\emptyset\emptyset\rangle$).

The setup of the quantum game begins with the choice of the initial state $|\Psi_0\rangle$. We assume that both players are in the state $|\text{o}\rangle$. The initial state of the two players is then given by $|\Psi_0\rangle = \hat{\mathcal{J}}\,|\text{oo}\rangle$, where the unitary operator $\hat{\mathcal{J}}$ is responsible for the possible entanglement of the two player system. The players' quantum decision (quantum strategy) is formulated with the use of a two parameter set of unitary 2×2 matrices:

$$\hat{\mathcal{U}}(\theta,\varphi) := \begin{pmatrix} e^{i\,\varphi}\cos(\frac{\theta}{2}) & \sin(\frac{\theta}{2}) \\ -\sin(\frac{\theta}{2}) & e^{-i\,\varphi}\cos(\frac{\theta}{2}) \end{pmatrix} \qquad (3.2)$$
$$\forall \quad \theta \in [0,\pi] \;\wedge\; \varphi \in [0,\tfrac{\pi}{2}] \qquad .$$

By arranging the parameters θ and φ a player is choosing his quantum strategy. The classical strategy o for example is selected by appointing $\theta = 0$ and $\varphi = 0$:

$$\hat{\text{o}} := \hat{\mathcal{U}}(0,0) = \begin{pmatrix} 1 & 0 \\ 0 & 1 \end{pmatrix} \quad , \qquad (3.3)$$

whereas the strategy $\emptyset$ is selected by choosing $\theta = \pi$ and $\varphi = 0$:

$$\hat{\emptyset} := \hat{\mathcal{U}}(\pi,0) = \begin{pmatrix} 0 & 1 \\ -1 & 0 \end{pmatrix} \quad . \qquad (3.4)$$

The tree of the open access quantum game is displayed in Fig. 3.3. After the two players have chosen their individual quantum strategies ($\hat{\mathcal{U}}_A := \hat{\mathcal{U}}(\theta_A,\varphi_A)$ and $\hat{\mathcal{U}}_B := \hat{\mathcal{U}}(\theta_B,\varphi_B)$) the disentangling operator $\hat{\mathcal{J}}^\dagger$ is acting to prepare the measurement of the scientists' state. The entangling and disentangling operator ($\hat{\mathcal{J}}, \hat{\mathcal{J}}^\dagger$; with $\hat{\mathcal{J}} \equiv \hat{\mathcal{J}}^\dagger$) is depending on one additional single parameter γ which is a measure of the entanglement of the system:

$$\hat{\mathcal{J}} := e^{i\,\frac{\gamma}{2}(\hat{\emptyset}\otimes\hat{\emptyset})} \;, \quad \gamma \in [0,\frac{\pi}{2}] \quad . \qquad (3.5)$$

The final state prior to detection therefore can be formulated as follows:

$$|\Psi_f\rangle = \hat{\mathcal{J}}^\dagger \left(\hat{\mathcal{U}}_A \otimes \hat{\mathcal{U}}_B\right) \hat{\mathcal{J}}\;|\text{oo}\rangle \quad . \qquad (3.6)$$

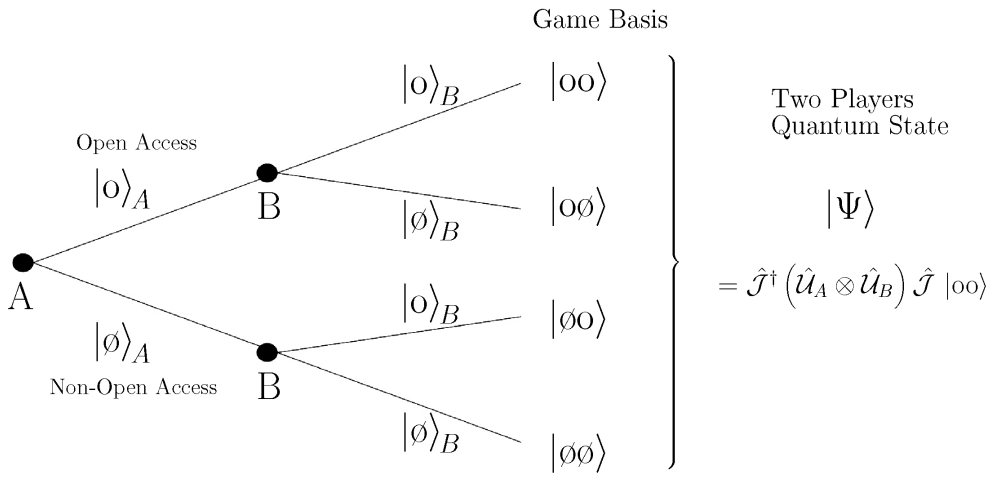

Figure 3.3.: Tree of the open access quantum game.

The expected payoff of the two scientists within the quantum version of the open access game depends on the payoff matrix (see Table 3.1) and on the joint probability to observe the four possible outcomes of the game:

$$\begin{aligned} \$_A &= (r+\delta)\,P_{\mathrm{oo}} + (r-\alpha)\,P_{\mathrm{o}\emptyset} + (r+\beta)\,P_{\emptyset\mathrm{o}} + r\,P_{\emptyset\emptyset} \\ \$_B &= (r+\delta)\,P_{\mathrm{oo}} + (r+\beta)\,P_{\mathrm{o}\emptyset} + (r-\alpha)\,P_{\emptyset\mathrm{o}} + r\,P_{\emptyset\emptyset} \\ &\quad \text{with:} \quad P_{\sigma\sigma'} = |\,\langle\sigma\sigma'|\Psi_f\rangle\,|^2 \;, \quad \sigma,\sigma' = \{\mathrm{o},\emptyset\} \quad . \end{aligned}$$

To visualize the payoffs in a three dimensional diagram it is neccessary to reduce the set of parameters in the final state: $|\Psi_f\rangle = |\Psi_f(\theta_A, \varphi_A, \theta_B, \varphi_B)\rangle \rightarrow |\Psi_f(t_A, t_B)\rangle$. We have used the same specific parameterization as Eisert et al. [66], where the two strategy angles θ and φ depend only on a single parameter $t \in [-1, 1]$. In our model $t_A, t_B = 1$ corresponds to strategy $\emptyset$, and $t_A, t_B = 0$ corresponds to strategy o. Negative t-values correspond to quantum strategies, where $\varphi > 0$.

Fig. 3.4 shows the general structure of the separation of strategy regions.

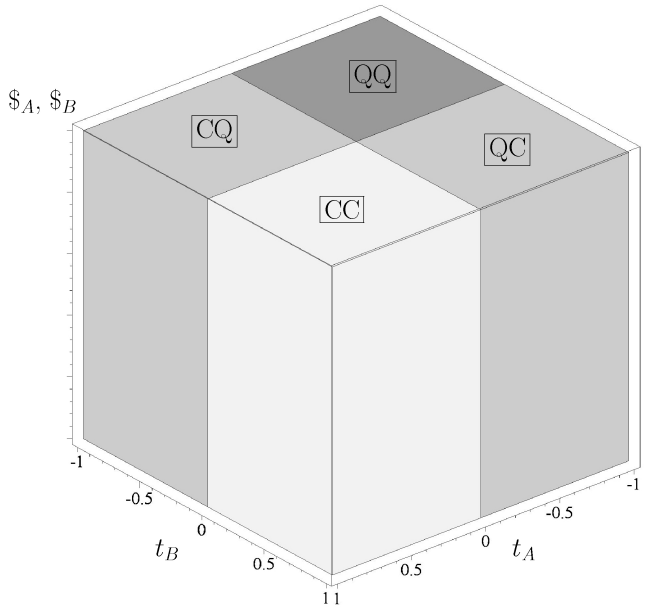

Figure 3.4.: Separation of the strategy space in four different regions; namely the absolute classical region CC, the absolute quantum region QQ, and the partially classical-quantum regions CQ and QC.

The whole strategy space is separated into four regions, namely the absolute classical region (CC: $t_A, t_B \geq 0$), the absolute quantum region (QQ: $t_A, t_B < 0$) and the two partially classical-quantum regions (CQ: $t_A \geq 0 \wedge t_B < 0$ and QC: $t_A < 0 \wedge t_B \geq 0$). In the following subsection we will present the main results of the different game settings of the open access quantum game. The outcomes of the different games are illustrated by visualizing the payoff surfaces of scientist A and scientist B as a function of their strategies t_A and t_B.

3.3.2. Potential Game Settings

Open Access as a Zero Sum Quantum Game

Using the simple payoff matrix (Table 3.2) and the quantum game formulation of section 3.3.1 we have calculated the expected payoff for the two scientists with and without entanglement. Fig. 3.5 depicts the expected payoff for scientist A

($\$_A$, intransparent surface) and scientist B ($\$_B$, wired surface) as a function of their strategies t_A and t_B in a separable quantum game ($\gamma = 0$).

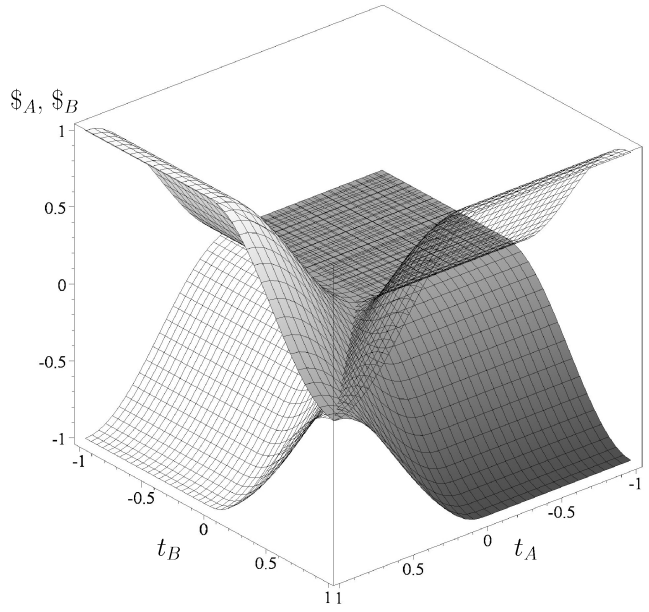

Figure 3.5.: Expected payoff of scientists A and B in a separable quantum game (payoff setting see Table 3.2).

The outcome of this separable quantum game is similar to the classical solution outlined in section 3.2.2. To illustrate this, we recall the definitions of dominant strategies and Nash equilibria and formulate them in respect to our possible quantum choices:

$(\theta_A^\star, \varphi_A^\star; \theta_B^\star, \varphi_B^\star)$ is a dominant quantum strategy if

$$\begin{aligned} \$_A(\hat{\mathcal{U}}_A^\star, \hat{\mathcal{U}}_B) &\geq \$_A(\hat{\mathcal{U}}_A, \hat{\mathcal{U}}_B) \quad \forall \ \hat{\mathcal{U}}_A \wedge \hat{\mathcal{U}}_B \\ \$_B(\hat{\mathcal{U}}_A, \hat{\mathcal{U}}_B^\star) &\geq \$_B(\hat{\mathcal{U}}_A, \hat{\mathcal{U}}_B) \quad \forall \ \hat{\mathcal{U}}_A \wedge \hat{\mathcal{U}}_B \quad . \end{aligned} \tag{3.7}$$

$(\theta_A^\star, \varphi_A^\star; \theta_B^\star, \varphi_B^\star)$ is a quantum Nash equilibrium if

$$\begin{aligned} \$_A(\hat{\mathcal{U}}_A^\star, \hat{\mathcal{U}}_B^\star) &\geq \$_A(\hat{\mathcal{U}}_A, \hat{\mathcal{U}}_B^\star) \quad \forall \ \hat{\mathcal{U}}_A \\ \$_B(\hat{\mathcal{U}}_A^\star, \hat{\mathcal{U}}_B^\star) &\geq \$_B(\hat{\mathcal{U}}_A^\star, \hat{\mathcal{U}}_B) \quad \forall \ \hat{\mathcal{U}}_B \quad . \end{aligned} \tag{3.8}$$

In the classical version of the game there exists one dominant strategy, namely (ø,ø), which corresponds to the parameter set ($\theta_A^\star = \pi, \varphi_A^\star = 0\,,\, \theta_B^\star = \pi, \varphi_B^\star = 0$). The expected payoff in this dominant strategy is equal to zero for both players ($\$_A(1,1) = \$_B(1,1) = 0$, see Fig. 3.5). Because of the validity of the following conditions, (ø,ø) is also a dominant strategy in the separable game:

$$\begin{aligned} \$_A(t_A = 1, \hat{\mathcal{U}}_B) = \cos\left(\tfrac{\theta_B}{2}\right)^2 \quad &\geq \quad \$_A(\hat{\mathcal{U}}_A, \hat{\mathcal{U}}_B) = \\ = \sin\left(\tfrac{\theta_A}{2}\right)^2 \cos\left(\tfrac{\theta_B}{2}\right)^2 - \cos\left(\tfrac{\theta_A}{2}\right)^2 \sin\left(\tfrac{\theta_B}{2}\right)^2 \quad &, \end{aligned} \tag{3.9}$$

$$\begin{aligned} \$_B(\hat{\mathcal{U}}_A, t_B = 1) = \cos\left(\tfrac{\theta_A}{2}\right)^2 \quad &\geq \quad \$_B(\hat{\mathcal{U}}_A, \hat{\mathcal{U}}_B) = \\ = \sin\left(\tfrac{\theta_B}{2}\right)^2 \cos\left(\tfrac{\theta_A}{2}\right)^2 - \cos\left(\tfrac{\theta_B}{2}\right)^2 \sin\left(\tfrac{\theta_A}{2}\right)^2 \quad &. \end{aligned} \tag{3.10}$$

The conditions (3.9) and (3.10) are easy to illustrate if one examines Fig. 3.5. To visualize condition (3.9) for example, one shall look at the intransparent surface and fix an arbitrary point on the surface, which is located on the curve $\$_A(1, t_B)$ (with $t_B \in [-1, 1]$). Condition (3.9) means, that if one varies t_A between all possible strategies ($t_A \in [-1, 1]$), while keeping t_B fixed, the payoff of player A ($\$_A$) will always decrease. In a similar way, condition (3.10) can be illustrated by considering the wired surface $\$_B(t_A, t_B)$.

Recapitulating the separable zero sum open access quantum game, one can say that no changes to the classical game are observable. Due to the dominance of strategy (ø,ø), both scientists will not perform open access.

The situation is entirely different in the maximally entangled version of the game.

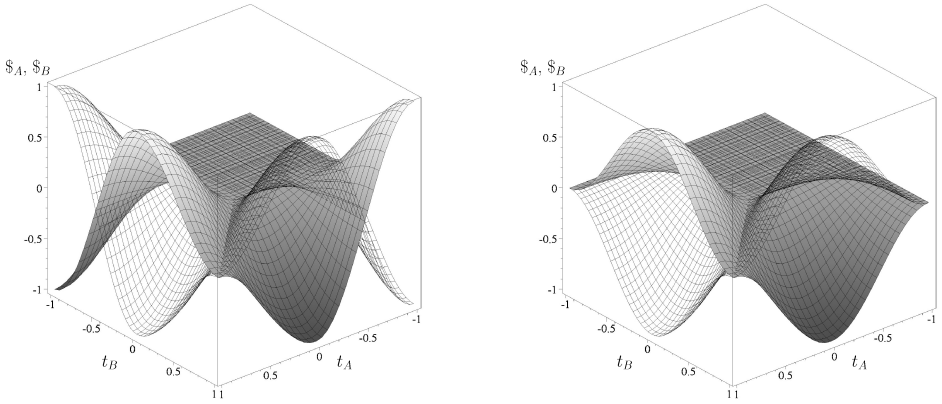

Figure 3.6.: Expected payoff of scientists A and B in a maximally entangled quantum game (left: $\gamma = \frac{\pi}{2}$) and in a partially entangled quantum game (right: $\gamma = \frac{\pi}{4}$). Payoff setting see Table 3.2.

In Fig. 3.6 (left) the expected payoff for scientist A ($\$_A$, intransparent surface) and scientist B ($\$_B$, wired surface) is visualized; in contrast to Fig. 3.5 the players are maximally entangled ($\gamma = \frac{\pi}{2}$). Because of the change in the payoff surfaces, the strategy (ø,ø) is neither a dominant strategy nor a Nash equilibrium any more. For example, if player B chooses the strategy ø, it would be advisable for player A to select the strategy $\hat{\mathcal{U}}_A(0, \pi/2) \hat{=} (t_A = -1)$. In contrast to the disappearance of the former Nash equilibrium (ø,ø), new Nash equilibria are observed in the maximally entangled game. The pure quantum strategy $\hat{\mathcal{Q}} := \hat{\mathcal{U}}(0, \pi/2) \hat{=} (t = -1)$ for instance is a Nash equilibrium because of the following conditions:

$$\begin{aligned} \$_A(t_A = -1, t_B = -1) = 0 \geq \\ -\sin\left(\tfrac{\theta_A}{2}\right)^2 = \$_A(\hat{\mathcal{U}}_A, t_B = -1) \quad \forall\ \theta_A \in [0, \pi] \quad , \\ \$_B(t_A = -1, t_B = -1) = 0 \geq \\ -\sin\left(\tfrac{\theta_B}{2}\right)^2 = \$_B(t_B = -1, \hat{\mathcal{U}}_A) \quad \forall\ \theta_B \in [0, \pi] \quad . \end{aligned}$$

By examining Fig. 3.6 (left) one can see that all quantum strategies with $t \leq -0.5$ belong to the set of possible Nash equilibria.

The results of the maximally entangled game show, that if quantum strategies are allowed, the scientists are not longer trapped in the strategy set (ø,ø). Nash equilibria exist only if both players choose a quantum strategy with $t_A, t_B \leq -0.5$.

For partially entangled situations ($0 < \gamma < \frac{\pi}{2}$), a boundary entanglement $\gamma_1 = \frac{\pi}{4}$ can be specified, where the Nash equilibrium (ø,ø) fades to the quantum equilibria $t_A, t_B \leq -0.5$. Fig. 3.6 (right) depicts the partially entangled quantum game, which is right at the edge of dissolving the Nash equilibrium (ø,ø). For all $\gamma \leq \frac{\pi}{4}$ the Nash equilibrium of the game is (ø,ø), whereas for $\gamma > \frac{\pi}{4}$ the outcome of the game is similar to the maximally entangled situation, although the range of the set of quantum Nash equilibria is smaller and varies from ($\gamma = \frac{\pi}{4}$: $t_A, t_B = -1$) to ($\gamma = \frac{\pi}{2}$: $-1 \leq (t_A, t_B) \leq -0.5$).

The Open Access Quantum Game as a Prisoners' Dilemma

We now focus on an open access game with a payoff matrix similar to a prisoners' dilemma (see Table 3.3). In difference to the zero sum game, discussed in the previous subsection, a dilemma occurs for both scientists. The players again are imprisoned in the strategy set (ø,ø), although a choice of (o,o) would be better for both of them. Fig. 3.7 illustrates this quandary in a graphic way (separable game with $\gamma = 0$). In contrast to Fig. 3.5, where the strategy sets (o,o) and (ø,ø) are on the same payoff level ($\$_A(\mathrm{o},\mathrm{o}) = \$_A(\emptyset,\emptyset) = 0$; same for player B), the payoff magnitudes are now different ($\$_A(\mathrm{o},\mathrm{o}) = 4$, $\$_A(\emptyset,\emptyset) = 3$; same for player B). The plane of the quantum-quantum region in Fig. 3.7 ($t_A, t_B \leq 0$) has moved upwards and has a higher payoff than the dominant strategy (ø,ø). There is again no difference between the classical outcome of the game and the separable quantum version: (ø,ø) remains to be a dominant strategy.

Increasing the entanglement factor γ to higher values leads to a qualitative change in the outcome of the game, if its value overruns $\gamma_1 := 2\arctan(\frac{\sqrt{3}-1}{\sqrt{3}+1})$. For $\gamma_1 < \gamma$ the strategy (ø,ø) ceases to be a unique dominant strategy, however (ø,ø) remains to be a Nash equilibrium if the entanglement-factor lies in the range $\gamma_1 < \gamma \leq \gamma_2 := \frac{\pi}{4}$. In this range, there exist two Nash equilibria, namely the former Nash equilibrium (ø,ø) and a new quantum Nash equilibrium ($\hat{\mathcal{Q}}_A, \hat{\mathcal{Q}}_B$), which corresponds to ($t_A = -1$, $t_B = -1$). Fig. 3.8 (left) shows the payoff

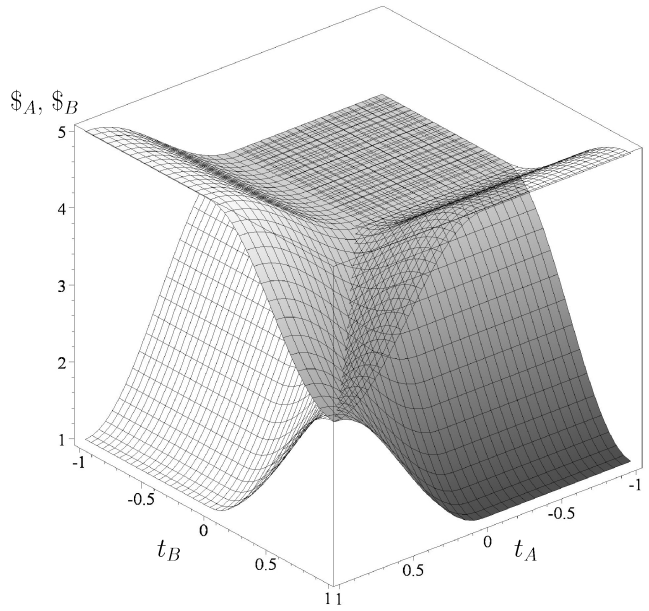

Figure 3.7.: Expected payoff of scientists A and B in a separable prisoners' dilemma quantum game (payoff setting see Table 3.3).

surfaces for both players at the entanglement barrier γ_1.

If one further increases γ, the strategy (ø,ø) even ceases to be a Nash equilibrium. For example, if $\gamma > \gamma_2$ and player B chooses the strategy ø, the best reward for player A would be the quantum strategy $\hat{\mathcal{Q}}_A$. Fig. 3.8 (right) depicts the payoff surfaces for both players for $\gamma = \gamma_2$.

For $\gamma > \gamma_2$ there exists only the quantum Nash equilibrium $(\hat{\mathcal{Q}}_A, \hat{\mathcal{Q}}_B)$, as one can see by looking at the maximally entangled situation (Fig. 3.9).

It should be mentioned, that our results are different from the results presented in [66] and [62], which is due to a different payoff matrix. For the separable and maximally entangled game there is no qualitative difference in the outcomes, whereas we want to point out, that we find different Nash equilibria for the partially entangled games (see Fig. 3.8). J. Du et al. found the two Nash equilibria ((($\hat{\mathcal{Q}}$,ø) and (ø,$\hat{\mathcal{Q}}$)) for $\arcsin(\sqrt{\frac{1}{5}}) < \gamma \leq \arcsin(\sqrt{\frac{2}{5}})$ [62], which is in clear contrast to our results. We therefore want to emphasize, that if one extends a prisoners' dilemma into a quantum region, the structure of the payoff matrix is

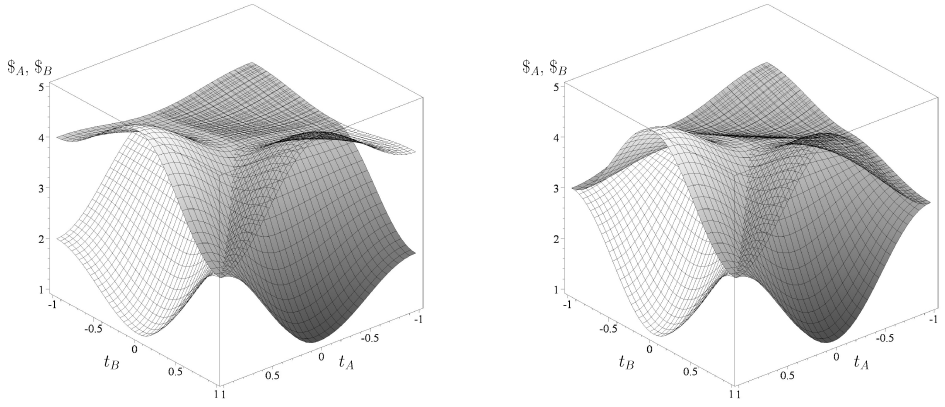

Figure 3.8.: Expected payoff of scientists A and B in partially entangled prisoners' dilemma quantum game (payoff setting see Table 3.3, left: $\gamma = 2\arctan(\frac{\sqrt{3}-1}{\sqrt{3}+1})$, right: $\gamma = \frac{\pi}{4}$).

important and seems to separate different types of quantum prisoners' dilemmas when varying the systems' entanglement.

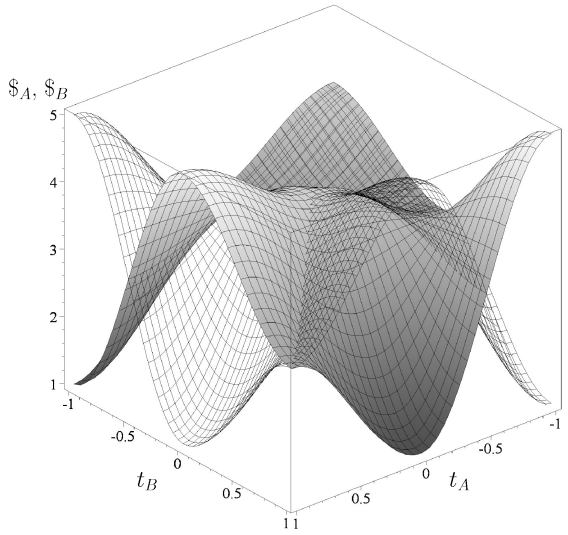

Figure 3.9.: Expected payoff of scientists A and B in a maximally entangled prisoners' dilemma quantum game (payoff setting see Table 3.3).

Open Access as a Stag Hunt Quantum Game

In contrast to the other separable games discussed in the previous subsections, the stag hunt quantum version of the open access game even shows advantages of using quantum strategies in the separable situation, where the strategical operations of the scientists are not entangled. In this case the QQ-plane of the payoffs for both players always lies above or equal to all other payoff values (see Fig. 3.10 (right)).

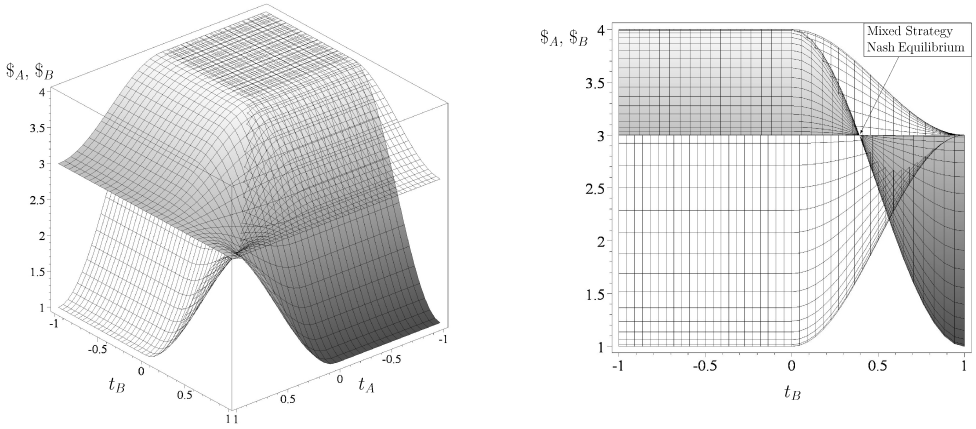

Figure 3.10.: Left: The expected payoff of scientists A and B in a separable stag hunt quantum game (payoff setting see Table 3.4). Right: The projection of the right figure onto the \$-t_B plane.

In addition to the three classical Nash equilibria ((ø,ø), (o,o) and $\frac{2}{3}$(o,o)), a set of new quantum Nash equilibria can be observed within the separable quantum game ($t_A, t_B < 0$). All quantum strategies that lie on the QQ-plane of Fig. 3.10 (left), ensure an identical, rather high payoff for both players ($\$_A(QQ) = \$_B(QQ) = 4$). Because of the absence of a dominant strategy and the complex structure of Nash equilibria, it is difficult to predict the outcome of the game. A risk conducted player may prefer the strategy ø, because this will guarantee him a payoff of 3. A payoff conducted player might be guided by the possibility of getting a greater payoff, and therefore will prefer either strategy o, or a quantum strategy $t < 0$. The mixed strategy Nash equilibrium $\frac{2}{3}$(o,o) can be visualized if one examines

the surfaces from a viewpoint parallel to the strategy space of player A (see Fig. 3.10 (left)). The character of a mixed Nash equilibrium ($t_A^\star$, $t_B^\star$) is that the gradients of the payoff surfaces vanish:

$$\begin{aligned} \frac{\partial \$_A}{\partial t_A}(t_A, t_B)\Big|_{t_B=t_B^\star} &\equiv 0\,, \quad \forall\ t_A \in [-1,1] \\ \frac{\partial \$_B}{\partial t_B}(t_A, t_B)\Big|_{t_A=t_A^\star} &\equiv 0\,, \quad \forall\ t_B \in [-1,1] \quad . \end{aligned} \tag{3.11}$$

$t_B^\star$ for example can be observed in the special projection of Fig. 3.10 (right), where the whole payoff surface of player A ($\$_A$) contracts to one single point. From our calculations we get the following mixed strategy Nash equilibrium ($t^\star = t_A^\star = t_B^\star = \frac{2}{\pi}\arcsin(\frac{1}{\sqrt{3}})$), which corresponds to the strategy $\frac{2}{3}$(o,o).

The maximally entangled stag hunt quantum game is displayed in Fig. 3.11.

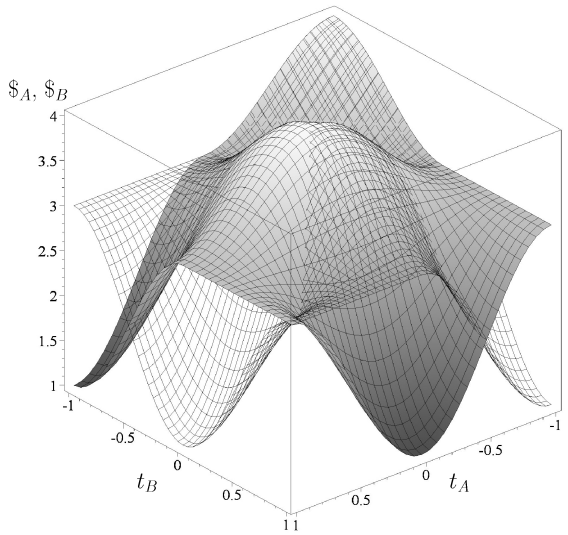

Figure 3.11.: Expected payoff of scientists A and B in a maximally entangled stag hunt quantum game (payoff setting see Table 3.4).

In this version of the game three Nash equilibria occur, namely (ø,ø), $\frac{2}{3}$(o,o) and ($\hat{\mathcal{Q}}_A, \hat{\mathcal{Q}}_B$). Although (ø,ø) technically remains to be a Nash equilibrium, no rational acting player would choose such a strategy, because the alternative of

the quantum strategy $\hat{\mathcal{Q}}$ would give him in any case a better or equal payoff:

$$\text{Quantum Strategy:}$$
$$\$_A(\hat{\mathcal{Q}}_A, t_B) \geq 3 \wedge \$_B(t_A, \hat{\mathcal{Q}}_B) \geq 3 \quad \forall\, t_A, t_B \in [-1, 1]$$
$$\text{Non-Open Access:}$$
$$\$_A(\emptyset, t_B) \leq 3 \wedge \$_B(t_A, \emptyset) \leq 3 \quad \forall\, t_A, t_B \in [-1, 1]$$

Furthermore it should be mentioned, that for all types of entanglement the mixed strategy Nash equilibrium $\frac{2}{3}$(o,o) persists at its former position.

In summary, we conclude that the players of a maximally entangled stag hunt quantum game will be in favor of performing the quantum strategy $\hat{\mathcal{Q}}$ over the non-open access strategy ø.

3.3.3. Manifestation of Quantum Strategies

We want to point out, that the measurable choice of the quantum strategy $\hat{\mathcal{Q}}$ in reality does not necessarily appear as the strategy o – albeit, if both players will choose $\hat{\mathcal{Q}}$, the measured outcome will be (o,o). To illustrate the role of entanglement and the nature of quantum strategies, we have fixed the strategy of scientist B to $\hat{\mathcal{U}}_B = \hat{\mathcal{U}}(\pi, 0) = \emptyset$, whereas we choose the strategy of scientist A to be a quantum strategy $\hat{\mathcal{U}}_A = \hat{\mathcal{U}}(\theta_A, \frac{\pi}{2})$. Fig. 3.12 displays the payoff for the players A and B as a function of θ_A and γ. Fig. 3.12 (left) depicts the calculations for the prisoners' dilemma game, whereas Fig. 3.12 (right) shows the results within the stag hunt quantum game. If the scientists' strategies are not entangled ($\gamma = 0$), the best respond for player A in the prisoners' dilemma game is the choice of $\theta_A = \pi$, which would result in the classical Nash equilibrium (ø,ø), giving both players the payoff 3. In contrast, if we focus on a situation where the scientists' strategies are maximally entangled ($\gamma = \frac{\pi}{2}$), the best respond for scientist A is $\theta_A = 0$, giving him a payoff of 5 and player B a payoff of 1. Player B could be amazed about his little payoff. To understand the real cause, we need to examine the joint probabilities of the measurable outcomes of the game. If player B selects the classical strategy ø and player A chooses the quantum

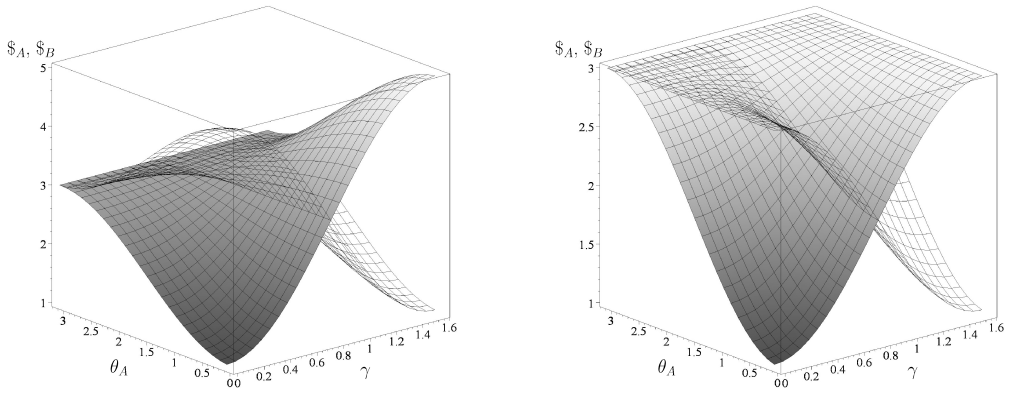

Figure 3.12.: Expected payoff of scientists A and B versus θ_A and γ. Player B has selected the classical strategy ø, whereas player A selects a quantum strategy $\hat{\mathcal{U}}_A = \hat{\mathcal{U}}(\theta_A, \frac{\pi}{2})$. The left picture shows the prisoners' dilemma case whereas the right picture depicts the stag hunt quantum game.

strategy $\hat{\mathcal{Q}}$, the joint probabilities result in the following outcomes:

$$\begin{aligned} |\langle \mathrm{oo}|\Psi_f\rangle|^2 &= |\langle \mathrm{øø}|\Psi_f\rangle|^2 = 0 \quad , \\ |\langle \mathrm{oø}|\Psi_f\rangle|^2 &= \cos(\gamma)^2, \quad |\langle \mathrm{øo}|\Psi_f\rangle|^2 = \sin(\gamma)^2 \quad . \end{aligned} \tag{3.12}$$

In Fig. 3.13 the non-zero probabilities $|\langle \mathrm{oø}|\Psi_f\rangle|^2$ and $|\langle \mathrm{øo}|\Psi_f\rangle|^2$ are plotted against the scientists' entanglement γ. The cause of the amazement of player B is that even though he chooses the strategy ø, the probability of measuring ø is zero if the entanglement γ is maximal. By using the quantum strategy $\hat{\mathcal{Q}}$ player A is able to switch the choice of player B. Within an entangled quantum game, it is not feasible to insist on a classically chosen strategy.

3.4. Summary

This article focuses the question why the open access model is only successfully adopted by a few scientific disciplines. We have constructed a game theoretical model, where the scientists' incentives where described with a reputation depen-

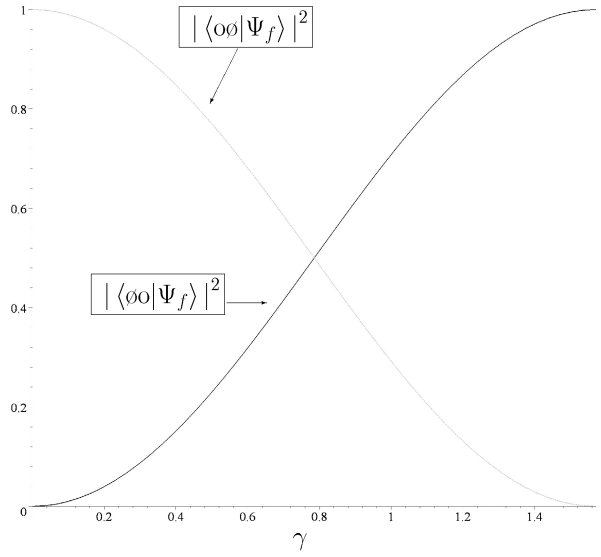

Figure 3.13.: Joint probabilities of the measurable outcomes as a function of γ. Player B chooses strategy $\emptyset$, whereas Player A chooses $\hat{Q}$.

dent payoff matrix. Three game settings where addressed, namely a zero sum game, the prisoners' dilemma and a stag hunt version of the open access game. By calculating the outcome of the games within a classical game theoretical framework, we have shown that in all cases the scientists face a dilemma situation: Considering a potential loss in reputation, incentives to perform open access are missing. These findings change, if quantum strategies are allowed. If the entanglement overruns a certain barrier, quantum strategies become superior to the former Nash equilibrium strategies. In none of the three different game settings the choice of traditional publishing remains to be a rational strategy for the players, if their strategical choices are maximally entangled. The results of this article therefore indicate one possible explanation of the differing publishing methods of scientific communities. In quantum game theory parlance one would say, that scientific disciplines, like mathematics and physics, which had been successful in realizing the open access model, consist of scientists, whose strategical operations are strongly entangled. In contrast, if a scientific community is still imprisoned in the Nash equilibrium of non-open access, there would be a lack

of entanglement between the strategical choices of the related scientists of the community.

Acknowledgments

We want to thank Jens Eisert for helpful discussions. This research is supported by grants from the German National Science Foundation (DFG) (Project "Scientific Publishing and Alternative Pricing Mechanisms", Grant No. GZ 554922). We gratefully acknowledge the financial support.

4. Article 2: Evolutionary Quantum Game Theory and Scientific Communication

Evolutionary Quantum Game Theory and Scientific Communication

Matthias Hanauske[a], Wolfgang König[a,b], and Berndt Dugall[c]
[a] *Institute of Information Systems,* [b] *House of Finance*
Goethe-University, Grüneburgplatz 1, 60323 Frankfurt/Main
[c] *Johann Christian Senckenberg University-Library*
Bockenheimer Landstr. 134-138, 60325 Frankfurt/Main

Figure 4.1.: Published version of this article is available through the conference internetpage of the "Second Brazilian Workshop of the Game Theory Society, in honor of John Nash, on occasion of the 60th anniversary of Nash equilibrium", which was held in São Paulo (Brazil) from the 29th July until the 4th August in the year 2010.

Abstract

Quantum game theory is a mathematical and conceptual amplification of classical game theory. The space of all conceivable decision paths is extended from the purely rational, measurable space in the Hilbertspace of complex numbers. Through the concept of a potential entanglement of the imaginary quantum strategy parts, it is possible to include corporate decision path, caused by cultural or moral standards. If this strategy entanglement is large enough, then, additional Nash-equilibria can occur, previously present dominant strategies could become nonexistent and new evolutionary stable strategies can appear. This article focuses on a quantum amplification of an evolutionary (2 player)-(2 strategy) - coordination game and shows, that

the different publication norms of scientific authors additionally depend on their strategic entanglement strength γ. If the strength of entanglement exceeds a certain value, a phase transition within the whole population occurs, reaching the global optimum of the underlying coordination game.

4.1. Introduction

In 1928 the main inventor of game theory - Johann (John) von Neumann - published the first article on game theory [234]. The first book about game theory was published in 1944 by von Neumann and Morgenstern [233]. Evolutionary game theory [216, 213, 214, 198, 166, 222, 198, 21, 108] was developed after J.M. Smith had found that the stationary solutions of the evolutionary differential equations are connected with game theory [212]. In the following years applications in respect to biological systems [209, 226, 148, 78, 171, 172] and socio-economic systems, e.g. "public good"-games [51], cultural or moral developments [68, 121], the evolution of languages [177], social learning [68], the evolution of social norms [23, 175], the financial crisis [114] and the evolution of social networks [222, 139, 67] came into the focus of research. In 1999 the first two articles on quantum games where published [165, 66]. In 2001 the first quantum game was realized on a quantum computer [62] (see also [190]). The extension to more than two players [28], the application to social networks [178, 111], social experiments [49, 176, 112] and first approaches towards an evolutionary quantum game theory [169, 95, 114][1] followed.

This article focuses on a simplified version of the open access game of scientific communication (for detail see [111]) and extends it to an evolutionary quantum coordination game. The payoff structure of the underlying game can be described by the payoff matrix illustrated in Table 4.1. The players are the authors of scientific articles, the two strategies represent the authors' choice between publishing open access (o) or not (ø), parameter r describes the increase of reputation achieved by an author, if he/she publishes a new paper, δ is an additional benefit if both authors publish open access and the parameter α

[1] ... - which is mathematically, most likely formulated with the use of the *von Neumann equation* -

A\B	o=s_1^B	ø=s_2^B
o=s_1^A	$(r+\delta, r+\delta)$	$(r-\alpha, r+\alpha)$
ø=s_2^A	$(r+\alpha, r-\alpha)$	(r, r)

Table 4.1.: Payoff of the underlying coordination game.

($\alpha < \delta$) is responsible for the potential increase or decrease of reputation if one author publishes open access and the other not (for detail see [111]).

4.2. Definitions and key aspects of classical evolutionary game theory

This section is dedicated to the introduction of the necessary definitions and fundamental basics of evolutionary game theory. In the following the presentation is constrained to the normal form of a symmetric (2 player)-(2 strategy) game Γ (for details see [108, 222]):

$$\begin{aligned} \Gamma &:= \left(\{A, B\}, \mathcal{S} \times \mathcal{S}, \hat{\$}_A, \hat{\$}_B \equiv \left(\hat{\$}^A\right)^T \right) \\ \mathcal{S} &= \{s_1, s_2\} \quad : \text{Set of pure strategies} \\ \hat{\$}_A &= \begin{pmatrix} \$_{11} & \$_{12} \\ \$_{21} & \$_{22} \end{pmatrix} \quad : \text{Payoff matrix of Player A} \end{aligned} \tag{4.1}$$

The mixed strategy payoff function of player A has the following structure[2]

$$\begin{aligned} \tilde{\$}^A : \tilde{\mathcal{S}} \times \tilde{\mathcal{S}} \to \mathbb{R}\,, \quad \tilde{\$}^A(\tilde{s}_1^A, \tilde{s}_1^B) = \$_{11}\tilde{s}_1^A\tilde{s}_1^B + \\ +\$_{12}\tilde{s}_1^A(1-\tilde{s}_1^B) + \$_{21}(1-\tilde{s}_1^A)\tilde{s}_1^B + \$_{22}(1-\tilde{s}_1^A)(1-\tilde{s}_1^B) \end{aligned} \tag{4.2}$$

, where $\tilde{s}_1^A, \tilde{s}_1^B \in [0,1]$ and $\tilde{s}_2^A = 1 - \tilde{s}_1^A$, $\tilde{s}_2^B = 1 - \tilde{s}_1^B$. Inserting the payoff matrix of the coordination game of Table 4.1 into equation (4.2) yields to the following structure of the mixed strategy payoff function ($\tilde{s}^A := \tilde{s}_1^A$ and $\tilde{s}^B := \tilde{s}_1^B$):

$$\tilde{\$}^A(\tilde{s}^A, \tilde{s}^B) = \delta\, \tilde{s}^A\tilde{s}^B + \alpha\left(\tilde{s}^B - \tilde{s}^A\right) + r \tag{4.3}$$

[2]The mixed strategy payoff function of player B can be constructed simply by interchanging the indices ^{A} and ^{B}.

The coordination game of Table 4.1 has two symmetric, pure Nash-equilibria ((o,o)= $(s_1^A, s_1^B) = (\tilde{s}^A = 1, \tilde{s}^B = 1)$ and (ø,ø)= $(s_2^A, s_2^B) = (\tilde{s}^A = 0, \tilde{s}^B = 0)$) and one symmetric mixed strategy Nash-equilibrium $(s^{A*}, s^{B*}) = (\tilde{s}^A = \frac{\alpha}{\delta}, \tilde{s}^B = \frac{\alpha}{\delta})$. (s^{A*}, s^{B*}) can be calculated using the fact that the partial derivative of the mixed strategy payoff function of player A vanishes at the value of the mixed strategy Nash-equilibrium:

$$\left.\frac{\partial \tilde{\$}^A(\tilde{s}^A, \tilde{s}^B)}{\partial \tilde{s}^A}\right|_{\tilde{s}^B = s^{B*}} = \delta s^{B*} - \alpha = 0 \;\Rightarrow\; s^{B*} = \frac{\alpha}{\delta} \tag{4.4}$$

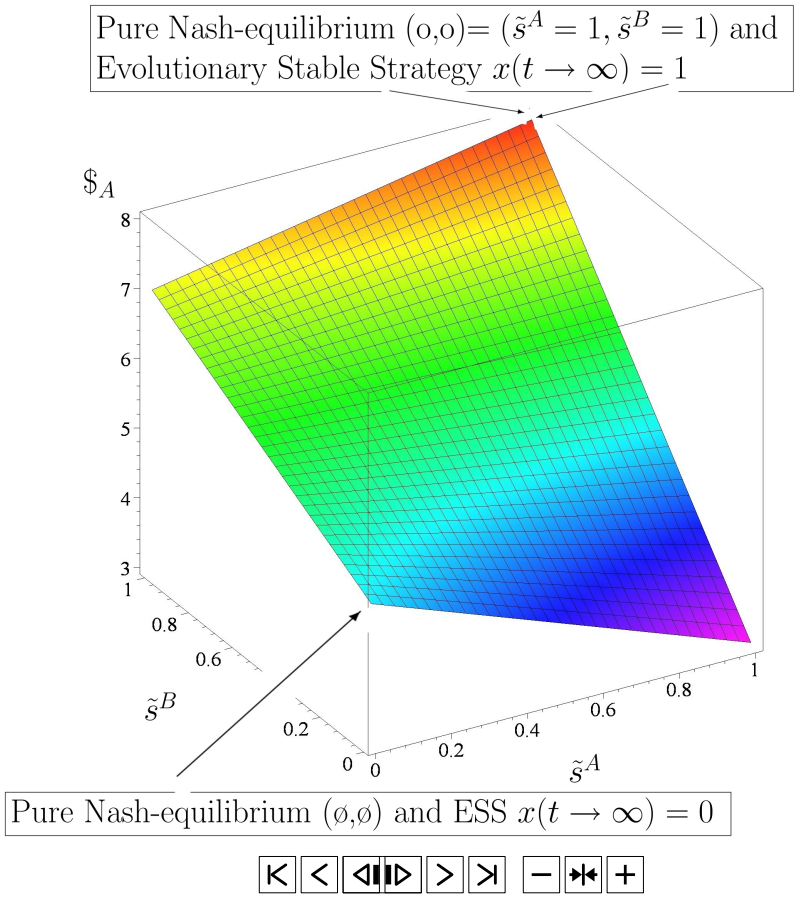

Figure 4.2.: Animation of the payoff function in mixed strategies.

The three Nash-equilibria of the underlying coordination game (Table 4.1, with $r = 5, \delta = 3$ and $\alpha = 2$) can be visualized (see Figure 4.2) by plotting the payoff of player A as a function of the mixed strategy of player A ($\tilde{s}^A$) and player B ($\tilde{s}^B$). The pure Nash-equilibrium (s_1^A, s_1^B) is actually present, because if one fixes the strategy of player B to $s_1^B = (\tilde{s}^B = 1)$ then the highest point on the payoff-surface for player A is realized, if he/she chooses s_1^A. The other pure Nash-equilibrium can be visualized the same way by fixing the strategy of player B to $s_2^B = (\tilde{s}^B = 0)$. The mathematical property of the mixed strategy Nash-equilibrium (equation (4.4)) is visualized in Figure 4.2 by a transformation of the figures' viewpoint, as the three dimensional payoff surface shrinks to one point at s^{B*}, if one looks in direction of the $\tilde{s}^A$-axis.[3]

To describe the time evolution of the repeated version of the game Γ, replicator dynamics were developed. Replicator dynamics, formulated within a system of differential equations, defines in which way the population vector $\vec{x} = (x_1, x_2)$ evolves in time. Each component $x_i = x_i(t)$ $(i = 1, 2)$ describes the time evolution of the fraction of different player types i in the whole population, where a type-i player is understood as an actor playing strategy s_i. The population vector has to fulfill the following conditions:

$$x_i(t) \geq 0 \quad \forall\, i = 1, 2\,,\ t \in \mathbb{R} \,\text{and}\, \sum_{i=1}^{2} x_i(t) = 1 \tag{4.5}$$

Because of condition (4.5), the population vector $\vec{x}(t) = (x_1(t), x_2(t))$ can be reduced to only one independent component ($x(t) := x_1(t)$, and $x_2(t) = 1 - x(t)$) and the replicator equation simplifies as follows:

$$\begin{aligned} \frac{dx}{dt} &= x\Big[(\$_{11} - \$_{21})(x - x^2) + (\$_{12} - \$_{22})(1 - 2x + x^2)\Big] \\ &= x\Big[(\delta + \alpha)x - \delta x^2 - \alpha\Big] := g(x) \end{aligned} \tag{4.6}$$

Figure 4.3 visualizes the time evolution of the population fraction $x(t)$ for several different starting values ($x_o := x(t = 0)$). The two symmetric, pure Nash-equilibria are the two evolutionary stable strategies (ESSs). Which of these ESSs is developed, depends on the value of the initial condition x_o. If x_o is above the

[3]The animations within this article are only viewable within its electronic version.

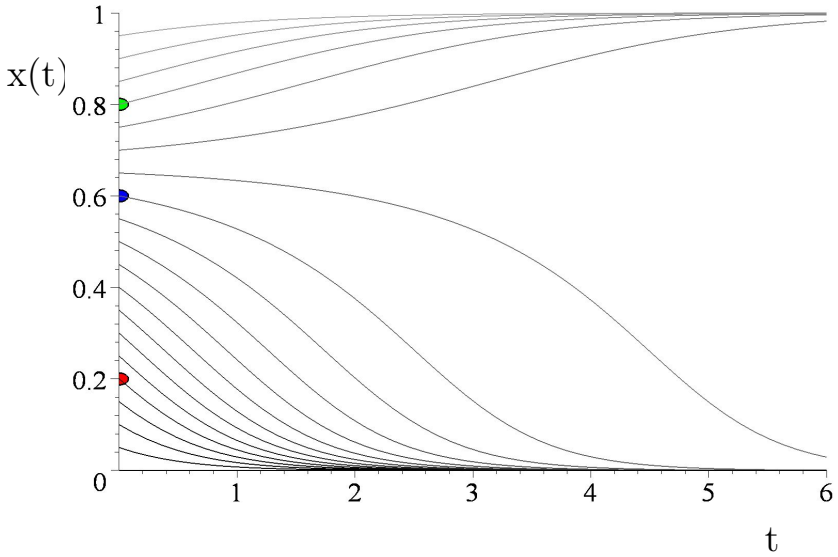

Figure 4.3.: Animation: Fraction of players choosing strategy s_1 =o as a function of time ($x(t)$) for different starting values $x(t=0)$. Results were calculated using the payoff matrix of Table 4.1 and the parameter set $r=5, \alpha=2$ and $\delta=3$.

value of the mixed strategy Nash-equilibrium ($x_o > \frac{\alpha}{\delta}$), the population will evolve to a community choosing solely the strategy s_1 ($x = \tilde{s}^A = \tilde{s}^B = 1$), whereas if $x_o < \frac{\alpha}{\delta}$ the population will asymptotical reach $x = 0$, which means that every player will choose strategy s_2 =∅. In respect to the application under focus, the results of the classical evolutionary game indicate, that if a scientific community has a traditional publication norm (e.g. almost all of the scientists do not use open access repositories) it is not possible to overcome the dilemma of the game, and the population remains in the ESS with the lower payoff.

4.3. Evolutionary Quantum Game Theory

In quantum game theory, the measurable pure classical strategies (s_1 and s_2) correspond to the orthonormal unit basis vectors $|s_1\rangle$ and $|s_2\rangle$ of the two dimensional complex space $\mathbb{C}^2$, the so called Hilbert space $\mathcal{H}_i$ of player i ($i = A, B$). A quantum strategy of a player i is represented as a general unit vector $|\psi\rangle_i$ in his/her strategic Hilbert space $\mathcal{H}_i$. The whole quantum strategy space $\mathcal{H}$ is

constructed with the use of the direct tensor product of the individual Hilbert spaces: $\mathcal{H} := \mathcal{H}_A \otimes \mathcal{H}_B$. The main difference between classical and quantum game theory is that in Hilbert space $\mathcal{H}$ correlations between the players' individual quantum strategies are allowed, if the two quantum strategies $|\psi\rangle_A \in \mathcal{H}_A$ and $|\psi\rangle_B \in \mathcal{H}_B$ are entangled. The overall state of the system we are looking at is described as a 2-player quantum state $|\Psi\rangle \in \mathcal{H}$. The four basis vectors of the Hilbert space $\mathcal{H}$ are defined as the classical game outcomes ($|s_1 s_1\rangle := (1,0,0,0)$, $|s_1 s_2\rangle := (0,-1,0,0)$, $|s_2 s_1\rangle := (0,0,-1,0)$ and $|s_2 s_2\rangle := (0,0,0,1)$). The setup of the quantum game begins with the choice of the initial state $|\Psi_0\rangle$. We assume that both players are in the state $|s_1\rangle$. The initial state of the two players is given by $|\Psi_0\rangle = \widehat{\mathcal{J}}\,|s_1 s_1\rangle$, where the unitary operator $\hat{\mathcal{J}}$ is responsible for the possible entanglement of the 2-player system (for details see [66, 111, 114]). The players' quantum decision (quantum strategy) is formulated with the use of a two parameter set of unitary 2×2 matrices:

$$\widehat{\mathcal{U}}(\theta,\varphi) := \begin{pmatrix} e^{i\,\varphi}\cos(\frac{\theta}{2}) & \sin(\frac{\theta}{2}) \\ -\sin(\frac{\theta}{2}) & e^{-i\,\varphi}\cos(\frac{\theta}{2}) \end{pmatrix} \qquad (4.7)$$
$$\forall \quad \theta \in [0,\pi] \;\wedge\; \varphi \in [0,\tfrac{\pi}{2}] \qquad .$$

By arranging the parameters θ and φ, a player chooses his quantum strategy. The classical strategy s_1 is selected by appointing $\theta = 0$ and $\varphi = 0$ ($\widehat{s_1} := \hat{\mathcal{U}}(0,0)$), whereas the strategy s_2 is selected by choosing $\theta = \pi$ and $\varphi = 0$ ($\widehat{s_2} := \hat{\mathcal{U}}(\pi,0)$); in addition, the quantum strategy $\widehat{Q}$ is given by $\widehat{Q} := \hat{\mathcal{U}}(0,\pi/2)$. After the two players have chosen their individual quantum strategies ($\hat{\mathcal{U}}_A := \hat{\mathcal{U}}(\theta_A,\varphi_A)$ and $\hat{\mathcal{U}}_B := \hat{\mathcal{U}}(\theta_B,\varphi_B)$) the disentangling operator $\widehat{\mathcal{J}}^\dagger$ is acting to prepare the measurement of the players' state. The entangling and disentangling operator ($\widehat{\mathcal{J}}, \widehat{\mathcal{J}}^\dagger$; with $\hat{\mathcal{J}} \equiv \hat{\mathcal{J}}^\dagger$) depends on one additional single parameter $\gamma \in [0,\pi/2]$ which is a measure of the strength of the entanglement of the system. Finally, the state prior to detection can therefore be formulated as follows:

$$|\Psi_f\rangle = \hat{\mathcal{J}}^\dagger \left(\hat{\mathcal{U}}_A \otimes \hat{\mathcal{U}}_B\right) \hat{\mathcal{J}}\;|s_1 s_1\rangle \qquad (4.8)$$

The expected payoff within a quantum version of a general 2-player game - which is an amplification of equation (4.2) - depends on the payoff matrix (see Table 4.1) and on the joint probability to observe the four observable outcomes

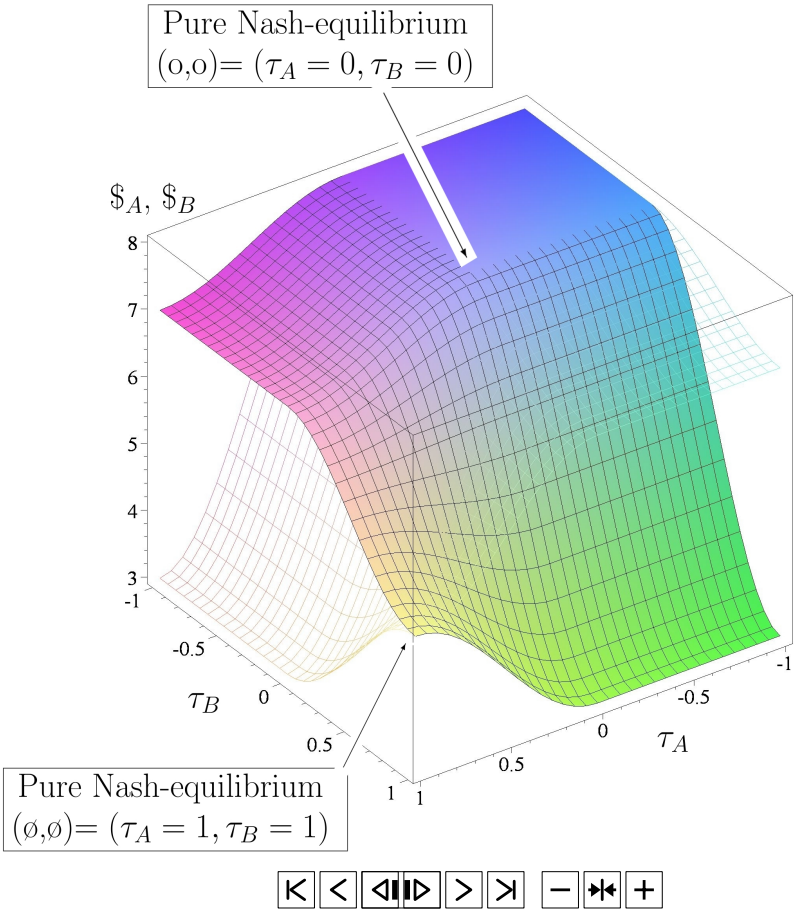

Figure 4.4.: Animation of the payoff surface of player A (solid) and player B (wired) as a function of their strategies τ_A and τ_B.

$P_{s_1s_1}, P_{s_1s_2}, P_{s_2s_1}$ and $P_{s_2s_2}$ of the game

$$\begin{aligned} \$_A &= \$_{11}\, P_{s_1s_1} + \$_{12}\, P_{s_1s_2} + \$_{21}\, P_{s_2s_1} + \$_{22}\, P_{s_2s_2} \\ \$_B &= \$_{11}\, P_{s_1s_1} + \$_{21}\, P_{s_2s_1} + \$_{12}\, P_{s_1s_2} + \$_{22}\, P_{s_2s_2} \\ \text{with:}\quad & P_{\sigma\sigma'} = |\langle \sigma\sigma' | \Psi_f \rangle|^2 \;, \quad \sigma, \sigma' = \{s_1, s_2\} \quad . \end{aligned} \tag{4.9}$$

To visualize the payoffs in a three dimensional diagram it is necessary to reduce the set of parameters in the final state: $|\Psi_f\rangle = |\Psi_f(\theta_A, \varphi_A, \theta_B, \varphi_B)\rangle \rightarrow |\Psi_f(\tau_A, \tau_B)\rangle$. Within the following diagram, the same specific parameterization as Eisert et al. [66] was used, where the two strategy angles θ and φ depend only

on a single parameter $\tau \in [-1, 1]$.[4] Positive τ-values represent pure and mixed classical strategies, whereas negative τ-values correspond to quantum strategies, where $\theta = 0$ and $\varphi > 0$. The whole strategy space is separated into four regions, namely the absolute classical region (CC: $\tau_A, \tau_B \geq 0$), the absolute quantum region (QQ: $\tau_A, \tau_B < 0$) and the two partially classical-quantum regions (CQ: $\tau_A \geq 0 \wedge \tau_B < 0$ and QC: $\tau_A < 0 \wedge \tau_B \geq 0$). Fig. 4.4 depicts the expected payoff for scientist A ($\$_A$, intransparent surface) and scientist B ($\$_B$, wired surface) as a function of their strategies τ_A and τ_B in a separable quantum game ($\gamma = 0$). The outcome of this separable quantum game is similar to the classical solution outlined in section 4.2. The animation in Figure 4.4 illustrates the change in the payoff surface, if one allows the strategic entanglement of the players to increase. For even tiny values of entanglement a new quantum Nash-equilibrium and additional ESS appears, for $\gamma > \frac{\pi}{4}$ the pure Nash-equilibrium (ø,ø) dissolves and the pure Nash-equilibrium (o,o) becomes the only observable ESS of the underlying game. A scientific community using a traditional publication norm can therefore overcome the dilemma of the game, if the strength of entanglement exceeds $\frac{\pi}{4}$. In such a case a spontaneous phase transition will occur reaching the global optimum of the underlying game.[5]

[4] The parameter τ corresponds to parameter t of [66].

[5] The electronic version of this article includes several dynamic animations. The LaTex-source files and the underlying Maple-worksheets of all the calculations performed, are freely downloadable on the following internet page http://evolution.wiwi.uni-frankfurt.de/BWGT2010/.

5. Article 3: Doves and Hawks in Economics Revisited: An evolutionary quantum game theory-based analysis of financial crises

Physica A 389 (2010) 5084–5102

Contents lists available at ScienceDirect

Physica A

journal homepage: www.elsevier.com/locate/physa

Doves and hawks in economics revisited: An evolutionary quantum game theory based analysis of financial crises

Matthias Hanauske [a,*], Jennifer Kunz [b], Steffen Bernius [a], Wolfgang König [c]

[a] Institute of Information Systems, Goethe-University, Grüneburgplatz 1, 60323 Frankfurt/Main, Germany
[b] Chair of Controlling & Auditing, Goethe-University, Grüneburgplatz 1, 60323 Frankfurt/Main, Germany
[c] House of Finance, Goethe-University, Grüneburgplatz 1, 60323 Frankfurt/Main, Germany

ARTICLE INFO

Article history:
Received 14 April 2009
Received in revised form 22 April 2010
Available online 15 June 2010

Keywords:
Evolutionary game theory
Quantum game theory
Hawk–dove game
Financial crisis

ABSTRACT

The last financial and economic crisis demonstrated the dysfunctional long-term effects of aggressive behaviour in financial markets. Yet, evolutionary game theory predicts that under the condition of strategic dependence a certain degree of aggressive behaviour remains within a given population of agents. However, as a consequence of the financial crisis, it would be desirable to change the "rules of the game" in a way that prevents the occurrence of any aggressive behaviour and thereby also the danger of market crashes. The paper picks up this aspect. Through the extension of the well-known hawk–dove game by a quantum approach, we can show that dependent on entanglement, evolutionary stable strategies also can emerge, which are not predicted by the classical evolutionary game theory and where the total economic population uses a non-aggressive quantum strategy.

Figure 5.1.: Published version of the article (Physica A 389 (2010) 5084-5102)[118].

Abstract

The last financial and economic crisis demonstrated the dysfunctional long-term effects of aggressive behaviour in financial markets. Yet, evolutionary game theory predicts that under the condition of strategic dependence a certain degree of aggressive behaviour remains within a given population of agents. However, as the consequences of the financial crisis exhibit, it would be desirable to change the "rules of the game" in a way that prevents the occurrence of any aggressive behaviour and thereby also the danger of market crashes. The paper picks up this aspect. Through the extension of the in literature well-known Hawk-Dove game by a quantum approach, we can show that dependent on entanglement, also evolutionary stable strategies can emerge, which are not predicted by classical evolutionary game theory and where the total economic population uses a non-aggressive quantum strategy.

5.1. Introduction

Economic developments often have been compared to biological evolutionary processes, as they converge to equilibria in an evolutionary manner (e.g. Hodgson, 1993; Dosi & Nelson, 1994; Dopfer, 2001 [126, 60, 59]). Actually, the conceptual ideas behind evolutionary theory were borrowed from early economic works, especially Malthus (1798) [161] (see e.g. Friedmann, 1998 [79]). Due to inter alia the application of evolutionary game theory, whose origin lies in biology (Maynard Smith, 1972, 1982 [212, 214]), evolutionary concepts came back into economics and organisational theory. Applications in respect to biological systems [209, 226, 148, 78, 171, 172, 83] and socio-economic systems, e.g. "public good"-games [51, 124], cultural or moral developments [68, 121], the evolution of languages [177], social learning [68], the evolution of social norms [23, 175] and the evolution of social networks [222, 139, 67, 225, 185, 245, 58] have been addressed in several research articles. One major topic in this evolutionary research field is the optimality of aggressive versus non-aggressive or cooperative behaviour (see e.g. for the tension of cooperative and non-cooperative behaviour Axelrod, 1997 [23]). In an economic context the notion of aggressive behaviour can be translated to the short-term oriented maximisation of individual utility without looking

after others, while cooperative behaviour comprises a more interactive and long-term oriented behaviour considering long-term, individual and/or group utility maximisation. Possible positive effects of the mentioned aggressive behaviour on economic welfare have been discussed since the earliest days of economics (Smith, 1776 [210]): The idea was that if each economic individual tries to maximise his/her utility without caring about other individuals, the whole welfare will also be maximal.

One instrument to analyse the long-term effects of this assumption is evolutionary game theory. Analogous to classical game theory it introduces the concept of strategic dependence among agents in an economic context. In such a situation the expected utility of one agent depends on the decisions of other agents. Evolutionary game theory provides an equilibrium in which the ratio of aggressive to non-aggressive agents is stable and that depends on the expected losses and gains of utility induced by the agents' decisions. For example, if the expected losses are high for two meeting aggressive agents, most members of the economic population – but not all of them – will behave in a none-aggressive, cooperative way (Osborne & Rubenstein, 1994 [174]). Hence, also in situations where severe losses are expected, if two aggressive agents meet, an economic population always will contain a certain degree of aggressive agents.

In economic reality, exactly this aspect can be observed, for example in the recent financial crisis: Each participant of financial transactions knew that highly risky financial products would increase the risk of the whole market portfolio and thereby augment the probability of a market crash resulting in huge losses. Nevertheless, several participants continued selling and buying these products in order to maximise their own, short-term utility resulting from high selling premiums and investment returns. Hence, these individuals followed an aggressive strategy. However, as the occurrence of the financial crisis exhibited, this behaviour can result in severe problems for the whole economic population. So, the question rises, whether there is a possibility to change the rules of the game in a way that protects populations from these severe problems by inhibiting the occurrence of aggressive behaviour.

To answer this question the classical concept of evolutionary game theory shall be extended by another game theoretical development that is currently discussed:

quantum games. The discussion of quantum games started with the work of Meyer (1999) [165] and Eisert et al. (1999) [66]. Meyer analysed the "penny flip" game and showed, that a player who selects a quantum strategy always wins this game. Eisert et al. (1999) concentrated on the prisoner dilemma and demonstrated that the players of this game could escape this dilemma if the entanglement of the prisoners' wave function is above a certain value. Since these leadoff articles several further applications of quantum games have been published. Marinatto & Weber (2000) [162] applied quantum games to the "battle of sexes" showing that entangled strategies will lead to a unique solution of this game. R.V. Mendes analysed the "quantum ultimatum game" and Hogg et al. investigated the quantum treatment of several different games, namely the "quantum treatment of public good economics" [48], the "quantum coordination game" [134] and "quantum auctions" [131]. Benjamin & Hayden [28] amplified the quantum game approach to a situation of multiple players. Piotrowski & Sladkowsky [178] used quantum games to examine market behaviour. In 2001 the first quantum game was realized on a quantum computer [62] (see also [190]). The application of quantum game theory to social experiments and experimental economics [49, 176, 112, 242, 38] and several review articles [97, 186, 240, 180, 155, 179, 181] followed. Hanauske et al. [111] based the analysis of the open access publishing behaviour in different scientific communities on a quantum game approach (see also [118]).

The combination of this quantum game approach and evolutionary game theory has been applied by [137, 95, 138, 169]. We add to this existing research a practical application of this type of game theory. Our results show that dependent on entanglement, also evolutionary stable strategies can emerge, which are not predicted by classical evolutionary game theory: The analysis exhibits the existence of a new, payoff dominant evolutionary stable strategy (ESS), where the whole economic population uses the non-aggressive quantum dove strategy. We interpret entanglement in this context as the objective influence of socio-economic context factors, while the application of quantum strategies exhibits the degree to which decision makers incorporate these factors into their decisions. This interpretation allows the derivation of consequences and shows the linkage of our study to other game theoretical analyses that also highlight the importance of the socio-economic context to the outcomes of games. For example, Sally [194]

discusses the notion of sympathy, a feeling that occurs when players get to know each other and that can lead to increasing cooperation in prisoners' dilemma games. T. Platkowski [184, 183] generalises classical evolutionary game theory by implementing additional parameters, which describe the complex personality profiles similar to Max Weber's ideal types of social actors. Analogical to this study additional evolutionary stable strategies have been found for specific parameter ranges.

The paper is structured as follows: We pick up the recent financial crisis as an example for the fruitful application of evolutionary quantum game theory. In order to do so, we have to select a group of participants in the financial transactions that finally lead to the crisis. We have chosen the group of inventors and sellers of the highly risky financial products. Their behaviour can be interpreted as the in theory well known Hawk-Dove game (Maynard Smith 1982, 1986 [214, 215]). Hence, in section 5.2 we develop a model that is based on this game type and comprises the relevant parts of the behaviour of these constructors and sellers to mirror the starting conditions of the financial crisis. In section 5.3 we transfer this model into a classical evolutionary game. Section 5.4 is dedicated to the quantum version of this game, while section 5.5 comprises the evolutionary quantum version. In section 5.6 we draw some conclusions from our findings. The paper closes with a summary in section 5.7.

5.2. The financial crisis as Hawk-Dove game

Financial crises in general and the last one especially, have their origin in highly speculative behaviour of market participants. In our analysis we focus on a specific population of market participants, who had a great part in the last crisis: constructors and sellers of financial products with different degrees of risk. They played an important role in the last crisis as follows:
This crisis grounded especially on the housing market in the United States. Based on the idea of continuously increasing prices for real estates, loans were also provided to borrowers, who actually could not afford buying a house. But under the premise of increasing house values, providing loans to these people seemed to be rational as they were backed by increasingly valuable real estates. Yet, these

loans did not remain with the lending credit institutes but they were bundled to portfolios together with loans of higher solvency. These portfolios then were sold to other banks as investment products. The idea behind these products is to spread risk among banks. Moreover, papers of higher risk also promise a higher return, which makes them attractive for speculative purposes. The buying banks often unbundled the loans and bundled them together with other loans to sell again parts of these newly created portfolios. These processes were repeated several times. So finally, the loans were scattered around the world. However, after the house prices started falling, the bad loans became obvious in these portfolios and caused losses. But, as the loans were scattered around the world, nobody really knew where which risk still remained and which bank would suffer next from a financial disorder. As a result of this, banks stopped providing credit to each other in order to prevent credit defaults. This trust crisis actually lead to the severe economic problems, as not only banks but also other firms got problems to receive credits for the continuation of their business.

Hence, one major driver of the crisis was the mentioned speculative investment products. The described portfolios had a considerable degree of complexity. In combination with the continuously spreading of risks among the same investors it was only a matter of time that the crisis had to start. However, although this was foreseeable dealing with this investment products continued. This scenario can be transferred to a model usable for evolutionary game theory as follows:
In line with the classical Hawk-Dove model two types of agents shall be considered: Doves follow a non-aggressive strategy. Transferred to the financial situation they are investment bankers who construct investment products of rather low risk and moderate expected return. These products lead to a moderate premium to the seller but have no negative long-term impact on the total market risk. Additionally, when selling their products to investors, doves remain with their contract conditions and do not try to make a deal by all means, e.g. promising unrealistic returns or omitting to point out severe risk factors of the investment product. In contrast, hawks follow an aggressive strategy. They represent those investment bankers, who are specialised on highly risky products with high expected returns. They also act aggressive to sell their products, which might end up in investment constructs that contain a destabilising potential to the financial market. Both types of agents “fight” for a pool of risk-neutral investors.

For simplification reasons, we assume that always only two agents fight for one investor, where both agents can be doves, or hawks, or one is a dove and one is a hawk.

If a dove and a hawk fight for one investor, the hawk will win, as he/she can offer a product with a higher expected return. If two doves meet, the investor will spread the investment equally, as it is assumed that both offer him/her the same conditions. If two hawks meet, the investor will also spread the investment equally, as again it is assumed that both hawks provide the same investment product. However, the payoffs of the players are quite different in all three cases and contain two parts.

The first part is the selling premium. This premium depends on the expected return of the sold investment product. In the first case, the dove gets nothing, as it cannot sell any product, while the hawk receives a high premium p_h. In the second case, both doves get half of the moderate premium p_m, as the investment sum is split up between both. In the last case, both hawks receive half of the high premium, as again the investment is split up.

The second part comprises a discount resulting from the fight of two players for one investor. In the first case, an aggressive and a non-aggressive investment banker meet. Here, no fight will take place, as the non-aggressive banker remains with his/her conditions and the investor prefers the product with the higher expected return. Hence, the aggressive banker has no reason to start any fight, since he/she can sell his/her product. Regarding the second case, again no fighting will be observed, as both bankers stay with their conditions and the investor just splits up the investment sum. Consequently, in the first and the second cases, no discount has to be considered. However, if two aggressive bankers meet, they will try to get the whole investment sum and start fighting for it. On the one hand, this can result in a lowering of selling prices. On the other hand, this ends in the construction of products which offer an even higher expected return but bear very high, partly hidden risks. These effects are totalled in a discount parameter d. Hence, both aggressive bankers receive half of the high premium minus this discount. The discount factor is an indicator for the degree of aggressiveness of the hawks and at the same time for the danger of the products resulting from the meeting of two hawks to cause a future crash due to

hidden risk. Table 5.1 summarises the payoff matrix.

A\B	Hawk	Dove
Hawk	$(\frac{p_h-d}{2}, \frac{p_h-d}{2})$	$(p_h, 0)$
Dove	$(0, p_h)$	$(\frac{p_m}{2}, \frac{p_m}{2})$

Table 5.1.: Payoff matrix for investment bankers A and B within the Hawk-Dove game. The parameters are defined as follows: p_h: high selling premium, d: disutility resulting from fighting and p_m: moderate selling premium.

To assure the payoff matrix to have the formal structure of a Hawk-Dove game the parameters of Table 5.1 should fulfil the inequation $p_h > p_m > 0 > \frac{p_h-d}{2}$, which means that the disutility d should be higher than the high selling premium p_h.

In sum, the following analyses concentrate on the appearance and possible prevention of aggressive behavioural patterns that may lead to a crisis. However, we do not explicitly model the occurrence of such a crisis.

5.3. The classical evolutionary game of doves and hawks

This section is dedicated to the introduction of the necessary definitions and fundamental basics of an evolutionary game. In the following the presentation is constrained to describe a symmetric two person, n–strategy game Γ (for details see [108, 166, 222, 235]):

$$\begin{aligned} \Gamma &:= \left(\{A, B\}, \mathcal{S} \times \mathcal{S}, \hat{\$}\right) && : \text{2-person game} \\ s &= (s_1, s_2, ..., s_n) \in \mathcal{S} && : \text{Set of pure strategies} \\ \hat{\$} &= \begin{pmatrix} \$_{11} & \$_{12} & ... & \$_{1n} \\ \$_{21} & \$_{22} & ... & \$_{2n} \\ ... & ... & ... & ... \\ \$_{n1} & \$_{n2} & ... & \$_{nn} \end{pmatrix} && : \text{Payoff matrix} \end{aligned} \tag{5.1}$$

To describe the time evolution of the repeated version of the game Γ, replicator dynamics were developed. Replicator dynamics, formulated within a system of differential equations, defines in which way the population vector $\vec{x} := (x_1, x_2, ..., x_n)$ evolves in time. Each component $x_i = x_i(t)$ $(i = 1, 2, ..., n)$ describes the time evolution of the fraction of different player types i in the whole population, where a type-i player is understood as an actor playing strategy s_i. The population vector $\vec{x}$ has to fulfil the normalising conditions of a unity vector

$$x_i(t) \geq 0 \quad \forall\, i = 1, 2, ..., n\,,\ t \in \mathbb{R} \,\text{and}\, \sum_{i=1}^{n} x_i(t) = 1. \tag{5.2}$$

The following first order system of differential equations of the population vector $\vec{x}(t) = (x_1(t), x_2(t), ..., x_n(t))$ is known as replicator dynamics (see [108, 222, 166, 235])

$$\frac{dx_i(t)}{dt} = x_i(t) \left[\underbrace{\sum_{l=1}^{n} \$_{il}\, x_l(t)}_{:=f_i(t)} - \underbrace{\sum_{l=1}^{n}\sum_{k=1}^{n} \$_{kl}\, x_k(t)\, x_l(t)}_{:=\bar{f}(t)} \right] \tag{5.3}$$

where $f_i(t)$ is the fitness of type i and $\bar{f}(t) = \sum_{i=1}^{n} f_i(t)$ is the avarage fitness of the whole population.

In the following the formal description is restricted to only two strategies $(i = 1, 2 \mathrel{\hat{=}} H, D)$. Because of condition (5.2), the population vector $\vec{x}(t) = (x_1(t), x_2(t))$ can be reduced to only one independent component $(x(t) := x_1(t)$ and $x_2(t) = 1 - x(t))$ and equation (5.3) simplifies as follows:

$$\frac{dx}{dt} = x \left[(\$_{11} - \$_{21})(x - x^2) + (\$_{12} - \$_{22})(1 - 2x + x^2) \right]$$

Inserting the parameters of the Hawk-Dove payoff matrix (see Table 5.1) gives the following differential equation:

$$\frac{dx}{dt} = \frac{1}{2}\,(p_h - p_m + d)\; x^3 + \left(p_m - \frac{3}{2} p_h - \frac{1}{2} d \right) x^2 + \left(p_h - \frac{1}{2} p_m \right) x \tag{5.4}$$

To show the consequences of equation (5.4) and to discuss and illustrate the main properties of the underlying Hawk-Dove game the payoff parameters of Table

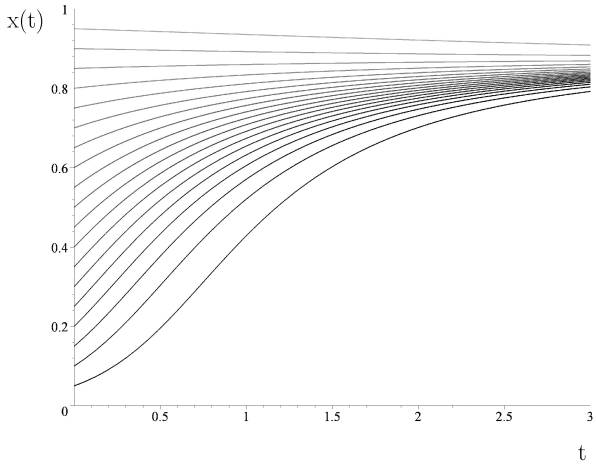

Figure 5.2.: Fraction of hawks x as a function of time t for different starting values $x(t = 0)$. Results were calculated using the parameter set $P1$ (low risk investment market).

5.1 have been set to three different parameter sets (see Table 5.2). Within the parameter sets the high and low selling premiums are fixed ($p_h = 5$ and $p_m = 3$), whereas the destabilising factor d is varied. In parameter set $P1$ the risk of destabilisation is only a little bit higher ($d = 6$) than the high selling premium, in parameter set $P2$ a medium value of the destabilising factor d that results from fighting was used ($d = 10$), and in set $P3$ the parameter d was chosen to a quite high value ($d = 20$).

Parameter setting	Risk of destabilisation	d	p_h	p_m
P1	LOW	6	5	3
P2	MEDIUM	10	5	3
P3	HIGH	20	5	3

Table 5.2.: Parameters of the three different sets of the underlying payoff matrix used to model the investment market of the Hawk-Dove game.

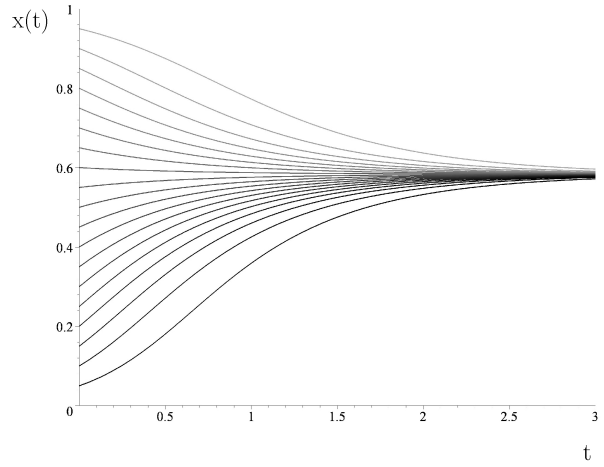

Figure 5.3.: Description like in Figure 5.2. Results were calculated using the parameter set $P2$ (medium risk investment market).

The evolution of the fraction of hawks $x(t)$ within the hawk-dove population is displayed in Figures 5.2, 5.3 and 5.4. Figure 5.2 shows $x(t)$ as a function of time for the parameter set $P1$, in which the different curves where calculated using various different starting values of the fraction of hawks at time zero ($x(0) = \frac{1}{20}, \frac{2}{20}, ..., \frac{19}{20}$). The Figure shows clearly that all population curves converge to one limit value $x_L := x(t \to \infty)$. Within parameter set $P1$ the fraction of hawks ends after some time always at $x_L = 0.86$, which means that the population of hawks and doves will be stable if it consists of 86% hawks and 14% doves. Parameter set $P1$ corresponds to a situation where the risk of a future crash of the whole investment market is expected to be quite low. Within such a situation the theory predicts that the relative number of investment bankers selling highly risky products (hawk strategy) is quite high (86%) and as a result the fraction of sellers offering products with moderate returns and a rather low risk is quite low (14%).

Within parameter set $P2$ the underlying investment market has a medium crashing risk. Figure 5.3 shows that for such a market the stable fraction of hawks (investment bankers selling highly risky products) has decreased ($x_L = 0.56$).

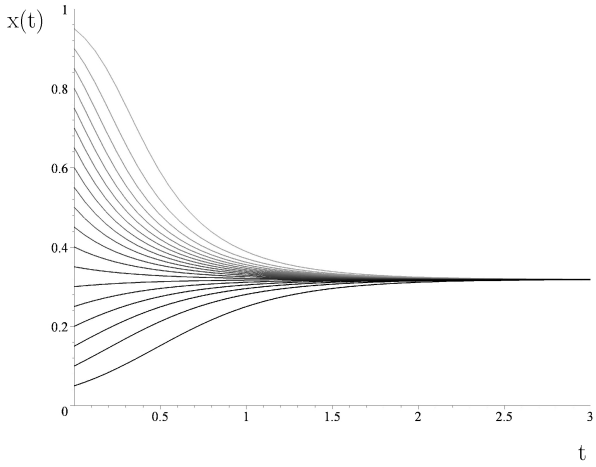

Figure 5.4.: Description like in Figure 5.2. Results were calculated using the parameter set $P3$ (high risk investment market).

Figure 5.4 shows the situation where aggressive behaviour will lead to an unstable market, in which it is very like that a future crash will occur. The players within such a highly risky market choose mainly a non risky dove strategy ($x_L = 0.34$), but still 34% of the investment bankers sell highly risky products.

To understand the simulated results more formally, the concept of evolutionary stable strategies is briefly explained in the following.

Taking a general symmetric 2-player game Γ with a payoff matrix $\hat{\$}$. A strategy $s^* \in \mathcal{S}$ is defined as an evolutionary stable strategy (ESS) if
a) (s^*, s^*) is a Nash equilibrium of the game
b) $\$(s, s) \leq \$(s^*, s) \ \forall \ s \in r(s^*)\,, \ s \neq s^*$

$r(s^*)$ is the best response function to the strategy s^* and $\$(s, s)$ describes the extended, mixed strategy payoff function. An evolutionary stable strategy s^* therefore needs to be a symmetric Nash equilibrium of the game and additionally the inequation b) should be fulfilled for any strategy s belonging to the set of best responses to s^* ($s \in r(s^*)$). To illustrate this definition we restrict the number of pure strategies to $n = 2$ and use the payoff matrix of Table 5.1. $x := s_1^A$ denotes

the probability of player A playing the aggressive strategy hawk, while $y := s_1^B$ defines the probability of player B playing strategy hawk. The mixed strategy payoff function has therefore the following structure:

$$\begin{aligned} \$(x,y) &= \$_{11}\, x\, y + \$_{12}\, x\,(1-y) + \$_{21}\,(1-x)\, y + \$_{22}\,(1-x)\,(1-y) \\ &= \frac{p_h - d}{2}\, x\, y + p_h\, x\,(1-y) + \frac{p_m}{2}\,(1-x)\,(1-y) \end{aligned} \tag{5.5}$$

Because of the symmetry of the game, the payoff of player A ($\$^A(x,y) = \$(x,y)$) and the payoff of player B are equal after variable transformation ($x \to y, y \to x$):

$$\$^A(x,y) = \$(x,y) \quad \text{and} \quad \$^B(x,y) = \$(y,x)$$

The two necessary conditions to prove the existence of a Nash equilibrium (x^*, y^*) in a 2-person 2-strategy game reduce therefore to one single condition [108, 222, 235]:

$$\begin{aligned} \$^A(x^*,y^*) &\geq \$^A(x,y^*) \quad \forall\ x \in [0,1] \\ \$^B(x^*,y^*) &\geq \$^B(x^*,y) \quad \forall\ y \in [0,1] \\ \Rightarrow \$(x^*,y^*) &\geq \$(x,y^*) \quad \forall\ x \in [0,1] \end{aligned} \tag{5.6}$$

The game has three Nash equilibria. Two are non symmetric pure Nash equilibria ($(x=1, y=0) \hat{=} (H,D)$ and $(x=0, y=1) \hat{=} (D,H)$) and one is a symmetric, mixed strategy Nash equilibrium ($x = \frac{p_m - 2p_h}{p_m - p_h - d}, y = \frac{p_m - 2p_h}{p_m - p_h - d}$). Definition (5.6) requires that in every Nash equilibrium the function $\mathcal{N} := \$(x^*,y^*) - \$(x,y^*)$ needs to be positive for all $x \in [0,1]$. Figure 5.5 shows $\mathcal{N}$ for the three Nash equilibria within a middle risk scenario (parameter set $P2$) and proves their existence, as all values are non negative.

To prove the existence of an evolutionary stable strategy, condition b) has to be fulfilled additionally for the mixed strategy Nash equilibrium. The best response of player A to the strategy $y^* = \frac{p_m - 2p_h}{p_m - p_h - d}$ is the set of all strategies $x \in [0,1]$, because $\$(x,y^*) = -\frac{(p_h - d)p_m}{2(p_h + d - p_m)}$ is independent of x. Condition b) therefore has to be checked for all $x \in [0,1] \setminus \{\frac{p_m - 2p_h}{p_m - p_h - d}\}$. x^* is an ESS if the function $\mathcal{G}(x^*, x)$

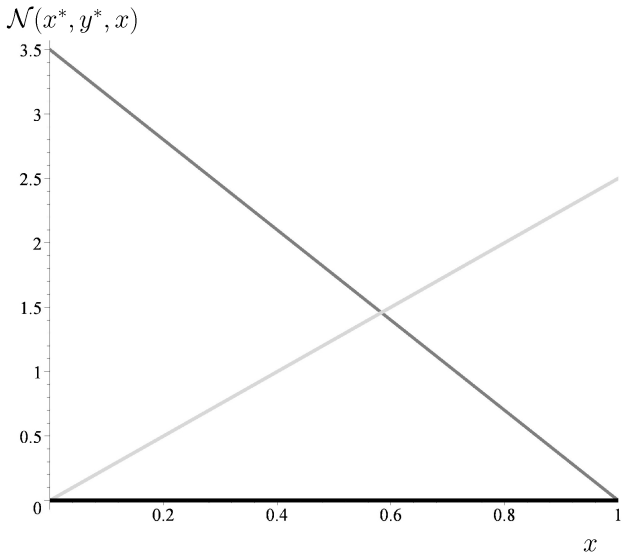

Figure 5.5.: $\mathcal{N}(x^*, y^*, x)$ for the three Nash equilibria as a function of x within the middle risk parameter setting $P2$. The dark grey line corresponds to the Nash equilibrium $(x^*, y^*) = (1, 0)$, the light grey line to $(x^*, y^*) = (0, 1)$ and the black line ($\mathcal{N} \equiv 0$) to the mixed strategy Nash equilibrium $(x^*, y^*) = (\frac{p_m - 2p_h}{p_m - p_h - d}, \frac{p_m - 2p_h}{p_m - p_h - d})$

fulfils the following condition:

$$\begin{aligned} \mathcal{G} &:= \$(x^*, x) - \$(x, x) \geq 0 \\ \forall\, x &\in [0,1] \setminus \{x^* = \tfrac{p_m - 2p_h}{p_m - p_h - d}\} \end{aligned} \tag{5.7}$$

Figure 5.6 shows $\mathcal{G}$ for the symmetric Nash equilibria $x^* = \frac{7}{2+d}$ ($p_h = 5, p_m = 3$) of the three different payoff parameter settings ($d = 6, 10, 20$). The null of the three curves corresponds to the evolutionary stable fraction of hawk strategies within the low ($d = 6$), middle ($d = 10$) and high ($d = 20$) risk settings. As the destabilisation risk d increases, the ESS $x^* = \frac{7}{2+d}$ (the fraction of hawks) decreases.

In sum, the results of the previous analysis based on evolutionary game theory suggest that dependent on the destabilisation factor the degree of aggressive

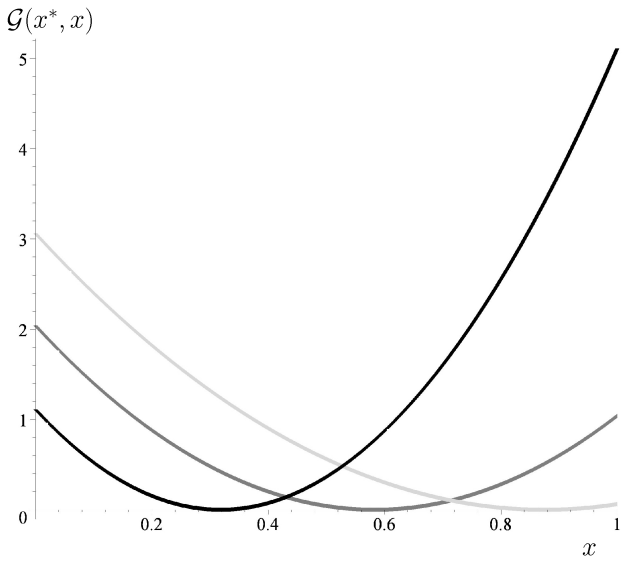

Figure 5.6.: $\mathcal{G}(x^*, x)$ for the three different parameter settings $P1$ ($x^* = \frac{7}{8}$, light grey curve), $P2$ ($x^* = \frac{7}{12}$, dark grey curve) and $P3$ ($x^* = \frac{7}{22}$, black curve).

agents varies, but even in case of highly risky markets aggressive behaviour will not vanish completely. This is exactly, what could be observed previously to the financial crisis: Although the risk of destabilisation in the investment market was obviously increasing for the last few years, the behaviour of some aggressive investment bankers did not change. However, instead of ending in a stable state, finally the market crashed and almost all aggressive agents disappeared from the population. This could have been prevented, if any aggressive behaviour were inhibited completely. Furthermore it should be remarked, that the players within this evolutionary game theoretical model are rewarded (punished) in each period of time and therefore realise immediately the benefit (risk) of their chosen strategy. However, in reality, the observation of an underlying negative utility of a disposed financial product (parameter d of Table 5.1) is usually time-delayed. The personal risk assessment within a market of increasing risk lags therefore always behind the real risk value.

It will be shown in this article that a quantum game theoretical formulation of

the Hawk-Dove game is able to induce exactly this result: within the subset of quantum dove strategies, it will be shown that if the strategy of all investment bankers is entangled above a certain value, a new evolutionary stable quantum strategy is possible, leading to an observed banker population offering solely non-aggressive investment products. Compared to the classical mixed strategy Nash equilibrium of the game, the new evolutionary stable quantum strategy is payoff dominant, if the strength of entanglement is above a certain value. To describe these phenomena in a more detailed way, the quantum game theory of doves and hawks is addressed within the following two sections.

5.4. The quantum game of doves and hawks

In quantum game theory, the measurable pure classical strategies (H and D) correspond to the orthonormal unit basis vectors $|H\rangle$ and $|D\rangle$ of the two dimensional complex space $\mathbb{C}^2$, the so called Hilbert space $\mathcal{H}_i$ of player i ($i = A, B$). A quantum strategy of a player i is represented as a general unit vector $|\psi\rangle_i$ in his strategic Hilbert space $\mathcal{H}_i$. The whole quantum strategy space $\mathcal{H}$ is constructed with the use of the direct tensor product of the individual Hilbert spaces: $\mathcal{H} := \mathcal{H}_A \otimes \mathcal{H}_B$. The main difference between classical and quantum game theory is that in the Hilbert space $\mathcal{H}$ correlations between the players' individual quantum strategies are allowed, if the two quantum strategies $|\psi\rangle_A \in \mathcal{H}_A$ and $|\psi\rangle_B \in \mathcal{H}_B$ are entangled. The overall state of the system we are looking at is described as a 2-player quantum state $|\Psi\rangle \in \mathcal{H}$. We define the four basis vectors of the Hilbert space $\mathcal{H}$ as the classical game outcomes ($|DD\rangle := (1, 0, 0, 0)$, $|DH\rangle := (0, -1, 0, 0)$, $|HD\rangle := (0, 0, -1, 0)$ and $|HH\rangle := (0, 0, 0, 1)$).

The setup of the quantum game begins with the choice of the initial state $|\Psi_0\rangle$. We assume that both players are in the state $|D\rangle$. The initial state of the two

players is given by

$$|\Psi_0\rangle \;=\; \widehat{\mathcal{J}}\,|DD\rangle \;=\; \begin{pmatrix} \cos\left(\frac{\gamma}{2}\right) \\ \\ 0 \\ \\ 0 \\ \\ i\sin\left(\frac{\gamma}{2}\right) \end{pmatrix} \quad , \tag{5.8}$$

where the unitary operator $\hat{\mathcal{J}}$ (see equation (5.13)) is responsible for the possible entanglement of the 2-player system. The players' quantum decision (quantum strategy) is formulated with the use of a two parameter set of unitary 2×2 matrices:

$$\begin{gathered} \widehat{\mathcal{U}}(\theta,\varphi) := \begin{pmatrix} e^{i\,\varphi}\cos(\frac{\theta}{2}) & \sin(\frac{\theta}{2}) \\ -\sin(\frac{\theta}{2}) & e^{-i\,\varphi}\cos(\frac{\theta}{2}) \end{pmatrix} \\ \forall \quad \theta \in [0,\pi] \;\wedge\; \varphi \in [0,\tfrac{\pi}{2}] \qquad . \end{gathered} \tag{5.9}$$

By arranging the parameters θ and φ, a player chooses his quantum strategy. The classical strategy D (Dove) is selected by appointing $\theta = 0$ and $\varphi = 0$:

$$\widehat{D} := \hat{\mathcal{U}}(0,0) = \begin{pmatrix} 1 & 0 \\ 0 & 1 \end{pmatrix} \quad , \tag{5.10}$$

whereas the strategy H (Hawk) is selected by choosing $\theta = \pi$ and $\varphi = 0$:

$$\widehat{H} := \hat{\mathcal{U}}(\pi,0) = \begin{pmatrix} 0 & 1 \\ -1 & 0 \end{pmatrix} \quad . \tag{5.11}$$

In addition, the quantum strategy $\widehat{Q}$ is given by

$$\widehat{Q} := \hat{\mathcal{U}}(0,\pi/2) = \begin{pmatrix} i & 0 \\ 0 & -i \end{pmatrix} \quad . \tag{5.12}$$

After the two players have chosen their individual quantum strategies ($\hat{\mathcal{U}}_A := \hat{\mathcal{U}}(\theta_A,\varphi_A)$ and $\hat{\mathcal{U}}_B := \hat{\mathcal{U}}(\theta_B,\varphi_B)$) the disentangling operator $\widehat{\mathcal{J}}^\dagger$ is acting to

prepare the measurement of the players' state. The entangling and disentangling operator ($\widehat{\mathcal{J}}, \widehat{\mathcal{J}}^{\dagger}$; with $\hat{\mathcal{J}} \equiv \hat{\mathcal{J}}^{\dagger}$) depends on one additional single parameter γ which measures the strength of the entanglement of the system:

$$\widehat{\mathcal{J}} := e^{i\,\frac{\gamma}{2}(\widehat{D}\otimes\widehat{D})} \;, \quad \gamma \in [0, \frac{\pi}{2}] \quad . \tag{5.13}$$

In the used representation, the entangling operator $\widehat{\mathcal{J}}$ has the following explicit structure:

$$\widehat{\mathcal{J}} := \begin{pmatrix} \cos\left(\frac{\gamma}{2}\right) & 0 & 0 & i\sin\left(\frac{\gamma}{2}\right) \\ 0 & \cos\left(\frac{\gamma}{2}\right) & -i\sin\left(\frac{\gamma}{2}\right) & 0 \\ 0 & -i\sin\left(\frac{\gamma}{2}\right) & \cos\left(\frac{\gamma}{2}\right) & 0 \\ i\sin\left(\frac{\gamma}{2}\right) & 0 & 0 & \cos\left(\frac{\gamma}{2}\right) \end{pmatrix} . \tag{5.14}$$

Finally, the state prior to detection can therefore be formulated as follows:

$$|\Psi_f\rangle = \hat{\mathcal{J}}^{\dagger}\left(\hat{\mathcal{U}}_A \otimes \hat{\mathcal{U}}_B\right)\hat{\mathcal{J}}\;|DD\rangle \quad . \tag{5.15}$$

The expected payoff within a quantum version of a general 2-player game depends on the payoff matrix (see Table 5.1) and on the joint probability to observe the four observable outcomes $P_{\mathrm{HH}}, P_{\mathrm{HD}}, P_{\mathrm{DH}}$ and P_{DD} of the game

$$\begin{aligned} \$_A \quad &= \$_{11}\,P_{\mathrm{HH}} + \$_{12}\,P_{\mathrm{HD}} + \$_{21}\,P_{\mathrm{DH}} + \$_{22}\,P_{\mathrm{DD}} \\ \$_B \quad &= \$_{11}\,P_{\mathrm{HH}} + \$_{21}\,P_{\mathrm{HD}} + \$_{12}\,P_{\mathrm{DH}} + \$_{22}\,P_{\mathrm{DD}} \\ \text{with:} \quad & P_{\sigma\sigma'} = |\,\langle\sigma\sigma'|\Psi_f\rangle\,|^2 \;, \quad \sigma,\sigma' = \{H, D\} \quad . \end{aligned} \tag{5.16}$$

It should be pointed out here, that an entangled 2-player quantum state does not mean at all that the persons themselves (or even the players' brains) are entangled. The process of quantum decoherence, with its quantum to classical transition, forbid such macroscopic entangled systems established from microscopic quantum particles [199, 140]. However, peoples' cogitations, represented as quantum strategies, could be associated within an abstract space. Although no measurable

accord is present between the players' strategy choices, the imaginary parts of their strategy wave functions might interact, if their individual states are entangled. In the context of the financial investment market, this quantum phenomenon might possibly be interpreted as a conjoint, psychological contract between the investment bankers aligning their strategies and resulting from social norms, moral standards and other impacts of socio-economic context factors. Such an alignment is now formulated as the appearance of a strongly entangled strategy effectuating the players to act more like a collective state.

To visualise the payoffs in a three dimensional diagram it is necessary to reduce the set of parameters in the final state: $|\Psi_f\rangle = |\Psi_f(\theta_A, \varphi_A, \theta_B, \varphi_B)\rangle \rightarrow |\Psi_f(\tau_A, \tau_B)\rangle$. Within the following diagrams we have used the same specific parameterisation as Eisert et al. [66], where the two strategy angles θ and φ depend only on a single parameter $\tau \in [-1, 1]$.[1] Positive τ-values represent pure and mixed classical strategies, whereas negative τ-values correspond to quantum strategies, where $\theta = 0$ and $\varphi > 0$. The whole strategy space is separated into four regions, namely the absolute classical region (CC: $\tau_A, \tau_B \geq 0$), the absolute quantum region (QQ: $\tau_A, \tau_B < 0$) and the two partially classical-quantum regions (CQ: $\tau_A \geq 0 \wedge \tau_B < 0$ and QC: $\tau_A < 0 \wedge \tau_B \geq 0$). It should be mentioned that within the (τ_A, τ_B) representation the set of possible strategies $\{(\theta, \varphi) \mid \theta \in [0, \pi]\,,\ \varphi \in [0, \frac{\pi}{2}]\}$ is reduced to the following specific subset:

$$\underbrace{\{(\tau\,\pi, 0) \mid \tau \in [0, 1]\}}_{\text{classical region C}} \ \wedge \ \underbrace{\{(0, \tau\,\frac{\pi}{2}) \mid \tau \in [-1, 0[\}}_{\text{quantum region Q}} \quad . \tag{5.17}$$

5.4.1. Quantum Dove Strategies

As the θ-value of the quantum region Q is fixed to zero, the possible quantum strategies can be understood as "Quantum Dove" strategies. In the following we will show results within this quantum dove strategy subset, where $\tau_A, \tau_B = 1$ corresponds to strategy H, and $\tau_A, \tau_B = 0$ corresponds to strategy D. All the results presented within this subsection where calculated using this quantum dove strategy subset.

[1] The parameter τ corresponds to parameter t of [66].

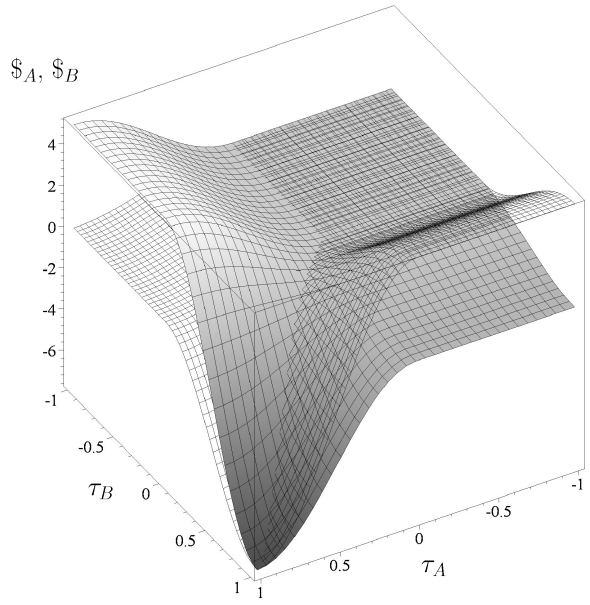

Figure 5.7.: Payoff surface of player A (solid) and player B (wired) as a function of their reduced strategies τ_A and τ_B within a non-entangled quantum game ($\gamma = 0$) using the quantum dove strategy subset and the high risk parameter setting $P3$.

Diagram 5.7 illustrates the outcomes of the high risk game setting by visualising the payoff surfaces of investment banker A (solid surface) and investment banker B (wired surface) as a function of their strategies τ_A and τ_B. In all of the presented three dimensional figures (within this subsection) the absolute quantum region QQ is projected in the back, whereas the absolute classical region CC is projected to the front. Figure 5.7 shows the result where no strategic entanglement is present ($\gamma = 0$). The diagram clearly exhibits that the non-entangled quantum game simply describes the classical version of the high risk Hawk-Dove game. For the case, that both players decide to play a quantum strategy ($\tau_A < 0 \wedge \tau_B < 0$) their payoff is equal to the case where both players choose the classical dove strategy D ($\$_A(D, D) = \$_A(\tau_A = 0, \tau_B = 0) = \frac{p_m}{2}$). The two classical non symmetric pure Nash equilibria ($(x = 1, y = 0)\hat{=}(H, D)$ and $(x = 0, y = 1)\hat{=}(D, H)$) correspond to the following τ-values: $(H, D)\hat{=}(\tau_A =$

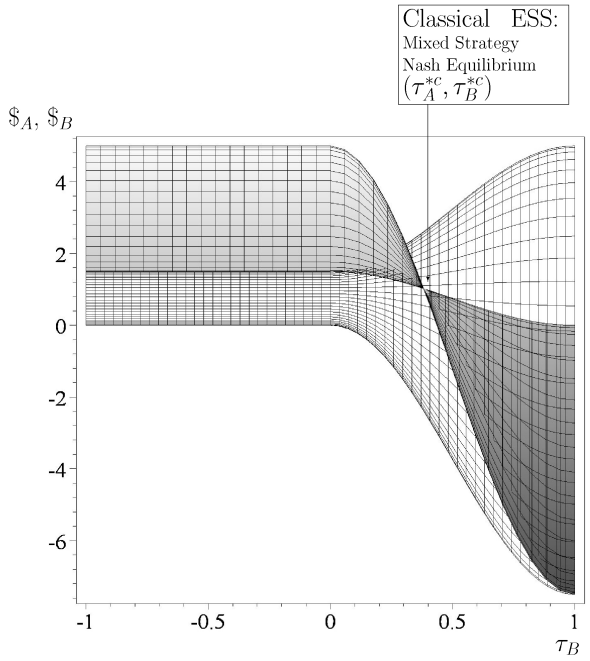

Figure 5.8.: Projection of the payoff surface of Figure 5.7 in direction of the τ_A-axis.

$1, \tau_B = 0)$ and $(D, H) \hat{=} (\tau_A = 0, \tau_B = 1)$. The ESS of the classical game (the mixed strategy Nash equilibrium $(x^* = \frac{p_m - 2p_h}{p_m - p_h - d}, y^* = \frac{p_m - 2p_h}{p_m - p_h - d})$ is equal to the strategy point $(\tau_A^{*c}, \tau_B^{*c}) = (\frac{2}{\pi}\arccos\Big(\sqrt{1 - \frac{p_m - 2p_h}{p_m - p_h - d}}\Big), \frac{2}{\pi}\arccos\Big(1 - \sqrt{\frac{p_m - 2p_h}{p_m - p_h - d}}\Big))$. At $(\tau_A^{*c}, \tau_B^{*c})$ the partial derivatives $\frac{\partial \$_A}{\partial \tau_A}(\tau_A, \tau_B^{*c})$ and $\frac{\partial \$_B}{\partial \tau_B}(\tau_A^{*c}, \tau_B)$ vanish for all possible strategy choices:

$$\begin{aligned} \frac{\partial \$_A}{\partial \tau_A}(\tau_A, \tau_B)\Big|_{\tau_B = \tau_B^{*c}} &= 0 \ \forall \ \tau_A \in [-1, 1] \\ \frac{\partial \$_B}{\partial \tau_B}(\tau_A, \tau_B)\Big|_{\tau_A = \tau_A^{*c}} &= 0 \ \forall \ \tau_B \in [-1, 1] \quad . \end{aligned} \tag{5.18}$$

This property of the classical ESS can be visualised by changing the projected viewpoint of the three dimensional surface. Figure 5.8 shows again the payoffs of the investment bankers within the non-entangled quantum game, whereas the projection of the picture is now along the τ_A-axis. As the partial derivative

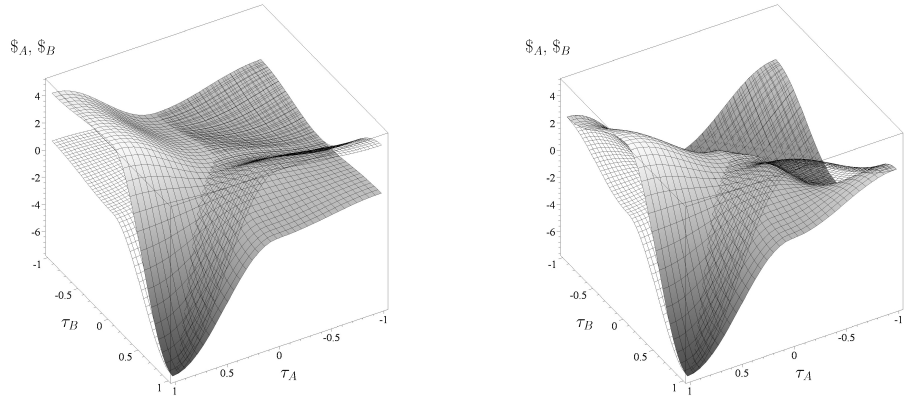

Figure 5.9.: Same description as Figure 5.7, whereas the left picture is calculated within a sparsely entangled quantum game ($\gamma = \frac{\pi}{8}$) and the right picture represents results within a medium entangled quantum game ($\gamma = \frac{\pi}{4}$).

$\frac{\partial \$_A}{\partial \tau_A}(\tau_A, \tau_B^{*c})$ vanishes for all τ_A-values, no gradient is observed at $\tau_B = \tau_B^{*c}$ and as a result the whole projected surface shrinks to one point (see Figure 5.8).

While the Figures 5.7 and 5.8 visualise the non-entangled quantum game, Figure 5.9 shows the payoff structure of a low (left picture, $\gamma = \frac{\pi}{8}$) and medium (right picture, $\gamma = \frac{\pi}{4}$) entangled high risk quantum game. The total classical region CC is equal to the non-entangled game (see Figure 5.7), whereas in all other regions the shape of the payoff surfaces $\$_A$ and $\$_B$ has changed. The classical ESS and one of the asymmetric, pure strategy Nash equilibria ($(H, D) \hat{=} (\tau_A = 1, \tau_B = 0)$) still remain present in both diagrams, whereas the other pure strategy Nash equilibrium $(D, H) \hat{=} (\tau_A = 0, \tau_B = 1)$ disappears even for a tiny strength of entanglement. A further increase of entanglement will even change the structure of the existing ESSs as a new, payoff dominant quantum ESS at $(\tau_A = -1, \tau_B = -1)$ appears for $\gamma > 0.99$.

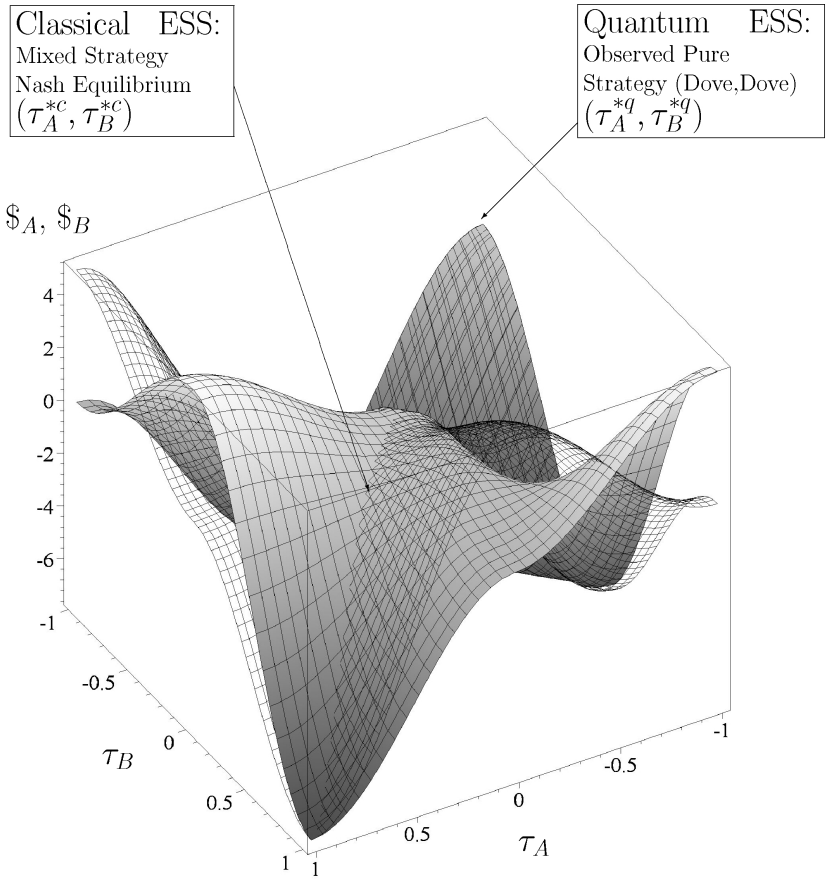

Figure 5.10.: Same description as Figure 5.7, whereas the results where calculated within a maximally entangled quantum game ($\gamma = \frac{\pi}{2}$) using parameter set $P3$.

Figure 5.10 shows the payoff structure of the maximally entangled ($\gamma = \frac{\pi}{2}$) high risk quantum game within the quantum dove strategy subset. The classical ESS and one of the asymmetric, pure strategy Nash equilibria ($(H, D) \hat{=} (\tau_A = 1, \tau_B = 0)$) still remain present, while the pure classical Nash equilibrium $(D, H) \hat{=} (\tau_A = 0, \tau_B = 1)$ has vanished. Beside the remaining classical ESS $(\tau_A^{*c}, \tau_B^{*c})$ a new quantum ESS ($(\tau_A^{*q}, \tau_B^{*q}) = (-1, -1)$) has been found for $\gamma > 0.99$. The point on the payoff surface, where both players choose the quantum ESS τ^{*q} is marked in Figure 5.10. Which of these equilibria will be chosen by the whole population, is

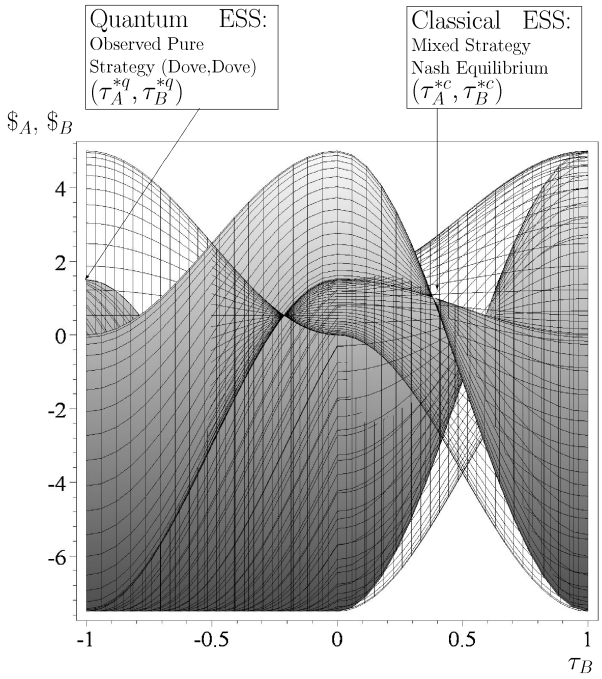

Figure 5.11.: Projection of the payoff surface 5.10 in direction of the τ_A-axis.

going to be addressed in section 5.5 when the time evolution of quantum games is going to be discussed. As the payoff of this new quantum ESS ($\$_A(\tau_A^{*q}, \tau_B^{*q}) = \frac{p_m}{2}$) is higher than the payoff of the classical ESS ($\$_A(\tau_A^{*c}, \tau_B^{*c}) \approx 1.02$), the fully entangled quantum players will likely asymptotically end within the new, payoff dominant quantum ESS. As the observable measurement of the strategy choice $(\tau_A^{*q}, \tau_B^{*q})$ is the strategy set where both players play the dove strategy D $((\tau_A^{*q}, \tau_B^{*q}) \hat{=} (D, D))$, fully entangled quantum players will likely end in a totally dove strategy population $(x = 0)$.

To visualise the payoff values of the two ESSs more explicit, Figure 5.11 projects the three dimensional surface of Figure 5.10 in direction of the τ_A-axis. As the partial derivative of the classical ESS is only zero in the CC-region of the 3-dimensional plot, the whole surface does not shrink to one point as in Figure 5.8.

5.4.2. Quantum Hawk Strategies

Within the previous subsection the set of possible strategies belong to the subset of quantum dove strategies whereas all the results presented within this subsection where calculated using the quantum hawk strategy subset. The corresponding quantum game restricted on a quantum hawk strategy subset is constructed as follows: We redefine the four basis vectors of the Hilbert space $\mathcal{H}$ as the following classical game outcomes ($|HH\rangle := (1,0,0,0)$, $|HD\rangle := (0,-1,0,0)$, $|DH\rangle := (0,0,-1,0)$ and $|DD\rangle := (0,0,0,1)$). The setup of the quantum game begins with the choice of the initial state $|\Psi_0\rangle$, where we assume that both players are in the state $|H\rangle$. The classical strategy H (Hawk) is now selected by appointing $\theta = 0$ and $\varphi = 0$ whereas the strategy D (Dove) is selected by choosing $\theta = \pi$ and $\varphi = 0$. Finally, the state prior to detection is formulated as follows

$$|\Psi_f\rangle = \hat{\mathcal{J}}^{\dagger}\left(\hat{\mathcal{U}}_A \otimes \hat{\mathcal{U}}_B\right)\hat{\mathcal{J}}\;|HH\rangle \quad , \tag{5.19}$$

where the entanglement operator $\widehat{\mathcal{J}}$ is formally given by $\widehat{\mathcal{J}} = e^{i\frac{\gamma}{2}(\widehat{H}\otimes\widehat{H})}$.

Within this quantum hawk strategy model $\tau_A, \tau_B = 1$ corresponds to strategy D, and $\tau_A, \tau_B = 0$ corresponds to strategy H. Negative τ-values correspond again to quantum strategies, where $\theta = 0$ and $\varphi > 0$. As the θ value of the quantum region Q is fixed to zero which corresponds now to the classical hawk strategy, the possible quantum strategies can be understood as "Quantum Hawk" strategies. In the following we will show results within this quantum-hawk strategy subset.

The two diagrams of Figure 5.12 illustrate the outcomes of the low and high risk game settings by visualising the payoff surfaces of investment banker A (solid surface) and investment banker B (wired surface) as a function of their strategies τ_A and τ_B. Because of visual reasons, in all of the presented three dimensional figures the absolute quantum region QQ is now projected in the front, whereas the absolute classical region is projected to the back. Figure 5.12 shows the result where no strategic entanglement is present ($\gamma = 0$), where the left figure depicts the low risk parameter case P1 and the right figure shows the calculated results within the high risk parameter setting P3. Both diagrams clearly show that the non-entangled quantum game simply describes the classical versions of the low and high risk Hawk-Dove games. For the case,

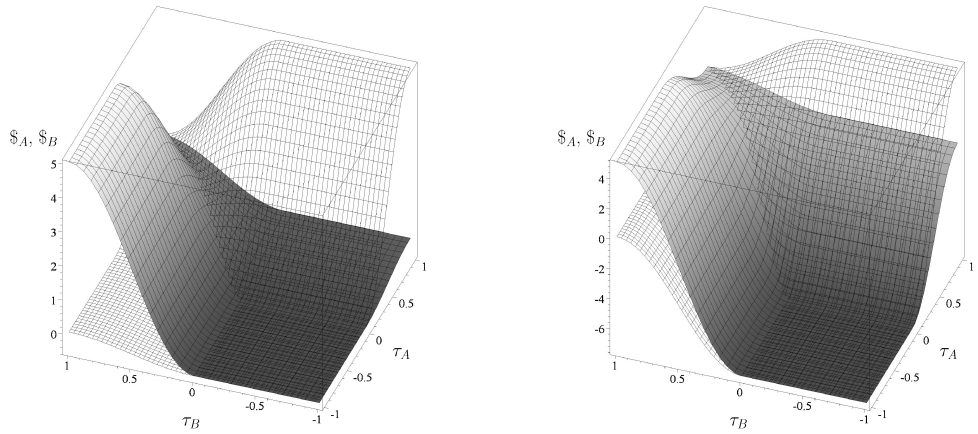

Figure 5.12.: Payoff surface of player A (solid) and player B (wired) as a function of their reduced strategies τ_A and τ_B within a non-entangled quantum game ($\gamma = 0$) using the quantum-hawk strategy subset. The left picture depicts the results of the low risk parameter set $P1$, whereas the right picture shows the results of the high risk setting $P3$.

that both players decide to play a quantum strategy ($\tau_A < 0 \wedge \tau_B < 0$) their payoff is the games lowest payoff which is equal to the case, where both players choose the hawk strategy H ($\$_A(H,H) = \$_A(\tau_A = 0, \tau_B = 0) = \frac{p_h - d}{2}$). The two classical non symmetric pure Nash equilibria ($(x = 1, y = 0) \hat{=} (H, D)$ and $(x = 0, y = 1) \hat{=} (D, H)$) correspond now to the following τ-values: $(H, D) \hat{=} (\tau_A = 0, \tau_B = 1)$ and $(D, H) \hat{=} (\tau_A = 1, \tau_B = 0)$. The ESS of the classical game (the mixed strategy Nash equilibrium) ($x^* = \frac{p_m - 2p_h}{p_m - p_h - d}, y^* = \frac{p_m - 2p_h}{p_m - p_h - d}$) is equal to the strategy point $(\tau_A^{*c}, \tau_B^{*c}) = (\frac{2}{\pi}\arccos\left(\sqrt{\frac{p_m - 2p_h}{p_m - p_h - d}}\right), \frac{2}{\pi}\arccos\left(\sqrt{\frac{p_m - 2p_h}{p_m - p_h - d}}\right))$. At $(\tau_A^{*c}, \tau_B^{*c})$ the partial derivatives $\frac{\partial \$_A}{\partial \tau_A}(\tau_A, \tau_B^{*c})$ and $\frac{\partial \$_B}{\partial \tau_B}(\tau_A^{*c}, \tau_B)$ vanish for all possible strategy choices.

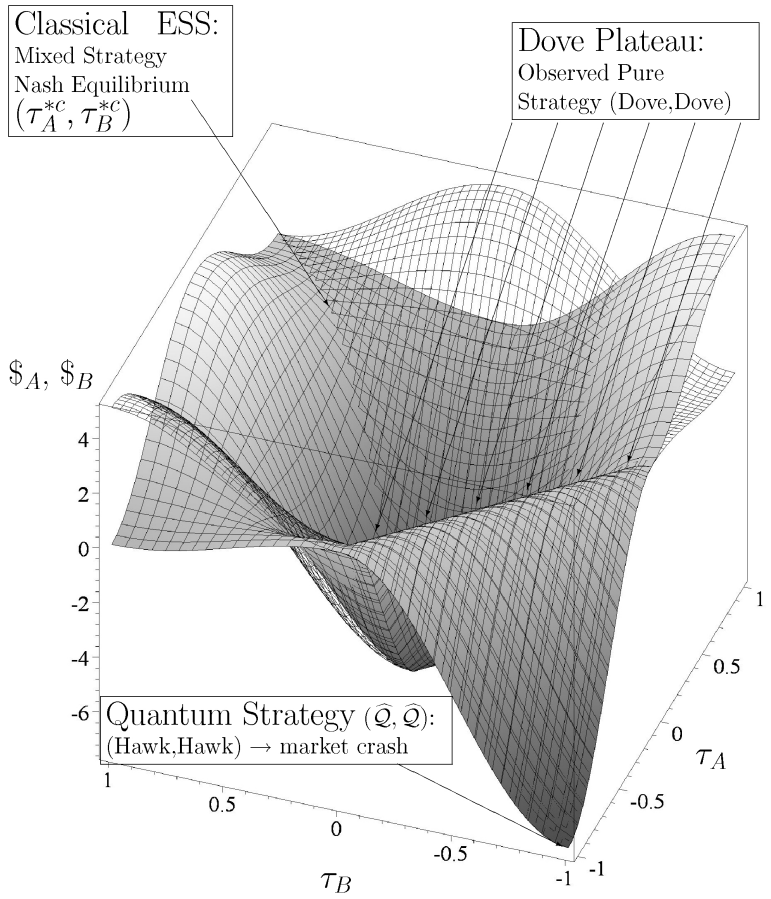

Figure 5.13.: Same description as Figure 5.12, whereas the results where calculated within a maximally entangled quantum game ($\gamma = \frac{\pi}{2}$) using parameter set $P3$.

Figure 5.13 shows the payoff structure of the maximally entangled ($\gamma = \frac{\pi}{2}$) high risk quantum game. The classical ESS and one of the asymmetric, pure strategy Nash equilibria ($(H, D) \hat{=} (\tau_A = 0, \tau_B = 1)$) still remain present, while the pure classical Nash equilibrium $(D, H) \hat{=} (\tau_A = 1, \tau_B = 0)$ has vanished. Beside the remaining classical ESS $(\tau_A^{*c}, \tau_B^{*c})$ a new quantum dove plateau has been found in the fully entangled quantum game. This new, relatively high payoff plateau is called the "dove plateau" because the observed measurement of a quantum strategy point at the top of it is the pure (D,D)-strategy and its payoff is $\frac{p_m}{2}$. It

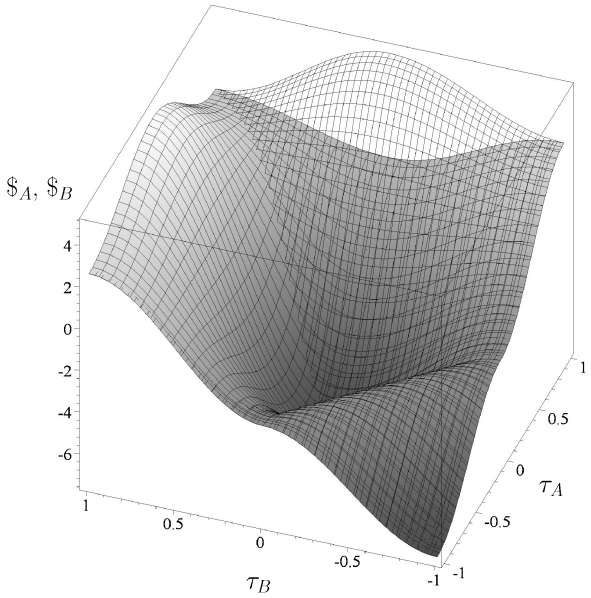

Figure 5.14.: Same description as Figure 5.12, whereas the results where calculated within a medium entangled quantum game ($\gamma = \frac{\pi}{4}$) using parameter set $P3$.

should be mentioned, that if both players decrease their τ-value further than the τ-value of the dove plateau their payoff extremely decrease. When the players choose the quantum strategy $\widehat{Q}$ ($\tau_A = -1, \tau_B = -1$) in the maximally entangled high risk game, their payoff is equal to the lowest possible and their observed action is the hawk strategy (H, H).

While the diagrams in Figure 5.12 visualise the non-entangled low and high risk quantum games, Figure 5.14 shows the payoff structure of the medium entangled ($\gamma = \frac{\pi}{4}$) high risk quantum game. The total classical region CC is equal to the non-entangled game (see Figure 5.12, right picture), whereas in all other regions the shape of the payoff surfaces $\$_A$ and $\$_B$ has changed. As the classical ESS and the asymmetric, pure strategy Nash equilibria ($(H, D)\hat{=}(\tau_A = 0, \tau_B = 1)$) and $(D, H)\hat{=}(\tau_A = 1, \tau_B = 0)$ still remain present, the outcome and the evolution of

such a medium entangled quantum game will not be different from the classical situation. However, a further increase of the strength of entanglement will change the structure of the existing Nash equilibria. For $\gamma \geq 1.15$ the pure classical Nash equilibrium $(D, H) \hat{=} (\tau_A = 1, \tau_B = 0)$ disappears and for $\gamma \geq 1.34$ the dove plateau at the QQ-region (see Figure 5.13) has a higher payoff than the payoff value of the classical ESS.

To summarise briefly the results of this section, we have shown on the one hand that within a highly entangled quantum version of the Hawk-Dove game a new, non-aggressive ESS appears, but on the other hand the results indicate that when both players use a quantum hawk strategy and increase the quantum degree of their strategy (φ) beyond the dove-plateau, their payoff suddenly extremely decrease due to market destabilisation.

5.5. The quantum evolutionary game of doves and hawks

In this section, the necessary conditions (a) and b), see section 5.3) for the existence of ESSs are adopted to prove the existence of the new quantum ESS τ^{*q}. The presented proof will be restricted to the maximally entangled game, but it can be shown, that it holds for any $\gamma > 0.99$. To illustrate that condition a) is fulfilled the pictures in Figure 5.15 depict the function $\mathcal{N}(\tau_A^*, \tau_B^*, \tau_A) := \$_A(\tau_A^*, \tau_B^*) - \$_A(\tau_A, \tau_B^*)$ versus τ_A for all symmetric and non-symmetric Nash equilibria. The left diagram in Figure 5.15 shows the results within the quantum dove strategy subset, whereas the curves in the right diagram of Figure 5.15 are calculated within the quantum hawk strategy subset. As all curves are always above zero they represent existent Nash equilibria. The function $\mathcal{N}(\tau_A^*, \tau_B^*, \tau_A)$ for the two non-symmetric Nash equilibria in the left picture ($\tau_A^* = -1, \tau_B^* = 1$ and $\tau_A^* = 1, \tau_B^* = 0$) are visualised using light grey curves, the classical mixed strategy, symmetric Nash equilibrium $\tau_A^* = \tau_B^* = \tau^{*c}$ is illustrated with the dark grey curve, whereas the symmetric pure quantum Nash equilibrium $\tau_A^* = \tau_B^* = \tau^{*q}$ is shown by using a black curve. The Figure shows clearly, that within the quantum dove strategy subset two symmetric Nash equilibria and therefore two potential ESSs are present. Within the quantum hawk strategy subset (see right diagram of Figure 5.15) only one symmetric Nash

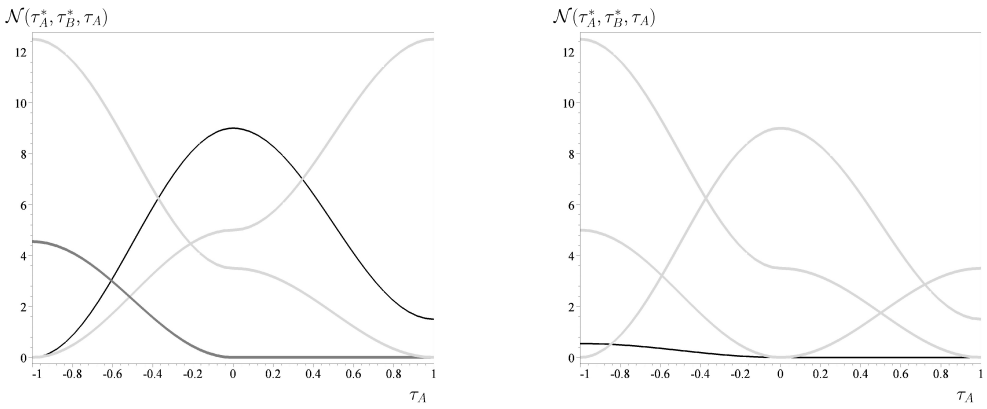

Figure 5.15.: $\mathcal{N}(\tau_A^*, \tau_B^*, \tau_A)$ as a function of τ_A. The light grey curves visualise the non-symmetric Nash equilibria, whereas the dark grey and black curves depict $\mathcal{N}$ for the symmetric Nash equilibria. The left picture shows the results calculated within the quantum dove strategy subset, whereas in the right picture the calculation within the quantum hawk strategy subset are visualised.

equilibrium, the classical ESS is present (black curve). The other three, light grey curves represent the pure, non-symmetric Nash equilibria ($\tau_A^* = 1, \tau_B^* = -1$, $\tau_A^* = -1, \tau_B^* = 0$ and $\tau_A^* = 0, \tau_B^* = 1$). To show that both of the symmetric Nash equilibria (τ^{*c} and τ^{*q}) are ESSs, condition b) has additionally to be checked. Similar as in section 5.3 a function $\mathcal{G}(\tau^*, \tau) := \$_A(\tau^*, \tau) - \$_A(\tau, \tau)$ is defined, which has to be greater than zero for all strategies belonging to the set of best responses within the quantum dove strategy subset. At first we will verify, if the classical mixed strategy Nash equilibrium τ^{*c} remains an ESS for the maximally entangled quantum game. If player B chooses the strategy τ^{*c}, the best response for player A are only strategies belonging to the CC-region, as the payoff of player A decreases within the QC-region (see Figure 5.10 in section 5.4). In the CC-region the derivative $\frac{\partial \$_A(\tau_A, \tau^{*c})}{\partial \tau_A}$ is equal to zero and as a result the set of best responses to the strategy τ^{*c} are all strategies belonging to the classical region ($r(\tau^{*c}) = [0, 1]$).

The two curves in Figure 5.16 describe the functions $\mathcal{G}(\tau^{*c}, \tau)$ (grey curve) and

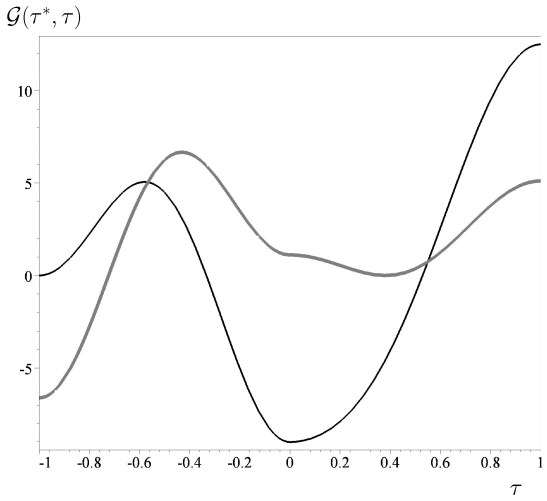

Figure 5.16.: $\mathcal{G}(\tau^{*q}, \tau)$ (black curve) and $\mathcal{G}(\tau^{*c}, \tau)$ (grey curve) as a function of τ within the quantum dove strategy subset.

$\mathcal{G}(\tau^{*q}, \tau)$ (black curve) as a function of the quantum strategy τ within the quantum dove strategy subset. As $\mathcal{G}(\tau^{*c}, \tau)$ is greater than zero for all strategies $\tau \in [0, 1]$, the classical mixed strategy Nash equilibrium τ^{*c} remains an ESS independent of the strength of entanglement. Secondly, we want to address the question whether the symmetric quantum Nash equilibrium τ^{*q} is indeed a new, additional ESS. If player B chooses the strategy $\tau^{*q} = -1$, the best response for player A is only again the strategy $\tau = -1$ and as a result condition b) is fulfilled, independently of the shape of the function $\mathcal{G}(\tau^{*q}, \tau)$. Which of the ESS will be finally reached by the whole population will most likely depend on the initial conditions and on the underlying time dependent quantum dynamics.

Quantum replicator dynamics (QRD), recently developed and discussed by E.G. Hidalgo [95, 96] (see also Toor et. al. [138, 169]) was formulated within the density matrix approach of quantum game theory [162]. QRD employs the von Neumann equation, which describes how a quantum density operator evolves in time. In order to reveal that the von Neumann equation is simply a quantum amplification of classical replicator dynamics (see equation (5.3)), Hidalgo had reformulated equation (5.3) to a matrix equation. Constraining to only two

possible pure strategies equation (5.3) can be formulated as follows [95]:

$$\frac{d}{dt}\widehat{X} = \left[\widehat{\Lambda}, \widehat{X}\right] \tag{5.20}$$
$$\widehat{X} := \begin{pmatrix} x_1 & \sqrt{x_1\, x_2} \\ \sqrt{x_2\, x_1} & x_2 \end{pmatrix} \quad \widehat{\Lambda} := \begin{pmatrix} \Lambda_{11} & \Lambda_{12} \\ \Lambda_{21} & \Lambda_{22} \end{pmatrix}$$
$$\Lambda_{ij} := \tfrac{1}{2} \sum_{k=1}^{n=2} \left(\$_{ik}\, x_k \sqrt{x_i\, x_j} - \sqrt{x_j\, x_i}\, \$_{jk}\, x_k \right)$$

, where the matrix $\widehat{X}$ is an amplification of the population vector $\vec{x} = (x_1, x_2)$, $\left[\widehat{a}, \widehat{b}\right] := \widehat{a}\widehat{b} - \widehat{b}\widehat{a}$ is the commutator of the two matrices $\widehat{a}$ and $\widehat{b}$ and $\widehat{\Lambda}$ is a payoff dependent (2×2)-matrix. The quantum amplification of classical replicator dynamics is realised by the substitution of $\widehat{X}$ to the density matrix $\widehat{\rho}$ and the interpretation of $\widehat{\Lambda}$ as the Hamilton Operator $\widehat{E}$ of the quantum system

$$E_{ij} := \frac{1}{2} \sum_{k=1}^{n=2} \left(\$_{ik}\, \rho_{kk}\, \rho_{ij} - \rho_{ji}\, \$_{jk}\, \rho_{kk} \right) \quad . \tag{5.21}$$

Quantum replicator dynamics as an extension of equation (5.3) and (5.20) is described with the von Neumann equation

$$\frac{d}{dt}\widehat{\rho} = \sigma \left[\widehat{E}, \widehat{\rho}\right] \quad , \tag{5.22}$$

where σ is a certain quantisation constant.[2] The mathematical structure of this ansatz has its origin in the Hamiltonian formulation of classical evolutionary game theory [127] and might be a special example of the multi-agent projector matrix formulation suggested by Gafiychuk and Prykarpatsky [82, 81]. The numerical simulation of equation (5.22) and therefore the time evolution of the Hawk-Dove quantum game will be addressed in a separate article.

5.6. Interpretation and consequences

With respect to the analysed strategy space the presented study provides the following results: Regarding the combination of classical and dove quantum

[2] The von Neumann equation usually describes how a quantum density operator $\widehat{\rho}$ evolves over time, where $\sigma := \frac{1}{i\hbar}$. In quantum replicator dynamics σ shall be deemed to be a certain complex constant.

strategies an additional ESS occurred in case of a high degree of entanglement. With respect to the combination of classical and hawk quantum strategies no additional ESS could be observed. Instead we found a dove-plateau and a steep reduction of payoffs behind this plateau.

With respect to the financial crisis especially the first finding is of interest. Obviously, the players did not behave in the way that a highly entangled quantum game would suggest, as a certain proportion of bankers continued their risk-seeking, aggressive behaviour resulting in a market crash. Hence, in this situation no or only relatively little entanglement of the individuals' decisions existed, which induced them to follow the classical ESS. Consequently, in order to induce the wished for behaviour - strict selection of non-aggressive strategies - one has to introduce a high degree of entanglement into this economic situation.

So far, in literature entanglement has been discussed from a more physical point of view. However, in order to derive consequences from the obtained results we want to propose one possibility to interpret it in an economic context. In this paper, entanglement has been termed a conjoint, psychological contract between the members of an economic population aligning their strategies. However, this contract is not the result of conscious negotiations but of general socio-economic factors influencing the agents simultaneously. These factors comprise moral standards, values, legal rules, joint experiences, a similar educational background, an established social norm etc. All these factors can drive the decision processes of different individuals into the same direction without the necessity that the individuals have to communicate to each other. The objective existence of these background factors can vary, which is reflected by the degree of the entanglement parameter.

As the results show, if a certain degree of entanglement is surpassed, a new ESS appears in the space of quantum dove strategies. Hence, then it is more rational for individuals to choose a quantum dove strategy instead of a classical mixed strategy. At this point also the notion of quantum strategies has to be interpreted in a more economic sense. We propose the following point of view: While the degree of the parameter γ exhibits the objective entanglement, i.e. the objectively observable influence of different socio-economic factors, the parameter φ, which has to be chosen by the agents when selecting a strategy, reflects the

degree to which an agent actually considers theses factors during the decision process. The higher the degree of this parameter is, the more attention the agent pays to these factors.

The results of the analysis point to the fact that if the degree of objective entanglement surpasses a certain threshold, it is rational for an agent to pay a lot of attention to the socio-economic factors and - in the context of the analysed situation - to play a non-aggressive strategy. In contrast, as long as entanglement is below this threshold, it is more rational for the agents to ignore these factors and play a classical evolutionary game. In sum, the degree of objective entanglement also will determine the degree of subjective attention paid by the agents toward this entanglement.

This is exactly the starting point for leading the agents' decisions into the wished for direction: So far, being greedy and aggressive was either not seen as negative or even accepted as an adequate behavioural strategy in the community of investment bankers. However, this behavioural code can be modified through different measures: One important instrument is education. By teaching adequate values and behavioural rules in the institutions that train future investment bankers or market participants in general the value basis of these individuals can be changed in a way that favours less aggressive behaviour. Moreover, the strong disapproval of aggressive behaviour from the general public outside this community can introduce pressure to align one's behaviour according to a less aggressive way. Furthermore, investment bankers were paid through bonus systems that rewarded aggressive and punished non-aggressive actions. Hence, under these incentive schemes a reduction of aggressive behaviour was impossible, since they also fostered the feeling that being aggressive was a positively valued behavioural strategy. In order to change this connotation legal structures - as another part of the socio-economic context - have to be modified in a way that prevents this kind of payment systems.

5.7. Summary

The last financial and economical crisis demonstrated the dysfunctional long-term effects of aggressive behaviour in financial markets. Starting from this observation,

this paper picked up a result of evolutionary game theory which states that under the condition of strategic dependence a certain degree of aggressive behaviour remains within a given population of agents and asked how one could change the "rules of the game" in a way that prevents the occurrence of any aggressive behaviour and thereby also the danger of market crashes. In order to answer this question we extended the in literature well-known evolutionary Hawk-Dove game by a quantum approach and analysed three scenarios in depth.

The resulting study exhibited that dependent on entanglement, also evolutionary stable strategies can emerge, which are not predicted by classical evolutionary game theory and where the total economic population uses a non-aggressive quantum strategy. Hence, the obtained outcomes point into a direction, how the mentioned "rules of the game" could be changed to prevent future crashes.

In order to make this mathematical result actually usable in an economic context, we additionally provided an interpretation of the outcomes of our study in the context of economic situations: We transformed the more physical notions *entanglement* and *quantum strategies* into concepts of the analysed economic situation. We interpret entanglement as the objective influence of socio-economic context factors, while in this context the application of quantum strategies exhibits the degree to which decision makers incorporate these factors into their decisions. Under this premise, our results point to the importance of deliberately changing existing socio-economic context factors and thereby influencing market participants. In this context, we explicitly mentioned the provision of a value basis that prevents aggressive behaviour through educational measures, the strengthening of disapproval regarding aggressive behaviour in an economic context through the general public and the change of the legal basis for the provision of variable payment systems.[3]

[3]This article is the second version of an original preprint which is downloadable from the ArXiv- and RePEc-Server [114]. The original article has been submitted to *Physica A*. We would like to thank the reviewers for their helpfull comments.

Acknowledgments

M.H. would like to thank John Forbes Nash Jr. for the inspiring discussion during the Third Congress of the Game Theory Society (Games 2008). The conversation initiated and motivated the author to broaden his work to an evolutionary context. J.K. wants to thank Carsten Heineke for helpful comments especially regarding the economic interpretation.

6. Article 4: Experimental Validation of Quantum Game Theory

Experimental Validation of Quantum Game Theory

Matthias Hanauske, Steffen Bernius, and Wolfgang König
Johann Wolfgang Goethe-University Frankfurt/Main
Institute of Information Systems
Mertonstr. 17, 60054 Frankfurt/Main

Berndt Dugall
Johann Christian Senckenberg University-Library
Bockenheimer Landstr. 134-138, 60325 Frankfurt/Main
(Dated: June 27, 2008)

Figure 6.1.: Published version of this article is available trough the internetpage of the the conference *Logic and the Foundations of Game and Decision Theory* (LOFT 2008) which was held in the year 2008 in Amsterdam.

Abstract

This article uses data from two experimental studies of two-person prisoner's dilemma games [34, 25] and compares the data with the theoretic predictions calculated with the use of a quantum game theoretical method. The experimental findings of the cooperation percentage indicate a strong connectivity with the properties of a novel function, which depends on the payoff parameters of the game and on the value of entanglement of the players' strategies. A classification scheme depending on four quantum cooperation indicators is developed to describe cooperation in real two-person games. The quantum indicators lead to results, which are more precise than the cooperation predictions derived from classical game theory.

6.1. Introduction

Quantum game theory (QGT)[1] has its origin in elementary particle physics and quantum information theory. In 1999 the first formulations of quantum game theory where presented by D. A. Meyer [165] and J. Eisert et al. [66]. Unknowing Meyers' results on the "Penny Flip" game, Eisert and colleagues focused on the prisoner's dilemma game. Within their quantum representation they where able to demonstrate that prisoners could escape from the dilemma, if the entanglement of the two-person quantum wave function lies above a certain value. In 2001 J. Du et al. [62] realized the first simulation of a quantum game on their nuclear magnetic resonance quantum computer. Later, in 2007 A. Zeilinger et al. accomplished a quantum game on a one-way quantum computer [190]. The application of quantum game theory to an existing social system, namely the publication network of scientists, was presented in M. Hanauske et al. [111]. The authors showed, that quantum game theory could give a possible explanation of the differing publishing methods of scientific communities. A validation of quantum game theoretical concepts by using experimental data of real two-person games was addressed in K.-Y. Chen and T. Hogg [49] (see also [176]). In contrast to the experimental data used in the present article, the authors of [49] used an experimental design, which includes a quantum version of the game. Our understanding of an inclusion of quantum strategies in the players' decisions is different, insofar as we interpret the whole process of a real game as a quantum game.

In this paper, on the one hand, we develop cooperation indicators derived from a quantum game theoretical approach, and on the other hand we address the following research question: *Compared to cooperation indicators based on classical game theory, how precise do "quantum" indicators predict the outcome of real person game experiments.*

Based on Eisert's two-player quantum protocol [66] and the concept of quantum Nash equilibria, four quantum cooperation indicators are defined. By using these indicators to predict the cooperation rates of real two-person games it will be shown that the quantum indicators lead to results, which are at least as good as

[1] An introduction into the main concepts of quantum game theory can be found at the online lecture notes (mostly in German) [102, 104, 107].

the cooperation predictions derived from classical game theory.

The present article is structured as follows: After presenting the main mathematical formulations used within the quantum game theoretical approach the "quantum" cooperation indicators are defined, visualized and compared with the classical indicators. Afterwards we address our research question and present the experimental validation of the cooperation predictions derived from quantum game theory. The paper ends with a short summary of the main findings.

6.2. Mathematics of QGT

The normal-form representation of a two-player game Γ, where each player (Player 1 $\hat{=}$ A, Player 2 $\hat{=}$ B) can choose between two strategies ($\mathcal{S}^A = \{s_1^A, s_2^A\}$, $\mathcal{S}^B = \{s_1^B, s_2^B\}$) is the classical grounding of the two-player quantum game focused on in this article. In our case the two strategies represent the players' choice between cooperating (not confess, C) or defecting (confess, D) in a prisoner's dilemma game. The whole strategy space $\mathcal{S}$ is composed with use of a Cartesian product of the individual strategies of the two players:

$$\mathcal{S} = \mathcal{S}^A \times \mathcal{S}^B = \{(\text{C,C}), (\text{C,D}), (\text{D,C}), (\text{D,D})\} \quad . \tag{6.1}$$

The payoff structure of a prisoner's dilemma game can be described by the following matrix:

A\B	C	D
C	(c,c)	(a,b)
D	(b,a)	(d,d)

Table 6.1.: General prisoner's dilemma payoff matrix.

The parameters a, b, c, and d should satisfy the following inequations [145, 34]

$$b > c > d > a \ , \quad 2\,c > a + b \quad . \tag{6.2}$$

In quantum game theory, the measurable classical strategies (C and D) correspond

to the orthonormal unit basis vectors $|C\rangle$ and $|D\rangle$ of the two dimensional complex space $\mathbb{C}^2$, the so called Hilbert space $\mathcal{H}_i$ of the player i ($i = A, B$). A quantum strategy of a player i is represented as a general unit vector $|\psi\rangle_i$ in his strategic Hilbert space $\mathcal{H}_i$. The whole quantum strategy space $\mathcal{H}$ is constructed with the use of the direct tensor product of the individual Hilbert spaces: $\mathcal{H} := \mathcal{H}_A \otimes \mathcal{H}_B$. The main difference between classical and quantum game theory is that in the Hilbert space $\mathcal{H}$ correlations between the players' individual quantum strategies are allowed, if the two quantum strategies $|\psi\rangle_A$ and $|\psi\rangle_B$ are entangled. The overall state of the system we are looking at is described as a two-player quantum state $|\Psi\rangle \in \mathcal{H}$. We define the four basis vectors of the Hilbert space $\mathcal{H}$ as the classical game outcomes ($|CC\rangle := (1,0,0,0)$, $|CD\rangle := (0,-1,0,0)$, $|DC\rangle := (0,0,-1,0)$ and $|DD\rangle := (0,0,0,1)$).

The setup of the quantum game begins with the choice of the initial state $|\Psi_0\rangle$. We assume that both players are in the state $|C\rangle$. The initial state of the two players is given by

$$|\Psi_0\rangle \;=\; \widehat{\mathcal{J}}\,|CC\rangle \;=\; \begin{pmatrix} \cos\left(\frac{\gamma}{2}\right) \\ \\ 0 \\ \\ 0 \\ \\ i\sin\left(\frac{\gamma}{2}\right) \end{pmatrix} \quad , \tag{6.3}$$

where the unitary operator $\hat{\mathcal{J}}$ (see equation (6.8)) is responsible for the possible entanglement of the two-player system. The players' quantum decision (quantum strategy) is formulated with the use of a two parameter set of unitary 2×2 matrices:

$$\widehat{\mathcal{U}}(\theta,\varphi) := \begin{pmatrix} e^{i\,\varphi}\cos(\frac{\theta}{2}) & \sin(\frac{\theta}{2}) \\ -\sin(\frac{\theta}{2}) & e^{-i\,\varphi}\cos(\frac{\theta}{2}) \end{pmatrix} \tag{6.4}$$
$$\forall \quad \theta \in [0,\pi] \;\wedge\; \varphi \in [0,\tfrac{\pi}{2}] \qquad .$$

By arranging the parameters θ and φ, a player chooses his quantum strategy.

The classical strategy C is selected by appointing $\theta = 0$ and $\varphi = 0$:

$$\widehat{\mathcal{C}} := \hat{\mathcal{U}}(0,0) = \begin{pmatrix} 1 & 0 \\ 0 & 1 \end{pmatrix} \quad , \tag{6.5}$$

whereas the strategy D is selected by choosing $\theta = \pi$ and $\varphi = 0$:

$$\widehat{\mathcal{D}} := \hat{\mathcal{U}}(\pi,0) = \begin{pmatrix} 0 & 1 \\ -1 & 0 \end{pmatrix} \quad . \tag{6.6}$$

In addition, the quantum strategy $\widehat{\mathcal{Q}}$ is given by

$$\widehat{\mathcal{Q}} := \hat{\mathcal{U}}(0,\pi/2) = \begin{pmatrix} i & 0 \\ 0 & -i \end{pmatrix} \quad . \tag{6.7}$$

After the two players have chosen their individual quantum strategies ($\hat{\mathcal{U}}_A := \hat{\mathcal{U}}(\theta_A, \varphi_A)$ and $\hat{\mathcal{U}}_B := \hat{\mathcal{U}}(\theta_B, \varphi_B)$) the disentangling operator $\widehat{\mathcal{J}}^\dagger$ is acting to prepare the measurement of the players' state. The entangling and disentangling operator ($\widehat{\mathcal{J}}, \widehat{\mathcal{J}}^\dagger$; with $\hat{\mathcal{J}} \equiv \hat{\mathcal{J}}^\dagger$) is depending on one additional single parameter γ which measures the strength of the entanglement of the system:

$$\widehat{\mathcal{J}} := e^{i\frac{\gamma}{2}(\widehat{\mathcal{D}} \otimes \widehat{\mathcal{D}})} \ , \quad \gamma \in [0, \frac{\pi}{2}] \quad . \tag{6.8}$$

The entangling operator $\widehat{\mathcal{J}}$ in the used representation has the following explicit structure:

$$\widehat{\mathcal{J}} := \begin{pmatrix} \cos\left(\frac{\gamma}{2}\right) & 0 & 0 & i\sin\left(\frac{\gamma}{2}\right) \\ 0 & \cos\left(\frac{\gamma}{2}\right) & -i\sin\left(\frac{\gamma}{2}\right) & 0 \\ 0 & -i\sin\left(\frac{\gamma}{2}\right) & \cos\left(\frac{\gamma}{2}\right) & 0 \\ i\sin\left(\frac{\gamma}{2}\right) & 0 & 0 & \cos\left(\frac{\gamma}{2}\right) \end{pmatrix} \tag{6.9}$$

Finally, the state prior to detection can therefore be formulated as follows:

$$|\Psi_f\rangle = \hat{\mathcal{J}}^\dagger \left(\hat{\mathcal{U}}_A \otimes \hat{\mathcal{U}}_B\right) \hat{\mathcal{J}} \; |CC\rangle \quad . \tag{6.10}$$

The expected payoff within a quantum version of a general two-player game, depends on the payoff matrix (see Table 6.1) and on the joint probability to observe the four observable outcomes $P_{\mathrm{CC}}, P_{\mathrm{CD}}, P_{\mathrm{DC}}$ and P_{DD} of the game:

$$\begin{aligned} \$_A \quad &= c\, P_{\mathrm{CC}} + a\, P_{\mathrm{CD}} + b\, P_{\mathrm{DC}} + d\, P_{\mathrm{DD}} \\ \$_B \quad &= c\, P_{\mathrm{CC}} + b\, P_{\mathrm{CD}} + a\, P_{\mathrm{DC}} + d\, P_{\mathrm{DD}} \\ \text{with:} \quad & P_{\sigma\sigma'} = |\, \langle \sigma\sigma' | \Psi_f \rangle \,|^2 \;\; , \quad \sigma, \sigma' = \{C, D\} \quad . \end{aligned} \tag{6.11}$$

It should be pointed out here, that an entangled two-player quantum state does not mean at all that the persons themselves (or even the players' brains) are entangled. The process of quantum decoherence, with its quantum to classical transition, forbid such macroscopic entangled systems established from microscopic quantum particles [199, 140]. However, peoples' cogitations, represented as quantum strategies, could be associated within an abstract space. Although no measurable accord is present between the players' strategy choices, the imaginary parts of their strategy wave functions might interact, if their individual states are entangled. This quantum phenomenon might possibly be interpreted as the ability of a player to empathize into the other players thinking lanes, which may be originated from similar historical or cultural background. Players with strongly entangled strategies appear to act more like a collective state.

6.3. Quantum Cooperation Indicators

Dominant quantum strategies and quantum Nash equilibria are formulated as follows:

$(\theta_A^\star, \varphi_A^\star; \theta_B^\star, \varphi_B^\star)$ is a dominant quantum strategy, if

$$\begin{aligned} \$_A(\widehat{\mathcal{U}}_A^\star, \widehat{\mathcal{U}}_B) \;&\geq\; \$_A(\widehat{\mathcal{U}}_A, \widehat{\mathcal{U}}_B) \qquad \forall \;\; \widehat{\mathcal{U}}_A \;\wedge\; \widehat{\mathcal{U}}_B \\ \$_B(\widehat{\mathcal{U}}_A, \widehat{\mathcal{U}}_B^\star) \;&\geq\; \$_B(\widehat{\mathcal{U}}_A, \widehat{\mathcal{U}}_B) \qquad \forall \;\; \widehat{\mathcal{U}}_A \;\wedge\; \widehat{\mathcal{U}}_B \quad . \end{aligned} \tag{6.12}$$

$(\theta_A^\star, \varphi_A^\star; \theta_B^\star, \varphi_B^\star)$ is a quantum Nash equilibrium, if

$$\begin{aligned} \$_A(\widehat{\mathcal{U}}_A^\star, \widehat{\mathcal{U}}_B^\star) &\geq \$_A(\widehat{\mathcal{U}}_A, \widehat{\mathcal{U}}_B^\star) \quad \forall \quad \widehat{\mathcal{U}}_A \\ \$_B(\widehat{\mathcal{U}}_A^\star, \widehat{\mathcal{U}}_B^\star) &\geq \$_B(\widehat{\mathcal{U}}_A^\star, \widehat{\mathcal{U}}_B) \quad \forall \quad \widehat{\mathcal{U}}_B \quad . \end{aligned} \tag{6.13}$$

We define the novel function $\mathcal{N}_A$ of player A in a two-player quantum game by

$$\begin{aligned} \mathcal{N}_A(\gamma) \quad := \quad & \int_{\theta_A=0}^{\pi} \int_{\varphi_A=0}^{\frac{\pi}{2}} \mathcal{N}_A(\widehat{\mathcal{Q}}_A^\star, \widehat{\mathcal{Q}}_B^\star, \theta_A, \varphi_A, \gamma)\, d\theta_A\, d\varphi_A - \\ & - \int_{\theta_A=0}^{\pi} \int_{\varphi_A=0}^{\frac{\pi}{2}} \mathcal{N}_A(\widehat{\mathcal{D}}_A^\star, \widehat{\mathcal{D}}_B^\star, \theta_A, \varphi_A, \gamma)\, d\theta_A\, d\varphi_A \ , \end{aligned} \tag{6.14}$$

where the functions $\mathcal{N}_A(\widehat{\mathcal{Q}}_A^\star, \widehat{\mathcal{Q}}_B^\star, \theta_A, \varphi_A, \gamma)$ and $\mathcal{N}_A(\widehat{\mathcal{D}}_A^\star, \widehat{\mathcal{D}}_B^\star, \theta_A, \varphi_A, \gamma)$ are given by

$$\begin{aligned} \mathcal{N}_A(\widehat{\mathcal{U}}_A^\star, \widehat{\mathcal{U}}_B^\star, \theta_A, \varphi_A, \gamma) = \\ \mathcal{N}_A(\widehat{\mathcal{U}}_A^\star, \widehat{\mathcal{U}}_B^\star, \widehat{\mathcal{U}}_A, \gamma) := \$_A(\widehat{\mathcal{U}}_A^\star, \widehat{\mathcal{U}}_B^\star, \gamma) - \$_A(\widehat{\mathcal{U}}_A, \widehat{\mathcal{U}}_B^\star, \gamma) \quad . \end{aligned} \tag{6.15}$$

A rather lengthy calculation gives the following analytic result for the function $\mathcal{N}(\gamma) := \mathcal{N}_A(\gamma) = \mathcal{N}_B(\gamma)$ of a two-player quantum game with a prisoner's dilemma payoff matrix:

$$\mathcal{N}(\gamma) = \frac{\pi^2}{16} \left[(1 + 3\cos(2\gamma))\,(a - b) + (5 - \cos(2\gamma))\,(c - d) \right] \tag{6.16}$$

For a separable game equation (6.16) reduces to $\mathcal{N}(\gamma = 0) = \frac{\pi^2}{16}(a - b + c - d)$. Restricting to games with a prisoner's dilemma game structure (see conditions 6.2) leads always to a negative value of $\mathcal{N}(\gamma = 0)$, which means that the classical limit of a quantum prisoner's dilemma game always yield to the classical Nash equilibrium of defection (strategy D). In the next but one section we will show the functions $\mathcal{N}(\gamma)$ for all games used in [34] (Fig. 6.4) and [25] (Fig. 6.5).

An integration of $\mathcal{N}(\gamma)$ from $\gamma = 0$ to $\gamma = \frac{\pi}{2}$ leads to a function $\mathcal{N}$, that depends solely on the payoff parameters (a, b, c, d).

$$\mathcal{N} := \int_{\gamma=0}^{\frac{\pi}{2}} \mathcal{N}(\gamma)\, d\gamma = \frac{\pi^3}{32} \left[a - b + 5\,(c - d) \right] \quad . \tag{6.17}$$

In the following, $\mathcal{N}$ will be used as the main cooperation indicator.[2] It is easy to show that the null of $\mathcal{N}(\gamma)$ is given by a specific threshold value $\gamma_\star$ of the entanglement:

$$\begin{aligned} \gamma_\star &:= \left\{\gamma \in [0, \frac{\pi}{2}] : \mathcal{N}(\gamma) = 0\right\} \\ \gamma_\star &= \frac{\pi}{2} - \frac{1}{2}\arccos\left(\frac{a - b + 5\,(c - d)}{3\,(a - b) - c + d}\right) . \end{aligned} \tag{6.18}$$

In addition to $\mathcal{N}$ and $\gamma_\star$, two other cooperation indicators are defined: γ_1 is defined as the entanglement barrier, for which the classical Nash equilibrium $|DD\rangle$ dissolves, and γ_2 is defined as the barrier where the new quantum Nash equilibrium $|QQ\rangle$ appears (for a detailed discussion of γ_1 and γ_2 see [111, 66]).

To visualize the quantum game theoretical foundations of our Ansatz and to illustrate the function $\mathcal{N}_A$ (see equation (6.14)) the two integration components $\mathcal{N}_A(\widehat{\mathcal{Q}}_A^\star, \widehat{\mathcal{Q}}_B^\star, \theta_A, \varphi_A, \gamma)$ and $\mathcal{N}_A(\widehat{\mathcal{D}}_A^\star, \widehat{\mathcal{D}}_B^\star, \theta_A, \varphi_A, \gamma)$ are displayed in Fig. 6.2 for six different γ-values. The grey surface depicts $\mathcal{N}_A(\widehat{\mathcal{D}}_A^\star, \widehat{\mathcal{D}}_B^\star, \theta_A, \varphi_A, \gamma)$ as a function of the decision angles θ_A and φ_A, whereas the wired white surface specifies $\mathcal{N}_A(\widehat{\mathcal{Q}}_A^\star, \widehat{\mathcal{Q}}_B^\star, \theta_A, \varphi_A, \gamma)$. In all of the presented illustrations the payoff structure of game 1 of [34] was used (a = 70, b = 100, c = 90 and d = 80).

[2] The cooperation percentage of a particular experiment should depend on the payoff parameters (a, b, c, d) of the game used in the experiment but will also be dependent on its specifications and given rules. The continuation probability δ used in the experiments of [34, 25] for example is such an additional input, which will change the resulting cooperation percentage. Within a quantum description of the experiment we interpret such additional specifications as a shift of the entanglement distribution ($\nu(\gamma)$) of the participators of the experiment. If we want to use $\mathcal{N}$ as a real cooperation indicator, it should also depend on the entanglement distribution $\nu(\gamma)$ ($\mathcal{N} = \int_{\gamma=0}^{\frac{\pi}{2}} \nu(\gamma)\,\mathcal{N}(\gamma)\,d\gamma$). We have neglected such an inclusion of the entanglement distribution, so that we can use $\mathcal{N}$ solely within experimental comparisons of equal specifications.

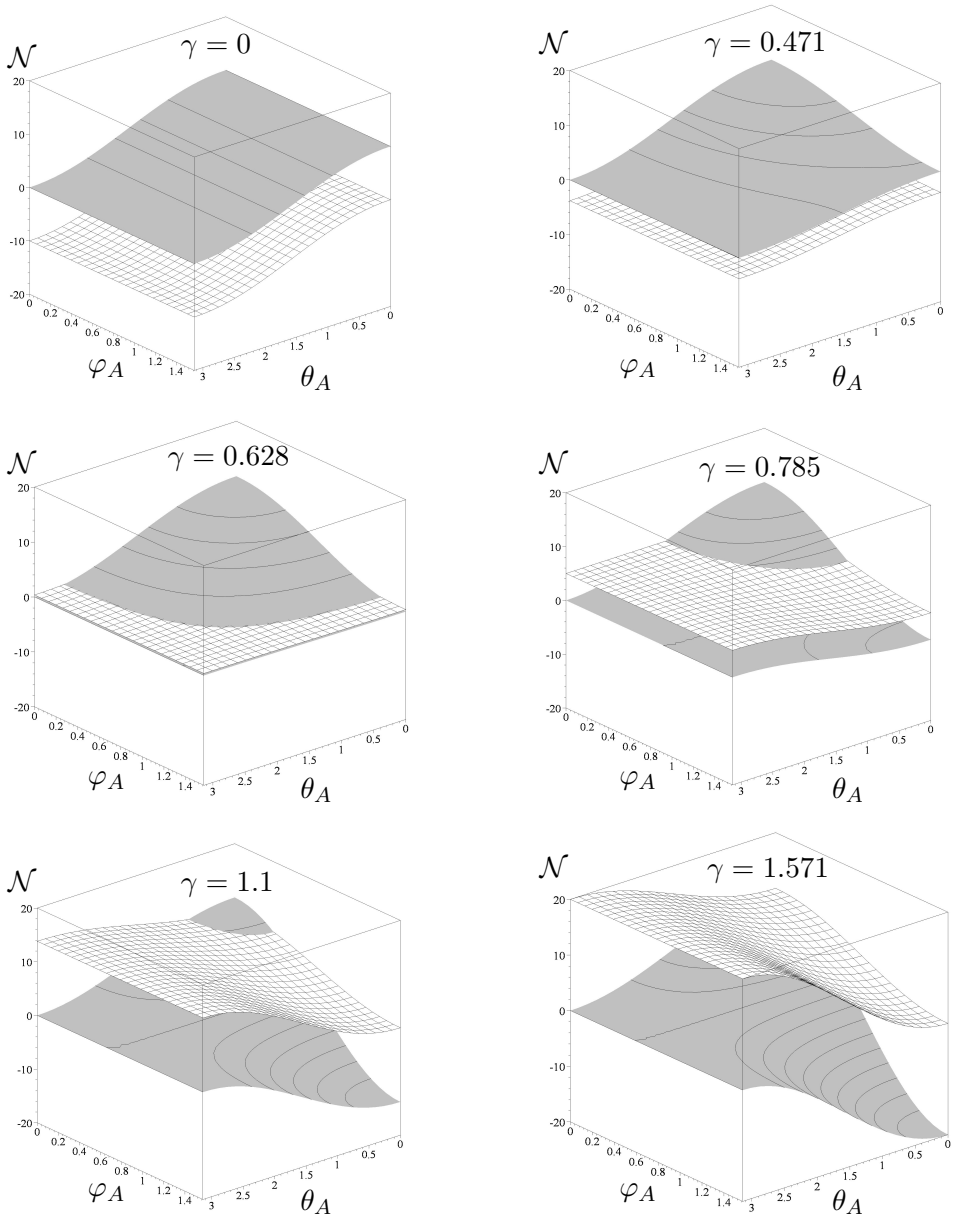

Figure 6.2.: Visualization of the surfaces $\mathcal{N}_A(\widehat{\mathcal{Q}}_A^\star, \widehat{\mathcal{Q}}_B^\star, \theta_A, \varphi_A, \gamma)$ (wired white) and $\mathcal{N}_A(\widehat{\mathcal{D}}_A^\star, \widehat{\mathcal{D}}_B^\star, \theta_A, \varphi_A, \gamma)$ (grey) as a function of the decision angles θ_A and φ_A for six different values of entanglement (γ-values). The figures were calculated using the payoff parameters of game 1 of [34] (a=70, b=100, c=90 and d=80).

The left picture at the top of Fig. 6.2 illustrates the separable situation, where no entanglement is present ($\gamma = 0$). For all possible decision angles the grey surface lies above zero, which means that the strategy $\widehat{\mathcal{D}}$ is a quantum Nash equilibrium (see equation (6.15) and definition (6.13)). The white surface lies in contrast always below the zero value, which reveals the futileness of the quantum strategy $\widehat{\mathcal{Q}}$ within the separable game. To calculate $\mathcal{N}_A(\gamma)$, the whole integration area of the grey surface is subtracted from the integration area of the white surface, which is anyway negative. For $\gamma = 0$, $\mathcal{N}_A$ becomes therefore highly negative ($\mathcal{N}_A(\gamma = 0) = -50$). The right picture at the top of Fig. 6.2 shows the resulting surfaces, in the case where the value of entanglement is low ($\gamma = \frac{3\pi}{20} \approx 0.471$). Due to the increase of entanglement both surfaces have converged, but from a qualitative viewpoint the resulting situation has not changed. The grey surface is still above the white surface and in addition, always above zero, which means that defection is still the only Nash equilibrium of the game. The left and right picture in the middle region of Fig. 6.2 shows the resulting surfaces for a further increase of entanglement (left: $\gamma = \frac{\pi}{5} \approx 0.628$ and right: $\gamma = \frac{\pi}{4} \approx 0.785$). For $\gamma = \frac{\pi}{5}$ the white surface lies always above zero, whereas the grey one is for a part of the surface somewhat below zero, which means that the old Nash equilibrium $\widehat{\mathcal{D}}$ has disappeared and the new Nash equilibrium $\widehat{\mathcal{Q}}$ has become present. The used γ-value ($\gamma \approx 0.628$) lies above the cooperation indicators γ_1 and γ_2, which are for this game both equal ($\gamma_1 = \gamma_2 = 0.615$). The integral $\mathcal{N}_A(\gamma = \frac{\pi}{5})$ is still sparsely negative, whereas the integral $\mathcal{N}_A(\gamma = \frac{\pi}{4})$ is positive. The left and right pictures in the lower region of Fig. 6.2 depict the situation where a strong entanglement is present. For the completely entangled game (right picture) the white surface lies always above the grey one and the integral $\mathcal{N}_A(\gamma = \frac{\pi}{4})$ reaches the largest value. Figure 6.2 on the one hand visualizes the structure of game 1 of [34] within a quantum extension of the game and on the other hand it illustrates the integration procedure introduced in equation (6.14). The shape and the location of the surfaces is important for understanding the properties of a given game and we will present and discuss the other games of [34, 25] in a detailed report [152]. The introduced way of integration when defining the function $\mathcal{N}_A(\gamma)$ is only one possibility of constructing a cooperation indicator for games with a symmetric payoff matrix. The definition of a more general function $\mathcal{N}_A(\gamma)$, which could in addition be used to describe asymmetric games

is remaining in employment [152]. Beside the concern of the present article to describe the extent of cooperation in real two-person games the authors think, that the quantum game theoretical method is by all means a valuable tool and new way of understanding the structure of a specific game.

6.4. Classical vs. Quantum Cooperation Indicators

The mathematical description of quantum game theory presented in the previous section is merely a simple one shot quantum game. In contrast, the experiments in [34, 25] are repeated versions of a prisoner's dilemma game. Within such repeated, extensive games the whole strategy sets should be used to describe the game's structure. Within this, primarily examination we neglect such differences by using only the period averaged value of the cooperation percentage C_p of the experiments [34, 25]. The mathematical formulations of a time dependent quantum game theory describing the dynamics of a population of players is to be working on. In the limit of a separable game such time dependent equations should fade to evolutionary game theoretical concepts and replicator dynamics [216, 213, 214, 166, 198].

The evolution of cooperation in repeated games depends on the payoff parameters of the game and the continuation probability δ.[3] Even though the theory of infinitely repeated games has been used to explain cooperation in a variety of environments it does not provide sharp predictions since there may be a multiplicity of equilibria [25].

In the classical theory of infinitely repeated games the standard lower bound on discount factors ($\underline{\delta}$) below which no player can ever cooperate on an equilibrium path of $\Gamma(\delta)$ depends simply on the payoff parameters b, c and d [193, 145]:

$$\underline{\delta} := \frac{b-c}{b-d} \quad . \tag{6.19}$$

[3]The present paper solely compares the classical theory of infinitely repeated games with the quantum approach. A comparison with the more general formulations based on negotiation and the axiomatic approach of two-player cooperative games [144] will be addressed in a separate article [152].

Cooperation can be achieved by some equilibrium if and only if the continuation probability δ is above or equal to the lower bound $\underline{\delta}$ ($\delta \geq \underline{\delta}$). On the other hand, it is possible to show, that cooperation can be achieved "easily" by a "tit-for-tat" strategy if and only if $\delta \geq \frac{b-c}{a-d}$ [145].

Blonski et al. have defined a new bound on the discount factors ($\delta^\star$), which includes the "sucker's payoff" (parameter "a" of the payoff matrix (see Table 6.1))

$$\delta^\star := \frac{b-a-c+d}{b-a} \quad . \tag{6.20}$$

The authors of [34] show in their article, that this indicator is able to predict the cooperation percentage much better than the standard indicator $\underline{\delta}$. It is remarkable, that $\gamma_\star$ and $\delta^\star$ are for a wide range of possible payoff parameters quite similar.

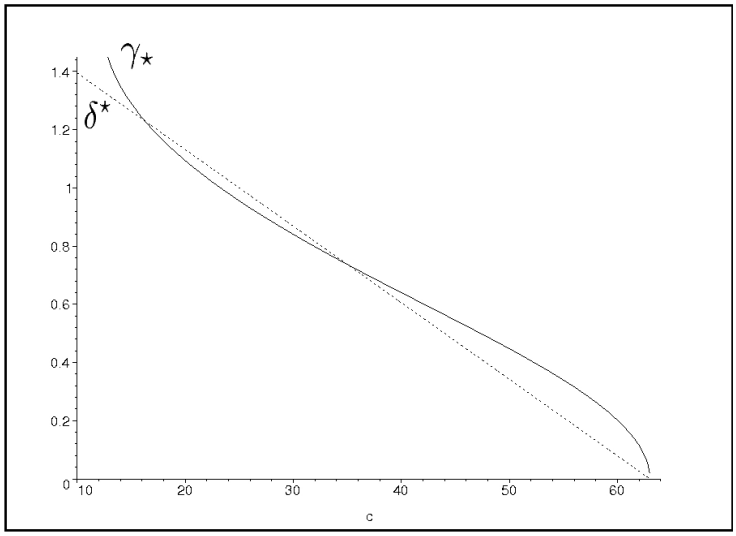

Figure 6.3.: $\delta^\star$ (dashed line, see [34]) and $\gamma_\star$ (solid curve) as a function of the payoff parameter c.

Figure 6.3 illustrates the similarities of the functions $\gamma_\star$ (solid curve) and $\delta^\star$ (dashed line) by varying the parameter c while keeping the other payoff parameters fixed as in the experimental settings of Dal Bó et. al. [25] ($a = 12, b = 50, d = 25$).

6.5. Experimental Validation

Different variations on the prisoner's dilemma game have been the subject of an enormous experimental interest since the 1950 experiment of Dresher and Flood [76, 145]. Most of the studies have focused on the finitely repeated prisoner's dilemma game [145]. In order to verify the theoretical predictions coming from a quantum game theoretical description it is useful to have data of three or more different payoff parameter settings in one experiment. Unfortunately [156, 206, 22] have only used less than three different payoffs in their studies. Another basic condition is the postulation that an entanglement of strategic choices consists only, if two persons play the game. The outstanding experiments accomplished by Roth and Murnighan [193, 167] had used an experimental setting where a player played against a computer program.[4] Other newer experimental studies have used additional game rules [46] or have analyzed all kinds of asymmetric games in their studies [205].

The experimental designs adopted in the studies [34, 25] are quite similar. Both experiments have used more than two payoff settings and were played by two real persons. Figure 6.4 shows the function $\mathcal{N}(\gamma)$ for the six different games used within the experiment [34]. For game 3 and 4 the functions $\mathcal{N}(\gamma)$ are not distinguishable from each other, because $\mathcal{N}(\gamma)$ depends only on the difference of the payoff parameters a and b (see equation (6.16)).

In the following we will briefly describe the design used in [34]. In each session a group of 20 undergraduate students have participated in the experiment, where they where able to win between 15 to 25 Euro. Ten couples where randomly matched at the beginning of a so called "stage game", whereupon the players could not meet the other one since their decisions where anonymously transmitted by computers. A stage game consisted of a given payoff matrix and a continuation probability δ. Six different payoff matrices (see Table 6.2) and three different continuation probabilities ($\delta = 0.5, 0.75, 0.875$) had been specified. During a stage game the continuation probability δ and the corresponding opponent did

[4] If we take the data from the experiment [167] to test the predictions derived from a quantum game theoretical approach, we do not get a good agreement. We think that the reason of this disagreement is that a player in this experiment played against a computer program and not against another player.

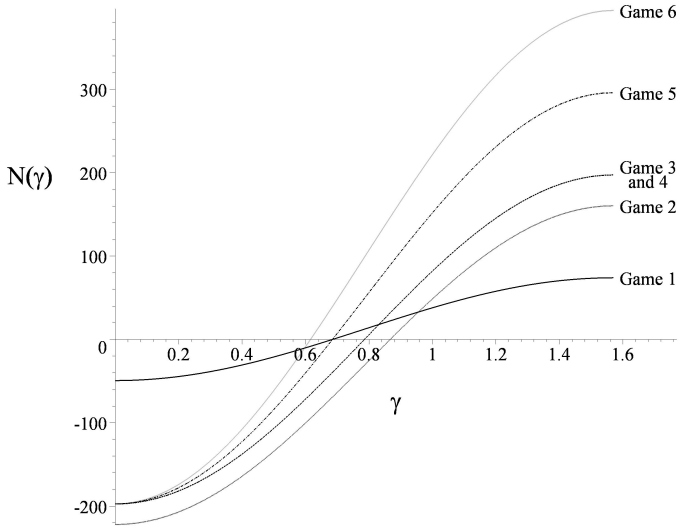

Figure 6.4.: $\mathcal{N}(\gamma)$ for the six different games used in the experiment [34]. The quantum cooperation indicator $\gamma_\star$ is the null of the respective functions, whereas $\mathcal{N}$ is calculated through the integral from $\gamma = 0$ to $\gamma = \pi$.

not change. Before every new round the computer picked randomly a probability $\delta^{'}$ from a uniform distribution ($\delta^{'} \in [0, 1]$) and the game was only continued if $\delta^{'} \leq \delta$. Every round consisted of a finite decision phase and an information phase that informed the players about the decision of their opponent and about the achieved payoff. The whole experiment lasted two to three hours.

The design of experiment [25] has only some minor modifications. For instance, the size of the groups of undergraduate students varied between 12 to 20 subjects, there were only two continuation probabilities ($\delta = 0.5, 0.75$) and three different payoff matrices (see Table 6.2) taken and the achieved payoffs varied between 16 to 43 Dollars. Figure 6.5 shows the function $\mathcal{N}(\gamma)$ for the three different games used within the experiment [25].

Quantum theoretical results of the games used in [34, 25] and their experimental data is summarized in Table 6.2 and partly visualized in Figure 6.6. The experimental data is based on the percentage of cooperating persons in all rounds.

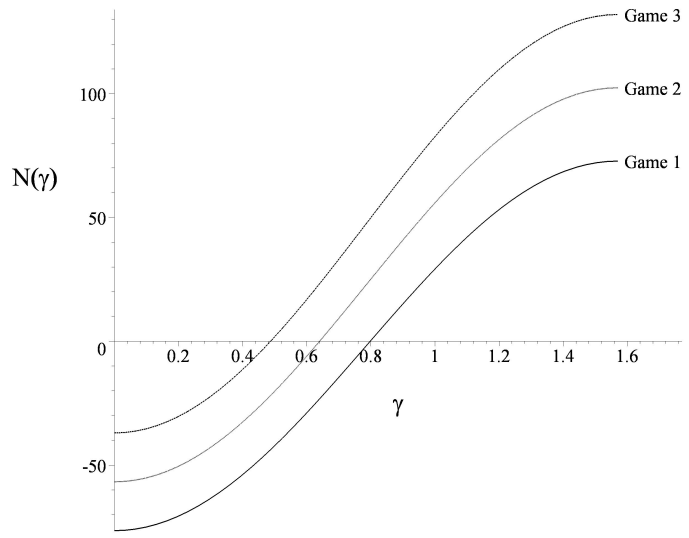

Figure 6.5.: $\mathcal{N}(\gamma)$ for the three different games used in the experiment [25].

[5] In the sixth column of Table 6.2 the experimental findings of the percentage of cooperating persons (C_p) of Blonski et al. [34] and Dal Bó. et al. [25] are denoted, whereas in the seventh column the cooperation rank of the games is quoted. The last rank in experiment [34] for example was found for game 2 ($C_p = 2.8\%$), whereas the lowest cooperation rank was achieved in game 6 ($C_p = 37.6\%$). The next two subsequent columns in Table 6.2 present the lower bounds on the discount factors coming from standard ($\underline{\delta}$) and extended ($\delta^\star$) classical game theory. The last four columns sum up the specified cooperation indicators calculated with the use of quantum game theory. $\mathcal{N}$ is considered as the most important indicator. Only if $\mathcal{N}$ is equal for two games, the indicator $\gamma_\star$ should be used to classify the cooperation rank. In the games 3 and 4 of [34] neither $\mathcal{N}$ nor $\gamma_\star$ provide distinguishable values. In such a case one can use γ_1 and γ_2 to classify the cooperation rank, where γ_1 is expected to be more important than γ_2 because in real two-person games decisions depend firstly on

[5] For comparison reasons we have used the data with $\delta = 0.75$ in both experiments. Besides the used payoff parameters, the discount factor δ is an important property in all of the experiments. As δ describes the abruption probability of the repeated games, it increases the individual entanglement of the persons, which results in a higher percentage of cooperation.

Experimental data of Blonski et. al. [34] and quantum theoretical results												
Game No.	a	b	c	d	C_p	Rank	$\underline{\delta}$	$\delta^\star$	γ_2	γ_1	$\gamma_\star$	$\mathcal{N}$
1	70	100	90	80	21.4 %	3	0.5	0.667	0.615	0.615	0.685	19.38
2	0	100	90	80	2.8 %	6	0.5	0.9	0.322	1.107	0.866	-48.45
3	30	130	90	70	15.4 %	4	0.667	0.8	0.685	0.685	0.785	0
4	0	100	90	70	13.4 %	5	0.333	0.8	0.322	0.991	0.785	0
5	0	120	90	50	37.0 %	2	0.429	0.667	0.524	0.702	0.685	77.52
6	0	140	90	30	37.6 %	1	0.625	0.786	0.641	0.481	0.615	155.03
Experimental data of Dal Bó et. al. [25] and quantum theoretical result												
Game No.	a	b	c	d	C_p	Rank	$\underline{\delta}$	$\delta^\star$	γ_2	γ_1	$\gamma_\star$	$\mathcal{N}$
1	12	50	32	25	7.6 %	3	0.72	0.816	0.759	0.625	0.798	-2.91
2	12	50	40	25	22.1 %	2	0.4	0.605	0.539	0.625	0.640	35.85
3	12	50	48	25	28.7 %	1	0.08	0.395	0.231	0.625	0.487	74.61

Table 6.2.: Quantum theoretical results and experimental data of Blonski et.al. [34] and Dal Bó et al. [25].

the real strategy choices and only secondly on their imaginary parts. In game 3 the classical Nash equilibrium $|DD\rangle$ disappears at $\gamma_1 = 0.685$, whereas in game 4 it vanishes at $\gamma_1 = 0.991$, which means that one expects to have more cooperating persons within game 3.

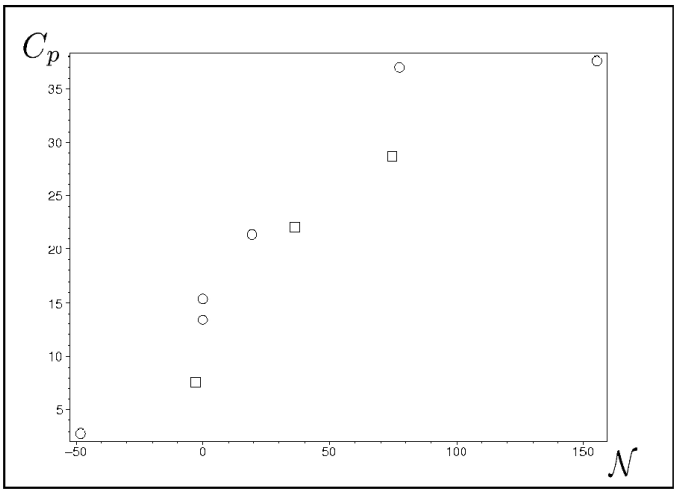

Figure 6.6.: Percentage of cooperating players (C_p) in experiment [34] (circles) and [25] (boxes) as a function of $\mathcal{N}$.

Figure 6.6 depicts the percentage of cooperating persons in both experiments as a function of $\mathcal{N}$. The diagram clearly shows, that an increase of cooperation comes along with an increase of $\mathcal{N}$.

It should be mentioned that the comparison of two different experiments is difficult, because besides the fixed payoff parameters and the abruption rate δ other experimental details could influence the persons' cooperation behavior. For instance the distribution of the persons strategic entanglement may depend on cultural characteristics or maybe influenced by the experimental design. The information communicated by the experimenter himself could subliminally or even consciously influence the entanglement distribution of the whole group. Fig. 6.6 indicates a small difference between the mean of the persons' entanglement in both experiments, because the cooperation percentage in [34] is always somewhat above experiment [25].

An increase (decrease) of δ influences the distribution of the players' entanglement,

which results in an increase (decrease) of C_p. The strong correlation between $\mathcal{N}$ and C_p for the specific games remains [152].

Our work does not contradict the results of [49], but we presume, that by implementing a specific quantum version of the prisoner's dilemma game, the experimenters have increased the strength of entanglement of the players' strategic decisions (and as a result the cooperation percentage C_p).

6.6. Summary

This article shows that a quantum extension of classical game theory is able to describe the experimental findings of two-person prisoner's dilemma games. A classification scheme was introduced to evaluate the cooperation hierarchy of prisoner's dilemma games. Four cooperation indicators where defined to predict the cooperation behavior. This quantum game theoretical approach was compared with predictions based on classical game theory and tested for two experimental settings. To answer our research question, we conclude that compared to cooperation indicators based on classical game theory the defined "quantum" indicators predict the outcome of real person game experiments very good.

Acknowledgments

We want to thank Peter Ockenfels and Matthias Blonski for helpful discussions. Furthermore we want to thank the referees for several helpful suggestions which had result in an improvement of the original article [29]. This research is supported by grants from the German National Science Foundation (DFG) (Project "Scientific Publishing and Alternative Pricing Mechanisms", Grant No. GZ 554922). We gratefully acknowledge the financial support.

7. Article 5: Evolutionary Game Theory and Complex Networks of Scientific Information

Abstract

The evolution of the socio-economic system of scientific information depend on the decision processes of its underlying system components. The mathematical model to describe the strategic decision of players within a socio-economic game is "game theory". "Evolutionary game theory" a time dependent dynamical extension of game theory, which itself attempts to mathematically capture behavior in strategic situations in which an individual's success in making choices depends on the choices of others. Evolutionary game theory focuses on the strategy evolution in populations to explain interdependent decision processes happening in biological or socio-economic systems. This chapter is about evolutionary game theory in the context of complex networks of scientific information. After a general introduction, the framework of evolutionary game theory is described in detail within this chapter. Two applications in respect to the evolution of scientific information are additionally discussed within this chapter.[1]

7.1. Introduction

The encounter of information science with the theory of complex networks is the main characteristic of a realistic model of science dynamics. Complex information networks and the social dimension of the network of researchers are combined in a multi-level network model which functions as the topological

[1]This article is reproduced in this thesis with permission by the publisher [117].

Table 7.1.: Major questions raised in this chapter and their answers.

Major questions raised	and their answers
1. Why should I deal with game theory?	By analysing the game structure of a specific decision problem, decision-makers can learn a lot about the problem they are involved in.
2. What is the difference between game theory and evolutionary game theory?	Evolutionary game theory focuses on the strategic decisions within a whole population of players, and describes the evolutionary, time-dependent dynamics of the population.
3. What do I need for a game-theoretical analysis?	You need only three things: The set of players, the set of available actions (strategies), and the payoff structure of the underlying game.
4. What are Nash equilibria, and evolutionary stable strategies?	These different equilibrium concepts will be defined, and explained in detail (see section 7.2). They are, e.g., important for the definition of the game classes.
5. What types of games are possible?	Symmetric and unsymmetric games. Symmetric games: "dominant games," "coordination games," and "anti-coordination games". Unsymmetric games: "corner class," "saddle class," and "center class".
6. How can evolutionary game theory be applied to science dynamics?	Two applications are discussed within this chapter. Subsection 7.3.1: "Scientific communication and the open access decision" and subsection 7.3.2: "Evolution of Hub-and-Spoke Communication Networks".
7. In the future, will scientific information be free of charge for everyone?	Scientists face a dilemma: Considering a potential loss in reputation, incentives to perform open access are missing (see subsection 7.3.1). Scientific publishers also face a dilemma, as they fear a profit loss within a totally "green-open-access publishing market" (see subsection 7.3.2).
8. Evolutionary game theory depends only on a few open parameters. How can that be? Isn't nature very complicated?	With the use of this simple model, one can learn a lot about the underlying game. However, some aspects are not included within classical evolutionary game theory. Some extensions of the classical theory ("Evolutionary Game Theory on Complex Networks" and "Evolutionary Quantum Game Theory") are discussed in section 7.4.

background of the whole market of scientific information. A main goal of academic research is the diffusion of new research results. This is achieved by interaction between scientists through reading and citing other authors' work [31]. Complex citation, co-authorship, and semantic networks have been evolved in reality, and the theoretical description of the dynamical behavior of these networks has been addressed in several chapters of this book. The evolution of the market of scientific information depends not only upon the researchers' actions, but also upon the actions of other actors involved in the knowledge-creation process (journals, libraries, funding agencies, etc.). For some years, the market of scientific publishing has been forced to make major changes in the process of distributing research results among scientists. First, the increase in digitalization brought a shift towards electronic publication, and second, shrinking library budgets in combination with a constant rise of journal prices have resulted in massive cancellations of journal subscriptions. In order to regain broad access to research findings, alternative ways of publishing scientific literature have been developed and have received increased attention. These new models are summarized under the term "Open Access (OA)" [29].

Within this chapter, the market of scientific information is modeled as a game between various actors involved in the knowledge-creation process. The main research goal of the chapter is to understand different publication norms within the scientific community, especially the description of the time evolution of the average strategic decision of different actor populations, using the framework of the evolutionary game theory. How can one include group behavior and social norms (which might be caused by cultural or moral standards) into the theory of population dynamics formulated within the evolutionary game theory? Evolutionary game theory on complex networks using agent-based computation methods and quantum game theory are recently developed models, and they will be discussed briefly at the end of this chapter (see section 7.4).

Within this chapter of the book *Models of Science Dynamics–Encounters between Complexity Theory and Information Science*, the framework of evolutionary game theory (EGT) is described in detail. After a general introduction and a discussion of a simple game-theoretical example, the grounding of EGT (section 7.2) and a brief literature review is presented. The formal mathematical model,

different concepts of equilibria, and various classes of evolutionary games will be defined, explained, and visualized. In section 7.3, two applications are presented. The first one (see subsection 7.3.1) focuses on the open-access game of scientific communication and extends it to an evolutionary game (for details, see [111, 118]). The second application (see subsection 7.3.2) focuses on the evolution of the interconnected network of scientific journals and scientific authors within a formal "Hub-and-Spoke Communication Network" model. The combination of evolutionary game theory with the theory of complex networks and the description of a new framework that includes group behavior and social norms into evolutionary population dynamics are briefly explained in section 7.4. The chapter ends with a short summary.

7.2. Evolutionary Game Theory

In 1928, the main inventor of game theory–Johann (John) von Neumann–published the first article on this important topic [234].[2] The first book about game theory was published in 1944 by von Neumann and Morgenstern [233]. Evolutionary game theory [216, 213, 214, 198, 166, 222, 198, 21, 108] was developed after J.M. Smith had found that stationary solutions to evolutionary differential equations are connected with game theory [212]. In the following years, applications in respect to biological systems [209, 226, 148, 78, 171, 172] and socio-economic systems–e.g., "public good" games [51], cultural or moral developments [68, 121], the evolution of languages [177], social learning [68], the evolution of social norms [23, 175], the financial crisis [114], and the evolution of social networks [222, 139, 67]–came into the focus of research.

7.2.1. Game theory: A simple example

The necessary definitions and fundamental basics of GT and EGT will be explained in the next subsection; however, the following section explains the use

[2] In principle, the groundings of GT go back to 1800 (e.g. Antoine-Augustin Cournot (1801–1877) and Francis Ysidro Edgeworth (1845–1926) [80]). Additionally, in the 1913, Ernst Zermelo had discussed the chess game using a backward-induction method [244]. However, the first formal, mathematical description of GT was developed by John von Neumann in the year 1928 [234].

of game-theoretical concepts with one simple example:

Two persons (Emma and Hans) have to make a decision. Each of them has to choose between two possible actions. For both of them it is an important decision, as they might get a great benefit (or a punishment) if they choose the "right" (or "wrong") decision. The amount of the potential benefit depends on the decisions of both persons and not only on the action of one. Unfortunately, they do not have any possibility of communicating with the other one to coordinate their actions.

GT is a mathematical concept used to analyze such decision states. Every quantitative mathematical model that tries to explain processes happening in nature begins with a definition of the necessary parameters. In the following, the parameter A or B (later also μ) will be used to describe a person, a player, a decision-maker, or even a firm or an animal. In the above example, the parameter A means "Emma" and the parameter B means "Hans". The parameter $\mathcal{S}^A$ will be used to describe the set of possible strategies (actions) available to Emma, whereas $\mathcal{S}^B$ describes the set of available actions of player "Hans." In the above example, this would be written as $\mathcal{S}^A = \left\{s_1^A, s_2^A\right\}$, as Emma can only choose between two possible actions namely, strategy one (s_1^A) and strategy two (s_2^A). The strategy space of Hans is written in a similar form: $\mathcal{S}^B = \left\{s_1^B, s_2^B\right\}$. The parameter U is used to quantify the potential benefit (or the amount of punishment) given to players after they have announced their final decisions.

In principle, to define a game Γ, one needs three things:

- Who is playing the game? Definition of the set of players:
  $\mathcal{I} = \{A, B, ...\} = \{\text{Emma}, \text{Hans}, ...\}$
- What can the players do? Definition of the set of actions (strategies) available for each player:
  $\mathcal{S}^A = \mathcal{S}^{\text{Emma}} = \left\{s_1^A, s_2^A, ...\right\}$ and $\mathcal{S}^B = \mathcal{S}^{\text{Hans}} = \left\{s_1^B, s_2^B, ...\right\}$
- How much can the players win or lose? Definition of the payoff structure of the game:
  $\hat{\mathcal{U}}^A = \hat{\mathcal{U}}^{\text{Emma}}$ and $\hat{\mathcal{U}}^B = \hat{\mathcal{U}}^{\text{Hans}}$

Every decision-maker who wants to analyse her/his decision problem (her/his

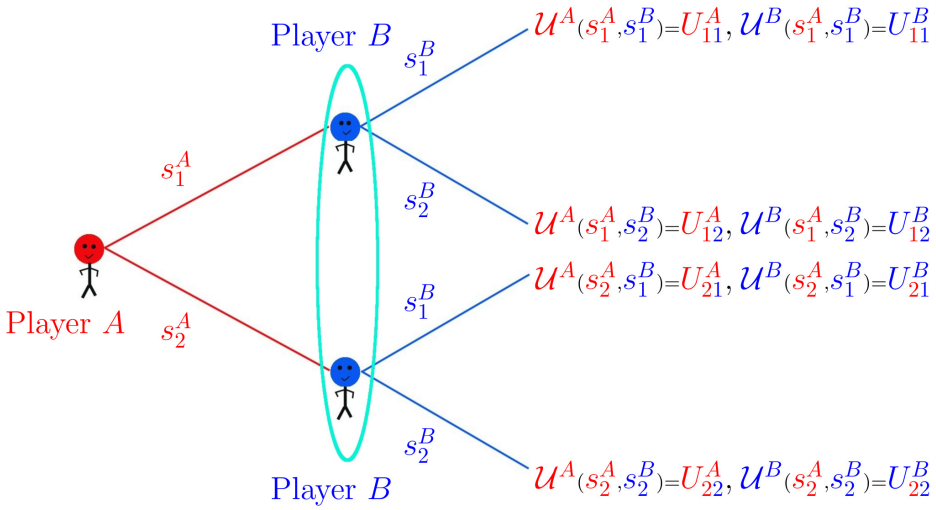

Figure 7.1.: Game tree of a (2 person)-(2 strategy) game with payoff for player A ($\mathcal{U}^A$) and player B ($\mathcal{U}^B$).

game) with game-theoretical concepts has to define these three things–therefore, the simple example is extended with the use of an additional little story. The binary decision of Emma (Player A) and Hans (Player B) could be "To stay" or "To go," or it could be simply to choose between two strategies (e.g., $\{buy, don't\, buy\}$, $\{left, right\}$, $\{above, below\}$, $\{s_1, s_2\}$). The benefit if both choose the strategy s_1 is very good for both of them, and the parameter U_{11} is used in the following to quantify this benefit. If Emma and Hans choose the strategy s_2, it will be bad for both of them, and the parameter U_{22} quantifies the value of punishment for both players. If Emma decides to stay (s_1^A) and Hans goes, the outcome for Hans will be even slightly better than the situation for him if both stay ($U_{11}^B < U_{12}^B$); the same holds true for Emma: ($U_{11}^A < U_{21}^A$). However, if Emma chooses the strategy s_2^A and Hans stays (strategy s_1^A), the outcome for Hans will be extremely bad ($U_{21}^B << U_{22}^B$); the same holds true for Emma: ($U_{12}^A << U_{22}^A$). Figure 7.1 visualizes this (two player)-(two strategy) game as a game tree with four possible payoff outcomes.

GT analyses such decision states, using mathematically defined equilibrium concepts. The most famous concept of this kind is called the "Nash equilibrium"

(NE). As player B does not know for sure what player A will do, he starts to think what would be the best for him, if player A chose the strategy s_1^A (staying): *"It would be good for me if player A stays and I stay, but in this case it would be even better for me to go."* After remaining a moment at this thought, player B starts to think in the other direction: *"If player A goes and I stay, it will be extremely bad for me–it is really advisable for me to go!"* Within the framework of classical GT, the predicted outcome of this example is that both players decide to go. In the language of game theory, the strategy s_2 is the only NE of this example, and as the game is a (two player)-(two strategy) normal-form game, s_2 is even a dominant strategy. To be more precise:

The strategy combination (s_2^A, s_2^B) is a Nash equilibrium because:

$$\begin{aligned} &\text{Nash equilibrium at } (s_2^A, s_2^B): \\ &\mathcal{U}^A(s_2^A, s_2^B) = U_{22}^A \geq \mathcal{U}^A(s^A, s_2^B) \quad \forall\ s^A \in \mathcal{S}^A = \left\{s_1^A, s_2^A\right\} \\ &\mathcal{U}^B(s_2^A, s_2^B) = U_{12}^B \geq \mathcal{U}^B(s_2^A, s^B) \quad \forall\ s^B \in \mathcal{S}^B = \left\{s_1^B, s_2^B\right\} \end{aligned} \tag{7.1}$$

The tragedy of this game is that after both players have made their decision, they are in a worse situation than when they had chosen the strategy s_1 ($U_{22}^A < U_{11}^A$ and $U_{22}^B < U_{11}^B$)–therefore, the game belongs formally to the class of prisoner's dilemma games (class of dominant games with a dilemma).

Depending on the payoff structure of the game ($\hat{\mathcal{U}}^A$ and $\hat{\mathcal{U}}^B$), different game classes and outcomes are possible. By analysing the game structure of a specific decision problem, decision makers can learn a lot about the problem they are involved in.

The simple example within this subsection was used to explain game-theoretical concepts. EGT uses these concepts, but focuses on the strategic decisions within a whole population of players. There exist not only one Emma and one Hans, but a whole group of players like Emma (group A) and a whole group of players like Hans (group B). They do not play the game only once–at each time increment the Emma's and the Hans's come together, play the game, receive their payoffs, and search the next game partner for the next time increment. The framework of EGT only needs one piece of additional information about the game Γ: What is the fraction of players within group A (group A) choosing strategy s_1^A (choosing

strategy s_1^B) at time zero–the initial value of the strategic decision of the whole population. Knowing the game Γ and the initial value, the framework of EGT is able to show the evolutionary dynamics of the population, and it gives answers about the thing everybody wants to know: "How is it going to the end?"

7.2.2. Definition and key aspects of evolutionary game theory

EGT is a time-dependent dynamical extension of "Game Theory" (GT), which itself is a mathematical toolbox to explain interdependent decision processes happening in biological or socio-economic systems. As the variety of different concepts in GT is very large, and the article is not meant to summarize only GT, the game-theoretical concepts presented in this article will only focus on "strategic-form games"[3], and the article does not discuss "extensive-form games" nor "cooperative games." In the following, the formal framework of the mixed extension of a (N player)-(m strategy) game in strategic form will be defined:

$$
\begin{aligned}
&\text{N-person game:} \quad \Gamma := \left(\mathcal{I}, \tilde{\mathcal{S}}, \tilde{\mathcal{U}}\right) \\
&\text{Set of players:} \quad \mathcal{I} = \{1, 2, ..., N\} \\
&\text{Pure strategy space:} \quad \mathcal{S} = \mathcal{S}^1 \times \mathcal{S}^2 \times ... \times \mathcal{S}^N \\
&\text{Pure strategy space of player } \mu \in \mathcal{I}: \quad \mathcal{S}^\mu = \left\{(s_1^\mu, s_2^\mu, ..., s_{m_\mu}^\mu)\right\} \\
&\text{Mixed-strategy space:} \quad \tilde{\mathcal{S}} = \tilde{\mathcal{S}}^1 \times \tilde{\mathcal{S}}^2 \times ... \times \tilde{\mathcal{S}}^N \\
&\text{Mixed-strategy space of player } \mu \in \mathcal{I}: \\
&\tilde{\mathcal{S}}^\mu = \left\{ (\tilde{s}_1^\mu, \tilde{s}_2^\mu, ..., \tilde{s}_{m_\mu}^\mu) \mid \sum_{i=1}^{m_\mu} \tilde{s}_i^\mu = 1, \tilde{s}_i^\mu \geq 0, i = 1, 2, ..., m_\mu \right\} \\
&\text{Number of strategies available for player } \mu \in \mathcal{I} \quad m_\mu \\
&\text{Mixed-strategy profile of player } \mu \in \mathcal{I}: \quad \tilde{s}^\mu = \left(\tilde{s}_1^\mu, \tilde{s}_2^\mu, ..., \tilde{s}_{m_\mu}^\mu\right)^T \in \tilde{\mathcal{S}}^\mu \\
&\text{Vector function of mixed payoffs:} \quad \tilde{\mathcal{U}} = \left(\tilde{\mathcal{U}}^1, \tilde{\mathcal{U}}^2, ..., \tilde{\mathcal{U}}^N\right) : \tilde{\mathcal{S}} \to \mathbb{R}^N \\
&\text{Mixed payoff for player } \mu \in \mathcal{I}: \\
&\tilde{\mathcal{U}}^\mu(\tilde{s}^1, \tilde{s}^2, ..., \tilde{s}^N) = \sum_{i_1=1}^{m_1} \sum_{i_2=1}^{m_2} ... \sum_{i_N=1}^{m_N} \mathcal{U}^\mu(s_{i_1}^1, s_{i_2}^2, ..., s_{i_N}^N) \prod_{\nu=1}^{N} \tilde{s}_{i_\nu}^\nu
\end{aligned}
\tag{7.2}
$$

[3]The category of "strategic-form games" is often also called "non-cooperative games".

Definition (7.2) expresses that three main quantities are necessary to define a (N player)-(m strategy) game in strategic form. The first quantity, the set of players $\mathcal{I}$, includes all of the actors involved in the underlying game. In respect to the focus of this book, $\mathcal{I}$ could be understood as the set of entities involved in the knowledge-creation process (subsets of $\mathcal{I}$: researchers, journals, libraries, funding agencies, etc.). The second quantity, the set of pure strategies $\tilde{\mathcal{S}}$, expresses all of the available strategies of all of the actors involved in the game. In principle, each actor $\mu \in \mathcal{I}$ could have her/his own set of available strategies ($\mathcal{S}^{\mu}$). If we focus again on a model of science, the different subgroups of $\mathcal{I}$ will have similar strategy spaces (strategy space of scholars, strategy space of journals, etc.). The set of mixed strategies of player μ ($\tilde{\mathcal{S}}^{\mu}$) is a mathematical amplification of the set of pure strategies ($\tilde{\mathcal{S}}^{\mu}$). The elements belonging to the set of mixed strategies ($\tilde{\mathbf{s}}^{\mu} = (\tilde{s}_1^{\mu}, \tilde{s}_2^{\mu}, ..., , \tilde{s}_{m_\mu}^{\mu}) \in \mathcal{S}^{\mu}$) consist of m_μ real numbers ($\tilde{s}_i^{\mu} \in [0,1] \; \forall \, i \in \{1, 2, ..., m_\mu\}$) and can be interpreted as the probability of player μ for choosing the pure strategy s_i^{μ}. The third quantity, the mixed strategy payoff function $\tilde{\mathcal{U}}$, is used to quantify the potential benefit (or the amount of punishment) given to the persons. The amount of the potential benefit (punishment) given to a player μ ($\tilde{\mathcal{U}}^{\mu}$) depends on the actions of all players and not only on the strategy decision of player μ.

To be more precise, the following part is constrained to the strategic form of an unsymmetric (or symmetric) (2 player)-(2 strategy) game Γ (for details, see [108, 222]):

$$(2 \times 2) \text{ game:} \quad \Gamma := \left(\{A, B\}, \mathcal{S}^A \times \mathcal{S}^B, \hat{\mathcal{U}}^A, \hat{\mathcal{U}}^B \right) \tag{7.3}$$

Set of pure strategies of player A and B:

$$\mathcal{S}^A = \left\{ s_1^A, s_2^A \right\}, \; \mathcal{S}^B = \left\{ s_1^B, s_2^B \right\}$$

Set of mixed strategies of player A and B:

$$\tilde{\mathcal{S}}^A = \left\{ \tilde{s}_1^A, \tilde{s}_2^A \right\}, \; \tilde{\mathcal{S}}^B = \left\{ \tilde{s}_1^B, \tilde{s}_2^B \right\}$$

Mixed payoff of player $\mu \in \{A, B\}$: $\quad \tilde{\mathcal{U}}^{\mu} : \left(\tilde{\mathcal{S}}^A \times \tilde{\mathcal{S}}^B \right) \to \mathbb{R}$

$$\tilde{\mathcal{U}}^{\mu}((\tilde{s}_1^A, \tilde{s}_2^A), (\tilde{s}_1^B, \tilde{s}_2^B)) = U_{11}^{\mu} \tilde{s}_1^A \tilde{s}_1^B + U_{12}^{\mu} \tilde{s}_1^A \tilde{s}_2^B + U_{21}^{\mu} \tilde{s}_2^A \tilde{s}_1^B + U_{22}^{\mu} \tilde{s}_2^A \tilde{s}_2^B$$

Payoff matrix for player A and B:

$$\hat{\mathcal{U}}^A = \begin{pmatrix} U_{11}^A & U_{12}^A \\ U_{21}^A & U_{22}^A \end{pmatrix}, \; \hat{\mathcal{U}}^B = \begin{pmatrix} U_{11}^B & U_{12}^B \\ U_{21}^B & U_{22}^B \end{pmatrix}$$

The set of mixed strategies of player A ($\tilde{\mathcal{S}}^A$) and player B ($\tilde{\mathcal{S}}^B$) is a mathematical amplification of the set of pure strategies ($\mathcal{S}^A$ and $\mathcal{S}^B$). The elements belonging to the set of mixed strategies ($\tilde{\mathbf{s}}^\mu = (\tilde{s}_1^\mu, \tilde{s}_2^\mu) \in \mathcal{S}^\mu$) of player $\mu = A, B$ consist of two real numbers ($\tilde{s}_1^\mu \in [0,1]$ and $\tilde{s}_2^\mu \in [0,1]$) and can be interpreted as the probability of player μ for choosing the strategy 1 ($\tilde{s}_1^\mu$) or 2 ($\tilde{s}_2^\mu$). For two-strategy games, the following normalization condition has to be fulfilled: $\tilde{s}_1^\mu + \tilde{s}_2^\mu = 1 \; \forall \, \mu = A, B$.

Due to the normalizing condition, it is possible to simplify the functional dependence of the mixed-strategy payoff function:

$$\begin{aligned} & \tilde{\mathcal{U}}^\mu : ([0,1] \times [0,1]) \to \mathbb{R} \\ \tilde{\mathcal{U}}^\mu(\tilde{s}^A, \tilde{s}^B) \;\; = \;\; & U_{11}^\mu \tilde{s}^A \tilde{s}^B + U_{12}^\mu \tilde{s}^A (1 - \tilde{s}^B) + \\ & + U_{21}^\mu (1 - \tilde{s}^A) \tilde{s}^B + U_{22}^\mu (1 - \tilde{s}^A)(1 - \tilde{s}^B) \,, \end{aligned} \tag{7.4}$$

where $\tilde{s}^A := \tilde{s}_1^A$, $\tilde{s}^B := \tilde{s}_1^B$, $\tilde{s}_2^A = 1 - \tilde{s}_1^A$ and $\tilde{s}_2^B = 1 - \tilde{s}_1^B$.

In the following, two fundamental equilibrium concepts are defined, namely the *equilibrium in dominant strategies* and the *Nash equilibrium*.

A strategy combination $(\tilde{s}^{A\dagger}, \tilde{s}^{B\dagger})$ is an equilibrium in dominant strategies if the following conditions are fulfilled:

$$\begin{gathered} \text{Equilibrium in dominant strategies:} \\ \tilde{\mathcal{U}}^\mu(\tilde{s}^{A\dagger}, \tilde{s}^{B\dagger}) \;\geq\; \tilde{\mathcal{U}}^\mu(\tilde{s}^A, \tilde{s}^B) \quad \forall \;\; \mu = A, B \text{ and } \quad \tilde{s}^A, \tilde{s}^B \in [0,1] \end{gathered} \tag{7.5}$$

A strategy combination $(\tilde{s}^{A*}, \tilde{s}^{B*})$ is called a Nash equilibrium if:

$$\begin{gathered} \text{Nash equilibrium:} \\ \tilde{\mathcal{U}}^A(\tilde{s}^{A*}, \tilde{s}^{B*}) \;\geq\; \tilde{\mathcal{U}}^A(\tilde{s}^A, \tilde{s}^{B*}) \quad \forall \;\; \tilde{s}^A \in [0,1] \\ \tilde{\mathcal{U}}^B(\tilde{s}^{A*}, \tilde{s}^{B*}) \;\geq\; \tilde{\mathcal{U}}^B(\tilde{s}^{A*}, \tilde{s}^B) \quad \forall \;\; \tilde{s}^B \in [0,1] \end{gathered} \tag{7.6}$$

An interior (mixed-strategy) NE $(\tilde{s}^{A\star}, \tilde{s}^{B\star})$ is a special case of the Definition 7.6, as the partial derivative of the mixed-strategy payoff function vanishes at the

value of the interior NE:

$$\text{Interior Nash equilibrium:} \tag{7.7}$$
$$\left.\frac{\partial \tilde{\mathcal{U}}^A(\tilde{s}^A,\tilde{s}^B)}{\partial \tilde{s}^A}\right|_{\tilde{s}^B=\tilde{s}^{B\star}} = 0 \quad \forall\ \tilde{s}^A \in [0,1]\ ,\ \tilde{s}^{B\star} \in]0,1[$$
$$\left.\frac{\partial \tilde{\mathcal{U}}^B(\tilde{s}^A,\tilde{s}^B)}{\partial \tilde{s}^B}\right|_{\tilde{s}^A=\tilde{s}^{A\star}} = 0 \quad \forall\ \tilde{s}^B \in [0,1]\ ,\ \tilde{s}^{A\star} \in]0,1[$$

The defined equilibrium concepts will be used in subsection 7.2.3 to classify games into different classes. The hitherto defined mathematical constructs can be used to analyze one-shot (2×2) games, while the following equations will describe the time evolution of the strategic behavior of a large group of players (population). At each time increment all of the individual players of the population search randomly for a partner to play a (2×2) game. Then, after the players have chosen their strategies and have received their payoffs, they search again for the next game partner. To describe the time evolution of such a repeated version of the game Γ, *replicator dynamics* has been developed. As the payoff matrices ($\hat{\mathcal{U}}^A$ and $\hat{\mathcal{U}}^B$) of the two persons playing the game are in general unsymmetric, the whole population of players separates into the two subpopulations "A" and "B." Replicator dynamics, formulated within a system of differential equations, defines in which way the population vector $\vec{x}^\mu = (x_1^\mu, x_2^\mu)$ evolves in time. Each component $x_i^\mu = x_i^\mu(t)$ ($i = 1, 2$ and $\mu = A, B$) describes the time evolution of the fraction of different player types i in the μ-subpopulation, where a type-i player is understood as an actor μ playing strategy s_i^μ. Similar to the normalizing condition of the mixed strategies, the two population vectors $\vec{x}^A$ and $\vec{x}^B$ have to fulfill the normalizing conditions of a unity vector:

$$x_i^\mu(t) \geq 0 \quad \text{and} \quad \sum_{i=1}^{2} x_i^\mu(t) = 1 \quad \forall\, i = 1, 2\,,\ t \in \mathbb{R},\ \mu = A, B. \tag{7.8}$$

The structure of the time evolution of the components of the two population vectors $\vec{x}^A(t) = (x_1^A(t), x_2^A(t)$ and $\vec{x}^B(t) = (x_1^B(t), x_2^B(t))$ is formulated through a system of differential equations, known as the equation of *Replicator Dynamics*

[21, 198, 166, 108, 222]:

$$\begin{aligned} \frac{dx_i^A(t)}{dt} &= x_i^A(t)\left[\sum_{l=1}^{2} U_{il}^A\, x_l^B(t) - \sum_{l=1}^{2}\sum_{k=1}^{2} U_{kl}^A\, x_k^A(t)\, x_l^B(t)\right] \\ \frac{dx_i^B(t)}{dt} &= x_i^B(t)\left[\sum_{l=1}^{2} U_{li}^B\, x_l^A(t) - \sum_{l=1}^{2}\sum_{k=1}^{2} U_{lk}^B\, x_l^A(t)\, x_k^B(t)\right] \end{aligned} \tag{7.9}$$

As the number of available strategies in our approach is restricted to two, it is possible to substitute the second strategy by using condition (7.8): $x_2^A = 1 - x_1^A$ and $x_2^B = 1 - x_1^B$. The system of differential equations (7.9) can therefore be formulated as follows ($x(t) := x_1^A(t)$, $y(t) := x_1^B(t)$):

$$\begin{aligned} \frac{dx(t)}{dt} &= \left(\underbrace{U_{11}^A - U_{21}^A}_{:=a^A} + \underbrace{U_{22}^A - U_{12}^A}_{:=b^A}\right)\left(x(t) - (x(t))^2\right)\, y(t) - \\ &\quad - \underbrace{\left(U_{22}^A - U_{12}^A\right)}_{:=b^A}\left(x(t) - (x(t))^2\right) = \\ &= \left(a^A + b^A\right)\left(x(t) - (x(t))^2\right)\, y(t) - b^A\left(x(t) - (x(t))^2\right) = \\ &=: g_A(x,y) \\ \frac{dy(t)}{dt} &= \left(\underbrace{U_{11}^B - U_{21}^B}_{:=a^B} + \underbrace{U_{22}^B - U_{12}^B}_{:=b^B}\right)\left(y(t) - (y(t))^2\right)\, x(t) - \\ &\quad - \underbrace{\left(U_{22}^B - U_{12}^B\right)}_{:=b^B}\left(y(t) - (y(t))^2\right) = \\ &= \left(a^B + b^B\right)\left(y(t) - (y(t))^2\right)\, x(t) - b^B\left(y(t) - (y(t))^2\right) = \\ &=: g_B(x,y) \end{aligned} \tag{7.10}$$

Equation (7.10) describes the time evolution of the strategic behavior of two separate subpopulations playing an unsymmetric bimatrix game. The fraction of players choosing strategy s_1 at time t of the subpopulation "A" is quantified by $x(t)$, whereas $y(t)$ describes the average strategic choice of subpopulation "B." The time evolution of the coupled system of differential equations (7.10) depends on the properties of the two functions $g_A(x,y)$ and $g_B(x,y)$ and on the initial conditions $x(t=0)$ and $y(t=0)$.

If we focus on a model of science, the two different subpopulations playing the evolutionary game could be, for example, the group of scholars (subpopulation "A") and the group of journals (subpopulation "B"). The two pure strategies of a member of the group A of researchers could be based on any relevant, recurring binary decision a scholar has to decide during her/his research lifetime (e.g., does she/he want to put her/his new article on a open-access repository). The two pure strategies of a member of the group B of journals could be any recurring binary decision a journal has to make (e.g., does the journal allow the authors to put their submitted article version on an open-access repository). The fraction of researchers choosing strategy $s_1^A \hat{=}$(put the article on an open-access repository) at time t is quantified by $x(t)$, where $x = 1$ corresponds to a situation where every scholar uses open-access repositories, and $x = 0$ means nobody uses them. Similarly, the fraction of journals choosing strategy $s_1^A \hat{=}$(allowing open-access repositories) at time t is quantified by $y(t)$, where $y = 1$ corresponds to a situation where every journal allows open-access repositories and $y = 0$ means no journal allows it. The two payoff matrices finally quantify the potential benefit to the researchers ($\hat{\mathcal{U}}^A$) and journals ($\hat{\mathcal{U}}^B$). This particular bimatrix game will be discussed in more detail within subsection 7.3.2.

By restricting the underlying payoff matrix to be symmetric ($\hat{\mathcal{U}}^A \equiv \left(\hat{\mathcal{U}}^B\right)^T$, $U_{lk} := U_{lk}^A = U_{kl}^B$), the two separate subpopulations (A and B) cannot be distinguished any more and the system of differential equations (7.9) simplifies as follows:

$$\begin{aligned} \frac{dx_i^A(t)}{dt} &= x_i^A(t) \left[\sum_{l=1}^{2} U_{il}\, x_l^B(t) - \sum_{l=1}^{2} \sum_{k=1}^{2} U_{kl}\, x_k^A(t)\, x_l^B(t) \right] \\ \frac{dx_i^B(t)}{dt} &= x_i^B(t) \left[\sum_{l=1}^{2} U_{il}\, x_l^A(t) - \sum_{l=1}^{2} \sum_{k=1}^{2} U_{kl}\, x_l^A(t)\, x_k^B(t) \right] \end{aligned} \tag{7.11}$$

Equation (7.11) indicates that the mathematical structures of the two population vectors $\vec{x}^A$ and $\vec{x}^B$ are identical, which simply means that a symmetric evolutionary game can be described by a single population vector $\vec{x} := \vec{x}^A = \vec{x}^B$. In respect to a model of science, this means that equation (7.11) can only be used for subgames with strategic decisions involving only one set of knowledge entities. Therefore the system of differential equations (7.11) reduces to one

single equation:

$$\frac{dx_i(t)}{dt} = x_i(t)\left[\underbrace{\sum_{l=1}^{2} U_{il}\, x_l(t)}_{:=f_i(t)} - \underbrace{\sum_{l=1}^{2}\sum_{k=1}^{2} U_{kl}\, x_k(t)\, x_l(t)}_{:=\bar{f}(t)}\right] \tag{7.12}$$

where $f_i(t)$ is the fitness of type i and $\bar{f}(t) = \sum_{i=1}^{2} f_i(t)$ is the average fitness of the whole population. Again, the overall vector $\vec{x} = (x_1(t), x_2(t))$ has to fulfill the normalizing conditions of a unity vector:

$$x_i(t) \geq 0 \;\; \forall\, i = 1,2 \quad \text{and} \quad \sum_{i=1}^{2} x_i(t) = 1 \;\; \forall\, t \in \mathbb{R} \quad . \tag{7.13}$$

For a symmetric game, equation (7.12) can therefore be simplified as follows:

$$\begin{aligned}
\frac{dx}{dt} &= x\Big[U_{11}(x - x^2) + U_{12}(1 - 2x + x^2) + \\
&\quad + U_{21}(x^2 - x) + U_{22}(2x - x^2 - 1)\Big] = \\
&= x\left[\underbrace{(U_{11} - U_{21})}_{:=a}(x - x^2) - \underbrace{(U_{22} - U_{12})}_{:=b}(1 - 2x + x^2)\right] = \\
&= x\Big[a(x - x^2) - b(1 - 2x + x^2)\Big] =: g(x) \\
&\quad \text{with:} \quad x = x(t) := x_1(t) \quad \text{and} \quad x_2(t) = (1 - x(t))
\end{aligned} \tag{7.14}$$

The function $x(t)$, describing the fraction of players choosing the strategy s_1 at time t, depends on the function $g(x)$ and on the initial starting value $x(t = 0)$. The stationary solution of the asymptotic behavior $\lim_{t\to\infty}(x(t))$ depends also on $g(x)$ and on the initial condition, and it is formalized within the mathematical concept of the *Evolutionary Stable Strategy* (ESS). For a general 2-player game Γ with the mixed payoff functions $\tilde{\mathcal{U}}^A$ and $\tilde{\mathcal{U}}^B$, a strategy combination $(\tilde{s}^{A*}, \tilde{s}^{B*}) \in ([0,1] \times [0,1])$ is defined as an (ESS) if:

a) $(\tilde{s}^{A*}, \tilde{s}^{B*})$ is a Nash equilibrium of the game

b) $\tilde{\mathcal{U}}^A(\tilde{s}^A, \tilde{s}^B) \leq \tilde{\mathcal{U}}^A(\tilde{s}^{A*}, \tilde{s}^B) \qquad \forall \quad \tilde{s}^A \in r^A(\tilde{s}^{B*})\,, \;\; \tilde{s}^B \neq \tilde{s}^{B*}$

$$\tilde{\mathcal{U}}^B(\tilde{s}^A, \tilde{s}^B) \leq \tilde{\mathcal{U}}^B(\tilde{s}^A, \tilde{s}^{B*}) \qquad \forall \quad \tilde{s}^B \in r^B(\tilde{s}^{A*}), \;\; \tilde{s}^A \neq \tilde{s}^{A*} \quad .$$

Let $r^B(\tilde{s}^A)$ and $r^A(\tilde{s}^B)$ signify the best response functions of players B and A to the strategy $\tilde{s}^A$ and $\tilde{s}^B$, respectively. An ESS $(\tilde{s}^{A*}, \tilde{s}^{B*})$ therefore needs to be a Nash equilibrium of the game, and also the inequations b) should be fulfilled for any strategy combination $(\tilde{s}^A, \tilde{s}^B)$ belonging to the set of best responses to $(\tilde{s}^{A*}, \tilde{s}^{B*})$.

This survey has focused on deterministic evolutionary game dynamics and has specially concentrated on replicator dynamics. Stochastic evolutionary game dynamics and adaptive or rational learning processes have not been discussed (for a detailed analysis, see e.g., [196]). The discussed evolutionary dynamics uses only the revision protocol of replicator dynamics and other possible types of dynamics (nonlinear payoff functions, general imitation dynamics, best-response dynamics, logit dynamics and Brown-von Neumann-Nash dynamics) were not discussed within this chapter either (for a detailed analysis, see e.g., [196, 128]). The conjunction of evolutionary game theory with the theory of complex networks using concepts from agent-based modeling is a new and interesting scientific topic, but it is not addressed within this chapter (for a detailed analysis, see e.g., [222, 128]).

7.2.3. Classes of evolutionary games

Within this subsection, the possible classes of (2 player)-(2 strategy) games are defined. The first part of this subsection focuses on classes of the symmetric version of the game Γ (see equation (7.14)), whereas the second part deals with the bimatrix version of the game (see equation (7.10)).

Classes of symmetric games

Following the classification scheme of [235] (see also [222]), only three classes of symmetric (2 player)-(2 strategy) games are possible, namely the dominant game class, the class of anti-coordination games, and the coordination game class. For $a < 0$ and $b > 0$ (see equation (7.14)), the game belongs to the class of dominant games having only one pure NE (s_1^A, s_1^B), which is also the dominant strategy and

the only ESS of the game. For $a, b < 0$, the game Γ is an anti-coordination game, having two pure, non-symmetric Nash equilibria ((s_1^A, s_2^B) and (s_2^A, s_1^B)), and one symmetric interior mixed strategy NE $(\tilde{s}^{A\star}, \tilde{s}^{B\star}) = (\frac{b}{a+b}, \frac{b}{a+b})$, which is the only ESS of the game. For $a, b > 0$, the game belongs to the coordination game class, having two pure symmetric Nash equilibria ((s_1^A, s_1^B) and (s_2^A, s_2^B)), which are the two possible ESSs, and one symmetric interior NE at $(\tilde{s}^{A\star}, \tilde{s}^{B\star}) = (\frac{b}{a+b}, \frac{b}{a+b})$. For $b < 0$ and $a > 0$, the game is again a dominant game, having only one pure NE and ESS at (s_2^A, s_2^B).

To illustrate these formal results and visualize the outcomes of the different game classes, this section presents the numerical simulations with different parameter settings of symmetric games. The parameter setting Set_1 belongs to the class of dominant games, parameter setting Set_2 belongs to the coordination game class, whereas the setting Set_3 describes an anti-coordination game. Table 7.2 summarizes the different parameters of the three sets.

Table 7.2.: Parameter values of the three different sets of symmetric games.

Setting	Class	U_{11}	U_{12}	U_{21}	U_{22}	a	b	Nash equilibria
Set_1	Dominant Class	10	4	12	5	-2	1	One pure Nash equilibrium (s_2^A, s_2^B)
Set_2	Coordination Class	10	4	9	5	1	1	Two pure Nash equilibria and one interior NE at $s^\star = \frac{1}{2}$
Set_3	Anti-Coord. Class	10	7	12	5	-2	-2	Two pure asymmetric Nash equilibria and one interior NE at $s^\star = \frac{1}{2}$

Dominant Games

Figure 7.2 visualizes the mixed-strategy payoff function $\tilde{\mathcal{U}}^A(\tilde{s}^A, \tilde{s}^B)$ (see equation (7.4)) for player A within parameter set Set_1.

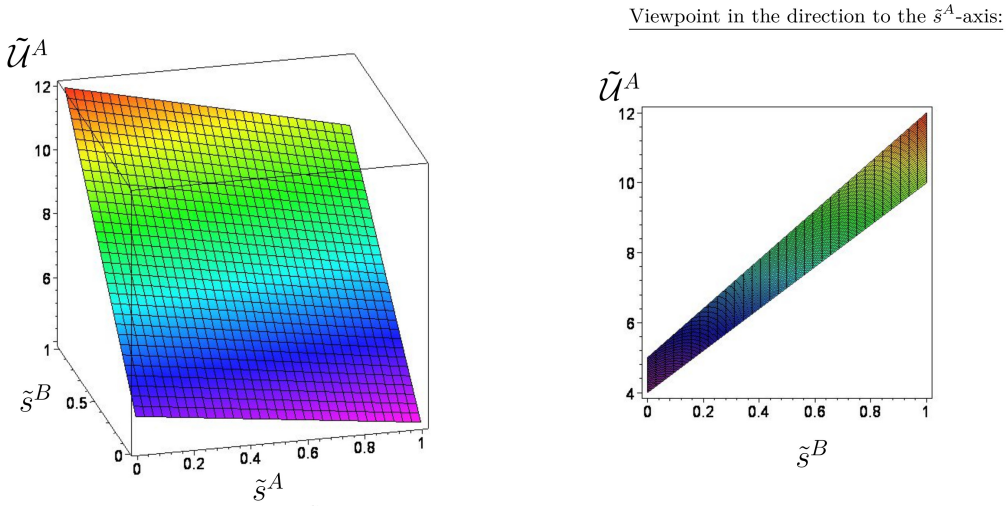

Figure 7.2.: Mixed-strategy payoff function $\tilde{\mathcal{U}}^A(\tilde{s}^A, \tilde{s}^B)$ for player A within parameter set Set_1 as a function of the mixed strategies of player A ($\tilde{s}^A$) and B ($\tilde{s}^B$).

The right picture shows a special projection of the surface in which the observer looks in the direction of the $\tilde{s}^A$-axis. The figure shows that the parameter set Set_1 belongs to the class of dominant games and that only one pure NE exists $((s_2^A, s_2^B) \hat{=} (\tilde{s}^A = 0, \tilde{s}^B = 0))$, which is the dominant strategy of the game. This property can be seen in the left picture of Figure 7.2 if one fixes the mixed strategy of player B to an arbitrary value ($\tilde{s}^B \in [0, 1]$). The best response for player A will always be the dominant strategy $s_2^A \hat{=} (\tilde{s}^A = 0)$. However, a dilemma appears within Set_1, as the payoff for the dominant strategy combination $(\tilde{\mathcal{U}}^A(\tilde{s}^A = 0, \tilde{s}^B = 0) = 5)$ is far below the highest point of the surface. If both players had chosen the strategy combination $(s_1^A, s_1^B) \hat{=} (\tilde{s}^A = 1, \tilde{s}^B = 1)$, it would have been much better for them $(\tilde{\mathcal{U}}^A(\tilde{s}^A = 1, \tilde{s}^B = 1) = 10)$. The structure of the game within parameter set Set_1 is comparable to a "prisoner's dilemma" game. As no interior NE is present within parameter set Set_1, the partial derivative (see

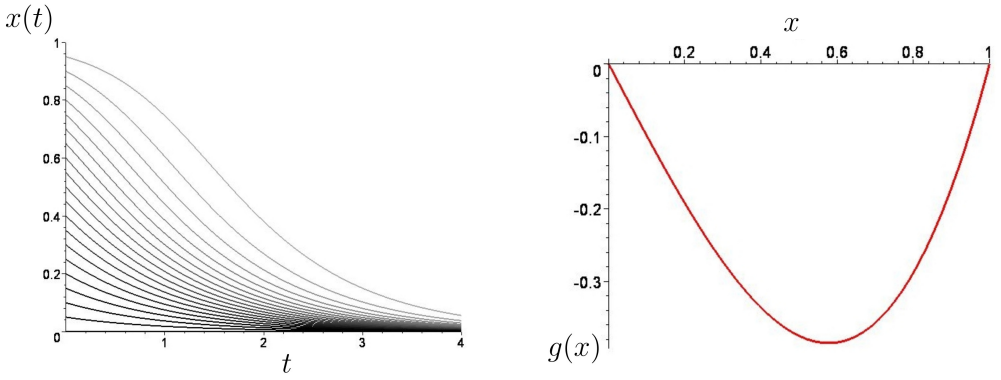

Figure 7.3.: Function $x(t)$, the fraction of players choosing the strategy s_1 at time t, for different initial conditions within parameter set Set_1 (left picture). The picture on the right shows the function $g(x)$, which determines the dynamical behavior of $x(t)$.

equation (7.7)) of $\tilde{\mathcal{U}}^A$ does not vanish within the given boundaries. The right picture of Figure 7.2 visualizes this fact as no cord-up point was found within the special $\tilde{s}^A$-projection.

The right picture of Figure 7.3 shows the function $g(x)$ within parameter set Set_1, whereas the left picture visualizes the numerical results of replicator dynamics ($x(t)$, see equation (7.14)) for several initial conditions of the population function ($x(t=0) = 0, 0.05, 0.1, ..., 0.95$). As the function $g(x)$ is negative for all $x \in]0,1[$, the fraction of players choosing the strategy s_1 ($x(t)$) will always decrease until everybody chooses the strategy s_2, independently of the initial condition.

Coordination Games

Within parameter set Set_2, the payoff $U_{21} = 9$ has decreased compared to the value of Set_1 ($U_{21} = 12$). Due to this decrease, the game class has shifted from the class of dominant games to the coordination game class. The game has now two pure, symmetric Nash equilibria ($(s_1^A, s_1^B) \hat{=} (\tilde{s}^A = 1, \tilde{s}^B = 1)$ and $(s_2^A, s_2^B) \hat{=} (\tilde{s}^A = 0, \tilde{s}^B = 0)$) and one interior mixed-strategy Nash equilibrium $((\tilde{s}^{A\star}, \tilde{s}^{B\star}) = (\frac{1}{2}, \frac{1}{2}))$. The apparency of the two pure Nash equilibria is visualized within the left picture of Figure 7.4. If player B is expected to choose a mixed strategy $\tilde{s}^B > s^\star$, the best response for player A is the pure strategy $s_1 \hat{=} \tilde{s}^A = 1$, whereas if player B is expected to choose a mixed-strategy $\tilde{s}^B < s^\star$, the best

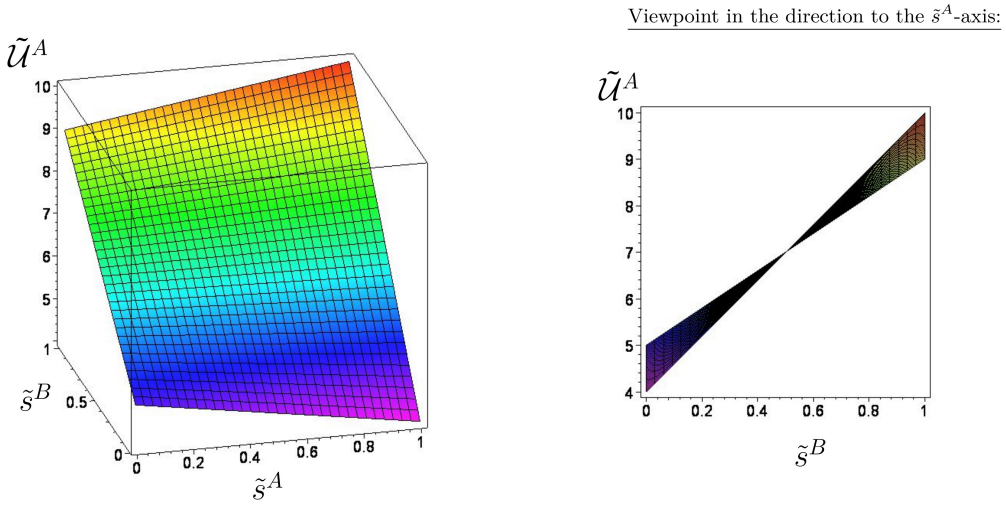

Figure 7.4.: Mixed-strategy payoff function $\tilde{\mathcal{U}}^A(\tilde{s}^A, \tilde{s}^B)$ for player A within parameter set Set_2 as a function of the mixed strategies for player A ($\tilde{s}^A$) and B ($\tilde{s}^B$).

response for player A is the pure strategy $s_2 \hat{=} \tilde{s}^A = 0$. The mixed-strategy Nash equilibrium is visualized within the right picture of Figure 7.4. Due to the fact that the partial derivative of the payoff surface for player A vanishes at the value of the mixed strategy NE, the whole surface shrinks to one point, if one projects the viewpoint in the direction to the $\tilde{s}^A$-axis (see the right picture of Figure 7.4).

The value of the mixed-strategy Nash equilibrium is equal to the zero point of the function $g(x)$ (see right picture of Figure 7.5). The function $g(x)$ (which determines the dynamical behavior of the population function $x(t)$) has, beside its negative region ($g(x) < 0 \; \forall \; x \in]0, s^\star[$), also a region where its value is positive ($g(x) > 0 \; \forall \; x \in]s^\star, 1[$). Due to this property, two evolutionary stable strategies emerge ($x(t \to \infty) = 0$ and $x(t \to \infty) = 1$). To which of these ESSs the population will evolve depends on the initial condition. If the fraction of s_1-player types at the initial time $t = 0$ is below the value of the mixed strategy NE ($x(0) < s^\star = 0.5$), the population will evolve to the ESS $\lim_{t\to\infty}(x(t)) = 0$, which corresponds to a population solely choosing the s_2-strategy. Only if the initial fraction is above the mixed strategy threshold ($x(0) > s^\star$), the population will end in the ESS $\lim_{t\to\infty}(x(t)) = 1$. The horizontal population path at $x(0.5) = 0.5$

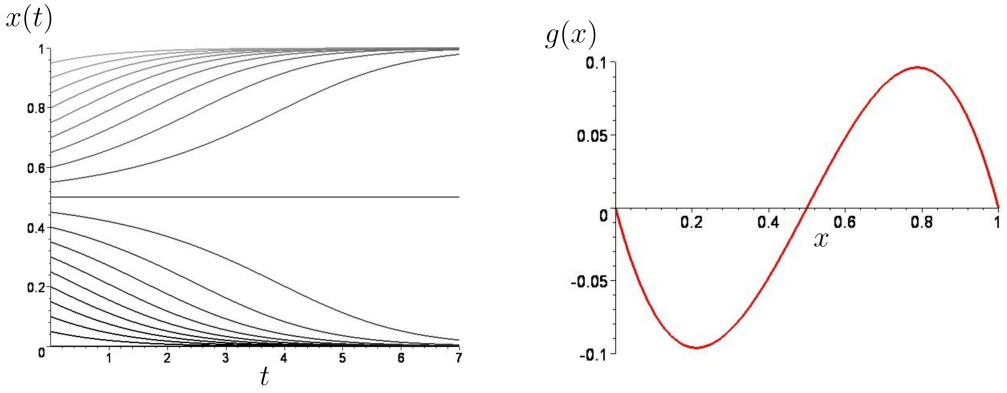

Figure 7.5.: Function $x(t)$, the fraction of players choosing the strategy s_1 at time t, for different initial conditions within parameter set Set_2 (left picture). The picture on the right shows the function $g(x)$, which determines the dynamical behavior of $x(t)$.

is an artefact of the numerical simulation and is not an ESS, as the solution is unstable in respect to infinitely small perturbations.

Anti-Coordination Games

Within parameter set Set_3, the payoff $U_{12} = 7$ has increased above the U_{22}-value (Set_3: $U_{22} = 5$). Due to this increase, the game class has shifted towards the class of anti-coordination games. Such games have two asymmetric pure Nash equilibria ((s_1^A, s_2^B) and (s_2^A, s_1^B)) and one interior mixed-strategy Nash equilibrium, which is the only ESS of such games. The apparency of the two asymmetric Nash equilibria is visualized within the left picture of Figure 7.6, whereas the mixed-strategy Nash equilibrium (Set_3: $s^\star = 0.5$) is visualized within the right picture.

The value of the mixed-strategy NE is again equal to the zero point of the function $g(x)$ (see right picture of Figure 7.7). The function $g(x)$ has now a positive region at $(g(x) > 0 \; \forall \; x \in]0, s^\star[)$ and a negative region at $(g(x) < 0 \; \forall \; x \in]s^\star, 1[)$. Independently of the specific value of the initial condition, the population will always asymptotically end in the ESS $x = s^\star = 0.5$ (see the left picture of Figure 7.7).

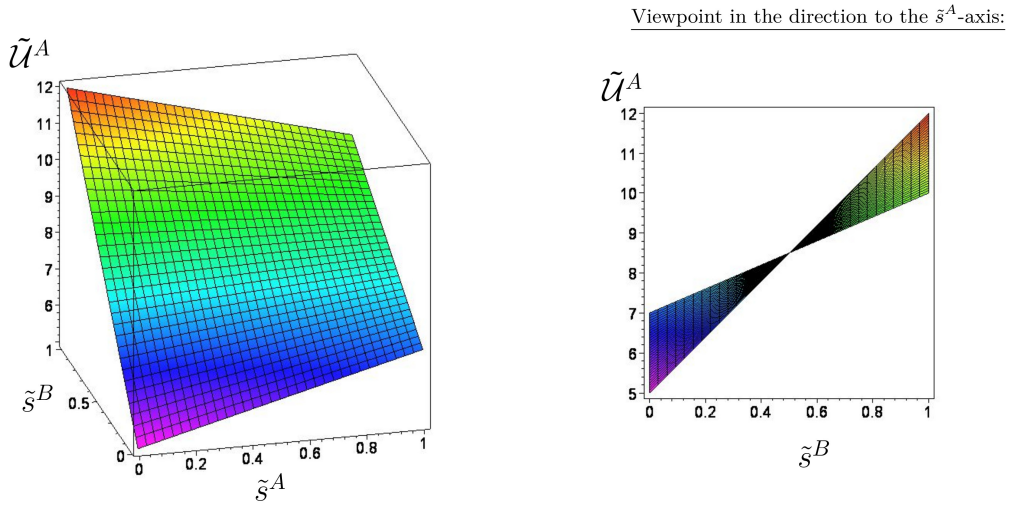

Figure 7.6.: Mixed-strategy payoff function $\tilde{\mathcal{U}}^A(\tilde{s}^A, \tilde{s}^B)$ for player A within parameter set Set_3 as a function of the mixed strategies for player A ($\tilde{s}^A$) and B ($\tilde{s}^B$).

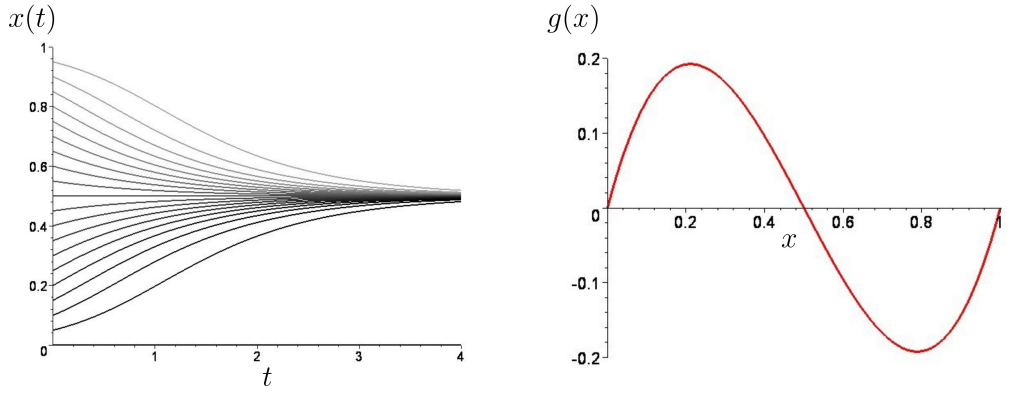

Figure 7.7.: Function $x(t)$, the fraction of players choosing the strategy s_1 at time t, for different initial conditions within parameter set Set_8 (left picture). The picture on the right shows the function $g(x)$, which determines the dynamical behavior of $x(t)$.

It was shown within this subsection that symmetric (2×2)-games can be separated

into three classes. However, if the number of available strategies increases, the number of possible classes also needs to be extended. Zeeman has defined 19 different game classes of symmetric (2×3)-games [243].

Classes of bimatrix games

This subsection summarizes the numerical results of the unsymmetric model, where two separate subpopulations play an evolutionary bimatrix game. Following the bimatrix classification scheme of Cressman [52] (see also [222]), again only three major[4] classes are possible within the unsymmetric version of the game Γ, namely the corner class, the center class and the saddle class. The game belongs to the saddle class if all of the parameters are positive ($a^A, b^A, a^B, b^B > 0$). Saddle-class games have an interior mixed-strategy Nash equilibrium at $(\tilde{s}^{A\star}, \tilde{s}^{B\star}) = (\frac{b^B}{a^B+b^B}, \frac{b^A}{a^A+b^A})$ and two pure, symmetric Nash equilibria $((s_1^A, s_1^B)$ and $(s_2^A, s_2^B))$, which are the two ESSs of the game. For $a^A, b^A > 0$ and $a^B, b^B < 0$ (or $a^A, b^A < 0$ and $a^B, b^B > 0$), the game describes a center-class game, having only one NE, namely the interior mixed-strategy NE at $(\tilde{s}^{A\star}, \tilde{s}^{B\star}) = (\frac{b^B}{a^B+b^B}, \frac{b^A}{a^A+b^A})$. Center-class games do not have any ESS, and the population trajectories are closed cycles. Corner-class games emerge if the parameters fulfill the following conditions: $a^A < 0 < b^A, b^B > 0, a^B \neq 0$ (or $a^B < 0 < b^B, b^A > 0, a^A \neq 0$). Such games have only one pure Nash equilibrium (s_2^A, s_2^B) (or (s_1^A, s_1^B)), which is the dominant strategy and the only ESS of the game.

To illustrate these theoretical results and visualize the outcomes of the different game classes, the parameters were fixed within four different game settings (see Table 7.3). The parameter setting Set_1^{us} belongs to the corner class of bimatrix games, the sets Set_2^{us} and Set_3^{us} are saddle-class games, and the last setting (Set_4^{us}) describes a game that belongs to the center class.

Corner class

The left picture of Figure 7.8 visualizes the mixed-strategy payoff function for player A–$\tilde{\mathcal{U}}^A(\tilde{s}^A, \tilde{s}^B)$: colored surface, see equation (7.4)–and player B–$\tilde{\mathcal{U}}^B(\tilde{s}^A, \tilde{s}^B)$: wired grey surface–within parameter set Set_1^{us}. The set Set_1^{us}

[4] Beside the three major (generic) classes there exist also degenerate cases, where one ore more of the parameters a^A, b^A, a^B and b^B are zero (see [222]).

Parameter setting	μ	Class of Game μ	$\$_{11}^{\mu}$	$\$_{12}^{\mu}$	$\$_{21}^{\mu}$	$\$_{22}^{\mu}$	a^{μ}	b^{μ}	Nash equilibria of Game μ	Game Class NE and ESS
Set_1^{us}	A:	Dominant Class	10	4	14	5	-4	1	One pure NE (s_2^A, s_2^B)	Corner Class
	B:	Dominant Class	10	12	2	5	-2	3	One pure NE (s_2^A, s_2^B)	One NE and ESS (s_2^A, s_2^B)
Set_2^{us}	A:	Coord. Class	10	4	9	5	1	1	Two pure NE, one int. NE $(s^\star = \frac{1}{2})$	Saddle Class
	B:	Coord. Class	10	7	4	5	3	1	Two pure NE, one int. NE $(s^\star = \frac{1}{4})$	Two ESSs (s_1^A, s_1^B), (s_2^A, s_2^B)
Set_3^{us}	A:	Anti-Co. Class	10	7	12	5	-2	-2	Two pure NE, one int. NE $(s^\star = \frac{1}{2})$	Saddle Class
	B:	Anti-Co. Class	10	12	9	5	-2	-4	Two pure NE, one int. NE $(s^\star = \frac{2}{3})$	Two ESSs (s_1^A, s_2^B), (s_2^A, s_1^B)
Set_4^{us}	A:	Coord. Class	10	4	7	5	3	1	Two pure NE, one int. NE $(s^\star = \frac{1}{4})$	Center Class
	B:	Anti-Co. Class	10	12	9	5	-2	-4	Two pure NE, one int. NE $(s^\star = \frac{2}{3})$	No NE nor a ESS

Table 7.3.: Parameter values of the four different sets of unsymmetric games.

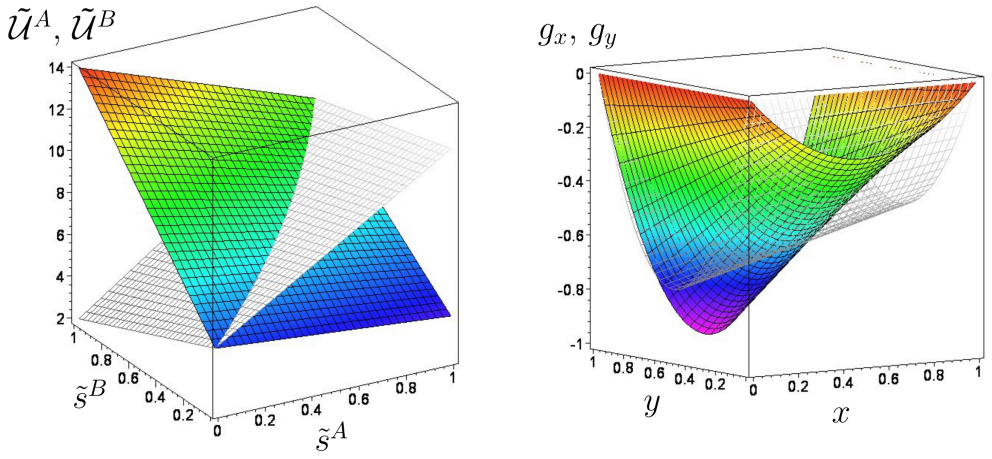

Figure 7.8.: Left picture: Mixed-strategy payoff function for player A ($\tilde{\mathcal{U}}^A(\tilde{s}^A, \tilde{s}^B)$, colored surface) and player B ($\tilde{\mathcal{U}}^B(\tilde{s}^A, \tilde{s}^B)$, wired grey surface) within parameter set Set_1^{us} as a function of the mixed strategies of player A ($\tilde{s}^A$) and B ($\tilde{s}^B$). Right picture: $g_x(x, y)$ (colored surface) and $g_y(x, y)$ (wired grey surface) as functions of the strategic population fractions of group A (x) and group B (y).

is similar to the symmetric parameter set Set_1 of a prisoner's dilemma game. In contrast to the set Set_1, the two game matrices for player A and B are unsymmetric ($U_{12}^A = 4 \neq 2 = U_{21}^B$ and $U_{21}^A = 14 \neq 12 = U_{12}^B$). The structure of the surfaces indicates that both groups have again only one NE, which is the dominant strategy $(s_2^A, s_2^B) \hat{=} (\tilde{s}^{A*} = 0, \tilde{s}^{B*} = 0)$.

The right picture of Figure 7.8 displays the two functions $g_x(x, y)$ (colored surface) and $g_y(x, y)$ (wired grey surface) that determine the dynamical behavior of the strategical decisions of group A ($x(t)$) and group B ($y(t)$) (see equation (7.10)). The amount of players choosing strategy s_1 will in both groups monotonically decrease and will–independently of the initial value–finally reach the only ESS ($x = 0, y = 0$), because the two surfaces are always below or equal to zero ($g_x(x, y) \leq 0$, $g_y(x, y) \leq 0 \ \forall \ x, y \in [0, 1]$).

The evolution of the strategic behavior of the two groups is visualized in Figure 7.9. The plot describes the numerical results of equation (7.10) for three different initial conditions, displayed through the three colored curves (xy-trajectories).

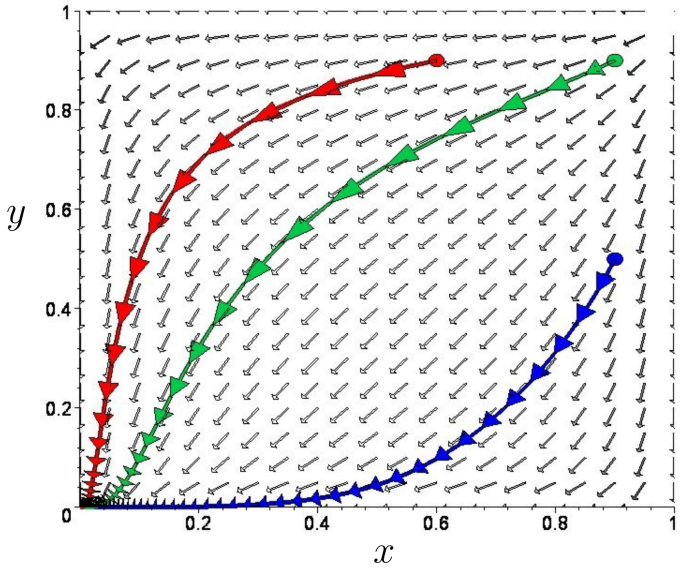

Figure 7.9.: Phase diagram of the xy-trajectories for three different initial conditions within parameter set Set_1^{us}. x describes the fraction of players within group A choosing the strategy s_1, while y is a similar fraction within group B.

The three trajectories are embedded in a field-plot phase diagram, where the little grey arrows describe the direction of a "strategic wind" the population has to follow during its time evolution. The three initial conditions $(x(0), y(0))$ are marked with colored circles at the beginning of the three curves. The several colored arrows which are on top of the trajectories describe the population movement for some intermediate time steps, where the length of arrows indicate the absolute value of the strategic change velocity within the population. Within Figure 7.9, the difference in the intermediate time steps ($\delta t = 0.125$) is equal for all three trajectories. The unsymmetric behavior of the trajectories is due to the unsymmetry of the parameter set. The green curve, for example, starts at a symmetric initial value ($x(0) = 0.9, y(0) = 0.9$), but as time evolves, it follows an unsymmetric evolution.

The interpretation of the results of Figure 7.9 is comparable to the results for the parameter set Set_1 of the symmetric model. Both population subgroups play a prisoner's dilemma game and the evolution of their strategical choice will finally–

independently of the initial condition–reach a state where everybody chooses the dominant strategy s_2. Similar to the symmetric model, the players face a dilemma, as the two populations evolve towards a low-payoff ESS ($\tilde{\mathcal{U}}^{\mu}(0,0) = 5 < 10 = \tilde{\mathcal{U}}^{\mu}(1,1)$). The game category belongs formally to the corner class. The velocity of the strategic change (length of the colored arrows) of the three trajectories differs slightly during the evolution. In the middle region of the trajectories, the velocity is the highest, whereas at the end (near to the ESS), the strategic change slows down very much.

Saddle class

Within the parameter set Set_2^{us}, both subpopulations play a coordination game. A bimatrix game that is composed of two coordination games always results in a saddle-class game.

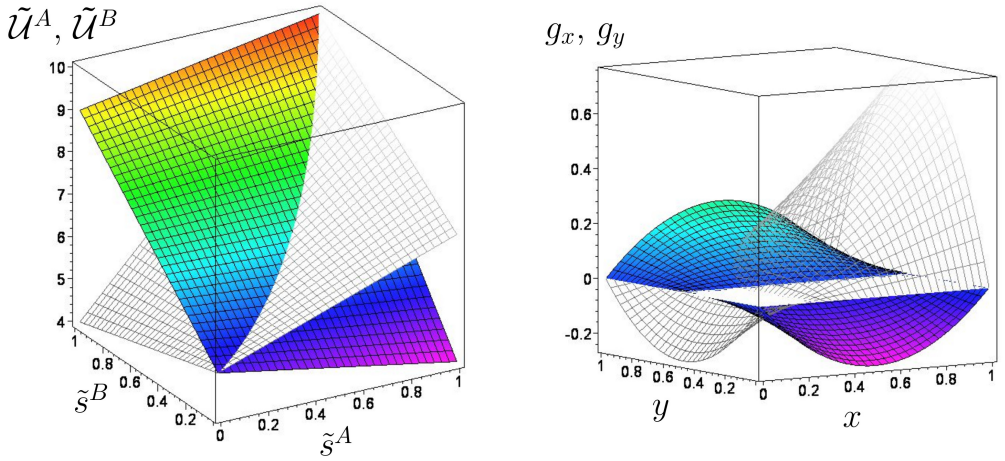

Figure 7.10.: Payoffs and functions $g_x(x,y)$ and $g_y(x,y)$ within set Set_2^{us}; similar to the description in Figure 7.8.

The structure of the payoff surfaces (see left picture in Figure 7.10) indicates that both groups have now two pure Nash equilibria ((s_1^A, s_1^B) and (s_2^A, s_2^B)). Additionally, there exists an interior mixed strategy NE ($(\tilde{s}^{A\star}, \tilde{s}^{B\star}) = (\frac{1}{2}, \frac{1}{4})$). To indicate the zero-level, an additional white plane was added to Figure 7.10 (right hand side). Within this parameter set, the two surfaces have regions where they have positive values ($g_x(x,y) > 0 \ \forall \ y \in]\tilde{s}^{B\star}, 1]$ and $g_y(x,y) > 0 \ \forall \ x \in]\tilde{s}^{A\star}, 1]$)

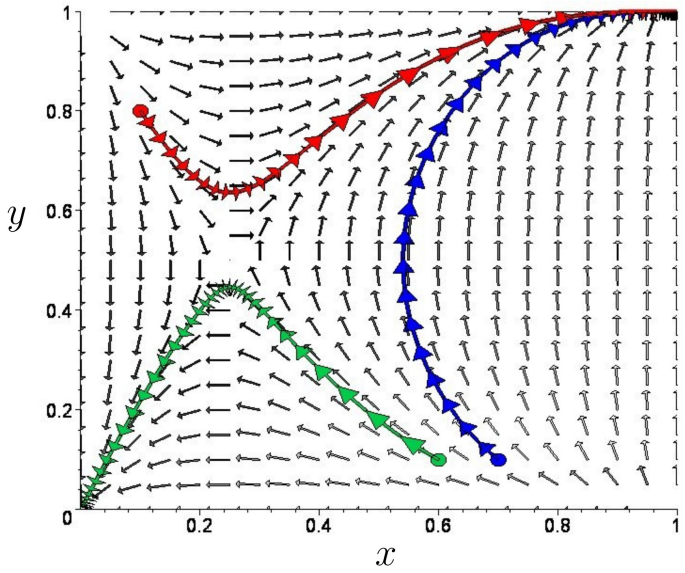

Figure 7.11.: Phase diagram for three different xy-trajectories within set Set_2^{us}; similar to the description in Figure 7.9.

and regions where they are negative ($g_x(x,y) < 0 \; \forall \; y \in]0, \tilde{s}^{B\star}[$ and $g_y(x,y) > 0 \; \forall \; x \in]0, \tilde{s}^{A\star}[$). The interior mixed strategy NE is exactly at the point where all of the three surfaces intersect. As all of the parameters (a^A, a^B, b^A, b^B) are positive, the game category belongs to the saddle class of bimatrix games and it has two symmetric ESSs.

The results of the evolutionary game of parameter set Set_2^{us} are visualized in Figure 7.11. As the strategic change velocities of the three different trajectories are quite different, the time steps (δt) between the colored arrows are not the same for the three different population paths. The red and green trajectories have the same time increment ($\delta t = 0.35$), whereas the arrows on the blue path are separated by a time lag of $\delta t = 2$. The strategic change of the blue population path is the slowest; starting from an initial condition ($x(0) = 0.7, y(0) = 0.1$), the fraction of players who choose the s_1-strategy monotonically decreases within group B ($y(t)$), while within group A ($x(t)$), the s_1-fraction first decreases and then increases until the whole population finally ends in the ESS $(s_1^A, s_1^B) \hat{=} (\tilde{s}^{A*} = 1, \tilde{s}^{B*} = 1)$ (all players choose the s_1-strategy). The red trajectory, which starts at the initial condition ($x(0) = 0.1, y(0) = 0.8$), also ends within the ESS (s_1^A, s_1^B). Its strategic

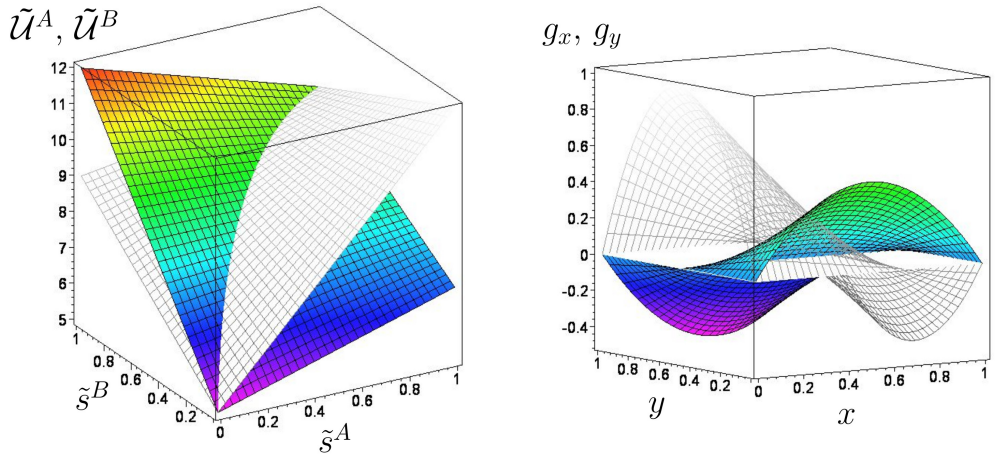

Figure 7.12.: Payoffs and functions $g_x(x, y)$ and $g_y(x, y)$ within set Set_3^{us}; similar to the description in Figure 7.8.

change velocity, however, slows down very much at the region near the interior NE. The initial condition of the green trajectory $(x(0) = 0.6, y(0) = 0.1)$ is only slightly different from the initial value of the blue curve; its evolution, however, is totally different. The s_1-fraction monotonically decreases within group A $(x(t))$, while within group B $(y(t))$, the s_1 fraction first increases and then decreases, until the whole population finally ends in the ESS $(s_2^A, s_2^B) \hat{=} (\tilde{s}^{A*} = 0, \tilde{s}^{B*} = 0)$ (all players choose the s_2-strategy). Similar to the red curve, the strategic change velocity slows down very much at the region near to the interior NE.

Parameter set Set_3^{us} is a saddle-class bimatrix game in which both subpopulations play an anti-coordination game. The structure of the payoff surfaces (see left picture in Figure 7.12) indicates that both groups have two asymmetric pure Nash equilibria $((s_1^A, s_2^B)$ and $(s_2^A, s_1^B))$ and one interior mixed strategy NE $((\tilde{s}^{A\star}, \tilde{s}^{B\star}) = (\frac{1}{2}, \frac{2}{3}))$. As all of the parameters (a^A, a^B, b^A, b^B) are negative, the game category belongs to the saddle class of bimatrix games, and it has two asymmetric ESSs.

The results of the evolutionary game of parameter set Set_3^{us} are visualized in Figure 7.12 and Figure 7.13. The time steps (δt) between the colored arrows are the same for all three population paths $(\delta t = 0.125)$.

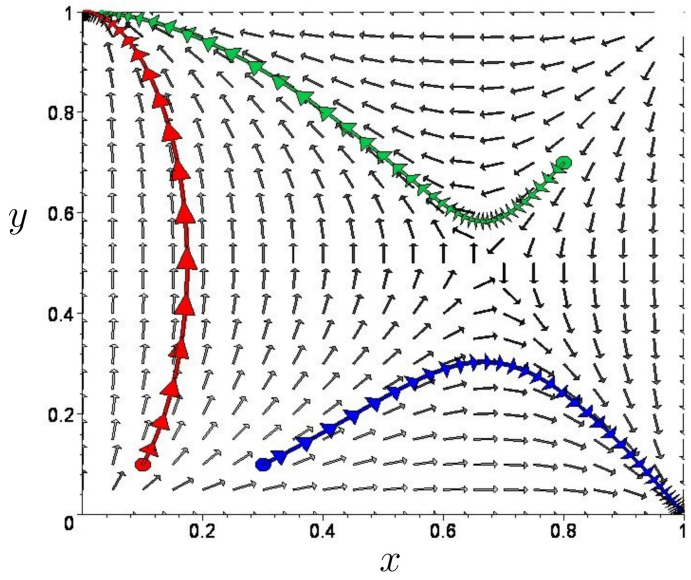

Figure 7.13.: Phase diagram for three different xy-trajectories within set Set_3^{us}; similar to the description in Figure 7.9.

Center class

Finally, the last parameter set (Set_4^{us}) belongs to the category of center-class games. Within parameter set Set_4^{us}, the subpopulation A plays a coordination game, while subpopulation B plays an anti-coordination game. The structure of the payoff surfaces (see left picture in Figure 7.14) indicates that there is only one interior mixed-strategy NE ($(\tilde{s}^{A\star}, \tilde{s}^{B\star}) = (\frac{1}{4}, \frac{2}{3})$).

The results of the evolutionary game of parameter set Set_4^{us} are visualized in Figure 7.15 and show that all of the trajectories cycle around the interior NE, which indicates the absence of an ESS. The time needed for one cycle is larger for bigger cycles and, as a result, the time steps (δt) between the colored arrows are the smallest for the blue trajectory ($\delta t = 6.5$) and the biggest for the red closed curve ($\delta t = 14.5$) (green: $\delta t = 8$).

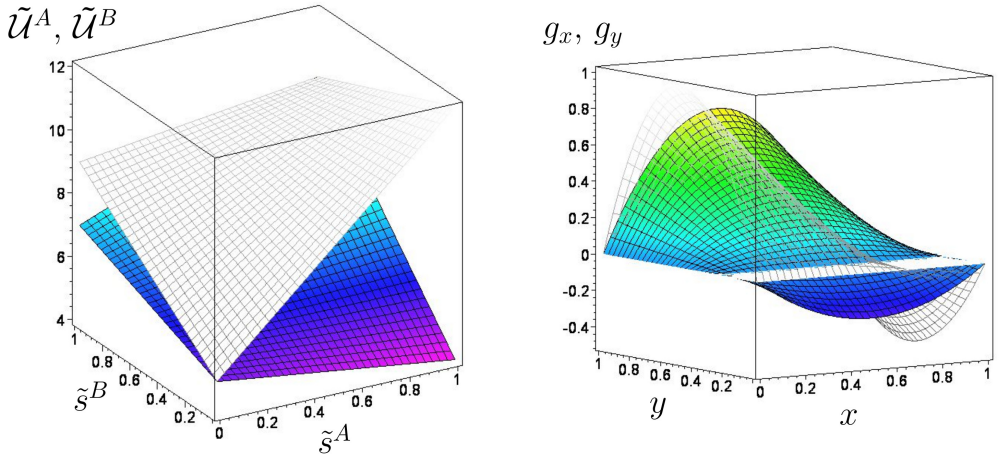

Figure 7.14.: Payoffs and functions $g_x(x, y)$ and $g_y(x, y)$ within set Set_4^{us}; similar to the description in Figure 7.8.

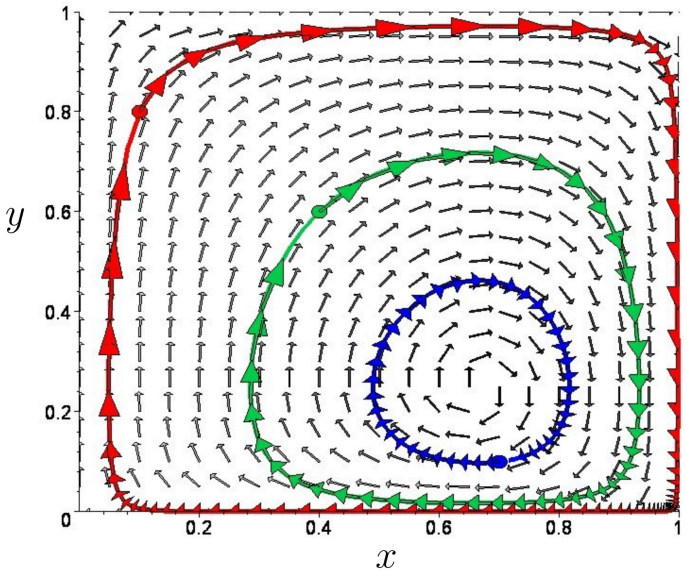

Figure 7.15.: Phase diagram for three different xy-trajectories within set Set_4^{us}; similar to the description in Figure 7.9.

7.3. Applications

In recent years, the market of scientific publishing faces several forces that may cause a major change of traditional market mechanisms. Currently, two main approaches have emerged. On the one hand, new open-access journals are brought to being, either through transformation of traditional journals or through creation of new titles. This approach is often called the "Golden Road to Open Access." On the other hand, authors may self-archive their articles in institutional or subject-based repositories, a model referred to as the "Green Road to Open Access" [123, 94]. The digital revolution of the information age and, in particular, the sweeping changes of scientific communication brought about by computing and novel communication technology, potentiate global, high-grade scientific information for free. The arXiv, for example, is the leading scientific communication platform, mainly for mathematics and physics, to which everyone in the world has free access on. In the following, we understand open-access publishing as the electronic publication of scientific information on a platform that provides access to this information for all potential users, without financial or other barriers. In contrast, most other scientific disciplines do not make use of open-access publishing, even though they support this model if asked for [77, 203]. Instead, they submit research papers to traditional journals that do not provide free access to their articles. Considering that the majority of scientists regard open-access publishing as superior to the traditional system, one may question why it is adopted only by a few disciplines.

7.3.1. Scientific communication and the open access decision

Based on the assumption that the main goal of scientists is the maximization of their reputation, we try to answer this question from the perspective of the producers of scientific information by using a game-theoretical approach. Scientific reputation originates mainly from two different sources: on the one hand, the citations to the articles of a scientist, and on the other hand, the reputation of the journals in which she/he publishes her/his articles [57]. Starting from a general symmetric (2 player)-(2 strategy) game Γ (see definition (7.4)), where two authors have to decide whether they publish open access or not,

different possible game settings are developed. This application focuses on a one-population model of an open-access game of scientific communication and extends it to an evolutionary game (for details, see [111, 118]).

To describe the underlying open-access game, we use a normal-form representation of a two-player game Γ where each player (Player 1 $\hat{=}$ A, Player 2 $\hat{=}$ B) can choose between two strategies ($\mathcal{S}^A = \{s_1^A, s_2^A\}$, $\mathcal{S}^B = \{s_1^B, s_2^B\}$). In our case, the two strategies represent the authors' choice between publishing open access (o) or not (ø). The whole strategy space $\mathcal{S}$ is composed with use of a Cartesian product of the individual strategies of the two players (scientists):

$$\mathcal{S} = \mathcal{S}^A \times \mathcal{S}^B = \{(\text{o,o}), (\text{o,ø}), (\text{ø,o}), (\text{ø,ø})\} \tag{7.15}$$

As outlined before, it is assumed that the main objective of scientists is the maximization of their reputation. In the following, we focus on a situation where the two scientists belong to a scientific community in which the open-access paradigm is not yet broadly adopted, and the publishers decline the acceptance of articles that are already accessible on an open access server. The payoff structure of this game is modeled by the following payoff matrix:

Table 7.4.: Researchers' open-access payoff matrix.

A\B	o	ø
o	$(r+\delta, r+\delta)$	$(r-\alpha, r+\beta)$
ø	$(r+\beta, r-\alpha)$	(r, r)

The actual reputation of the two scientists is represented by a single parameter r [5]. If both players decide to publish their papers only in traditional journals (ø,ø), their reputation r does not change. If only one of the two players chooses the open-access strategy ((ø,o) or (o,ø)), the parameters α and β ($\alpha, \beta \geq 0$) describe the decrease and the increase of the scientists' reputation, depending on the selected strategy. By modeling the payoff in this way, it is assumed that the reputation of the player who performs open access decreases if the other player

[5] By using this formalization, we assume that both scientists are on a similar level of reputation. If they would have different "starting" reputation values, the game would be unsymmetric.

simultaneously decides not to publish open access. This can be explained by the fact that in "non-open-access communities," reputation is mainly defined through the reputation of the journals in which a scientist publishes. Thus, if performing open-access (making publication in traditional journals impossible), the scientist has no chance to gain journal-related reputation anymore. On the other hand, the parameter β describes the potential increase of reputation of a scientist who refuses to perform open-access, while the other player selects the open-access strategy. The parameter δ represents the potential benefit in the case that both players choose the open-access strategy (o,o). The payoff for each player then is $r + \delta$. In this case, it is assumed that if both players choose the open-access strategy, the publishers are forced to accept articles for publication even if they are already accessible (see also the application discussed in subsection 7.3.2). Then, scientists can gain reputation both through the reputation of the journal they publish in and through the increase of citations due to a broader accessibility [157, 122, 70].

As the presented open-access game is a symmetric game and the parameter $b = \alpha$ is positive, the underlying game class depends only on the sign of the parameter $a = \delta - \beta$. For $\delta > \beta$, the game belongs to the class of coordination games, whereas for $\delta < \beta$, the game has the structure of a dominant game with a dilemma. For example, if the payoff parameters are fixed to the values $\alpha = 1$, $\beta = 2.25$, and $\delta = 0.25$ ($a = -2$ and $b = 1$), the results of the open-access game would be identical to the parameter setting Set_1 of the dominant game presented in subsection 7.2.3. Although the payoff for both players would be higher if they chose the strategy set (o,o), they are stuck within the Nash equilibrium (ø,ø). This outcome describes the paradox situation of many scientific disciplines: On the one hand, scientists realize that they would benefit if all players adopt open access, but on the other hand, no player has an individual incentive to change. For $\alpha = 1$, $\beta = 0.25$, and $\delta = 1.25$ ($a = 1$ and $b = 1$), the game belongs to the class of coordination games, and its corresponding results are also discussed in subsection 7.2.3 (see parameter setting Set_2). In contrast to set Set_1, this game has two pure Nash equilibria ((o,o) and (ø,ø)) and one mixed-strategy Nash equilibrium $\frac{1}{2}$(o,o). (o,o) is payoff dominant, whereas (ø,ø) is the risk-dominant pure Nash equilibrium. The mixed-strategy Nash equilibrium $\frac{1}{2}$(o,o) implies that one scientist has the incentive to choose non-open-access if she/he expects the

probability of the other player to choose non-open-access to be higher than 50 % (for further details see [111]). As $b = \alpha > 0$, the class of the open-access game cannot be parameterized as an anti-coordination game.

7.3.2. Evolution of Hubs- and Spokes Communication Networks

Within this subsection, the interconnected network of scientific journals and researchers is modeled as an unsymmetric bimatrix game. This application is an example of a more general analysis of a "Hub-and-Spoke Communication Network," which is currently under investigation [113]. The main actors within the scientific communication network are the authors of scientific articles (Spokes, population group A) and the scientific journals (Hubs, population group B). Following the approach of Habermann [98], but restricting the focus to green open access, the researchers have two possible strategies $\{s_1^A, s_2^A\} = \{\text{o},\emptyset\} \hat{=} \{$*publishing open access*, *conventional publishing*$\}$. Within the underlying game, the group of scientific journals have the following two strategies: $\{s_1^B, s_2^B\} = \{\text{o},\emptyset\} \hat{=} \{$*accept open access*, *decline open access*$\}$.

Table 7.5.: Payoff matrix of the "Author(A)-Journal(B)" open-access bimatrix game.

A\B	o	ø
o	$(r+\delta+I \ , \ r-\kappa)$	$(r+\delta \ , \ 0)$
ø	$(r+I \ , \ r)$	$(r-P+I \ , \ r+P)$

Table 7.5 describes one possible way of a parameterization of the "Author(A)-Journal(B)" open-access bimatrix game (see also [98] for another kind of parameterization). Similar to what was introduced in subsection 7.3.2, the parameter r describes the reputation of the scientist and the parameter δ quantifies the author's potential benefit if she/he chooses the open-access strategy o. The parameter I describes the author's additional increase in reputation if she/he publishes her/his new article within the journal (e.g., the journal's impact factor). Parameter κ is meant as a quantity that measures the journal's hypothetical payoff decrease due to fears of a totally green-open-access publishing market.

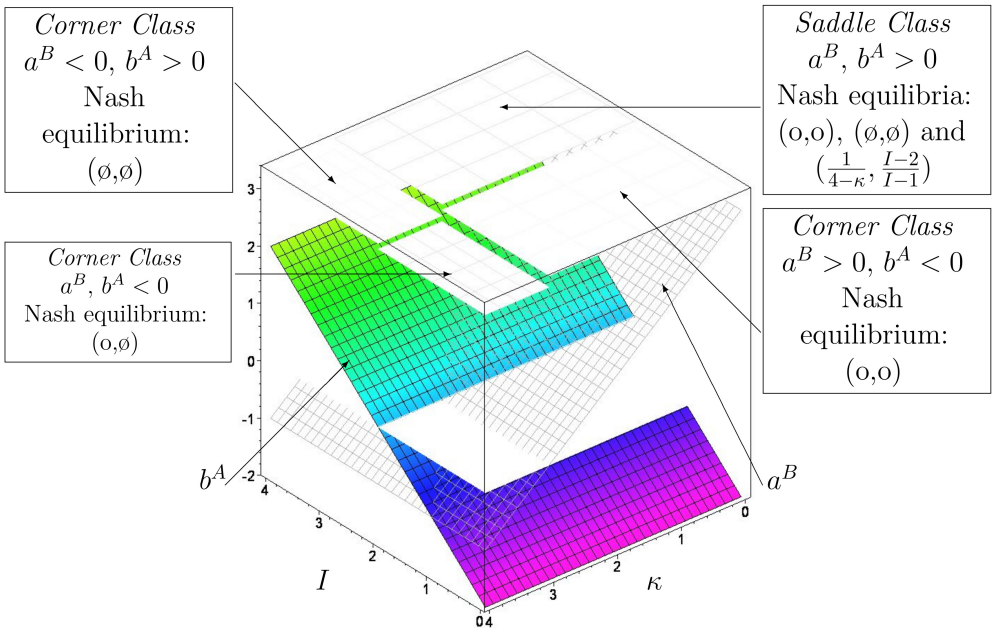

Figure 7.16.: $b^A = I - 2$ (solid, colored surface) and $a^B = 3 - \kappa$ (wired surface) as a function of the parameters I and κ. The other parameters are fixed to the values: $\delta = 1$, $r = 3$ and $P = 1$.

Finally, the parameter P quantifies the possibility of an extraordinary journal price increase due to the journal's market power in a totally conventional publishing market. Taking the parameterization of Table 7.5, the underlying class is only dependent on the following parameters: $a^A = \delta$, $b^A = I - P - \delta$, $a^B = r - \kappa$, and $b^B = P$. Because $a^A = \delta > 0$ and $b^B = P > 0$, the game category cannot belong to the center-class games [6]. For $b^A, a^B > 0$ ($r > \kappa, I > P + \delta$), the game's category belongs to the saddle-class having two pure, symmetric Nash equilibria ($(s_1^A, s_1^B) \hat{=}$(o,o) and $(s_2^A, s_2^B) \hat{=}$(ø,ø)) and one mixed strategy NE at $((\tilde{s}^{A\star}, \tilde{s}^{B\star}) = (\frac{P}{r-\kappa+P}, \frac{I-P-\delta}{I-P}))$. The outcome of such a parameterization is comparable to the results discussed in subsection 7.2.3 (parametration set Set_2^{us}). For all other parameterizations, the category of the author-journal open-access game belongs to the corner class. For ($b^A < 0$ and $a^B > 0$), the only NE is (o,o), for ($b^A > 0$ and $a^B < 0$), the only NE is (ø,ø), and finally for ($a^B, b^A < 0$), there

[6] Other parameterizations do, however, result in open-access center-class games [98].

exists only the asymmetric NE (o,ø).

To visualize these outcomes, Figure 7.16 shows the different possible classes within the author-journal open-access game for a certain parameterization. The solid, colored surface depicts the parameter b^A as a function of the two payoff parameters κ and I (the other parameters were fixed to the following values: $\delta = 1$, $r = 3$ and $P = 1$). The wired grey surface depicts the parameter a^B, and the solid white surface indicates the zero level. The point where all of the three surfaces intersect ($b^A(\kappa^\circ, I^\circ) = a^B(\kappa^\circ, I^\circ) = 0 \;\rightarrow \kappa^\circ = 3\,,\; I^\circ = 2$) defines the class boundary. Only for $\kappa > \kappa^\circ\,,\; I > I^\circ$ is a saddle-class game is realized, whereas in all of the other parameterizations, only one NE and ESS is possible, as the game belongs under such parametrisations to the corner class (for details see [118]).

7.4. Summary and Outlook

One of the main criticism of EGT is the fact that the theory is based on a totally connected network of an infinitely large number of actors, where every player (in each time interval) chooses her/his game partner randomly. In reality, the players are often organized in groups, and even within these groups the players often are not fully connected to all of the group members. The theory of social grouping in decision-based interacting complex networks is one of the most interesting topics within the presented research field. *Evolutionary Game Theory on Complex Networks* is a more realistic framework to simulate population dynamics; however, it often needs a variety of additional parameters to classify the network topologies and updating rules (see e.g., [222, 166]).

A second, more recently developed model that tries to implement social grouping into classical[7] evolutionary game theory is *Evolutionary Quantum Game Theory*. Quantum game theory is a mathematical and conceptual amplification of classical game theory. The space of all conceivable decision paths is extended from the purely rational, measurable space in the Hilbertspace of complex numbers.

[7] Following the scientific classification of the physical literature, the notation "classical" is used to describe the scientific sub-discipline that do not use "quantum" concepts to describe the underlying natural processes (example in physics: *Classical Mechanics* vs. *Quantum Mechanics*).

Through the concept of a potential entanglement of the imaginary quantum strategy parts, it is possible to include corporate decision paths, caused by cultural or moral group standards. In quantum game theory, players may cooperate, depending on the degree of entanglement γ among players. The notion of entanglement is perhaps most clearly expressed in terms of Adam Smith's classical concept of sympathy or "fellow feeling," which is a cornerstone of Smith's understanding of individual behavior [119]. In his "*Theory of Moral Sentiments*" (1759) [220], Smith claims that there is a general tendency for fellow-feeling among human beings, whereas the greater the strength of fellow-feeling is, the more closely related the individuals are. For example, there tends to be more fellow-feeling between friends than between acquaintances, and more between close relatives than between distant ones. Fellow-feeling as the human capacity to emphasize and become entangled with others is inversely related to the perceived and felt distance, whereas distance has been interpreted in terms of psychological and physical distance [194]. It can be shown that Emma and Hans are able to escape the dilemma if their strength of fellow-feeling (strength of strategic entanglement) is high enough to overcome the game's γ-threshold. If this strategy entanglement is large enough, then additional Nash equilibria can occur, previously present dominant strategies could become nonexistent, and new evolutionary stable strategies might appear (see e.g., [110]).

Within this chapter, the framework of classical EGT has been described in detail. After a general introduction and a brief literature review, the groundings of EGT (section 7.2) have been explained in detail. The formal mathematical model, the different concepts of equilibria, and the various classes of evolutionary games have been defined, explained, and visualized to understand the main ideas of EGT. Additionally, in section 7.3 two applications have been discussed:

- Application 1: Scientific communication and the open-access decision (see subsection 7.3.1)

- Application 2: Evolution of Hub-and-Spoke Communication Networks (see subsection 7.3.2)

Take away box

By analysing the game structure of a specific decision problem, policy-makers can learn a lot about the problems they attempt to address. To analyse the problem game theoretically, you need only three things:

- Who is playing the game? Definition of the set of players.
- What can the players do? Definition of the set of actions (strategies) available for each player.
- How much can the players win or lose? Definition of the payoff structure of the underlying game.

If the decision problem can be modelled as a symmetric (two player)-(two strategy) game and you know the payoff structure (define the parameters U_{11}, U_{12}, U_{21} and U_{22} and calculate $a := U_{11} - U_{21}$ and $b := U_{22} - U_{12}$), your game belongs to the following class:

- $b < 0$ and $a > 0$ (or $b > 0$ and $a < 0$): Dominant class
- $a, b > 0$: Coordination class
- $a, b < 0$: Anti-coordination class

If your game belongs to the dominant class and there is no dilemma, use the dominant strategy. If your game belongs to the dominant class and there is a dilemma (or it belongs to the coordination class with a high and low Nash equilibrium, or to the anti-coordination class with a dilemma), you have to think about how much fellow-feeling you have with your game partner–perhaps your socio-economic system is strong enough to escape the game's dilemma.

Anhang A

A.I. Analytische Lösung des Barabasi-Albert Modell

Im Folgenden soll ein einfaches Modell der Erzeugung eines skalenfreien Netzwerks beschrieben werden (das sogenannte „Barabasi-Albert Modell“). In dem zugrundeliegenden Netzwerkmodell beschränkt man die Komplexität auf drei wesentliche Eigenschaften und lässt sowohl ein zeitliches Anwachsen der Anzahl der Netzwerkknoten, eine Anfangsattraktivität $A^{(0)}$, als auch ein bevorzugtes Anlagern (engl.: „preferential attachment“) der Netzwerkkanten an attraktivere Knoten zu. Dorogovtsev, Mendes, und Samukhin [217] konnten in diesem Modell zeigen, dass die Verteilung der Anzahl der Verbindungen pro Knoten $P(k)$ analytisch angegeben werden kann. Der in diesem Artikel beschrittene analytische Weg basiert auf dem folgendem „Master equation“-Ansatz der Verteilungsfunktion $p\left(k_i, i, t\right)$ des Verlinkungsgrades k_i des Netzwerkknotens i zurzeit t.

$$
\begin{aligned}
& p\left(k_i, i, t+1\right) = \Pi\left(k_i, t\right)\, p\left(k_i, i, t\right) + \left[1 - \Pi\left(k_i, t\right)\right] p\left(k_i - 1, i, t\right) + O\left(\frac{p}{t^2}\right) \\
& \Pi\left(k_i, t\right) := \left[1 - \frac{k_i + A^{(0)}}{\left(1 + \frac{A^{(0)}}{m}\right) t}\right] \; : \text{ Verlinkungswahrscheinlichkeit} \\
& m \; : \text{ Anzahl der ausgehenden Verlinkungen pro Knoten} \\
& k_i \; : \text{ Anzahl der eingehenden Verlinkungen des Knotens i} \\
& A_i := k_i + A^{(0)} \; : \text{ Attraktivität des Knotens i .}
\end{aligned}
\tag{A.1}
$$

Die Lösung der Gleichung erfolgt mittels Z-Transformation (näheres siehe [217]):

$$
p(k_i, i, t) = \frac{\Gamma(k_i + A^{(0)})}{\Gamma(A^{(0)})\, k_i!} \left(\frac{i}{t}\right)^{\frac{A^{(0)}}{1 + \frac{A^{(0)}}{m}}} \left[1 - \left(\frac{i}{t}\right)^{\frac{1}{1 + \frac{A^{(0)}}{m}}}\right]^{k_i} . \tag{A.2}
$$

Für die stationäre Verteilungsfunktion $P(k) = P(k, t \to \infty)$ der eingehenden Verlinkungen ergibt sich schließlich:

$$\begin{aligned} P(k) &= P(k, t \to \infty) \quad \text{, wobei} \quad P(k,t) = \frac{1}{t} \sum_{i=1}^{t} p(k_i, i, t) \\ P(k) &= \frac{(1 + \frac{A^{(0)}}{m})\,\Gamma(1 + \frac{(m+1)\,A^{(0)}}{m})\,\Gamma(k_i + A^{(0)})}{\Gamma(A^{(0)})\,\Gamma(k_i + 2 + \frac{(m+1)\,A^{(0)}}{m})} \end{aligned} \tag{A.3}$$

Überträgt man dieses mathematische Modell z.B. auf die Netzwerkstrukturen des wissenschaftlichen Informationsmarktes (näheres siehe [3, 4, 7, 152]), so muss man zunächst definieren um welche Knoten- und Verlinkungsart es sich handelt. Man könnte z.B. die Autoren (Wissenschaftler) als die Knoten ansehen und als Verlinkungsart z.B. die Zitationen oder Koautorenschaften verstehen, welche dann eine Art von Kooperationsverhalten zwischen den jeweiligen Wissenschaftlern darstellen würde. Als Knotenart könnte man auch die einzelnen Artikel ansehen, wobei man dann bei der Beschreibung der Zitatsverlinkungen eine explizite Zeitabhängigkeit in den „Master equation"-Ansatz (Gleichung (A.1)) einbeziehen muss, da die Zitationswahrscheinlichkeit eines Artikels ebenfalls von seinem Alter abhängt [99].

$$\Pi\,(k_i, t, \tau_i) \;\sim\; (k_i)^{\alpha} (\tau_i)^{\beta} \tag{A.4}$$

Numerische Berechnungen (näheres siehe [99, 100, 101]) zeigen Phasenübergänge zwischen den möglichen Netzwerktopologien („Kleine Welt", „Exponentiell" und „Skalenfrei") in Abhängigkeit der Parameter α und β. Neben der jeweiligen Topologie des betrachteten Netzwerks ist zusätzlich auch die Informationsdiffusion in komplexen Netzwerken von Bedeutung (siehe z.B. [35, 170]).

Appendix B

B.I. Payoff transformations and strategic equivalent games

There are two kinds of payoff transformations that leave the main characteristics of the game (the corresponding Nash equilibria, the best response functions and the ESS's) unchanged. Games with payoff matrices that differ only by such transformations are named strategic equivalent.

B.I.1. Positive affine transformations

A positive affine transformation of a payoff function $\tilde{\$}^{\mu}(\tilde{s}^A, \tilde{s}^B)$ is defined as follows:

$$\tilde{\$}^{\mu|}(\tilde{s}^A, \tilde{s}^B) = (\tilde{s}^A)^T \alpha^{\mu} \hat{\$}^{\mu} \tilde{s}^B + \beta^{\mu} \,, \;\; \alpha^{\mu} \in \mathbb{R}^+ \,, \;\; \beta^{\mu} \in \mathbb{R} \quad \forall \; \mu = A, B \qquad \text{(B.1)}$$

The Nash equilibria, the best response functions and the ESS's of the corresponding game are unaffected by such a transformation. In the following, this property will be exemplarily proven in the case of the unaffection of the Nash equilibria of the game. By using the definition of a NE, the condition for the transformed game writes as follows:

$$\begin{aligned}
\tilde{\$}^{A|}(\tilde{s}^{A*}, \tilde{s}^{B*}) &= (\tilde{s}^{A*})^T \alpha^A \hat{\$}^A \tilde{s}^{B*} + \beta^A \quad \geq \\
&\geq (\tilde{s}^A)^T \alpha^A \hat{\$}^A \tilde{s}^{B*} + \beta^A = \tilde{\$}^{A|}(\tilde{s}^A, \tilde{s}^{B*}) \qquad \forall \quad \tilde{s}^A \in \tilde{\mathcal{S}}^A \\
\tilde{\$}^{B|}(\tilde{s}^{A*}, \tilde{s}^{B*}) &= (\tilde{s}^{A*})^T \alpha^B \hat{\$}^B \tilde{s}^{B*} + \beta^B \quad \geq \\
&\geq (\tilde{s}^{A*})^T \alpha^B \hat{\$}^B \tilde{s}^B + \beta^B = \tilde{\$}^{B|}(\tilde{s}^{A*}, \tilde{s}^B) \qquad \forall \quad \tilde{s}^B \in \tilde{\mathcal{S}}^B
\end{aligned}$$

These inequations can be simplified to the Nash equilibrium conditions of an untransformed game by simple mathematical transformations:

$$\begin{aligned}
(\tilde{s}^{A*})^T \alpha^A \hat{\$}^A \tilde{s}^{B*} + \beta^A &\geq (\tilde{s}^A)^T \alpha^A \hat{\$}^A \tilde{s}^{B*} + \beta^A \quad \Big| -\beta^A \\
\Leftrightarrow \quad \alpha^A (\tilde{s}^{A*})^T \hat{\$}^A \tilde{s}^{B*} &\geq \alpha^A (\tilde{s}^A)^T \hat{\$}^A \tilde{s}^{B*} \quad | \div (\alpha^A) \\
\Leftrightarrow \quad (\tilde{s}^{A*})^T \hat{\$}^A \tilde{s}^{B*} &\geq (\tilde{s}^A)^T \hat{\$}^A \tilde{s}^{B*} \\
\Leftrightarrow \quad \tilde{\$}^A (\tilde{s}^{A*}, \tilde{s}^{B*}) &\geq \tilde{\$}^A (\tilde{s}^A, \tilde{s}^{B*}) \qquad \forall \quad \tilde{s}^A \in \tilde{\mathcal{S}}^A
\end{aligned}$$

Similarly for the inequations of player B.

Positive affine transformations therefore do not change the main characteristics of the game, however they might change the dynamic behavior of the game. To illustrate this fact, a positive affine transformation (see equation (B.1), with $\alpha^\mu = \alpha$ and $\beta^\mu = 0$)[1]) was used, which acts on a simple payoff matrix, having only two free parameters:

$$\hat{\$} = \begin{pmatrix} \$_I & 0 \\ 0 & \$_{II} \end{pmatrix} \longrightarrow \hat{\$}^| = \begin{pmatrix} \alpha\$_I & 0 \\ 0 & \alpha\$_{II} \end{pmatrix} \quad . \tag{B.2}$$

Using the transformed payoff $\hat{\$}^|$ within the replicator dynamics of equation (2.18) it is possible to compare the effect of the affine transformation as a simple time-scaling behavior:

$$\begin{aligned}
\frac{dx(t)}{dt} &= x\left[\alpha\$_I(x - x^2) + \alpha\$_{II}(1 - 2x + x^2)\right] \qquad \text{(B.3)} \\
\Leftrightarrow \frac{dx(t)}{d\tilde{t}} := \frac{1}{\alpha}\frac{dx(t)}{dt} &= x\left[\$_I(x - x^2) + \$_{II}(1 - 2x + x^2)\right] \\
\text{with:} \qquad \tilde{t} := \alpha t \quad &\rightarrow \quad \frac{dx(t)}{d\tilde{t}} = \frac{dx(t)}{dt}\frac{dt}{d\tilde{t}} = \frac{dx(t)}{dt}\frac{1}{\alpha}
\end{aligned}$$

Equation (B.3) shows that although the main structure of the game did not change, positive affine transformations of the kind (B.2) change the dynamics. The transformed dynamic equation (B.3) is similar to untransformed, only if one introduces a new time scale $\tilde{t} := \alpha t$.

[1] The parameter β^μ of the positive affine transformation do not change the dynamical behavior of the population at all and is set to zero for simplicity.

B.I.2. Local payoff shifts

The main properties of a game do not change under a second kind of transformation, the so called *local shift* of the payoff function. The payoff matrix $\left(\hat{\$}^A\right)^{|_k}$ ($\left(\hat{\$}^B\right)^{|_k}$) of the transformed game is modified only in the k-th column (in k-th row) by addition of an arbitrary constant $c \in \mathbb{R}$.

$$\begin{aligned}
\left(\hat{\$}^A\right)^{|_k} &= \begin{pmatrix} \$^A_{11} & \$^A_{12} & \dots & \$^A_{1k}+c & \dots & \$^A_{1m_B} \\ \$^A_{21} & \$^A_{22} & \dots & \$^A_{2k}+c & \dots & \$^A_{2m_B} \\ \dots & \dots & \dots & \dots & \dots & \dots \\ \$^A_{m_A1} & \$^A_{m_A2} & \dots & \$^A_{m_Ak}+c & \dots & \$^A_{m_Am_B} \end{pmatrix} \\
\left(\hat{\$}^B\right)^{|_k} &= \begin{pmatrix} \$^B_{11} & \$^B_{12} & \dots & \$^B_{1m_B} \\ \$^B_{21} & \$^B_{22} & \dots & \$^B_{2m_B} \\ \dots & \dots & \dots & \dots \\ \$^B_{k1}+c & \$^B_{k2}+c & \dots & \$^B_{km_B}+c \\ \dots & \dots & \dots & \dots \\ \$^B_{m_A1} & \$^B_{m_A2} & \dots & \$^B_{m_Am_B} \end{pmatrix}
\end{aligned} \tag{B.4}$$

To illustrate that the Nash equilibria of the transformed game are equal to the corresponding untransformed game the number of strategies is reduced to only two ($m_A = m_B = 2$). The payoff matrix of player A is locally shifted only in the first column ($\left(\hat{\$}^A\right)^{|_1}$) by addition of an arbitrary constant $c \in \mathbb{R}$. Using the explicit formulation of the mixed payoff function (2.5), the Nash equilibrium inequation of player A within the locally shifted game can be simplified as follows

$$\begin{aligned}
& \tilde{\$}^{A|_1}(\tilde{s}^{A*}, \tilde{s}^{B*}) = (\tilde{s}^{A*})^T \left(\hat{\$}^A\right)^{|_1} \tilde{s}^{B*} \geq \\
& \geq (\tilde{s}^A)^T \left(\hat{\$}^A\right)^{|_1} \tilde{s}^{B*} = \tilde{\$}^{A|_1}(\tilde{s}^A, \tilde{s}^{B*}) \qquad \forall \quad \tilde{s}^A \in \tilde{\mathcal{S}}^A \\
\Leftrightarrow \quad & \left(\tilde{s}^{A*}_1, \tilde{s}^{A*}_2\right) \begin{pmatrix} (\$^A_{11}+c) & \$^A_{12} \\ (\$^A_{21}+c) & \$^A_{22} \end{pmatrix} \begin{pmatrix} \tilde{s}^{B*}_1 \\ \tilde{s}^{B*}_2 \end{pmatrix} \geq \\
& \geq \left(\tilde{s}^A_1, \tilde{s}^A_2\right) \begin{pmatrix} (\$^A_{11}+c) & \$^A_{12} \\ (\$^A_{21}+c) & \$^A_{22} \end{pmatrix} \begin{pmatrix} \tilde{s}^{B*}_1 \\ \tilde{s}^{B*}_2 \end{pmatrix}
\end{aligned}$$

Using equation (2.5) it follows:

$$
\begin{aligned}
\Leftrightarrow \quad & (\$_{11}^A + c)\tilde{s}_1^{B*}\tilde{s}_1^{A*} + \$_{12}^A\tilde{s}_2^{B*}\tilde{s}_1^{A*} + (\$_{21}^A + c)\tilde{s}_1^{B*}\tilde{s}_2^{A*} + \$_{22}^A\tilde{s}_2^{B*}\tilde{s}_2^{A*} \geq \\
& \geq (\$_{11}^A + c)\tilde{s}_1^{B*}\tilde{s}_1^{A} + \$_{12}^A\tilde{s}_2^{B*}\tilde{s}_1^{A} + (\$_{21}^A + c)\tilde{s}_1^{B*}\tilde{s}_2^{A} + \$_{22}^A\tilde{s}_2^{B*}\tilde{s}_2^{A} \\
\Leftrightarrow \quad & \underbrace{\$_{11}^A\tilde{s}_1^{B*}\tilde{s}_1^{A*} + \$_{12}^A\tilde{s}_2^{B*}\tilde{s}_1^{A*} + \$_{21}^A\tilde{s}_1^{B*}\tilde{s}_2^{A*} + \$_{22}^A\tilde{s}_2^{B*}\tilde{s}_2^{A*}}_{(\tilde{s}^{A*})^T\hat{\$}^A\tilde{s}^{B*}} + c\,\tilde{s}_1^{B*}\underbrace{(\tilde{s}_1^{A*} + \tilde{s}_2^{A*})}_{=1} \geq \\
& \geq \underbrace{\$_{11}^A\tilde{s}_1^{B*}\tilde{s}_1^{A} + \$_{12}^A\tilde{s}_2^{B*}\tilde{s}_1^{A} + \$_{21}^A\tilde{s}_1^{B*}\tilde{s}_2^{A} + \$_{22}^A\tilde{s}_2^{B*}\tilde{s}_2^{A}}_{(\tilde{s}^{A})^T\hat{\$}^A\tilde{s}^{B*}} + c\,\tilde{s}_1^{B*}\underbrace{(\tilde{s}_1^{A} + \tilde{s}_2^{A})}_{=1} \\
\Leftrightarrow \quad & (\tilde{s}^{A*})^T\hat{\$}^A\tilde{s}^{B*} + c\,\tilde{s}_1^{B*} \geq (\tilde{s}^{A})^T\hat{\$}^A\tilde{s}^{B*} + c\,\tilde{s}_1^{B*} \quad \Big| -(c\,\tilde{s}_1^{B*}) \\
\Leftrightarrow \quad & \tilde{\$}^A(\tilde{s}^{A*}, \tilde{s}^{B*}) \geq \tilde{\$}^A(\tilde{s}^{A}, \tilde{s}^{B*}) \qquad \forall \quad \tilde{s}^A \in \tilde{\mathcal{S}}^A \quad : \text{unshifted inequation}
\end{aligned}
$$

Similarly for local shifts of the second column ($\left(\left(\hat{\$}^A\right)^{|_2}\right)$).

To show explicitly that *local payoff shifts* do not change the dynamical behavior of replicator dynamics (see equation (2.18)), the equation is rearranged as follows:

$$
\begin{aligned}
\frac{dx(t)}{dt} &= x(t)\left[\$_{11}x(t) + \$_{12}(1 - x(t)) - \bar{\$}\right] \\
&= x\left[\$_{11}(x - x^2) + \$_{12}(1 - 2x + x^2) + \$_{21}(x^2 - x) + \$_{22}(2x - x^2 - 1)\right] \\
&= x\left[\underbrace{(\$_{11} - \$_{21})}_{:=\$_I}(x - x^2) + \underbrace{(\$_{22} - \$_{12})}_{:=\$_{II}}(1 - 2x + x^2)\right] \qquad \text{(B.5)} \\
& \quad x = x(t) := x_1(t) \quad \rightarrow \quad x_2(t) = (1 - x(t)) \\
& \quad \tilde{\$} := \$_{11}\,x(t)^2 + (\$_{12} + \$_{21})\,x(t)(1 - x(t)) + \$_{22}\,(1 - x(t))^2
\end{aligned}
$$

The time derivative of the population function depends only on two parameters ($\$_I := \$_{11} - \$_{21}$ and $\$_{II} := \$_{22} - \$_{12}$, see equation (B.5)). The underlying reason for this behavior is the invariance of the games structure in respect to *local payoff shifts*. As previously explained, it is possible to change the payoff matrix without effecting the games' main characteristics. Using iteratively the following two

payoff shifts

$$\hat{\$} = \begin{pmatrix} \$_{11} & \$_{12} \\ \$_{21} & \$_{22} \end{pmatrix} \longrightarrow \hat{\$}^{|} = \begin{pmatrix} \$_{11} - \$_{21} & \$_{12} \\ 0 & \$_{22} \end{pmatrix} \longrightarrow$$
$$\hat{\$}^{||} = \begin{pmatrix} \$_{11} - \$_{21} & 0 \\ 0 & \$_{22} - \$_{12} \end{pmatrix} =: \begin{pmatrix} \$_{I} & 0 \\ 0 & \$_{II} \end{pmatrix} \tag{B.6}$$

The dynamic evolution of a (2×2)-game depends therefore only on the two payoff parameters $\$_I$ and $\$_{II}$ and these two parameters are identical to the parameters a and b of the transformed game (see table 2.1). Using this fact, it is possible to categorize such games into four game classes (see [235] and [222]), where two classes are mathematically identical modulo a relabeling of the two pure strategies.

B.II. Results for classical symmetric (2x2) games

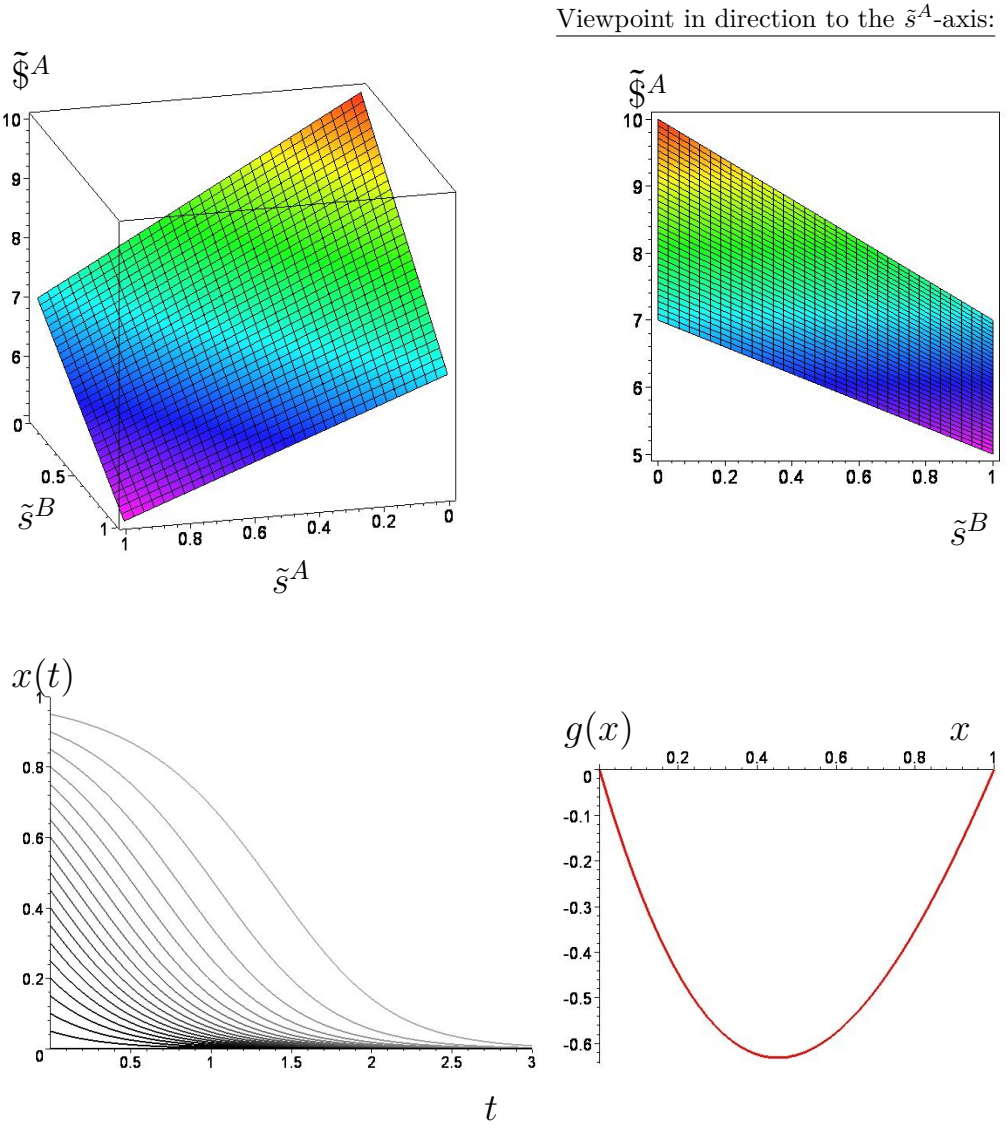

Figure B.1.: Results for the classical game of parameter set Set_1.

Description of figure B.1

The picture in the left upper row shows the mixed strategy payoff function $\tilde{\$}^A(\tilde{s}^A, \tilde{s}^B)$ for player A within parameter set Set_1 as a function of the mixed strategies of player A ($\tilde{s}^A$) and B ($\tilde{s}^B$). The right picture in the upper row shows a special projection of the surface, in which the observer looks in direction of the $\tilde{s}^A$-axis. The lower row depicts $x(t)$, the fraction of players choosing the strategy s_1 at time t for different initial conditions ($x(t=0) = 0, 0.05, 0.1, ..., 0.95$) within parameter set Set_1 (left picture). The right picture shows the function $g(x)$, which determines the dynamical behavior of $x(t)$. The figures show that the game's category of parameter set Set_1 belongs to the class of dominant games and that only one pure NE exists ($(s_2^A, s_2^B) \hat{=} (\tilde{s}^A = 0, \tilde{s}^B = 0)$), which is the dominant strategy of the game. As no interior NE is present within parameter set Set_1 the partial derivative (see equation (2.11)) of $\tilde{\$}^A$ does not vanish within the given boundaries. The right picture in the upper row visualizes this fact as no cord-up point was found within the special $\tilde{s}^A$-projection. As the function $g(x)$ is positive for all $x \in]0, 1[$, the fraction of players choosing the strategy $s_1 = s_1^A = s_1^B$ ($x(t)$) will always decrease until everybody chooses the strategy s_2, independently on the initial condition.

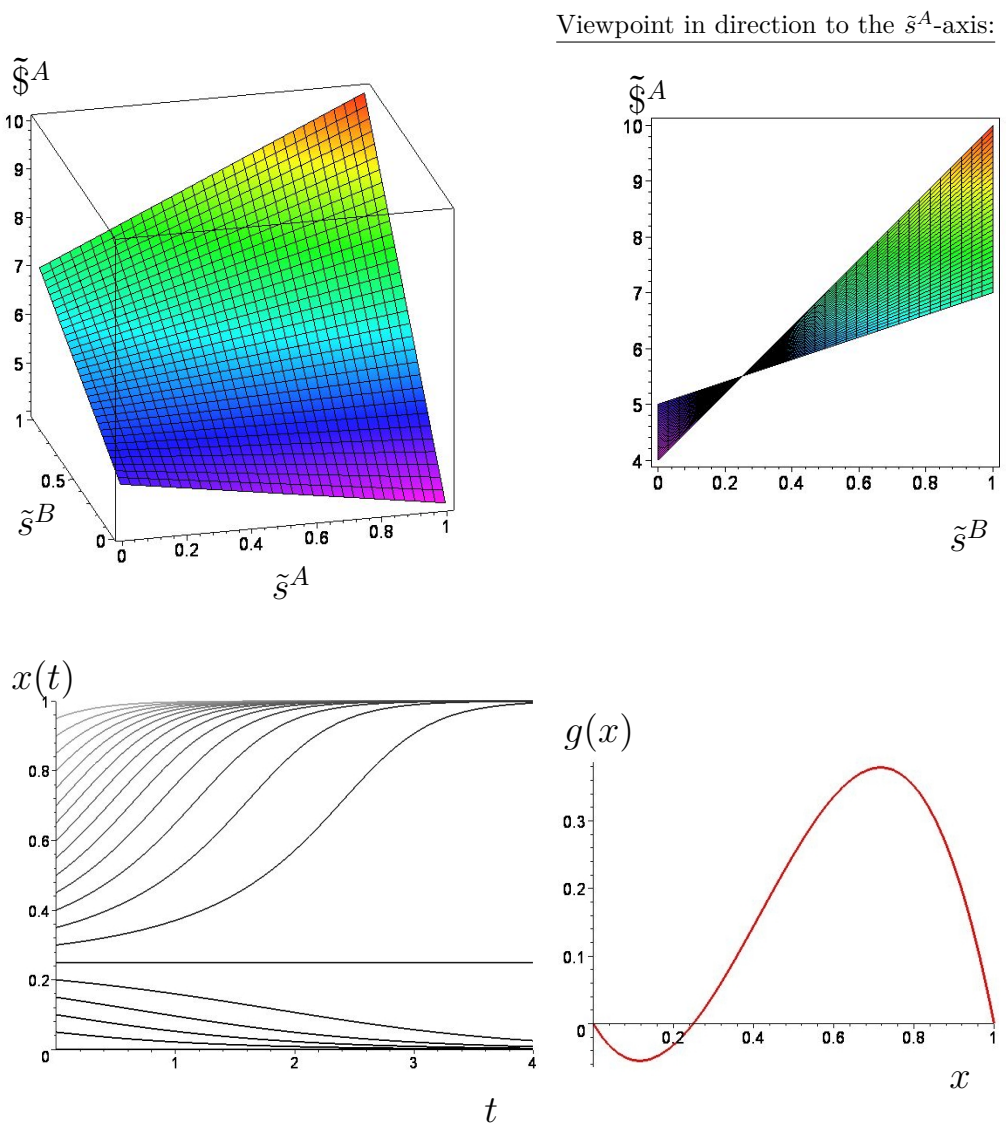

Figure B.2.: Results for the classical game of parameter set Set_5.

Description of figure B.2

The picture in the left upper row shows the mixed strategy payoff function $\tilde{\$}^A(\tilde{s}^A, \tilde{s}^B)$ for player A within parameter set Set_5 as a function of the mixed strategies of player A ($\tilde{s}^A$) and B ($\tilde{s}^B$). The right picture in the upper row shows a special projection of the surface, in which the observer looks in direction of the $\tilde{s}^A$-axis. The lower row depicts $x(t)$, the fraction of players choosing the strategy s_1 at time t for different initial conditions ($x(t=0) = 0, 0.05, 0.1, ..., 0.95$) within parameter set Set_5 (left picture). The right picture shows the function $g(x)$, which determines the dynamical behavior of $x(t)$. The figures show that the game's category of parameter set Set_5 belongs to the class of coordination games with two pure symmetric Nash equilibria ($(s_1^A, s_1^B) \hat{=} (\tilde{s}^A = 1, \tilde{s}^B = 1)$ and $(s_2^A, s_2^B) \hat{=} (\tilde{s}^A = 0, \tilde{s}^B = 0)$) and one interior mixed strategy NE ($(\tilde{s}^{A\star}, \tilde{s}^{B\star}) = (\frac{1}{4}, \frac{1}{4})$). Due to the fact that the partial derivative of the payoff surface for player A vanishes at the value of the mixed strategy NE, the whole surface shrinks to one point if one projects the viewpoint in direction to the $\tilde{s}^A$-axis (see right picture in the upper row). The value of the mixed strategy NE is equal to the zero point of the function $g(x)$ (see right picture in the lower row). $g(x)$ (which determines the dynamical behavior of the population function $x(t)$) has, beside its negative region ($g(x) < 0 \; \forall \; x \in]0, s^\star[$) also a region where its value is positive ($g(x) > 0 \; \forall \; x \in]s^\star, 1[$). Due to this property two ESS emerge ($x(t \to \infty) = 0$ and $x(t \to \infty) = 1$). To which of these ESS's the population will evolve depends on the initial condition. If the fraction of s_1-player types at the initial time $t = 0$ is below the value of the mixed strategy NE ($x(0) < s^\star = 0.25$) the population will evolve to the ESS $x(t \to \infty) = 0$, which corresponds to a population sorely choosing the s_2-strategy. Only if the initial fraction is above the mixed strategy threshold ($x(0) > s^\star$) the population will end in the ESS $x(t \to \infty) = 1$. The horizontal population path at $x(t) = 0.25$ is an artefact of the numerical simulation and is not an ESS, as the solution is unstable in respect to infinitely small perturbations.

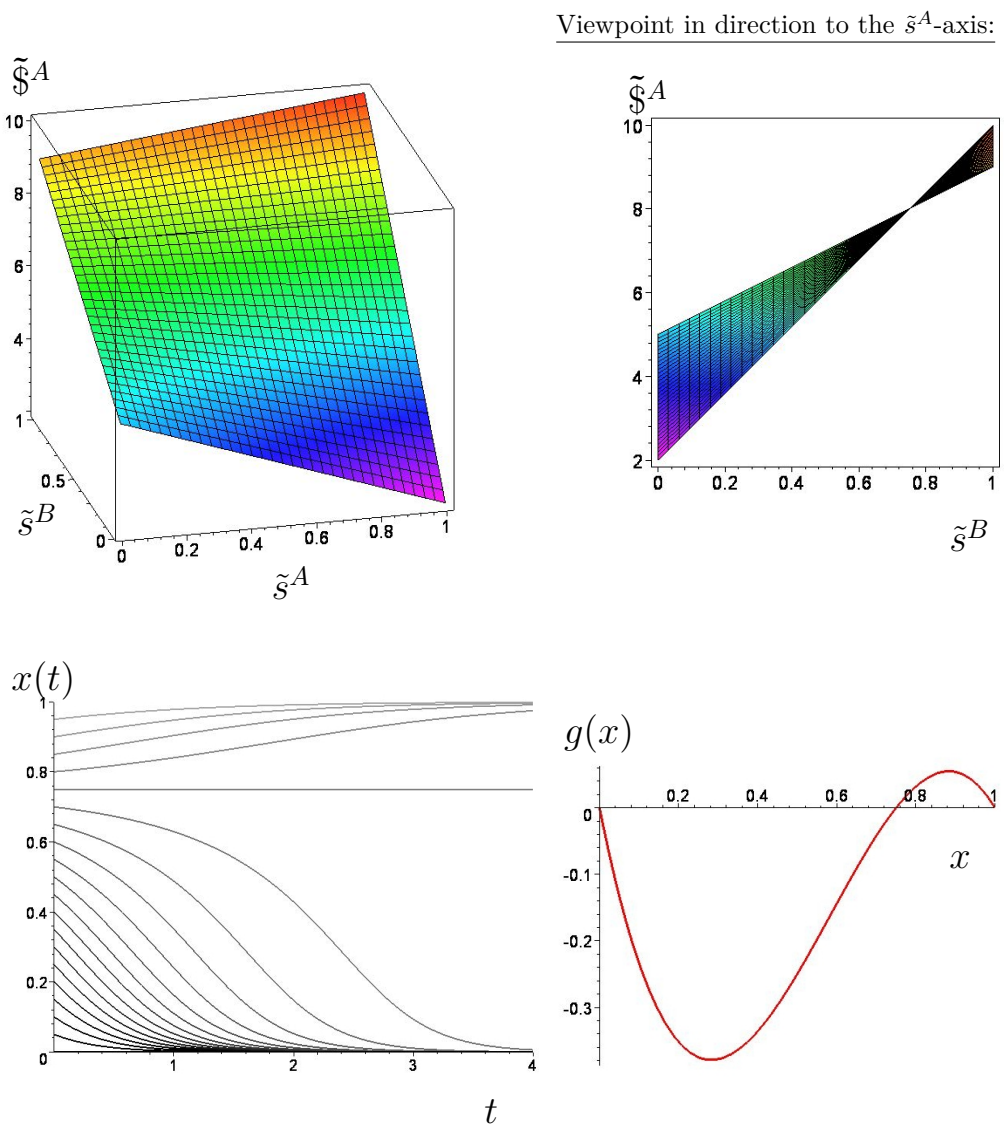

Figure B.3.: Results for the classical game of parameter set Set_6.

Description of figure B.3

The picture in the left upper row shows the mixed strategy payoff function $\tilde{\$}^A(\tilde{s}^A, \tilde{s}^B)$ for player A within parameter set Set_6 as a function of the mixed strategies of player A ($\tilde{s}^A$) and B ($\tilde{s}^B$). The right picture in the upper row shows a special projection of the surface, in which the observer looks in direction of the $\tilde{s}^A$-axis. The lower row depicts $x(t)$, the fraction of players choosing the strategy s_1 at time t for different initial conditions ($x(t=0) = 0, 0.05, 0.1, ..., 0.95$) within parameter set Set_6 (left picture). The right picture shows the function $g(x)$, which determines the dynamical behavior of $x(t)$. The figures show that the game's category of parameter set Set_6 belongs to the class of coordination games with two pure symmetric Nash equilibria ($(s_1^A, s_1^B) \hat{=} (\tilde{s}^A = 1, \tilde{s}^B = 1)$ and $(s_2^A, s_2^B) \hat{=} (\tilde{s}^A = 0, \tilde{s}^B = 0)$) and one interior mixed strategy NE ($(\tilde{s}^{A\star}, \tilde{s}^{B\star}) = (\frac{3}{4}, \frac{3}{4})$). Due to the fact that the partial derivative of the payoff surface for player A vanishes at the value of the mixed strategy NE, the whole surface shrinks to one point if one projects the viewpoint in direction to the $\tilde{s}^A$-axis (see right picture in the upper row). The value of the mixed strategy NE is equal to the zero point of the function $g(x)$ (see right picture in the lower row). $g(x)$ (which determines the dynamical behavior of the population function $x(t)$) has, beside its negative region ($g(x) < 0 \; \forall \; x \in]0, s^\star[$) also a region where its value is positive ($g(x) > 0 \; \forall \; x \in]s^\star, 1[$). Due to this property two ESS emerge ($x(t \to \infty) = 0$ and $x(t \to \infty) = 1$). To which of these ESS's the population will evolve depends on the initial condition. If the fraction of s_1-player types at the initial time $t = 0$ is below the value of the mixed strategy NE ($x(0) < s^\star = 0.75$) the population will evolve to the ESS $x(t \to \infty) = 0$, which corresponds to a population sorely choosing the s_2-strategy. Only if the initial fraction is above the mixed strategy threshold ($x(0) > s^\star$) the population will end in the ESS $x(t \to \infty) = 1$. The horizontal population path at $x(t) = 0.75$ is an artefact of the numerical simulation and is not an ESS, as the solution is unstable in respect to infinitely small perturbations.

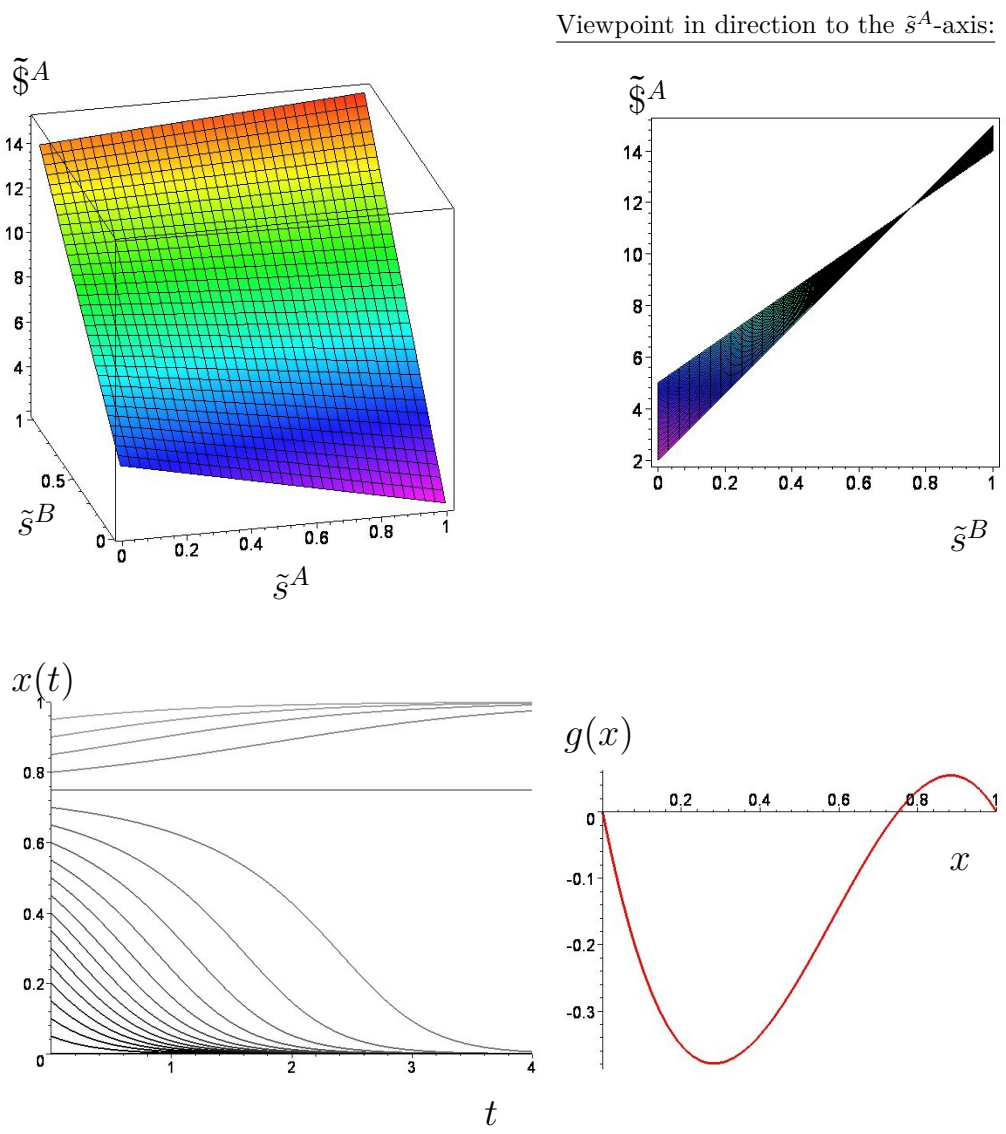

Figure B.4.: Results for the classical game of parameter set Set_7.

Description of figure B.4

The picture in the left upper row shows the mixed strategy payoff function $\tilde{\$}^A(\tilde{s}^A, \tilde{s}^B)$ for player A within parameter set Set_7 as a function of the mixed strategies of player A ($\tilde{s}^A$) and B ($\tilde{s}^B$). The right picture in the upper row shows a special projection of the surface, in which the observer looks in direction of the $\tilde{s}^A$-axis. The lower row depicts $x(t)$, the fraction of players choosing the strategy s_1 at time t for different initial conditions ($x(t=0) = 0, 0.05, 0.1, ..., 0.95$) within parameter set Set_7 (left picture). The right picture shows the function $g(x)$, which determines the dynamical behavior of $x(t)$. The figures show that the game's category of parameter set Set_7 belongs to the class of coordination games with two pure symmetric Nash equilibria ($(s_1^A, s_1^B) \hat{=} (\tilde{s}^A = 1, \tilde{s}^B = 1)$ and $(s_2^A, s_2^B) \hat{=} (\tilde{s}^A = 0, \tilde{s}^B = 0)$) and one interior mixed strategy NE ($(\tilde{s}^{A\star}, \tilde{s}^{B\star}) = (\frac{3}{4}, \frac{3}{4})$). Due to the fact that the partial derivative of the payoff surface for player A vanishes at the value of the mixed strategy NE, the whole surface shrinks to one point if one projects the viewpoint in direction to the $\tilde{s}^A$-axis (see right picture in the upper row). The value of the mixed strategy NE is equal to the zero point of the function $g(x)$ (see right picture in the lower row). $g(x)$ (which determines the dynamical behavior of the population function $x(t)$) has, beside its negative region ($g(x) < 0 \; \forall \; x \in]0, s^\star[$) also a region where its value is positive ($g(x) > 0 \; \forall \; x \in]s^\star, 1[$). Due to this property two ESS emerge ($x(t \to \infty) = 0$ and $x(t \to \infty) = 1$). To which of these ESS's the population will evolve depends on the initial condition. If the fraction of s_1-player types at the initial time $t = 0$ is below the value of the mixed strategy NE ($x(0) < s^\star = 0.75$) the population will evolve to the ESS $x(t \to \infty) = 0$, which corresponds to a population sorely choosing the s_2-strategy. Only if the initial fraction is above the mixed strategy threshold ($x(0) > s^\star$) the population will end in the ESS $x(t \to \infty) = 1$. The horizontal population path at $x(t) = 0.75$ is an artefact of the numerical simulation and is not an ESS, as the solution is unstable in respect to infinitely small perturbations. The strategy sets Set_6 and Set_7 have identical properties, as the payoff parameters of the payoff-transformed games ($a = 1$ and $b = 3$, see table 2.1) have the same values. The mixed strategy payoff surfaces for these two parameter sets are however quite different (see upper left picture in the figures B.3 and B.4).

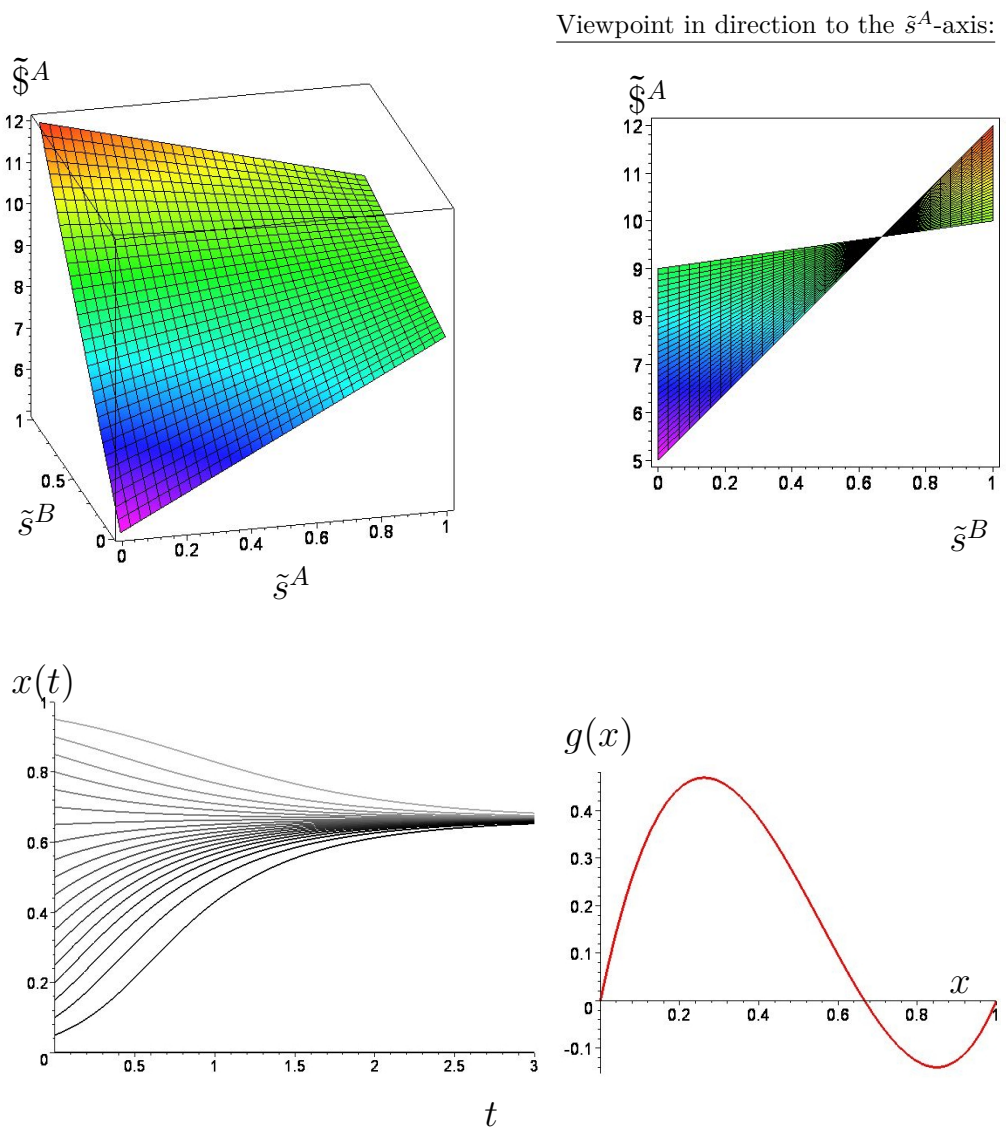

Figure B.5.: Results for the classical game of parameter set Set_9.

Description of figure B.5

The picture in the left upper row shows the mixed strategy payoff function $\tilde{\$}^A(\tilde{s}^A, \tilde{s}^B)$ for player A within parameter set Set_9 as a function of the mixed strategies of player A ($\tilde{s}^A$) and B ($\tilde{s}^B$). The right picture in the upper row shows a special projection of the surface, in which the observer looks in direction of the $\tilde{s}^A$-axis. The lower row depicts $x(t)$, the fraction of players choosing the strategy s_1 at time t for different initial conditions ($x(t=0) = 0, 0.05, 0.1, ..., 0.95$) within parameter set Set_9 (left picture). The right picture shows the function $g(x)$, which determines the dynamical behavior of $x(t)$. The figures show that the game's category of parameter set Set_9 belongs to the class of anti-coordination games with two pure unsymmetric Nash equilibria ($(s_1^A, s_2^B) \hat{=} (\tilde{s}^A = 1, \tilde{s}^B = 0)$ and $(s_2^A, s_1^B) \hat{=} (\tilde{s}^A = 0, \tilde{s}^B = 1)$) and one interior mixed strategy NE ($(\tilde{s}^{A\star}, \tilde{s}^{B\star}) = (\frac{2}{3}, \frac{2}{3})$). Due to the fact that the partial derivative of the payoff surface for player A vanishes at the value of the mixed strategy NE, the whole surface shrinks to one point if one projects the viewpoint in direction to the $\tilde{s}^A$-axis (see right picture in the upper row). The value of the mixed strategy NE is equal to the zero point of the function $g(x)$ (see right picture in the lower row). $g(x)$ (which determines the dynamical behavior of the population function $x(t)$) has, beside its negative region ($g(x) < 0 \; \forall \; x \in]s^\star, 1[$) also a region where its value is positive ($g(x) > 0 \; \forall \; x \in]0, s^\star[$). Due to this property only one ESS emerge ($x(t \to \infty) = \frac{2}{3}$, independent on the initial condition $x(t=0)$.

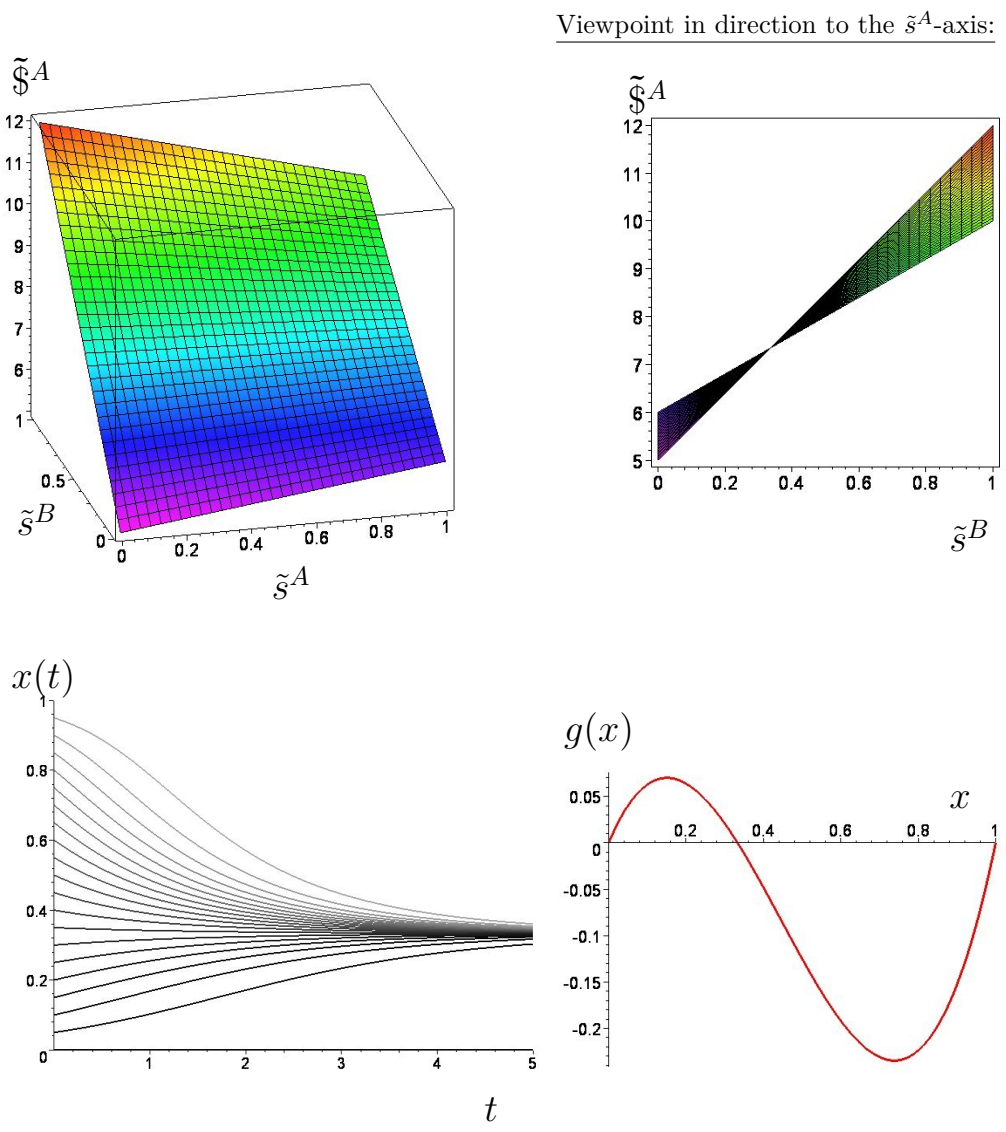

Figure B.6.: Results for the classical game of parameter set Set_{10}.

Description of figure B.6

The picture in the left upper row shows the mixed strategy payoff function $\tilde{\$}^A(\tilde{s}^A, \tilde{s}^B)$ for player A within parameter set Set_{10} as a function of the mixed strategies of player A ($\tilde{s}^A$) and B ($\tilde{s}^B$). The right picture in the upper row shows a special projection of the surface, in which the observer looks in direction of the $\tilde{s}^A$-axis. The lower row depicts $x(t)$, the fraction of players choosing the strategy s_1 at time t for different initial conditions ($x(t=0) = 0, 0.05, 0.1, ..., 0.95$) within parameter set Set_{10} (left picture). The right picture shows the function $g(x)$, which determines the dynamical behavior of $x(t)$. The figures show that the game's category of parameter set Set_{10} belongs to the class of anti-coordination games with two pure unsymmetric Nash equilibria ($(s_1^A, s_2^B) \hat{=} (\tilde{s}^A = 1, \tilde{s}^B = 0)$ and $(s_2^A, s_1^B) \hat{=} (\tilde{s}^A = 0, \tilde{s}^B = 1)$) and one interior mixed strategy NE ($(\tilde{s}^{A\star}, \tilde{s}^{B\star}) = (\frac{1}{3}, \frac{1}{3})$). Due to the fact that the partial derivative of the payoff surface for player A vanishes at the value of the mixed strategy NE, the whole surface shrinks to one point if one projects the viewpoint in direction to the $\tilde{s}^A$-axis (see right picture in the upper row). The value of the mixed strategy NE is equal to the zero point of the function $g(x)$ (see right picture in the lower row). $g(x)$ (which determines the dynamical behavior of the population function $x(t)$) has, beside its negative region ($g(x) < 0 \; \forall \; x \in]s^\star, 1[$) also a region where its value is positive ($g(x) > 0 \; \forall \; x \in]0, s^\star[$). Due to this property only one ESS emerge ($x(t \to \infty) = \frac{1}{3}$, independent on the initial condition $x(t=0)$.

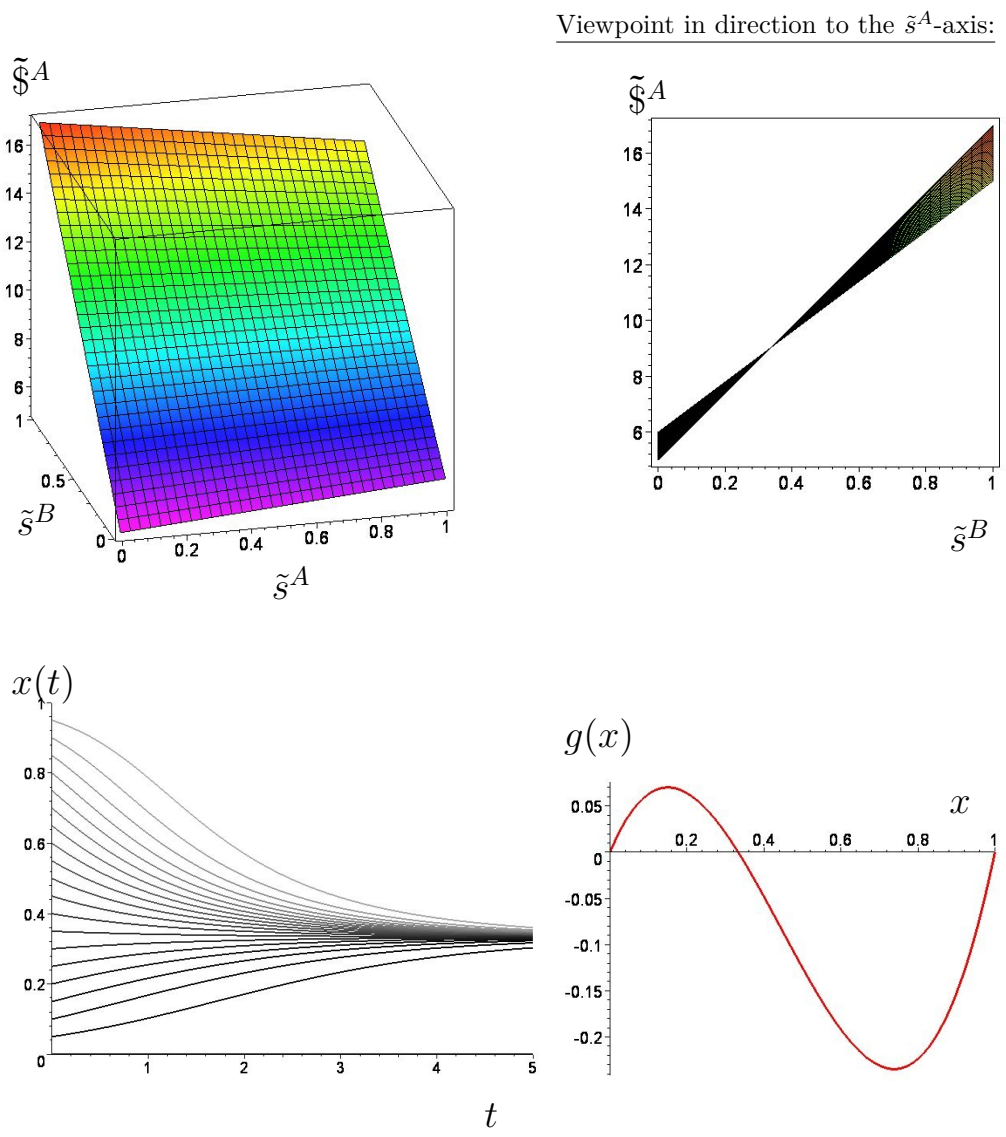

Figure B.7.: Results for the classical game of parameter set Set_{11}.

Description of figure B.7

The picture in the left upper row shows the mixed strategy payoff function $\tilde{\$}^A(\tilde{s}^A, \tilde{s}^B)$ for player A within parameter set Set_{11} as a function of the mixed

strategies of player A ($\tilde{s}^A$) and B ($\tilde{s}^B$). The right picture in the upper row shows a special projection of the surface, in which the observer looks in direction of the $\tilde{s}^A$-axis. The lower row depicts $x(t)$, the fraction of players choosing the strategy s_1 at time t for different initial conditions ($x(t=0) = 0, 0.05, 0.1, ..., 0.95$) within parameter set Set_{11} (left picture). The right picture shows the function $g(x)$, which determines the dynamical behavior of $x(t)$. The figures show that the game's category of parameter set Set_{10} belongs to the class of anti-coordination games with two pure unsymmetric Nash equilibria ($(s_1^A, s_2^B) \hat{=} (\tilde{s}^A = 1, \tilde{s}^B = 0)$ and $(s_2^A, s_1^B) \hat{=} (\tilde{s}^A = 0, \tilde{s}^B = 1)$) and one interior mixed strategy NE ($(\tilde{s}^{A\star}, \tilde{s}^{B\star}) = (\frac{1}{3}, \frac{1}{3})$). Due to the fact that the partial derivative of the payoff surface for player A vanishes at the value of the mixed strategy NE, the whole surface shrinks to one point if one projects the viewpoint in direction to the $\tilde{s}^A$-axis (see right picture in the upper row). The value of the mixed strategy NE is equal to the zero point of the function $g(x)$ (see right picture in the lower row). $g(x)$ (which determines the dynamical behavior of the population function $x(t)$) has, beside its negative region ($g(x) < 0 \; \forall \; x \in]s^\star, 1[$) also a region where its value is positive ($g(x) > 0 \; \forall \; x \in]0, s^\star[$). Due to this property only one ESS emerge ($x(t \to \infty) = \frac{1}{3}$, independent on the initial condition $x(t=0)$. The strategy sets Set_{10} and Set_{11} have identical properties, as the payoff parameters of the payoff-transformed games ($a = -2$ and $b = -1$, see table 2.1) have the same values. The mixed strategy payoff surfaces for these two parameter sets are however quite different (see upper left picture in the figures B.6 and B.7).

B.III. Results for classical symmetric (2x3) games

Within this part of the appendix the properties and classification scheme of symmetric (2×3)-games are defined and discussed. To describe the time evolution of the repeated version of the game Γ (see definition (2.3)) with more than two available strategies, the system of replicator dynamics is generalized as follows. Replicator dynamics, formulated within a system of differential equations, defines in which way the two population vectors $\vec{x}^A := (x_1^A, x_2^A, ..., x_{m_A}^A)$ and $\vec{x}^B := (x_1^B, x_2^B, ..., x_{m_B}^B)$ evolves in time. Each component $x_i^\mu = x_i^\mu(t)$ ($i = 1, 2, ..., m_\mu$, $\mu = A, B$) describes the time evolution of the fraction of different player types i in the whole population composed of the two different groups of players ($\mu = A, B$).

A type-i player of the group $\mu = A, B$ is understood as an actor μ playing strategy s_i^μ. The population vector $\vec{x}^\mu$ has to fulfill the normalizing conditions of a unity vector

$$\begin{aligned} & x_i^\mu(t) \geq 0 \quad \forall\, i = 1, 2\,,\ \mu = A, B\,,\ t \in \mathbb{R} \\ & \sum_{i=1}^{m_\mu} x_i^\mu(t) = 1 \quad \forall\, \mu = A, B \quad . \end{aligned} \tag{B.7}$$

The following first order system of differential equations of the population vector $\vec{x}^\mu(t) = (x_1^\mu(t), x_2^\mu(t), ..., x_{m_\mu}^\mu(t))$ is known as replicator dynamics of a general bimatrix game (see [166, 198])

$$\begin{aligned} \frac{dx_i^A(t)}{dt} &= x_i^A(t) \left[\underbrace{\sum_{l=1}^{m_B} \$_{il}^A\, x_l^B(t)}_{:=f_i^A(t)} - \underbrace{\sum_{l=1}^{m_B}\sum_{k=1}^{m_A} \$_{kl}^A\, x_k^A(t)\, x_l^B(t)}_{:=\bar{f}^A(t)} \right] \\ \frac{dx_i^B(t)}{dt} &= x_i^B(t) \left[\underbrace{\sum_{l=1}^{m_A} \$_{li}^B\, x_l^A(t)}_{:=f_i^B(t)} - \underbrace{\sum_{l=1}^{m_B}\sum_{k=1}^{m_A} \$_{lk}^B\, x_l^A(t)\, x_k^B(t)}_{:=\bar{f}^B(t)} \right] \end{aligned} \tag{B.8}$$

where $f_i^\mu(t)$ is the fitness of type i within the μ-player population and $\bar{f}^\mu(t) = \sum_{i=1}^{m_\mu} f_i^\mu(t)$ is the average fitness of the whole μ-player population.

Assuming that the number of available strategies for player A and player B are equal ($m_A = m_B := m$) and restricting their payoffs to be identical (symmetric payoff matrices: $\hat{\$}^A = (\hat{\$}^B)^T$, $\$_{lk}^A = \$_{kl}^B := \$_{lk}$) equation (B.8) becomes

$$\begin{aligned} \frac{dx_i^A(t)}{dt} &= x_i^A(t) \left[\sum_{l=1}^{m} \$_{il}\, x_l^B(t) - \sum_{l=1}^{m}\sum_{k=1}^{m} \$_{kl}\, x_k^A(t)\, x_l^B(t) \right] \\ \frac{dx_i^B(t)}{dt} &= x_i^B(t) \left[\sum_{l=1}^{m} \$_{il}\, x_l^A(t) - \sum_{l=1}^{m}\sum_{k=1}^{m} \$_{kl}\, x_l^A(t)\, x_k^B(t) \right] \quad . \end{aligned} \tag{B.9}$$

As the two equations of (B.9) are identical, the system of differential equations reduces to a single set of equations with only one population vector $\vec{x}(t) =$

$(x_1(t), x_2(t), ..., x_m(t))$:

$$\frac{dx_i(t)}{dt} = x_i(t) \left[\sum_{l=1}^{m} \$_{il}\, x_l(t) - \sum_{l=1}^{m} \sum_{k=1}^{m} \$_{kl}\, x_k(t)\, x_l(t) \right] \tag{B.10}$$

The overall population vector $\vec{x}(t)$ has to fulfill the following condition

$$x_i(t) \leq 0 \;\; \forall\, i = 1, 2, ..., m \quad \text{and} \quad \sum_{i=1}^{m} x_i(t) = 1 \;\; \forall\, t \in \mathbb{R} \quad . \tag{B.11}$$

Starting from the differential equation (B.10) and restricting the set of available strategies to three $m = 3$, the following system of differential equations describes the dynamical behavior of a (2×3)-game:

$$\begin{aligned}
\dot{x_1} = \frac{dx_1(t)}{dt} &= x_1(t) \left[\sum_{l=1}^{3} \$_{1l}\, x_l(t) - \sum_{l=1}^{3} \sum_{k=1}^{3} \$_{kl}\, x_k(t)\, x_l(t) \right] \\
\dot{x_2} = \frac{dx_2(t)}{dt} &= x_2(t) \left[\sum_{l=1}^{3} \$_{2l}\, x_l(t) - \sum_{l=1}^{3} \sum_{k=1}^{3} \$_{kl}\, x_k(t)\, x_l(t) \right] \\
\dot{x_3} = \frac{dx_3(t)}{dt} &= x_3(t) \left[\sum_{l=1}^{3} \$_{3l}\, x_l(t) - \sum_{l=1}^{3} \sum_{k=1}^{3} \$_{kl}\, x_k(t)\, x_l(t) \right]
\end{aligned} \tag{B.12}$$

By using local payoff shifts it is possible to transform the payoff matrix $\hat{\$}$ to a diagonal free matrix $\hat{\$}^{|}$ without effecting the main characteristics and the dynamical behavior of the game:

$$\hat{\$} = \begin{pmatrix} \$_{11} & \$_{12} & \$_{13} \\ \$_{21} & \$_{22} & \$_{23} \\ \$_{31} & \$_{32} & \$_{33} \end{pmatrix} \qquad \longrightarrow \tag{B.13}$$

$$\hat{\$}^{|} = \begin{pmatrix} 0 & \$_{12} - \$_{22} & \$_{13} - \$_{33} \\ \$_{21} - \$_{11} & 0 & \$_{23} - \$_{33} \\ \$_{31} - \$_{11} & \$_{32} - \$_{22} & 0 \end{pmatrix} =: \begin{pmatrix} 0 & \$_a & \$_b \\ \$_c & 0 & \$_d \\ \$_e & \$_f & 0 \end{pmatrix}$$

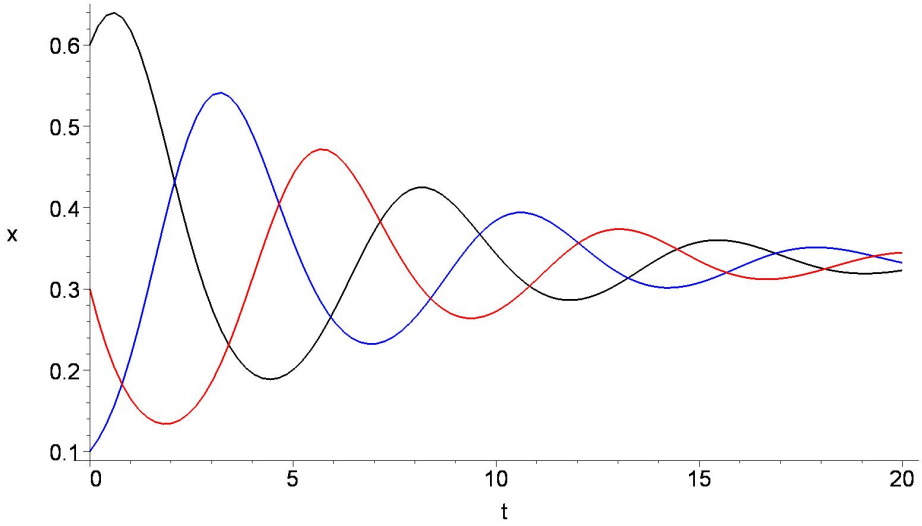

Figure B.8.: Time evolution of the three components of the population vector $\vec{x}(t)$ within a (2×3)-game (payoff parameters $\$_a = 2, \$_b = -1, \$_c = -1, \$_d = 2, \$_e = 2, \$_f = -1$, Zeeman class 1). The blue curve describes the x_1-component, the red curve the x_2-component and the black curve the x_3-component of the population vector. The initial condition $\vec{x}(0) = (0.1, 0.3, 0.6)$ was used for the numerical analysis.

With the use of the transformation (B.13), equation (B.12) simplifies:

$$\begin{aligned} \dot{x_1} &= x_1 \left[\$_a\, x_2 + \$_b\, x_3 - \bar{G}\right] \\ \dot{x_2} &= x_2 \left[\$_c\, x_1 + \$_d\, x_3 - \bar{G}\right] \\ \dot{x_3} &= x_3 \left[\$_e\, x_1 + \$_f\, x_2 - \bar{G}\right] \qquad \text{(B.14)} \\ \text{with:} \qquad \bar{G} &:= (\$_a + \$_c)\, x_1\, x_2 + (\$_b + \$_e)\, x_1\, x_3 + (\$_d + \$_f)\, x_2\, x_3 \end{aligned}$$

The evolution of the three dimensional population vector $\vec{x}(t) = (x_1(t), x_2(t), x_3(t))$ depends therefore on the six payoff parameters $(\$_a, \$_b, \$_c, \$_d, \$_e, \$_f)$ and on its initial condition $\vec{x}(t = 0)$. In general there is a great variety of different game types and there can be up to three stable ESS's within one game. To exemplify one evolution and describe how this evolution is visualized using a barycentric coordinate system, the following specific payoff parameters

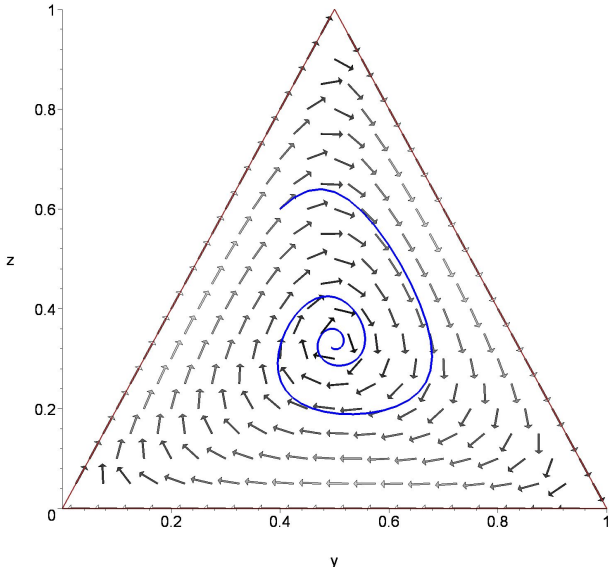

Figure B.9.: Vector field $\vec{F}$ and time evolution of the population vector $\vec{x}(t)$ within a two dimensional barycentric coordinate system (initial condition $\vec{x}(0) = (0.1, 0.3, 0.6) \hat{=} (y = 0.4, z = 0.6)$, payoff parameters $\$_a = 2, \$_b = -1, \$_c = -1, \$_d = 2, \$_e = 2, \$_f = -1$, Zeeman class 1).

($\$_a = 2, \$_b = -1, \$_c = -1, \$_d = 2, \$_e = 2, \$_f = -1$) and initial condition $\vec{x}(0) = (0.1, 0.3, 0.6)$ are used. The time dependence of the three components of the population vector are calculated numerically and the results are shown in figure B.8. The figure shows, that all of the three population components oscillate around a fixed point attractor, which is the mixed NE of the game $\hat{\vec{x}} = (\frac{1}{3}, \frac{1}{3}, \frac{1}{3})$.

To visualize the evolution of the population with only one curve barycentric coordinates are commonly used. Within (2×3)-games the following coordinate transformation is used to map the population vector $\vec{x}$ onto a triangle:

$$y := x_1 + \frac{x_3}{2}, \quad z := x_3 \tag{B.15}$$

Within the two dimensional barycentric coordinate system, the pure population state $(x_1 = 1, x_2 = 0, x_3 = 0)$ is mapped onto the left lower corner of the triangle at $(y = 0, z = 0)$, the state $(x_1 = 0, x_2 = 1, x_3 = 0)$ is mapped to the right lower corner at $(y = 1, z = 0)$ and the population state $(x_1 = 0, x_2 = 0, x_3 = 1)$ is

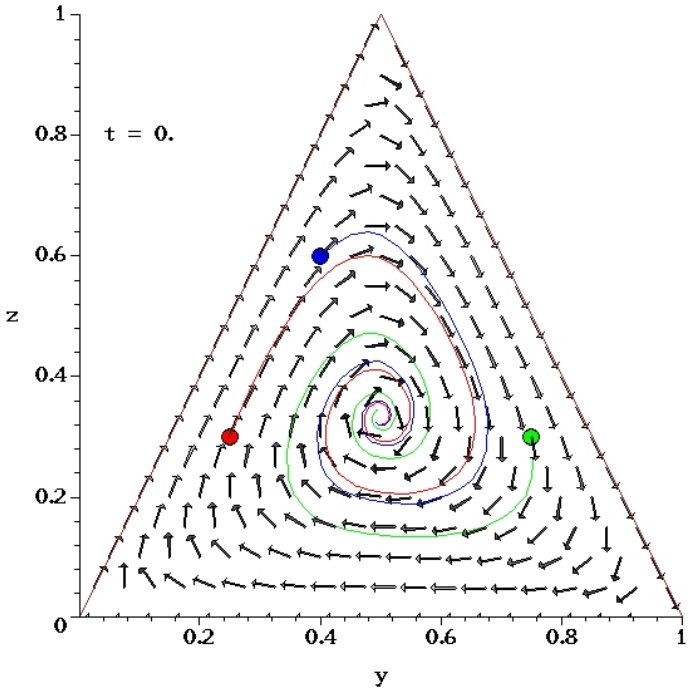

Figure B.10.: Animation of the time evolution of the population vector $\vec{x}(t)$ within a two dimensional barycentric coordinate system (payoff parameters $\$_a = 2, \$_b = -1, \$_c = -1, \$_d = 2, \$_e = 2, \$_f = -1$, Zeeman class 1). The colored trajectories describe the numerical results of three different initial condition (blue: $\vec{x}(0) = (0.1, 0.3, 0.6) \hat{=} (y = 0.4, z = 0.6)$, red: $\vec{x}(0) = (0.1, 0.6, 0.3) \hat{=} (y = 0.25, z = 0.3)$ and green: $\vec{x}(0) = (0.6, 0.1, 0.3) \hat{=} (y = 0.75, z = 0.3)$.

mapped onto $(y = \frac{1}{2}, z = 1)$ (see figure B.9).

The corresponding forces $\vec{F} = (F_1, F_2, F_3)$ which act on the population vector $\vec{x}$ are defined as the components of their time derivatives $\dot{\vec{x}}$:

$$\begin{aligned} F_1 &= x_1 \left[\$_a\, x_2 + \$_b\, x_3 - \bar{G} \right] \\ F_2 &= x_2 \left[\$_c\, x_1 + \$_d\, x_3 - \bar{G} \right] \\ F_3 &= x_3 \left[\$_e\, x_1 + \$_f\, x_2 - \bar{G} \right] \end{aligned} \tag{B.16}$$

Similar to the population vector, the vector $\vec{F} = \vec{F}(\vec{x})$ can be transformed into

barycentric coordinates

$$\vec{F} = \vec{F}(\vec{x}) = \begin{pmatrix} F_1(x_1, x_2, x_3) \\ F_2(x_1, x_2, x_3) \\ F_3(x_1, x_2, x_3) \end{pmatrix} \qquad \longrightarrow \tag{B.17}$$

$$\vec{F} = \vec{F}(y, z) = \begin{pmatrix} F_y(y, z) = F_1(y, z) + \frac{F_3(y,z)}{2} \\ F_z(y, z) = F_3(y, z) \end{pmatrix}$$

Figure B.9 shows these vectorfields for the game discussed within figure B.8. When a vector gets darker the time derivative of the population vector increases. The blue curve within figure B.9 shows the evolution of the population vector (see figure B.8) within the barycentric coordinate system.

The trajectory of the population vector starts at $\vec{x}(0) = (0.1, 0.3, 0.6) \hat{=} (y = 0.4, z = 0.6)$ and spirals in towards the mixed strategy NE $\hat{\vec{x}} = (\frac{1}{3}, \frac{1}{3}, \frac{1}{3}) \hat{=} (y = 0.5, z = \frac{1}{3})$, which is the fixed point attractor of the underlying differential equation. At every point of the trajectory the evolution follows the path of the vectorfield at that point. It can be shown, that this fixed point is the only ESS of the system and any possible initial condition will finally converge to this fixed point attractor. To illustrate the dynamics of the evolutionary paths, the animated figure B.10 shows the trajectories of three numerical simulations having three different initial conditions. The animation shows that all of the three different population paths converge to the fixed point attractor.

As shown by this example, the structure of the vectorfields and the possible population trajectories within the barycentric coordinate system depend strongly on the parameters of the payoff matrix. Zeeman has defined 19 different game classes of (2×3)-games. All of these classes have at least one ESS, some have two and actually one game class (*class:* -10_2, $\$_a = -3, \$_b = -1, \$_c = -3, \$_d = -1, \$_e = -1, \$_f = -1$) has three ESS. The animated figure B.11 shows the structure of the vectorfields and three possible population trajectories within the Zemann class -10_2. Each of the trajectories converges to a different ESS. The ESS's of this game are the fixed point attractors of the three pure Nash equilibria, which are situated at the edges of the triangle of the barycentric coordinate system.

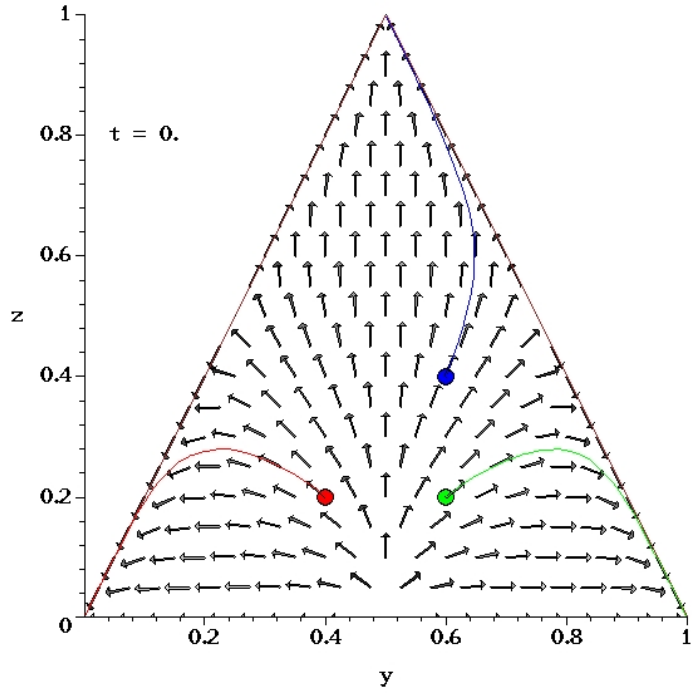

Figure B.11.: Animation of the time evolution of the population vector $\vec{x}(t)$ within a two dimensional barycentric coordinate system (payoff parameters $\$_a = -3, \$_b = -1, \$_c = -3, \$_d = -1, \$_e = -1, \$_f = -1$, Zeeman class -10_2). The colored trajectories describe the numerical results of three different initial condition (blue: $\vec{x}(0) = (0.4, 0.2, 0.4) \hat{=} (y = 0.6, z = 0.4)$, red: $\vec{x}(0) = (0.3, 0.5, 0.2) \hat{=} (y = 0.4, z = 0.2)$ and green: $\vec{x}(0) = (0.5, 0.3, 0.2) \hat{=} (y = 0.6, z = 0.2)$.

An other example is the so called generalized "Rock-Scissors-Paper" game, which has the following payoff matrix (see [235])

$$\hat{\$} = \begin{pmatrix} 1 & 2+a & 0 \\ 0 & 1 & 2+a \\ 2+a & 0 & 1 \end{pmatrix} \longrightarrow \hat{\$}^{|} = \begin{pmatrix} 0 & 1+a & -1 \\ -1 & 0 & 1+a \\ 1+a & -1 & 0 \end{pmatrix} \quad , \quad \text{(B.18)}$$

where the parameter a determines the equivalence class of the game. Figure B.12 depicts the vector field and trajectory structure of the three possible equivalence class of the generalized Rock-Scissors-Paper game.

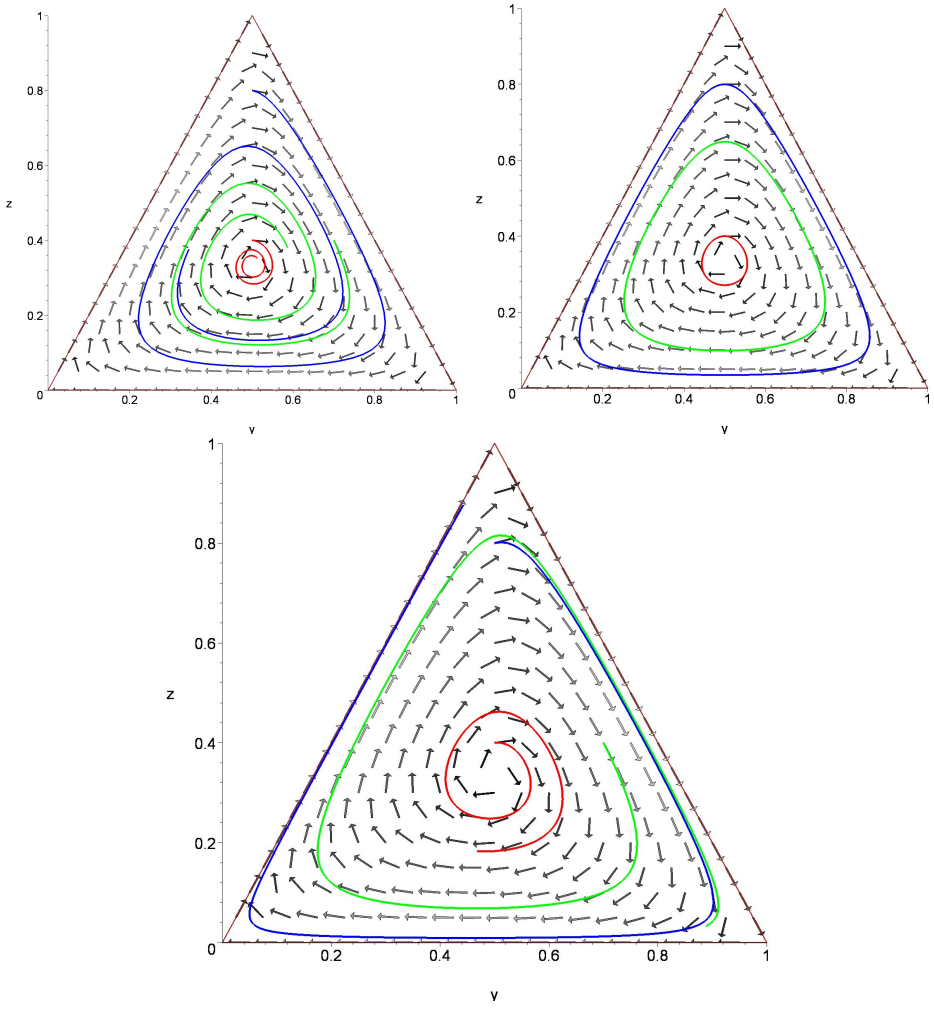

Figure B.12.: Vector field $\vec{F}$ and time evolution of the population vector $\vec{x}(t)$ within a two dimensional barycentric coordinate system for the generalized Rock-Scissors-Paper game. Payoff parameters $\$_a = 1+a, \$_b = -1, \$_c = -1, \$_d = 1+a, \$_e = 1+a, \$_f = -1$ (left picture $a = -0.1$, middle picture $a = 0$ and right picture $a = 0.1$.

B.IV. Results for classical unsymmetric (2x2) games

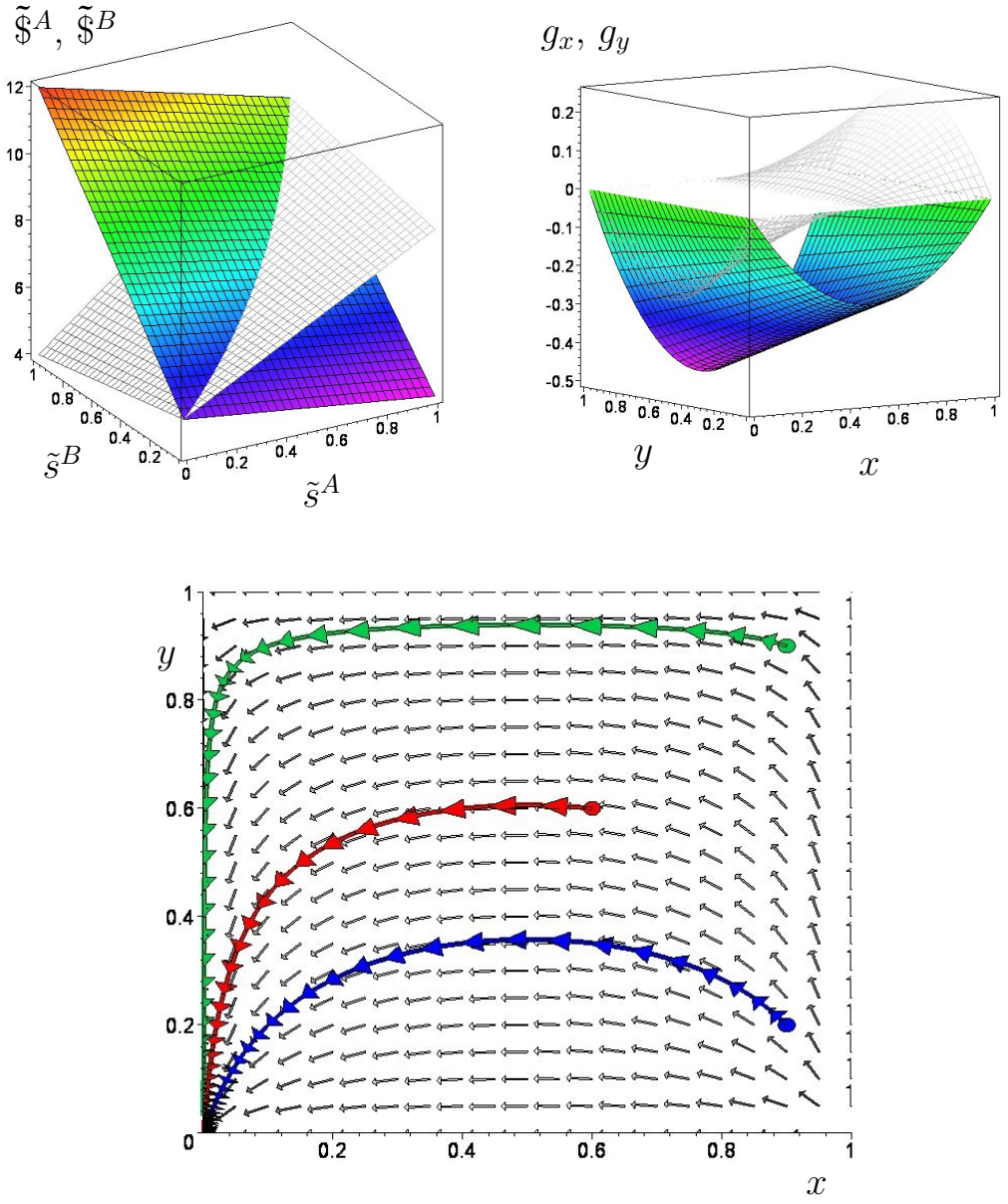

Figure B.13.: Results for the classical unsymmetric game of setting Set_3^{us}.

Description of figure B.13

Upper row, left picture: Mixed strategy payoff function for player A ($\tilde{\$}^A(\tilde{s}^A, \tilde{s}^B)$, colored surface) and player B ($\tilde{\$}^B(\tilde{s}^A, \tilde{s}^B)$, wired grey surface) within parameter set Set_3^{us} as a function of the mixed strategies of player A ($\tilde{s}^A$) and B ($\tilde{s}^B$). Upper row, right picture: $g_x(x, y)$ (colored surface) and $g_y(x, y)$ (wired grey surface) as a function of the strategic population fractions of group A (x) and group B (y). Lower row: Phase diagram of the xy-trajectories for three different initial conditions within parameter set Set_3^{us}. x describes the fraction of players within group A choosing the strategy s_1, while y is a similar fraction within group B. Parameter set Set_3^{us} is a combination of a prisoner's dilemma game (subpopulation A) with a game belonging to the coordination class (subpopulation B). The only NE of the game is the strategy combination ($\tilde{s}^A = 0, \tilde{s}^B = 0$). As the function $g_x(x, y)$ is always below zero, the amount of players (within group A) choosing strategy s_1 will monotony decrease as time goes by, and will finally reach the only ESS ($x(t \to \infty) = 0$,$y(t \to \infty) = 0$), independent on the initial condition. The three trajectories are embedded in a field plot phase diagram, where the little grey arrows describe the direction of a "strategic wind" the population has to follow during its time evolution. The three initial conditions $(x(0), y(0))$ are marked with colored circles at the beginning of the three curves. The several colored arrows, which are on top of the trajectories describe the population's movement for some intermediate time steps, where the length of arrows indicate the absolute value of the strategic change velocity within the population. The difference in the intermediate time steps ($\delta t = 0.2$) is equal for all of the three trajectories. Both population subgroups play a dominant game and the evolution of their strategical choice will finally - independent on the initial condition - reach a state, where everybody chooses the dominant strategy s_2. The game category belongs therefore formally to the corner class.

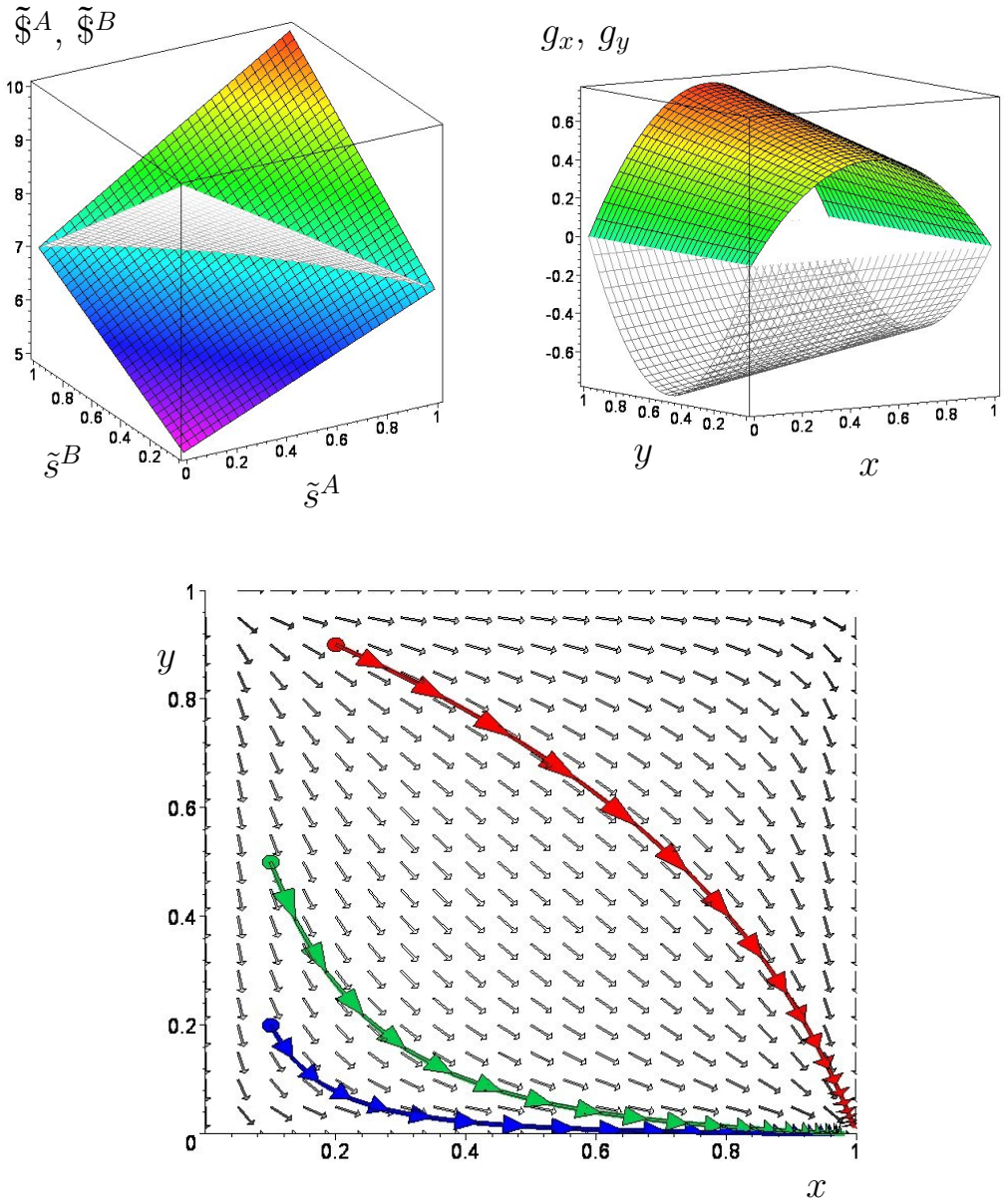

Figure B.14.: Results for the classical unsymmetric game of parameter setting Set_4^{us}.

Description of figure B.14

Same description as figure B.13. Parameter set Set_4^{us} is a combination of two dominant games with different underlying dominant strategies ($\tilde{s}^{A\star} = 1$ and $\tilde{s}^{B\star} = 0$). The only NE of the game is the unsymmetric strategy combination ($\tilde{s}^A = 1, \tilde{s}^B = 0$). As the function $g_x(x, y)$ is always above zero ($g_y(x, y)$ is always below zero) the amount of players choosing strategy s_1 will monotony increase in group A (monotony decrease in group B) as time goes by, and will finally reach the only ESS ($x(t \to \infty) = 1$,$y(t \to \infty) = 0$), independent on the initial condition. The three trajectories are embedded in a field plot phase diagram, where the little grey arrows describe the direction of a "strategic wind" the population has to follow during its time evolution. The three initial conditions $(x(0), y(0))$ are marked with colored circles at the beginning of the three curves. The several colored arrows, which are on top of the trajectories describe the population's movement for some intermediate time steps, where the length of arrows indicate the absolute value of the strategic change velocity within the population. The difference in the intermediate time steps ($\delta t = 0.15$) is equal for all of the three trajectories. Both population subgroups play a dominant game and the evolution of their strategical choice will finally - independent on the initial condition - reach a state, where everybody in group A chooses the dominant strategy s_1 and everybody in group B chooses the dominant strategy s_2. The game category belongs therefore formally to the corner class.

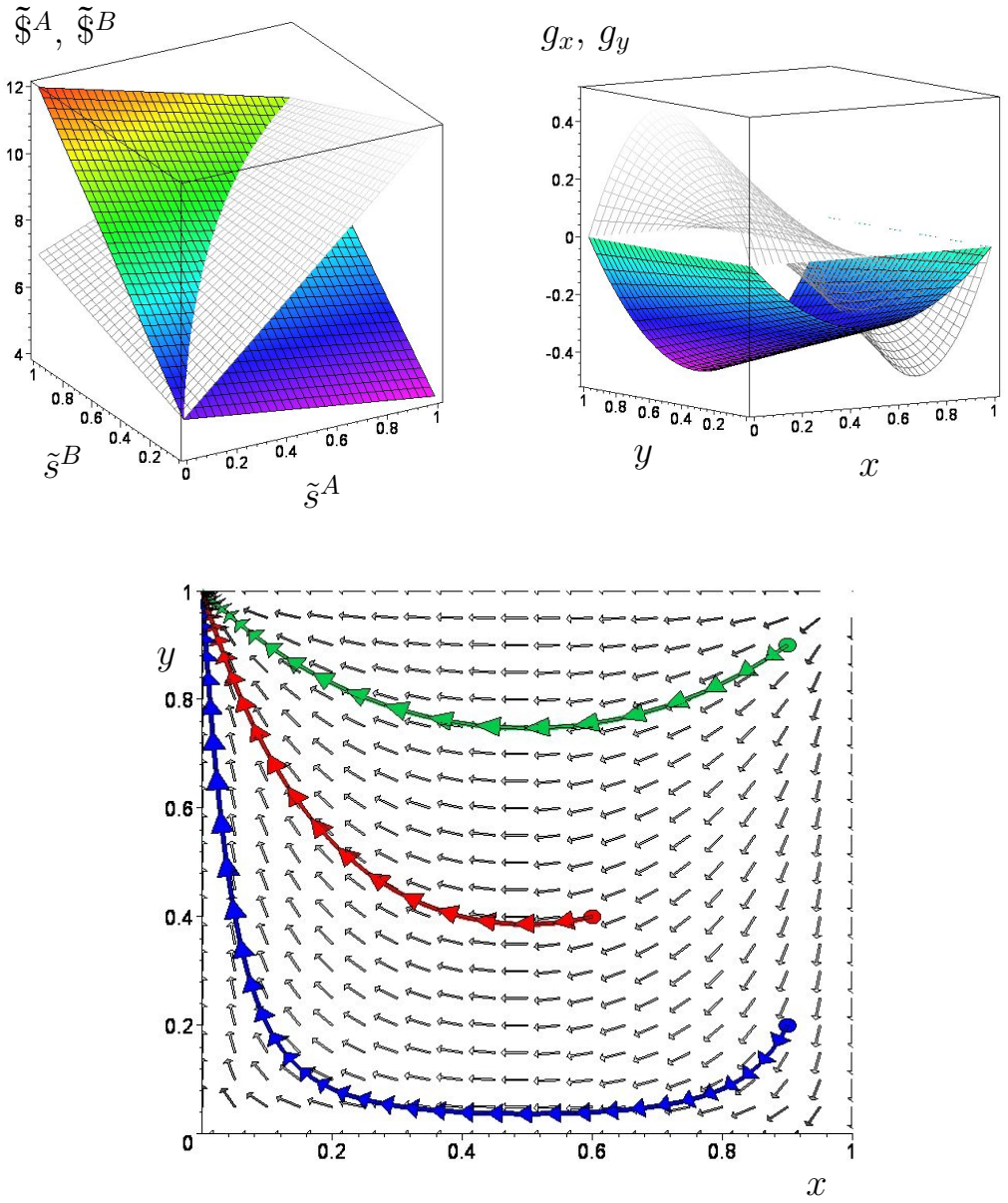

Figure B.15.: Results for the classical unsymmetric game of parameter setting Set_5^{us}.

Description of figure B.15

Same description as figure B.13. Parameter set Set_5^{us} is a combination of a dominant game (subpopulation A) with a game belonging to the anti-coordination class (subpopulation B). The only NE of the game is the unsymmetric strategy combination ($\tilde{s}^A = 0, \tilde{s}^B = 1$). As the function $g_x(x, y)$ is always below zero, the amount of players choosing strategy s_1 will monotony decrease in group A as time goes by, and will finally reach the only ESS ($x(t \to \infty) = 0$,$y(t \to \infty) = 1$), independent on the initial condition. The three trajectories are embedded in a field plot phase diagram, where the little grey arrows describe the direction of a "strategic wind" the population has to follow during its time evolution. The three initial conditions $(x(0), y(0))$ are marked with colored circles at the beginning of the three curves. The several colored arrows, which are on top of the trajectories describe the population's movement for some intermediate time steps, where the length of arrows indicate the absolute value of the strategic change velocity within the population. The difference in the intermediate time steps ($\delta t = 0.175$) is equal for all of the three trajectories. The evolution of the strategical choice will finally - independent on the initial condition - reach a state, where everybody in group A chooses the dominant strategy s_2 and everybody in group B chooses the strategy s_1. The game category belongs therefore formally to the corner class.

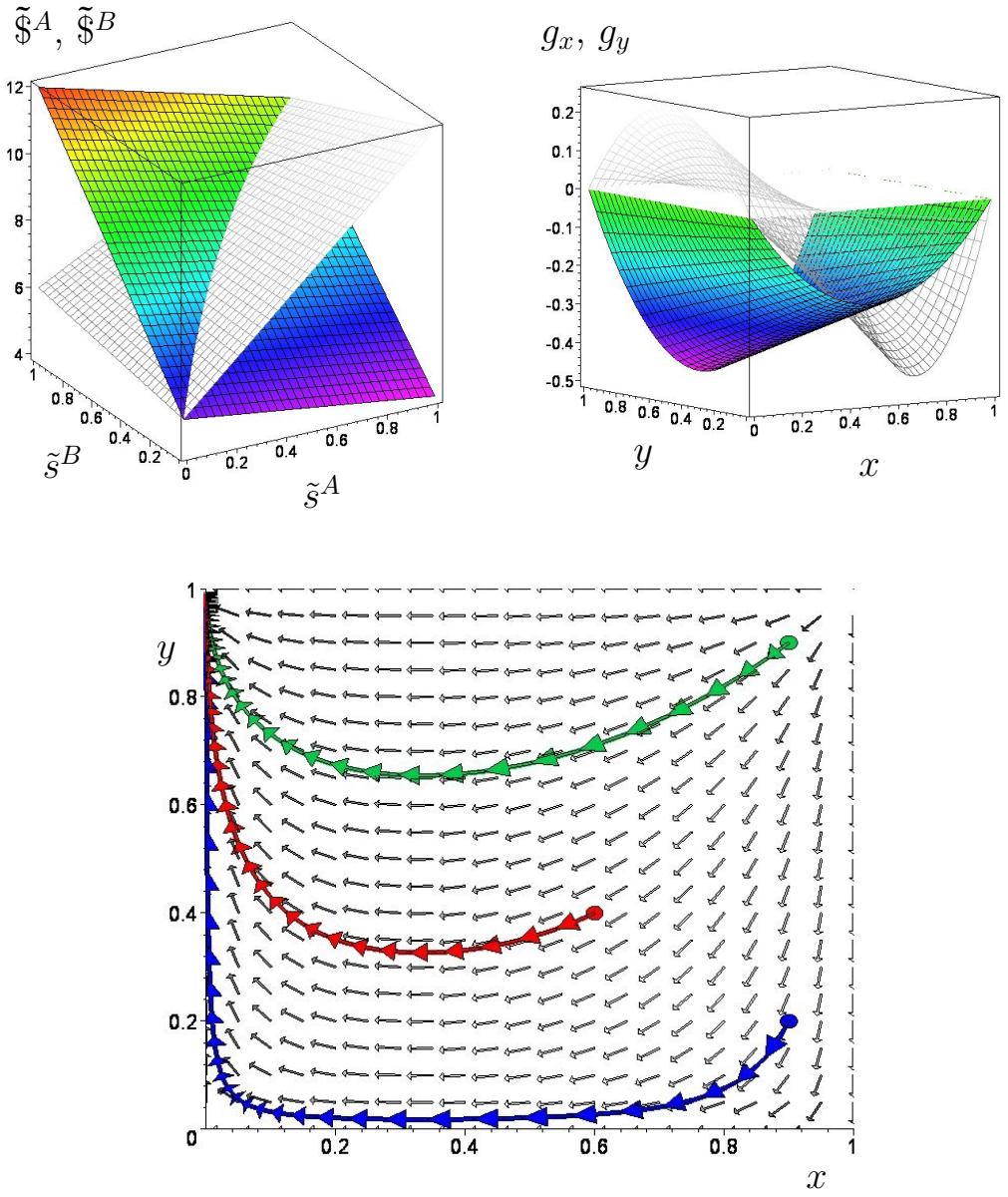

Figure B.16.: Results for the classical unsymmetric game of parameter setting Set_6^{us}.

Description of figure B.16

Same description as figure B.13. Parameter set Set_6^{us} is a combination of a dominant game (subpopulation A) with a game belonging to the anti-coordination class (subpopulation B). The only NE of the game is the unsymmetric strategy combination ($\tilde{s}^A = 0, \tilde{s}^B = 1$). As the function $g_x(x, y)$ is always below zero, the amount of players choosing strategy s_1 will monotony decrease in group A as time goes by, and will finally reach the only ESS ($x(t \to \infty) = 0$,$y(t \to \infty) = 1$), independent on the initial condition. The three trajectories are embedded in a field plot phase diagram, where the little grey arrows describe the direction of a "strategic wind" the population has to follow during its time evolution. The three initial conditions $(x(0), y(0))$ are marked with colored circles at the beginning of the three curves. The several colored arrows, which are on top of the trajectories describe the population's movement for some intermediate time steps, where the length of arrows indicate the absolute value of the strategic change velocity within the population. The difference in the intermediate time steps is different for the three trajectories ($\delta t = 0.175$ for the red and green trajectories and $\delta t = 0.3$ for the blue trajectory). The evolution of the strategical choice will finally - independent on the initial condition - reach a state, where everybody in group A chooses the dominant strategy s_2 and everybody in group B chooses the strategy s_1. The game category belongs therefore formally to the corner class.

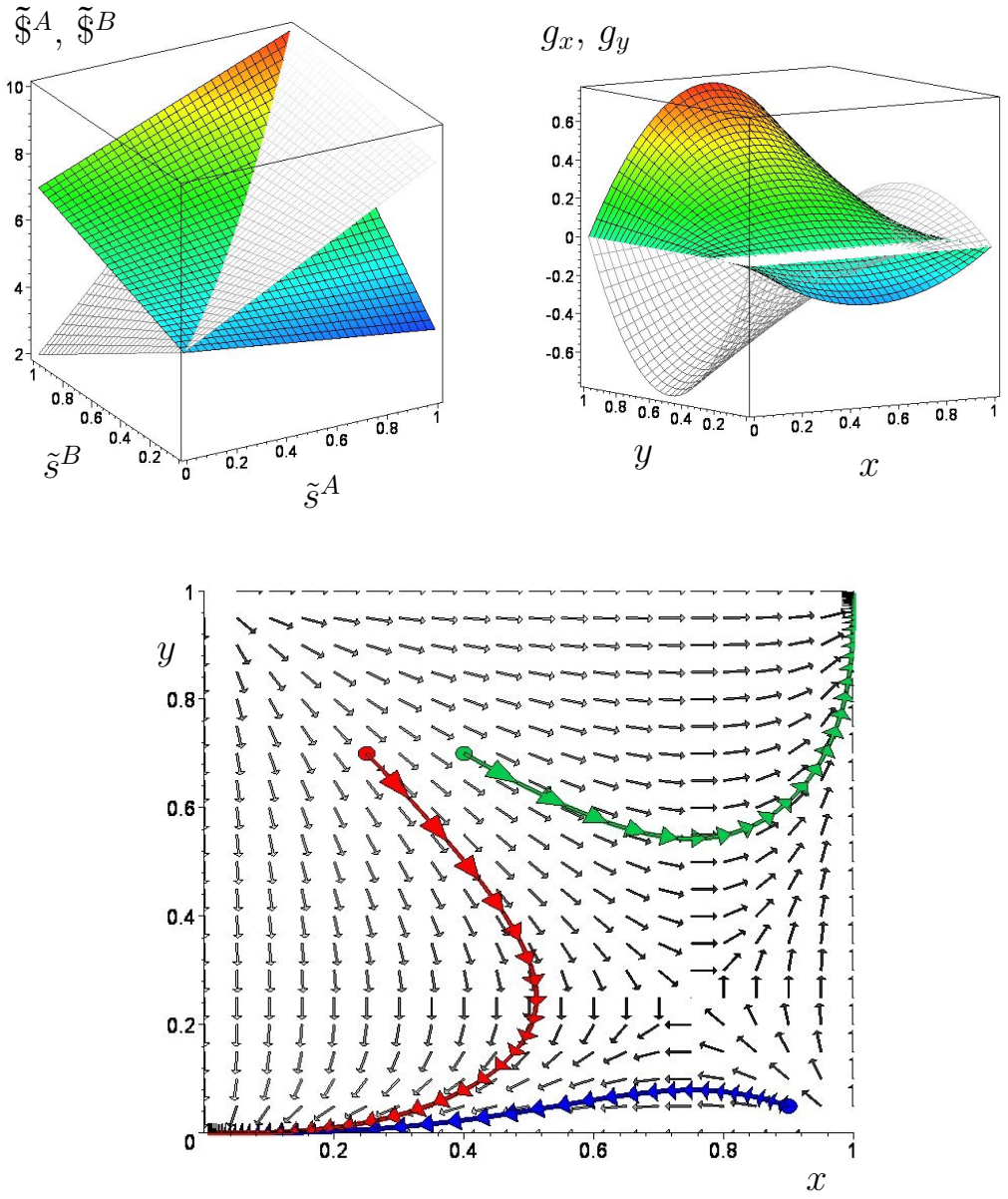

Figure B.17.: Results for the classical unsymmetric game of parameter setting Set_8^{us}.

Description of figure B.17

Same description as figure B.13. Parameter set Set_8^{us} is a combination of two coordination games with different underlying mixed strategy Nash equilibria ($\tilde{s}^{A\star} = \frac{1}{4}$ and $\tilde{s}^{B\star} = \frac{3}{4}$). The two symmetric pure Nash equilibria of the game are the strategy combinations ($\tilde{s}^A = 1, \tilde{s}^B = 1$) and ($\tilde{s}^A = 0, \tilde{s}^B = 0$). Both functions, $g_x(x, y)$ and $g_y(x, y)$, have regions where they are above and below zero. Dependent on the initial condition, the population will finally reach one of the two possible ESS ($(x(t \to \infty) = 0$,$y(t \to \infty) = 0)$ or $(x(t \to \infty) = 1$,$y(t \to \infty) = 1)$). The three trajectories are embedded in a field plot phase diagram, where the little grey arrows describe the direction of a "strategic wind" the population has to follow during its time evolution. The three initial conditions $(x(0), y(0))$ are marked with colored circles at the beginning of the three curves. The several colored arrows, which are on top of the trajectories describe the population's movement for some intermediate time steps, where the length of arrows indicate the absolute value of the strategic change velocity within the population. The difference in the intermediate time steps ($\delta t = 0.2$) is equal for all of the three trajectories. The evolution of the strategical choice will finally - dependent on the initial condition - reach a state, where everybody chooses the strategy s_1 (green trajectory) or everybody chooses the strategy s_2 (red and blue trajectory). The game category belongs therefore formally to the saddle class.

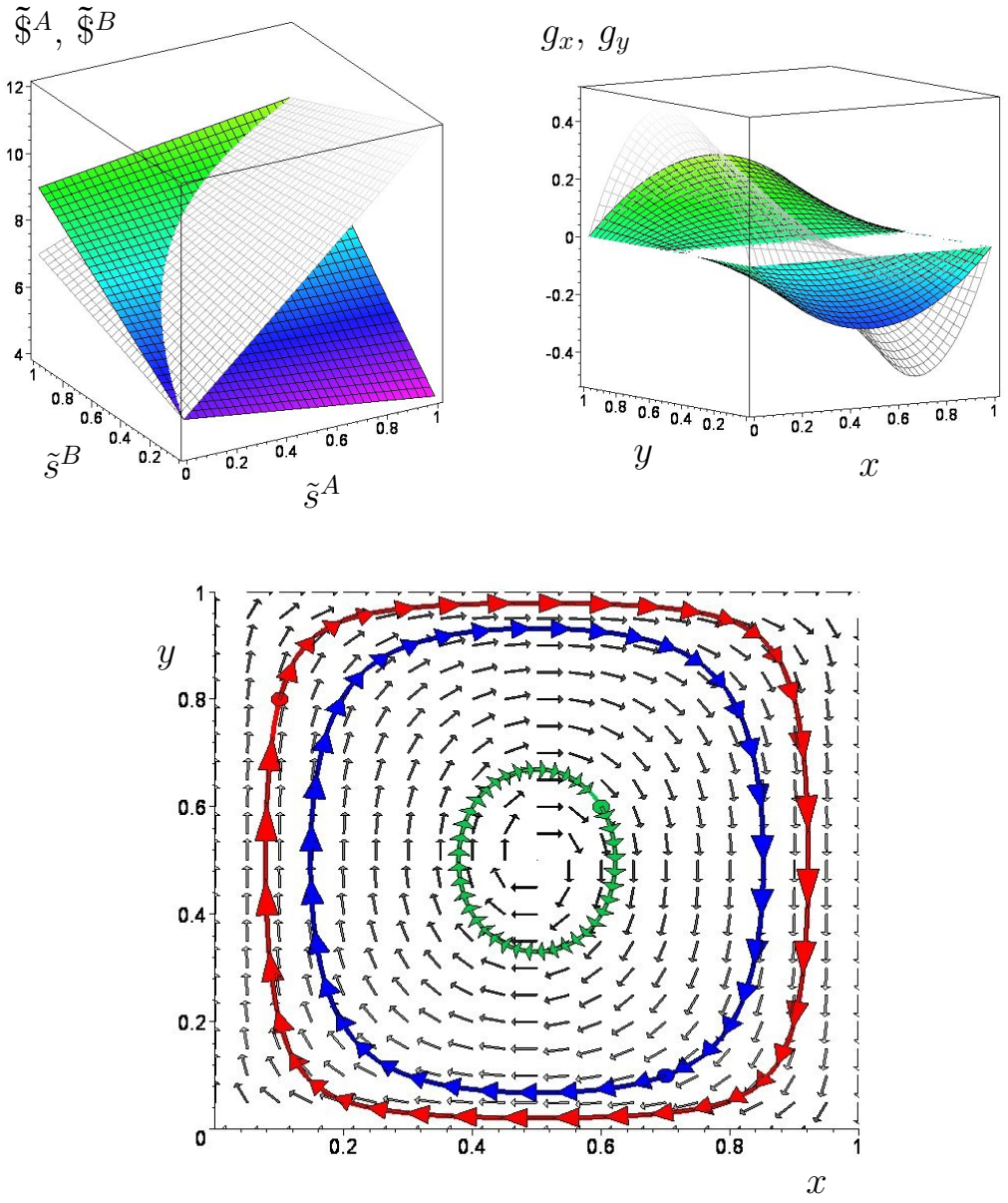

Figure B.18.: Results for the classical unsymmetric game of parameter setting Set_{10}^{us}.

Description of figure B.18

Same description as figure B.13. Parameter set Set_{10}^{us} is a combination of a coordination game (subpopulation A) with a game belonging to the anti-coordination class (subpopulation B). The game does not have any pure NE, however the underlying mixed strategy NE of the game is ($\tilde{s}^{A\star} = \frac{1}{2}$ and $\tilde{s}^{B\star} = \frac{1}{2}$). Both functions, $g_x(x, y)$ and $g_y(x, y)$, have regions where they are above and below zero. Independent on the initial condition, the population will never reach an ESS. The three trajectories are embedded in a field plot phase diagram, where the little grey arrows describe the direction of a "strategic wind" the population has to follow during its time evolution. The three initial conditions $(x(0), y(0))$ are marked with colored circles at the beginning of the three curves. The several colored arrows, which are on top of the trajectories describe the population's movement for some intermediate time steps, where the length of arrows indicate the absolute value of the strategic change velocity within the population. The difference in the intermediate time steps is different for the three trajectories ($\delta t = 13.5$ for the red, $\delta t = 9$ for the green and $\delta t = 11.5$ for the blue trajectory). Due to the absence of an ESS, all of the trajectories cycle around the interior NE, where the time which is needed for one cycle is larger for bigger cycles. The game category belongs therefore formally to the center class.

B.V. Analytical expression for the γ-thresholds

Within this part of the appendix the two entanglement thresholds γ_1 and γ_2 are calculated for general symmetric (2×2)-games. In the following the underlying symmetric (2×2) game has the following payoff parameters

$$\$_{11} := \$_{11}^A = \$_{11}^B,\ \$_{22} := \$_{22}^A = \$_{22}^B,\ \$_{12} := \$_{12}^A = \$_{21}^B,\ \$_{21} := \$_{21}^A = \$_{12}^B \quad .$$

B.V.1. Entanglement threshold γ_1

In the following it is supposed, that the underlying game has a classical NE at the strategy combination $(s_2^A, s_2^B) \hat{=} (\tau_A = 1, \tau_B = 1)$. The entanglement threshold γ_1 is defined as the entanglement barrier, for which the classical NE dissolves. For $\gamma \geq \gamma_1$, the best response to the strategy $s_2^B \hat{=} \tau_B = 1$ for player A is no

longer the strategy $s_2^A \hat{=} \tau_A = 1$, as $\$_A(\tau_A = -1, \tau_B = 1, \gamma)$ is now higher than $\$_A(\tau_A = 1, \tau_B = 1, \gamma) = \$_{22}$. The specific value of γ_1 can therefore be calculated using the following equation:

$$\$_{22} - \$_A(\tau_A = -1, \tau_B = 1, \gamma_1) = 0 \tag{B.19}$$

A rather comprehensive calculation results in the following expression:

$$\$_{22} - 4\,\$_{21}\left(\sin(\frac{\gamma_1}{2})\right)^2\left(\cos(\frac{\gamma_1}{2})\right)^2 - \$_{12}\left[\left(\sin(\frac{\gamma_1}{2})\right)^2 - \left(\cos(\frac{\gamma_1}{2})\right)^2\right]^2 = 0$$

The solution of this equation finally gives:

$$\begin{aligned} \gamma_1 &= 2\arctan(\mathcal{Y}, \mathcal{X}) \qquad (B.20)\\ \mathcal{Y} &:= -\frac{\sqrt{(\$_{12} - \$_{21})\left(\$_{12} - \$_{21} + \sqrt{(\$_{21})^2 - \$_{21}\$_{12} - \$_{21}\$_{22} + \$_{12}\$_{22}}\right)}}{\sqrt{2}\,(\$_{12} - \$_{21})}\\ \mathcal{X} &:= \sqrt{\frac{\$_{21} - \$_{12} + \sqrt{(\$_{21})^2 - \$_{21}\$_{12} - \$_{21}\$_{22} + \$_{12}\$_{22}}}{\sqrt{2}\,(\$_{21} - \$_{12})}} \end{aligned}$$

B.V.2. Entanglement threshold γ_2

In the following it is supposed, that (for low values of entanglement) the underlying game has semi classical-quantum NE at the strategy combination $(\tau_A = 1, \tau_B = -1)$. The entanglement threshold γ_2 is defined as the entanglement barrier, for which the new quantum NE at $(\tau_A = -1, \tau_B = -1)$ appears. For $\gamma \geq \gamma_2$, the best response to the strategy $\tau_B = -1$ for player A is no longer the strategy $s_2^A \hat{=} \tau_A = 1$, as $\$_A(\tau_A = -1, \tau_B = -1, \gamma)$ is now higher than $\$_A(\tau_A = 1, \tau_B = -1, \gamma)$. The specific value of γ_2 can therefore be calculated using the following equation:

$$\$_A(\tau_A = 1, \tau_B = -1, \gamma_2) - \$_A(\tau_A = -1, \tau_B = -1, \gamma_2) = 0 \tag{B.21}$$

Again, a rather comprehensive calculation results in the following expression:

$$\$_{11} - 4\,\$_{12}\left(\sin(\frac{\gamma_2}{2})\right)^2\left(\cos(\frac{\gamma_2}{2})\right)^2 - \$_{21}\left[\left(\cos(\frac{\gamma_2}{2})\right)^2 - \left(\sin(\frac{\gamma_2}{2})\right)^2\right]^2 = 0$$

The solution of this equation finally gives:

$$\begin{aligned} \gamma_2 &= 2\arccos\left(\mathcal{Z}\right) \qquad \text{(B.22)} \\ \mathcal{Z} &:= \frac{\sqrt{(\$_{21}-\$_{12})\left(\$_{21}-\$_{12}+\sqrt{(\$_{12})^2-\$_{21}\$_{12}+\$_{21}\$_{11}-\$_{12}\$_{11}}\right)}}{\sqrt{2}\,(\$_{21}-\$_{12})} \end{aligned}$$

B.VI. Results for symmetric (2x2) quantum games

Description of figure B.19

Payoff surfaces of player A as a function of the reduced s_1-quantum strategies τ_A and τ_B for different strength of entanglement γ using the parameter setting Set_1. The diagrams where calculated using the following entanglement values: $\gamma = 0$ (upper left picture), $\gamma = \frac{\pi}{10}$ (upper right picture), $\gamma = \frac{\pi}{5}$ (middle left picture), $\gamma = \frac{3\pi}{10}$ (middle right picture), $\gamma = \frac{2\pi}{5}$ (lower left picture) and $\gamma = \frac{\pi}{2}$ (lower right picture). As outlined in subsection 2.4.3 the dominant strategy within the non-entangled game is at $(\tau_A = 1, \tau_B = 1)$ which corresponds to the classical dominant strategy (s_2^A, s_2^B) of parameter setting Set_1. Due to the absence of a dilemma, an increase of entanglement does not change the structure of the existing Nash equilibria and dominant strategy of the game and as a result the γ-thresholds (see appendix B.V) do not exist.

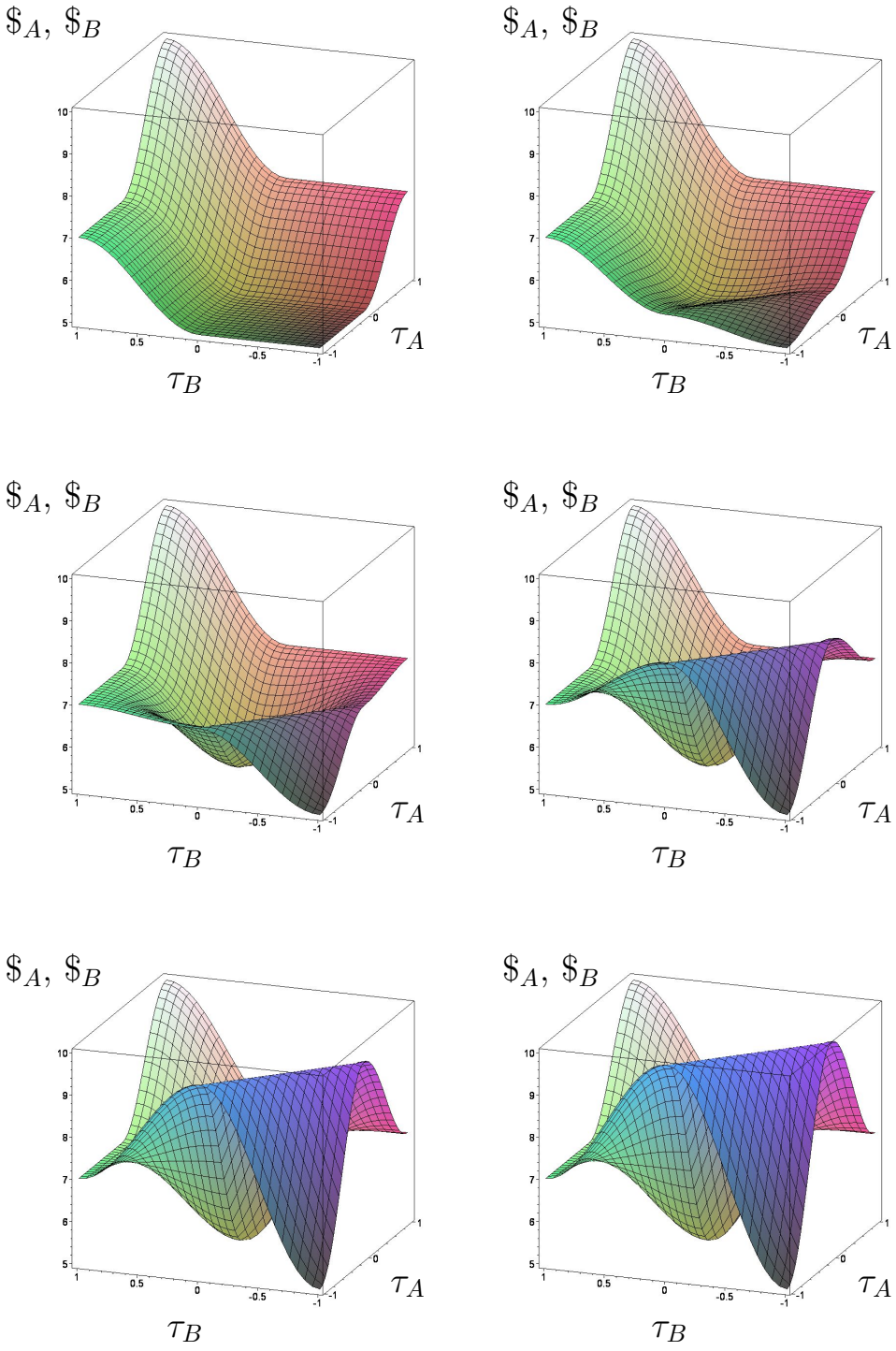

Figure B.19.: Results for the quantum game of parameter setting Set_1.

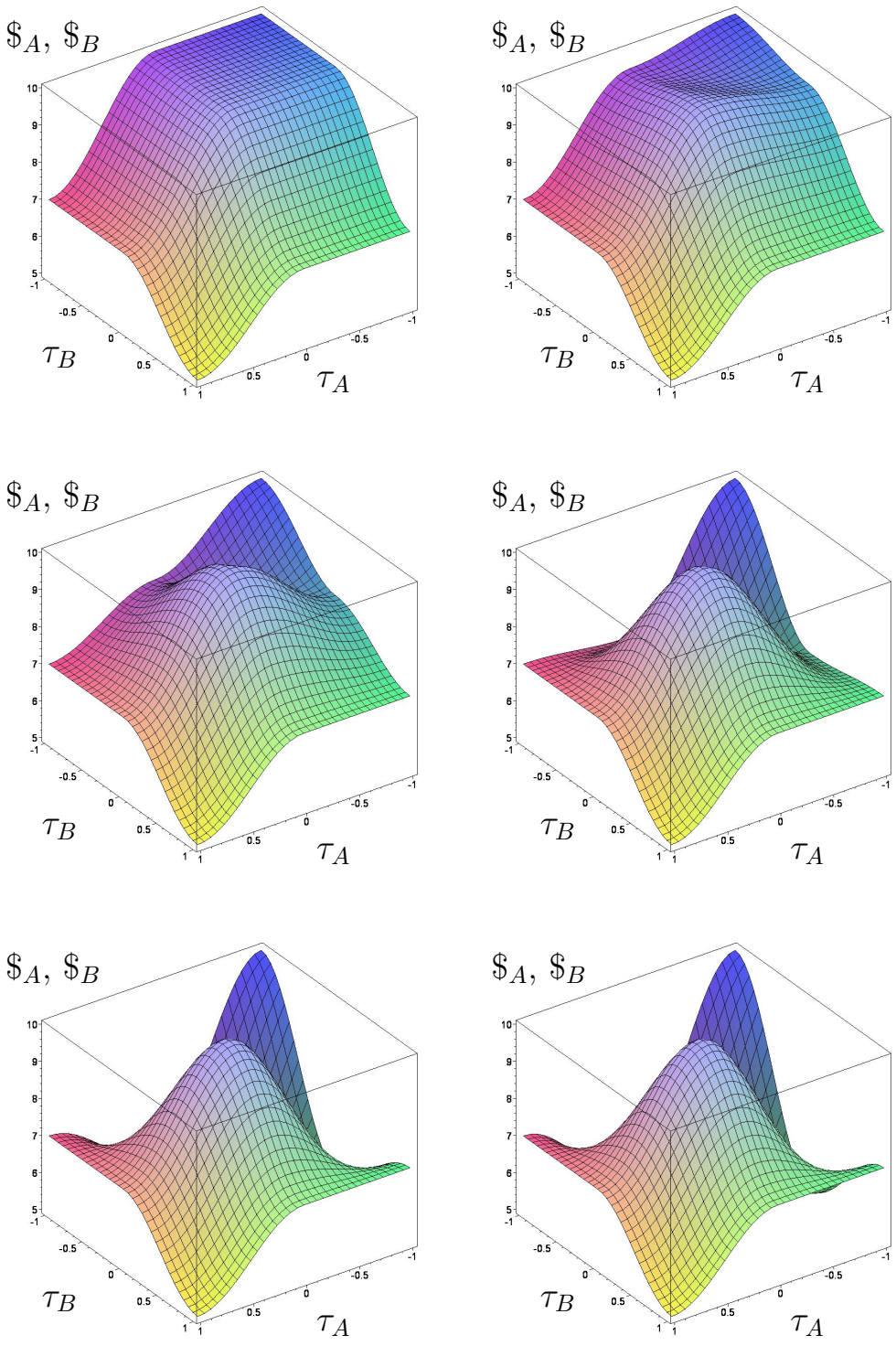

Figure B.20.: Results for the quantum game of parameter setting Set_2.

Description of figure B.20

Payoff surfaces of player A as a function of the reduced s_1-quantum strategies τ_A and τ_B for different strength of entanglement γ using the parameter setting Set_2. The diagrams where calculated using the same γ-values as figure B.19. As outlined in subsection 2.4.3 the dominant strategy within the non-entangled game is at $(\tau_A = 0, \tau_B = 0)$ which corresponds to the classical dominant strategy (s_1^A, s_1^B) of parameter setting Set_2. Due to the absence of a dilemma, an increase of entanglement does not change the structure of the existing Nash equilibria and dominant strategy of the game and as a result the γ-thresholds (see appendix B.V) do not exist.

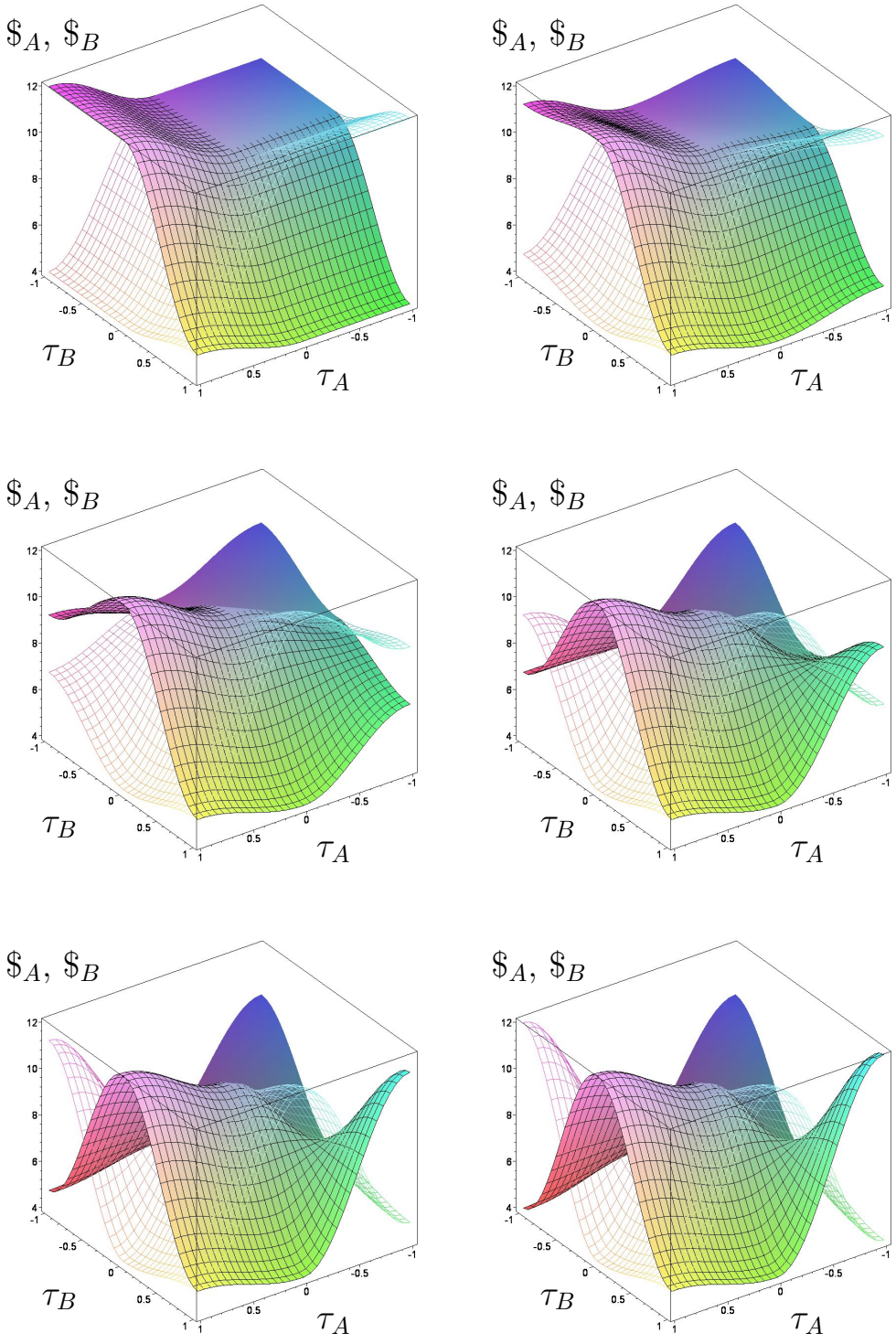

Figure B.21.: Results for the quantum game of parameter setting Set_3.

Description of figure B.21

Payoff surface of player A (solid) and player B (wired) as a function of their reduced s_1-quantum strategies τ_A and τ_B for different strength of entanglement γ using the parameter setting Set_3. The diagrams where calculated using the same γ-values as figure B.19. As outlined in subsection 2.4.3 the dominant strategy within the non-entangled game is at $(\tau_A = 0, \tau_B = 0)$, which corresponds to the classical dominant strategy (s_2^A, s_2^B) of parameter setting Set_3. The entanglement barrier for which the classical NE dissolves is $\gamma_1 \approx 0.3614$, whereas the entanglement threshold for which the new quantum NE at $(\tau_A = -1, \tau_B = -1)$ appears is $\gamma_2 \approx 0.5236$. Players with a strategic entanglement value $\gamma \geq \gamma_2$ escape the dilemma as they see the advantage of the quantum strategy combination $(\widehat{Q}_A, \widehat{Q}_B)$, which is observed (measured) as both are playing the classical strategy s_1.

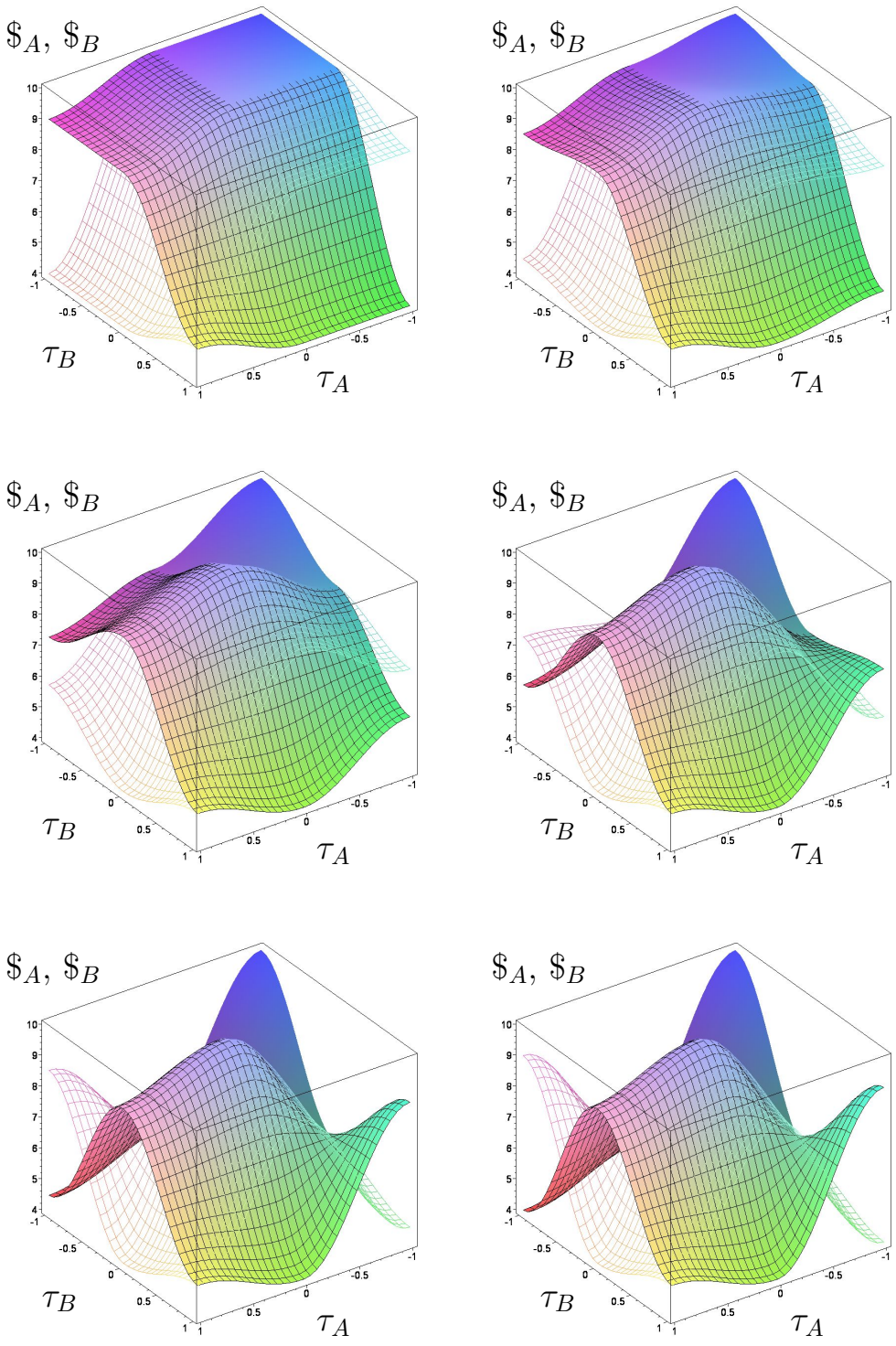

Figure B.22.: Results for the quantum game of parameter setting Set_4.

Description of figure B.22

Payoff surface of player A (solid) and player B (wired) as a function of their reduced s_1-quantum strategies τ_A and τ_B for different strength of entanglement γ using the parameter setting Set_4. The diagrams where calculated using the same γ-values as figure B.19. The non-entangled quantum game is identical to the classical version of the underlying coordination game parameterized trough parameter setting Set_4. For the case, that both players decide to play a quantum strategy $(\tau_A < 0 \wedge \tau_B < 0)$ their payoff is equal to the case where both players choose the classical pure strategy s_1 ($\$_A(\tau_A = 0, \tau_B = 0) = 10$), with the overall highest possible payoff. The classical pure Nash equilibria correspond to the following τ-values: $(s_1^A, s_1^B) \hat{=} (\tau_A = 0, \tau_B = 0)$ and $(s_2^A, s_2^B) \hat{=} (\tau_A = 1, \tau_B = 1)$, whereas the classical mixed strategy equilibrium is at: $\tau^\star = \frac{2}{\pi}\arccos(\sqrt{\frac{1}{2}})$. Even for tiny values of entanglement a new quantum NE appears $(\widehat{Q}, \widehat{Q} \hat{=} (\tau_A = -1, \tau_B = -1))$. The entanglement barrier for which the low payoff classical NE dissolves is $\gamma_1 \approx 0.4636$. For $\gamma \geq \gamma_1$ the game's only NE and ESS is the new quantum ESS.

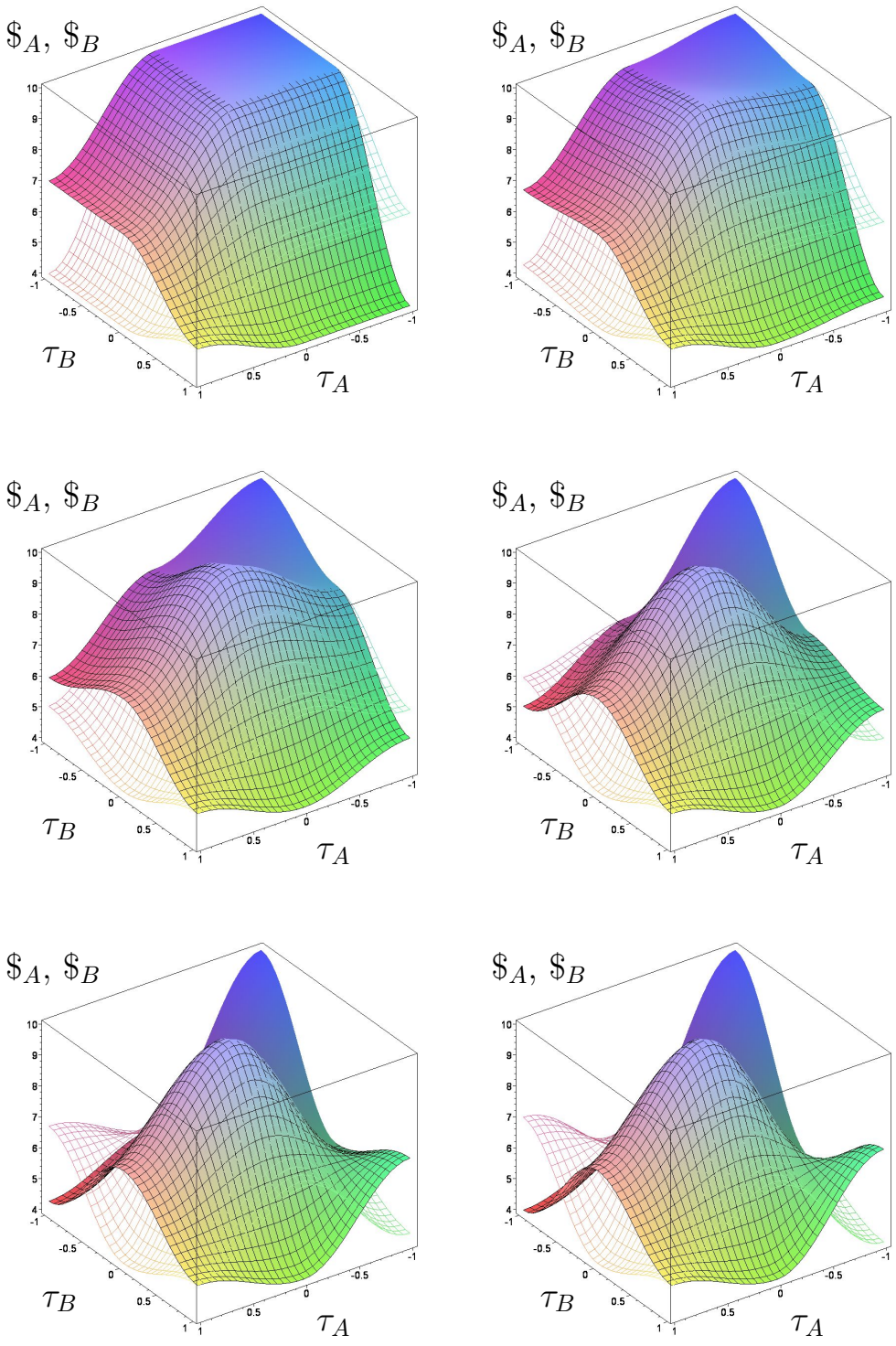

Figure B.23.: Results for the quantum game of parameter setting Set_5.

Description of figure B.23

Payoff surface of player A (solid) and player B (wired) as a function of their reduced s_1-quantum strategies τ_A and τ_B for different strength of entanglement γ using the parameter setting Set_5. The diagrams where calculated using the same γ-values as figure B.19. As outlined in subsection 2.4.3, the non-entangled quantum game is identical to the classical version of the underlying coordination game parameterized trough parameter setting Set_5. For the case, that both players decide to play a quantum strategy ($\tau_A < 0 \wedge \tau_B < 0$) their payoff is equal to the case where both players choose the classical pure strategy s_1 ($\$_A(\tau_A = 0, \tau_B = 0) = 10$), with the overall highest possible payoff. The classical pure Nash equilibria correspond to the following τ-values: $(s_1^A, s_1^B) \hat{=} (\tau_A = 0, \tau_B = 0)$ and $(s_2^A, s_2^B) \hat{=} (\tau_A = 1, \tau_B = 1)$, whereas the classical mixed strategy equilibrium is at: $\tau^\star = \frac{2}{\pi}\arccos(\sqrt{\frac{1}{4}})$. Even for tiny values of entanglement a new quantum NE appears ($\widehat{Q}, \widehat{Q} \hat{=} (\tau_A = -1, \tau_B = -1)$). The entanglement barrier for which the low payoff classical NE dissolves is $\gamma_1 \approx 0.6155$. For $\gamma \geq \gamma_1$ the game's only NE and ESS is the new quantum ESS.

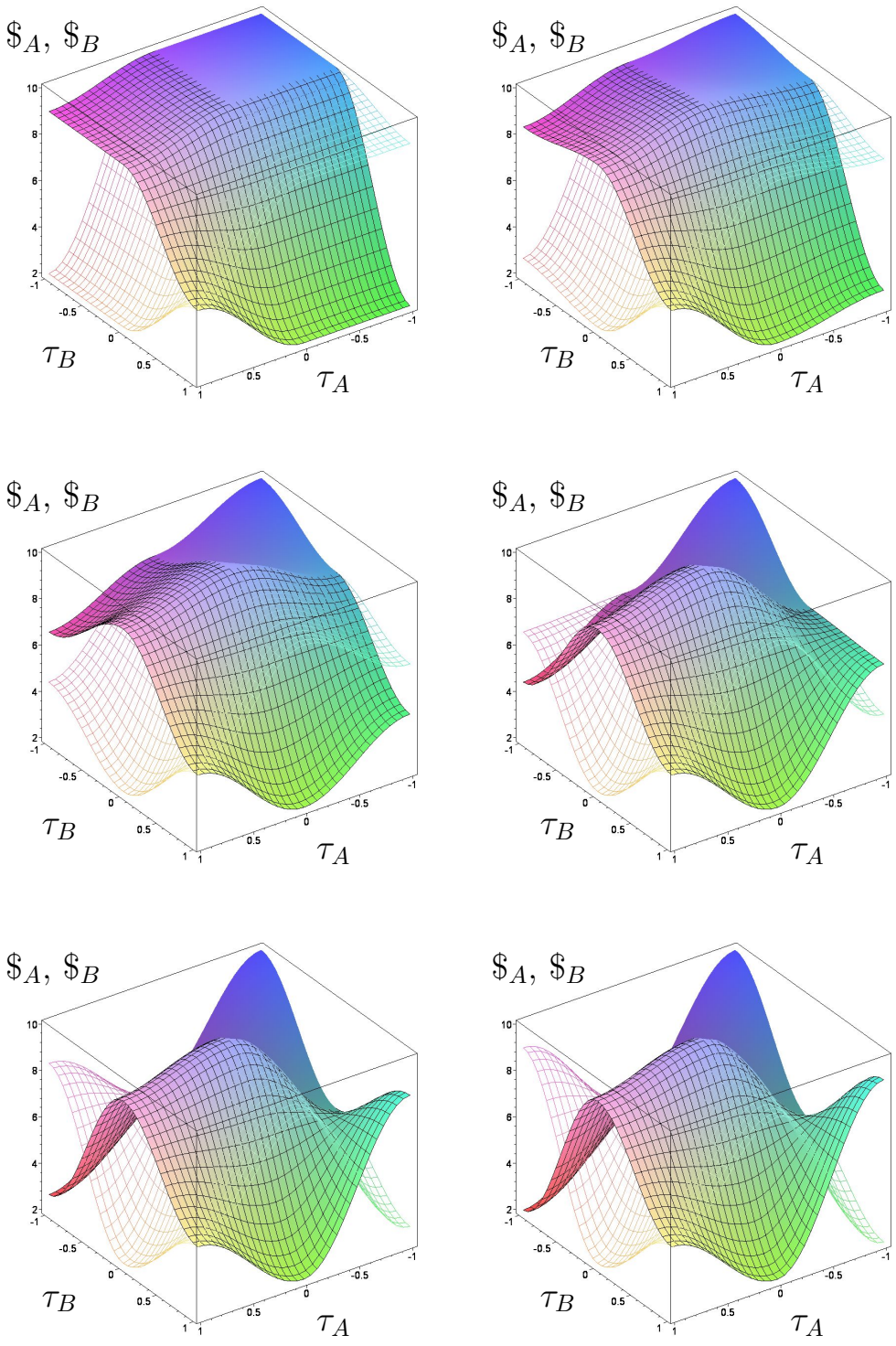

Figure B.24.: Results for the quantum game of parameter setting Set_6.

Description of figure B.24

Payoff surface of player A (solid) and player B (wired) as a function of their reduced s_1-quantum strategies τ_A and τ_B for different strength of entanglement γ using the parameter setting Set_6. The diagrams where calculated using the same γ-values as figure B.19. The non-entangled quantum game is identical to the classical version of the underlying coordination game parameterized trough parameter setting Set_6. For the case, that both players decide to play a quantum strategy $(\tau_A < 0 \wedge \tau_B < 0)$ their payoff is equal to the case where both players choose the classical pure strategy s_1 ($\$_A(\tau_A = 0, \tau_B = 0) = 10$), with the overall highest possible payoff. The classical pure Nash equilibria correspond to the following τ-values: $(s_1^A, s_1^B) \hat{=} (\tau_A = 0, \tau_B = 0)$ and $(s_2^A, s_2^B) \hat{=} (\tau_A = 1, \tau_B = 1)$, whereas the classical mixed strategy equilibrium is at: $\tau^\star = \frac{2}{\pi}\arccos(\sqrt{\frac{3}{4}})$. Even for tiny values of entanglement a new quantum NE appears $(\widehat{Q}, \widehat{Q} \hat{=} (\tau_A = -1, \tau_B = -1))$. The entanglement barrier for which the low payoff classical NE dissolves is $\gamma_1 \approx 0.7137$. For $\gamma \geq \gamma_1$ the game's only NE and ESS is the new quantum ESS.

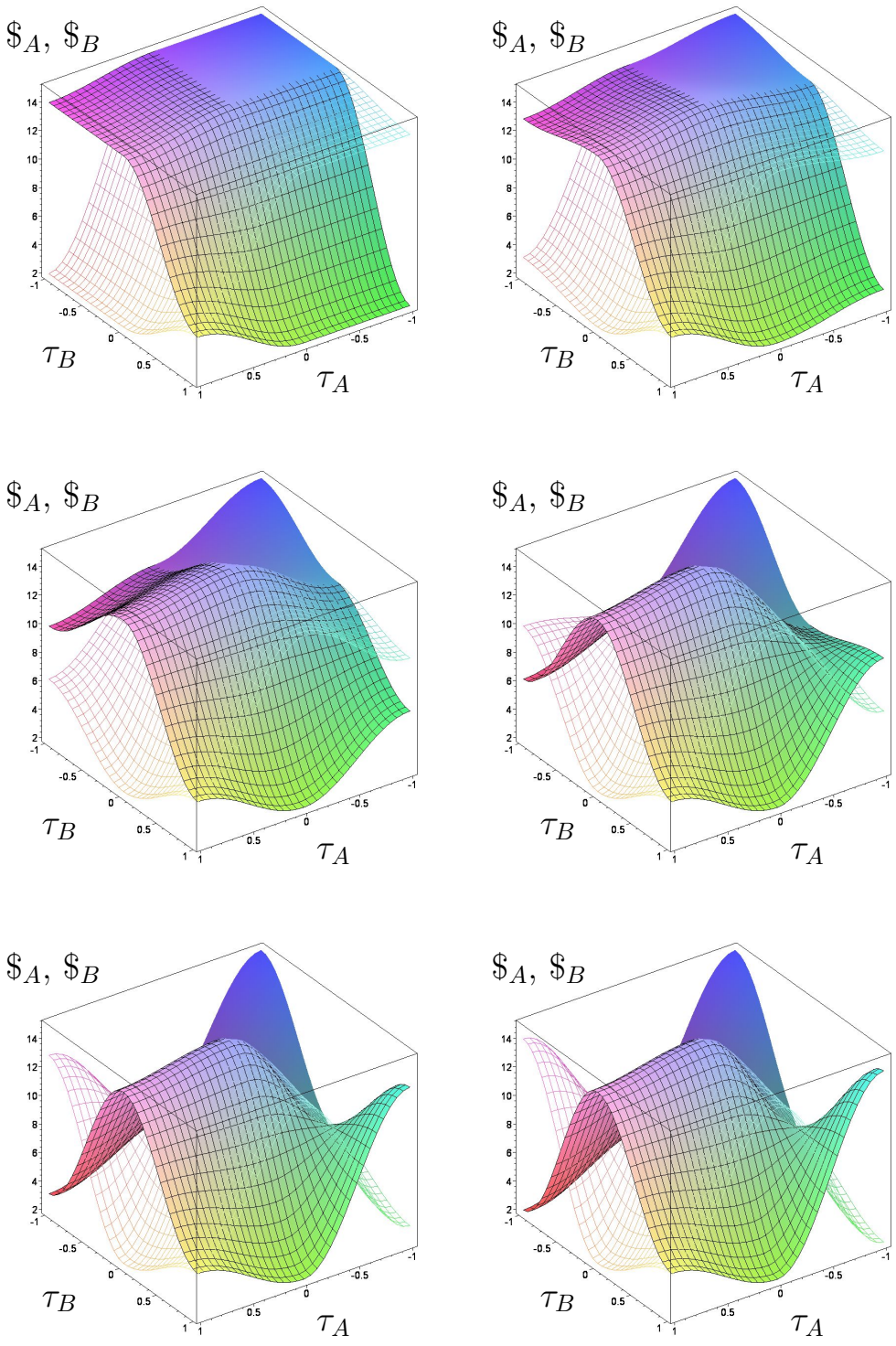

Figure B.25.: Results for the quantum game of parameter setting Set_7.

Description of figure B.25

Payoff surface of player A (solid) and player B (wired) as a function of their reduced s_1-quantum strategies τ_A and τ_B for different strength of entanglement γ using the parameter setting Set_7. The diagrams where calculated using the same γ-values as figure B.19. The non-entangled quantum game is identical to the classical version of the underlying coordination game parameterized trough parameter setting Set_7. For the case, that both players decide to play a quantum strategy $(\tau_A < 0 \wedge \tau_B < 0)$ their payoff is equal to the case where both players choose the classical pure strategy s_1 ($\$_A(\tau_A = 0, \tau_B = 0) = 10$), with the overall highest possible payoff. The classical pure Nash equilibria correspond to the following τ-values: $(s_1^A, s_1^B) \hat{=} (\tau_A = 0, \tau_B = 0)$ and $(s_2^A, s_2^B) \hat{=} (\tau_A = 1, \tau_B = 1)$, whereas the classical mixed strategy equilibrium is at: $\tau^\star = \frac{2}{\pi}\arccos(\sqrt{\frac{3}{4}})$. Even for tiny values of entanglement a new quantum NE appears $(\widehat{Q}, \widehat{Q} \hat{=} (\tau_A = -1, \tau_B = -1))$. The entanglement barrier for which the low payoff classical NE dissolves is $\gamma_1 \approx 0.5236$. For $\gamma \geq \gamma_1$ the game's only NE and ESS is the new quantum ESS. While the outcome predictions of the classical version of Set_6 and Set_7 are identical, the quantum versions give different results for both parameter sets. This fact illustrates that the existence of NE in quantum games is not invariant under linear payoff transformations (see table 2.1).

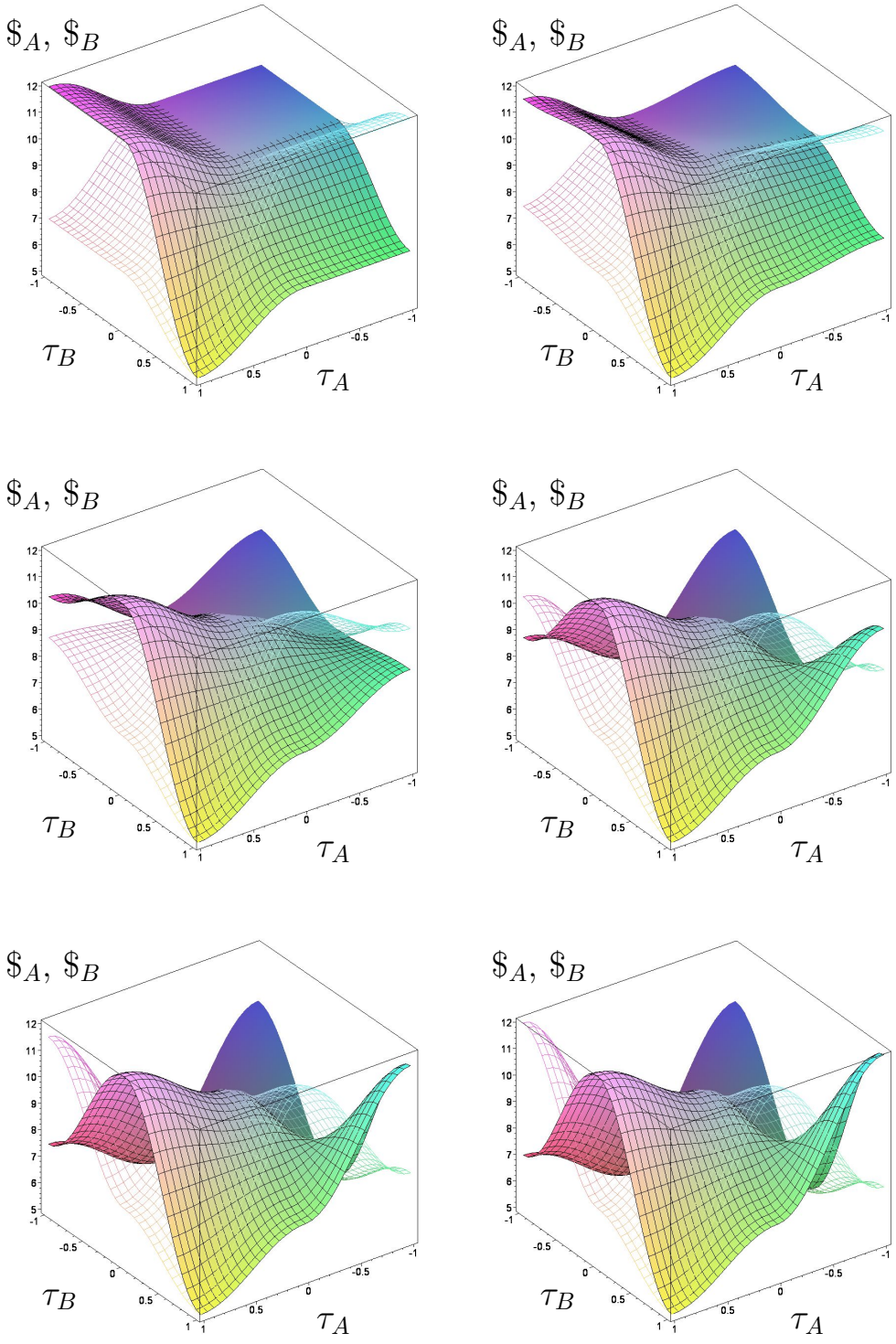

Figure B.26.: Results for the quantum game of parameter setting Set_8.

Description of figure B.26

Payoff surface of player A (solid) and player B (wired) as a function of their reduced s_1-quantum strategies τ_A and τ_B for different strength of entanglement γ using the parameter setting Set_8. The diagrams where calculated using the same γ-values as figure B.19. The non-entangled quantum game is identical to the classical version of the underlying anti-coordination game parameterized trough parameter setting Set_8. For the case, that both players decide to play a quantum strategy ($\tau_A < 0 \wedge \tau_B < 0$) their payoff is equal to the case where both players choose the classical pure strategy s_1 ($\$_A(\tau_A = 0, \tau_B = 0) = 10 = \$_B(\tau_A = 0, \tau_B = 0)$). The classical pure, asymmetric Nash equilibria correspond to the following τ-values: $(s_1^A, s_2^B) \hat{=} (\tau_A = 0, \tau_B = 1)$ and $(s_2^A, s_1^B) \hat{=} (\tau_A = 1, \tau_B = 0)$, whereas the classical mixed strategy equilibrium is at: $\tau^\star = \frac{2}{\pi}\arccos(\sqrt{\frac{1}{2}}) = \frac{1}{2}$. The results indicate, that beside the classical mixed strategy ESS a new quantum ESS appears at a specific γ-value ($\gamma_2 \approx 0.6847$).

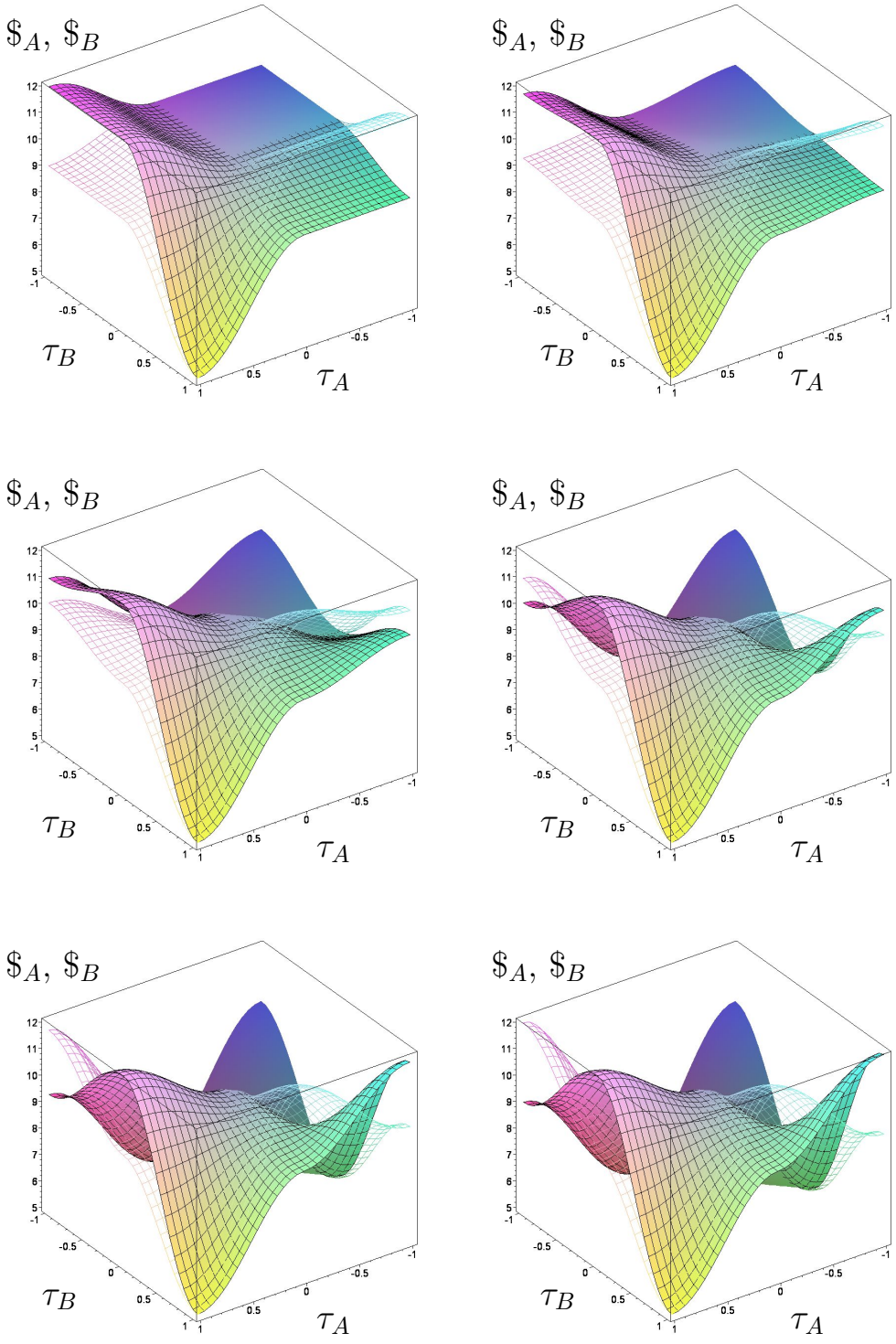

Figure B.27.: Results for the quantum game of parameter setting Set_9.

Description of figure B.27

Payoff surface of player A (solid) and player B (wired) as a function of their reduced s_1-quantum strategies τ_A and τ_B for different strength of entanglement γ using the parameter setting Set_9. The diagrams where calculated using the same γ-values as figure B.19. The non-entangled quantum game is identical to the classical version of the underlying anti-coordination game parameterized trough parameter setting Set_9. For the case, that both players decide to play a quantum strategy ($\tau_A < 0 \wedge \tau_B < 0$) their payoff is equal to the case where both players choose the classical pure strategy s_1 ($\$_A(\tau_A = 0, \tau_B = 0) = 10 = \$_B(\tau_A = 0, \tau_B = 0)$). The classical pure, asymmetric Nash equilibria correspond to the following τ-values: $(s_1^A, s_2^B) \hat{=} (\tau_A = 0, \tau_B = 1)$ and $(s_2^A, s_1^B) \hat{=} (\tau_A = 1, \tau_B = 0)$, whereas the classical mixed strategy equilibrium is at: $\tau^\star = \frac{2}{\pi}\arccos(\sqrt{\frac{2}{3}})$. The results indicate, that beside the classical mixed strategy ESS a new quantum ESS appears at a specific γ-value ($\gamma_2 \approx 0.9553$).

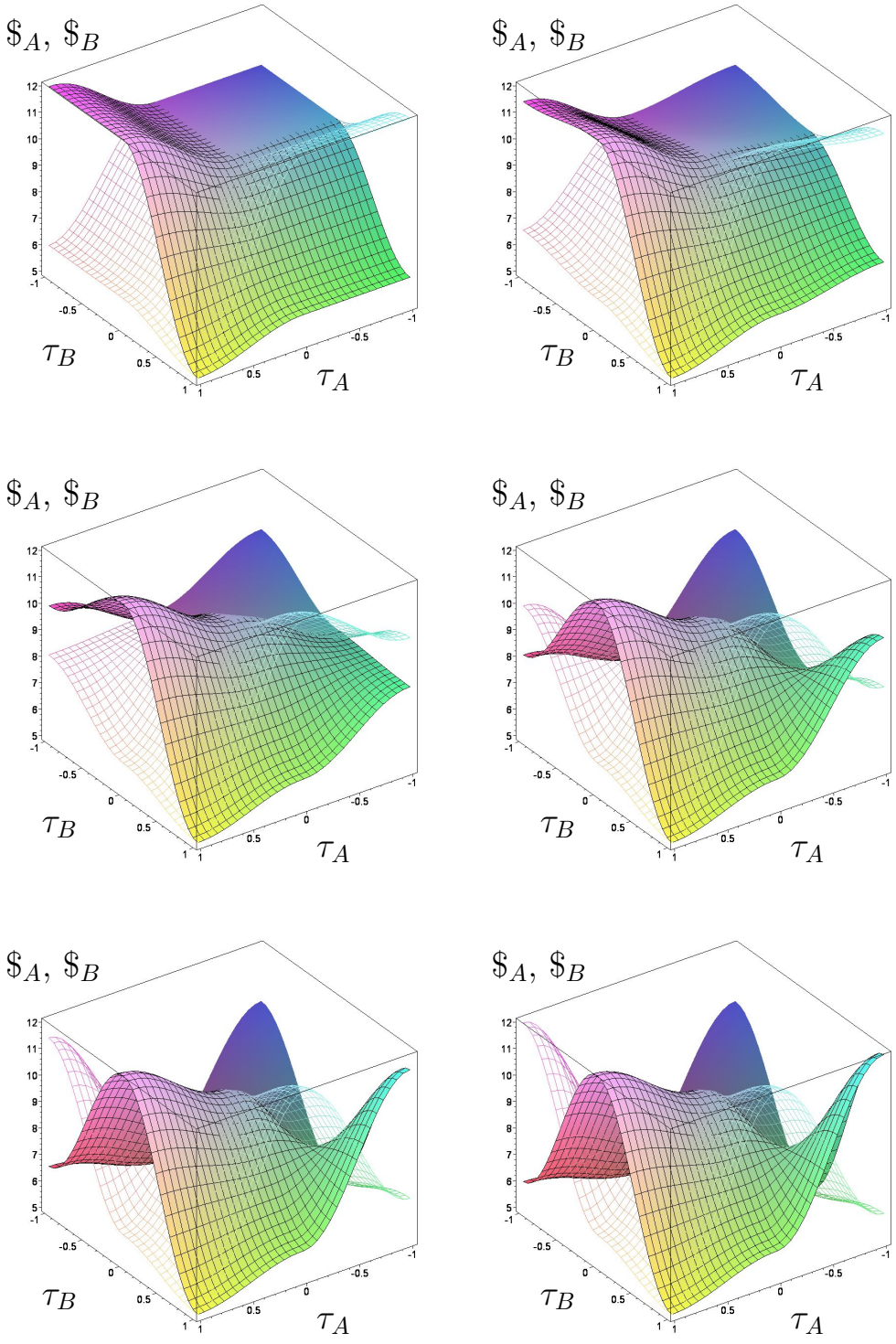

Figure B.28.: Results for the quantum game of parameter setting Set_{10}.

Description of figure B.28

Payoff surface of player A (solid) and player B (wired) as a function of their reduced s_1-quantum strategies τ_A and τ_B for different strength of entanglement γ using the parameter setting Set_{10}. The diagrams where calculated using the same γ-values as figure B.19. The non-entangled quantum game is identical to the classical version of the underlying anti-coordination game parameterized trough parameter setting Set_{10}. For the case, that both players decide to play a quantum strategy ($\tau_A < 0 \wedge \tau_B < 0$) their payoff is equal to the case where both players choose the classical pure strategy s_1 ($\$_A(\tau_A = 0, \tau_B = 0) = 10 = \$_B(\tau_A = 0, \tau_B = 0)$). The classical pure, asymmetric Nash equilibria correspond to the following τ-values: $(s_1^A, s_2^B) \hat{=} (\tau_A = 0, \tau_B = 1)$ and $(s_2^A, s_1^B) \hat{=} (\tau_A = 1, \tau_B = 0)$, whereas the classical mixed strategy equilibrium is at: $\tau^\star = \frac{2}{\pi}\arccos(\sqrt{\frac{1}{3}})$. The results indicate, that beside the classical mixed strategy ESS a new quantum ESS appears at a specific γ-value ($\gamma_2 \approx 0.6155$).

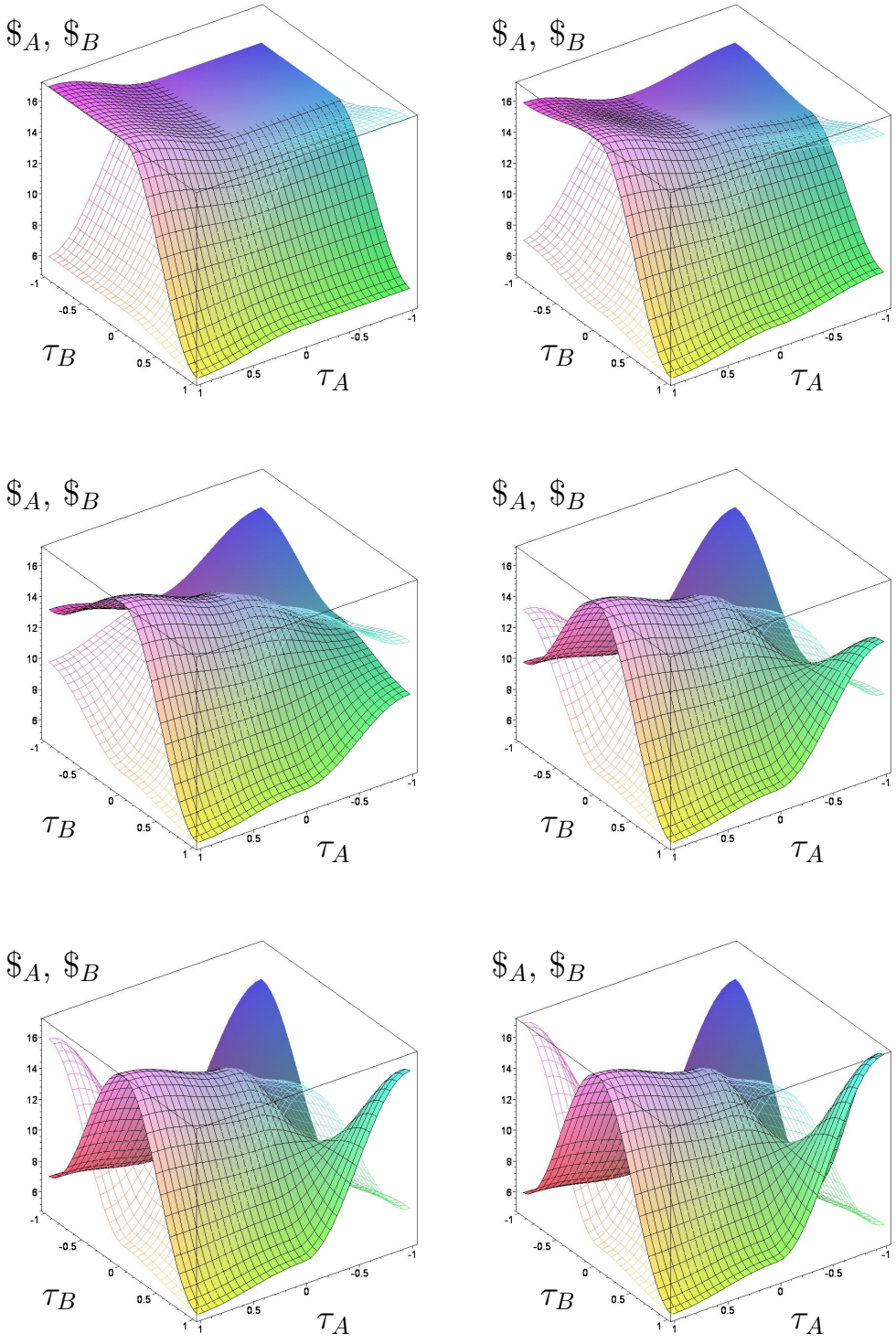

Figure B.29.: Results for the quantum game of parameter setting Set_{11}.

Description of figure B.29

Payoff surface of player A (solid) and player B (wired) as a function of their reduced s_1-quantum strategies τ_A and τ_B for different strength of entanglement γ using the parameter setting Set_{11}. The diagrams where calculated using the same γ-values as figure B.19. The non-entangled quantum game is identical to the classical version of the underlying anti-coordination game parameterized trough parameter setting Set_{11}. For the case, that both players decide to play a quantum strategy ($\tau_A < 0 \wedge \tau_B < 0$) their payoff is equal to the case where both players choose the classical pure strategy s_1 ($\$_A(\tau_A = 0, \tau_B = 0) = 10 = \$_B(\tau_A = 0, \tau_B = 0)$). The classical pure, asymmetric Nash equilibria correspond to the following τ-values: $(s_1^A, s_2^B) \hat{=} (\tau_A = 0, \tau_B = 1)$ and $(s_2^A, s_1^B) \hat{=} (\tau_A = 1, \tau_B = 0)$, whereas the classical mixed strategy equilibrium is at: $\tau^\star = \frac{2}{\pi}\arccos(\sqrt{\frac{1}{3}})$. The results indicate, that beside the classical mixed strategy ESS a new quantum ESS appears at a specific γ-value ($\gamma_2 \approx 0.4405$).

Bibliography

[1] *The handbook of experimental economics*. Princeton Univ. Press, Princeton, N.J, 1995.

[2] 5th frankfurt scientific symposium: Is there any progress in alternative publishing? 2004. http://wiap.wiwi.uni-frankfurt.de/5thsymp/.

[3] Zwischenberichte, DFG-Projekt WIAP. 2006.

[4] Abschlussbericht: DFG-Projekt WIAP. 2007.

[5] Verlängerungsantrag (Projekt WIAP). 2007.

[6] Abschlussbericht: DFG-Projekt WIAP (Verlängerungsphase). 2008.

[7] Zwischenbericht: DFG-Projekt WIAP (Verlängerungsphase). 2008. .

[8] D. Aerts. Quantum particles as conceptual entities: A possible explanatory framework for quantum theory. *Foundations of science*, 14(4):361–411, 2009.

[9] D. Aerts. Quantum structure in cognition. *Journal of Mathematical Psychology*, 53(5):314–348, 2009.

[10] D. Aerts. A potentiality and conceptuality interpretation of quantum physics. *Arxiv preprint arXiv:1005.3767*, 2010.

[11] D. Aerts. Interpreting quantum particles as conceptual entities. *International Journal of Theoretical Physics*, pages 1–21, 2010.

[12] D. Aerts, S. Aerts, J. Broekaert, and L. Gabora. The violation of Bell inequalities in the macroworld. *Foundations of Physics*, 30(9):1387–1414, 2000.

[13] D. Aerts, S. Aerts, and L. Gabora. Experimental evidence for quantum structure in cognition. *Quantum Interaction*, pages 59–70, 2009.

[14] D. Aerts, J. Broekaert, and L. Gabora. A case for applying an abstracted quantum formalism to cognition. *New Ideas in Psychology*, 2010.

[15] D. Aerts and B. D'Hooghe. Classical logical versus quantum conceptual thought: Examples in economics, decision theory and concept theory. *Quantum Interaction*, pages 128–142, 2009.

[16] D. Aerts and B. D'Hooghe. A quantum-conceptual explanation of violations of expected utility in economics. *Arxiv preprint arXiv:1004.2525*, 2010.

[17] D. Aerts, B. D'Hooghe, and E. Haven. Quantum Experimental Data in Psychology and Economics. *Int. J. Theor. Phys.*, 49:2971–2990, 2010.

[18] Reka Albert and Albert-Laszlo Barabasi. Statistical mechanics of complex networks. *Reviews of Modern Physics*, 74:47, 2002. cond-mat/0106096.

[19] Reka Albert, Hawoong Jeong, and Albert-Laszlo Barabasi. The diameter of the world wide web. *Nature*, 401:130, 1999. cond-mat/9907038.

[20] J.B. Altepeter, M.A. Hall, M. Medic, M. Patel, D.A. Meyer, and P. Kumar. Experimental Realization of a Multi-Player Quantum Game. In *Nonlinear Optics: Materials, Fundamentals and Applications*. Optical Society of America, 2009.

[21] Erwin Amann. *Evolutionäre Spieltheorie*. Physica-Verlag, 1999.

[22] James Andreoni and John H. Miller. Rational Cooperation in the Finitely Repeated Prisoner's Dilemma: Experimental Evidence. *The Economic Journal*, 103(418):570–585, 1993.

[23] R. Axelrod. *The complexity of cooperation: Agent-based models of conflict and cooperation*. The Princeton University Press, Princeton, 1997.

[24] Petro Dal B*ó*. Cooperation under the Shadow of the Future: Experimental Evidence from Infinetely Repeated Games. *The American Economic Review*, 95(5):1591–1604, 2005.

[25] Petro Dal B*ó* and Guillaume R.Fréchette. The Evolution of Cooperation

in Infinitely Repeated Games: Experimental Evidence. *Working Paper*, 2007. e-print.

[26] E. Ben-Porath and M. Kahneman. Communication in Repeated Games with Costly Monitoring. *Games and Economic Behavior*, 44:227–250, 2003.

[27] Simon C. Benjamin and Patrick M. Hayden. Coment on "quantum games and quantum strategies". *Physical Review Letters*, 87(6):69801, 2001. arXiv:quant-ph/0003036v1.

[28] Simon C. Benjamin and Patrick M. Hayden. Multi-player quantum games. *Physical Review A*, 64:030301, 2001. arXiv:quant-ph/0007038v2.

[29] S. Bernius and M. Hanauske. WI - Schlagwort: Open Access. *Wirtschaftsinformatik*, 49:456–459, 2007.

[30] S. Bernius and M. Hanauske. Open Access to Scientific Literatur - Increasing citations as an incentive for authors to make their publications freely accessible. 2009. In: Proceedings of the 42. Annual Hawaii International Conference on System Sciences (CD-ROM), Computer Society Press.

[31] S. Bernius, M. Hanauske, B. Dugall, and W. König. Exploring the Effects of a Transition to Open Access: Insights from a Simulation Study. 2010. submitted to JASIST.

[32] S. Bernius, M. Hanauske, R. Fladung, and B. Dugall. Determinanten des Zeitschriftenpreises - Eine explorative Studie der Zusammenhänge zwischen dem Preis einer wissenschaftlichen Zeitschrift und den Kennzahlen Journal Impact Factor, Zitate, Nutzung und Preis. *ABI-Technik*, 26:38–54, 2006.

[33] S. Bernius, M. Hanauske, W. König, and B. Dugall. Open Access Modells and their Implications for the Players on the Scientific Publishing Market. *Economic Analysis and Policy (EAP)*, 39:103–115, 2009. EAP.

[34] Matthias Blonski, Peter Ockenfels, and Giancarlo Spagnolo. Co-operation in Infinitely Repeated Games: Extending Theory and Experimental Evidence. *Working Paper*, 2007. e-print.

[35] S. Boccaletti, V. Latora, Y. Moreno, M. Chavez, and D.-U. Hwang. Complex networks: Structure and dynamics. *Physics Reports*, 424:175–308, 2006.

[36] Iris Bohnet and S. Bruno Frey. Social Distance and other-regarding Behavior in Dictator Games: Comment. *American Economic Review*, 89(1), 1999.

[37] M. Bonitz, E. Bruckner, and Andrea Scharnhorst. Characteristics and impact of the matthew effect for countries. *Scientometrics*, 40(3), 1997.

[38] A. Brandenburger. The relationship between quantum and classical correlation in games. *Games and Economic Behavior*, 69(1):175–183, 2010.

[39] P. Bruza, J.R. Busemeyer, and L. Gabora. Introduction to the special issue on quantum cognition. *Journal of Mathematical Psychology*, 53(5):303–305, 2009.

[40] J. Busemeyer. Introduction to Quantum Probability for Social and Behavioral Scientists. *Quantum Interaction*, pages 1–2, 2009.

[41] J. Busemeyer and R. Franco. What is The Evidence for Quantum Like Interference Effects in Human Judgments and Decision Behavior? *Neuro-Quantology*, 8(4):S48, 2010.

[42] J.R. Busemeyer, Z. Wang, and J.T. Townsend. Quantum dynamics of human decision-making. *Journal of Mathematical Psychology*, 50(3):220–241, 2006.

[43] D. Butler. Open-access journal hits rocky times. *Nature*, 44:914, 2006.

[44] Colin Camerer. *Behavioral game theory experiments in strategic interaction.* Russell Sage [u.a.], New York [u.a.], 2003.

[45] C. Chang. Business models for open access journals publishing. *Online Information Review*, 30 (6):699–713, 2006.

[46] G. Charness, G. R. Fréchette, and Cheng-Zhong Qin. Endogenous transfers in the Prisoner's Dilemma gama: An experimental test of cooperation and coordination. *Games and Economic Behavior*, 60:287–306, 2007.

[47] R. Chellappa and N. Saraf. Alliances, Rivalry and Firm Performance in Enterprise Systems Software Markets: A Social Network Approach. *Information Systems Research*, 2010. (forthcoming).

[48] Kay-Yut Chen, T. Hogg, and R. Beaulsoleil. A Quantum Treatment of Public Goods Economics. *Quantum Information Processing*, 1(6), 2002.

[49] Kay-Yut Chen and Tad Hogg. How well do people play a quantum prisoner's dilemma? *Quant.Inf.Process.*, 5:43–67, 2006.

[50] Q. Chen, Y. Wang, J.T. Liu, and K.L. Wang. N-player quantum minority game. *Physics Letters A*, 327(2-3):98–102, 2004.

[51] C. Clemens and T. Riechmann. Evolutionary Dynamics in Public Good Games. *Computational Economics*, 28:399–420, 2006.

[52] R. Cressman. *Evolutionary Dynamics and Extensive Form Games*. MIT Press, 2003.

[53] R. Crow. The case for institutional repositories. a sparc position paper. *The Scholarly Publishing & Academic Resources Coalition, Washington, D.C.*, 2002.

[54] R. Crow and H. Goldstein. Guides to Business Planning for Launching a New Open Access Journal. *Open Society Institute, Edition 2*, 2003. pdf.

[55] J.A. de Barrosa and P. Suppes. Quantum mechanics, interference, and the brain. *Journal of Mathematical Psychology*, 53:306–313, 2009.

[56] J.J. de Farias Neto. Quantum Battle of Sexes Revisited. 2009. arXiv:quant-ph/0408019.

[57] T. Dewett and A.S. Denisi. *Scientometrics*, 60:249, 2004.

[58] Anne-Ly Do and Thilo Gross. Patterns of cooperation: fairness and coordination in networks of interacting agents. arXiv:0902.2954v2.

[59] K. Dopfer. *Evolutionary economics: program and scope*. Kluwer Academic Publishers, Boston, 2001.

[60] G. Dosi and R. R. Nelson. An introduction to evolutionary theories in economics. *Journal of Evolutionary Economics*, 4:153–172, 1994.

[61] J. Du, X. Xu, H. Li, X. Zhou, and R. Han. Entanglement playing a dominating role in quantum games. *Physics Letters A*, 289(1-2):9–15, 2001.

[62] Jiangfeng Du, Hui Li, Xiaodong Xu, Mingjun Shi, Jihui Wu, Xianyi Zhou, and Rongdian Han. Experimental realization of quantum games on a quantum computer. *Physical Review Letters*, 88:137902, 2002. arXiv:quant-ph/0104087v3.

[63] Holger Ebel and Stefan Bornholdt. Coevolutionary games on networks. *Physical Review E*, 66:056118, 2002.

[64] A. Einstein, B. Podolsky, and N. Rosen. Can Quantum-Mechanical Description of Physical Reality Be Considered Complete? *Physical Review*, 47:777–780, 1935.

[65] J. Eisert and M. Wilkens. Quantum games. *Journal of Modern Optics*, 47:2543, 2000. arXiv:quant-ph/0004076.

[66] J. Eisert, M. Wilkens, and M. Lewenstein. Quantum games and quantum strategies. *Physical Review Letters*, 83:3077, 1999. arXiv:quant-ph/9806088v3.

[67] Elinor Ostrom et al. A General Framework for Analyzing Sustainability of Social-Ecological Systems. *Science*, 325:419, 2009.

[68] Magnus Enquist and Stefano Ghirlanda. Evolution of social learning does not explain the origin of human cumulative culture. *Journal of Theoretical Biology*, 246:129–135, 2007.

[69] EU. Study on the economic and technical evolution of the scientific publication markets in europe. *DG Research*, 2006.

[70] Eysenbach. Citation advantage of open access articles. *PLoS Biol*, 4(5), 2006.

[71] Ernst Fehr and Simon Gächter. Fairness and Retaliation: The Economics of Reciprocity. *The Journal of Economic Perspectives*, 14(3):159, 2000.

[72] Rainer B. Fladung. *Scientific Communication.* ibidem-Verlag, 2007.

[73] Rainer B. Fladung, Berndt Dugall, and Wolfgang König. Ökonomie der elektronischen Literaturversorgung. *Wirtschaftsinformatik*, 46(4):256–272, 2004.

[74] Adrian P. Flitney and Derek Abbott. An introduction to quantum game theory. *Fluctuation and Noise Letters*, 2:R175, 2002. arXiv:quant-ph/0208069.

[75] A.P. Flitney and D. Abbott. An introduction to quantum game theory. *Fluctuation and Noise Letters*, 2(4):R175–R187, 2002.

[76] M. M. Flood. Some experimental games. *Management Science*, 5:5–26, 1958.

[77] Deutsche Forschungsgemeinschaft. Publication strategies in transformation? *DFG*, 2006.

[78] Hunter B. Fraser, Aaron E. Hirsh, Lars M. Steinmetz, Curt Scharfe, and Marcus W. Feldman. Evolutionary Rate in the Protein Interaction Network. *Science*, 296:750–752, 2002.

[79] D. Friedman. On economic applications of evolutionary game theory. *Journal of Evolutionary Economics*, 8:15–43, 1998.

[80] Fritz Söllner. *Die Geschichte des ökonomischen Denkens*. Springer, 2001.

[81] Vasyl V. Gafiychuk and Anatoliy K. Prykarpatsky. Replicator - Mutator Evolutionary Dynamics. *Journal of Nonlinear Mathematical Physics*, 11(3):350–360, 2004.

[82] Vasyl V. Gafiychuk and Anatoliy K. Prykarpatsky. Replicator Dynamics and Mathematical Description of Multi-Agent Interaction in Complex Systems. *Journal of Nonlinear Mathematical Physics*, 11(1):113–122, 2004.

[83] Tobias Galla. Independence and interdependence in the nest-site choice by honeybee swarms: Agent-based models, analytical approaches and pattern formation. *Journal of Theoretical Biology*, 262(1):186–196, 2010.

[84] L.S. Gao and B. Iyer. Partnerships between Software Firms: Is There Value from Complementarities? *HICSS Proceedings*, page 386, 2008.

[85] Markus M. Geipel and Frank Schweitzer. Software change dynamics: evidence from 35 java projects. 2009. Proceedings of the the 7th joint meeting of the European software engineering conference.

[86] M. Getz. Academic Pricing: Networks and Prices. *Proceedings of the ACRL 9th National Conference 1999*, 1999.

[87] J.B. Glattfelder and S. Battiston. Backbone of complex networks of corporations: The flow of control. *Phys. Rev. E*, 80:036104, 2009.

[88] W. Paul Glimcher. *Neuroeconomics: Decision making and the brain*. Academic Press, Amsterdam, 1. ed. edition, 2009.

[89] P. Gooden, M. Owen, and S. Simon. Scientific Publishing: Knowledge is Power. *Morgan Stanley Equity Research*, 2002. www-link.

[90] J. Orlin Grabbe. An introduction to quantum game theory, 2005. arXiv:quant-ph/0506219.

[91] W. Greiner. *Quantum Mechanics*. Springer, 1989.

[92] W. Greiner. *Thermodynamics and Statistical Physics*. Springer, 1989.

[93] Thilo Gross, Lars Rudolf, Simon A. Levin, and Ulf Dieckmann. Generalized Models Reveal Stabilizing Factors in Food Webs. *Science 7*, 325(5941):747 – 750, 2009.

[94] J. Guedon. The "green" and "gold" roads to open access: The case for mixing and matching. *Serials Review*, 30 (4):315–328, 2004.

[95] Esteban Guevara. Quantum Replicator Dynamics. *Physica A*, 369/2:393–407, 2006. arXiv:quant-ph/0510238v7.

[96] Esteban Guevara. Quantum Games and the Relationships between Quantum Mechanics and Game Theory. 2008. arXiv:0803.0292v1.

[97] Hong Guo, Juheng Zhang, and Gary J. Koehler. A survey of quantum games. *Decision Support Systems*, 46(1):318–332, 2008.

[98] K. Habermann and L. Habermann. An evolutionary game-theoretic approach to open access. 2009. arXiv:0903.4562v1.

[99] Kamalika Basu Hajra and Parongama Sen. Phase transitions in an aging network. *Physical Review E*, 70:056103, 2004. arXiv:cond-mat/0406332v1.

[100] Kamalika Basu Hajra and Parongama Sen. Aging in citation networks. *Physica A*, 346(1-2):44–48, 2005. arXiv:cond-mat/0409017v1.

[101] Kamalika Basu Hajra and Parongama Sen. Modelling aging characteristics in citation networks. *Physica A*, 368(2):575–582, 2006.

[102] M. Hanauske. Quanten-Spieltheorie und deren mögliche Anwendungsfelder. 2007. *Vortrag bei der Parmenides Foundation, München* (Folien des Vortrags).

[103] M. Hanauske. Open Access Geschäftsmodelle und evolutionär stabile Strategien (Open Access business models and evolutionary stable strategies). 2008. *Open-Access-Tage 2009 in Konstanz (07.10.2009)*, (Programm und Folien).

[104] M. Hanauske. Quantum Game Theory and Co-operation. 2008. *Vortrag im "Applied Microeconomics and Organisations Seminar", Frankfurt* (Folien des Vortrags).

[105] M. Hanauske. Quantum Game Theory and Co-operation. 2008. *Vortrag im "Applied Microeconomics and Organisations Seminar", Frankfurt*, (Folien des Vortrags).

[106] M. Hanauske. Quantum Game Theory and Cooperation. 2008. *Third World Congress of the Game Theory Society, Chicago(Evanston), USA, 13-17 July 2008*, (Folien des Vortrags).

[107] M. Hanauske. Über die Anwendbarkeit von Quanten-Spieltheoretischen Konzepten in realen 2x2-Entscheidungssituationen. 2008. *Vortrag im Rahmen der DPG Frühjahrstagung (Symposium Game theory in dynamical systems), Berlin* (Folien des Vortrags).

[108] M. Hanauske. Advances in Evolutionary Game Theory. 2009. *Lecture at the "Université Lumière Lyon 2" in Lyon, France (MINERVE Exchange Program); Slides and additional material.*

[109] M. Hanauske. Neue Entwicklungen in der evolutionären Spieltheorie. 2009. *Vorlesung im Rahmen des MINERVE Dozenten-Austauschprogramms an der "Université Lumière Lyon 2" in Lyon, Frankreich; Folien und diverse Zusatzmaterialien.*

[110] M. Hanauske. Evolutionary Quantum Game Theory. 2011. *PHD-Thesis.*

[111] M. Hanauske, S. Bernius, and B. Dugall. Quantum Game Theory and Open Access Publishing. *Physica A*, 382(2):650–664, 2007. arXiv:physics/0612234.

[112] M. Hanauske, S. Bernius, W. König, and B. Dugall. Experimental Validation of Quantum Game Theory. *Accepted paper at the conference "Logic and the Foundations of Game and Decision Theory" (LOFT 2008), Amsterdam*, 2008. arXiv:0707.3068v1.

[113] M. Hanauske, T. Huber, T.Kude, and et.al. Evolutionary Quantum Game Theory and Hubs- and Spoke-Networks. 2010. in preparation.

[114] M. Hanauske, J. Kunz, S. Bernius, and W. König. Doves and hawks in economics revisited: An evolutionary quantum game theory-based analysis of financial crises. *Physica A*, 389:5084 – 5102, 2009. arXiv:0904.2113, RePEc:pra:mprapa:14680 and SSRN_{id}:1597735.

[115] M. Hanauske, J. Kunz, and et.al. Quantum Game Theory and the Evolution of Social Norms in Firms. 2010. submitted to the *Journal of Economic Theory*.

[116] Matthias Hanauske. Black Holes and the German Reichstag. *Physics World*, 36(7):1947–1959, 2005.

[117] Matthias Hanauske. Evolutionary Game Theory and Complex Networks of Scientific Information. 2011. Article is going to be published as a chapter in the book *"Models of science dynamics - Encounters between complexity theory and information science"*, Spinger book in the Complexity series, Editors: Andrea Scharnhorst, Katy Börner and Peter van den Besselaar.

[118] Matthias Hanauske, Wolfgang König, and Berndt Dugall. Evolutionary Quantum Game Theory and Scientific Communication. 2010. Accepted article at the "Second Brasilian Workshop of the Game Theory Society", http://evolution.wiwi.uni-frankfurt.de/BWGT2010/.

[119] Matthias Hanauske and Sebastian Schäfer. Fellow-Feeling and Cooperation (A quantum game theory-based analysis of a prisoner's dilemma experiment). 2009. The article has been originated from the phd-seminar „Experimental Economics" organised by Prof. Kosfeld, (unpublished).

[120] C. B. Harley. Learning the evolutionary stable strategy. *J. Theoret. Biol.*, 89:611–633, 1981.

[121] William Harms and Brian Skyrms. Evolution of Moral Norms. Oxford Handbook on the Philosophy of Biology ed. Michael Ruse.

[122] Harnad and Brody. *D-Lib Magazine*, 10, 2004.

[123] S. Harnad. Fast-forward on the green road to open access: The case against mixing up green and gold. *Ariadne*, 42, 2005. www-link.

[124] C. Hauert, A. Traulsen, H. Brandt, M.A. Nowak, and K. Sigmund. Punishing and abstaining for public goods in finite populations. *Biological Theory*, 3:114, 2008.

[125] E.G. Hildalgo. The why of the applicability of statistical physics to economics. *arXiv:physics/0609088*.

[126] G. M. Hodgson. *Economics and Evolution: Bringing Life back into Economics*. The University of Michigan Press, Ann Arbor, 1993.

[127] J. Hofbauer. Evolutionary dynamics for bimatrix games: A Hamiltonian system? *Journal of Mathematical Biology*, 34:675–688, 1996.

[128] J. Hofbauer and K. Sigmund. Evolutionary game dynamics. *Bulletin of the American mathematical Society*, 40(4):479–519, 2003.

[129] Elizabeth Hoffman, Kevin McCabe, and L. Vernon Smith. Social Distance and Other-Regarding Behavior in Dictator Games. *The American Economic Review*, 86(3), 1996.

[130] A. (ed). Michael Hogg. *Social identity sociological and social psychological perspectives*. American Sociological Assoc., Washington, DC, 2003.

[131] T. Hogg, P. Harsha, and Kay-Yut Chen. Quantum Auctions. *Int. J. of Quantum Information*, 5:751–780, 2007.

[132] P. Huang, M. Ceccagnoli, C. Forman, and D.J. Wu. When Do ISVs Join a Platform Ecosystem? Evidence from the Enterprise Software Industry. *ICIS Proceedings*, 2009.

[133] B.A. Huberman and T. Hogg. Quantum solution of coordination problems. *Quantum Information Processing*, 2(6):421–432, 2003.

[134] Bernado A. Huberman and Tad Hogg. Quantum Solution of Coordination Problems. *Quantum Information Processing*, 2(6), 2003. arXiv:quant-ph/0306112v1.

[135] A. Iqbal and AH Toor. Evolutionarily stable strategies in quantum games. *Physics Letters A*, 280(5-6):249–256, 2001.

[136] Azhar Iqbal. Investigations in quantum games using EPR-type set-ups, 2006. arXiv:quant-ph/0604188.

[137] Azhar Iqbal and Derek Abbott. Non-factorizable joint probabilities and evolutionarily stable strategies in the quantum prisoner's dilemma game. *Physics Letters A*, 373(30):2537–2541, 2009. arXiv:0902.2889v2.

[138] Azhar Iqbal and A. H. Toor. Equilibria of Replicator Dynamics in Quantum Games. 2001. arXiv:quant-ph/0106135v2.

[139] M. A. Janssen and E. Ostrom. Governing Social-Ecological Systems.

[140] E. Joos, H. D. Zeh, C. Kiefer, D. Giulini, J. Kupsch, and I. O. Stamatescu. *Decoherence and the Appearance of a Classical World in Quantum Theory.* Springer, 2003.

[141] John F. Nash Jr. Equilibrium Points in N-person Games. *Proceedings of the National Academy of Sciences*, 36:48–49, 1950.

[142] John F. Nash Jr. The Bargaining Problem. *Econometrica*, 18:155–162, 1950.

[143] John F. Nash Jr. Non-Cooperative Games. *The Annals of Mathematics*, 54(2):286–295, 1951.

[144] John F. Nash Jr. Two-Person Cooperative Games. *Econometrica*, 21:128–140, 1953.

[145] J. H. Kagel and A. E. Roth. *Handbook os Experimental Economics.* Princeton University Press, 1995.

[146] M. Kandori. Introduction to Repeated Games with Private Monitoring. *Journal of Economic Theory*, 102:1–15, 2002.

[147] V. Kargin. On coordination games with quantum correlations. *International Journal of Game Theory*, 37(2):211–218, 2008.

[148] Benjamin Kerr, Margaret A. Riley, Marcus W. Feldman, and Brendan J. M. Bohannan. Local dispersal promotes biodiversity in a real-life game of rock paper scissors. *Nature*, 418, 2002.

[149] Markus Kinateder. Repeated Games Played in a Network. 2008. *Vortrag im "Applied Microeconomics and Organisations Seminar", Frankfurt* (Related online article).

[150] D. King and C. Tenopir. Evolving Journal Costs: implications for publishers, libraries, and readers. *Learned Publishing*, 12:251–258, 1999.

[151] E. Klarreich. Playing by quantum rules. *Nature*, 414(6861):244–245, 2001.

[152] W. König, S. Bernius, and M. Hanauske. Netzwerke in der Wissenschaft - Auswirkungen von Open Access auf die Verbreitung von Forschungsergebnissen. 2008. In: Kortzfleisch, Harald F. O.; Bohl, Oliver (Hrsg.): Wissen, Vernetzung, Virtualisierung ; Josef Eul Verlag, Lohmar.

[153] Michael Kosfeld, Ernst Fehr, and Jörgen W. Weilbull. The revealed Prisoners Dilemma Game. 2005. Unpublished, preliminary Version (December 2005).

[154] T. Kude and J. Dibbern. Tight versus Loose Organizational Coupling within Inter-Firm Networks in the Enterprise Software Industry. The Perspective of Complementors. *AMCIS Proceedings*, page 666, 2009.

[155] S.E. Landsburg. Quantum game theory. *Notices-American Mathematical Society*, 51(4):394–402, 2004.

[156] Lester B. Lave. An Empirical Approach to the Prisoner's Dilemma Game. *The Quarterly Journal of Economics*, 76(3):424–436, 1962.

[157] S. Lawrence. Free online availability substantially increases the paper's impact. *Nature*, 411(6837):521, 2001.

[158] S. Lehmann, B. Lautrup, and A. D. Jackson. Citation networks in high energy physics. *Physical Review E*, 68:026113, 2003. arXiv:physics/0211010.

[159] D.K. Levine. Quantum games have no news for economists. *Manuscript. Quarterly 45 pp*, 51:208–211, 2005.

[160] Z. Liao, G. Qin, L. Hu, S. Li, N. Xu, and J. Du. Static and evolutionary quantum public goods games. *Physics Letters A*, 372(20):3586–3590, 2008.

[161] T. R. Malthus. *An essay on the principle population as it aects the future improvement of society with remarks on the speculations of Mr. Godwin, M. Condorcet and other writers.* Johnson, London, 1798.

[162] Luca Marinatto and Tullio Weber. A quantum approach to static games of complete information. *Physics Letters A*, 272:291, 2000. arXiv:quant-ph/0004081v2.

[163] M.J. McCabe. Law Serials Pricing and Mergers: A Portfolio Approach. *Contributions to Economic Analysis and Policy*, 3:1, 2004.

[164] R. Vilela Mendes. Quantum Games and social norms: The quantum ultimatum game. *Quantum Information Processing*, 4:1–12, 2005. arXiv:quant-ph/0208167v1.

[165] David A. Meyer. Quantum strategies. *Physical Review Letters*, 82:1052, 1999. arXiv:quant-ph/9804010v1.

[166] Jacek Miekisz. Evolutionary game theory and population dynamics. 2007. arXiv:q-bio/0703062v1.

[167] J. K. Murnighan and A. E. Roth. Expecting Continued Play in Prisoner's Dilemma Games. *Journal of Conflict Resulution*, 27(2):279–300, 1983.

[168] A. Nawaz and AH Toor. Evolutionarily Stable Strategies in Quantum Hawk–Dove Game. *Chinese Physics Letters*, 27:050303, 2010.

[169] Ahmad Nawaz and A.H.Toor. Evolutionarily Stable Strategies in Quantum Hawk-Dove Game. 2001. arXiv:quant-ph/0108075v3.

[170] M. E. J. Newman. Spread of epidemic disease on networks. *Physical Review E*, 66:016128, 2002.

[171] Martin A. Nowak and Karl Sigmund. Bacterial game dynamics. *Nature*, 418, 2002.

[172] Martin A. Nowak and Karl Sigmund. Evolutionary Dynamics of Biological Games. *Science*, 303:793–799, 2003.

[173] A. Okerson. A Librarian's View of Some Economic Issues in Electronic Scientific Publishing. *Proceedings of the UNESCO Invitational Meeting on the Future of Scientific Information*, 1996. .

[174] M. J. Osborne and A. Rubinstein. *A course in game theory.* MIT Press, Cambridge, Massachusetts, 1994.

[175] Elinor Ostrom. Collective Action and the Evolution of Social Norms. *The Journal of Economic Perspectives*, 14:137–158, 2000.

[176] Novroz Papel. Quantum games: States of play. *Nature*, 445:144–146, 2007.

[177] Christina Pawlowitsch. Finite populations choose an optimal language. *Journal of Theoretical Biology*, 249:606–616, 2007.

[178] E. W. Piotrowski and J. Sladkowski. Quantum Market Games. *Physica A*, 312:208, 2002. arXiv:quant-ph/0104006v1.

[179] E. W. Piotrowski and Jan Sladkowski. The next stage: quantum game theory. *Progress in Mathematical Physics Research*, 2003. arXiv:quant-ph/0308027v1.

[180] E. W. Piotrowski and Jan Sladkowski. Quantum Game Theory in Finance. *Quantitative Finance*, 4:1–7, 2004. arXiv:quant-ph/0406129v1.

[181] E. W. Piotrowski and Jan Sladkowski. Quantum auctions: Facts and myths. *Physica A*, 387(15):3949–3953, 2008. arXiv:0709.4096v1.

[182] E.W. Piotrowski and J. Sładkowski. An invitation to quantum game theory. *International Journal of Theoretical Physics*, 42(5):1089–1099, 2003.

[183] T. Platkowski. Coorperation in Two-Person Evolutionary Games with Complex Personality Profiles. 2010. unpublished.

[184] T. Platkowski and J. Poleszczuk. Operant Response Theory of social interactions. *eJournal of Biological Science*, 1(1), 2009.

[185] J. Poncela, J. Gomez-Gardenes, A. Traulsen, and Y. Moreno. Evolutionary game dynamics in a growing structured population. *New Journal of Physics*, 11:083031, 2009.

[186] E. M. Pothos and J. R. Busemeyer. A quantum probability explanation for violations of 'rational' decision theory. *Proc. R. Soc. B*, 276(1665):2171–2178, 2009.

[187] E.M. Pothos and J.R. Busemeyer. A quantum probability explanation for violations of "rational"decision theory. *Proceedings of the Royal Society B: Biological Sciences*, 276(1665):2171, 2009.

[188] E.M. Pothos, G. Perry, P.J. Corr, M.R. Matthew, and J.R. Busemeyer. Understanding cooperation in the Prisoner's Dilemma game. *Personality and Individual Differences*, 2010.

[189] Tobias Preis, Sebastian Golke, Wolfgang Paul, and Johannes J. Schneider. Statistical analysis of financial returns for a multiagent order book model of asset trading. *Phys. Rev. E*, 76:016108, 2007.

[190] Robert Prevedel, Andre Stefanov, Philip Walther, and Anton Zeilinger. Experimental realization of a quantum game on a one-way quantum computer. *New Journal of Physics*, 9:205, 2007. arXiv:0708.1129v1.

[191] S. Redner. How Popular is Your Paper? An Empirical Study of the Citation Distribution. *The European Physical Journal B*, 4:131, 1998. cond-mat/9804163.

[192] Jörg Reichardt and Stefan Bornholdt. Clustering of sparse data via network communities - a prototype study of a large online market of social interactions. *J. Stat. Mech.*, page P06016, 2007.

[193] A. E. Roth and J. K. Murnighan. Equilibrium Behavior and Repeated Play of the Prisoner's Dilemma. *Journal of Mathematical Psychology*, 17:189–198, 1978.

[194] D. Sally. On sympathy and games. *Journal of Economic Behavior and Organization*, 44(1):1–30, 2001.

[195] D. Sally. Conversation and Cooperation in Social Dilemmas: A Meta-

Analysis of Experiments from 1958 to 1992. *Rationality and Society*, 7(1):58, 2009. http://rss.sagepub.com/cgi/content/abstract/7/1/58.

[196] W.H. Sandholm. *Population Games and Evolutionary Dynamics*. MIT Press, 2010.

[197] L.J. Savage. *The foundations of statistics*. Wiley, 1954.

[198] Walter Schlee. *Einführung in die Spieltheorie*. Vieweg, 2004.

[199] Maximilian Schlosshauer. Decoherence, the measurement problem, and interpretations of quantum mechanics. *Rev. Mod. Phys.*, 76:1267–1305, 2004. arXiv:quant-ph/0312059v4.

[200] C. Schmid, A.P. Flitney, W. Wieczorek, N. Kiesel, H. Weinfurter, and L.C.L. Hollenberg. Experimental implementation of a four-player quantum game. *New Journal of Physics*, 12:063031, 2010.

[201] Johannes J. Schneider and Christian Hirtreiter. The Impact of Election Results on the Member Numbers of the Large Parties in Bavaria and Germany. *Int. J. Mod. Phys. C*, 16:1165–1215, 2005.

[202] Jan C. Scholz and Martin O.W. Greiner. Topology control with IPD network creation games. *New Journal of Physics*, 9:185, 2007.

[203] S. Schroter, L. Tite, and R. Smith. Perceptions of open access publishing: interviews with journal authors. *BMJ*, 330(7494):756, 2005.

[204] W. Scott, C. Aders, and R. Beusch. Fachverlage in Deutschland - Aktuelle Entwicklung und deren Auswirkung auf den Deutschen Markt. 2003.

[205] R. Selten and T. Chmura. Stationary concepts for experimental 2x2-games. *The American Economic Review*, 98(3):938–966, 2008.

[206] Reinhard Selten and Rolf Stoecker. End behavior in sequences of finite Prisoner's Dilemma supergames A learning theory approach. *Journal of Economic Behavior and Organization*, 7(1):47–70, March 1986.

[207] K. Amartya Sen. Rational Fools: A Critique of the Behavioral Foundations of Economic Theory. *Philosophy*, 6(4), 1977.

[208] Jia Shao, Sergey V. Buldyrev, Lidia A. Braunstein, Shlomo Havlin, and

H. Eugene Stanley. Structure of shells in complex networks. *Phys. Rev. E*, 80:036105, 2009.

[209] B. Sinervo and C.M. Lively. The rock-paper-scissors game and the evolution of alternative male. *Nature*, 380, 1996.

[210] A. Smith. *An inquiry into the nature and causes of the wealth of nations*. Strahan and Cadell, London. Reprint in Oxford University Press, Oxford 1993, 1776.

[211] Adam Smith. *The theory of moral sentiments*. Prometheus Books, Amherst, NY, 2000.

[212] J. Maynard Smith. Game theory and the evolution of fighting. pages 8–28, 1972. *On Evolution*, Edinburgh University Press.

[213] J. Maynard Smith. The theory of games and the evolution of animal conflicts. *J. Theor. Biol.*, 47:209–221, 1974.

[214] J. Maynard Smith. *Evolution and the Theory of Games*. Cambridge University Press, 1982.

[215] J. Maynard Smith. Evolutionary game theory. *Physica D*, 22:43–49, 1986.

[216] J. Maynard Smith and G.R. Price. The logic of animal conflicts. *Nature*, 246:15–18, 1973.

[217] A.N. Samukhin S.N. Dorogovtsev, J.F.F. Mendes. Structure of Growing Networks: Exakt Solution of the Barabasi-Albert's Model. *Phys. Rev. Lett.*, 85:4633, 2000. arXiv:cond-mat/0004434.

[218] J.F.F. Mendes S.N. Dorogovtsev. Evolution of networks. *Adv. Phys.*, 51:1079, 2002. cond-mat/0106144.

[219] SQW. Economic analysis of scientific research publishing. *Wellcome Trust, Cambridgeshire*, 2003.

[220] Robert Sugden. Beyond sympathy and empathy: Adam Smith's concept of fellow-feeling. *Economics*, 18(1):63, 2002.

[221] ZW Sun. The Rule for Evolution of Cooperation in Quantum Games. *Acta Physica Polonica A*, 116:135, 2009.

[222] G. Szab*ó* and G. F*á*th. Evolutionary games on graphs. *Physics Reports*, 446:97–216, 2007. arXiv:cond-mat/0607344v3.

[223] G. Tananbaum. Of wolves and boys: the scholarly communication crisis. *Learned Publishing*, 16(4):284–289, 2003.

[224] Tenopir and King. Towards electronic journals. *SLA Publishing, Washington DC*, 2000.

[225] A. Traulsen, C. Hauert, H. de Silva, M.A. Nowak, and K. Sigmund. Exploration dynamics in evolutionary games. *Proc. Natl. Acad. Sci.*, 106:709–712, 2009.

[226] P.E. Turner and L. Chao. Prisoner's dilemma in an RNA virus. *Nature*, 398, 1999.

[227] A. Tversky and E. Shafir. The disjunction effect in choice under uncertainty. *Psychological Science*, 3(5):305, 1992.

[228] S. J. van Enk. Quantum and classical game strategies. *Physical Review Letters*, 84(4):789, 2000.

[229] S. J. van Enk and R. Pike. Classical rules in quantum games. *Physical Review A*, 66:024306, 2002. arXiv:quant-ph/0203133.

[230] F. Vega-Redondo, M. Marsili, and R. Slanina. Cooperation, and Search in Social Networks. *Journal of the European Economic Association*, 3:628–638, 2005.

[231] G. T. Vickers and C. Cannings. On the Definition of an Evolutionarily Stable Strategy. *J. Theoret. Biol.*, 129:349–353, 1987.

[232] J. von Neumann. *Mathematische Grundlagen der Quantenmechanik*. Springer, 1932.

[233] J. von Neumann and O. Morgenstern. *The Theory of Games and Economic Behaviour*. Princeton University Press, 1947.

[234] Johann (John) von Neumann. Zur Theorie der Gesellschaftsspiele. *Mathematische Annalen*, 100:295–300, 1928.

[235] J.W. Weibull. *Evolutionary Game Theory*. The MIT Press, 1995.

[236] S. White and C. Creaser. Scholarly Journal Prices: Selected Trends and Comparisons. *LISU, Loughborough*, 2004.

[237] C. Woll. Bibliotheken als Dienstleister im Publikationsprozess - Herausforderungen und Chancen alternativer Formen des wissenschaftlichen Publizierens. 2006. VDM Verlag Dr. Müller, Saarbrücken.

[238] T. Yamagishi, S. Terei, T. Kiyonari, N. Mifune, and S. Kanazawa. The social exchange heuristic. *Rationality and Society*, 19(3):259–298, 2007.

[239] Toshio Yamagishi and Nobihiro Mifune. Does Shared Group Membership Promote Altruism?: Fear, Greed, And Reputation. *Rationality and Society*, (20):2–30, 2008.

[240] V. I. Yukalov and D. Sornette. Physics of risk and uncertainty in quantum decision making. *The European Physical Journal B*, 71(4), 2009. arXiv:0812.2388v2.

[241] VI Yukalov and D. Sornette. Quantum decision theory as quantum theory of measurement. *Physics Letters A*, 372(46):6867–6871, 2008.

[242] O.G. Zabaleta and C.M. Arizmendi. Quantum dating market. *Physica A*, 2010. Article in Press arXiv:1003.1153v1 .

[243] E.C. Zeeman. Population Dynamics from Game Theory. *Lecture Notes in Mathematics*, 819:471–497, 1980.

[244] Ernst Zermelo. Über eine Anwendung der Mengenlehre auf die Theorie des Schachspiels. *Proceedings of the Fifth International Congress of Mathematicians*, pages 501–504, 1913.

[245] Vinko Zlatic, Gourab Ghoshal, and Guido Caldarelli. Hypergraph topological quantities for tagged social networks. *Phys. Rev. E*, 80:036118, 2009. arXiv:0905.0976v1.

List of Figures

1.1. Spielbaum eines (2 Personen)-(2 Strategien) Spiels mit den Auszahlungsfunktionen für Spieler A ($\$^A$) und Spieler B ($\$^B$). 7

1.2. Reellwertige und imaginäre Komponenten des zweidimensionalen Quantenspinors $|\psi\rangle_A = \widehat{\mathcal{U}}(\theta_A, \varphi_A) \left| s_1^A \right\rangle$ des Spielers A als Funktion der Quantenstrategien θ_A und φ_A. 18

1.3. Spielbaum eines (2 Personen)-(2 Strategien) Quantenspiels. . . . 20

1.4. Visualisierungsraum der quantentheoretisch erweiterten Auszahlung \$ als Funktion der reduzierten s_1-Quantenstrategien τ_A des Spielers A und τ_B des Spielers B. 23

1.5. Parametersatz Set_A: Auszahlungsfunktion $\tilde{\$}^A(\tilde{s}^A, \tilde{s}^B)$ des Spielers A als Funktion der gemischten Strategie des Spielers A ($\tilde{s}^A$) und des Spielers B ($\tilde{s}^B$). 27

1.6. Links: $x(t)$, Anteil der Spieler die zurzeit t die Strategie s_1 wählen für unterschiedliche Anfangswerte berechnet im Parametersatz Set_A. Rechts: $g(x)$, Reproduktionsdynamik bestimmende Funktion. 28

1.7. Quantentheoretisch erweiterte Auszahlung $\$_A$ des Spielers A (untransparente Fläche) und $\$_B$ des Spielers B (transparente Fläche) als Funktion der reduzierten s_1-Quantenstrategien τ_A des Spielers A und τ_B des Spielers B in einem unverschränktem Quantenspiel ($\gamma = 0$) unter Verwendung des Parametersatzes Set_A. 29

1.8. Quantentheoretisch erweiterte Auszahlungsfunktion (wie in Abbildung 1.7 beschrieben). Die beiden Diagramme stellen die Resultate von Quantenspielen im Parametersatz Set_A mit einem mittleren Verschränkungswert dar (linke Seite: $\gamma = \frac{\pi}{10}$, rechte Seite: $\gamma = \frac{\pi}{5}$). 31

1.9. Quantentheoretisch erweiterte Auszahlungsfunktion (wie in Abbildung 1.7 beschrieben). Die beiden Diagramme stellen die Resultate von Quantenspielen im Parametersatz Set_A mit einem hohen Verschränkungswert dar (linke Seite: $\gamma = \frac{3\pi}{10}$, rechte Seite: $\gamma = \frac{\pi}{2}$). . 32

1.10. Parametersatz Set_B: Auszahlungsfunktion $\tilde{\$}^A(\tilde{s}^A, \tilde{s}^B)$ des Spielers A als Funktion der gemischten Strategie des Spielers A ($\tilde{s}^A$) und des Spielers B ($\tilde{s}^B$). 33

1.11. Links: $x(t)$, Anteil der Spieler die zurzeit t die Strategie s_1 wählen für unterschiedliche Anfangswerte berechnet im Parametersatz Set_B. Rechts: $g(x)$, Reproduktionsdynamik bestimmende Funktion. 34

1.12. Quantentheoretisch erweiterte Auszahlung $\$_A$ des Spielers A (untransparente Fläche) und $\$_B$ des Spielers B (transparente Fläche) als Funktion der reduzierten s_1-Quantenstrategien τ_A des Spielers A und τ_B des Spielers B in einem unverschränktem Quantenspiel ($\gamma = 0$) unter Verwendung des Parametersatzes Set_B. 35

1.13. Quantentheoretisch erweiterte Auszahlungsfunktion (wie in Abbildung 1.12 beschrieben). Die beiden Diagramme stellen die Resultate von Quantenspielen im Parametersatz Set_B mit einem mittleren Verschränkungswert dar (linke Seite: $\gamma = \frac{\pi}{10}$, rechte Seite: $\gamma = \frac{\pi}{5}$). 36

1.14. Quantentheoretisch erweiterte Auszahlungsfunktion (wie in Abbildung 1.12 beschrieben). Die beiden Diagramme stellen die Resultate von Quantenspielen im Parametersatz Set_B mit einem hohen Verschränkungswert dar (linke Seite: $\gamma = \frac{3\pi}{10}$, rechte Seite: $\gamma = \frac{\pi}{2}$). 37

1.15. Parametersatz Set_C: Auszahlungsfunktion $\tilde{\$}^A(\tilde{s}^A, \tilde{s}^B)$ des Spielers A als Funktion der gemischten Strategie des Spielers A ($\tilde{s}^A$) und des Spielers B ($\tilde{s}^B$). 38

1.16. Links: $x(t)$, Anteil der Spieler die zurzeit t die Strategie s_1 wählen für unterschiedliche Anfangswerte berechnet im Parametersatz Set_C. Rechts: $g(x)$, Reproduktionsdynamik bestimmende Funktion. 39

1.17. Quantentheoretisch erweiterte Auszahlung $\$_A$ des Spielers A (untransparente Fläche) und $\$_B$ des Spielers B (transparente Fläche) als Funktion der reduzierten s_1-Quantenstrategien τ_A des Spielers A und τ_B des Spielers B in einem unverschränktem Quantenspiel ($\gamma = 0$) unter Verwendung des Parametersatzes Set_C. 40

1.18. Quantentheoretisch erweiterte Auszahlungsfunktion (wie in Abbildung 1.17 beschrieben). Die beiden Diagramme stellen die Resultate von Quantenspielen im Parametersatz Set_C mit einem mittleren (linke Seite: $\gamma = \frac{\pi}{5}$) und einem hohen (rechte Seite: $\gamma = \frac{2\pi}{5}$) Verschränkungswert dar. 41

1.19. Linke Seite: Auszahlungsfunktion in gemischten Strategien für Spieler A ($\tilde{\$}^A(\tilde{s}^A, \tilde{s}^B)$, farbige Fläche) und Spieler B ($\tilde{\$}^B(\tilde{s}^A, \tilde{s}^B)$, graue Fläche) berechnet im unsymmetrischen Parametersatz Set_7^{us} als Funktion der gemischten Strategien des Spielers A ($\tilde{s}^A$) und Spielers B ($\tilde{s}^B$). Rechte Seite: $g_x(x, y)$ (farbige Fläche) und $g_y(x, y)$ (transparente graue Fläche) in Abhängigkeit der durchschnittlichen strategischen Wahl der Teilpopulation A (x) und B (y). 44

1.20. Phasendiagramm der xy-Trajektorien für drei unterschiedliche Anfangsbedingungen im Parametersatz Set_7^{us}. x beschreibt den Anteil der Spieler aus Gruppe A, die die Strategie s_1 wohingegen y denselben Anteil der Spieler aus Gruppe B bezeichnet. 45

2.1. Game tree of a (2 person)-(2 strategy) game with payoff for player A ($\$^A$) and player B ($\$^B$). 58

2.2. Mixed strategy payoff function $\tilde{\$}^A(\tilde{s}^A, \tilde{s}^B)$ for player A within parameter set Set_2 as a function of the mixed strategies of player A ($\tilde{s}^A$) and B ($\tilde{s}^B$). 74

2.3. $x(t)$, fraction of players choosing the strategy s_1 at time t for different initial conditions within parameter set Set_2 (left picture). The picture on the right shows the function $g(x)$, which determines the dynamical behavior of $x(t)$. 75

2.4. Mixed strategy payoff function $\tilde{\$}^A(\tilde{s}^A, \tilde{s}^B)$ for player A within parameter set Set_3 as a function of the mixed strategies of player A ($\tilde{s}^A$) and B ($\tilde{s}^B$). 75

2.5. $x(t)$, fraction of players choosing the strategy s_1 at time t for different initial conditions within parameter set Set_3 (left picture). The picture on the right shows the function $g(x)$, which determines the dynamical behavior of $x(t)$. 76
2.6. Mixed strategy payoff function $\tilde{\$}^A(\tilde{s}^A, \tilde{s}^B)$ for player A within parameter set Set_4 as a function of the mixed strategies for player A ($\tilde{s}^A$) and B ($\tilde{s}^B$). 77
2.7. $x(t)$, fraction of players choosing the strategy s_1 at time t for different initial conditions within parameter set Set_4 (left picture). The picture on the right shows the function $g(x)$, which determines the dynamical behavior of $x(t)$. 78
2.8. Mixed strategy payoff function $\tilde{\$}^A(\tilde{s}^A, \tilde{s}^B)$ for player A within parameter set Set_8 as a function of the mixed strategies for player A ($\tilde{s}^A$) and B ($\tilde{s}^B$). 79
2.9. $x(t)$, fraction of players choosing the strategy s_1 at time t for different initial conditions within parameter set Set_8 (left picture). The picture on the right shows the function $g(x)$, which determines the dynamical behavior of $x(t)$. 80
2.10. Left picture: Mixed strategy payoff function for player A ($\tilde{\$}^A(\tilde{s}^A, \tilde{s}^B)$, colored surface) and player B ($\tilde{\$}^B(\tilde{s}^A, \tilde{s}^B)$, wired grey surface) within parameter set Set_1^{us} as a function of the mixed strategies of player A ($\tilde{s}^A$) and B ($\tilde{s}^B$). Right picture: $g_x(x, y)$ (colored surface) and $g_y(x, y)$ (wired grey surface) as a function of the strategic population fractions of group A (x) and group B (y). 85
2.11. Phase diagram of the xy-trajectories for three different initial conditions within parameter set Set_1^{us}. x describes the fraction of players within group A choosing the strategy s_1, while y is a similar fraction within group B. 86
2.12. Payoffs and functions $g_x(x, y)$ and $g_y(x, y)$ within set Set_2^{us}; similar description as in figure 2.10. 87
2.13. Phase diagram for three different xy-trajectories within set Set_2^{us}; similar description as in figure 2.11. 88
2.14. Payoffs and functions $g_x(x, y)$ and $g_y(x, y)$ within set Set_7^{us}; similar description as in figure 2.10. 89

2.15. Phase diagram for three different xy-trajectories within set Set_7^{us}; similar description as in figure 2.11. 90

2.16. Payoffs and functions $g_x(x,y)$ and $g_y(x,y)$ within set Set_9^{us}; similar description as in figure 2.10. 91

2.17. Phase diagram for three different xy-trajectories within set Set_9^{us}; similar description as in figure 2.11. 92

2.18. Payoffs and functions $g_x(x,y)$ and $g_y(x,y)$ within set Set_{11}^{us}; similar description as in figure 2.10. 93

2.19. Phase diagram for three different xy-trajectories within set Set_{11}^{us}; similar description as in figure 2.11. 94

2.20. Real and imaginary values of the spinor components of the state $|\psi\rangle_A = \widehat{\mathcal{U}}(\theta_A, \varphi_A) \left| s_1^A \right\rangle$ as a function of the two strategy angles θ_A and φ_A. 100

2.21. Payoff visualization space as a function of the reduced s_1-quantum strategies τ_A of player A and τ_B of player B. 103

2.22. Payoff surface of player A (solid) and player B (wired) as a function of their reduced s_1-quantum strategies τ_A and τ_B within a non-entangled quantum game ($\gamma = 0$) using the parameter setting Set_3 of the dominant prisoner's dilemma game. 107

2.23. Payoff surface of player A (solid) and player B (wired) as a function of their reduced s_1-quantum strategies τ_A and τ_B within two low-entangled quantum games (Left: $\gamma = \frac{\pi}{10}$, Right: $\frac{\pi}{5}$) using the parameter setting Set_3. 108

2.24. Payoff surface of player A (solid) and player B (wired) as a function of their reduced s_1-quantum strategies τ_A and τ_B within two highly-entangled quantum games (Left: $\gamma = \frac{3\pi}{10}$, Right: $\frac{\pi}{2}$) using the parameter setting Set_3. 109

2.25. Payoff surface of player A as a function of the reduced s_1-quantum strategies τ_A and τ_B within a non-entangled ($\gamma = 0$, left picture) and maximally entangled quantum game ($\gamma = \frac{\pi}{2}$, right picture) using the parameter setting Set_2. 110

2.26. Payoff surface of player A as a function of the reduced s_1-quantum strategies τ_A and τ_B within a non-entangled ($\gamma = 0$, left picture) and maximally entangled quantum game ($\gamma = \frac{\pi}{2}$, right picture) using the parameter setting Set_1. 111
2.27. Payoff surface of player A (solid) and player B (wired) as a function of their reduced s_1-quantum strategies τ_A and τ_B within a non-entangled quantum game ($\gamma = 0$) using the parameter setting Set_5 of an coordination game. 112
2.28. Payoff surface of player A (solid) and player B (wired) as a function of their reduced s_1-quantum strategies τ_A and τ_B within two low-entangled quantum games (Left: $\gamma = \frac{\pi}{10}$, Right: $\frac{\pi}{5}$) using the parameter setting Set_5. 113
2.29. Payoff surface of player A (solid) and player B (wired) as a function of their reduced s_1-quantum strategies τ_A and τ_B within two highly-entangled quantum games (Left: $\gamma = \frac{3\pi}{10}$, Right: $\frac{\pi}{2}$) using the parameter setting Set_5. 114
2.30. Payoff surface of player A (solid) and player B (wired) as a function of their reduced s_1-quantum strategies τ_A and τ_B within a non-entangled quantum game ($\gamma = 0$) using the parameter setting Set_8 of an anti-coordination game. 115
2.31. Payoff surface of player A (solid) and player B (wired) as a function of their reduced s_1-quantum strategies τ_A and τ_B within a low-entangled (Left: $\gamma = \frac{\pi}{5}$) and a highly entangled quantum (Right: $\gamma = \frac{2\pi}{5}$) using the parameter setting Set_8. 116
2.32. The thresholds γ_1 (blue line) and γ_2 (red line) of the example game as a function of the payoff parameter α. 120

3.1. Published version of the article (Physica A 382 (2007) 650-664) [111]. 123
3.2. Classical tree of the open access game. 126
3.3. Tree of the open access quantum game. 133
3.4. Separation of the strategy space in four different regions; namely the absolute classical region CC, the absolute quantum region QQ, and the partially classical-quantum regions CQ and QC. 134

3.5. Expected payoff of scientists A and B in a separable quantum game (payoff setting see Table 3.2). 135
3.6. Expected payoff of scientists A and B in a maximally entangled quantum game (left: $\gamma = \frac{\pi}{2}$) and in a partially entangled quantum game (right: $\gamma = \frac{\pi}{4}$). Payoff setting see Table 3.2. 137
3.7. Expected payoff of scientists A and B in a separable prisoners' dilemma quantum game (payoff setting see Table 3.3). 139
3.8. Expected payoff of scientists A and B in partially entangled prisoners' dilemma quantum game (payoff setting see Table 3.3, left: $\gamma = 2\arctan(\frac{\sqrt{3}-1}{\sqrt{3}+1})$, right: $\gamma = \frac{\pi}{4}$). 140
3.9. Expected payoff of scientists A and B in a maximally entangled prisoners' dilemma quantum game (payoff setting see Table 3.3). 140
3.10. Left: The expected payoff of scientists A and B in a separable stag hunt quantum game (payoff setting see Table 3.4). Right: The projection of the right figure onto the \$-t_B plane. 141
3.11. Expected payoff of scientists A and B in a maximally entangled stag hunt quantum game (payoff setting see Table 3.4). 142
3.12. Expected payoff of scientists A and B versus θ_A and γ. Player B has selected the classical strategy ø, whereas player A selects a quantum strategy $\hat{\mathcal{U}}_A = \hat{\mathcal{U}}(\theta_A, \frac{\pi}{2})$. The left picture shows the prisoners' dilemma case whereas the right picture depicts the stag hunt quantum game. 144
3.13. Joint probabilities of the measurable outcomes as a function of γ. Player B chooses strategy ø, whereas Player A chooses $\hat{\mathcal{Q}}$. 145

4.1. Published version of this article is available through the conference internetpage of the "Second Brazilian Workshop of the Game Theory Society, in honor of John Nash, on occasion of the 60th anniversary of Nash equilibrium", which was held in Sãao Paulo (Brazil) from the 29th July until the 4th August in the year 2010. 147
4.2. Animation of the payoff function in mixed strategies. 150
4.3. Animation: Fraction of players choosing strategy s_1 =o as a function of time ($x(t)$) for different starting values $x(t = 0)$. Results were calculated using the payoff matrix of Table 4.1 and the parameter set $r = 5, \alpha = 2$ and $\delta = 3$. 152

4.4. Animation of the payoff surface of player A (solid) and player B (wired) as a function of their strategies τ_A and τ_B. 154

5.1. Published version of the article (Physica A 389 (2010) 5084-5102)[118]. 157
5.2. Fraction of hawks x as a function of time t for different starting values $x(t=0)$. Results were calculated using the parameter set $P1$ (low risk investment market). 166
5.3. Description like in Figure 5.2. Results were calculated using the parameter set $P2$ (medium risk investment market). 167
5.4. Description like in Figure 5.2. Results were calculated using the parameter set $P3$ (high risk investment market). 168
5.5. $\mathcal{N}(x^*, y^*, x)$ for the three Nash equilibria as a function of x within the middle risk parameter setting $P2$. The dark grey line corresponds to the Nash equilibrium $(x^*, y^*) = (1, 0)$, the light grey line to $(x^*, y^*) = (0, 1)$ and the black line ($\mathcal{N} \equiv 0$) to the mixed strategy Nash equilibrium $(x^*, y^*) = (\frac{p_m - 2p_h}{p_m - p_h - d}, \frac{p_m - 2p_h}{p_m - p_h - d})$ 170
5.6. $\mathcal{G}(x^*, x)$ for the three different parameter settings $P1$ ($x^* = \frac{7}{8}$, light grey curve), $P2$ ($x^* = \frac{7}{12}$, dark grey curve) and $P3$ ($x^* = \frac{7}{22}$, black curve). 171
5.7. Payoff surface of player A (solid) and player B (wired) as a function of their reduced strategies τ_A and τ_B within a non-entangled quantum game ($\gamma = 0$) using the quantum dove strategy subset and the high risk parameter setting $P3$. 176
5.8. Projection of the payoff surface of Figure 5.7 in direction of the τ_A-axis. 177
5.9. Same description as Figure 5.7, whereas the left picture is calculated within a sparsely entangled quantum game ($\gamma = \frac{\pi}{8}$) and the right picture represents results within a medium entangled quantum game ($\gamma = \frac{\pi}{4}$). 178
5.10. Same description as Figure 5.7, whereas the results where calculated within a maximally entangled quantum game ($\gamma = \frac{\pi}{2}$) using parameter set $P3$. 179
5.11. Projection of the payoff surface 5.10 in direction of the τ_A-axis. . 180

5.12. Payoff surface of player A (solid) and player B (wired) as a function of their reduced strategies τ_A and τ_B within a non-entangled quantum game ($\gamma = 0$) using the quantum-hawk strategy subset. The left picture depicts the results of the low risk parameter set $P1$, whereas the right picture shows the results of the high risk setting $P3$. 182

5.13. Same description as Figure 5.12, whereas the results where calculated within a maximally entangled quantum game ($\gamma = \frac{\pi}{2}$) using parameter set $P3$. 183

5.14. Same description as Figure 5.12, whereas the results where calculated within a medium entangled quantum game ($\gamma = \frac{\pi}{4}$) using parameter set $P3$. 184

5.15. $\mathcal{N}(\tau_A^*, \tau_B^*, \tau_A)$ as a function of τ_A. The light grey curves visualise the non-symmetric Nash equilibria, whereas the dark grey and black curves depict $\mathcal{N}$ for the symmetric Nash equilibria. The left picture shows the results calculated within the quantum dove strategy subset, whereas in the right picture the calculation within the quantum hawk strategy subset are visualised. 186

5.16. $\mathcal{G}(\tau^{*q}, \tau)$ (black curve) and $\mathcal{G}(\tau^{*c}, \tau)$ (grey curve) as a function of τ within the quantum dove strategy subset. 187

6.1. Published version of this article is available trough the internetpage of the the conference *Logic and the Foundations of Game and Decision Theory* (LOFT 2008) which was held in the year 2008 in Amsterdam. 193

6.2. Visualization of the surfaces $\mathcal{N}_A(\widehat{\mathcal{Q}}_A^\star, \widehat{\mathcal{Q}}_B^\star, \theta_A, \varphi_A, \gamma)$ (wired white) and $\mathcal{N}_A(\widehat{\mathcal{D}}_A^\star, \widehat{\mathcal{D}}_B^\star, \theta_A, \varphi_A, \gamma)$ (grey) as a function of the decision angles θ_A and φ_A for six different values of entanglement (γ-values). The figures were calculated using the payoff parameters of game 1 of [34] (a=70, b=100, c=90 and d=80). 201

6.3. $\delta^\star$ (dashed line, see [34]) and $\gamma_\star$ (solid curve) as a function of the payoff parameter c. 204

6.4. $\mathcal{N}(\gamma)$ for the six different games used in the experiment [34]. The quantum cooperation indicator $\gamma_\star$ is the null of the respective functions, whereas $\mathcal{N}$ is calculated through the integral from $\gamma = 0$ to $\gamma = \pi$. 206

6.5. $\mathcal{N}(\gamma)$ for the three different games used in the experiment [25]. . 207

6.6. Percentage of cooperating players (C_p) in experiment [34] (circles) and [25] (boxes) as a function of $\mathcal{N}$. 209

7.1. Game tree of a (2 person)-(2 strategy) game with payoff for player A ($\mathcal{U}^A$) and player B ($\mathcal{U}^B$). 216

7.2. Mixed-strategy payoff function $\tilde{\mathcal{U}}^A(\tilde{s}^A, \tilde{s}^B)$ for player A within parameter set Set_1 as a function of the mixed strategies of player A ($\tilde{s}^A$) and B ($\tilde{s}^B$). 227

7.3. Function $x(t)$, the fraction of players choosing the strategy s_1 at time t, for different initial conditions within parameter set Set_1 (left picture). The picture on the right shows the function $g(x)$, which determines the dynamical behavior of $x(t)$. 228

7.4. Mixed-strategy payoff function $\tilde{\mathcal{U}}^A(\tilde{s}^A, \tilde{s}^B)$ for player A within parameter set Set_2 as a function of the mixed strategies for player A ($\tilde{s}^A$) and B ($\tilde{s}^B$). 229

7.5. Function $x(t)$, the fraction of players choosing the strategy s_1 at time t, for different initial conditions within parameter set Set_2 (left picture). The picture on the right shows the function $g(x)$, which determines the dynamical behavior of $x(t)$. 230

7.6. Mixed-strategy payoff function $\tilde{\mathcal{U}}^A(\tilde{s}^A, \tilde{s}^B)$ for player A within parameter set Set_3 as a function of the mixed strategies for player A ($\tilde{s}^A$) and B ($\tilde{s}^B$). 231

7.7. Function $x(t)$, the fraction of players choosing the strategy s_1 at time t, for different initial conditions within parameter set Set_8 (left picture). The picture on the right shows the function $g(x)$, which determines the dynamical behavior of $x(t)$. 231

7.8. Left picture: Mixed-strategy payoff function for player A ($\tilde{\mathcal{U}}^A(\tilde{s}^A, \tilde{s}^B)$, colored surface) and player B ($\tilde{\mathcal{U}}^B(\tilde{s}^A, \tilde{s}^B)$, wired grey surface) within parameter set Set_1^{us} as a function of the mixed strategies of player A ($\tilde{s}^A$) and B ($\tilde{s}^B$). Right picture: $g_x(x, y)$ (colored surface) and $g_y(x, y)$ (wired grey surface) as functions of the strategic population fractions of group A (x) and group B (y). 234

7.9. Phase diagram of the xy-trajectories for three different initial conditions within parameter set Set_1^{us}. x describes the fraction of players within group A choosing the strategy s_1, while y is a similar fraction within group B. 235

7.10. Payoffs and functions $g_x(x, y)$ and $g_y(x, y)$ within set Set_2^{us}; similar to the description in Figure 7.8. 236

7.11. Phase diagram for three different xy-trajectories within set Set_2^{us}; similar to the description in Figure 7.9. 237

7.12. Payoffs and functions $g_x(x, y)$ and $g_y(x, y)$ within set Set_3^{us}; similar to the description in Figure 7.8. 238

7.13. Phase diagram for three different xy-trajectories within set Set_3^{us}; similar to the description in Figure 7.9. 239

7.14. Payoffs and functions $g_x(x, y)$ and $g_y(x, y)$ within set Set_4^{us}; similar to the description in Figure 7.8. 240

7.15. Phase diagram for three different xy-trajectories within set Set_4^{us}; similar to the description in Figure 7.9. 240

7.16. $b^A = I - 2$ (solid, colored surface) and $a^B = 3 - \kappa$ (wired surface) as a function of the parameters I and κ. The other parameters are fixed to the values: $\delta = 1$, $r = 3$ and $P = 1$. 245

B.1. Results for the classical game of parameter set Set_1. 256

B.2. Results for the classical game of parameter set Set_5. 258

B.3. Results for the classical game of parameter set Set_6. 260

B.4. Results for the classical game of parameter set Set_7. 262

B.5. Results for the classical game of parameter set Set_9. 264

B.6. Results for the classical game of parameter set Set_{10}. 266

B.7. Results for the classical game of parameter set Set_{11}. 268

B.8. Time evolution of the three components of the population vector $\vec{x}(t)$ within a (2×3)-game (payoff parameters $\$_a = 2, \$_b = -1, \$_c = -1, \$_d = 2, \$_e = 2, \$_f = -1$, Zeeman class 1). The blue curve describes the x_1-component, the red curve the x_2-component and the black curve the x_3-component of the population vector. The initial condition $\vec{x}(0) = (0.1, 0.3, 0.6)$ was used for the numerical analysis. 272

B.9. Vector field $\vec{F}$ and time evolution of the population vector $\vec{x}(t)$ within a two dimensional barycentric coordinate system (initial condition $\vec{x}(0) = (0.1, 0.3, 0.6) \hat{=} (y = 0.4, z = 0.6)$, payoff parameters $\$_a = 2, \$_b = -1, \$_c = -1, \$_d = 2, \$_e = 2, \$_f = -1$, Zeeman class 1). 273

B.10. Animation of the time evolution of the population vector $\vec{x}(t)$ within a two dimensional barycentric coordinate system (payoff parameters $\$_a = 2, \$_b = -1, \$_c = -1, \$_d = 2, \$_e = 2, \$_f = -1$, Zeeman class 1). The colored trajectories describe the numerical results of three different initial condition (blue: $\vec{x}(0) = (0.1, 0.3, 0.6) \hat{=} (y = 0.4, z = 0.6)$, red: $\vec{x}(0) = (0.1, 0.6, 0.3) \hat{=} (y = 0.25, z = 0.3)$ and green: $\vec{x}(0) = (0.6, 0.1, 0.3) \hat{=} (y = 0.75, z = 0.3)$. 274

B.11. Animation of the time evolution of the population vector $\vec{x}(t)$ within a two dimensional barycentric coordinate system (payoff parameters $\$_a = -3, \$_b = -1, \$_c = -3, \$_d = -1, \$_e = -1, \$_f = -1$, Zeeman class -10_2). The colored trajectories describe the numerical results of three different initial condition (blue: $\vec{x}(0) = (0.4, 0.2, 0.4) \hat{=} (y = 0.6, z = 0.4)$, red: $\vec{x}(0) = (0.3, 0.5, 0.2) \hat{=} (y = 0.4, z = 0.2)$ and green: $\vec{x}(0) = (0.5, 0.3, 0.2) \hat{=} (y = 0.6, z = 0.2)$. . 276

B.12. Vector field $\vec{F}$ and time evolution of the population vector $\vec{x}(t)$ within a two dimensional barycentric coordinate system for the generalized Rock-Scissors-Paper game. Payoff parameters $\$_a = 1 + a, \$_b = -1, \$_c = -1, \$_d = 1 + a, \$_e = 1 + a, \$_f = -1$ (left picture $a = -0.1$, middle picture $a = 0$ and right picture $a = 0.1$. 277

B.13. Results for the classical unsymmetric game of setting Set_3^{us}. . . . 278

B.14. Results for the classical unsymmetric game of parameter setting Set_4^{us}. 280

B.15. Results for the classical unsymmetric game of parameter setting Set_5^{us}. 282
B.16. Results for the classical unsymmetric game of parameter setting Set_6^{us}. 284
B.17. Results for the classical unsymmetric game of parameter setting Set_8^{us}. 286
B.18. Results for the classical unsymmetric game of parameter setting Set_{10}^{us}. 288
B.19. Results for the quantum game of parameter setting Set_1. 293
B.20. Results for the quantum game of parameter setting Set_2. 294
B.21. Results for the quantum game of parameter setting Set_3. 296
B.22. Results for the quantum game of parameter setting Set_4. 298
B.23. Results for the quantum game of parameter setting Set_5. 300
B.24. Results for the quantum game of parameter setting Set_6. 302
B.25. Results for the quantum game of parameter setting Set_7. 304
B.26. Results for the quantum game of parameter setting Set_8. 306
B.27. Results for the quantum game of parameter setting Set_9. 308
B.28. Results for the quantum game of parameter setting Set_{10}. 310
B.29. Results for the quantum game of parameter setting Set_{11}. 312

List of Tables

1.1. Allgemeine 2×2 Auszahlungsmatrix der Spieler A und B 16
1.2. Parameterwerte der drei symmetrischen Beispielspiele 25
1.3. (2×2)-Auszahlungsmatrix der Spieler A und B im Parametersatz Set_7^{us}. 43
1.4. Allgemeine Auszahlungsmatrix des „Open Access“-Publikationsspiels. 47
1.5. Allgemeine Auszahlungsmatrix des „Autoren-Journal“ „Open Access“-Bimatrixspiels. 50
1.6. Auszahlungsmatrix der Investmentbanker A und B im Falke-Taube Spiel. 51

2.1. Symmetric payoff matrix after payoff transformation. 70
2.2. Unsymmetric payoff matrix after payoff transformation. 71
2.3. Parameter values of the first seven different sets of symmetric games belonging to the dominant and coordination class. 72
2.4. Parameter values of the last four different sets of symmetric games belonging to the anti-coordination class. 73
2.5. Parameter values of the first two sets of unsymmetric games. . . 81
2.6. Parameter values for set Set_{3-5}^{us} of unsymmetric games. 82
2.7. Parameter values for set Set_{6-8}^{us} of unsymmetric games. 83
2.8. Parameter values for set Set_{9-11}^{us} of unsymmetric games. 84

3.1. General open access payoff matrix. 127
3.2. Open access payoff matrix with reputation as a relative quantity. 128
3.3. Open access payoff matrix within the prisoners' dilemma setting. 129
3.4. Open access payoff matrix within the stag hunt setting. 130

4.1. Payoff of the underlying coordination game. 149

5.1. Payoff matrix for investment bankers A and B within the Hawk-Dove game. The parameters are defined as follows: p_h: high selling premium, d: disutility resulting from fighting and p_m: moderate selling premium. 164
5.2. Parameters of the three different sets of the underlying payoff matrix used to model the investment market of the Hawk-Dove game. 166

6.1. General prisoner's dilemma payoff matrix. 195
6.2. Quantum theoretical results and experimental data of Blonski et.al. [34] and Dal Bó et al. [25]. 208

7.1. Major questions raised in this chapter and their answers. 212
7.2. Parameter values of the three different sets of symmetric games. 226
7.3. Parameter values of the four different sets of unsymmetric games. 233
7.4. Researchers' open-access payoff matrix. 242
7.5. Payoff matrix of the "Author(A)-Journal(B)" open-access bimatrix game. 244

Erklärung:

Ich habe die vorgelegte Dissertation selbst verfaßt und dabei nur die von mir angegebenen Quellen und Hilfsmittel benutzt. Alle Textstellen, die wörtlich oder sinngemäß aus veröffentlichten oder nicht veröffentlichten Schriften entnommen sind sowie alle Angaben, die auf mündlichen Auskünften beruhen, sind als solche kenntlich gemacht.

Frankfurt am Main, den 10.12.2010 Matthias Hanauske